

SQUAT EXERCISE BIOMECHANICS DURING SHORT-RADIUS CENTRIFUGATION

by

KEVIN RONALD DUDA

B.S. Aerospace Engineering (2001)
Embry-Riddle Aeronautical University

S.M. Aeronautics and Astronautics (2004)
Massachusetts Institute of Technology

Submitted to the Department of Aeronautics and Astronautics
in partial fulfillment of the requirements for the degree of

DOCTOR OF PHILOSOPHY IN AERONAUTICS AND ASTRONAUTICS

at the

MASSACHUSETTS INSTITUTE OF TECHNOLOGY

February 2007

© 2007 Massachusetts Institute of Technology
All rights reserved.

Signature of Author: _____

Department of Aeronautics and Astronautics
December 13, 2006

Accepted by: _____

Jaime Peraire
Professor of Aeronautics and Astronautics
Chair, Committee on Graduate Students

SQUAT EXERCISE BIOMECHANICS DURING SHORT-RADIUS CENTRIFUGATION

by

KEVIN RONALD DUDA

DOCTOR OF PHILOSOPHY IN AERONAUTICS AND ASTRONAUTICS

at the

MASSACHUSETTS INSTITUTE OF TECHNOLOGY

Certified by: _____
Laurence R. Young, Sc.D.
Apollo Program Professor of Astronautics
Professor of Health Sciences and Technology
Massachusetts Institute of Technology
Thesis Supervisor

Accepted by: _____
Jeffrey A. Hoffman, Ph.D.
Professor of the Practice of Aeronautics and Astronautics
Massachusetts Institute of Technology

Accepted by: _____
Dava J. Newman, Ph.D.
Professor of Aeronautics and Astronautics and Engineering Systems
Massachusetts Institute of Technology

Accepted by: _____
Lars Oddsson, Dr. Med. Sci.
Research Associate Professor
Boston University

Accepted by: _____
Charles M. Oman, Ph.D.
Senior Lecturer, Department of Aeronautics and Astronautics
Massachusetts Institute of Technology

SQUAT EXERCISE BIOMECHANICS DURING SHORT-RADIUS CENTRIFUGATION

by

KEVIN RONALD DUDA

Submitted to the Department of Aeronautics and Astronautics
on December 13, 2006 in Partial Fulfillment of the
Requirements for the Degree of Doctor of Philosophy in
Aeronautics and Astronautics

Abstract

Artificial gravity (AG) created by short-radius centrifugation is a promising countermeasure to the physiological de-conditioning that results from long-duration spaceflight. However, as on Earth, gravity alone does not ensure fitness. We will need to supplement passive exposure to AG with physical exercise to achieve a comprehensive countermeasure. Before AG exercise can be deemed safe and effective, we must understand how Coriolis accelerations and a gravity gradient affect our biomechanics and how centrifuge-based exercises differ from Earth-upright ones.

Two experiments were designed to investigate the squat biomechanics while upright in the laboratory and while lying supine on a horizontal, clockwise-rotating short-radius centrifuge at speeds up to 30 revolutions per minute. Constant force springs provided additional resistive force up to 25% of body weight. Dependent measure included the three-dimensional position of the left and right knee, left and right foot reaction forces, and muscle activity. We investigated the Coriolis-induced mediolateral knee perturbations and the sensory-motor after-effects from a multiple repetition protocol. The upright and centrifuge biomechanics were compared for similarities and differences between them. In addition, a two-dimensional kinematic model was developed to predict foot reaction forces, Coriolis accelerations, and joint torques.

Our results show that mediolateral knee travel during the AG squats was 1.0 to 2.0 centimeters greater than Earth-upright squats. Increasing the rotation rate or adding resistive force did not affect the results. The peak foot forces increased with rotation rate, but rarely exceeded 200% body weight. The ratio of left-to-right foot force during centrifugation was non-constant and approximately sinusoidal, suggesting a postural correction for the Coriolis accelerations. There was a qualitative difference in the foot force vs. knee angle profile between upright and centrifuge-supine because of the centripetal acceleration. Muscle activity, however, was qualitatively similar between the conditions. The kinematic model was used to evaluate the exercise safety and extend the results to larger-radius centrifuges. We conclude that centrifugation provides a unique and challenging environment for exercise and that a brief artificial gravity squat can be carried out safely. The results are extended to cycle ergometry, when possible, and recommendations are made for future AG squat protocols.

Supported by NASA Grant NNN04HD64G and the MIT-Italy Program Progetto Roberto Rocca.

Thesis Supervisor: Laurence R. Young, Sc.D.
Title: Apollo Program Professor of Aeronautics and Astronautics and
Professor of Health Sciences and Technology

Acknowledgments

First, and most important of all, I would like to thank my family. I wouldn't have been able to do this without them. Their love and support have made me who I am, and their packaged-up leftovers and homemade cookies kept me fed after my many weekend visits home. I'll never forget what they've given me over the years.

A big appreciation goes out to my thesis committee: Larry Young, Chuck Oman, Lars Oddsson, Dava Newman, and Jeff Hoffman. Their collective insight and expertise made it a pleasure to work with them, and their guidance helped keep me on the beaten path.

I am especially thankful to Larry Young for giving me the opportunity to work on this project and being supportive of my research interests. His endless knowledge, infectious enthusiasm, and superb instructional skills were a great asset to this entire process. In particular, I'm thinking of the time he helped improve my skiing technique by explaining it in terms of centripetal acceleration and gravito-inertial forces – both terms used in my research.

Big thanks to Chuck Oman for introducing me to the MVL and its history of human spaceflight experiments. From my Day 1 at MIT, his support and enthusiasm have made it a great pleasure to work with him. He has this incredible ability to give you mid-course corrections to keep you on track with simple suggestions. It's comforting to know that an expert in human navigation knows how to keep you from getting lost.

Lars Oddsson has provided me with the all-important knowledge of sports physiology and biomechanics. He has been enormously helpful. It was always a pleasure to meet with him, not only because of his top notch instructional and advising skills, but because it gave me an excuse to travel to Kenmore Square – a place full of Boston Red Sox and New England Patriots World Championship memories.

A great source of inspiration has come from Dava Newman and Jeff Hoffman. Although I did not work as closely with them as the other members of my committee, their experience,

enthusiasm and passion for what they do, and their dedication to teaching made learning from them a pleasure.

Thomas Jarchow has been uber helpful and supportive. His intuitive knowledge and clever ways of solving problems made everything seem do-able. Statistics has never been so fun with Alan Natapoff. Learning from Alan, has made me a better data analyzer, and more importantly, a better writer. Liz Zotos, our administrative assistant, has helped in so many ways – from ordering glue sticks to pricing flights for me to travel to Italy. I can't thank her enough. Michele Tagliabue from the Politecnico di Milano welcomed me to his laboratory in Italy gave me a great taste of Italian culture.

After being in Florida for four years and missing the New England winters, my choosing to return to Massachusetts was not fun the first winter back. The friends I have made here warmed the entire city, so that even the multiple blizzards seemed tropical. Jessica Edmonds always put a smile on my face, made me have fun on the weekends, and kept me well-fed when I was buried in work. Jessica Marquez was my first officemate, and has become a great friend. She tolerates my humor and gives the right advice on everything. David Benveniste keeps me up-to-date on his travels with risqué postcards from around the world. Neil Ruiz was a fantastic roommate for 4 years, gym partner, and friend. Will Ouimet always reminded me that anything and everything can be turned into a competition. John Mills has been a rock-solid friend with a level-head. Dan Burns always had the sunflower seeds. Dave Quinn never let me forget how angry someone can get. Joe Contrada always knew when to share his Red Sox season tickets. Geoff Huntington knows how to put on a party and get friends together. My buddies from Embry-Riddle, Gene St. Clair, Zack Craig, Tim Meckley, Chris Schott, Craig Delaney, Tom Booth, and all those guys for camping trips and weekend excursions around the country.

Many thanks to the NASA JSC International Multi-disciplinary Artificial Gravity (IMAG) Project (NASA Grant NNJ04HD64G) and the MIT-Italy Program Progetto Roberto Rocca for making this work possible.

Table of Contents

Abstract	5
Acknowledgments.....	7
Table of Contents	9
List of Figures	11
List of Tables	18
Chapter 1: Introduction.....	19
Motivation	20
Problem Statement.....	20
Research Aims	21
Thesis Outline.....	22
Contributions	23
Chapter 2: Background Literature	25
Spaceflight-Related Physiological De-Conditioning.....	26
Exercise Countermeasures for Spaceflight Related De-Conditioning.....	33
Biomechanics of the Squat Exercise.....	40
Artificial Gravity Exercise as a Countermeasure	42
Chapter 3: Exercise and Motion Capture Equipment	47
Linear Back-Slider.....	47
Constant Force Spring Assembly	51
Upright Exercise Device.....	54
SMART Motion Capture Equipment.....	57
Chapter 4: Biomechanical Modeling.....	59
Predicting Coriolis Accelerations.....	59
Estimating Foot Reaction Forces.....	65
Estimating Joint Torques	68
Chapter 5: Squat Biomechanics Experiments.....	73
Equipment and Materials.....	73
Experimental Methods.....	75
Chapter 6: Analysis and Results.....	93
Experiment 1	93
Experiment 2	118
Chapter 7: Discussion.....	148
Kinematics.....	148
Kinetics.....	152
Muscle Activity	161
Motion Sickness and Perceived Effort	166
AG Squat Exercise Protocol Design.....	168

Future Work.....	170
Chapter 8: Conclusions and Recommendations	172
References.....	178
Appendix A: Biographical Sketch.....	188
Appendix B: MVL Centrifuge Technical Description.....	190
Appendix C: AG Exercise Device Drawings.....	197
Appendix D: Biomechanical Model Calculations.....	207
Appendix E: COUHES Informed Consent	209
Appendix F: Rating of Perceived Exertion Scale (Borg Scale).....	217
Appendix G: Surface EMG Electrode Placement	219
Appendix H: Thesis Defense Slides.....	223
Appendix I: Individual Data	241

List of Figures

Figure 1. A qualitative depiction of the rate of adaptation of various human physiological systems to the weightless environment of orbital space flight. Image modified from [12]..... 26

Figure 2. Percentage of muscle volume lost during bed rest unloading [14]. The data suggests that muscle volume lost during bed rest reaches a plateau after ~100 days for most muscles studies. Interestingly, the psoas shows an increase in bed rest, yet often shows a decrease following spaceflight. 29

Figure 3. Summarized reductions in bone mineral density (BMD) by skeletal site [14]..... 32

Figure 4. Exercise countermeasure program for long-duration space flights [14]..... 34

Figure 5. “Preferred Strain History.” The grey line interpolates the data points indicating the number of loading cycles at a particular microstrain sufficient for maintenance of bone mass for a variety of animal species (including the human tibia). Bed rest unloading and microgravity likely results in microstrains that are below the grey line, whereas an increase in activity (impact or resistance exercises) produces microstrains higher than the preferred strain history. “m-values” on the plot are the slopes of the various regions; $m = 4.5$ represents the majority of the loading cycles. Image modified from [49]..... 35

Figure 6. ISS iRED exercise countermeasure program [14]..... 38

Figure 7. Modern spaceflight resistive exercise devices. The image on the left shows the interim resistive exercise device (iRED) (image from [65]). The image on the right is the advanced resistive exercise device (ARED) (image from [68])..... 39

Figure 8. Adaptation of the sensory-motor system to arm reaching movements before, during, and after centrifugation [11]. 43

Figure 9. Three-dimensional assembly views of the backslider frame (left), shoulder harness (top right), and shoulder pad (bottom right). All individual components are fabricated from steel and welded together to form the assemblies. 49

Figure 10. Full three-dimensional conceptualization of the backslider assembly for addition onto the centrifuge. The shoulder harness assembly is bolted to the slider frame with the shoulder pads inserted. The linear pillow-block bearings are attached to the slider frame and then attached to the precision linear rails. The rails are then attached to aluminum sheet stock for rigid attachment to the centrifuge structure. Not shown on here are: 1) the end-stop collars on the precision rails, 2) HDPE surface on top of the slider assembly, and 3) foam padding on the slider assembly and shoulder pads. 50

Figure 11. SolidWorks three-dimensional concept of the constant force spring assembly mounted to the centrifuge foot plate. The constant force spring array is mounted to the top horizontal Unistrut®, and the two vertical Unistrut® U-channels are bolted to the centrifuge foot plate. The springs are connected to the load distributor via eye bolts. Two steel cables are fastened to the load distributor and are routed around the two pulleys and under the foot plate to the backslider assembly..... 53

Figure 12. Plot of the subject’s 1-G upright body weight versus the weight of the subject when lying supine on the centrifuge with the constant force springs set to provide body weight resistance. In approximately half of the cases, the constant force spring load was a little more than their body weight.

However, in general, we are able to apply resistive forces within 10% of the subjects normal body weight. Best fit line has a slope of 0.954 with an intercept of -2.27 pounds, $R^2 = 0.681$. $N = 15$ 54

Figure 13. Upright exercise device. This image shows the configuration of the device when fully assembled. This setup requires the removal of the foot plate from the centrifuge. The Unistrut® frame with the back slider attached is securely clamped to the centrifuge foot plate. The whole assembly is then tilted backwards approximately 20-degrees for subject comfort when exercising. The back slider assembly is counterweighted and the constant force springs can be adjusted for the desired resistive load. 56

Figure 14. SMART System basic equipment. 1) Front of the computer and video synchronization hub. The door on the front of the computer opens downward to reveal the power switch, CD-ROM, CD-RW, and floppy drive. The power switch for the synchronization hub is also on the front. 2) Rear view of the computer and synchronization hub. 3) Front and back of the camera unit with a 3.6-mm lens. 4) Power and data cable for the camera units. 5) Camera unit on tripod. 6) Calibration axis. 57

Figure 15. SMART motion capture equipment mounted on-board the MIT short-radius centrifuge. All equipment and power sources were on the rotating device. Computer equipment and cables were strapped securely to the centrifuge. The four camera units (not shown in this picture) were rigidly mounted to the four corners at approximately 1.0-meter (39.4 in.) from the centrifuge surface. 58

Figure 16. Two-dimensional three-link segment for approximation of the squat biomechanics. The full calculations and definition of variables is located in the Appendix. 60

Figure 17. Coriolis accelerations on the approximate center of mass locations of both the thigh and shin during 0.5-Hz cadence artificial gravity squats. 61

Figure 18. Coriolis acceleration-induced joint torques on the knee and hip in the frontal plane. 62

Figure 19. Coriolis acceleration on the right shin from one cycle while exercising at 23-RPM. The accelerometer was located 0.13 m (5.1 in.) below the knee joint (30% of the length of the shin). Positive acceleration is in the medial direction. Curve-fit parameters: $a = 0.1$ G, $\omega = 2.7$ rad/sec, $c = -0.004$ G, $R^2 = 0.80$, $SSE = 0.39$ 63

Figure 20. Coriolis acceleration on the right thigh while exercising at 23-RPM. The accelerometer was located 0.17 m (6.7 in.) above the knee joint (40% of the length of the thigh). Positive acceleration is in the medial direction. Curve-fit parameters: $a = 0.16$ G, $\omega = 2.6$ rad/sec, $c = -0.01$ G, $R^2 = 0.74$, $SSE = 1.1$ 64

Figure 21. Left: Measured and predicted foot reaction forces during a 23-RPM supine squat. Right: Measured and predicted foot reaction forces over a 20 second window during a 23-RPM supine squat. Root-mean-square error (RMSE) = 40 N (8.95 lbs.) 67

Figure 22. Left: Measured and predicted foot reaction forces during a 30-RPM supine squat. Right: Measured and predicted foot reaction forces over a 20 second window during a 30-RPM supine squat. Root-mean-square error (RMSE) = 30 N (6.59 lbs.) 67

Figure 23. Biomechanical approximation for calculating frontal plane knee torque of a single leg. 69

Figure 24. Estimation of a single leg knee torque in the frontal plane. 70

Figure 25. Ligaments, cartilage, and menisci of the right knee.	71
Figure 26. Left: Centrifuge linear back-slider with shoulder pads installed. The calibration axis is shown on the back-slider. Right: The foot plate of the centrifuge with the modified Kettler Vario Mini Stepper attached. The subjects feet are strapped to independent foot holds on the stepper. Single axis force sensors are located underneath each foot. The stepper foot holds are locked into a symmetric position by the 2-in. by 4-in. piece of lumber. Four of the springs in the constant force spring assembly are deflected in this image.	74
Figure 27. Experiment 1 conditions for investigating Aim #1 and #2. The 0-RPM, 0% resistance condition (pink cell) was used to look for after-effects. The 0-RPM, 1-BW (green cell) is a baseline measure for comparing the conditions when the centrifuge is rotating (blue cells).	77
Figure 28. Anatomical locations of the muscles we recorded EMG from. Top left: Vastus medialis, vastus lateralis, rectus femoris. Top right: Tibialis anterior. Bottom right: Medial and lateral gastrocnemius, soleus. Images from [110].	79
Figure 29. EMG electrode placement on the lower leg. Left: electrode placement on the soleus, medial gastrocnemius, and lateral gastrocnemius of the left and right leg. Right: electrode placement on the tibialis anterior of the left and right leg.	80
Figure 30. Maximum voluntary isometric contraction (MVIC) testing for the soleus (upper left), tibialis anterior (upper right), and gastrocnemius (bottom).	82
Figure 31. Electrode placement on the vastus lateralis, vastus medialis, and rectus femoris of the left and right leg. The EMG junction boxes are shown on the subjects left and right hip.	82
Figure 32. Maximum voluntary isometric contraction (MVIC) testing for the vastus lateralis, vastus medialis, and rectus femoris. The right leg was tested first, followed by the left leg.	83
Figure 33. Subject performing a supine squat on-board the centrifuge. Left: Subject is “standing” against either their artificial gravity weight or constant force spring resistance. Right: Subject is the knee flexed position against either their artificial gravity weight or constant force spring resistance.	85
Figure 34. Side-views of a subject performing a supine squat on-board the centrifuge. Left: Subject is “standing” against either their artificial gravity weight or constant force spring resistance. Right: Subject is the knee flexed position against either their artificial gravity weight or constant force spring resistance.	86
Figure 35. Experimental conditions for testing Hypothesis #3 (primary) and expanding on the conditions for testing Hypothesis #1 (secondary).	89
Figure 36. Subject performing an upright squat. Left: Subject is standing against either their body weight or body weight plus constant force spring resistance. Right: Subject is the knee flexed position against either their body weight or body weight plus constant force spring resistance.	92
Figure 37. Exemplary data for the two-dimensional frontal plane motion of the left and right knee during a set of eight repetitions while rotating at 23 RPM clockwise. We see the start and end position of the left and right knee, as well as the maximum medial and lateral deflection of the knee during each repetition. During descent, the left knee deflects laterally (right knee medially) and during ascent, the left knee deflects medially (right knee laterally). The maximum medial-lateral travel of the knee is the	

absolute value of the difference between the maximum lateral deflection and the maximum medial deflection during each repetition for the left and right knees individually. 94

Figure 38. Maximum medial-lateral travel of the knees during each experimental phase. Both knees averaged together. Data from 14 (7 male, 7 female) of the 15 subjects is shown. Mean +/- SEM..... 95

Figure 39. Time history of the maximum total medial-lateral deflection. The left and right knee are averaged together. The experimental phases are presented sequentially, along with the repetition numbers within each phase. There are a total of 112 squat repetitions in this experiment. Data for all 15 subjects is shown. Mean +/- SEM. 96

Figure 40. "Standing Weight" of the subject as a percentage of their 1-G upright weight. Phase 2 is the weight of the subjects provided by the constant force springs. Phases 3 and 5 are the artificial gravity weight of the subject plus the artificial gravity weight of the back slider. Data for all 15 subjects (all 15 for Phases 1, 2, 3 and 4, 14 of 15 for Phase 5) is shown. Mean +/- SEM..... 97

Figure 41. Average peak foot reaction force during each repetition of the squat as a percentage of each subject's 1-G upright weight. Data for 15 subjects is shown. Mean +/- SEM..... 98

Figure 42. Definition of knee flexion and extension angles. Top: Knee flexion (positive angles, ϕ). Bottom: Knee extension (negative angles, $-\phi$). 99

Figure 43. Ratio of left foot reaction force to right foot reaction force minus 1.0 as a function of knee angle. Left: 0-RPM, 100% body weight resistance (Phase 2), Middle: 23-RPM (Phase 3), Right: 30-RPM (Phase 5). Data for all 15 subjects is shown. Mean +/- SEM..... 101

Figure 44. Ratio of left to right foot force minus 1.0 for the 23-RPM (left) and 30-RPM (right) squat conditions. Each of the five sets is plotted individually. Data from 14 of the 15 subjects is shown. Mean +/- SEM..... 102

Figure 45. Total foot reaction force (sum of left and right leg) during each repetition expressed as a percentage of the subject's 1-G upright body weight. Left: 0-RPM, 100% body weight resistance (Phase 2), Middle: 23-RPM (Phase 3), Right: 30-RPM (Phase 5). Mean +/- SEM for 14 subjects is shown..... 103

Figure 46. Raw EMG of the right vastus lateralis during MVIC testing. Muscle activity [Volts] is shown as a function of time [seconds]. 104

Figure 47. Rectified EMG of the right vastus lateralis during MVIC testing (i.e., rectified signal from Figure 46). Muscle activity [Volts] is shown as a function of time [seconds]..... 105

Figure 48. 500-ms moving average (250-ms overlap) of the rectified EMG of the right vastus lateralis during MVIC testing (i.e., moving average of data in Figure 47). Muscle activity [Volts] is shown as a function of time [seconds]. 105

Figure 49. Percentage of maximum voluntary isometric contraction (%MVIC) with the Knee Angle (degrees) overlaid versus time (seconds). The 1 degree window over which the %MVIC data is averaged is shown (e.g., 60 degrees knee angle)..... 106

Figure 50. Soleus muscle activity. Values are presented as a ratio of the left soleus %MVIC at each knee angle divided by right soleus %MVIC minus one. Data for all 15 subjects is shown. Mean +/- SEM. . 108

Figure 51. Lateral gastrocnemius muscle activity. Values are presented as a ratio of the left lateral gastrocnemius %MVIC at each knee angle divided by right lateral gastrocnemius %MVIC minus one. Data for all 15 subjects is shown. Mean +/- SEM. 109

Figure 52. Medial gastrocnemius muscle activity. Values are presented as a ratio of the left medial gastrocnemius %MVIC at each knee angle divided by right medial gastrocnemius %MVIC minus one. Data for all 15 subjects is shown. Mean +/- SEM. 110

Figure 53. Tibialis anterior muscle activity. Values are presented as a ratio of the left tibialis anterior %MVIC at each knee angle divided by right tibialis anterior %MVIC minus one. Data for all 15 subjects is shown. Mean +/- SEM. 111

Figure 54. Vastus lateralis muscle activity. Values are presented as a ratio of the left vastus lateralis %MVIC at each knee angle divided by right vastus lateralis %MVIC minus one. Data for all 15 subjects is shown. Mean +/- SEM. 112

Figure 55. Vastus medialis muscle activity. Values are presented as a ratio of the left vastus medialis %MVIC at each knee angle divided by right vastus medialis %MVIC minus one. Data for all 15 subjects is shown. Mean +/- SEM. 113

Figure 56. Rectus femoris muscle activity. Values are presented as a ratio of the left rectus femoris %MVIC at each knee angle divided by right rectus femoris %MVIC minus one. Data for all 15 subjects is shown. Mean +/- SEM. 114

Figure 57. Histogram of subjective reports of motion sickness. Left: 23 RPM (Phase 3). Right: 30 RPM (Phase 5). 115

Figure 58. Maximum total medial-lateral travel of the knees. Group A deflections are shown sequentially in the Phase Index. Group B phases are re-arranged so that they are plotted against the similar experimental conditions in Group A. Within each cluster of three Phases, the additional resistance is zero (left bar), 10% body weight (middle bar), and 25% body weight (right bar). Data from 12 (8 male, 2 female) of the 13 subjects is shown. Mean +/- SEM. 119

Figure 59. Maximum total medial-lateral deflection of the knee as a function of upright and centrifuge supine conditions. Data from 12 (8 male, 2 female) of the 13 subjects is shown. Mean +/- SEM. 120

Figure 60. Postural effect on the maximum total medial-lateral deflection of the knees. Two postures: Upright (0% body weight additional resistance – Phase 1) and Supine (100% body weight resistance – Phase 5). Left and right legs combined. Data shows 12 of the 13 subjects. Mean +/- SEM. 121

Figure 61. Maximum total medial-lateral deflection of the knee during the pre- and post-centrifugation trials. Eight repetitions while lying supine without any additional resistance were averaged together. Data from all 13 subjects is shown. Mean +/- SEM. 122

Figure 62. "Standing Weight" of the subject as a percentage of their 1-G upright weight. Group A deflections are shown sequentially in the Phase Index. Group B phases are re-arranged so that they are plotted against the similar experimental conditions in Group A. Data for 12 of the 13 subjects. Mean +/- SEM. 123

Figure 63. Left: "Standing weight" of the subject as a percentage of their 1-G upright weight for males and females. We see the interaction between rotation rate and gender in Phase Indices 6 thru 13. Data for

12 of the 13 subjects is shown. Mean +/- SEM. Right: “Standing weight” of the subject as a percentage of their 1-G upright weight. Both groups averaged together. Data for 12 of the 13 subjects is shown. Mean +/- SEM. 124

Figure 64. Peak foot reaction forces (percentage of 1-G upright standing weight). Group A deflections are shown sequentially in the Phase Index. Group B phases are re-arranged so that they are plotted against the similar experimental conditions in Group A. Within each cluster of three Phases, the additional resistance is zero (left bar), 10% body weight (middle bar), and 25% body weight (right bar). Data from 12 of 13 subjects is shown. Mean +/- SEM. 125

Figure 65. Left: Peak force as a percentage of 1-G upright weight during each repetition for subjects in Group A and B. We see the RPM * Group effect in Phase Indices 11 thru 13. Data for 12 of the 13 subjects is shown. Mean +/- SEM. Right: Peak force as a percentage of 1-G upright weight. Both groups averaged together. Data for 12 of the 13 subjects is shown. Mean +/- SEM. 126

Figure 66. Ratio of left foot force to right foot force minus one as a function of knee excursion angle. Data from 12 of the 13 subjects are shown. Mean +/- SEM. 130

Figure 67. Total foot reaction force (percentage of 1-G upright body weight) as a function of knee angle. Data from 12 of the 13 subjects are shown. Mean +/- SEM. 132

Figure 68. Total foot reaction force as a function of knee angle. The knee angles during flexion and extension are averaged together. Data from 12 of 13 subjects is shown. Mean +/- SEM. 133

Figure 69. Soleus muscle activity (%MVIC) plotted as a function of knee angle. Mean +/- SEM. 136

Figure 70. Lateral gastrocnemius muscle activity (%MVIC) plotted as a function of knee angle. Mean +/- SEM. 137

Figure 71. Medial gastrocnemius muscle activity (%MVIC) plotted as a function of knee angle. Mean +/- SEM. 138

Figure 72. Tibialis anterior muscle activity (%MVIC) plotted as a function of knee angle. Mean +/- SEM. 139

Figure 73. Vastus lateralis muscle activity (%MVIC) plotted as a function of knee angle. Mean +/- SEM. 140

Figure 74. Vastus medialis muscle activity (%MVIC) plotted as a function of knee angle. Mean +/- SEM. 141

Figure 75. Rectus femoris muscle activity (%MVIC) plotted as a function of knee angle. Mean +/- SEM. 142

Figure 76. Borg rating of perceived physical exertion. Groups A and B are plotted separately. Within each cluster of three phases (Upright, 23-RPM, and 30-RPM), there are increasing levels of resistance (0-, 10-, and 25-% of 1-G upright body weight). Data for all 13 subjects is shown. Mean +/- SEM. 143

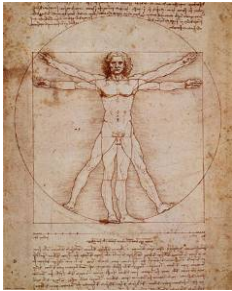
Figure 77. Histogram of the subjective reports of motion sickness at 23-RPM (Left; Phase Indices 6, 7, 8) and 30-RPM (Right; Phase Indices 11, 12, 13). Data for all 13 subjects. 144

Figure 78. Ground reaction force as a ratio of body weight for various terrestrial, centrifuge, and space-based activities. ISS Treadmill Running and 30-RPM AG Squats depict the peak forces and not the time-course of the ground reaction force, as with the other illustrated activities. Figure modified from [114].	155
Figure 79. Inertial and gravity/centripetal contributions to foot reaction forces. Kinematic data recorded from the supine squats was used to plot the ratio of the inertial force to gravity/centripetal force throughout one squat cycle.	157
Figure 80. Difference in mean total foot reaction forces (% body weight) at each of the flexion angles. Multiple conditions are shown where the foot reaction forces were thought to be similar. Data from 12 of 13 subjects is shown. Mean +/- SEM.	158
Figure 81. Difference in %MVIC between experimental conditions of the left soleus at various knee angles.	164
Figure 82. Vastus medialis %MVIC (triangles) as a function of knee angle (degrees). Muscle activity is from a 12-RM strength training protocol. Modified from [78].	165
Figure 83. Accelerations on the otoliths organs from a 0.5-Hz squat with 0.5-m amplitude. Earth gravity is constant in the nasal-occipital direction. Top left: Inter-aural Coriolis accelerations. Top right: Dorsal-ventral inertial and centripetal accelerations. Bottom left: Coriolis-induced swing of the GIF vector in the transverse plane. Bottom right: Inertial/centripetal-induced swing of the GIF in the sagittal plane.	167
Figure 84. Maximum average mediolateral knee travel while upright, supine, and while rotating at 23 and 30 RPM. Data from Experiment 2. All levels of resistance averaged together while upright and while rotating. Mean +/- SEM.	173
Figure 85. Maximum average mediolateral knee travel without rotation and after a forty repetition artificial gravity squat protocol at 23 and 30 RPM. Mean +/- SEM.	174
Figure 86. Left: Left-to-right foot force ratio minus 1.0 during 30 RPM squats. Mean +/- SEM. Right: Inter-aural Coriolis acceleration during 0.5 Hz squats. This figure illustrates the fact that the foot force compensation is 180 degrees out of phase with the Coriolis accelerations. Although the abscissas of the graphs are different units (degrees vs. time), both plots represent one cycle of the squat.	174
Figure 87. Left: Standing force as a percentage of body weight while standing upright, and lying supine at 23 and 30 RPM squats (Experiment 2). N = 12. Mean +/- SEM. Right: Peak force as a percentage of body weight during upright squats, and AG supine squats at 23 and 30 RPM (Experiment 2). N = 12. Mean +/- SEM.	175

List of Tables

Table 1. Centrifuge linear back-slider design guidelines.....	48
Table 2. Constant force spring assembly design guidelines.	51
Table 3. Upright exercise device design guidelines.....	55
Table 4. Experiment 1 phases. Rotation rates are in revolutions per minute (RPM). Resistance is a percentage of 1-G upright body weight (BW).	77
Table 5. Anatomical functions of the muscles we recorded EMG from, and the percentage of type I (slow-twitch) fibers [14]. Data is not available for the rectus femoris, vastus medialis, or tibialis anterior.	80
Table 6. Experiment 2 protocol. Resistance is a percentage of 1-G body weight. RPM = Revolutions per minute (centrifuge rotation rate). BW = Body weight.	88
Table 7. Statistical analyses results for Experiment 1: Knee Kinematics and Foot Forces. [$p < 0.05$] ...	116
Table 8. Statistical analyses results for Experiment 1: Muscle Activity. [$p < 0.05$].....	117
Table 9. Comparison of mean standing foot reaction forces across conditions. The conditions where the mean standing foot reaction forces are not significantly different from one another are highlighted, with p-values shown.....	124
Table 10. Comparison of mean peak foot reaction forces (% body weight) during the exercise repetitions across conditions. The conditions where the mean peak foot reaction forces appear similar to one another are highlighted, with p-values shown.	128
Table 11. Statistical analyses results for Experiment 2: Knee Kinematics, Foot Forces, Borg Effort. [$p < 0.05$]	145
Table 12. Statistical analyses results for Experiment 2: HMR Muscle Activity.....	146
Table 13. Contrast table for the soleus %MVIC data. Out of the 12 knee angles we tested, the number of knee angles that are not significantly different between the conditions compared. The matching conditions where at least nine of the twelve knee angles produce similar activity are highlighted.....	164

Chapter 1: Introduction



*“...we may overlook the element not listed on the chart.
Its importance, so obvious. Its presence is simply understood.
The missing element is the human element.
And when we add it to the equation, the chemistry changes...”*
Dow Chemical Company Television Commercial

Many people perceive space travel as something that is technologically easy, something that happens every day. The large number of engineers and scientists that work in the space industry know differently, and smaller subsets of those who work the human aspects of space flight know how challenging every flight can be. Despite over forty-five years of human space travel, the physiological challenges we face during both short- and long-duration flights are well known, but inadequately mitigated.

When entering the weightless environment of orbital space flight, the human body begins to adapt to the new stresses imposed on it. Those stresses, initiated primarily by the lack of gravity, cause physiological de-conditioning that includes bone loss, muscle atrophy, cardiovascular alterations, and neurovestibular disturbances [1]. Many of these changes pose no health threat for life in microgravity, yet they result in physiological systems that are changed, or de-conditioned, relative to their Earth-normal levels. As a result of this de-conditioning, “performance of mission related physical activities may be impaired due to loss of muscle mass, strength, and endurance associated with prolonged exposure to hypogravity [2],” especially on a Mars mission, which could take 600 to 1,500 days roundtrip [3].

In-flight resistive and cardiovascular exercise devices have been used as a countermeasure to mitigate physiological de-conditioning since the Skylab missions in the 1970s. These exercises along with resistive garments and lower body negative pressure (LBNP) are inadequate for preventing these adaptations and preparing the crew-members for Earth return. Artificial gravity has been proposed as a multi-system countermeasure that replaces the mechanical loading countermeasure devices with inertial loading from short-radius centrifugation.

Motivation

Artificial gravity (AG) created by short-radius centrifugation is a promising countermeasure, since it attempts to prevent the de-conditioning from occurring rather than treating the de-conditioned state [4, 5]. However, as on Earth, gravity alone does not ensure fitness. We will likely need to supplement passive exposure to AG with physical exercise. This combination could be effective in achieving a comprehensive countermeasure and some form of exercise may also be required to avoid syncope on-board the centrifuge.

Before AG exercise can be deemed safe and effective, we must first understand the effects that a rotating environment has on our biomechanics. The majority of the previous studies investigating AG exercise as a countermeasure have focused on the response and adaptation of cardiovascular system [6-10], with little mention of biomechanics (e.g., foot forces and muscle activation) and Coriolis forces. These forces may cause unwanted, and potentially harmful, perturbations in our body segments [10, 11] and torques in our joints during repetitive, high cadence motions. It may be possible to physically compensate for those perturbations so that our movements are not significantly affected, but this adaptation may negatively affect our post-rotation performance [11]. Even though we are compensating for the perturbations during rotation, the induced torque still exists. The demonstration that artificial gravity exercises, both resistive and cardiovascular, are physically safe from an operational and physiological point of view is necessary for implementation and acceptance by the astronauts.

Problem Statement

Artificial gravity alone will likely be insufficient in both preventing the spaceflight-related de-conditioning and assuring fitness. The squat exercise will supplement our physiological responses to tonic gravity, and benefit the bone, muscle, and cardiovascular systems. We hypothesize that AG exercise is required to achieve an adequate comprehensive countermeasure, but we must first overcome the challenges of exercising within a rotating environment.

Before AG exercise can be implemented, we must first understand the effects a rotating environment and a gravity gradient have on our biomechanics, and how those biomechanics may differ from those when we are Earth upright. We must also understand the joint forces and torques that arise from these types of exercises.

Research Aims

The squat is one type of resistive exercise that could have significant musculoskeletal and cardiovascular benefits when combined with AG. The studies presented in this thesis were designed to investigate the biomechanical responses (leg kinematics, foot reaction forces, muscle activity) to AG squats while lying supine on the centrifuge, and how those compare with Earth upright squats. For all of these studies, the subject's feet were kept fixed and the head and torso moved linearly either along the radius of centrifuge or along an Earth-vertical slider device. Understanding exercise biomechanics within a rotating environment is necessary for the development and implementation of safe and optimal AG exercise protocols.

This research program was designed to determine a set of artificial gravity exercise parameters by 1) quantifying Coriolis-induced mediolateral knee deflections when performing supine squats on the centrifuge, 2) determine the magnitude and duration of post-rotatory mediolateral knee perturbations following repetitive squats on-board the centrifuge, and 3) determine the centrifuge exercise parameters (rotation rate, additional resistance) that produce similar biomechanical responses (foot reaction forces, muscle activity) to Earth-upright squats. The details of each specific research aim and the governing hypotheses follow.

Aim #1: Coriolis-Induced Knee Deflections

To quantify the magnitude of Coriolis-induced mediolateral knee deflections during the supine squat on-board the centrifuge. Identify whether that deflection increases with rotation rate while holding exercise cadence constant. Additional resistive force will be added during the squat and will allow us to determine whether those mediolateral knee deflections are affected by this resistance at a particular rotation rate and exercise cadence. The higher force, and therefore greater muscle activity, will stiffen the leg and reject the perturbing Coriolis forces.

Hypothesis #1: Mediolateral knee deflections will increase with increasing rotation rate, while keeping exercise cadence constant. Additional resistance at a particular rotation rate and exercise cadence will reduce those deflections.

Aim #2: Biomechanical Adaptation and Post-Rotatory Effects

Determine if repetitive supine squat exercises on-board the centrifuge result in sensory-motor adaptation. Previous research with arm pointing during centrifugation (e.g., [11]) suggests that

there may be an increase in mediolateral knee travel during the during post-centrifugation supine squat exercises compared with no-rotation.

Hypothesis #2: Following a 40 repetition centrifuge squat protocol, the knees will continue to be perturbed after rotation has stopped due to adaptation to the Coriolis forces.

Aim #3: AG and Upright Squat Biomechanics Comparison

We aim to define centrifuge-based squat exercise protocols based on the similarities and differences in the biomechanical data sets between AG supine squats and Earth upright squats. Similar foot reaction forces and muscle activity between the upright and centrifuge-supine squat conditions will allow us to define artificial gravity squat exercise parameters.

Aim #4: Predicting Coriolis Accelerations and Foot Reaction Forces

Create a two-dimensional model for predicting the Coriolis accelerations acting on the upper and lower leg, as well as the vestibular system during AG supine squats. The estimation of accelerations will be used to predict the induced joint torques on the knee and hip. We will use these joint forces and torques to make estimates on injury risk, especially those related to repetitive motions. It will also allow us to determine the inertial contributions to foot reaction forces while on-board the centrifuge.

Thesis Outline

This thesis documents the design and implementation of artificial gravity exercise hardware as well as the research program for evaluating the biomechanical responses to performing a squat on-board the MIT short-radius centrifuge. The next chapter, Chapter 2, provides an overview of the physiological adaptations associated with spaceflight and the countermeasures used to mitigate those adaptations. A review of previous artificial gravity exercise literature is also presented.

This research was made possible by collaboration with the Politecnico di Milano Laboratory for Biomedical Technologies, supported by the MIT-Italy Program. In Chapter 3 we discuss the motion capture equipment that was exchanged during this collaboration as well as the exercise hardware that was used in these experiments.

Chapter 4 begins discussions on the quantitative effects of exercising within a rotating environment. These effects include a gravity gradient and the Coriolis accelerations. We describe a two-dimensional model for predicting Coriolis accelerations, and using the resulting forces to predict frontal plane knee torques. The magnitude and frequency of this joint torque is discussed in context of potential knee injuries.

Two experiments were designed and conducted to test the three hypotheses previously outlined. Chapter 5 details the experimental equipment and setup, the design, as well as the methods and procedures. The following chapter, Chapter 6, presents the results from the two experiments. The two experiments, although they have similar measures, are discussed independently.

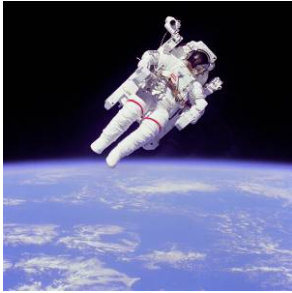
The final two chapters, Chapters 7 and 8, discuss our results and put them in context of previous work in either artificial gravity exercise, or squat biomechanics. We mention the effects, both short- and long-term from exercising within a rotating environment, as well as methods to reduce the effects of Coriolis accelerations. Recommendations are made for implementing AG squats as a countermeasure.

Contributions

The major contributions of this dissertation include:

1. Quantifying artificial gravity biomechanics, which includes the kinematics of the leg, foot reaction forces, and muscle activity. Recommendations for future exercise programs are made based on comparisons between upright centrifuge supine squat exercises.
2. Modeling the kinematics and kinetics of the squat for predicting foot reaction forces and the Coriolis accelerations acting on the body during AG exercises. Estimations on joint torques and repetitive motion injury risk.
3. The design and implementation of resistive exercise equipment for use on-board the MVL short-radius centrifuge and for upright exercises in the laboratory. Several pieces of this equipment were designed for permanent installation on the centrifuge to support current and future studies.

Chapter 2: Background Literature



*“Once you have tasted flight,
you will forever walk the earth with
your eyes turned skyward, for there
you have been, and there you will
always long to return.”*

Leonardo da Vinci

Exercise devices have been flown on spacecraft since Gemini IV, and widely used since Skylab. Various devices have been designed, tested, and implemented. None, however, are adequate in completely mitigating the physiological de-conditioning seen in the astronauts when they return to Earth. Exercising in space often requires special restraints or harnesses to keep you in contact with the exercise equipment. These restraints may prevent you from making “natural” movements and causing changes in your biomechanics. As a result, the physiological responses to exercise in space may differ greatly from those on Earth. These differing physiological responses may not contribute to the maintenance of normal Earth activities, such as locomotion.

Artificial gravity, a century-old concept for protecting space travelers from physiological de-conditioning, may be the multi-system countermeasure we have long searched for. Centrifugation, however, does not come without its own challenges – whether they are technical, sensory-motor, or neurovestibular. Understanding and overcoming these challenges is an important step along the way.

In this Chapter, a review of the physiological changes that result from space flight is presented, along with current exercise countermeasures. The biomechanics of human movement, and more specifically, the squat exercise, are summarized and discussed in terms of the benefits and complications of exercising during centrifugation.

Spaceflight-Related Physiological De-Conditioning

Shortly after entering the weightless environment of orbital space flight, the human body begins to adapt to the new stresses imposed on it. These adaptations include, but are not limited to, bone loss, muscle atrophy, cardiovascular alterations, and neurovestibular disturbances [1]. Each system has been shown to adapt with a qualitatively different time course (Figure 1). Some have been quantified during space flights up to 6-months in duration, whereas others have no known “0-G Set Point.” Each system also recovers to their “1-G Set Point” after returning to Earth at a different pace, ranging from days (neurovestibular) to years (bone). Some data, particularly bone loss, indicates that physiological adaptation to- and recovery from- spaceflight is individual specific, and may depend on previous flight experience.

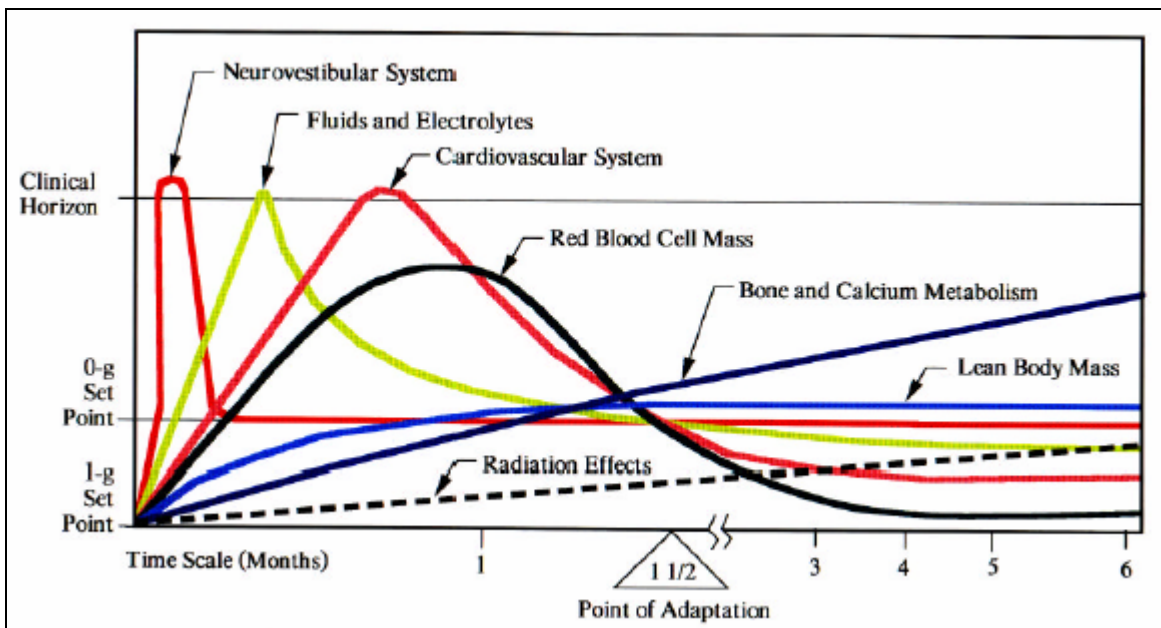


Figure 1. A qualitative depiction of the rate of adaptation of various human physiological systems to the weightless environment of orbital space flight. Image modified from [12].

Neurovestibular Disturbances

Nearly three-quarters of astronauts experience symptoms of space motion sickness (SMS)¹ upon entering orbit [13], but symptoms rarely last more than three days. The occurrence of SMS is popularly explained by sensory conflict theory, which hypothesizes that “it is not the stimulation of any particular sensory modality that leads to motion sickness, but instead a conflict between senses or between a sense and past experience that leads to the sickness [14].” In normal

¹ Also referred to as space adaptation syndrome (SAS), or simply space sickness.

everyday situations on Earth we experience no motion sickness or orientation illusions [15] because our sensory systems all agree on the same interpretation of our orientation with respect to the surrounding environment. In space the semi-circular canals and vision continue to provide accurate information, but the otoliths no longer have a tonic input signaling gravity or body tilt, and the feet are rarely in contact with a surface. Cumulatively, this results in a conflict between the senses and may lead to SMS.

Neurovestibular disturbances also manifest themselves when returning to a gravitational environment, primarily in terms of postural instability [16] and gait ataxia [17, 18]. The balance system relies on information from the otoliths, semi-circular canals, vision, proprioception, as well as local reflex arcs [19]. Changes in neuromuscular function (muscle fiber changes, activation potential changes), muscle atrophy, and orthostatic intolerance may also contribute to post-flight posture and stability. The system, however, does recover rapidly. The recovery of postural equilibrium following short-duration spaceflight has been modeled as a double exponential [16]. The initial rapid re-adaptation has a time constant on the order of 2.7 hours, whereas the slower, secondary, re-adaptation phase shows a time constant of approximately 100 hours (4 days).

Cardiovascular Alterations

Post-flight orthostatic intolerance and reduced exercise capacity are the two well-known consequences of cardiovascular de-conditioning. There are a number of mechanisms hypothesized as the cause of orthostatic intolerance [20]. The most common hypotheses include hypovolemia, alterations in venous compliance, and changes in the baroreflex gain. Within hours of entering weightlessness, leg volume decreases because of the fluid shift from the lower extremities to the upper body and results in a “puffy face [21].” This proximal fluid shift is sensed as an increase in body fluid by the baroreceptors in the carotid artery and aorta, which is compensated for by increasing urinary excretion [22]. A decrease in circulating blood volume is measurable within a few hours of chronic stimulation of the baroreceptors. Hypovolemia during spaceflight has been reported as high as 20% after 36 hours into the mission, and remained at that level after one week [23]. Venous compliance in the legs is also increased because the mechanisms responsible for venous return do not have to work against the hydrostatic gradient normally present when standing upright in Earth-gravity. This includes a reduction in

sympathetic activity [24] (either centrally or peripherally) as well as a reduction in the performance of the skeletal muscle pump [19] due to leg muscle inactivity and atrophy.

Exposure to weightlessness significantly reduces aerobic power ($VO_{2,max}$), even in the presence of exercise countermeasures. In ground-based spaceflight analogs, the absence of exercise countermeasures has resulted in reductions in aerobic power as high as 16% after 10 days of bed rest, and these reductions may increase to as much as 25% with longer-duration bed rest [23]. During 8-14 days of weightlessness, astronauts who did not exercise showed a 21% reduction, and those who did exercise showed an 18% reduction in aerobic power compared to pre-flight [25, 26]. Reduced stroke volume and cardiac output, likely the result of hypovolemia, are considered the primary factors contributing to lower $VO_{2,max}$. Exercise capacity does recover rather quickly after short-duration spaceflight. Cardiac output and stroke volume recover to baseline values between 24 and 48 hours after landing [26]. Aerobic power, however, takes about one week to fully recover after short flights, even when actively taking part in an interval training protocol following spaceflight.

Muscle Sarcopenia

The muscular system, used for locomotion, postural control, and balance, is significantly affected by spaceflight due to the unloading, the lack of a need for balance, and changes in locomotor strategies in a weightless environment [27]. Different muscles are affected differently, and may be associated with the magnitude of the muscular unloading [28]. Muscle changes associated with spaceflight include alterations in fiber type, reductions in muscle volume, and losses in (isokinetic) strength. Many factors can influence muscle sarcopenia, such as disuse, under-nutrition, psychological or physical stress, oxidative stress, and hormones [14].

Human muscle is composed of type I (slow twitch), type IIA (fast, fatigue-resistant), and type IIX (fast, fatigable) fibers – named after the myosin heavy chains (MHC) that predominate within the cells. Type I fibers (e.g., soleus, which is 90% type I) are affected the most by unloading, since they are typically subjected to a tonic stimulation on Earth. Evidence suggests that the soleus fibers both reduce their size and begin adopting a type II isoform during spaceflight [14]. The quadriceps muscles, however, have been studied much more extensively during spaceflight. In astronauts following a 5-11 day mission, the vastus lateralis fibers

expressing fast myosin heavy chains (type II) increased as much as 11% and the slow (type I) fibers were decreased by 16% in the post-flight biopsies compared with pre-flight [25, 28]. However, there are large inter-subject differences in fiber-type alterations and muscle atrophy.

The greatest loss in muscle mass occurs in the lower extremities and postural muscles (Figure 2) whereas the upper body (e.g., arms) muscles seem to remain relatively unaffected. As much as a 10% loss in the deep muscles of the lower back was reported after an 8 day shuttle mission [29]. Unloading initiates a protein breakdown in the muscles, a hypotrophic process that eventually leads to a reduction in muscle volume. Muscle volume losses on landing day following the long-duration spaceflights (16-28 week Shuttle/Mir missions) were often twice as large as those during the short-duration flights (17 day shuttle flight) [30]. It is quite evident that the longer the time in space, the greater the loss in muscle volume. In bed rest, there is evidence to suggest that muscle loss plateaus after approximately 120 days, but these results are specific to each muscle group (see Figure 2). Recovery time is quite different between long- and short-duration flights. After approximately 10 days, muscles loss during the 17 day flight returned to within 5% of the pre-flight values. However, it took approximately four weeks for the muscle loss during the Shuttle/Mir flights to return to baseline levels.

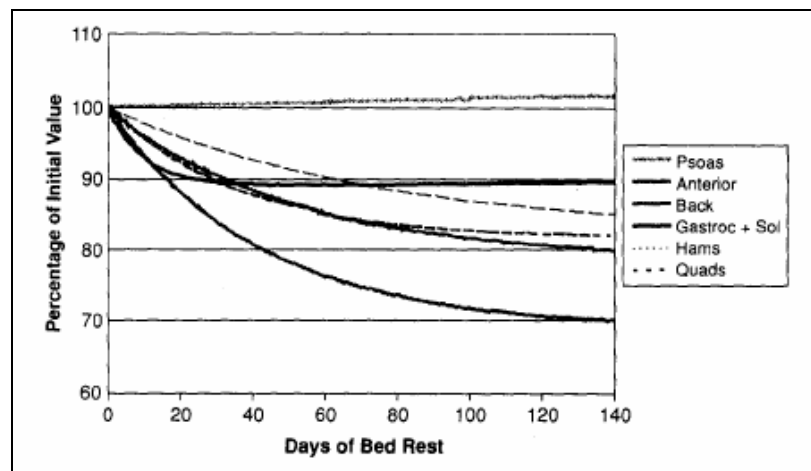


Figure 2. Percentage of muscle volume lost during bed rest unloading [14]. The data suggests that muscle volume lost during bed rest reaches a plateau after ~100 days for most muscles studies. Interestingly, the psoas shows an increase in bed rest, yet often shows a decrease following spaceflight.

Following short-duration flights, research has shown a 20-50% reduction in leg and trunk muscle force [23, 25]. It has been noted that “the decline in peak force production in skeletal muscle

groups of the lower extremities has been consistently greater than average reduction in CSAs² of the total muscle compartment and fiber size [23].” The reductions in strength during bed rest without exercise are quite astounding. Losses on the order of 0.6% per day in the muscles of the lower extremities and 0.4% per day in the arm muscles [23]. Even though the arm muscle volume is relatively unchanged during unloading, we still see reductions in force production. This implies some form of neuromuscular control changes in these muscle groups.

Post-flight strength testing relies heavily on the equipment and joint angular velocity used during the tests. Astronauts (or bed rest subjects) may train with a particular exercise device pre-flight, but these machines are not available in-flight, leading to losses in muscle strength specific to the testing motions. Thus, care is required when performing and interpreting the strength testing data, in part due to the well-documented effects of training specificity [19]. However, subjects who ran on a treadmill during a short-duration mission showed some improvement in maximum force production in the gastrocnemius during post-flight testing even though they did not explicitly train those specific motions pre- or in-flight [25].

There is evidence that the muscles may experience an increased level of fatigability during 1-G activities following spaceflight [28]. This could be due to changes in muscle fiber isoform, or it could be due to the neural changes requiring greater motor unit activation to complete the task. It may also be linked to cardiovascular de-conditioning – hypovolemia and/or reduced sympathetic tone of the vasculature. However, the selective loss of contractile elements relative to mitochondria, and shorter capillary diffusion distance may help to delay the onset of fatigue. The bottom line is that there are many factors that play into the evaluation of our exercise protocols, and each must be considered during analysis.

Reductions in Bone Mineral Density

The bone architecture is constantly remodeling itself and adapting to the stresses from the surrounding environment. The gravitational unloading during spaceflight, along with other stresses within the orbiting laboratory (e.g., low light and high ambient CO₂ concentrations), result in increased bone resorption and decreased bone formation. Urinary calcium excretion is

² Cross-sectional areas (CSAs)

one of the common markers of bone resorption, and it may increase by 60 to 70% within the first few days upon entering weightlessness [14]. Data from Skylab indicated that 0.3% of total body calcium was lost in a 30 day period (0.5% during 30 day bed rest) [31].

The net result of increased bone resorption and urinary calcium excretion is a reduction in bone mineral density³ (BMD). BMD is a common measure used to quantify bone mass and mechanical properties, such as stiffness and strength, by correlating these measurements with *in vitro* tests of animal or cadaveric bones. Astronauts may lose a significant amount of bone during spaceflight, even during flights less than 2 weeks (e.g., lumbar vertebrae) [32]. The lower spine and hip can lose 1-2% BMD per month, whereas the upper arm may show a slight increase on the order of 0.1% per month (Figure 3) [14, 33, 34]. Comparatively speaking, the reduction in BMD for a post-menopausal woman is on the order of 1-2% per year (National Health and Nutrition Examination Survey (NHANES) III). Similar to aging, bone loss increases linearly with spaceflight duration, with no known plateau. Of the astronauts and cosmonauts who flew on Mir or ISS, more than half of them had a greater than 10% loss in BMD in at least one skeletal site, and roughly a quarter of the cosmonauts had a 15-20% reduction in BMD in at least one site [35].

³ BMD is quantified in terms of areal density (g/cm^2), rather than volumetric density (g/cm^3) due to the measurement techniques.

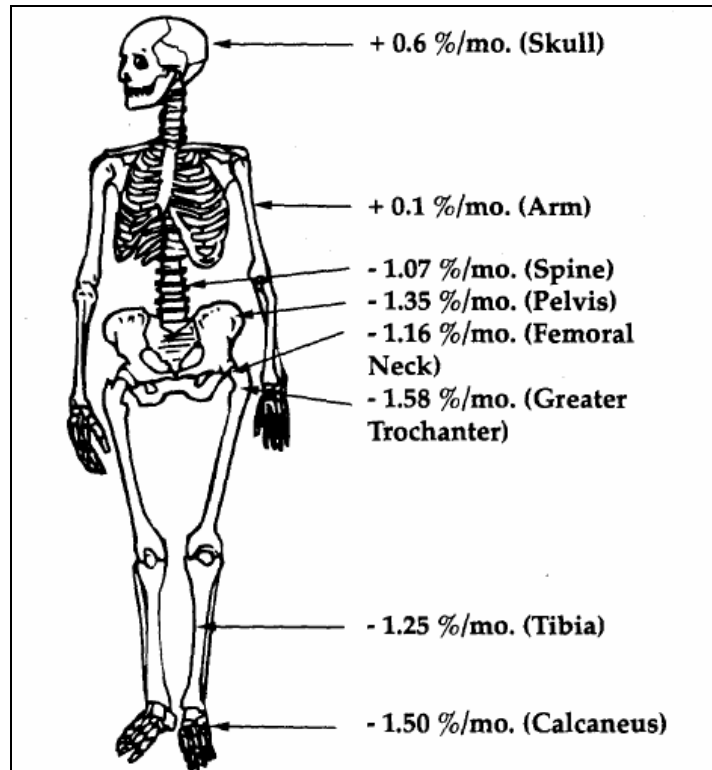


Figure 3. Summarized reductions in bone mineral density (BMD) by skeletal site [14].

The recovery of BMD after returning from spaceflight takes much longer than it took to lose it. For example, a regionalized 12% loss in bone during 4.5 months on the Mir was still at a 6% deficit one year after return to Earth⁴ [14, 36, 37]. Of the ISS and Mir astronaut and cosmonaut data (4-6 months in weightlessness), it took between 4 and 10 months to recover half of the lost bone, depending on the skeletal site. Therefore, based on this recovery rate, it is estimated to take nearly 3 years to recover 94% of the bone lost during a long-duration spaceflight.

There are a number of serious health risks associated with dramatic bone loss. First, the elevated calcium levels in the urine may lead to the formation of kidney stones. There have been 14 documented episodes in the American space program (4 pre-flight, 10 post-flight), and 4 in the Russian program (1 in-flight, 3 post-flight) [38]. Fracture risk is another health-related issue. Once the astronauts return to a terrestrial environment, the risk of bone fracture during locomotion, or even a fall, is elevated due to the reduction in BMD. Schaffner assessed hip

⁴ NASA Johnson Space Center (JSC) Bone and Mineral Laboratory has defined a “recovery half-life” for each skeletal site. The half-life indicates the time required (days or years) to recover 50% of the lost bone.

fracture risk⁵ using computational modeling following exposure to 0, 6, and 12 months of weightlessness and then returning to either Earth or Martian gravity levels [39]. He concluded that, on average, the risk of fracture increased 10% following a return to Earth after 12 months in weightlessness. The risk of fracture on Mars after similar exposures to weightlessness was found to be slightly less than Earth baseline due to the Martian (3/8 G) gravity.

Exercise Countermeasures for Spaceflight Related De-Conditioning

The first flight manifested exercise device was flown on Gemini IV [40], and others have been used extensively for resistive and cardiovascular conditioning since Skylab missions in the 1970s. Despite regular exercise during long-duration spaceflight, we still see reductions in BMD, muscular strength, cardiovascular conditioning, and postural stability when the astronauts return to Earth.

On the ISS, U.S. astronauts are supposed to spend approximately 2.5 hours per day, at least six days per week, exercising in an attempt to prevent this de-conditioning [14, 41]. Typically, they exercise twice a day: one session of resistive exercise, and one session of aerobic/anaerobic exercise (Figure 4) [14]. The training protocols, which alternate among several devices, are designed specific to the capabilities of each crewmember [42]. These include a treadmill, a cycle ergometer, and a resistive exercise device (RED) [43], which are the core exercise devices in the U.S. space program today. Other countermeasures are used in the Russian program. Each piece of equipment is designed to counteract a specific physiological system, sometimes several systems (e.g., treadmill – cardiovascular, bone, muscle, and possibly neurovestibular [44]). We do not have a realized countermeasure that targets and prevents de-conditioning in all physiological systems simultaneously.

⁵ Ratio of applied load to the failure load. High risk of fracture if close to, or greater than 1.0. Low risk is well below 1.0.

- 2.5 hours per day, 6 days per week, consisting of set-up and stowage (10 min each), cool-down and personal hygiene (20 min each), aerobic/anaerobic exercise (30 min each), and resistive exercise (60 min)
 - Day 1: 60 min—lower limb resistance exercise, 30 min—treadmill
 - Day 2: 60 min—lower limb resistance exercise, 30 min—treadmill
 - Day 3: 60 min—lower/upper limb resistance exercise, 30 min—cycle
 - Day 4: 60 min—lower limb resistance exercise, 30 min—treadmill
 - Day 5: 60 min—lower limb resistance exercise, 30 min—treadmill
 - Day 6: 60 min—lower/upper limb resistance exercise, 30 min—cycle
 - Day 7: Active rest
- May be accelerated or increased before entry—with increased exercise times
- No exercise 24 hours before the periodic fitness evaluation

Figure 4. Exercise countermeasure program for long-duration space flights [14].

General cardiovascular and musculoskeletal exercise protocols for maintenance of, or even improvement in, performance are dramatically different. For cardiorespiratory fitness, the American College of Sports Medicine (ACSM) recommends “intensities within the range of 60% to 80% HRR⁶ or 77% to 90% HR_{max}⁷ ...when combined with an appropriate frequency and duration of training [45].” The duration and frequency should be for at least 20-minutes per session three to five days per week. A resistance program designed to “elicit improvement in both muscular strength and endurance” should include 8-12 repetitions of at least 3 sets at a high intensity (approximate momentary muscular fatigue). Each muscle group should be exercised “2 to 3 nonconsecutive days per week and if possible, perform a different exercise for the muscle group every two to three sessions.”

When considering exercise regimens for increasing bone strength they should follow three generally accepted rules [46]: 1) provide dynamic, rather than static, loading. The bone cells are sensitive to the hydrostatic pressure gradients within the lacunar-canalicular network of the bones during dynamic loading, which promotes osteogenesis [47]. 2) Only a short duration of mechanical loading is necessary to initiate the adaptive response. Increasing the duration of skeletal loading does not yield proportional increases in bone mass [46]. 3) Bone cells become desensitized when mechanical-loading sessions are prolonged [48]. It has been proposed that bone requires a “preferred strain history” in order to maintain mass [49]. That is, a certain number of cycles on the bone with a particular surface strain magnitude will maintain the mass

⁶ Heart rate reserve (HRR). The difference between the current heart rate and the projected maximum heart rate (HR_{max} [beats per minute] = 220 – age [in years]).

⁷ Maximum heart rate [beats per minute] = 220 – age [years].

of the bone (Figure 5). This has been the basis of the work using 30-Hz low magnitude mechanical vibration to prevent bone loss in osteoporotic women [50].

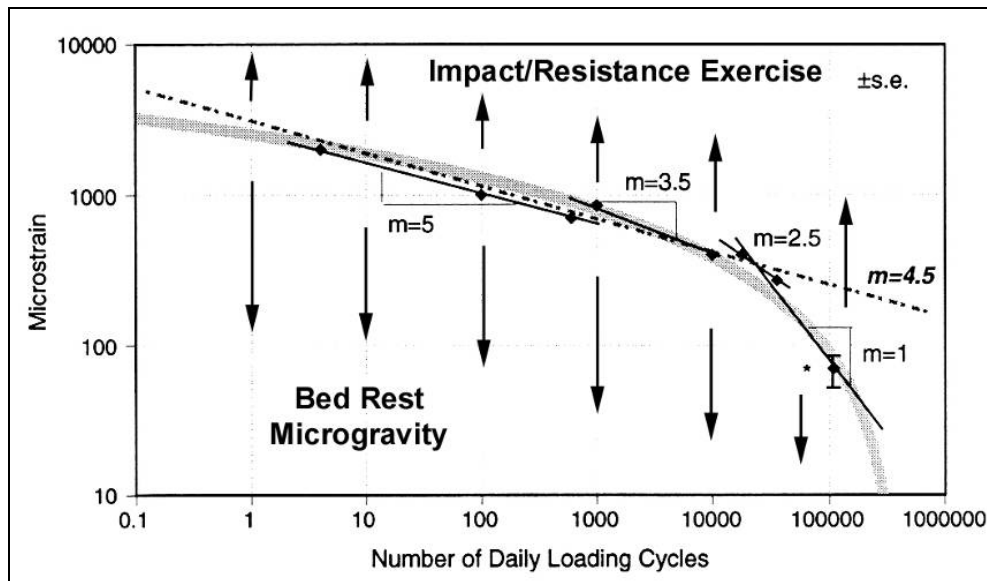


Figure 5. “Preferred Strain History.” The grey line interpolates the data points indicating the number of loading cycles at a particular microstrain sufficient for maintenance of bone mass for a variety of animal species (including the human tibia). Bed rest unloading and microgravity likely results in microstrains that are below the grey line, whereas an increase in activity (impact or resistance exercises) produces microstrains higher than the preferred strain history. “m-values” on the plot are the slopes of the various regions; $m = 4.5$ represents the majority of the loading cycles. Image modified from [49].

It is difficult, however, to evaluate the effectiveness of the exercises performed on the ISS because of the many confounding variables which include stress, nutrition, sleep, psychological state, etc. Our ground-based evaluations of the exercises attempt to control for these factors. It is also difficult to control and monitor exercise intensity/duration and compliance. A NASA flight rule that required exercise on all missions lasting more than 10 days made it difficult to make a comparison between the exercise prescription and control groups [25]. Other factors include medical privacy standards and making generalizations about the astronaut population with small sample sizes.

Cycle Ergometry

Cycle ergometers have been widely used during long-duration space flights in an attempt to maintain cardiovascular fitness and aerobic power. In ground-based spaceflight analogs, the absence of exercise countermeasures has resulted in a 16% reduction in aerobic power after 10 days of bed rest, and up to 25% reductions after longer periods of inactivity [23]. Intense 30 minute bouts of supine cycle ergometry (up to 90% of $VO_{2,max}$) five days per week during 30

days of bed rest maintained $VO_{2,max}$ at pre-bed rest levels [51]. It has also been reported that isotonic cycle ergometry is more effective at maintaining plasma volume and fluid balance⁸ compared to muscular strength and endurance (isokinetic) exercises during 30 days of bed rest [52].

During short-duration (< 2 weeks) shuttle missions, peak VO_2 had declined by 21% in control astronauts, and 18% in the astronauts who cycled 20 minutes per day, three days per week at 60% of the pre-flight maximum work rate [25]. Other experiments have shown smaller reductions, on the order of a 13% reduction in aerobic power following spaceflight. Similar reductions were seen during the Apollo program and during Skylab, $VO_{2,max}$ did not decrease [23].

Cycle ergometers have been primarily employed as a cardio-pulmonary countermeasure. They have been proposed as an addition to short-radius centrifugation to maintain muscular volume during simulated microgravity [53]. As they are designed now, they do not provide any impact loading to the skeletal system. Recent work had been done to incorporate high-frequency mechanical vibration to the pedals [54].

Treadmills

Aerobic and anaerobic treadmill running has also been used in an attempt to preserve aerobic capacity in space [55]. On landing day, following Shuttle flights up to two weeks in duration, $VO_{2,max}$ in treadmill exercisers was not significantly reduced (3% reduction) compared to pre-flight values [25, 55]. The more intense exercise protocol prescribed for the treadmill exercises is better at preventing reduction in aerobic power compared with cycle ergometers.

There are few published studies evaluating the efficacy of treadmill exercises in preventing spaceflight (or bed rest) cardiovascular de-conditioning. This is likely due to the fact that treadmill running is not easily accomplished while maintaining a horizontal posture on Earth. The Cleveland Clinic Center for Space Medicine has developed a zero-gravity locomotion simulator (ZLS) [56] to incorporate treadmill locomotion as part of a bed rest countermeasure program to compare the results of the ISS Foot Experiment [57].

⁸ Fluid balance is defined as fluid intake minus urinary output.

It has often been suggested that treadmill running is important during spaceflight because of the high impact loads during heel strike – important for stimulating bone remodeling. When we run on Earth, the peak ground reaction forces often exceed 260% of our body weight, whereas on the ISS⁹ these forces rarely exceed 160% of body weight [58]. Characteristically, the shape of the ground reaction force profile when running in 0-G with the subject loading device (SLD) is similar to that of 1-G [59], but the bungees of the SLD were not designed to provide sufficient force to mimic 1-G impact forces.

Resistance Devices

It is operationally important during spaceflight to maintain muscle size and strength at or near pre-flight levels [60], particularly in the event of emergency egress. Several studies have shown that resistance training, which requires high muscle forces, is an effective stimulus to increase muscle volume, muscle strength, and BMD [61, 62]. As a result, resistance exercise has been proposed and incorporated as a countermeasure to prevent muscle sarcopenia and reductions in BMD during space flight [63] and bed rest unloading [35].

Onboard the ISS, the interim resistance exercise device (iRED) allows the astronauts to perform a variety of exercises (Figure 6). The maximum resistive force of the iRED is approximately 380 pounds, which is attained by adding bungees to the maximum allowable resistance [43]. An effective 0-G resistance exercise device should be able to provide resistance exceeding twice one's body weight [64], which is often not accomplished by the iRED. Additionally, the peak ground reaction forces (GRFs) with the iRED during 0-G testing in parabolic flight were less than half of that during 1-G, due to the lack of body weight contributing to GRF [65], highlighting another limitation of the current countermeasure.

⁹ The ISS treadmill is called the Treadmill Vibration Isolation System (TVIS). It includes an active damping system to reduce the transmittal of the high frequency foot reaction forces to the spacecraft structure – to preserve the true micro-gravity environment of the orbiting laboratory. This system is very complicated and frequently does not operate properly. This treadmill frequently operates as a self-powered treadmill with passive mechanical damping (i.e., springs), similar to the Russian treadmill.

Exercise	Day 1	Day 2	Day 3	Day 4	Day 5	Day 6
Deadlift	X		X		X	
Bent over rows	X		X		X	
Straight leg deadlift	X		X		X	
Squat	X		X		X	
Heel raises	X		X		X	
Shoulder press		X				X
Rear raises		X				
Front raises		X				
Hip abduction		X				X
Hip adduction		X				X
Bicep curls				X		
Tricep kickbacks				X		
Upright rows				X		
Hip flexion				X		
Hip extension				X		
Lateral raises						X
Front raises						X

The resistance exercises are performed on a device that has pulleys and a shoulder harness to provide the resistance. Early in the mission the goal is 12–15 repetitions maximum (RM) for the resistance exercises, progressing to 4–6 RM later in the mission. The exercise program is as follows: aerobic conditioning—2 days/week, 1 hour/session; resistive exercise—6 days/week, 1 hour/session; interval training—4 days/week, 1 hour/session; extravehicular training—as needed.

Figure 6. ISS iRED exercise countermeasure program [14].

Recent data from ISS expeditions indicates that the iRED exercise program is not effective in maintaining BMD in the regions that are most affected by unloading [37]. In a 16-week ground-based study comparing the strength training benefits of the iRED with those of free weight exercises¹⁰, lumbar BMD increases were significantly greater with the free weights (4.2% increase vs. no change with iRED) [66]. There are two possibilities for this difference: reduced peak reaction force with the iRED and the linear force-tension properties of the iRED [67]. In a separate study comparing the iRED with a Smith machine, it was reported that “because the mass moved with the Smith machine¹¹ was much greater than that moved with the iRED, the effects of acceleration upon GRF will be different [67].” This was part of the motivation for developing the advanced resistive exercise device (ARED). The ARED utilizes vacuum cylinders and flywheels to provide a more “Earth-like” feel to the exercise as well as expanding the exercise capability over the iRED [68].

¹⁰ Subjects were able to improve their one-repetition maximum (1-RM) squat strength by approximately 22% with the iRED.

¹¹ An exercise device that includes a bar with linear bearings on either end of the bar, and the bearings run on steel shafts providing vertical linear motion.

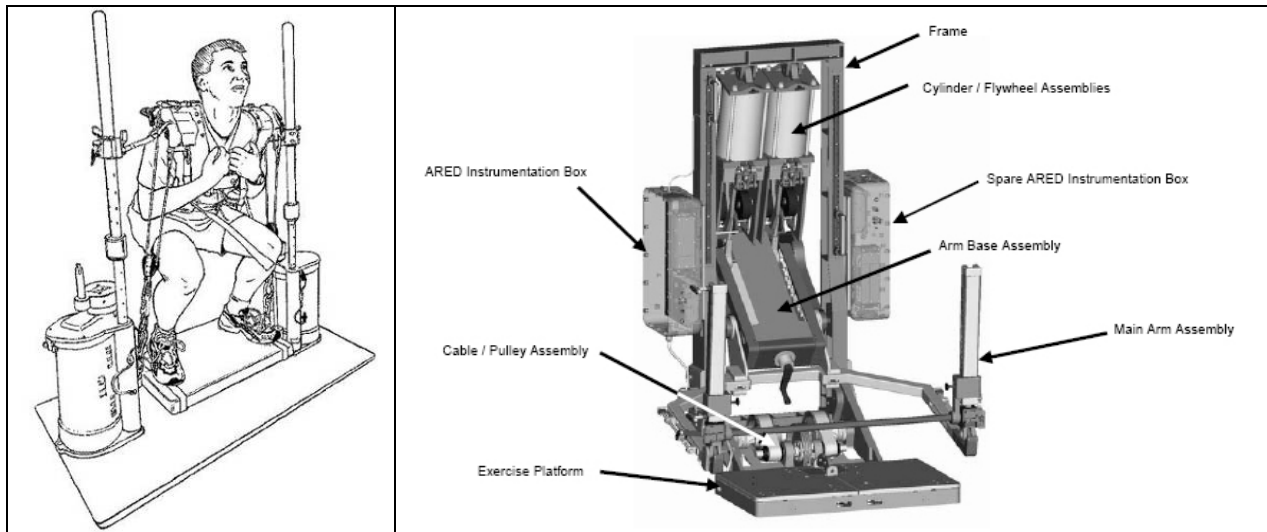


Figure 7. Modern spaceflight resistive exercise devices. The image on the left shows the interim resistive exercise device (iRED) (image from [65]). The image on the right is the advanced resistive exercise device (ARED) (image from [68]).

Resistance exercise has also been evaluated as a countermeasure to muscle sarcopenia and bone loss during simulated microgravity [35, 69-71]. An exercise program consisting of supine squats and calf raises using a flywheel exercise device [72] mitigated reductions in quadriceps and triceps surae muscle volume during 29- [71] and 84 days [70] of bed rest¹². A more extensive exercise program during 17-weeks of bed rest using a “multi-gym¹³” resulted a significant gain in quadriceps muscle volume, gastrocnemius and soleus volume decreased [35]. This indicates that the triceps surae may require a different exercise or perhaps a tonic stimulation to prevent sarcopenia of the slow-twitch fibers.

The effect of bed rest unloading on muscle strength has been widely studied [23, 35, 45, 60, 69-71, 73, 74]. However, only a few recent studies have investigated the effects of resistance training on maintenance of strength. The maintenance, or even increase, in strength during certain exercises depends strongly on the intensity and frequency of the exercise program [45, 75]. In many instances, it is difficult to interpret the benefits of the program because the pre- and post-training isokinetic strength testing is fundamentally different from the training exercises.

¹² The countermeasure was more effective in maintaining muscle volume of the knee extensors than the plantar flexors.

¹³ Horizontal Exercise Machine (HEM). Resistance is provided by weight plates and cable pulleys for transferring force.

Strength training may have additional benefits besides maintenance of bone and muscle. Recent data suggests that combining strength and balance training¹⁴ increases balance function [76] as assessed by the functional mobility test (FMT) [77]. The FMT “subject’s step over and duck under obstacles along with negotiating a series of pylons set up on a base of 10 centimeter thick medium density foam [44].” The performance increase in the FMT after strength training highlights the possibility of “multi-modal effects” from a particular exercise.

Other Devices

A number of countermeasures have been developed and used in an attempt to prevent muscle atrophy and strength loss during spaceflight. In addition to the treadmill, cycle ergometer, and the iRED, the Russians have used passive stretch garments (Russian “Penguin Suit”) and electrical stimulation. Chronic passive stretch has been shown to maintain muscle mass in animals during unloading [14] and has been reported to increase fiber number (hyperplasia) in humans [19]. The “Penguin suit” has “rubber bands woven into the fabric, extending from the shoulders to the waist and from the waist to the lower extremities, to produce tension on antigravity muscles [23].” Data on the effectiveness of the Russian system of countermeasures is scarcely available, making it hard to argue for or against it.

Electrical stimulation is frequently used during physical therapy and other forms of rehabilitation to promote muscle growth [14]. In addition to promoting muscle growth, prolonged electrical activation of muscles has also been shown to induce changes in fiber type (type II to I) [19]. To date, only cosmonauts have been known to include electrical stimulation as part of their countermeasure program. However, there are no known results on the benefits of electrical stimulation alone on muscle hypotrophy.

Biomechanics of the Squat Exercise

The squat is a closed kinetic chain exercise (CKCE) – “the terminal or distal segment is opposed by ‘considerable resistance’ [78].” It is primarily an exercise for the extensor muscles at the ankle, knee, hip, and trunk even though we normally think of it as an exercise for the big leg muscles – the quadriceps, hamstrings, and gastrocnemius. The co-contraction of these muscles is

¹⁴ Performing supine squats with the feet on a balance board and the subjects back on an air-bearing floor. Resistive force is provided by a cable-pulley system that connects to weighted plates.

believed to enhance knee stability. The squat is both an eccentric and concentric¹⁵ exercise for the single-joint muscles involved. It has been suggested that the eccentric portion of the exercise provides the most efficient resistive exercise as a countermeasure for muscle atrophy and dysfunction [60]. This is because eccentric contractions provide a high level of force development independent of the speed of contraction. Even though strength can be maintained, or even improved, with only eccentric training, “concentric training is preferable for development of concentric strength and eccentric training is preferable for development of eccentric strength [75].”

Kinematics and Kinetics

The leg is a multi-segmented system and the kinematics and kinetics depend on the spatial positioning of the feet relative to the hip [79, 80]. Despite the three-dimensionality of the squat exercise, the work on whole-body kinematics and kinetics of the squat is primarily two-dimensional [78, 81, 82]. A significant amount of this work has been dedicated to investigating hip and knee torques, with some emphasis on ground reaction forces and joint forces. The internal forces act on the ligaments of the knee, for example, are also affected during the squat exercise [83].

The anterior cruciate ligament (ACL), posterior cruciate ligament (PCL), tibiofemoral, and patellofemoral forces have been approximated in the sagittal plane during a squat and leg press. Peak PCL and ACL forces can reach as high as 1.5 to 2.0 times body weight during the dynamic squat with resistance as high as 1,335 N (300 lbs.)¹⁶. In this study [78], there was no modeling of the medial or lateral collateral ligaments (MCL or LCL), since they provide mediolateral knee stability (frontal plane) and this model was two-dimensional in the sagittal plane.

Three-dimensional models of the ligaments and musculature within and surrounding the knee have been created to assess ligament function during various loading conditions [85, 86],

¹⁵ During a concentric exercise, the muscle that is contracting is also shortening; it's successfully overpowering the resistance. By contrast, during an eccentric exercise, the muscle that is working is simultaneously lengthening. For example, the quadriceps during a squat – “downward” phase = eccentric, “upward” phase = concentric. Vice versa for the hamstrings.

¹⁶ It has been reported that the ultimate load of the human femur-ACL-tibia complex is as high as 2,160 N [84]. This indicates a factor of safety of approximately 1.2 for a 890 N (200 lb.) man with peak ACL tensile forces of 1,780 N (twice body weight).

including walking [87, 88]. Several other three-dimensional models of the knee have been developed to investigate the loading profiles during skiing injuries. However, no three-dimensional models are known to investigate the forces and moments during the squat.

Muscle Activation

Muscle activity, measured through surface electromyography (EMG), of the dynamic squat exercise has been recorded and compared with the leg press. Escamilla and others [78] recorded EMG activity from the quadriceps (vastus lateralis, vastus medialis, rectus femoris), hamstrings (biceps femoris), and gastrocnemius (medial head). They did not record muscle activity of the soleus or tibialis anterior muscles. The soleus is of interest to us because of its susceptibility to spaceflight de-conditioning. Numerous studies have quantified muscle activity about the knee during the dynamic squat (see [89] for references). Different muscles are activated differently depending on the feet positioning, the knee flexion angle, and the strength of the contraction, which depends on the magnitude of the external resistance [78, 79, 89]. .

Artificial Gravity Exercise as a Countermeasure

The use of artificial gravity created by centrifugation to counter the effects of weightlessness was first proposed over 100 years ago by Konstantin Tsiolkovsky, the Russian space visionary [90, 91]. At the time of Tsiolkovsky's publications, we had no first hand experience with the magnitude and consequences of human physiological de-conditioning in space. Today, we have a fairly good understanding of the physiological systems that are susceptible, the magnitude of the de-conditioning, and the consequences of returning to Earth in a de-conditioned state for missions less than six months in duration [1, 2].

After more than 30 years of very intermittent AG research, there have been no conclusions on fundamental operating parameters (such as radius and rotation rate) [5], despite having a well known design space. Hill and Schnitzer [92] were the first to propose desirable operating parameters – an artificial gravity “comfort zone” – which “defines the rotational characteristics that would be used in conjunction with interpretation of physiological response (comfort zone) to size a manned space station.” They concluded that an upper limit on the angular velocity of the spacecraft of 4 revolutions per minute (RPM), based on the occurrence of vestibular disturbances. For nearly 40 years, it had been assumed that “10-RPM was considered to be near

the upper limits of angular velocity to which man might adapt without impractical side effects [93].” However, it has been recently shown that the human vestibular system can adapt to rotation rates over twice the previously considered upper limit [94]. Current work is aimed at investigating adaptation at rotation speeds as high as 30 RPM [95].

Sensorimotor Adaptation

In addition to vestibular adaptation to high rotation rates, the sensory-motor system has been shown to adapt to centrifugation [11]. In finger pointing experiments, the first movement during rotation tends to be deflected in the direction of the Coriolis force¹⁷. After a series of reaches, the subjects learn to compensate for the perturbing force and the movements were straight and accurate (as before rotation) (Figure 8). Adaptation occurred over a shorter time-scale if reaching movements were made in the light so that the subject could see their arm movements. Post-rotation, the arm movements continued to compensate for the Coriolis force resulting in pointing perturbations that were symmetric to those that had originally occurred during rotation. This post-rotatory compensation typically lasted 15 movements. Similar studies have been performed with toe pointing [96].

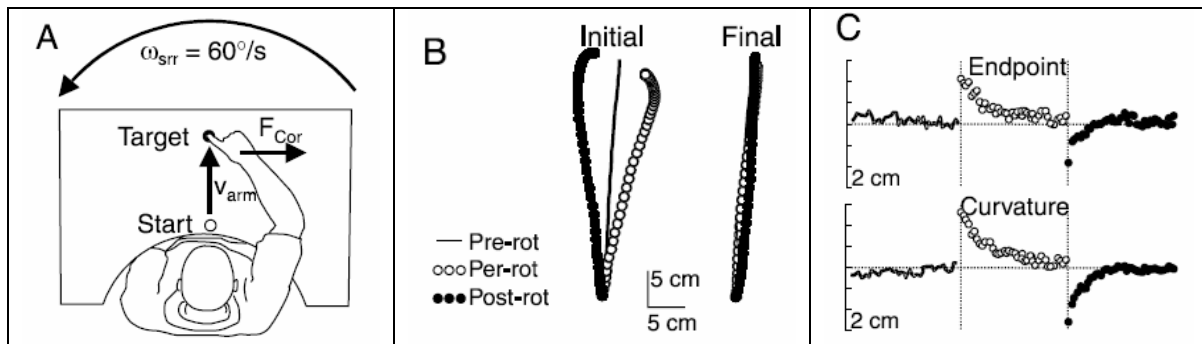


Figure 8. Adaptation of the sensory-motor system to arm reaching movements before, during, and after centrifugation [11].

The motor movements in these studies can be classified as an open kinetic chain, where the terminal or distal segment is not fixed in space, or opposed by any resistance. CKCEs, such as those proposed for artificial gravity exercise, will still pre-dispose the arm or legs to Coriolis forces during movements, but the perturbations will act on the intermediate segment rather than

¹⁷ $\vec{F}_{Coriolis} = -2m(\vec{\omega} \times \vec{v})$ where m is the mass of the moving object, v is the linear velocity, and ω is the angular velocity of the rotating reference frame.

the distal point. The time course of any adaptation and after-effects will likely depend on performance feedback (proprioceptive or visual) during the centrifugation trials – shorter adaptation period with feedback.

Artificial Gravity Exercise

The potential benefits of artificial gravity exercise at preventing physiological de-conditioning during simulated weightlessness were first reported in the early 1970s by Hoche and Graybiel [97]. Since then, exercise has been successfully combined with motor-driven centrifuges [7-10, 53, 97], and is an integral part of those that are human-powered [6, 98-100]. The human-powered centrifuges are cycle-driven and may be configured in such a way that the subject is lying horizontally on their side [99], lying horizontally on their back [98], or pedaling along the gravito-inertial acceleration of a pendulous arm [100]. With a motor-driven centrifuge, the subject may be configured in any number of positions, and offers the benefit of studying human performance over long periods of time.

Current literature on artificial gravity exercise¹⁸ as a countermeasure to spaceflight de-conditioning has primarily investigated cycle ergometry and stair stepping, with one older study investigating treadmill walking [97]. The results have focused on short-term hemodynamic and metabolic responses to both self-powered and passive centrifugation [6, 8, 98], preventing cardio-respiratory de-conditioning [7, 9], and the maintenance of muscle volume [53] during simulated microgravity. In particular, it was reported that heart rate was significantly higher during self-powered centrifugation than when passively rotated at the same Gz stimulus (greater than +3 Gz), with no effect on blood pressure [6], [98]. Active centrifugation seemingly also lowered the slope of the heart rate with Gz¹⁹ compared with passive centrifugation, indicating the importance of the skeletal muscle pump helping with venous return.

¹⁸ The majority of the work has focused on short-radius centrifugation, where the subject's head is typically near the center of rotation and the feet are approximately 2.0 meters from the rotation axis. These short-radius systems require high rotation rates (and generate larger Coriolis accelerations with a large gravity gradient from head-to-toe) to provide sufficient G-loading. Larger radius centrifuges could be spun at lower rotation rates to provide the same G-loading (and therefore lesser Coriolis accelerations and smaller gravity gradients).

¹⁹ When pedaling, heart rate increased slower with Gz stimulus than when not pedaling.

Aiding the venous return during centrifugation, whether it be the skeletal muscle pump or another mechanism, may be responsible for increasing the “Anti-G score”²⁰ in exercising compared with passive trials [8]. The increased venous return is also reflected by an increase in thoracic fluid during exercise trials. A similar result during exposure to lower body negative pressure (LBNP) – the skeletal muscle pump from dynamic leg exercises, such as the calf-raise, improved tolerance to LBNP [101].

Operationally, treadmill walking at one-half Earth gravity²¹ was not adequate to maintain LBNP tolerance, the duration of volitional exercise, or plasma volume during 14 days of bed rest. More recently, it was reported that 1.2 Gz at the level of heart with bouts of 60 Watt (W) cycle ergometry during two weeks of bed rest reduced losses in plasma volume, reduced the fluid shift from the thorax to the leg during centrifugation, and increased orthostatic tolerance during 30-deg head up tilt [7]. Thigh muscle volume has been reportedly maintained during 20 days of bed rest with bouts 60 W cycle ergometry during centrifugation protocols that included 0.8-1.4 Gz at the heart (2.9-5.0 Gz at feet) [9]. However, there were still significant reductions in maximum voluntary contraction force following reambulation. A significant shortcoming in a majority of the cited work is the failure to state the magnitude as well as where the G-level was measured along the longitudinal axis of the body²². The most recent work, however, seems to realize the importance of the location of the “1 G centripetal acceleration” along the axis of the body, and frequently cites the location.

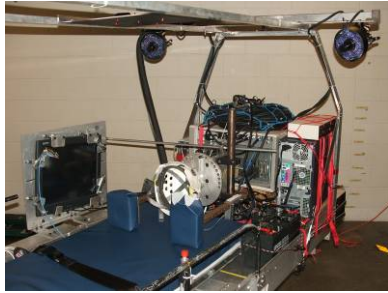
Coriolis forces will affect our motor control and limb movements during exercise on-board the centrifuge. Some work has been done regarding the challenges of locomotion, jumping, or even climbing stairs in a rotating environment [102, 103]. However, in these studies, there was no mention of if, or how, Coriolis forces may have affected the biomechanics or performance of the subjects while exercising, or if they may have affected their results. Biomechanical after effects, may also be present, but were not reported. In addition to the Coriolis force effects, the gravity gradient along the centrifuge may also affect performance and should be accounted for.

²⁰ Defined as the sum of the magnitude of the gravity vector toward the leg (+Gz) multiplied by the time of centrifugation (sec) for the load to the endpoint in order to quantify orthostatic tolerance.

²¹ Man’s center of mass at a radius of 19.5 feet, rotation at 8.7 +/- 0.1 RPM generated a force approximately 15% less than 0.5 Gz at head level and 15% more at the feet.

²² Iwase et al. has stated a “max of 2 G-load at the heart level.”

Chapter 3: Exercise and Motion Capture Equipment



*“Good designs let you,
bad designs make you.”*
Unknown

Over the years, there have been many different exercise devices built for orbiting laboratories, reusable space vehicles, and ground-based evaluation. The development of exercise equipment for use on-board the MIT short-radius centrifuge [4] had to meet certain design and performance requirements in order to meet the research program goals. In this Chapter, the design and implementation of the exercise equipment is described. This equipment includes the sliding backrest, constant force spring assembly, and the mounting of the motion analysis cameras and related equipment. The motion analysis cameras were loaned to us from the Politecnico di Milano Laboratory for Biomedical Technologies through a grant from the Roberto Rocca Project within the MIT-Italy Program.

Linear Back-Slider

In order to accommodate the current resistive type exercises and perhaps, a future aerobic exercise such as cycle ergometry or stair stepping, a new back-slider was designed. This new back slider²³ is a welded Unistrut® frame with a shoulder pad assembly that moves smoothly along two precision linear rails. Foam padding on the frame and shoulder pads ensures comfort to the subject when lying supine or on their side. We identified several design requirements and performance specifications for the back slider device. A brief overview of the design and operation is documented in this section. The detailed engineering drawings and SolidWorks 2001^{PLUS} three-dimensional renderings for the device can be found in the Appendix.

²³ This backslider replaced the previous device [11] because it could not accommodate the resistive loads of this current research program.

Requirements

Before designing the linear back-slider for resistance exercises, several requirements were outlined. These requirements included the weight, longitudinal, lateral and torsional rigidity, load bearing capability, range of motion, comfort, and safety.

Table 1. Centrifuge linear back-slider design guidelines.

Requirement	Notes
Weight	The back-slider must not weigh more than 445 N (100 lbs.) An excessive weight addition to the centrifuge would make it difficult to balance the cantilevered arm and put the device in danger of overloading the axial bearings in the support shaft.
Rigidity	The assembly must be able to withstand any Coriolis-induced lateral forces with an 890 N (200 lb.) subject on the slider (up to 535 N (120 lbs.)). The torsional rigidity of the backslider frame must prevent the linear bearings from binding on the precision rails and reducing performance.
Load bearing capability	The two shoulder pads, which are also connected to the backslider frame, must be able to withstand 890 N (200 lbs.) (445 N on each pad) from the constant force springs (maximum subject weight) plus the artificial gravity weight of that same 445 N subject during the peak foot reaction forces of a 0.5 Hz squat at 30 revolutions per minute (approx 1,560 N (350lbs.)). Therefore, the shoulder pads / frame assembly must be able to withstand up to 2,450 N (550 lbs.)
Range of motion	The slider must move at least 61 cm (24 in.) along the radius of the centrifuge. This allows a subject who is at the maximum height for participation to achieve at least 90 degrees of knee flexion during the supine squat.
Adjustability	The shoulder pads must be adjustable along the longitudinal axis of the slider frame in increments of 1-in. This allows for accommodation of subjects of multiple heights with varying anthropometric proportions.
Comfort	The slider must have enough padding on the surface and shoulder pads so that the subject is free from discomfort when lying supine on the slider for periods up to 1-hr. The shoulder pads must prevent discomfort at “pressure points” on the shoulder during the maximum loading of the device (2,450 N).
Safety	The device must operate safely and provide no harm to the subject over the entire research program. The frame must provide for attachments of a safety harness. All connection points and moving parts where a subject could injury an extremity must be hidden or clearly marked.
Cost	The cost of the materials and associated assembly must be kept to less than \$2,000

Design

The backslider frame and assembly were designed using SolidWorks 2001^{PLUS} computer aided design software (SolidWorks Corporation). The backslider is a multi-part assembly of commercial-off-the-shelf components. All parts, including the linear rails and bearings, were obtained through McMaster-Carr’s® online store (<http://www.mcmaster.com>). The complete list of parts and materials for constructing this back-slider, as well as the constant force spring assembly (described later), are listed in the Appendix.

The slider frame is made of 4.1 cm (1.625 in.) welded Unistrut® steel U-channel (Figure 9). The channel faces outward along the perimeter of the frame to allow for mounting of additional research and safety equipment. Two steel plates are welded to the “top” of the back-slider to provide additional bending rigidity when the shoulder pad assembly is attached. Steel L-brackets span laterally at two locations. These provide adequate torsional and lateral rigidity, and provide a mounting platform for the linear bearings. U-slots are cut out of the L-brackets to allow the backslider to move close to the centrifuge surface when riding on the precision rails. Multiple holes are drilled along the two longitudinal U-channels for attachment of a high density polyethylene (HDPE) sheet, which is then covered in foam for padded comfort.

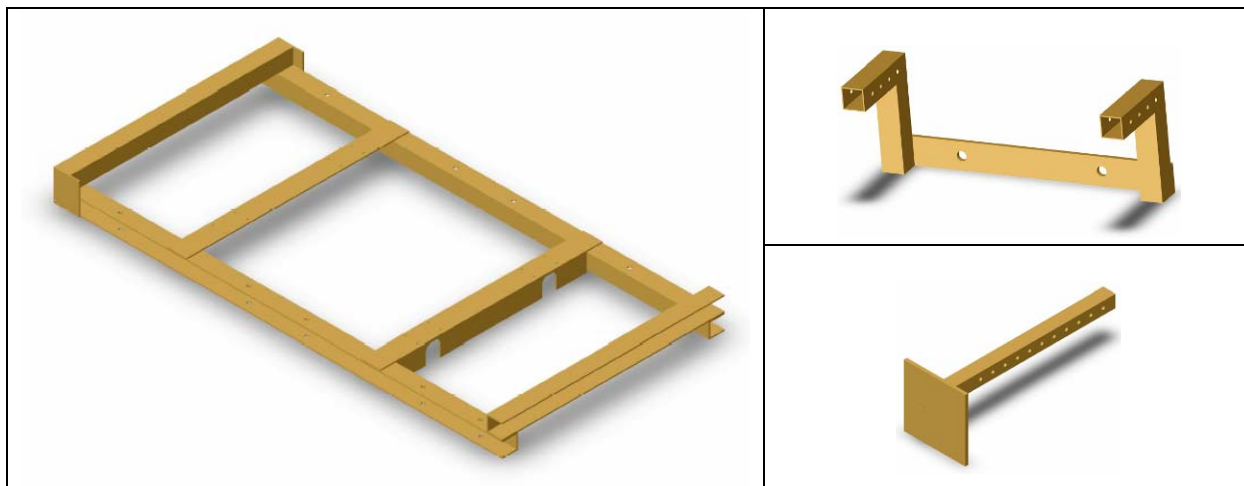


Figure 9. Three-dimensional assembly views of the backslider frame (left), shoulder harness (top right), and shoulder pad (bottom right). All individual components are fabricated from steel and welded together to form the assemblies.

When assembled, the shoulder harness is bolted to the back-slider frame and each of the shoulder pads slide into the shoulder harness. The multiple holes (each 2.54 cm (1 in.) apart) on the shoulder harness and shoulder pad allow for adjustment. The shoulder pad is locked in place by two T-handle quick-release pins on each of the assemblies. The linear rails are bolted to aluminum sheet stock, which is then bolted to the centrifuge structure via aluminum L-brackets. This ensures that the device will not become detached from the centrifuge. Stoppers are placed on each end of the linear rails to prevent the backslider from sliding off the rails during operation. Two eye-bolts are mounted to the frame closest to the subject’s feet to connect the steel cables from the constant force spring assembly.

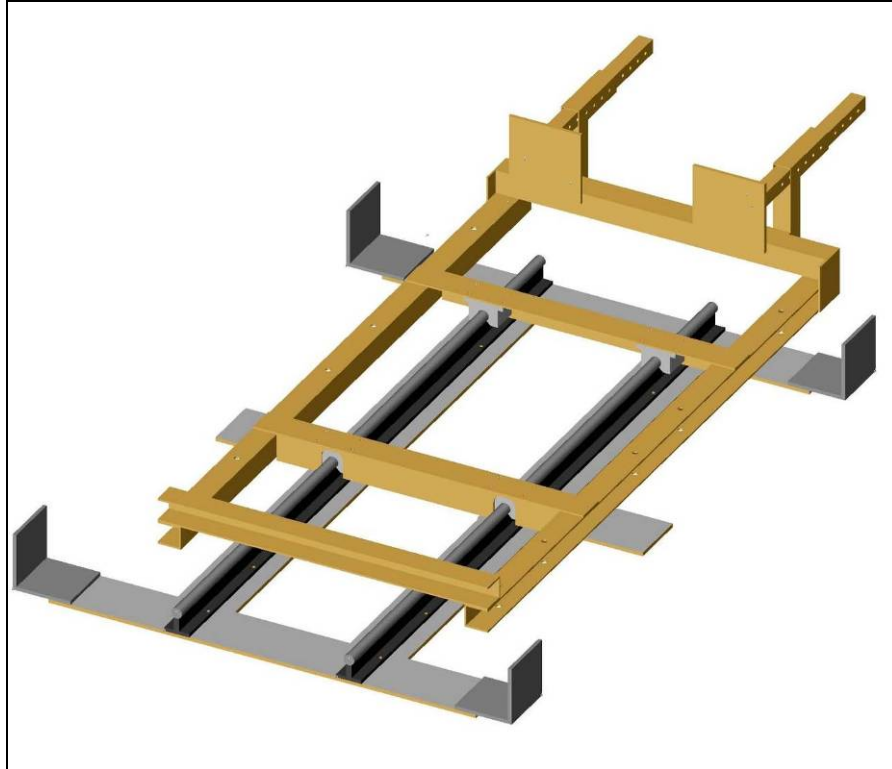


Figure 10. Full three-dimensional conceptualization of the backslider assembly for addition onto the centrifuge. The shoulder harness assembly is bolted to the slider frame with the shoulder pads inserted. The linear pillow-block bearings are attached to the slider frame and then attached to the precision linear rails. The rails are then attached to aluminum sheet stock for rigid attachment to the centrifuge structure. Not shown on here are: 1) the end-stop collars on the precision rails, 2) HDPE surface on top of the slider assembly, and 3) foam padding on the slider assembly and shoulder pads.

Performance

The use of the back-slider in an experimental setting has shown that it meets all of the design requirements and operates with adequate performance. It is comfortable and no subjects sustained any injuries during its operation. The slider has a maximum range of motion of 63.5 cm (25 in.) and moves nearly frictionless throughout that entire range. The shoulder pads are adjustable in 2.54 cm (1 in.) increments to accommodate all subjects. The moveable portion of the back-slider has a mass of approximately 25 kilograms (55.1 lbs.). The center of mass is approximately 38 cm (15 in.) from the end closest to the centrifuge axis of rotation. It is not counterweighted, and therefore this off-axis mass adds to the foot reaction forces of the subject when the centrifuge is spinning.

Constant Force Spring Assembly

In order to provide an additional resistive force to the subject during artificial gravity supine squats, we needed to design and build a device to give this additional load to the subject. This spring assembly is a Unistrut® frame with several constant force springs that has the capability of providing a resistive force up to 1,110 N (250 lbs.) in 22 N (5 lb) increments. It was mounted to the existing foot plate on the centrifuge. A cable and pulley system connects the springs to the back-slider.

Requirements

Before designing the constant force spring assembly, several design requirements were outlined. These requirements take into account the desired performance outcome based on the current and future research goals at the onset of this work. These include the weight, force increment and range, deflection range, and safety.

Table 2. Constant force spring assembly design guidelines.

Requirement	Notes
Weight	The weight must not exceed 220 N (50 lbs.) A large weight addition to the centrifuge at such a great distance from the center of rotation would make it difficult to counterbalance the assembly. It must not overload the axial bearings within the centrifuge support shaft.
Force range	The resistance assembly should be able to provide a force of up to 1,110 N (250 lbs) in at least 22 N (5 lb) increments. This would allow us to apply resistance up to the maximum weight of our subjects (890 N), and resistance within 22 N (5 lbs) of the weight of all our subjects.
Deflection range	The assembly must be able to provide a resistive force over the entire range of motion of the back-slider. This will allow a resistive force to be applied to all knee flexion angles to at least 90 degrees for all of our subjects.
Safety	The device must operate safely and provide no harm to the subject over the more than one thousand repetitions required to complete this research program. All connections and moving parts must be hidden from the subject or clearly marked.
Cost	The cost of the materials and associated assembly must be kept to less than \$500.

Design

The constant force spring assembly was designed using SolidWorks 2001^{PLUS} computer aided design software (SolidWorks Corporation). By in large, it is a multi-part assembly of commercial-off-the-shelf components. All parts were obtained through McMaster-Carr's® online store (<http://www.mcmaster.com>). It was designed to be rigidly attached to the moveable footplate already on the centrifuge. The constant force springs were chosen over a traditional weight stack because of the significant force-to-weight advantage.

This constant force spring assembly is composed of a three segments of 4.1 cm (1.625 in.) Unistrut® U-channel that is connected by two L-brackets. Three large U-bolts support the thirteen constant force springs (4 x 40 lbs., 2 x 25 lbs., 4 x 10 lbs., 3 x 5 lbs.). Bushings for each of the constant force springs were cut from high density polyethylene (HDPE) stock to align the axis of rotation of all springs. Flanges cut out of 32 mm (0.125 in.) aluminum sheet were screwed to either side of the constant force spring and bushing assembly to ensure that each spring unraveled and raveled onto itself. Each of the springs could be independently connected to a load-distributor (2.54 cm (1 in.) square steel tube) via eye bolts and carabiners. The load distributor is a 2.54 cm (1 in.) square steel tube that is used to take the multiple spring connections and transmit the load via two steel cables to the back-slider. It has HDPE dowels on either end to fit within the U-channel, which acts as a vertical guide for the load distributor. The steel cables are each routed around a pulley and underneath the foot plate. The pulleys are attached to the bottom backside of the foot plate.

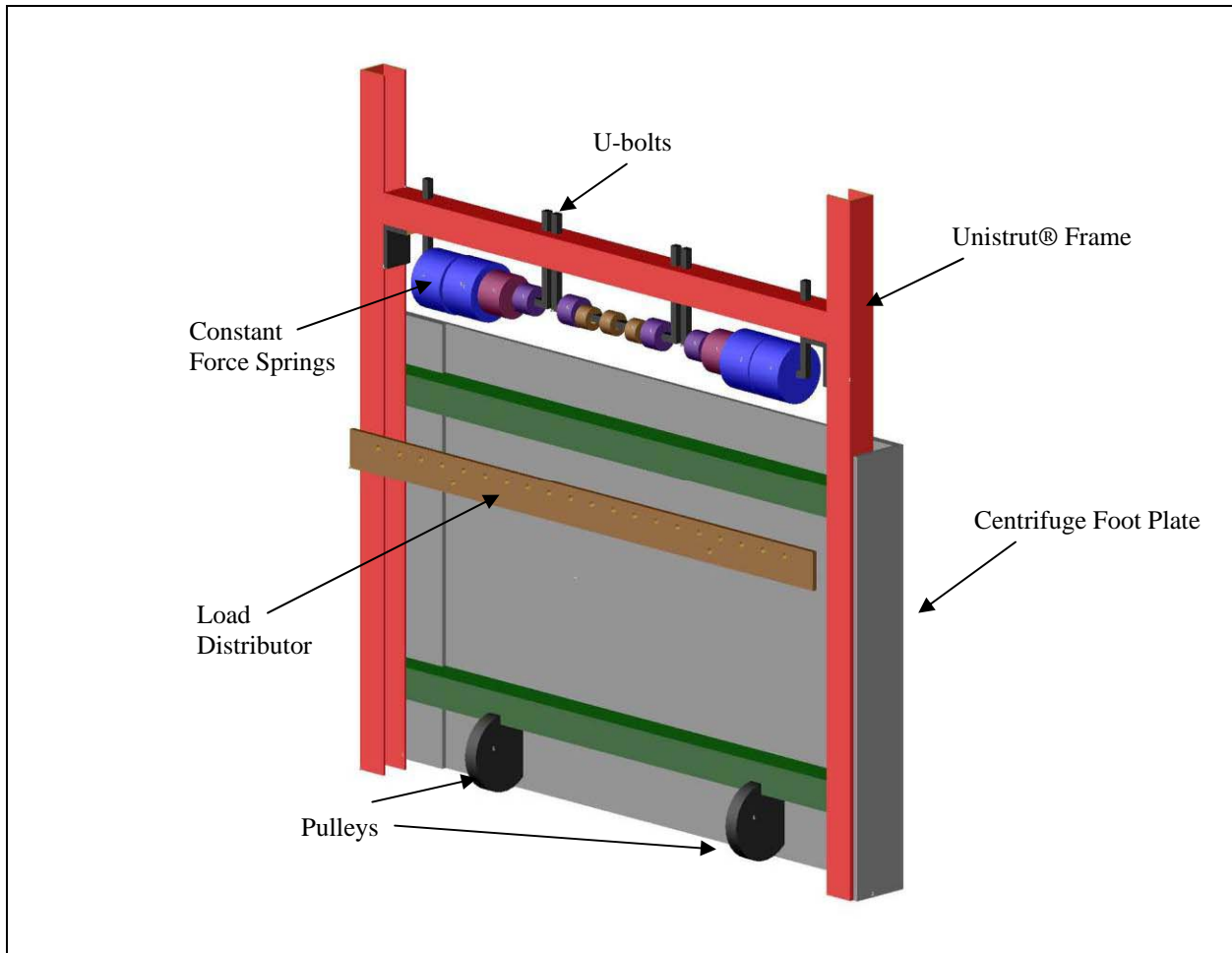


Figure 11. SolidWorks three-dimensional concept of the constant force spring assembly mounted to the centrifuge foot plate. The constant force spring array is mounted to the top horizontal Unistrut®, and the two vertical Unistrut® U-channels are bolted to the centrifuge foot plate. The springs are connected to the load distributor via eye bolts. Two steel cables are fastened to the load distributor and are routed around the two pulleys and under the foot plate to the backslider assembly.

Performance

The use of the constant force spring assembly has shown that it has the capability to provide resistive forces in 22 N (5 lb) increments up to a maximum of 1,110 N (250 lbs.) We chose 22 N increments because it was the smallest feasible increment to both provide resistive force equivalent to body weight as well as resistive force in a variety of increments²⁴. The force can be applied over the entire 63.5 cm (25 in.) travel of the back slider. The entire assembly weighs approximately 178 N (40 lbs.) Subjects indicated that the use of the device was adequate and no injuries were sustained during the operation.

²⁴ 22 N (5 lb.) increments are also common to fitness center equipment.

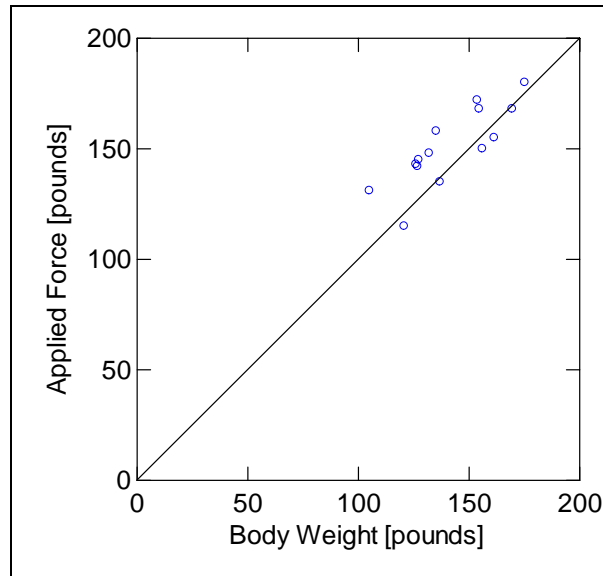


Figure 12. Plot of the subject’s 1-G upright body weight versus the weight of the subject when lying supine on the centrifuge with the constant force springs set to provide body weight resistance. In approximately half of the cases, the constant force spring load was a little more than their body weight. However, in general, we are able to apply resistive forces within 10% of the subjects normal body weight. Best fit line has a slope of 0.954 with an intercept of -2.27 pounds, $R^2 = 0.681$. N = 15.

Upright Exercise Device

One of the research aims of this work was to compare supine squats on the centrifuge with upright squats in the laboratory. Therefore, it was necessary to construct an upright exercise device for testing. We decided to make use of the centrifuge footplate and constant force spring assembly already built, as well as the previous back-slider assembly that was replaced with the newer version.

Requirements

Requirements for the design and construction for this device were outlined during the concept phase. As with all of our research equipment, we are concerned with accommodating a wide range of subjects with comfortable equipment that is safe.

Table 3. Upright exercise device design guidelines.

Requirement	Notes
Weight	This device needed to be assembled and disassembled by not more than two people within the laboratory due to lack of available floor space.
Load bearing capability	This device must sustain loads similar to those on the centrifuge. The slider frame and shoulder harness assembly must be able to withstand loads up to 2,450 N (550 lbs.)
Range of motion	The range of motion of the linear slider must be equal to or greater than the centrifuge back-slider.
Adjustability	The upright exercise device must have the same or greater adjustability as the centrifuge back-slider. Again, this ensures that the centrifuge and upright exercise device can accommodate the maximum number of subjects.
Comfort	This device must be as comfortable as, or more comfortable than, the centrifuge backslider under the same loading conditions.
Safety	The construction and operation of this device must not pose any safety concerns to the subject. All connections and moving parts must be hidden from the subject or clearly marked.
Cost	The construction of this device must make use of already available components and the cost must be kept to a minimum

Design

The upright exercise device was designed and realized through the use of the previous back-slider assembly, 4.1 cm (1.625 in.) Unistrut ® U-channel, and related Unistrut® components (Figure 13). The existing back slider was mounted to a Unistrut® frame with the U-channels facing outward around the perimeter. This frame was designed to carry the entire resistive load since the previous back slider assembly had the bearings mounted to a 1.27 cm (0.5 in.) plywood sheet, which was not sufficient for load bearing. The precision rails, which the bearings and back slider moved upon, were each bolted along parallel-mounted U-channel.

This device was also designed to interface with the existing resistive exercise components: the same shoulder harness and pad assembly as on the centrifuge back-slider and the centrifuge foot plate and constant force spring assembly. After removing the footplate from the centrifuge, the upright back slider was attached to the footplate. Unistrut® supports were attached to the footplate to tilt the entire assembly 20 degrees. This tilt made it more comfortable for the subject to perform the squats, and made the device more similar to a traditional hack-squat machine found in many fitness centers. Eye bolts on the back-slider frame connected to the same steel cables to provide the additional resistance. The back-slider assembly in this configuration weighed approximately 200 N (45 lbs.) Through another steel cable and pulley system, we were able to counterbalance the back slider so that it had an apparent weight less than 22 N (5 lbs.)

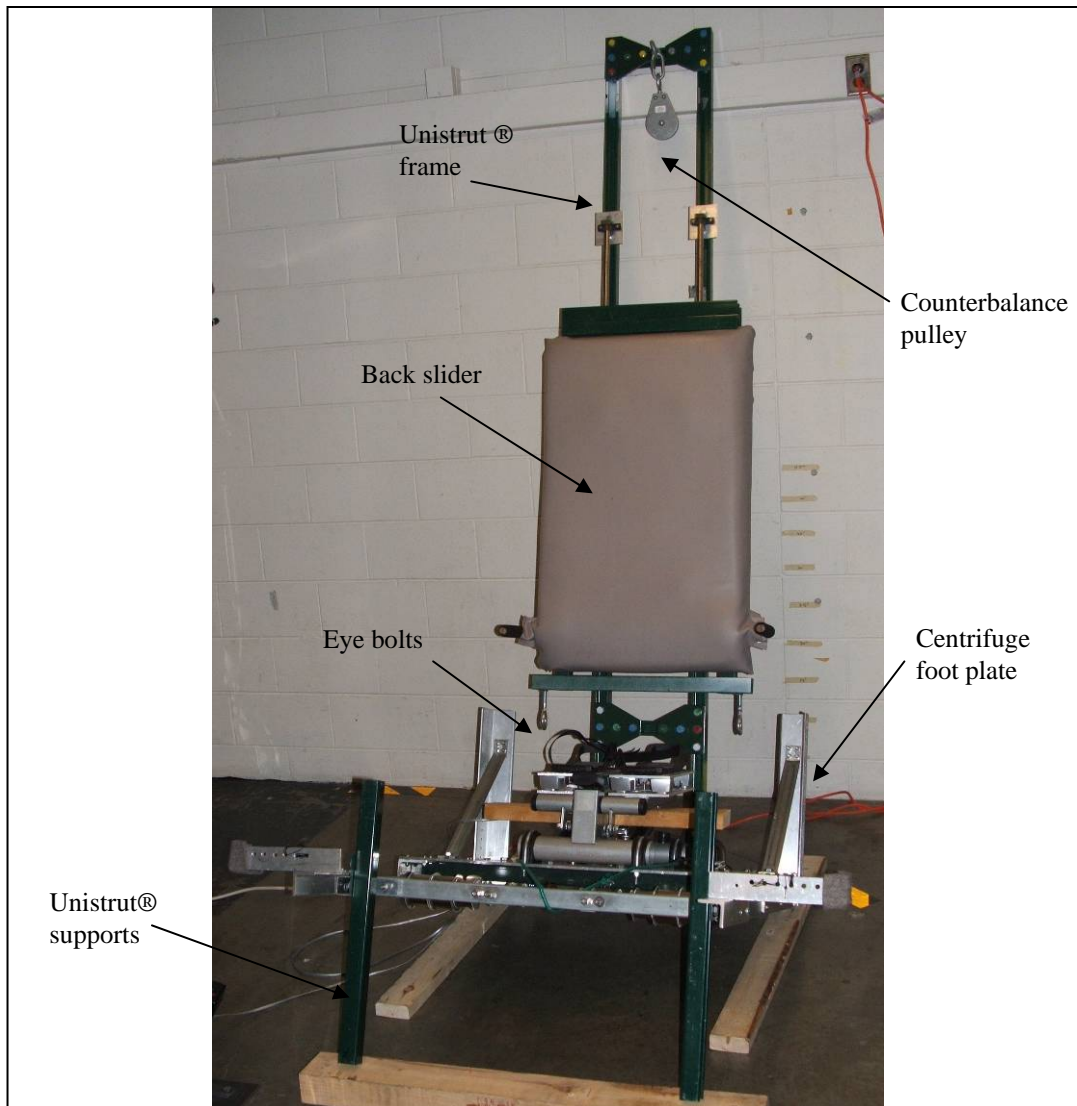


Figure 13. Upright exercise device. This image shows the configuration of the device when fully assembled. This setup requires the removal of the foot plate from the centrifuge. The Unistrut® frame with the back slider attached is securely clamped to the centrifuge foot plate. The whole assembly is then tilted backwards approximately 20-degrees for subject comfort when exercising. The back slider assembly is counterweighted and the constant force springs can be adjusted for the desired resistive load.

Performance

We were able to successfully design and construct an upright exercise device that allowed a setup very similar to that on-board the centrifuge. The slider range of motion is 61 cm (24 in.), 2.54 cm (1 in.) shorter than the centrifuge slider, but still allows our tallest subjects (1.95 m) to achieve at least 90 degrees of knee flexion during the squat. Subjects mentioned no discomfort during the exercises and none sustained any injuries during operation.

SMART Motion Capture Equipment

In order to quantify the kinematics of the legs during the squat exercises, we needed to install motion capture equipment on-board the centrifuge. The SMART motion capture equipment (BTS, Inc.) is a commercially available infrared camera system that includes the cameras, an infrared light-emitting diode (LED) ring, camera synchronization hub, and personal computer (PC) for data collection. The system was on loan to us from the Politecnico di Milano Laboratory for Biomedical Technologies (TBMLab) as part of a research collaboration funded by the Roberto Rocca Project within the MIT-Italy Program²⁵.

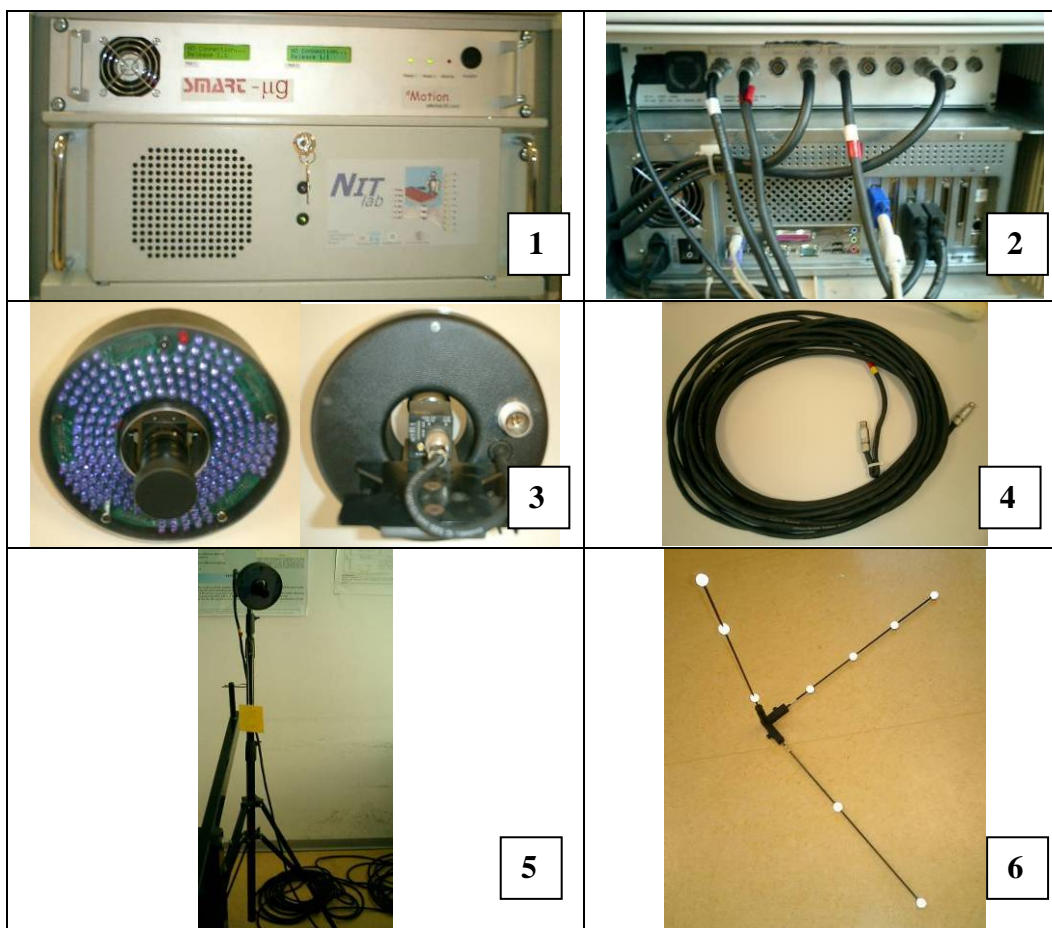


Figure 14. SMART System basic equipment. 1) Front of the computer and video synchronization hub. The door on the front of the computer opens downward to reveal the power switch, CD-ROM, CD-RW, and floppy drive. The power switch for the synchronization hub is also on the front. 2) Rear view of the computer and synchronization hub. 3) Front and back of the camera unit with a 3.6-mm lens. 4) Power and data cable for the camera units. 5) Camera unit on tripod. 6) Calibration axis.

²⁵ MIT-Italy Program: <http://web.mit.edu/mit-italy/>
Progetto Roberto Rocca: <http://web.mit.edu/mit-italy/partnerships/rocca.html>

We attached one camera to each of the four corners of the centrifuge. Camera placement was driven by the lens field-of-view (40° H x 36° V). The synchronization hub and PC were placed on the short-arm of the centrifuge. Power was supplied by two 12-Volt seal lead acid batteries (12V 35 Ah, UB12350, Universal Battery) arranged in series, which was then converted to 120 Volt 60 Hz AC power via a power converter (S300-124, Go Power! Electric, Inc.).

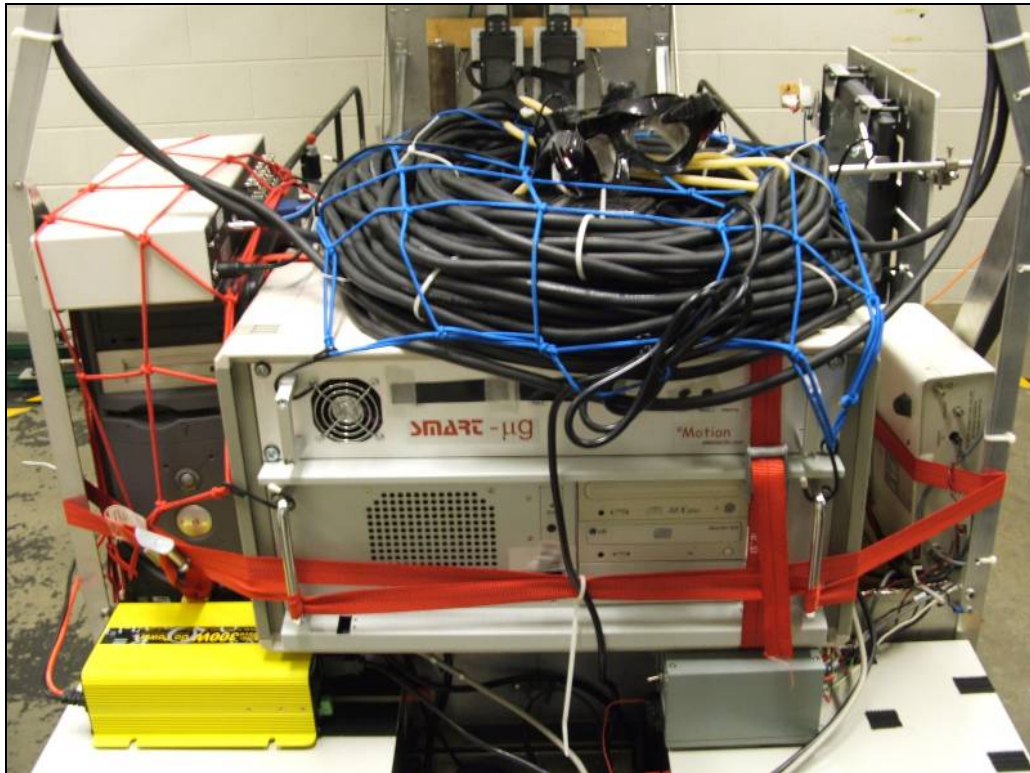


Figure 15. SMART motion capture equipment mounted on-board the MIT short-radius centrifuge. All equipment and power sources were on the rotating device. Computer equipment and cables were strapped securely to the centrifuge. The four camera units (not shown in this picture) were rigidly mounted to the four corners at approximately 1.0 meter (39.4 in.) from the centrifuge surface.

Chapter 4: Biomechanical Modeling



*"Those who have knowledge, don't predict.
Those who predict, don't have knowledge. "*
Lao Tzu, 6th Century BC Chinese Poet

There are two great minds that have put their names on the governing principles that make this research program both interesting and challenging. Gaspard-Gustave de Coriolis, a French mathematician, is best known for the work bearing his name. This “effect” is an acceleration produced when an object moves within a rotating environment. Sir Isaac Newton prescribed three laws of motion. His second law, in which the acceleration of an object is directly proportional to the net force acting on it, is the underlying principle for the success of centrifugation as a countermeasure to space flight de-conditioning. The artificial gravity environment, where the acceleration level changes depending on how far you are from the axis of rotation, is a unique environment in which to operate. The application of the “Coriolis effect” and Newton’s 2nd Law to the kinematics of the artificial gravity supine squat allows us to 1) predict the magnitude and direction of the Coriolis forces which deflect our legs during each repetition, and 2) predict the foot reaction forces during each repetition.

Predicting Coriolis Accelerations

The linear movement of any object within a rotating environment results in a Coriolis acceleration. If this acceleration acts on an object with mass, we get a Coriolis force, which is expressed as $\vec{F}_{Coriolis} = -2m(\vec{\omega} \times \vec{v})$ where m is the mass of the moving object, v is the linear velocity, and ω is the angular velocity of the rotating reference frame. In this section, we developed and validated a two-dimensional mathematical model of the leg press biomechanics to predict the magnitude and direction of these Coriolis accelerations while exercising in artificial gravity.

Biomechanical Methods

The kinematics of the body during a leg press while lying supine was modeled as a three-link segment (Figure 16). The three links are the torso, thigh and shin, with the ankle and knee modeled as hinge joints. From the geometry, the equations of motion for the two-link segment can be formulated (see the Appendix for full calculations).

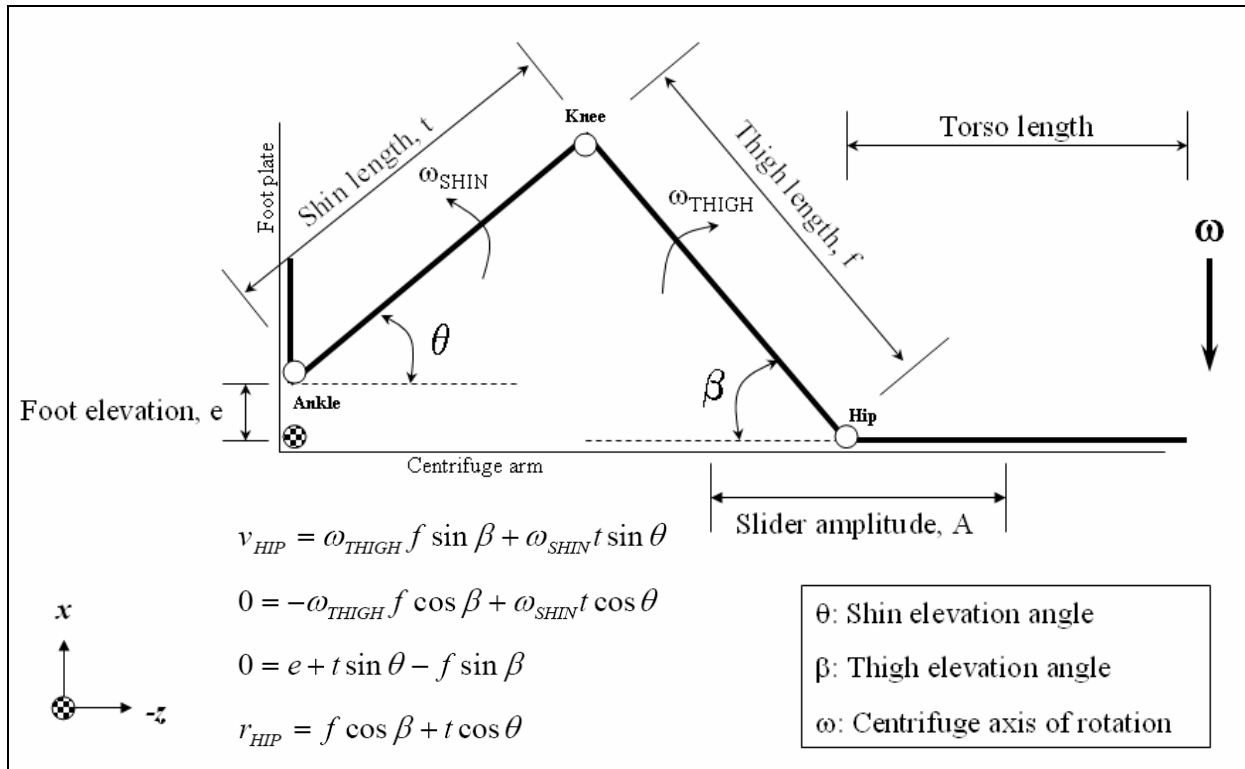
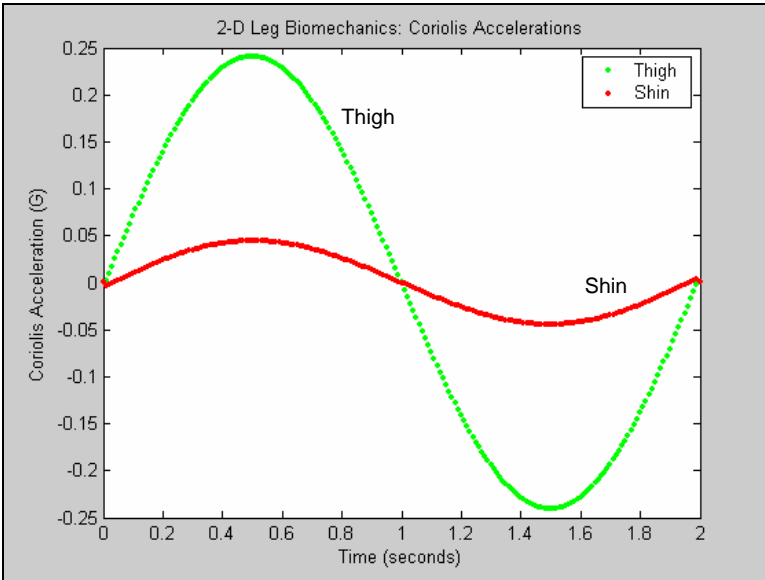


Figure 16. Two-dimensional three-link segment for approximation of the squat biomechanics. The full calculations and definition of variables is located in the Appendix.

The following are predictions of Coriolis accelerations on both the shin and thigh during one repetition (cycle) of the squat (Figure 17). The model parameters are important in determining the magnitude of the Coriolis accelerations, which are specific to a particular location on each limb.



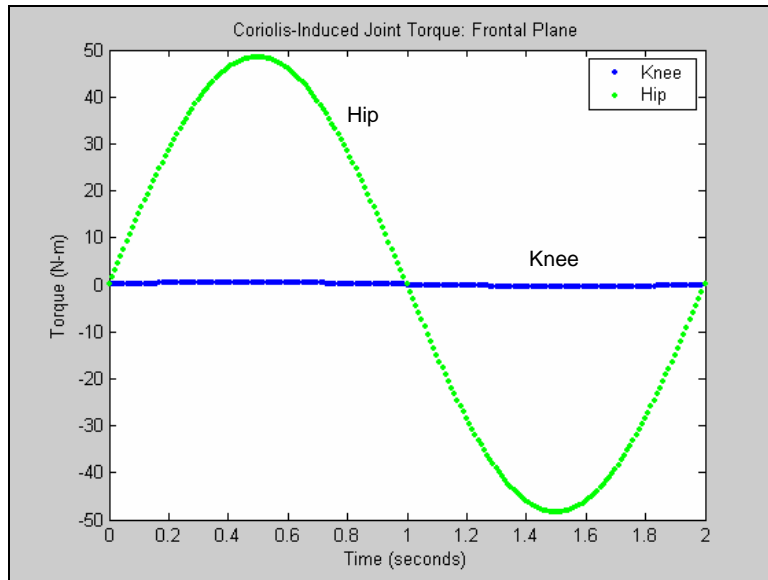
Model parameters:

$f = 0.46$ m (thigh length)
 $t = 0.43$ m (shin length)
 $e = 0.05$ m (foot elevation)
 $\omega = 23$ RPM (centrifuge rotation)
frequency = 0.5 Hz ($T = 2$ seconds)
 $A = 0.381$ m (slider amplitude)

Shin center of mass = 0.29 m from ankle
 Thigh center of mass = 0.15 m from hip

Figure 17. Coriolis accelerations on the approximate center of mass locations of both the thigh and shin during 0.5-Hz cadence artificial gravity squats.

It is important to note that the Coriolis accelerations of the thigh and shin in Figure 17 are only different in magnitude; they are not out of phase with each other. The magnitude difference is the result of the geometry of the problem, which causes a torque about the knee joint in the frontal plane. Torques, however, are mass dependent. Therefore, to estimate the joint torques, we chose mass parameters similar to those estimated by Yeadon [104], which require several anthropometric measurements.



Model parameters:

$f = 0.46$ m (thigh length)
 $t = 0.43$ m (shin length)
 $e = 0.05$ m (foot elevation)
 $\omega = 23$ RPM (centrifuge rotation)
frequency = 0.5 Hz ($T = 2$ seconds)
 $A = 0.381$ m (slider amplitude)

Shin center of mass = 0.29 m from ankle
 Thigh center of mass = 0.15 m from hip

150 lb male (68-kg)
 Thigh mass = 8.0 kg
 Shin mass = 5.1 kg
 Torso mass = 37.5 kg

Figure 18. Coriolis acceleration-induced joint torques on the knee and hip in the frontal plane.

The knee and hip joint torques, in the frontal plane, reach their maximum magnitude when the difference in Coriolis accelerations is at its greatest (Figure 18). Note the striking difference in torque magnitude between the knee and hip. This is attributable to the large mass of the torso compared with either the thigh or shin. However, in the situation with the subject supine on the back-slider, the majority of the hip torque is absorbed by the friction against the back-slider. There is virtually no torque (0.6 Nm) about the knee due to the small differences in both Coriolis accelerations and mass between the thigh and shin.

Validating the Biomechanical Models

To validate the model predictions, we attached a small accelerometer (Crossbow CXL02LF3) to the right leg (shin (0.13 m from knee) and thigh (0.17 m from knee)) of a subject whom we then asked to perform self-paced two-second cadence (0.5 Hz) squats while rotating on the centrifuge at 23 revolutions per minute (RPM) (2.41 radians per second). The self-paced exercise cadence was at approximately 0.4 Hz. The parameters and location of the accelerometers on the subject's leg are listed in Figure 18. Data was sampled at 120Hz via a laptop computer (Pentium 4, 1.6 GHz) onboard the centrifuge. One cycle of the squat for the shin and the thigh was curve fit to a sinusoid of the form $a_{Coriolis} = a \sin(\omega t) + c$ via the MATLAB 6.5 Curve Fitting Toolbox (The

Mathworks, Inc.)²⁶. The maximum magnitude of the Coriolis acceleration, a , was pre-determined from the biomechanical model using the actual placement of the accelerometer on the subject, whereas the exercise frequency, ω , was determined from the one-repetition cycle time in the actual data. The constant, c , was a free parameter in the curve fit. Positive acceleration is in the medial direction of the right leg.

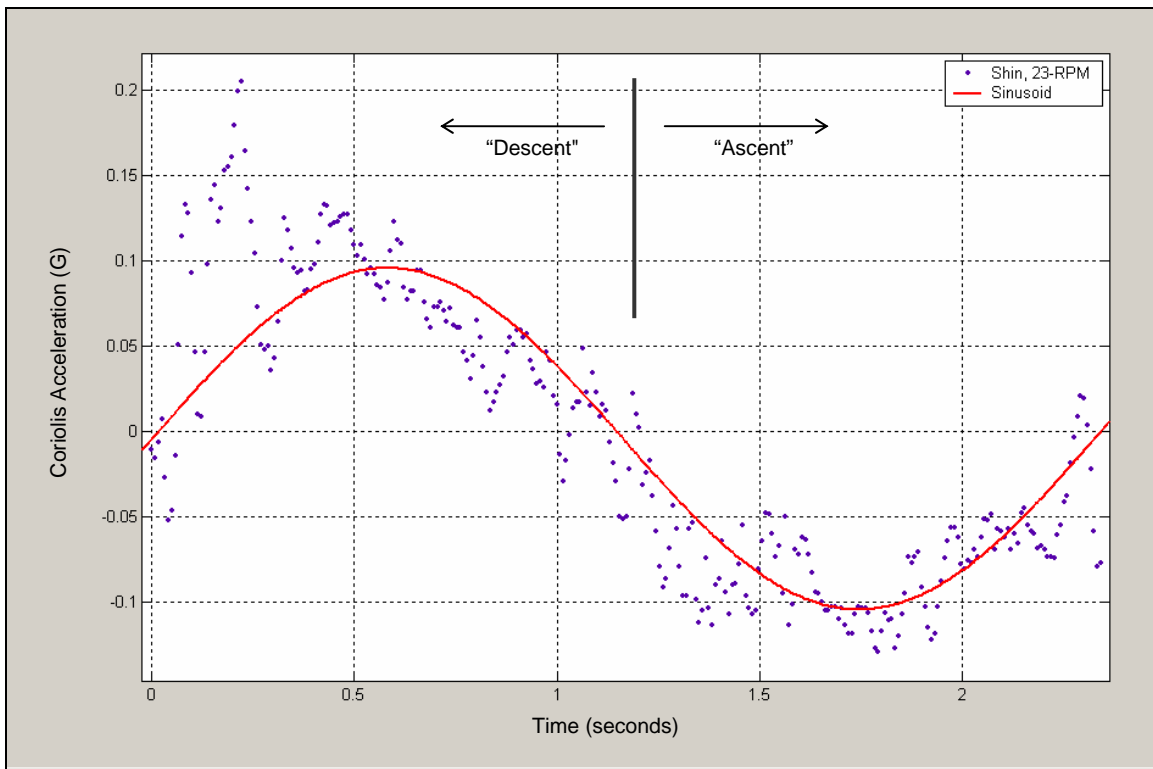


Figure 19. Coriolis acceleration on the right shin from one cycle while exercising at 23-RPM. The accelerometer was located 0.13 m (5.1 in.) below the knee joint (30% of the length of the shin). Positive acceleration is in the medial direction. Curve-fit parameters: $a = 0.1$ G, $\omega = 2.7$ rad/sec, $c = -0.004$ G, $R^2 = 0.80$, SSE = 0.39.

Figure 19 shows typical shin accelerometer data with the sinusoidal curve fit overlaid. At the beginning of the exercise cycle, the curve fit underestimates the acceleration data. This is a result of the Coriolis acceleration causing a medial biomechanical perturbation of the shin, which in turn causes the accelerometer to tilt in the same direction as the Coriolis acceleration. Therefore, the accelerometer records the Coriolis acceleration and a fraction of gravity²⁷, which causes the curve fit to underestimate the magnitude of the acceleration data.

²⁶ a = maximum amplitude [G], ω = exercise frequency [rad/sec], c = curve fitting constant [G].

²⁷ The acceleration due to gravity is the sine of the angle between the local vertical and the plane defined by the hip, knee, and ankle.

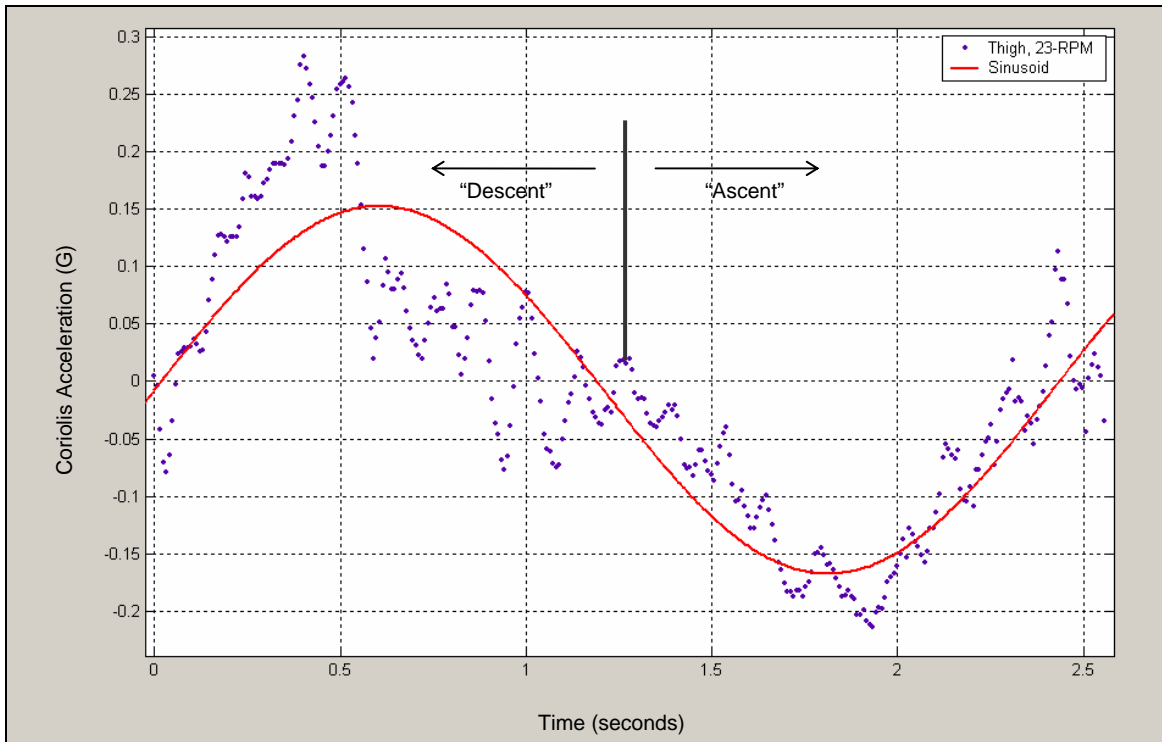


Figure 20. Coriolis acceleration on the right thigh while exercising at 23-RPM. The accelerometer was located 0.17 m (6.7 in.) above the knee joint (40% of the length of the thigh). Positive acceleration is in the medial direction. Curve-fit parameters: $a = 0.16$ G, $\omega = 2.6$ rad/sec, $c = -0.01$ G, $R^2 = 0.74$, $SSE = 1.1$

The thigh accelerometer data with the curve fit overlaid is shown in Figure 20. Once again, at the beginning of the repetition, the measured acceleration overshoots the predicted Coriolis acceleration due to the tilting of the subject's thigh, which is also the result of a biomechanical perturbation caused by the Coriolis acceleration.

Discussion

We have created a two-dimensional biomechanical model to approximate the Coriolis accelerations on the thigh and shin during artificial gravity supine squats. The motion of each limb is often three-dimensional, depending on the feet position and orientation relative to the trunk. However, the feet position during this study resulted in nearly two-dimensional motion of the leg²⁸.

²⁸ In this validation study, just as in the experiments presented in this dissertation, the feet were positioned the same distance apart for all subjects, regardless of height or leg length.

The method of attachment of the accelerometer to the subject’s leg may have introduced an unknown amount of noise. The subject wrapped a Velcro band around their leg with the accelerometer attached. This likely allowed the accelerometer to move (rotate) with respect to the limb. Also, without corroborating the two-dimensional nature of the biomechanics, it is difficult to estimate how much of the scatter in the data is due to the accelerometer tilting with the leg. The goodness of each fit (R^2 values) indicates that these sources of noise were not exceptionally large and that there were no gross errors in the biomechanical model.

Estimating Foot Reaction Forces

Exercising in artificial gravity, an environment where the subject’s “weight” changes with the distance from the center of rotation provides a unique opportunity to predict the foot reaction forces during a squat motion. The development of methods for estimating foot reaction forces during centrifuge squats will help us in determining centrifuge and exercise parameters for future exercise protocol design.

Biomechanical Methods

The application of Newtonian mechanics to a two-dimensional three-segment model, such as that in Figure 16, allows us to estimate the foot reaction forces during supine squats on-board the centrifuge, or perhaps upright. To make such estimations we need to know the mass of the object moving and how fast that object is accelerating: $\vec{F} = \sum_{i=1}^n m_i \vec{a}_i$. The mass, m , remains constant. Acceleration, however, is the sum of the centripetal acceleration and acceleration of each i^{th} segment itself within the rotating frame: $a_i = r_{cm,i} \omega_c^2 + a_{cm,i}$, where $r_{cm,i}$ is the distance of the i^{th} segment center of mass from the axis of rotation, ω_c is the centrifuge angular velocity, and $a_{cm,i}$ is the acceleration of the i^{th} segment center of mass relative to the moving centrifuge..

We used the human anthropometric and inertia model, developed by Yeadon [104], to estimate the mass of each of nine body segments. These nine segments include the upper arm, lower arm, palm, fingers, upper leg, lower leg, foot, toes, and torso. From approximately forty anthropometric measurements, we are able to derive the length, mass, and center of mass for each segment. Yeadon claims that the absolute error in this mass estimation by this model is less

than 3%. From our experience, the error may be as high as 5% due to taking the measurements over (snug fitting) clothes and by small changes in measurement location.

Estimating the acceleration of each segment is a bit more challenging. On the centrifuge, we must know how far the center of mass of each segment is from the axis of rotation, and how fast that center of mass is accelerating. To do so, we make use of two synchronized measures: the linear back-slider position (potentiometer, measurement frequency = 1 kHz) and lateral tibial condyle position (SMART motion capture system, measurement frequency = 120 Hz). From the back-slider location along the radius of the centrifuge, we can infer the center of mass position of the torso, upper and lower arms, palms, and fingers. The tibial condyle (knee) location, combined with the backslider location, allows us to estimate the position of the upper and lower leg center of mass. The feet and toes remain at a fixed distance from the centrifuge axis of rotation. The mass and center of mass location of the back-slider is known.

We differentiate the position of each segment's center of mass with respect to time twice to get the segment acceleration. Although we are capable of determining the three-dimensional acceleration profile of the upper and lower legs, we are only interested in the acceleration along radius of the centrifuge.

Validating the Biomechanical Methods

We attached reflective markers to the lateral tibial condyle of the left and right legs and had the subject perform several self-paced squats at 23- and 30 RPM. From measured positions of the ankles, knees, and back-slider, as well as the position relationship between the center of mass of each body segment, we were able to estimate the foot reaction forces. The actual foot reaction forces were measured by custom built and calibrated force sensors under the left and right foot.

The differentiation process introduces quite a bit of noise to the signal, particularly the contribution from the motion capture system. This is seen by the spikes in the estimated data (Left: Figure 21 and Left: Figure 22). There is also a noticeable separation between the measured and predicted foot reaction forces before and after rotation. This is due to the properties of the force sensors themselves. They do not read accurately at low force levels. We see that when the total force is approximately 220 N (50 lbs.) (110 N (25 lbs.) per sensor), the

measured and predicted values appear to match up well. Therefore, to validate our estimations,

we calculated the root-mean-square error, $RMSE = \sqrt{\frac{1}{N} \sum_{i=1}^N \left(\hat{F}_i - \bar{F}_i \right)^2}$ over a 20 second window

that included the peak forces during the squat (Right: Figure 21 and Right: Figure 22). This window was first averaged by using a 20 millisecond moving average window with 10 ms overlap to remove the spikes in the data. At 23 RPM, we see that the RMSE is roughly 40 N (9 lbs.), and at an artificial gravity “standing weight” of 445 N (100 lbs.), this is approximately a 9% error in our estimation. The error at 30-RPM is quite a bit lower, 31 N (7 lb.) error at an AG weight of 690 N (155 lbs.), which leaves us with a 4.5% estimation error.

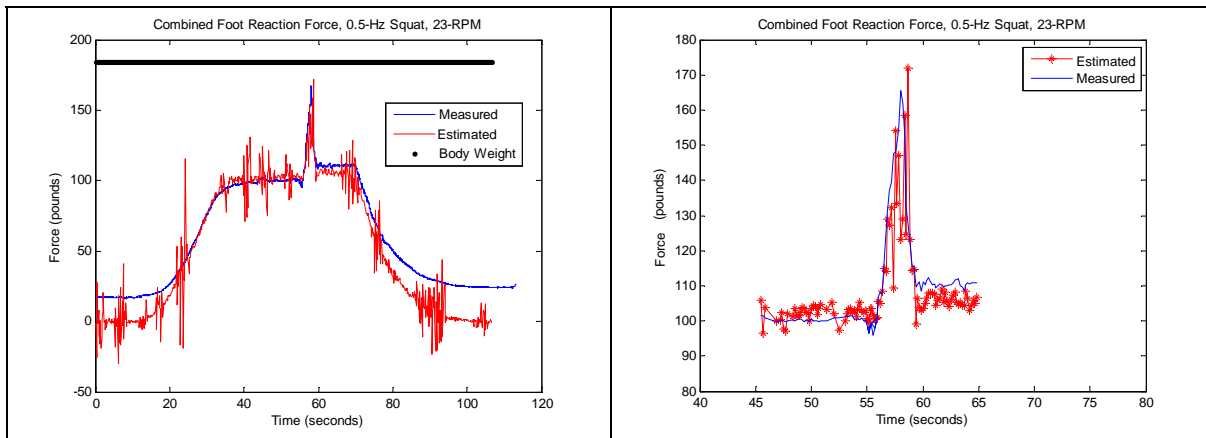


Figure 21. Left: Measured and estimated foot reaction forces during a 23 RPM supine squat. Right: Measured and estimated foot reaction forces over a 20 second window during a 23 RPM supine squat. Root-mean-square error (RMSE) = 40 N (8.95 lbs.)

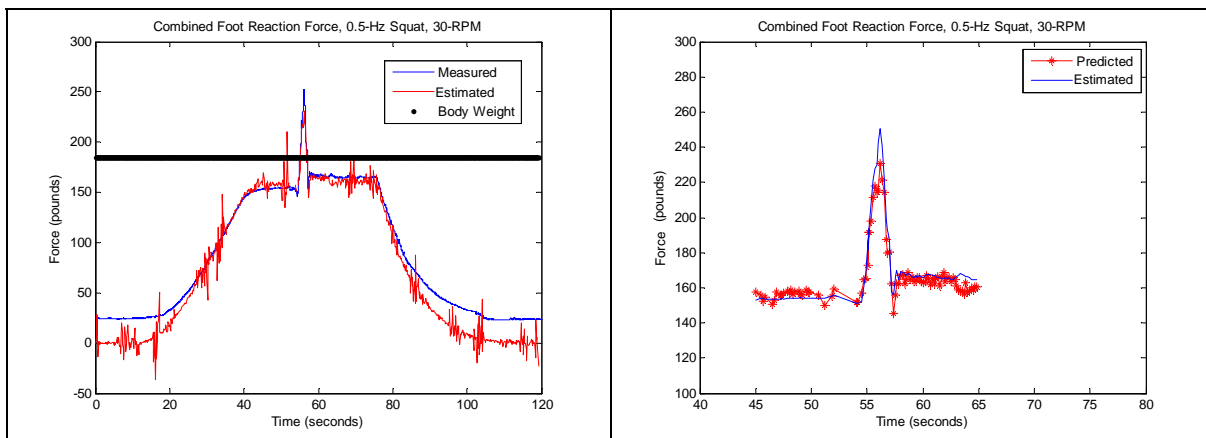


Figure 22. Left: Measured and estimated foot reaction forces during a 30 RPM supine squat. Right: Measured and estimated foot reaction forces over a 20 second window during a 30 RPM supine squat. Root-mean-square error (RMSE) = 30 N (6.59 lbs.)

Discussion

We have used a two-dimensional model as a basis to estimate the foot reaction forces. Even though the movement of each leg is, in large part, three dimensional during the AG supine squats, our predictions are fairly accurate. For these two estimations, there was 4 to 9% error. If we factor in the error of the mass and inertia measurements, as well as the error in the measurement systems, we could have an extremely accurate method for predicting the foot reaction forces during the squat exercise.

There is quite a bit of noise in the estimated foot forces. This noise is primarily from differentiating the motion capture data. Although the calibration error was less than one millimeter, the lower sampling rate (120 Hz) compared with the back slider position (1 kHz) likely introduced the noise. However, after averaging the data, we see that there is a relatively smooth representation of the foot reaction forces as a function of time.

The validation only looked at a twenty second window that included the peak forces during the exercise because of the limitations of the foot force sensors. The way they are designed prevents them from measuring accurately at forces below 110 N (25 lbs.) If we were to calculate the RMSE over the entire duration of the centrifuge acceleration and deceleration profile, then the error would be artificially inflated by this measurement limitation.

Estimating Joint Torques

Exercising while supine on a rotating horizontal centrifuge introduces two types of torques in the frontal plane of the knee joint: mechanical and Coriolis-induced. The mechanical torque is determined by the spatial position of the knee relative to the line of action of the foot reaction forces. The relative velocity of the thigh and shin, as well as the rotation rate of the centrifuge, result in Coriolis torques. In this section, we present a first-approximation to the magnitude and relative contribution of each of these knee torques.

Mechanical Torque

To estimate the mechanical frontal torque at the knee joint, we take, once again, a two-dimensional three-link model of the body (Figure 23). This model approximates the torque in

one knee, by taking the mass segments of a half-body. We use the same segment mass properties and anthropometric measurements as in the prediction of the Coriolis-induced torques. The calculations of the torque are made under conditions considered “worst case.” That is, the subject has a foot reaction force equal to twice their body weight (one body weight reaction force under each foot) and a maximum lateral deflection of the knee of 8 cm²⁹. Based on these assumptions, we are able to estimate the knee torque across several medial-lateral knee positions (Figure 24). With an 8 cm lateral deflection of the knee, we can expect to see knee torques as high as 34 Nm.

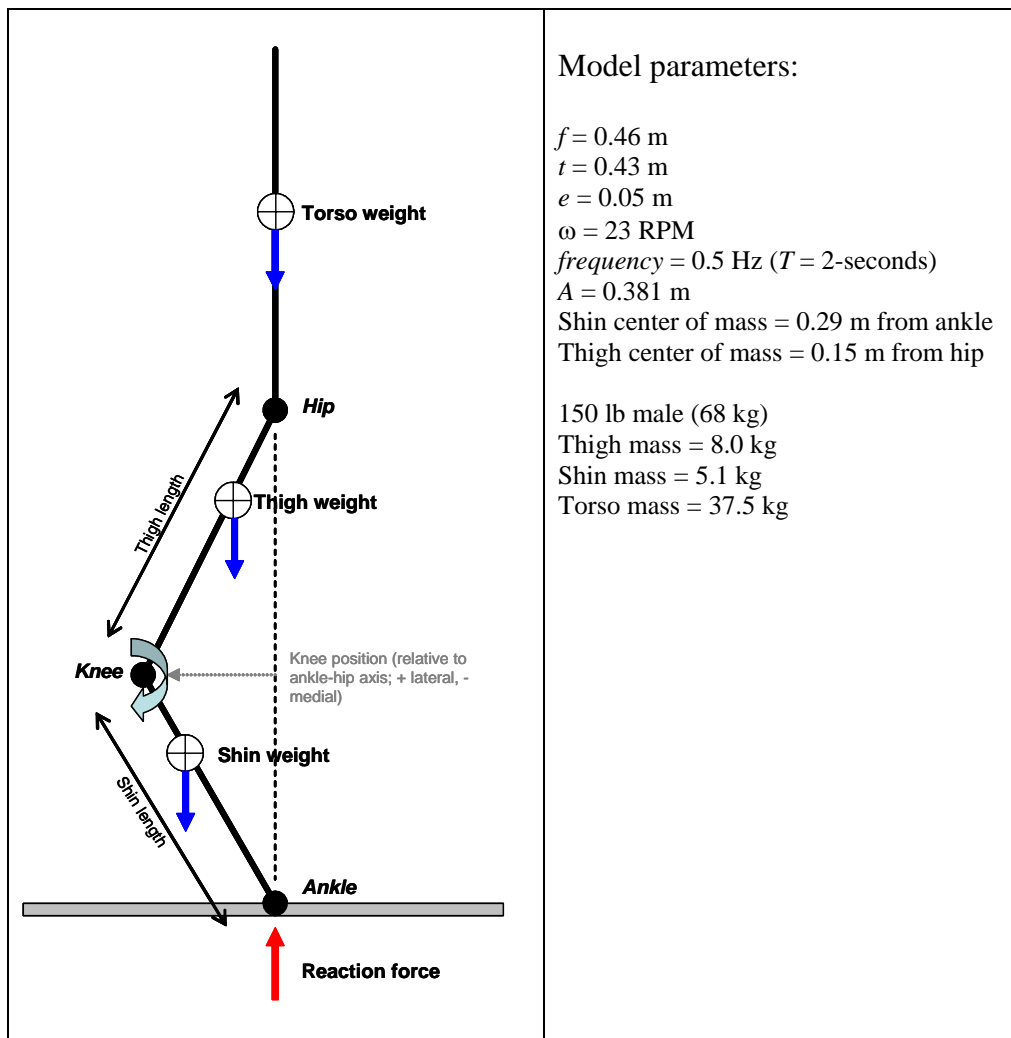


Figure 23. Biomechanical approximation for calculating frontal plane knee torque of a single leg.

²⁹ These numbers are representative of extreme conditions from the data collected in the experiments later discussed in this thesis.

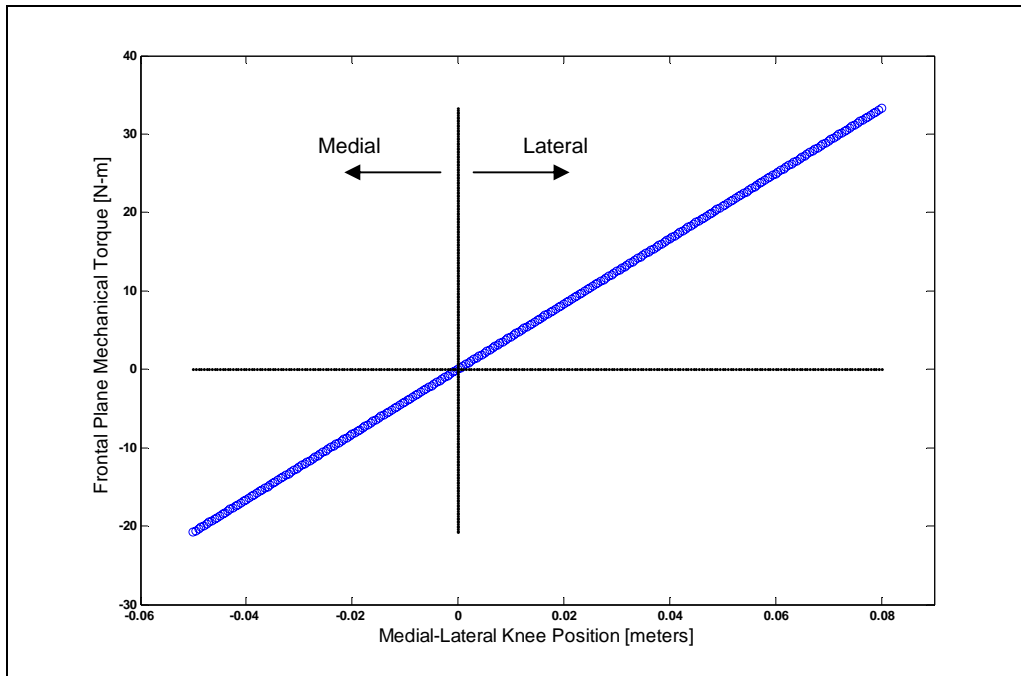


Figure 24. Estimation of a single leg knee torque in the frontal plane.

Coriolis Torque

We have previously estimated the Coriolis-induced frontal-plane knee torque from the two-dimensional three-link model (see Figure 16). We found that a squat at a 0.5 Hz cadence during 30 RPM centrifugation induces a torque up to 0.6 Nm in a subject with the anthropometric measurements we specified. This is approximately 2% of the total frontal-plane torque.

Discussion

We have estimated the contributions of mechanics and Coriolis forces on the frontal-plane torque at the knee joint. The Coriolis torque is approximately 2% of the total torque at the knee. Coriolis is partly responsible for the mechanical torque, since it is these forces that deflect the knee medially and laterally during repetitions of the supine squat on-board a rotating centrifuge.

Throughout the squat you would have to use hip the hip adductors to resist lateral knee deflection and hip abductors to resist medial knee deflection to maintain knee-in-space stability. In order to maintain internal knee stability, this torque must be passively resisted by the medial and lateral collateral ligaments (MCL and LCL) (Figure 25) and actively by co-contraction of the quadriceps and hamstrings. Each of these ligaments (MCL and LCL) have rather different

mechanical properties [105, 106]. Failure loads of the MCL have been reported as low as 1.0 kN and as low as 0.24 kN in the LCL. If we assume the width of the knee joint is 10 cm and the torque axis is through the center of the joint, then the moment arm to the LCL and MCL is approximately 5 cm. Therefore, with a 34 Nm torque, the tensile force on the LCL is roughly 680 N. Mechanically speaking, this is greater than the failure loads of the ligament. However, this is not the actual load transmitted to this structure. Absorption of the load in the cartilage and muscular activation of the vastus medialis, vastus medialis, and biceps femoris also work to stabilize the knee, indicating the complex nature of active (e.g., muscle) and passive (e.g., ligaments) elements.



Figure 25. Ligaments, cartilage, and menisci of the right knee.

It is likely not the single occurrence of these joint forces and torques that makes them harmful, but rather the repeated occurrence – overuse injuries³⁰. During stationary cycling motions with the feet rigidly attached to the pedals, the biomechanics of the motion result in frontal plane torques at the knee up to 30 Nm [107]. This repetitive, low magnitude torque, that results from improper foot positioning (internal / external rotation of the foot) and anatomical variations (such as hip width) may cause medial and lateral knee pain [108], and is believed to be the design

³⁰ “Overuse injuries occur when a tissue accumulates damage caused by repetitive submaximal loading. Repetitive activity fatigues a specific structure, such as tendon or bone [108].

driver of swiveling cycling cleats³¹. The number of repetitive motions (cycles) during a squat workout is many orders of magnitude less than the pedal revolutions during a cycle workout; however, this is something that should be considered in the case of repeated squat exercise during centrifugation by an astronaut on a long-duration mission.

³¹ <http://www.cptips.com/knee.htm>

Chapter 5: Squat Biomechanics Experiments



*“No amount of experimentation can ever prove me right;
a single experiment can prove me wrong.”*
Albert Einstein

We defined two separate experiments to investigate the research aims previously outlined. These experiments involved a number of repetitive squat exercises both while lying supine on the centrifuge and while standing upright in the laboratory. In this section, we briefly describe the research equipment used, as well as the experimental design and procedures.

Equipment and Materials

All experiments were conducted on the MIT Man-Vehicle Laboratory short-radius centrifuge (SRC). The centrifuge was modified to allow resistive squat exercises when rotating at speeds up to 30 RPM. Motion capture equipment was added to the centrifuge to record the kinematics of the legs during exercise, surface electromyography (EMG) recorded muscle activity, and left and right foot forces were recorded from custom built strain gauges.

MVL Short-Radius Centrifuge

The MIT SRC is a 3.04 meter long rotating horizontal bed that can rotate continuously at speeds up to 30 RPM (180 degrees per second) [4, 10, 109]. The subject rotation radius is 2.13 meters and can accommodate individuals who are 1.82 meters or less in height. Typically, subjects are supine with their head at or near the axis of rotation. Rotation is about an earth-vertical axis.

A DC motor (1.0 HP, Browning) and motor controller (Browning LWS Series LW second generation) were responsible for driving the centrifuge rotation. Rotation rate may be controlled either manually or via a PC. The controller limited the maximal angular acceleration to 0.17 degrees per second squared (deg/sec^2) until a constant angular velocity is reached. On-board power was provided by two 24 Volt uninterruptible power supplies (UPS) (SF-6030, 300Wh) and two 12 Volt sealed lead batteries (12V 35A-hr, UB12350, Universal Battery) arranged in

series. A switched ATX computer power supply running off 24Volts (Orion, 300DX/24) provided the different voltages for the various measurement equipment. The two UPS units and a power converter (S300-124, Go Power! Electric, Inc.) provided 120-Volt 60-Hz AC power on-board the centrifuge.

Exercise Equipment

The exercise equipment for this experiment consisted of the linear backslider with shoulder pads, a constant force spring assembly, and a foot plate with a modified stair stepper (Kettler Vario Mini Stepper) (Figure 26). The stair stepper has force sensors attached to each of the independent foot holds, and the foot holds can be locked into a symmetric position for squat exercises. The subjects' feet were strapped to each of the foot holds on the stepper for safety.

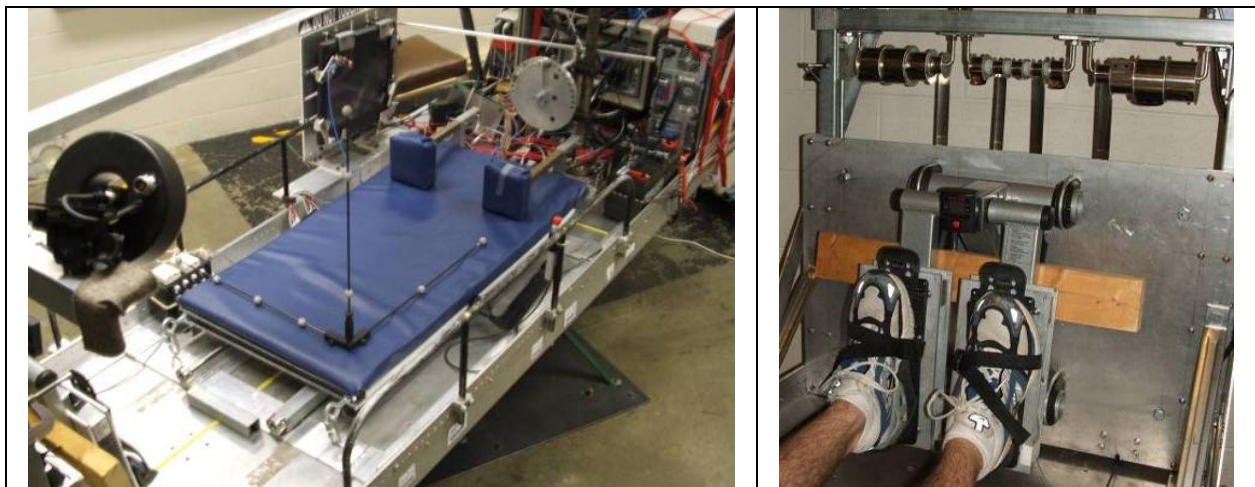


Figure 26. Left: Centrifuge linear back-slider with shoulder pads installed. The calibration axis is shown on the back-slider. Right: The foot plate of the centrifuge with the modified Kettler Vario Mini Stepper attached. The subjects feet are strapped to independent foot holds on the stepper. Single axis force sensors are located underneath each foot. The stepper foot holds are locked into a symmetric position by the 2 in. by 4 in. piece of lumber. Four of the springs in the constant force spring assembly are deflected in this image.

Data Acquisition

The data acquisition PC on-board the centrifuge was controlled remotely by the experiment operator through a wireless internet connection running PC-Anywhere (Version 11.5, Symantec). The PC is set up to record up to 32 analog (16 bit) and up to 96 digital signals (PCI-6229, National Instruments, Inc.) and surface electromyography data (Bagnoli-16, DelSys, Inc., PCI-6034E, National Instruments, Inc.) Data acquisition rate was 1.0 kHz, and was saved to the hard disk and downloaded for analysis after the experiment has been completed. The switching

power supply frequency of 68 kHz required each of the data acquisition channels be low pass filtered using a simple resistor-capacitor (R-C) circuit with a cutoff frequency of 32 kHz.

Sensory-Motor and Biomechanical Recording

There are two devices used for recording the kinematics of the squat exercise. A linear string potentiometer (Model LX-PA-30, UniMeasure, Inc.) was mounted to the centrifuge structure and the back-slider. The second piece of equipment is the SMART motion capture system (previously described). In short, this system includes several camera units, a personal computer, and a video synchronization hub. Two reflective markers were placed on the body, and data recorded through the calibrated cameras allowed us to reconstruct the three-dimensional position of the reflective markers.

Surface Electromyography

We used a DelSys Bagnoli-16 (DelSys, Inc., Boston, MA) surface electromyography (EMG) system with DE-2.1 single differentiation surface electrodes. These electrodes have 1.0 cm spacing between each electrode. The amplifier bandwidth was from 20 to 450 Hz with an input voltage of 12 VDC at 1.5 Amps. The amplitude of the raw EMG as recorded at the electrodes was expressed in millivolts. The skin was cleansed with rubbing alcohol before attaching the electrodes. We did not measure the contact impedance between the skin and electrodes.

Experimental Methods

We conducted two separate experiments to investigate the kinematics, kinetics, and muscle activity during artificial gravity squats. Experiment 1 was designed to quantify the kinematics and kinetics during a multiple repetition protocol, as well as any post-rotatory effects on the same exercise movements. In Experiment 2, we investigated the effects of additional constant force resistance on AG exercise kinematics and kinetics, and compared the centrifuge supine responses with those during Earth upright. In this section we outline the experiment design, participants, and procedures.

Experiment 1

The first experiment was designed in support of Aim #1 and #2 – to investigate the knee perturbations from Coriolis forces during centrifuge squats, and to look for after-effects during

squat motions when the centrifuge has stopped. We also recorded foot reaction forces and muscle activity.

Participants

Fifteen subjects, seven male and eight female, between the ages of 19 and 39 took part in the experiment. They were selected from a population that regularly participates in some form of exercise, and screened free of a recent history of injuries that could be exacerbated by performing resistive squat exercises. Two subjects had previous experience with AG exercise. One subject was not able to complete all portions of the experiment due to fatigue. None failed to complete the experiment because of motion sickness symptoms or discomfort. All participants gave informed consent in accordance with the MIT committee on the use of humans as experimental subjects (COUHES). They were compensated \$10 per hour, when applicable. None possessed prior knowledge of the goals of the experiment, or expected results. Each subject completed the experiment in three hours or less, and the time on the centrifuge was typically one hour or less.

Experiment Design

Experiment 1 is a within-subject complete block repeated measures design. All subjects took part in each of the six phases (Table 4). Each phase includes one of three centrifuge rotation rates (0-, 23-, and 30 RPM) and has one or five sets of eight repetitions, each consisting of one squat. Eight self-paced 0.5 Hz cadence (2 seconds per repetition: 1 second “descent”, 1 second “ascent”) repetitions were performed before and after rotation, and forty repetitions were completed during rotation. A single cadence was chosen because of the natural feel to that frequency, which makes it comfortable to self-pace. Subjects were instructed on the cadence. They did not synchronize their movements with a pacing device, such as a metronome.

Phase 1 provided baseline measures when lying supine and Phase 2 replicated upright squats by adding resistance equivalent to their body weight. The subsequent phases during rotation were of interest to measure the knee position and muscle activity during centrifugation. “Standing” periods of one minute separated each set during rotation. We did not add additional resistance because of the fatiguing nature of the multiple set and multiple repetition protocol. The 30 RPM squats always followed the 23 RPM squats because of the fatigue concern. The 0 RPM phases

after each rotation phase investigated any post-rotatory after-effects on the supine squat biomechanics. All exercises during rotation were performed in darkness with eyes closed. Subjects did not get visual feedback of their leg position. Figure 27 outlines the conditions that were examined and contrasted to allow us to test Hypothesis #1 and #2.

Table 4. Experiment 1 phases. Rotation rates are in revolutions per minute (RPM). Resistance is a percentage of 1-G upright body weight (BW).

Phase	RPM	Resistance	Repetitions	Notes
1	0	0%	8	Reference
2	0	BW	8	Body weight reference
3	23	0%	40 (5 sets of 8 reps)	First rotation speed
4	0	0%	8	Post-effects of first speed
5	30	0%	40 (5 sets of 8 reps)	Second rotation speed
6	0	0%	8	Post-effects of second speed

Centrifuge RPM Resistance (% 1-BW)	0, Supine	23	30
	0	1-set 8-reps (pre, post)	5-sets 8-reps (per)
100	1-set 8-reps (pre)		

Figure 27. Experiment 1 conditions for investigating Aim #1 and #2. The 0-RPM, 0% resistance condition (pink cell) was used to look for after-effects. The 0-RPM, 1-BW (green cell) is a baseline measure for comparing the conditions when the centrifuge is rotating (blue cells).

Procedure

Before the subject arrived at the laboratory, the surface EMG electrodes were cleansed with gauze pads and rubbing alcohol. Two-sided adhesive was affixed to the surface that attaches to the subject. We also went through the calibration sequence for the four SMART motion capture cameras. The calibration ensured that the error in position estimation was less than 1.0 mm.

When each subject arrived for participation, they were introduced to the experiment – the background, the goals, and the equipment. We asked them to carefully read the informed consent document, ask any questions that they may have, and sign indicating they agreed to participate. There was also a subject compensation form and a brief medical history questionnaire to screen each participant free of a recent history of injuries that could be exacerbated by performing the squat exercises.

After completing all the initial paperwork, the subjects changed into athletic shorts and sneakers, if they were not already wearing them. We first recorded their weight. The EMG junction boxes were clipped to the waistband on their shorts and then we began preparing the skin for attaching the surface electrodes. The muscles activity we were interested in recording was that of the soleus, medial and lateral gastrocnemius, tibialis anterior, vastus lateralis, vastus medialis, and rectus femoris. We did not record the muscle activity of the biceps femoris because the supine posture on the centrifuge put the hamstrings in contact with the back-slider surface, which continually interfered with the recording. The anatomical locations of the muscles are shown in Figure 28, and their function is listed in Table 5.

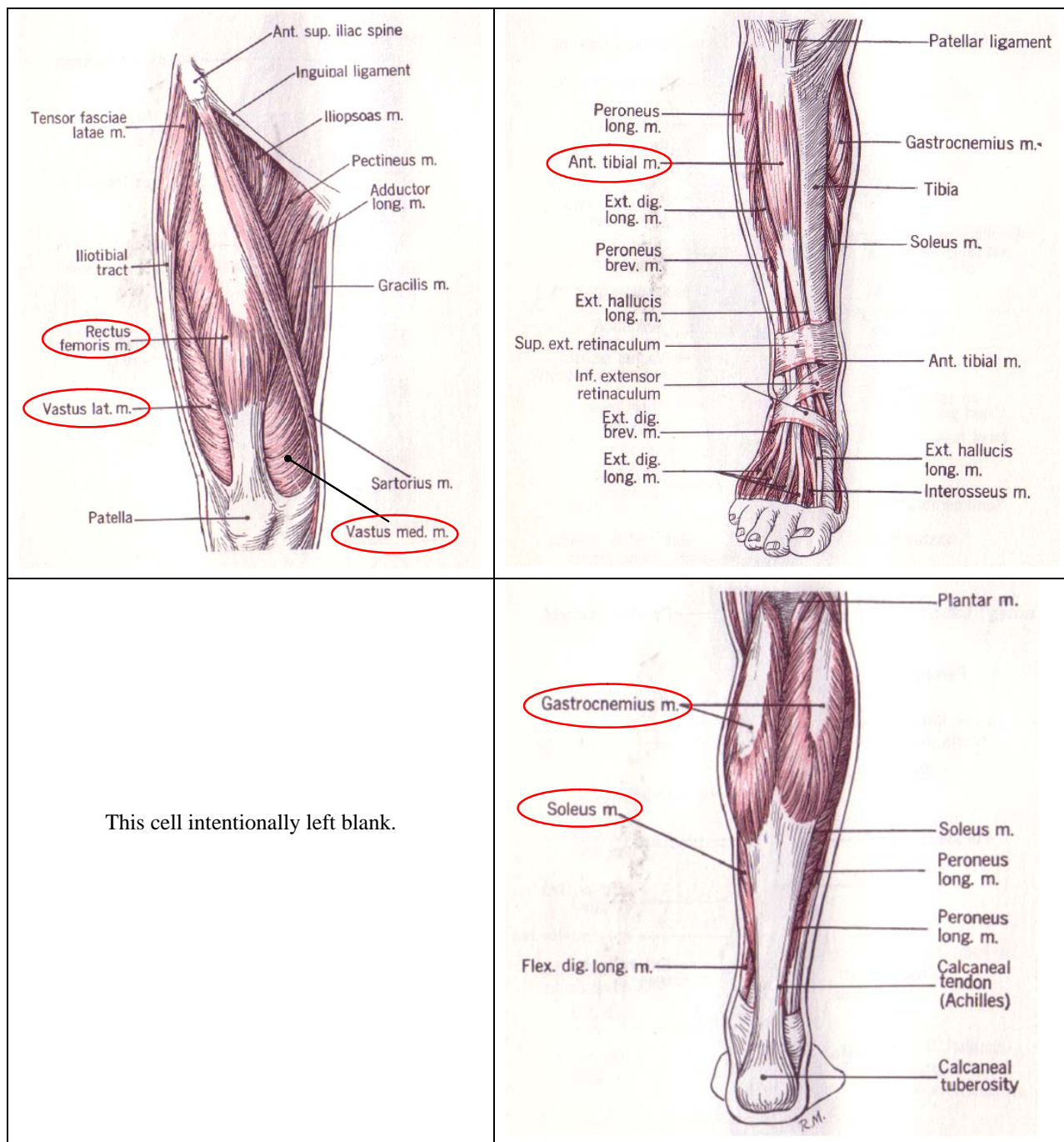


Figure 28. Anatomical locations of the muscles we recorded EMG from. Top left: Vastus medialis, vastus lateralis, rectus femoris. Top right: Tibialis anterior. Bottom right: Medial and lateral gastrocnemius, soleus. Images from [110].

Table 5. Anatomical functions of the muscles we recorded EMG from, and the percentage of type I (slow-twitch) fibers [14]. Data is not available for the rectus femoris, vastus medialis, or tibialis anterior.

Muscle	Action	Fiber type
Rectus femoris	Knee extensor; hip flexor	---
Vastus medialis	Knee extensor	---
Vastus lateralis	Knee extensor	42% type I
Tibialis anterior	Dorsiflexes foot	---
Medial gastrocnemius	Knee flexor; plantar flexes foot	55% type I
Lateral gastrocnemius	Knee flexor; plantar flexes foot	55% type I
Soleus	Plantar flexes foot	90% type I

The skin over each muscle of interest, location specified by Basmajian and Blumenstein [111], was thoroughly cleansed with a gauze pad and rubbing alcohol. There was no shaving or abrading. Each electrode was affixed to the skin using two-sided adhesive tape. We then placed several strips of medical tape over the electrode and skin to ensure that it would not be inadvertently pulled loose. The opposite end of the electrode cable was then connected to the junction box. This was repeated for the soleus, medial and lateral head of the gastrocnemius, and tibialis anterior on the left and right legs (Figure 29). After attaching the electrodes to the lower leg muscles, we cleansed the right elbow with a gauze pad and rubbing alcohol before attaching the reference electrode.

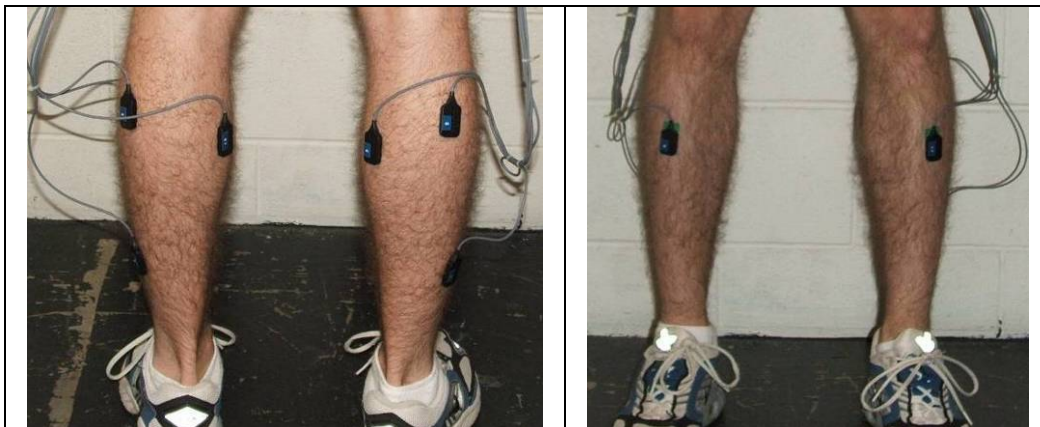


Figure 29. EMG electrode placement on the lower leg. Left: electrode placement on the soleus, medial gastrocnemius, and lateral gastrocnemius of the left and right leg. Right: electrode placement on the tibialis anterior of the left and right leg.

After a brief warm-up period and stretching, we then asked the subject to perform a series of maximum voluntary isometric contractions (MVIC) for each of the muscle groups. This allowed us to record the muscle activity during maximum contraction for normalization, to a percentage of MVIC, of the exercise-related muscle activity. We used the arrangement outlined by Konrad

[112] for each MVIC exercise. The equipment and a subject demonstration are shown in Figure 30. For these muscles of the lower leg, the MVIC testing order was: right soleus, left soleus, right gastrocnemius, left gastrocnemius, right tibialis anterior, left tibialis anterior. Each MVIC was performed by slowly increasing the contraction to maximum over three seconds, holding the maximum contraction for approximately three seconds, and then slowly relaxing the contraction over three seconds. This procedure was repeated three times for the right and left leg.

For the soleus, the subject was seated, with their knee at 90 degrees flexion and ankle half-way plantar-flexed. They were asked to perform a unilateral plantar flexion of the foot against the Unistrut® frame. A wooden block was placed underneath the metal frame to help distribute the pressure on the leg and a foam pillow was placed between the wooden block and the subject's leg for comfort. We tested the medial and lateral head of the gastrocnemius simultaneously. The subject was seated with their leg extended and foot against the wall. We asked them to perform a unilateral plantar flexion of the foot while the experimenter firmly held the back of the chair. The tibialis anterior was again tested unilaterally. The subject was seated with their foot flat on the floor. Foam padding was placed on top of the foot and then the Unistrut® frame was then placed on top of the foam. The experimenter applied manual resistance to ensure the dorsal flexion of the foot was isometric.

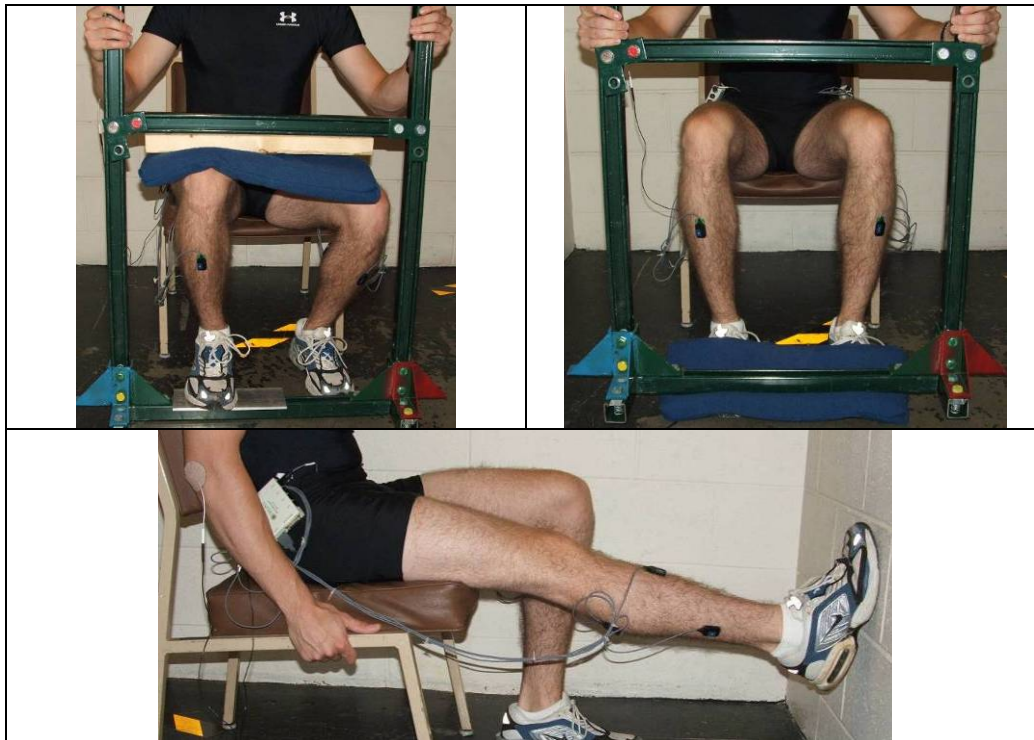


Figure 30. Maximum voluntary isometric contraction (MVIC) testing for the soleus (upper left), tibialis anterior (upper right), and gastrocnemius (bottom).

After completing the MVIC testing for the lower leg muscles, we then attached the electrodes to the vastus lateralis, vastus medialis, and rectus femoris of the left and right legs. Again, the location (specified by Basmajian and Blumenstein) was cleansed with gauze pads and alcohol and electrodes were attached to the skin using two-sided adhesive and medical tape (Figure 31).



Figure 31. Electrode placement on the vastus lateralis, vastus medialis, and rectus femoris of the left and right leg. The EMG junction boxes are shown on the subjects left and right hip.

After attachment of the electrodes to three of the quadriceps muscles, we had the subjects perform MVICs. Again, we used the arrangement outlined by Konrad [112] for each MVIC exercise. The setup is shown in Figure 32. The subject sat in the chair, with their knee at approximately 90 degrees flexion with their toe against the wall. They performed unilateral isometric leg extensions with the experimenter holding the back of the chair to make sure it did not move during the contractions.



Figure 32. Maximum voluntary isometric contraction (MVIC) testing for the vastus lateralis, vastus medialis, and rectus femoris. The right leg was tested first, followed by the left leg.

After performing the MVIC testing, we re-iterated the components of the centrifuge, its operation including the emergency stop button, and the experiment protocol. We described the 0-20 motion sickness scale to the subjects, and advised them that if their motion sickness were to reach 10 or 12 out of 20, we would terminate the experiment. The subject was then assisted onto the centrifuge by the experimenter. They were supine on the linear back-slider with their shoulders comfortably against the pads, and the feet strapped into the left and right foot holds on the stair-stepper. The safety belt was strapped over their torso, all EMG cables were connected, and they were handed a trigger button³². We then affixed the reflective markers for the motion capture on the left and right lateral tibial condyle. The subjects were then instructed on the self-paced exercise cadence: *“We’d like you to perform the squats at a two-second pace. That is, take one second to go “down” in the squat, and one second to go back “up,” and briefly pause*

³² The trigger button was connected to an infrared LED circuit, the on-board data acquisition system, and the DelSys EMG unit. When the button was pressed, it completed a 5-Volt circuit, which started the EMG recording, illuminated an IR LED that was seen by the SMART motion capture system, and was recorded by the on-board DAQ. As a result, this ensured that the three systems were all time synchronized within 2-milliseconds. The button was typically depressed by the subject for 500 to 1,000-ms.

for one second before starting the next repetition. Go down as far as you comfortably can in the squat, but be sure that you keep the two-second pace.” They performed several practice trials with the supervision of the experimenter before starting the experiment. When their performance was deemed satisfactory, the computers were turned on and confirmed the data recording. The experimenter always instructed to them when to click the trigger button, and when to start the exercises.

Phase 1 consisted of performing a set of eight squat repetitions with the centrifuge stationary, and no resistance. At the end of every set, whether spinning or not, we asked them their level of motion sickness. We then connected the constant force spring assembly to provide resistance equivalent to their body weight (Phase 2). With the centrifuge still stationary, we asked them to perform a set of eight repetitions. After completing this phase, the constant force spring assembly was disconnected.

Before starting the rotation phases, the centrifuge was manually walked around for one revolution to ensure that there were no cables or obstructions that interrupt the centrifuge operation. With the lights in the room off, the centrifuge was then spun up to 23 RPM, not exceeding 0.17 deg/sec^2 (0.002 rad/sec^2) angular acceleration. When instructed, the subject completed five sets of eight squat repetitions (40 repetitions total) against their artificial gravity weight (Phase 3). The centrifuge was slowed down (angular deceleration less than $0.17^\circ/\text{sec}^2$ (0.002 rad/sec^2)) and stopped after completing the forty repetitions.

With the centrifuge at a complete stop, we asked the subject to complete a set of eight repetitions of the supine squat (Phase 4). The centrifuge was then spun up to 30 RPM, under the same angular acceleration limits, and the subjects were asked to complete five sets of eight squat repetitions against their artificial gravity weight (Phase 5). The centrifuge was slowed down and stopped after the five sets. The subject then completed a set of eight repetitions with the centrifuge stationary (Phase 6).

After Phase 6, we powered down the centrifuge control software and secured the centrifuge. With the subject still supine on the back-slider, we removed the EMG electrodes and the motion

tracker markers. The safety harness was unbuckled and the feet unstrapped. The back slider was locked in place and the subject was assisted off of the centrifuge. We took the anthropometric measurements [104] and de-briefed the subject on their experience before they left the laboratory.

Post-experiment clean-up included cleansing the surface EMG electrodes with gauze and rubbing alcohol, and stowing them. The batteries on-board the centrifuge were charged. The data was downloaded from each computer and written to a CD for subsequent analysis.

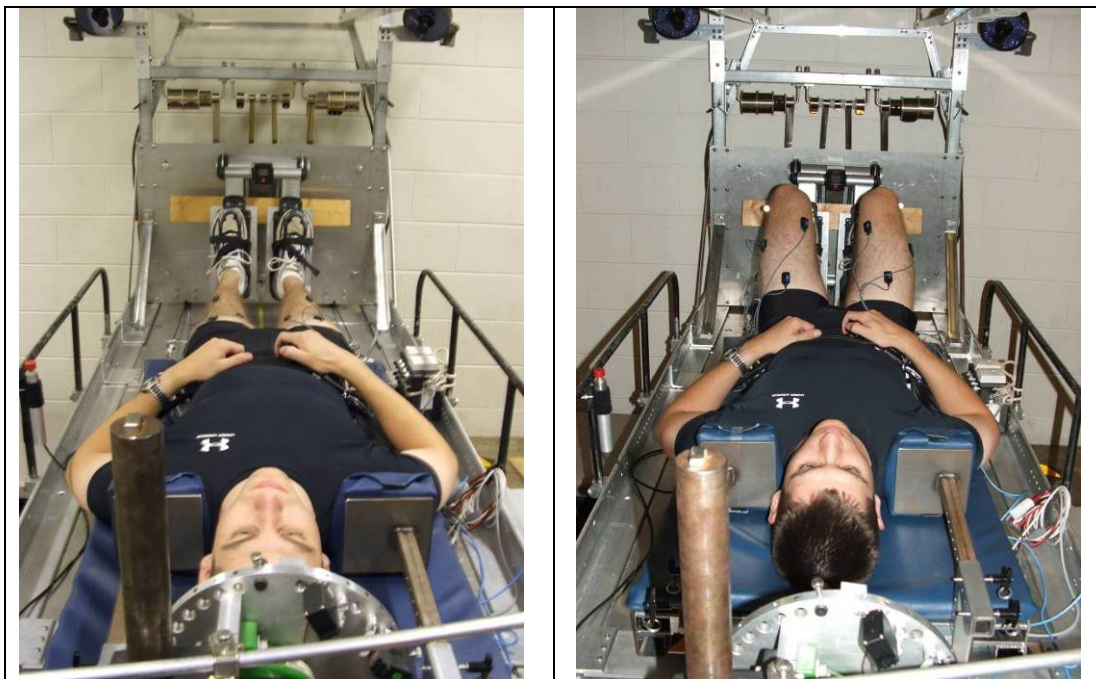


Figure 33. Subject performing a supine squat on-board the centrifuge. Left: Subject is “standing” against either their artificial gravity weight or constant force spring resistance. Right: Subject is the knee flexed position against either their artificial gravity weight or constant force spring resistance.

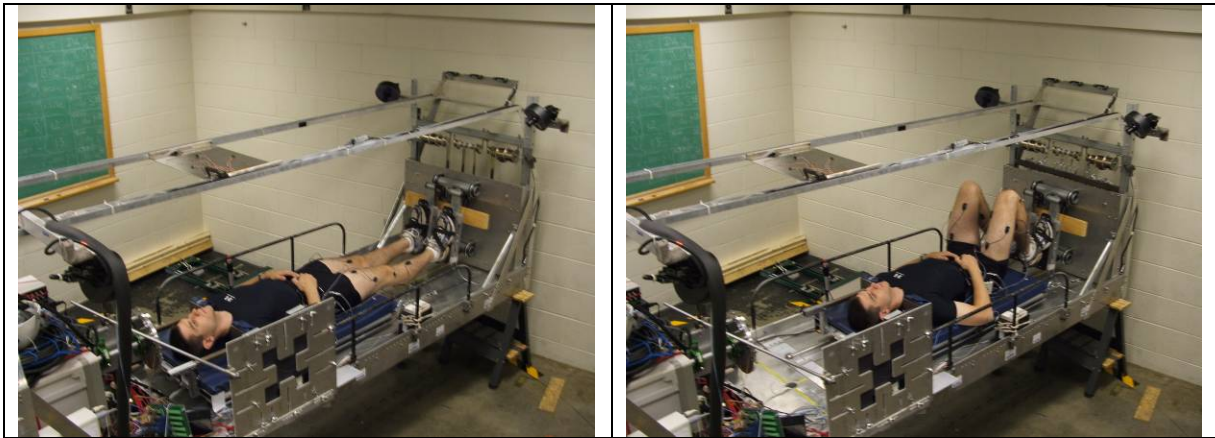


Figure 34. Side-views of a subject performing a supine squat on-board the centrifuge. **Left:** Subject is “standing” against either their artificial gravity weight or constant force spring resistance. **Right:** Subject is the knee flexed position against either their artificial gravity weight or constant force spring resistance.

Experiment 1 Summary

Experiment 1 follows a within-subject complete block repeated measure design. All subjects took part in all portions of the experiment in the same order – there was no randomization or balancing in the presentation of conditions. Independent variables included the rotation rate, magnitude of the resistive force, and squat exercise repetition and set number. These are all fixed factors. The dependent variables included the foot reaction forces (left and right foot), left and right knee three-dimensional position, surface EMG from the 14 leg muscles (7 in each leg), and subjective reports of motion sickness. The blocking factor, the subjects, was considered random.

Experiment 2

Experiment 2 was designed to compare and contrast the muscle activity, knee biomechanics, and foot reaction forces during artificial gravity supine squats with upright squats. This data was used, primarily, for Aim #3, and secondarily to expand on the Experiment 1 conditions. Subjects exercised at a single cadence while standing upright or while lying supine. They were spun at several centrifuge rotation rates, and had several levels of additional resistance.

Participants

Thirteen subjects, 9 male and 5 female, between the ages of 19 and 39 years participated in Experiment 2. All participants were selected from a population that regularly participates in some form of exercise, and screened free of a recent history of injuries that could be exacerbated by performing resistive squat exercises. Eight subjects had taken part in Experiment 1. None of the subjects failed to complete the experiment because of fatigue, discomfort, or motion sickness. None possessed prior knowledge of the goals of the experiment, or expected results. They all gave informed consent in accordance with the MIT COUHES. The experiment was typically completed in four hours or less, with centrifugation time less than one hour. Compensation was \$10 per hour, when applicable.

Experiment Design

Experiment 2 is also follows a within-subjects complete block repeated measures design. Table 6 outlines the research plan, which was divided into 14 phases. Each phase consists of one set of eight squat repetitions at a 0.5 Hz cadence (2 seconds per repetition: 1-second “descent,” 1 second “ascent”). Subjects were pseudo-randomly assigned to one of two groups (A or B). Group A took part in the upright portion of the study, then 23 RPM, followed by the 30 RPM centrifugation. Group B took part in the upright portion of the study, then 30 RPM, followed by 23 RPM. This balanced any centrifuge rotation order effects. Within each rotation rate, the level of resistance always increased to minimize fatigue. The upright squats always preceded the centrifuge squats. All subjects took part in all phases.

Table 6. Experiment 2 protocol. Resistance is a percentage of 1-G body weight. RPM = Revolutions per minute (centrifuge rotation rate). BW = Body weight.

Phase	Group A	Group B	Comments
1	Upright, 0%	Upright, 0%	1-set, 8 reps, 0.5 Hz cadence
2	Upright, 10%	Upright, 10%	
3	Upright, 25%	Upright, 25%	
4	0-RPM, 0%	0-RPM, 0%	Pre-study of first centrifuge speed
5	0-RPM, 1-BW	0-RPM, 1-BW	Difference between Phase 1 and Supine
6	23-RPM, 0%	30-RPM, 0%	
7	23-RPM, 10%	30-RPM, 10%	
8	23-RPM, 25%	30-RPM, 25%	
9	0-RPM, 0%	0-RPM, 0%	Post-study of first centrifuge speed
10	0-RPM, 0%	0-RPM, 0%	Pre-study of second centrifuge speed
11	30-RPM, 0%	23-RPM, 0%	
12	30-RPM, 10%	23-RPM, 10%	
13	30-RPM, 25%	23-RPM, 25%	
14	0-RPM, 0%	0-RPM, 0%	Post-study of second centrifuge speed

Figure 35 depicts the experimental conditions that were examined and contrasted. The 23- and 30 RPM cells with 0-, 10-, and 25% BW resistance (blue) allowed us to expand on the conditions explored in Experiment 1 to test Hypothesis #1. The 0 RPM Supine, 0% resistance condition (pink cell) was as a pre- and post-rotation baseline measure. The magnitude of the knee deflections recorded during (blue) and after (pink, post) rotation were compared to those recorded before (pink, pre) rotation. The nine cells with the cross hatching (23- and 30 RPM, Upright, 0, 10, and 25% BW resistance) are the primary focus of Experiment 2. The Upright, 0%-resistance and Supine, 1 BW conditions (beige cells) allowed us to determine any fundamental differences between the Earth upright squats and supine squats with 1-BW resistance. For the Supine 1 BW case (not spinning), we were also interested in knowing whether medial-lateral knee position during the supine squat was affected by additional resistance.

Centrifuge RPM Resistance (% 1 BW)	0, Supine	23	30	0, Upright
0	8-reps (pre, post)	8-reps (per)	8-reps (per)	8-reps (pre)
10		8-reps (per)	8-reps (per)	8-reps (pre)
25		8-reps (per)	8-reps (per)	8-reps (pre)
100	8-reps (pre)			

Figure 35. Experimental conditions for testing Hypothesis #3 (primary) and expanding on the conditions for testing Hypothesis #1 (secondary).

Procedure

Before the subject arrived, we removed two of the SMART cameras from the foot plate assembly and placed them on tripods. The foot plate assembly (foot plate, stair stepper, constant force springs) was removed from the centrifuge and placed on the floor in the laboratory. The upright slider device, with shoulder pads, was attached to the footplate and we counterbalanced the back-slide. After the upright exerciser was set up, the surface EMG electrodes were cleansed with gauze pads and rubbing alcohol and two-sided adhesive was affixed to the surface that will be attached to the subject. We went through the calibration sequence for the two SMART motion capture cameras. Two cameras were used for the upright exercises because of the simplicity and flexibility of operating in the laboratory. The calibration ensured that the error in position estimation was less than 1.0 mm.

When each subject arrived for participation, they were introduced to the experiment – the background, goals, and the equipment. We asked them to carefully read informed consent document, ask any questions that they may have, and sign indicating they agreed to participate. We also asked them to complete a brief medical history questionnaire to screen them free of any

recent history of injuries that could be exacerbated by performing the squat exercises, as well as a subject compensation form. After completing all the initial paperwork, the subjects changed into athletic shorts and sneakers, if they were not already wearing them. We first recorded their weight before clipping the EMG junction boxes to the waistband on their shorts. The same EMG electrode attachment procedure and MVIC testing as in Experiment 1 was used.

After performing the MVIC testing, we introduced the subject to the upright exercise device, its operation, and the experimental protocol. We described the 0-20 motion sickness scale to the subjects, and advised them that if their motion sickness were to reach 10 to 12 / 20, we would terminate the experiment. We also described the 6-20 Borg physical exertion scale (see Appendix). After each set, whether upright or on-board the centrifuge, we asked the subject to report their motion sickness and level of effort. While on the upright exercise device, the subjects were instructed on the self-paced exercise cadence: *“We’d like you to perform the squats at a two-second pace. That is, take one second to go “down” in the squat, and one second to go back “up,” and briefly pause for one second before starting the next repetition. Go down as far as you comfortably can in the squat, but be sure that you keep the two-second pace.”* They performed several practice trials with the supervision of the experimenter before starting the experiment. When their performance was deemed satisfactory, the computers were turned on and we confirmed data recording. The experimenter depressed the data synchronization trigger button during the upright exercises.

All subjects, whether they were in Group A or B, conducted the upright exercises before centrifugation. Phase 1 consisted of performing a set of eight squat repetitions without any additional resistance. We then connected the constant force springs to provide resistance equivalent to 10% of their body weight for eight repetitions (Phase 2). The constant force springs were then arranged so that they provided 25% body weight resistance for a third set of eight repetitions (Phase 3). The subjects were given approximately a 45 minute break between Phases 3 and 4 for disassembling the upright exercise device and placing the footplate back on the centrifuge. The SMART cameras were removed from the tripods and put back on the centrifuge, and all four on-board cameras were calibrated.

In Phase 4 subjects completed a set of eight squat repetitions with the centrifuge stationary against no resistance. We then connected the constant force spring assembly to provide resistance equivalent to their body weight, and asked them to perform a set of eight repetitions (Phase 5). After completing this set, the constant force spring assembly was disconnected. Phases 6 thru 8 were at 23 RPM for subjects in Group A, and at 30-RPM for those in Group B. Subjects performed eight repetitions against their AG weight in Phase 6, eight repetitions against AG weight plus 10% body weight in Phase 7, and eight repetitions against AG weight plus 25% body weight in Phase 8. The centrifuge was slowed and stopped between each Phase to adjust the constant force spring resistance. The next two phases, 9 and 10, were two sets of eight repetitions with the centrifuge stationary against no resistance (similar to Phase 4). Phases 11 thru 13 were at 30 RPM for subjects in Group A, and at 23 RPM for those in Group B. Subjects performed eight repetitions against their AG weight in Phase 11, eight repetitions against AG weight plus 10% body weight in Phase 12, and eight repetitions against AG weight plus 25% body weight in Phase 13. The centrifuge was, once again, stopped between each Phase to adjust the constant force spring resistance. The last phase, Phase 14, was a set of eight repetitions with the centrifuge stationary with no resistance.

At the end of the experiment we powered down the centrifuge control software and secured the centrifuge in the laboratory. With the subject still supine on the back-slider, we removed the EMG electrodes and motion tracker markers. The safety harness was unbuckled and the feet unstrapped. The back-slider was locked in place and the experimenter assisted the subject off the centrifuge. Anthropometric measurements were recorded before the subject left the laboratory. Post-experiment clean-up included cleansing the surface EMG electrodes with gauze and rubbing alcohol, and stowing them. The data was downloaded from each computer and written to a CD for subsequent analysis.

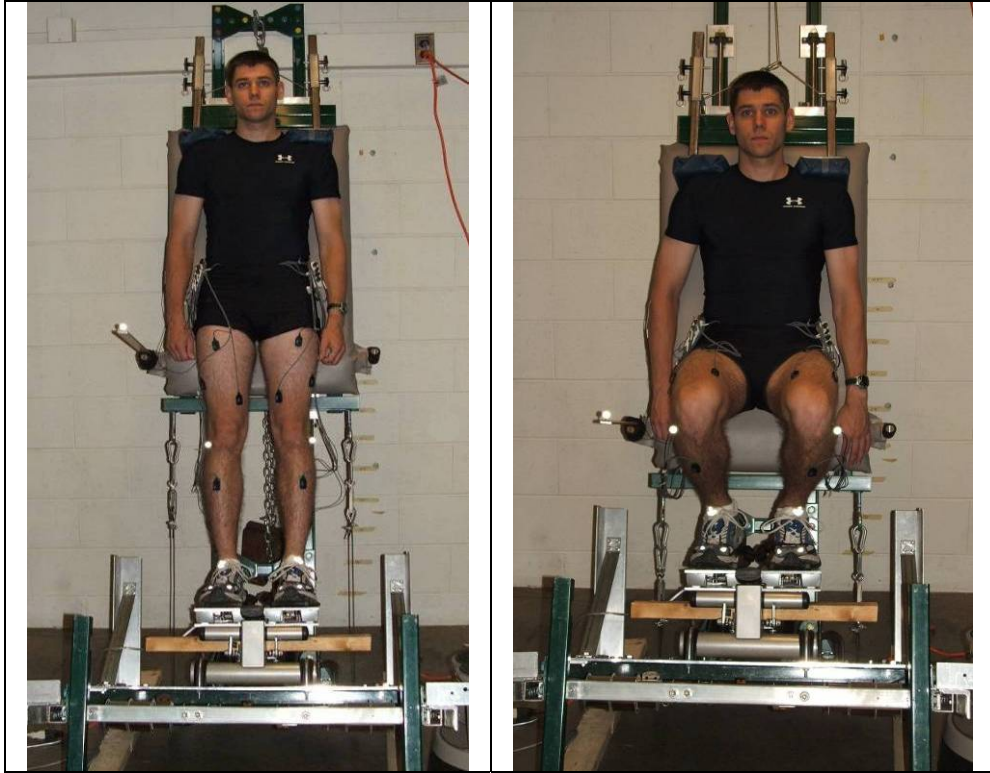
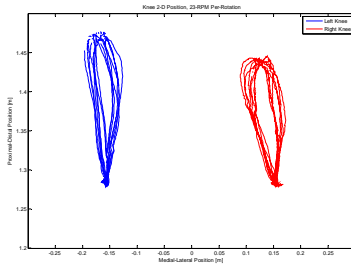


Figure 36. Subject performing an upright squat. Left: Subject is standing against either their body weight or body weight plus constant force spring resistance. Right: Subject is the knee flexed position against either their body weight or body weight plus constant force spring resistance.

Experiment 2 Summary

Experiment 2 also follows a within-subject complete block repeated measure design. All subjects took part in all portions of the experiment. However, we pseudo-randomly assigned the subjects to one of two groups: Group A or Group B, to balance the groups, approximately, for height, weight, and gender. Independent variables included the assigned group, rotation rate (upright, 23 or 30 RPM), magnitude of the resistive force (0, 10, 25% body weight), and squat exercise repetition number. These are all fixed factors. The dependent variables included the foot reaction forces (left and right foot), left and right knee three-dimensional position, surface EMG from the 14 leg muscles (7 in each leg), subjective reports of motion sickness, and Borg ratings of perceived physical exertion. The blocking factor, the subjects, was considered random.

Chapter 6: Analysis and Results



"Not everything that counts can be counted, and not everything that can be counted counts."
Albert Einstein

In this section, we present the results of the two experiments. For our statistical analysis, all effects are considered significant at $p < 0.05$ unless otherwise stated. When an ANOVA was used, the residuals were inspected to check the Fisher assumptions: e.g., normally distributed with zero mean. We used SYSTAT v.11 statistical software (SPSS Software, Inc.) for all of our analyses.

Experiment 1

The aim of Experiment 1 was to quantify the kinematics and kinetics of multiple repetitions of the centrifuge supine squat. We tested 15 subjects (8 male, 7 female) between the ages of 19 and 39 years. All subjects completed Phases 1 through 4. One subject (Subject 8) could not complete the squats at 30 RPM (Phase 5), and therefore, we do not have Phase 5 and 6 data for that subject. There were also several instances when the surface EMG electrode became partially detached from the skin which resulted in lost data. The EMG data was not analyzed in these instances. The statistical results are tabulated at the end of the Experiment 1 results (Table 7 and Table 8).

Leg Kinematics

The motion capture system made it possible to record the three-dimensional kinematics of the left and right lateral tibial condyle during each repetition. For our configuration, with the subjects lying supine on a horizontal centrifuge, the Coriolis accelerations tended to deflect the thigh and shin medially and laterally. From this position-data, we identified the maximum total

mediolateral motion of the knee³³ (Figure 37). Quantitatively, this parameter is the sum of the maximum medial travel and the maximum lateral travel of each knee during each repetition. The data was analyzed using a repeated measures analysis of variance (ANOVA). In this statistical model, the fixed effects were experimental phase (1..6), gender (male or female), and leg (left or right). The blocking factor, subjects, was considered random.

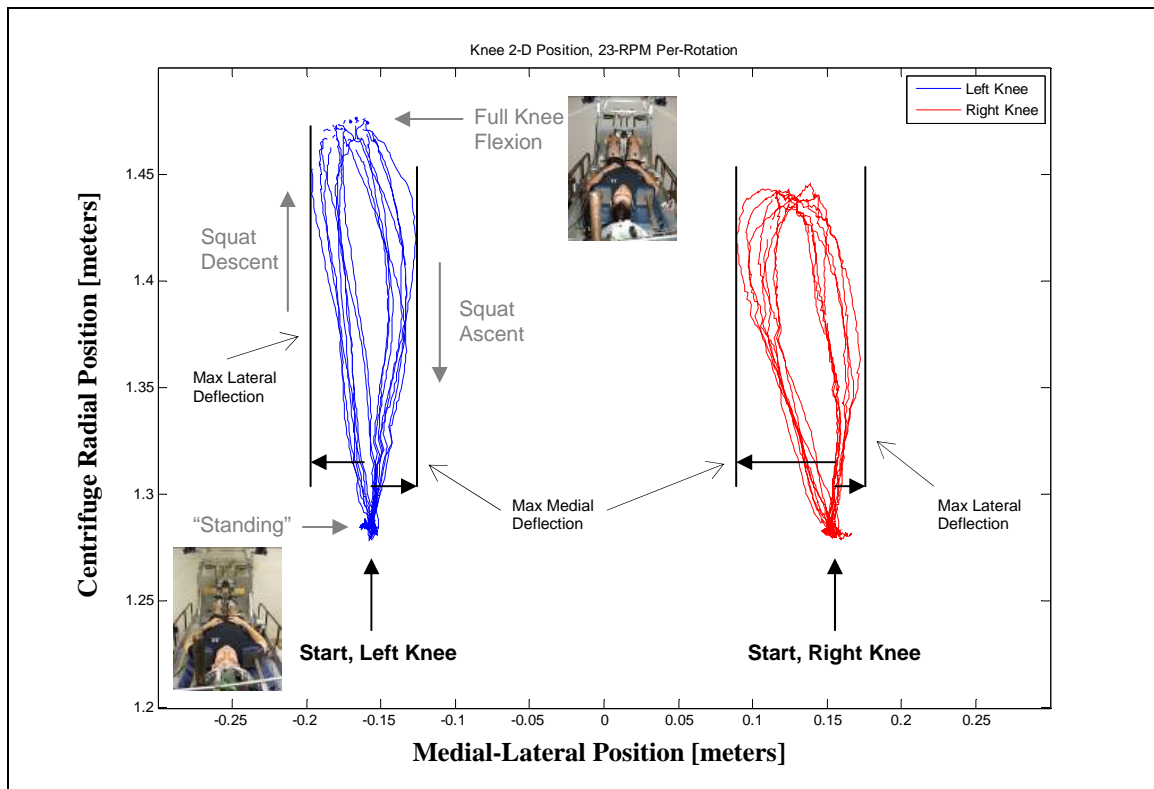


Figure 37. Exemplary data for the two-dimensional frontal plane motion of the left and right knee during a set of eight repetitions while rotating at 23 RPM clockwise. We see the start and end position of the left and right knee, as well as the maximum medial and lateral deflection of the knee during each repetition. During descent, the left knee deflects laterally (right knee medially) and during ascent, the left knee deflects medially (right knee laterally). The maximum medial-lateral travel of the knee is the absolute value of the difference between the maximum lateral deflection and the maximum medial deflection during each repetition for the left and right knees individually.

Figure 38 shows the maximum mediolateral travel of the legs during each of the experimental phases. We found that the maximum mediolateral deflections during centrifugation at 23- and 30 RPM (Phase 3 and 5) were both significantly greater than the 1-G body weight resistance without centrifugation (Phase 2) (Phase 2 < 3: $p = 0.004$, Phase 2 < 5: $p = 0.005$). This data

³³ Although the position tracker markers were placed on the left and right lateral tibial condyle, we project that position to the patella. Therefore, we describe all parameters as the deflection of the knee rather than the deflection of the lateral tibial condyle.

supports our hypothesis (Hypothesis #1) that centrifugation causes greater medial-lateral deflections of the knee. We found no significant difference between the two rotation speeds (Phase 3 v. 5: n.s.). This does not support our hypothesis (Hypothesis #1) that a higher rotation rate, keeping cadence constant, will induce greater medial-lateral deflections. In fact, the deflections at 30 RPM (Phase 5) are slightly smaller than at 23-RPM (Phase 3), indicating that the increased apparent body weight during the higher rotation rate may have suppressed the mediolateral deflections.

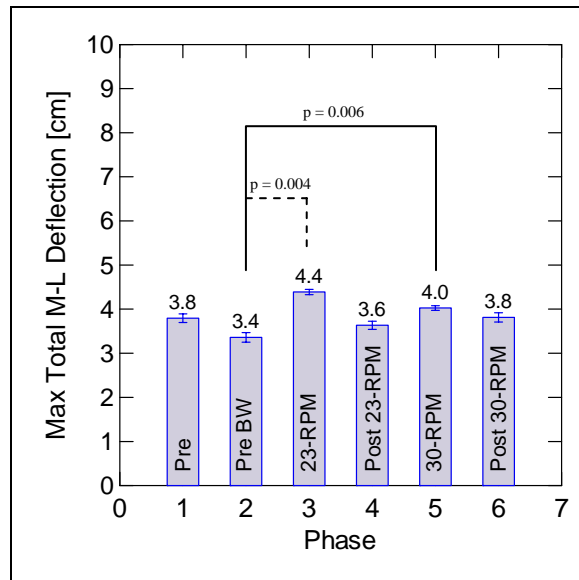


Figure 38. Maximum medial-lateral travel of the knees during each experimental phase. Both knees averaged together. Data from 14 (7 male, 7 female) of the 15 subjects is shown. Mean +/- SEM.

The maximum mediolateral knee travel of the knee after centrifugation was not significantly different from those without centrifugation (Phase 1 vs. 4: n.s., Phase 1 vs. 6: n.s.). This data does not support the hypothesis (Hypothesis #2) that repetitive squats during centrifugation will cause increased mediolateral knee travel after rotation compared to squats without centrifugation.

A plot of the individual repetitions across all of the experiment phases shows some interesting trends (Figure 39). There is an initial large deflection in the knees during the first few repetitions of the 23 RPM supine squats (first few repetitions in Phase 3). The subjects then begin to compensate for the Coriolis accelerations, and therefore reduce the medial-lateral deflections over time. However, using a Hierarchical Mixed Regression (HMR), the maximum medial-lateral travel did not decrease with repetition (23 RPM, Phase 3), but the travel during the first

set of eight repetitions was slightly greater than during the second ($p = 0.067$). During the 30 RPM squats (Phase 5) the maximum total medial-lateral deflection increased with repetition number ($p < 0.0005$), which may be a result of increasing fatigue.

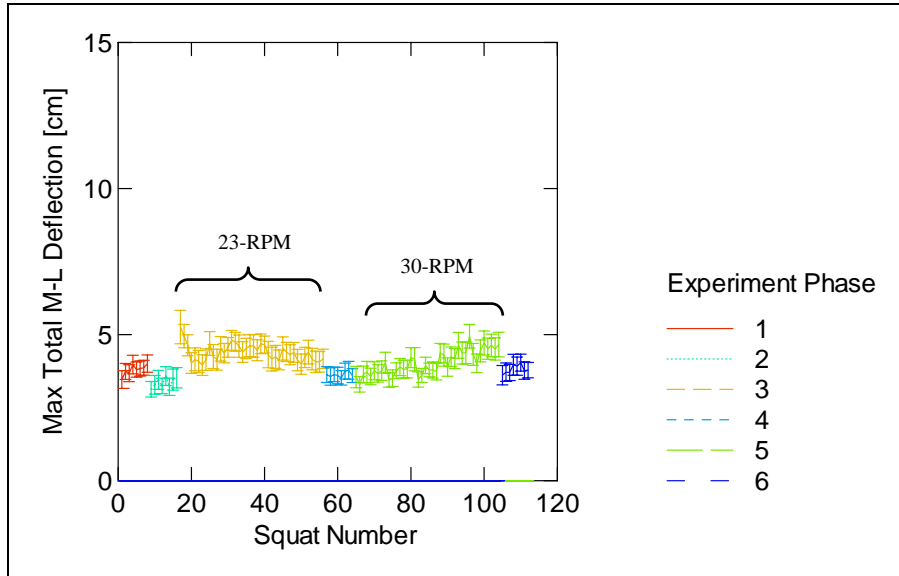


Figure 39. Time history of the maximum total medial-lateral deflection. The left and right knee are averaged together. The experimental phases are presented sequentially, along with the repetition numbers within each phase. There are a total of 112 squat repetitions in this experiment. Data for all 15 subjects is shown. Mean +/- SEM.

Foot Reaction Forces

Foot reaction forces were measured in one-dimension perpendicular to the foot plate. The force sensors are not pre-tensioned, therefore they read erroneous until a minimum force (approximately 133 N (30 lbs.)) is reached. In these analyses, we only consider the phases where subjects were “weighted” – Phases 2, 3, and 5. The “standing weight” and peak foot forces were also analyzed using a repeated measures ANOVA, with experimental phase (2, 3, 5) and gender (male or female) as the only fixed factors. When analyzing the foot forces (ratio of left to right, or total foot forces) as a function of knee angle, the fixed factors included experimental phase (2, 3, 5), gender (male or female), squat direction (ascent or descent), knee angle (15..90 degrees), and footedness (left or right dominant). Subjects, was once again the random factor in the statistical models.

“Standing Weight”

The total foot reaction force prior to beginning each set of squat exercises was expressed as a percentage of the subject’s 1-G upright body weight (Figure 40). We found that the “standing weight” 23 RPM was less than when supine with body weight resistance ($p < 0.0005$) and that 30 RPM “standing weight” was greater than when supine with body weight resistance ($p < 0.0005$). Females tended to be standing against a greater percentage of their body weight during rotation compared with males ($p = 0.008$), likely because of smaller body heights and lower centers of mass.

The foot forces when the subject was supine with body weight resistance (Phase 2) were slightly less than 1-G body weight. On average, the constant force spring assembly loaded the subjects to 93% of their body weight, which was significantly different from 100% (t-test, $p = 0.014$).

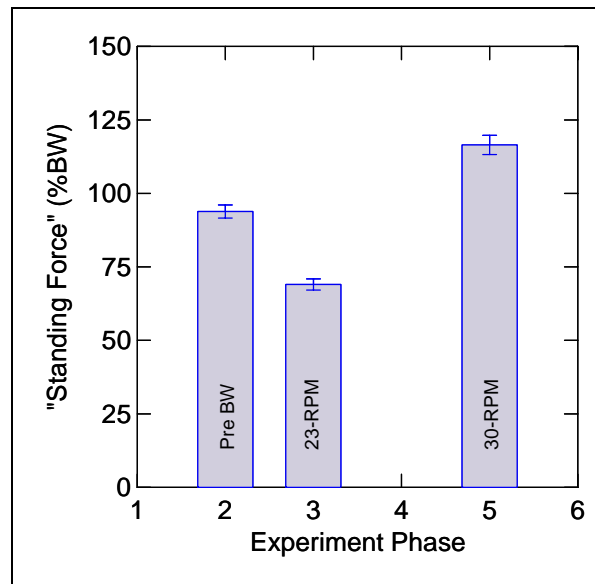


Figure 40. “Standing Weight” of the subject as a percentage of their 1-G upright weight. Phase 2 is the weight of the subjects provided by the constant force springs. Phases 3 and 5 are the artificial gravity weight of the subject plus the artificial gravity weight of the back slider. Data for all 15 subjects (all 15 for Phases 1, 2, 3 and 4, 14 of 15 for Phase 5) is shown. Mean +/- SEM.

Peak Foot Forces

The peak foot reaction forces during each repetition were also expressed as a percentage of the subject’s 1 G standing body weight. Again, we found that the peak force at 23 RPM was less than when supine with body weight resistance ($p < 0.0005$) and that the 30 RPM peak force was greater when than supine with body weight resistance ($p < 0.0005$).

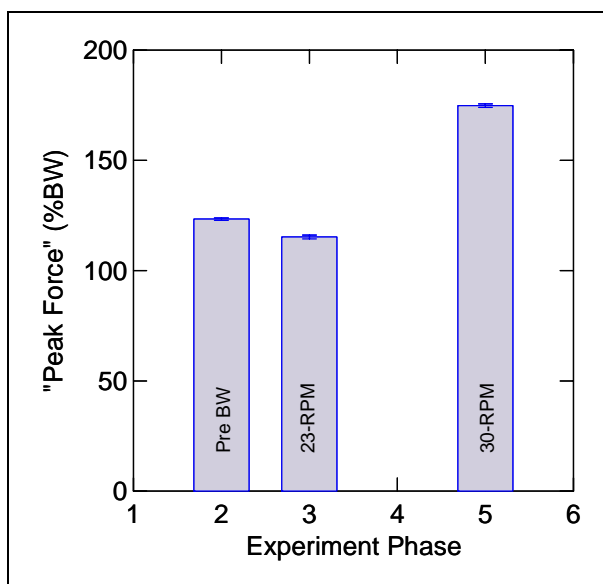


Figure 41. Average peak foot reaction force during each repetition of the squat as a percentage of each subject’s 1-G upright weight. Data for 15 subjects is shown. Mean +/- SEM.

Individual Foot Force as a Function of Knee Angle

We used the position of the knee and back-slider position potentiometer to calculate the knee angle during each repetition, and then expressed the foot force as a function of knee angle. First, let us define the convention used for reporting knee angles (Figure 42). The subject begins the squat at 0 degrees knee angle (“standing”). During the descent phase, the knee flexes and the knee angle increases until full flexion is reached. These are positive angles. Then, the knee extends and the angle begins to decrease from the maximum angle reached during descent. The angles during ascent are negative angles.

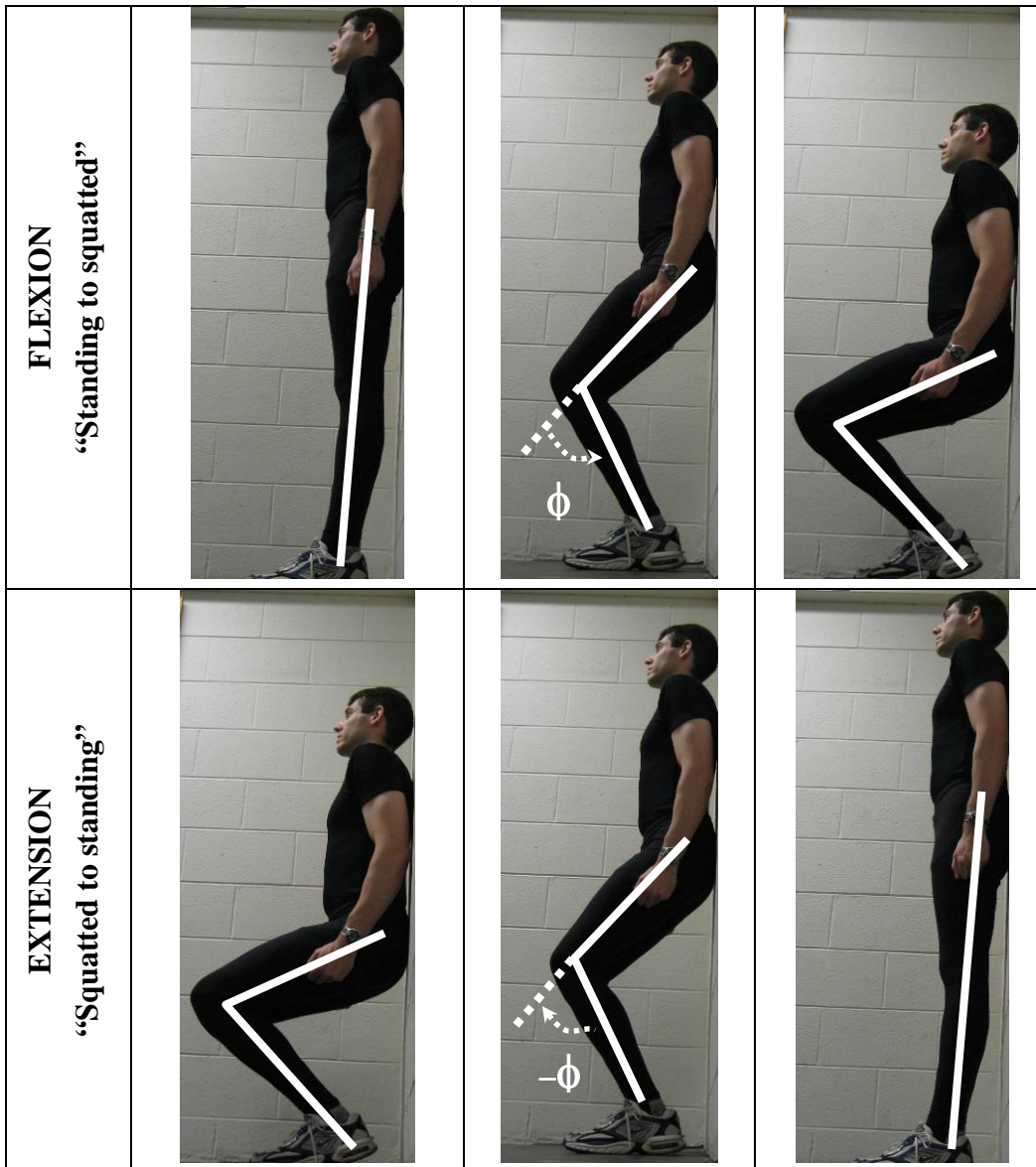


Figure 42. Definition of knee flexion and extension angles. Top: Knee flexion (positive angles, ϕ). Bottom: Knee extension (negative angles, $-\phi$).

The ratio of the left to right foot force minus one³⁴ ($\text{Left} / \text{Right} - 1$) is shown as a function of knee angle in Figure 43. The ratio is equal to zero when there is equal force on the left and right foot, greater than zero when there is more force on the left foot, and less than zero when there is more force on the right foot. The order of the knee angles in Figure 43, are such that one cycle of the squat is read from left to right. That is, the subjects starts standing upright, then descends

³⁴ One was subtracted from ratio of left force divided by right force to easily show a transition from left foot dominance to right foot dominance as a crossing of a horizontal line at zero. This ratio also offers the advantage of being a non-dimensional parameter.

in the squat (knee flexion: positive angles), reaches full flexion (90 degrees), then begins to ascend in the squat (knee extension: negative angles), and finally ends standing upright.

Across all conditions, the left to right foot force ratio is significantly greater while descending than ascending ($p < 0.0005$). The probable explanation is that during rotation as the subject descends their apparent weight increases from centripetal acceleration, which makes it more difficult and fatiguing on the right leg to ascend with a large asymmetry. We also found that, on average, females tended to put more weight on their left foot in the “weighted” conditions (Phases 2, 3, and 5), and at nearly all knee angles. It is not, e.g., the result of a single subject dominating the trend since all females exhibited this left foot dominance. Also, we cannot attribute the effect to footedness: only one female subject indicated that she was left footed.

During rotation (Phases 3 and 5), the subjects put more force on their right foot than left when ascending from full knee flexion, but put more force on the left foot when ascending without rotation (Phase * Direction). We also see that the foot force ratio during centrifugation (Phases 3 and 5) was nearly sinusoidal across knee angles, and was approximately linear without rotation and body weight resistance (Phase 2). Consequently, the magnitude of the ratio is greater at mid-flexion/extension angles than when near full extension or flexion (Phase * Knee Angle).

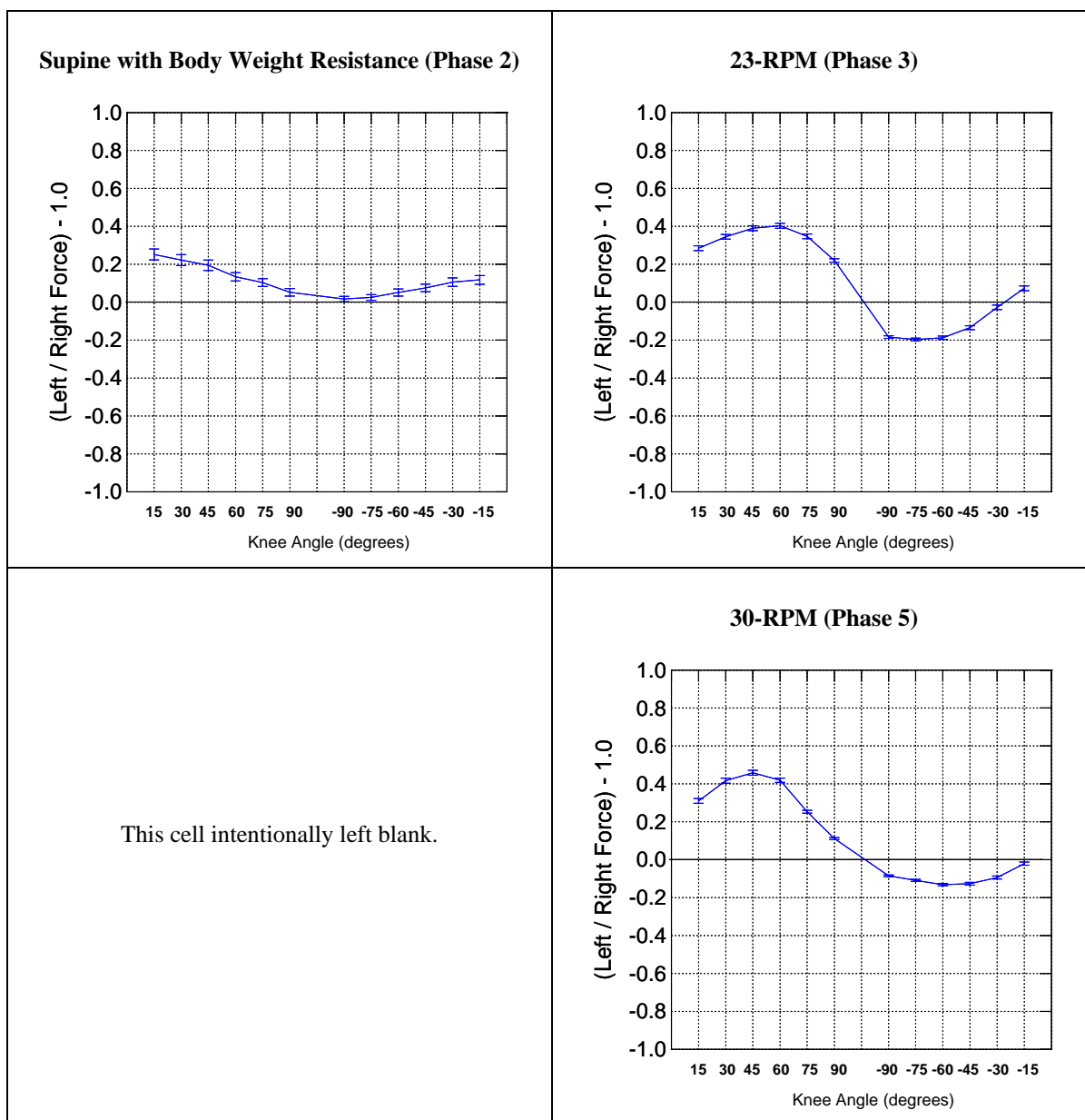


Figure 43. Ratio of left foot reaction force to right foot reaction force minus 1.0 as a function of knee angle. Left: 0-RPM, 100% body weight resistance (Phase 2), Middle: 23-RPM (Phase 3), Right: 30-RPM (Phase 5). Data for all 15 subjects is shown. Mean +/- SEM.

Figure 44 shows that set-to-set change in the magnitude of the foot force ratio vs. knee angle. Using a hierarchical mixed regression, we found a significant main effect of exercise set ($p = 0.005$) at 23 RPM (Phase 3). The asymmetry grows during the descent phase (knee flexion), but is little changed during the ascent. However, this is not the case for the 30 RPM squats.

Although there is also a main effect of exercise set ($p < 0.0005$), the asymmetry grows during the descent and shrinks during the ascent.

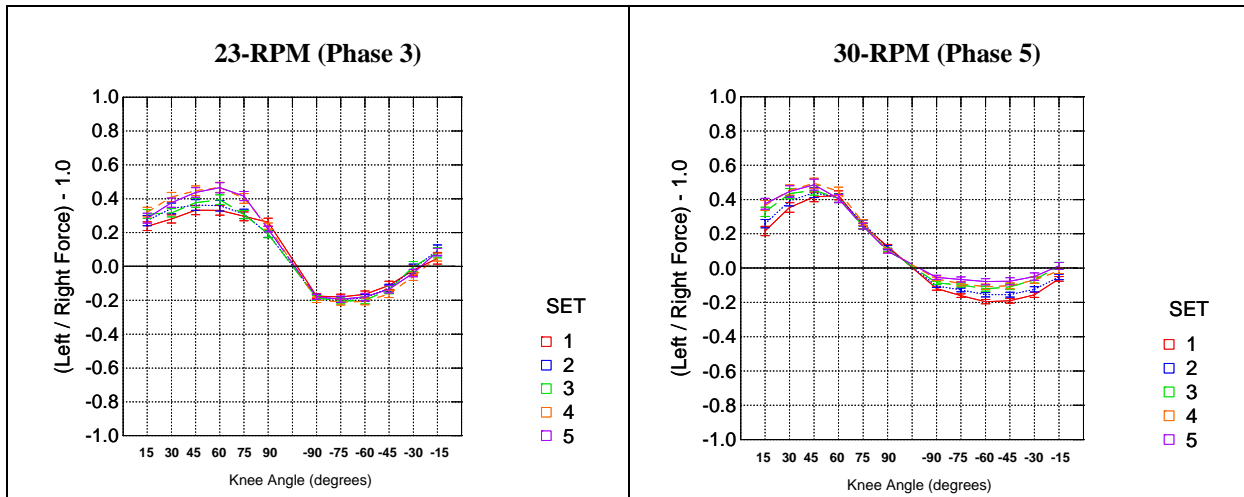


Figure 44. Ratio of left to right foot force minus 1.0 for the 23-RPM (left) and 30-RPM (right) squat conditions. Each of the five sets is plotted individually. Data from 14 of the 15 subjects is shown. Mean \pm SEM.

Total Foot Force as a Function of Knee Angle

We also expressed the sum of the left and right foot forces as a function of knee angle. In Figure 45, we plot the total foot reaction force, expressed as a percentage of 1 G upright body weight, at each knee angle. Immediately, no rotation condition with body weight resistance (Phase 2), we see an asymmetry between ascent and descent. As expected, we see a reduced foot reaction force during descent and an increased foot reaction force during ascent due to the inertial acceleration of the body. This is something that we do not see during centrifugation when exercising at the same cadence. The foot forces during rotation (Phases 3 and 5) show a striking symmetry about full knee extension (0 degree knee angle).

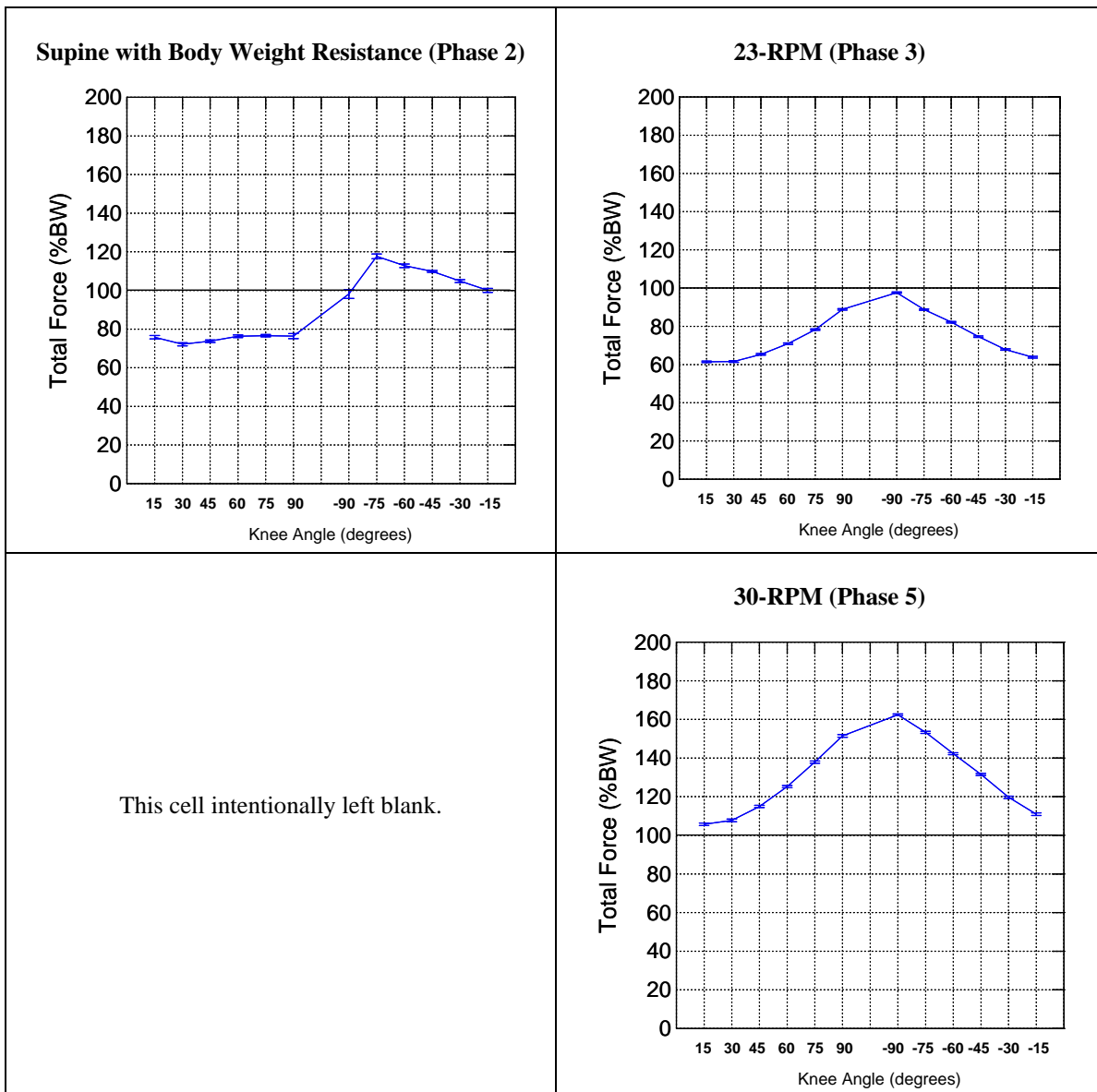


Figure 45. Total foot reaction force (sum of left and right leg) during each repetition expressed as a percentage of the subject’s 1-G upright body weight. Left: 0-RPM, 100% body weight resistance (Phase 2), Middle: 23-RPM (Phase 3), Right: 30-RPM (Phase 5). Mean +/- SEM for 14 subjects is shown.

The total foot force, across all knee angles, was greater at 30 RPM (Phase 5) compared with either no centrifugation with body weight resistance (Phase 2) or 23 RPM (Phase 3) ($p = 0.019$). The no-rotation condition with body weight resistance (Phase 2) was not significantly different from 23-RPM (Phase 3). We also found the foot reaction forces to be greater during knee extension (ascent) than during descent ($p < 0.0005$). During ascent, the body’s inertial and centripetal accelerations add, but during descent they tend to cancel. The qualitative difference between the body weight resistance (approximately sinusoidal, Phase 2) and the centrifuge

(approximately parabolic, Phases 3 and 5) indicates that the effect of exercising in an environment with a gravity gradient.

Surface Electromyography

We used surface electromyography (EMG) to record the muscle activity in seven muscles of the left and right leg. These muscles were the soleus, medial and lateral gastrocnemius, tibialis anterior, vastus medialis and lateralis, and rectus femoris. The anatomical location and function of each muscle as well as the surface electrode placement is described in the Methods section.

The EMG data was normalized to the recordings collected during the series of maximum voluntary isometric contractions (MVIC). We first rectified the raw EMG, and then used a 500 ms moving average window to reduce the data. The reference maximum voltage during the maximum contractions was then taken as the mean amplitude of the highest signal portion with 500 ms duration [112].

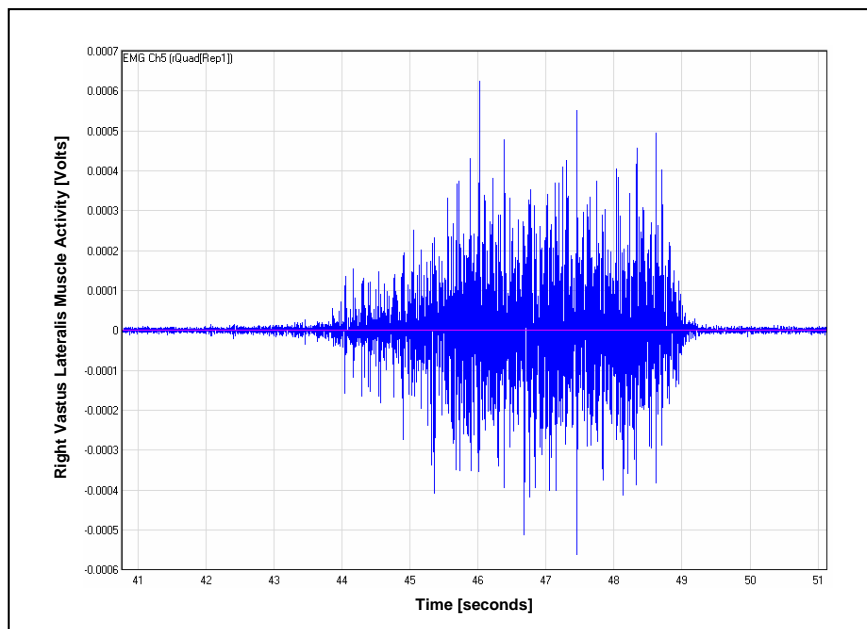


Figure 46. Raw EMG of the right vastus lateralis during MVIC testing. Muscle activity [Volts] is shown as a function of time [seconds].

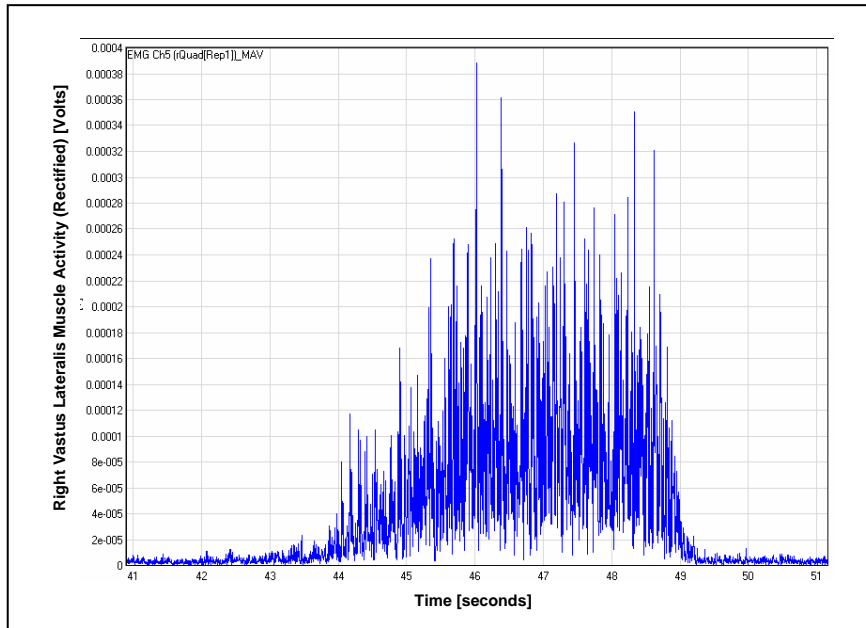


Figure 47. Rectified EMG of the right vastus lateralis during MVIC testing (i.e., rectified signal from Figure 46). Muscle activity [Volts] is shown as a function of time [seconds].

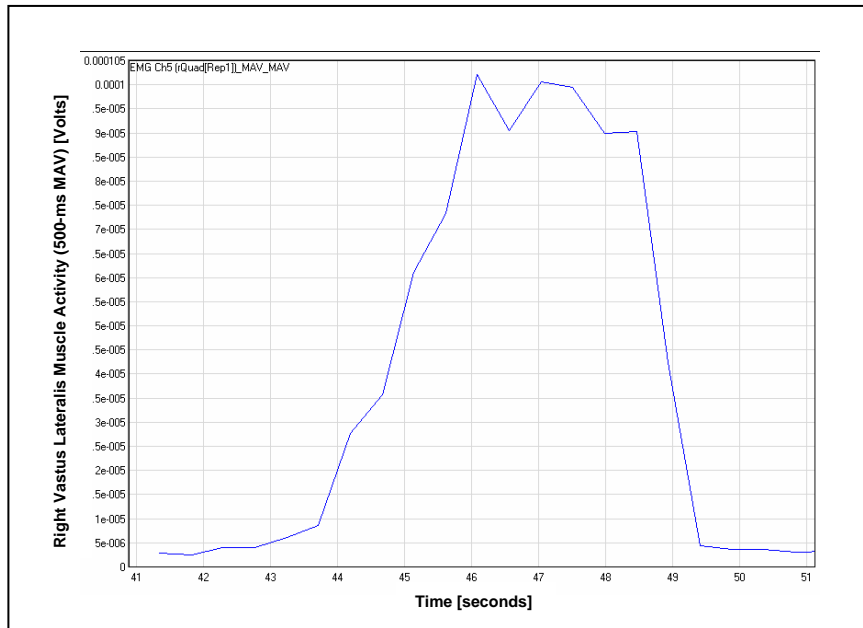


Figure 48. 500-ms moving average (250-ms overlap) of the rectified EMG of the right vastus lateralis during MVIC testing (i.e., moving average of data in Figure 47). Muscle activity [Volts] is shown as a function of time [seconds].

We then divided the rectified raw EMG signal recorded during the experimentation by the reference maximum obtained during MVIC testing. This normalized the recording and allowed

us to express the data as a percentage of the MVIC (%MVIC)³⁵. The %MVIC EMG was then combined with the knee and back-slider position data to obtain the %MVIC as a function of knee angle (Figure 49). The %MVIC was then extracted at 0.5 degrees leading and lagging each of the knee angles of interest (15, 30, 45, 60, 75, 90 degrees flexion and extension). For example, at 60 degrees knee flexion, we extracted the %MVIC between 59.5 and 60.5 degrees. This extracted data was then averaged over that 1 degree window and reported as the %MVIC at that particular knee angle.

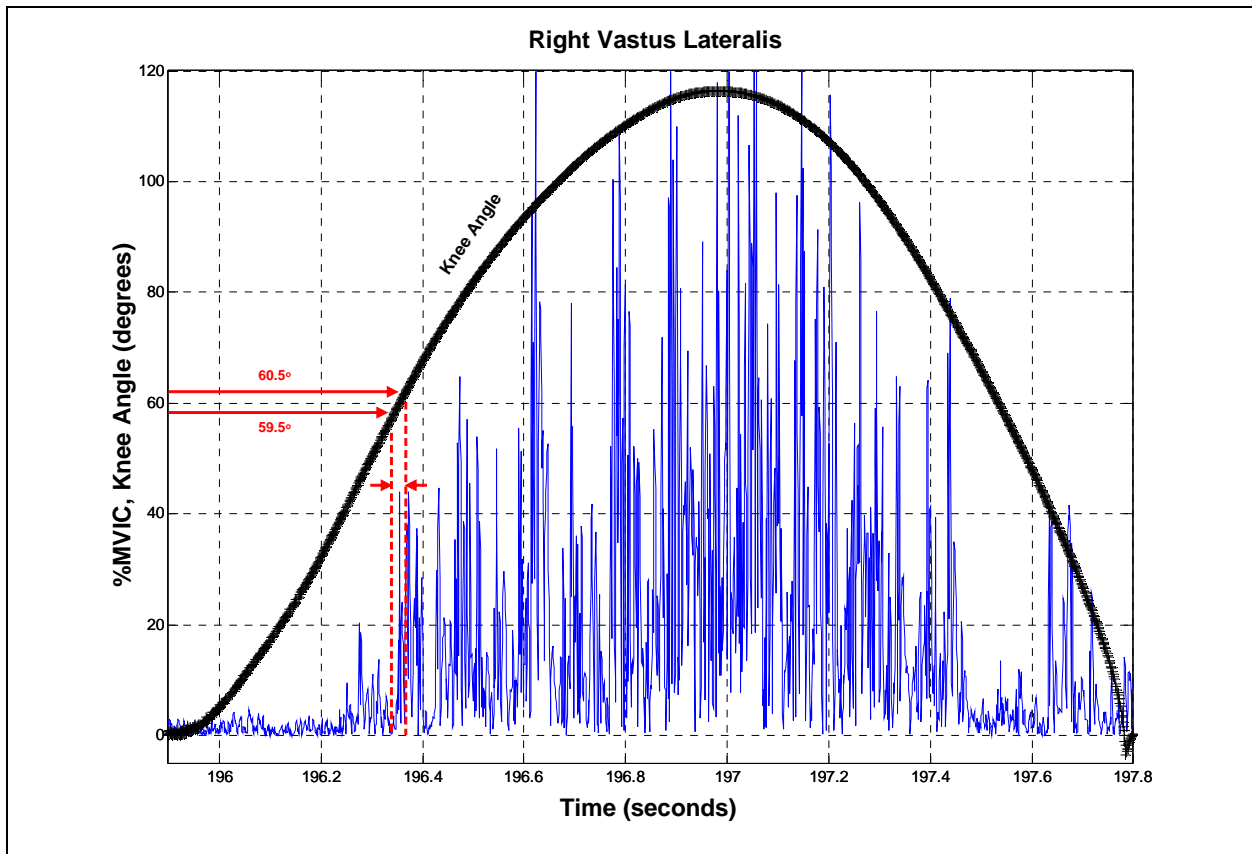


Figure 49. Percentage of maximum voluntary isometric contraction (%MVIC) with the Knee Angle (degrees) overlaid versus time (seconds). The 1 degree window over which the %MVIC data is averaged is shown (e.g., 60 degrees knee angle)

³⁵ Throughout the experimentation, there were several instances (less than 1% of the data) when the electrodes were recording erroneously during the experiment. The accuracy of the recording was particularly sensitive to the contact between the electrode and the skin. When the electrode and skin became separated, a significant amount of noise was introduced. These cases were identified and not included in the analysis.

The analysis of the EMG data in Experiment 1 is aimed at investigating the ascent/descent asymmetry in the ratio of the left to right leg, for each of the muscle groups. The analysis of the individual muscle activity across conditions is reserved for Experiment 2.

In several of the muscle groups (soleus, vastus medialis, and vastus lateralis), we see a trend in the ratio of left to right muscle activity similar to that seen with the foot reaction forces (Figure 50 thru Figure 56). This trend, however, is not seen in all of the muscle groups. We conducted a Hierarchical Mixed Regression (HMR) on the left to right leg EMG ratio minus one for each of the muscle groups. During rotation, the muscle activity was averaged over each of the five sets, since there was no apparent difference between the sets. This reduction in the data set made it possible to run the statistical models on the left to right leg muscle activity ratio. In all of the muscle groups, the muscle activity tended to increase with knee angle ($p < 0.016$), and there was no difference between males and females or whether the subject was left or right foot dominant. In the following muscle-by-muscle analyses, we discuss the significance of rotation rate (supine with body weight resistance, 23 RPM, or 30 RPM) and squat direction (ascent or descent).

Soleus

During centrifugation, we see that the ratio of left to right leg muscle activity shows an asymmetry similar to the left to right foot force ratio (Figure 50). That is, there is significantly more activity in the left leg during squat descent and more activity in the right leg during squat ascent ($p = 0.023$). We found that, on average, the ratio during centrifugation (23- or 30 RPM) was greater than without rotation and supine with body weight resistance ($p < 0.0005$) (Phase 2). There was not a difference between 23- and 30 RPM.

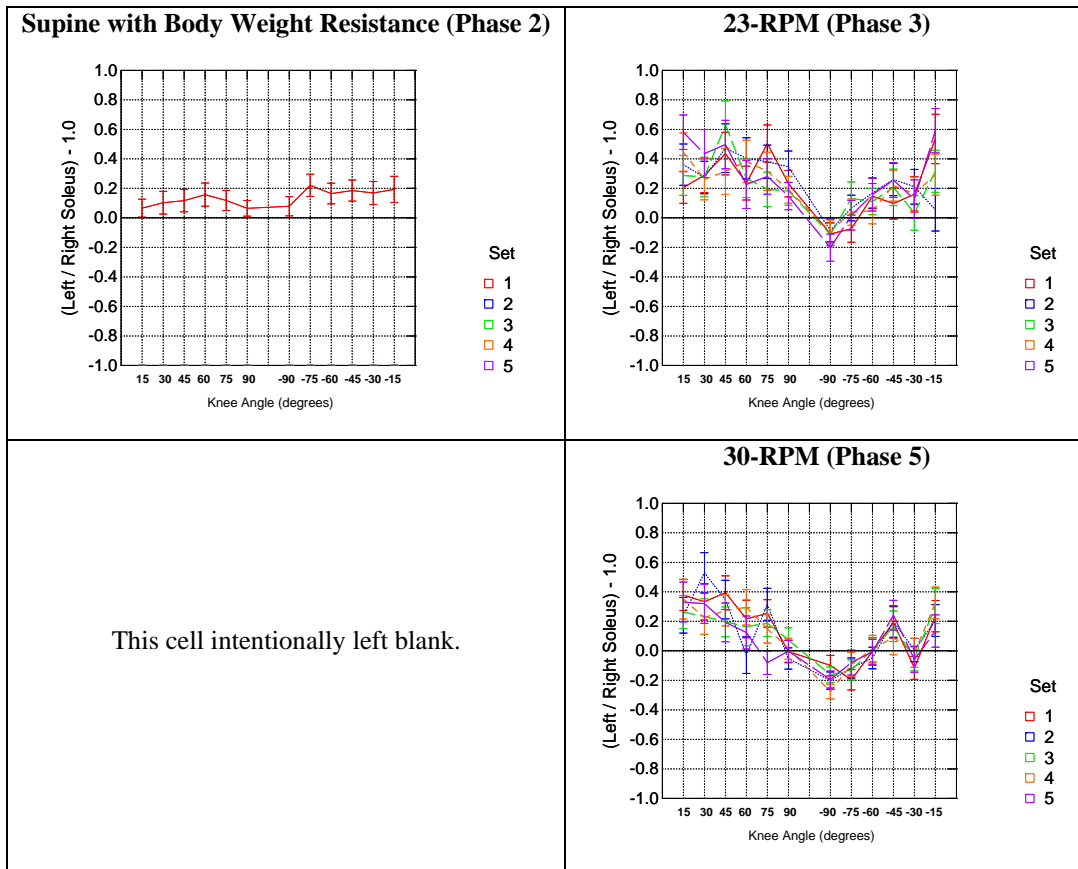


Figure 50. Soleus muscle activity. Values are presented as a ratio of the left soleus %MVIC at each knee angle divided by right soleus %MVIC minus one. Data for all 15 subjects is shown. Mean +/- SEM.

Lateral Gastrocnemius

During centrifugation, we see an asymmetry in the ratio of the left to right leg muscle activity as a function of knee angle (Figure 51). That is, that the muscle activity ratio is greater during ascent than descent ($p = 0.0001$). On average, the ratio during the supine squats with body weight resistance (Phase 2) is not significantly different from 23 RPM (Phase 3). However, subjects tend to put more force on their left leg during 30 RPM (Phase 5) than the other two conditions ($p = 0.002$).

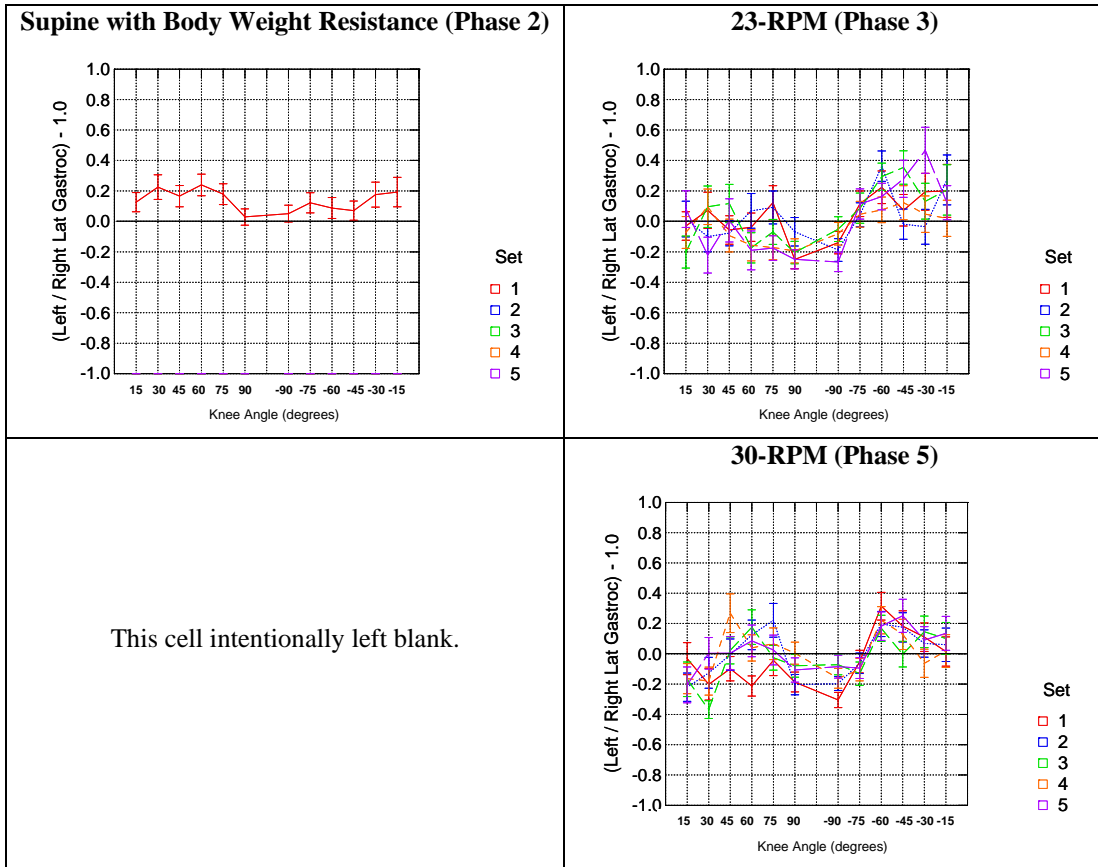


Figure 51. Lateral gastrocnemius muscle activity. Values are presented as a ratio of the left lateral gastrocnemius %MVIC at each knee angle divided by right lateral gastrocnemius %MVIC minus one. Data for all 15 subjects is shown. Mean +/- SEM.

Medial Gastrocnemius

The medial gastrocnemius shows an interesting trend of near consistent dominance of the right leg during centrifugation (Figure 52). In this muscle, the ratio of left to right leg muscle activity was slightly greater during ascent than descent ($p = 0.004$). There was no difference between supine with body weight resistance (Phase 2) or centrifugation (23- or 30 RPM) (Phase 3 or 5).

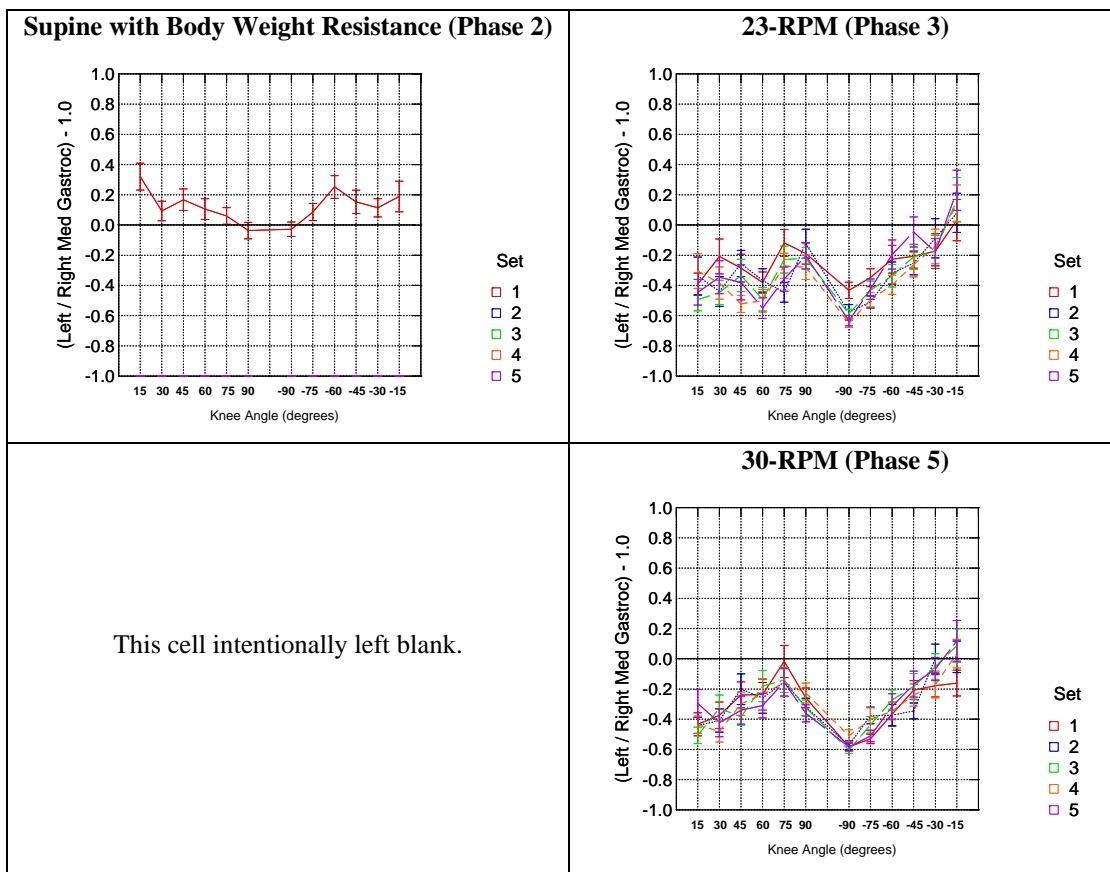


Figure 52. Medial gastrocnemius muscle activity. Values are presented as a ratio of the left medial gastrocnemius %MVIC at each knee angle divided by right medial gastrocnemius %MVIC minus one. Data for all 15 subjects is shown. Mean +/- SEM.

Tibialis Anterior

Upon first inspection, we see no obvious trends in the left to right leg muscle activity across conditions (Figure 53). Our analysis, however, revealed that the ratio was greater during knee flexion (descent) than during knee extension (ascent) ($p = 0.002$). There was no significant difference between the body weight supine squats (Phase 2) and centrifugation (Phase 3 or 5).

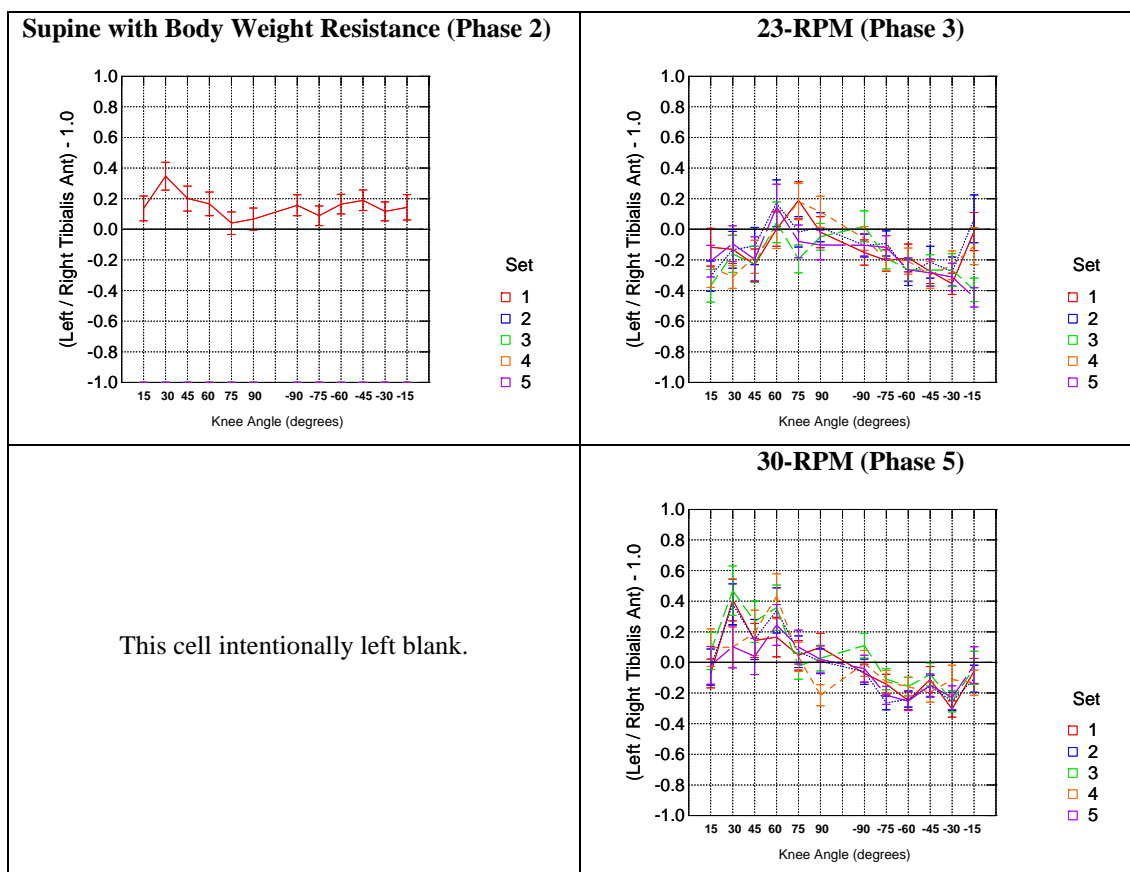


Figure 53. Tibialis anterior muscle activity. Values are presented as a ratio of the left tibialis anterior %MVIC at each knee angle divided by right tibialis anterior %MVIC minus one. Data for all 15 subjects is shown. Mean +/- SEM.

Vastus Lateralis

The ratio of left to right leg activity shows a prominent asymmetry similar to the foot reaction force ratio (Figure 54). We found that the ratio during descent was greater than ascent ($p < 0.0005$), and this ratio was greater during centrifugation (23- and 30 RPM) than without centrifugation and body weight resistance (Phase 2) ($p < 0.0005$). There was no significant difference between 23- and 30 RPM.

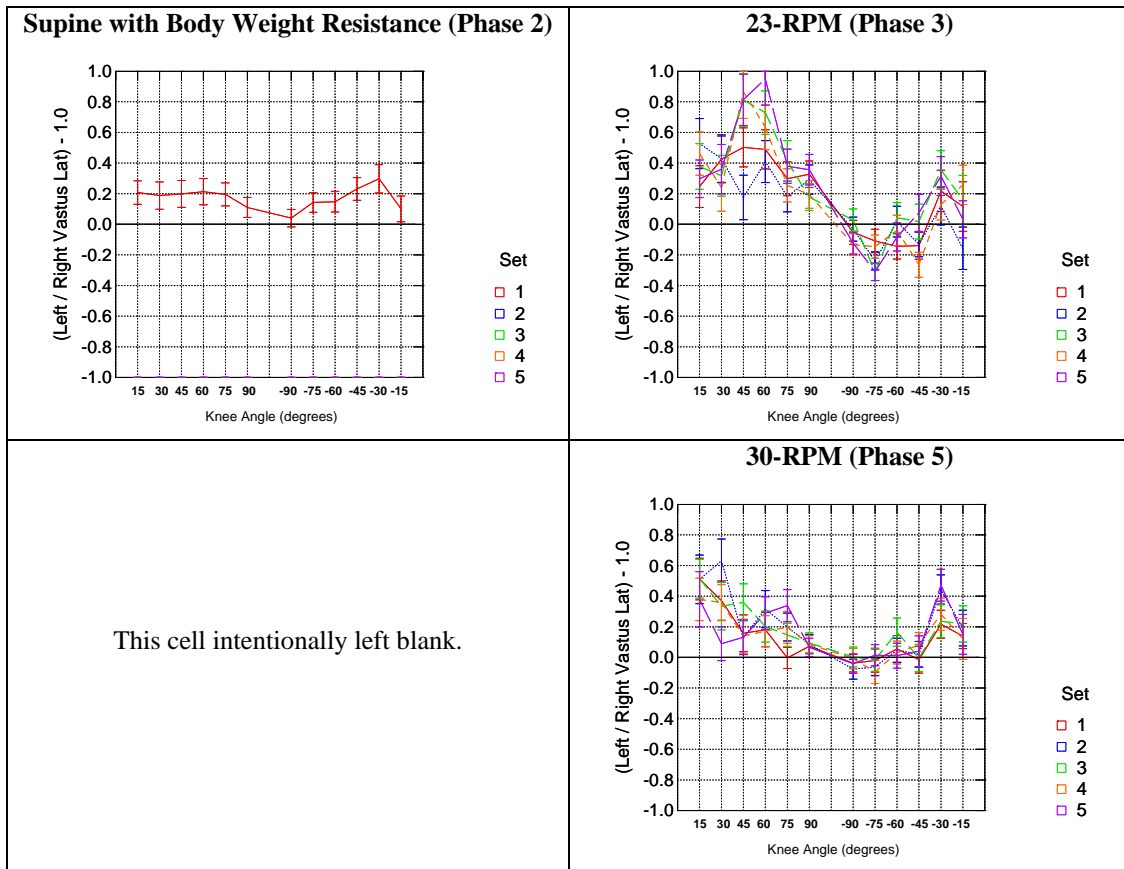


Figure 54. Vastus lateralalis muscle activity. Values are presented as a ratio of the left vastus lateralalis %MVIC at each knee angle divided by right vastus lateralalis %MVIC minus one. Data for all 15 subjects is shown. Mean +/- SEM.

Vastus Medialis

The vastus medialis also shows the left to right leg muscle activity ratio asymmetry between knee flexion and extension during the squat (Figure 55). Again, we found that the ratio was greater during knee flexion than extension ($p < 0.0005$). 23 or 30 RPM centrifugation led to a generally greater ratio than while lying supine and squatting against body weight resistance (Phase 2). There was no difference between the two rotation rates.

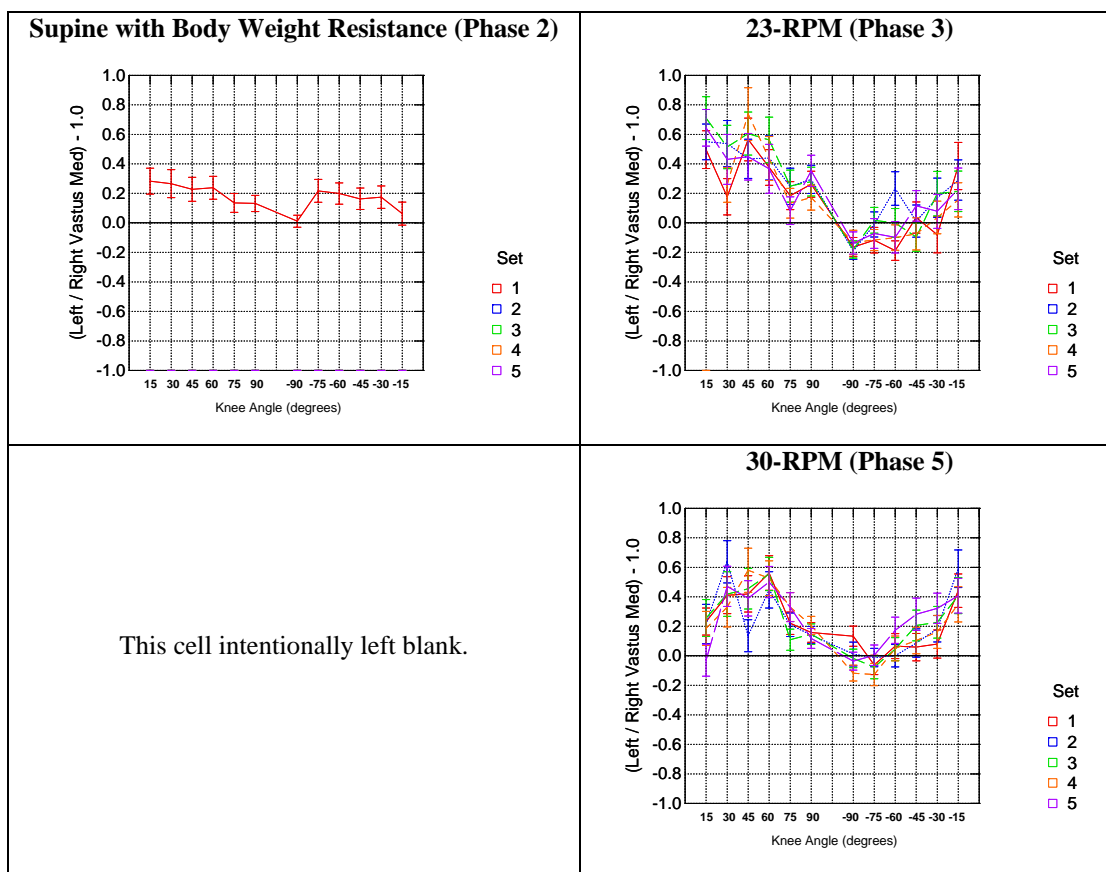


Figure 55. Vastus medialis muscle activity. Values are presented as a ratio of the left vastus medialis %MVIC at each knee angle divided by right vastus medialis %MVIC minus one. Data for all 15 subjects is shown. Mean +/- SEM.

Rectus Femoris

Upon first inspection, the rectus femoris does not show a left to right leg muscle activity ratio asymmetry as a function of knee angle (Figure 56). However, the statistics revealed a trend that is opposite to that exhibited by the foot force ratio: greater during ascent than descent ($p < 0.0005$). Additionally, we found that, on average, the ratio was the smallest when supine with body weight resistance (Phase 2), slightly greater at 23 RPM ($p < 0.0005$), and still greater at 30 RPM ($p < 0.0005$).

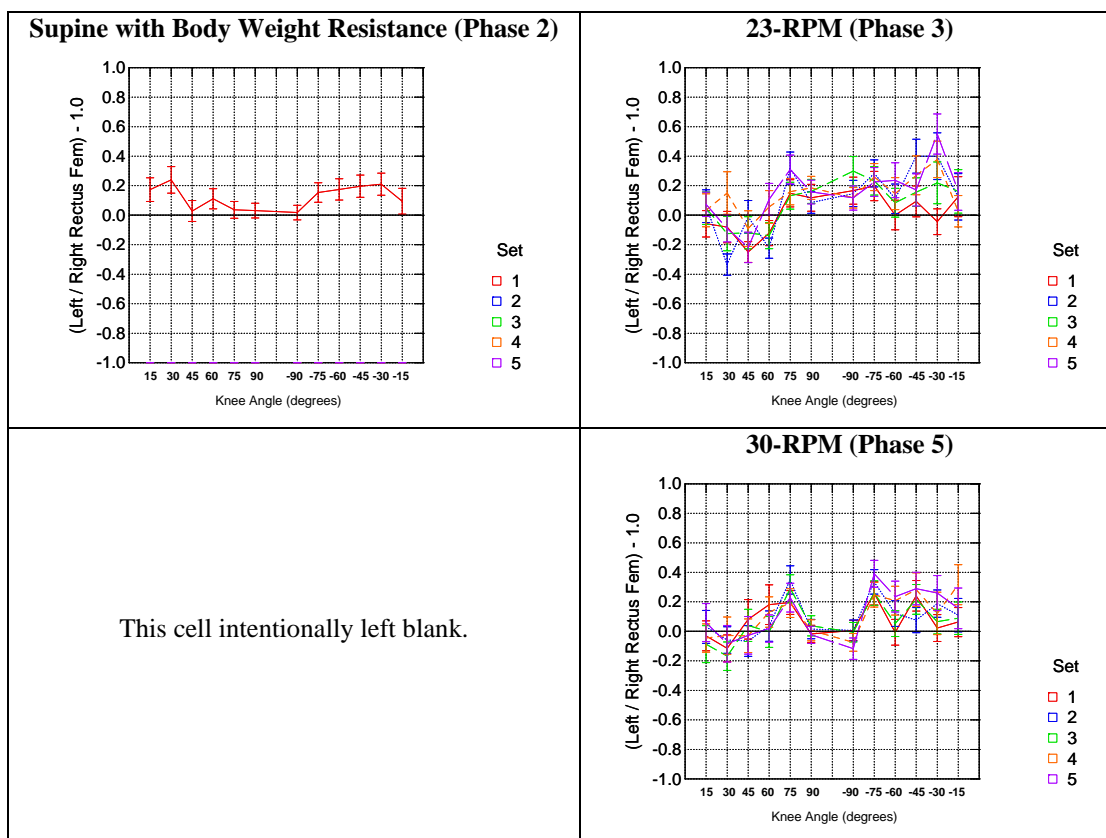


Figure 56. Rectus femoris muscle activity. Values are presented as a ratio of the left rectus femoris %MVIC at each knee angle divided by right rectus femoris %MVIC minus one. Data for all 15 subjects is shown. Mean +/- SEM.

Motion Sickness

We asked the subjects to report their level of motion sickness (MS) on the 0-20 scale after each set. Figure 57 shows a histogram of the motion sickness reports at each rotation rate. The greatest motion sickness report in this experiment was 5 out of 20, which occurred once during the 30 RPM squats (Phase 5). No motion sickness was reported before or after rotation (Phases 1, 2, 4, or 6). A Kruskal-Wallis nonparametric test was used to analyze the motion sickness reports. We found that the MS was greater during the 23-RPM squats (Phase 3) than before rotation (Phase 2, $p = 0.012$), and the 30 RPM squats (Phase 5) produced greater MS reports than the 23 RPM squats (Phase 3, $p = 0.004$).

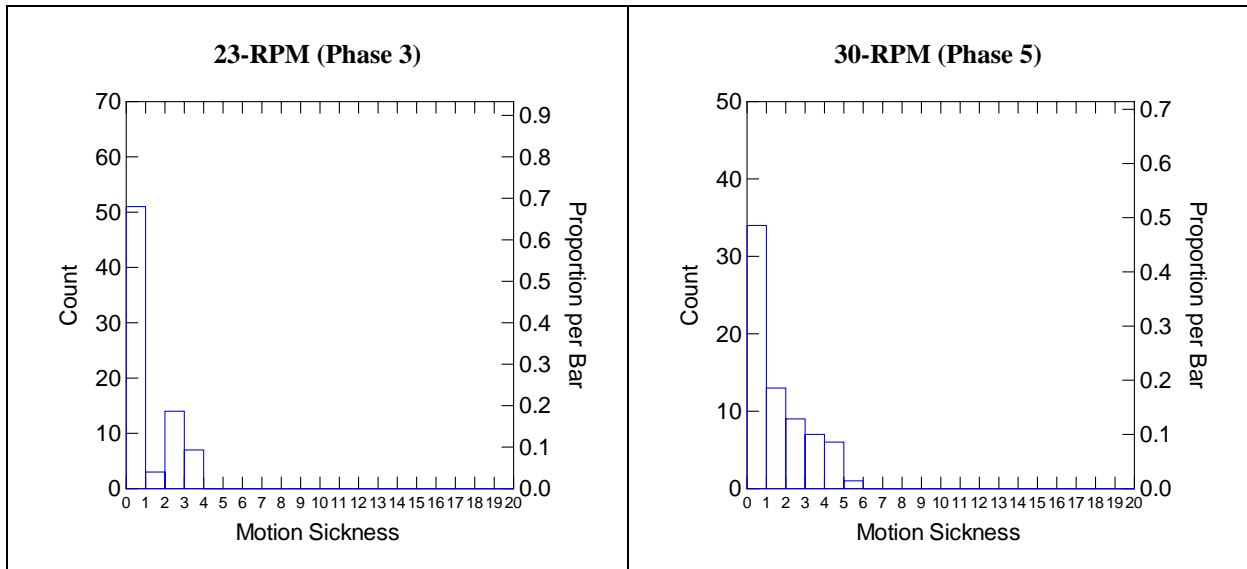


Figure 57. Histogram of subjective reports of motion sickness. Left: 23 RPM (Phase 3). Right: 30 RPM (Phase 5).

Tabulation of Experiment 1 Statistical Results

In this section, we tabulate the dependent and independent variables in our statistical analyses. These analyses summarize the statistical claims in the presentation of Experiment 1 results. Significant and non-significant results are listed. The statistically significant results have the p-values highlighted.

Table 7. Statistical analyses results for Experiment 1: Knee Kinematics and Foot Forces. [p < 0.05]

Dependent variable	Independent Variable	Parameter	DOF	Value	p-Value
Maximum M-L knee travel	Phase (1..6)	F	5, 60	4.701	0.001
	Gender (Male, Female)	F	1, 12	0.520	0.485
	Leg (Left, Right)	F	1, 12	0.769	0.398
Standing weight	Phase (2, 3, 5)	F	2, 24	125.8	< 0.0005
	Gender (Male, Female)	F	1, 12	10.14	0.008
	Phase * Gender	F	2, 24	6.039	0.008
Peak foot forces	Phase (2, 3, 5)	F	2, 26	435.4	< 0.0005
	Gender (Male, Female)	F	1, 12	0.01	0.976
	Repetition (1..8)	F	7, 84	12.31	< 0.0005
Individual foot forces as a function of knee angle	Phase (2, 3, 5)	F	2, 22	0.054	0.948
	Gender (Male, Female)	F	1, 11	11.64	0.005
	Squat direction (Ascent, Descent)	F	1,12	37.52	< 0.0005
	Knee Angle (15..90)	F	5, 60	4.75	0.001
	Footedness (L, R dominant foot)	F	1, 11	0.002	0.965
	Repetition (1..8)	F	7, 77	1.379	0.226
	Phase * Knee Angle	F	22,264	4.39	< 0.0005
Phase * Direction	F	2, 24	13.45	< 0.0005	
Total foot forces as a function of knee angle	Phase (2, 3, 5)	F	2, 22	4.795	0.019
	Gender (Male, Female)	F	1, 11	2.755	0.125
	Squat direction (Ascent, Descent)	F	1,11	53.12	< 0.0005
	Knee Angle (15..90)	F	5, 55	4.79	0.001
	Footedness (L, R dominant foot)	F	1, 11	3.617	0.084
	Phase * Direction	F	2, 22	22.746	< 0.0005
	Phase * Knee Angle	F	10, 110	2.481	0.010

Table 8. Statistical analyses results for Experiment 1: Muscle Activity. [$p < 0.05$]

Muscle Group	Independent Variable	Regression Type	p-Value
Soleus	Phase (2, 3, 5)	HMR	< 0.0005
	Squat Direction	HMR	0.023
	Knee Angle	HMR	< 0.0005
	Gender	HMR	0.057
	Footedness	HMR	0.876
Lateral Gastrocnemius	Phase (2, 3, 5)	HMR	0.008
	Squat Direction	HMR	0.001
	Knee Angle	HMR	< 0.0005
	Gender	HMR	0.170
	Footedness	HMR	0.525
Medial Gastrocnemius	Phase (2, 3, 5)	HMR	0.583
	Squat Direction	HMR	0.004
	Knee Angle	HMR	< 0.0005
	Gender	HMR	0.769
	Footedness	HMR	0.658
Tibialis Anterior	Phase (2, 3, 5)	HMR	0.525
	Squat Direction	HMR	0.002
	Knee Angle	HMR	0.016
	Gender	HMR	0.988
	Footedness	HMR	0.080
Vastus Lateralis	Phase (2, 3, 5)	HMR	< 0.0005
	Squat Direction	HMR	< 0.0005
	Knee Angle	HMR	< 0.0005
	Gender	HMR	0.204
	Footedness	HMR	1.000
Vastus Medialis	Phase (2, 3, 5)	HMR	< 0.0005
	Squat Direction	HMR	< 0.0005
	Knee Angle	HMR	< 0.0005
	Gender	HMR	0.591
	Footedness	HMR	0.729
Rectus Femoris	Phase (2, 3, 5)	HMR	< 0.0005
	Squat Direction	HMR	< 0.0005
	Knee Angle	HMR	< 0.0005
	Gender	HMR	0.395
	Footedness	HMR	0.795

Experiment 2

The aim of Experiment 2 was to define a set of centrifuge-based resistance exercise parameters (resistance, rotation rate) that gave similar biomechanical results to upright exercises. We tested a total of 13 subjects (9 male, 4 female) between the ages of 19 and 30 years. All subjects completed the experiment. We were not able to accurately reconstruct the upright knee position data for Subject 4 due to errors in the calibration. Therefore, we do not have synchronized foot forces, EMG, or knee position data for this subject when exercising upright. As in Experiment 1, instances where the EMG signal was deemed noisy and erroneous were not considered for analysis. Tabulation of the statistical results of Experiment 2 is at the end of this section (Table 11 and Table 12).

Leg Kinematics

We used the same motion capture equipment to record the left and right lateral tibial condyle position during the upright and centrifuge supine squats. This data was used primarily to determine how adding resistance to the squat exercise during centrifugation affects the Coriolis-induced medial and lateral perturbations of the knees. The same parameter as in Experiment 1 was analyzed: maximum total mediolateral travel of the left and right knee. We also analyzed the repeated measures data using an ANOVA. The fixed effects in the model were the rotation rate (upright, 23 RPM, 30 RPM), leg (left or right), group (A or B), gender (male or female), experience (experienced or naïve), and resistance (0, 10, or 25% body weight). Subjects were the blocking factor, and considered a random factor in this model.

Maximum Total Medial-Lateral Travel

Figure 58 shows the maximum medial-lateral travel of the legs (averaged together) during the upright and centrifugation portions of the experiment (nine of the fourteen experimental phases). We analyzed the data using a repeated measures ANOVA. As we hypothesized, the total mediolateral travel of the knees was greater during centrifugation (Upright < 23- or 30 RPM, $p < 0.020$), but increasing the rotation rate did not increase the medial-lateral travel (23 v. 30 RPM, $p = 0.237$). Within each set, the knee travel increased with repetition ($p = 0.007$). This could be an early indication of fatigue, similar to what we saw during the 30 RPM squats in Experiment 1.

We hypothesized that the additional resistance during centrifugation would reduce the magnitude of the mediolateral knee travel. However, there was no evidence of a reduction in knee travel with resistance. We did find a significant interaction between the rotation rate and resistance, which would support our hypothesis, but this effect is dominated by a single condition. At 30-RPM and 25% body weight resistance (Phase Index 13), the knee travel was greater than any of the other resistance and rotation rate conditions (seen in Figure 58).

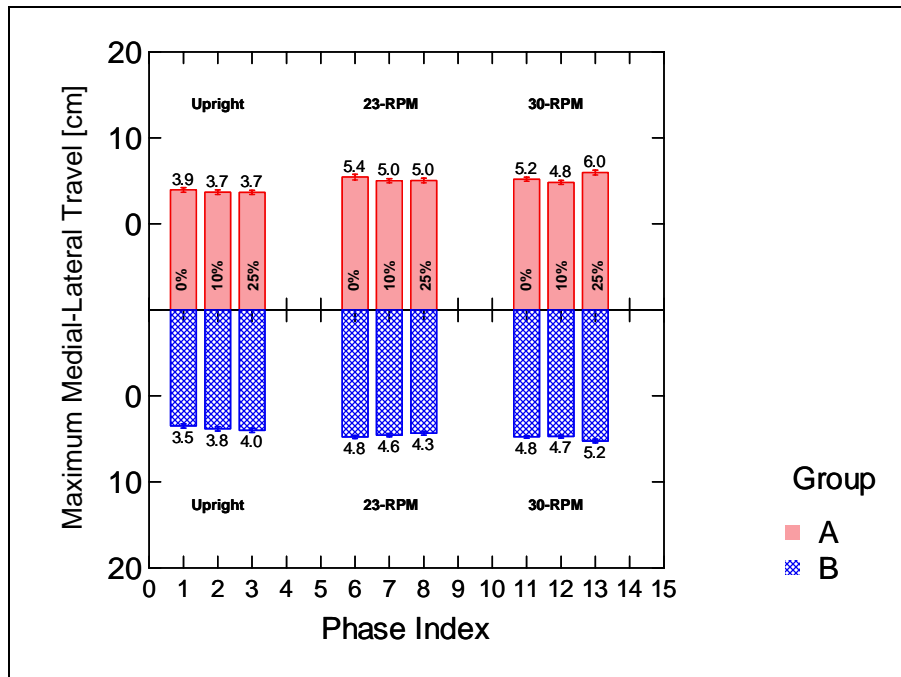


Figure 58. Maximum total mediolateral travel of the knees. Group A deflections are shown sequentially in the Phase Index. Group B phases are re-arranged so that they are plotted against the similar experimental conditions in Group A. Within each cluster of three Phases, the additional resistance is zero (left bar), 10% body weight (middle bar), and 25% body weight (right bar). Data from 12 (8 male, 2 female) of the 13 subjects is shown. Mean +/- SEM.

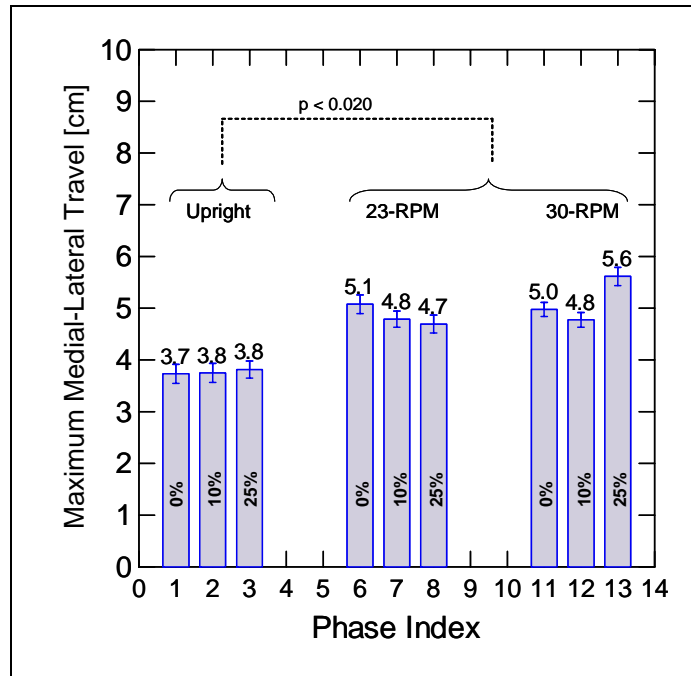


Figure 59. Maximum total mediolateral deflection of the knee as a function of upright and centrifuge supine conditions. Data from 12 (8 male, 2 female) of the 13 subjects is shown. Mean +/- SEM.

Upright vs. Supine Squats

Under the aims of Experiment 2, we were interested in any fundamental differences between the upright and supine exercise conditions under similar resistive loads. Therefore, we compared the upright condition without any additional resistance (Phase 1) with the supine condition with body weight resistance (Phase 5) in order to identify any differences in the leg kinematics (Figure 60). We found the maximum mediolateral knee travel was slightly greater while supine than upright (t-test, $p = 0.036$).

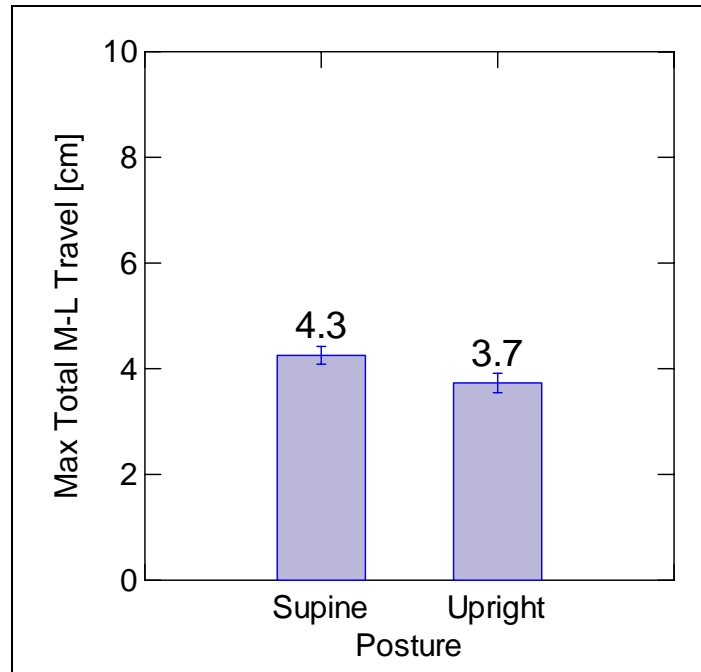


Figure 60. Postural effect on the maximum total mediolateral deflection of the knees. Two postures: Upright (0% body weight additional resistance – Phase 1) and Supine (100% body weight resistance – Phase 5). Left and right legs combined. Data shows 12 of the 13 subjects. Mean +/- SEM.

After Effects

Even though we found no evidence of significant kinematic after-effects in Experiment 1, we still looked for an effect in Experiment 2 because of the different experimental conditions between pre- and post-rotatory testing. A t-test found no significant difference in the maximum mediolateral travel between pre- and post 23 RPM squat motions ($p = 0.220$), nor was there a significant difference between pre- and post 30 RPM ($p = 0.578$) (Figure 61).

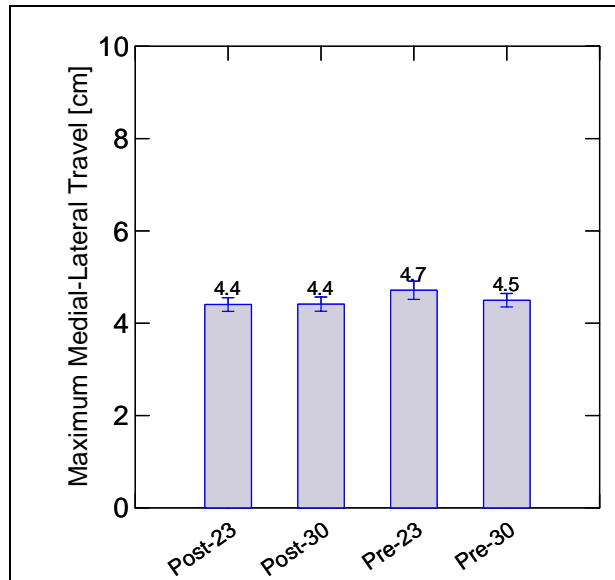


Figure 61. Maximum total medial-lateral deflection of the knee during the pre- and post-centrifugation trials. Eight repetitions while lying supine without any additional resistance were averaged together. Data from all 13 subjects is shown. Mean +/- SEM.

Foot Reaction Forces

Foot reaction forces were measured the same way as in Experiment 1, in one dimension perpendicular to the foot plate. In the following analyses, we only considered the cases where the subject was exercising upright or when the centrifuge was rotating (i.e., Phases 1, 2, 3, 6, 7, 8, 11, 12, and 13). Data from twelve of the thirteen subjects was analyzed since we did not have synchronized foot force data for Subject 4. Similar to Experiment 1, the “standing weight,” peak foot forces, and knee-angle-specific foot forces (ratio of left to right or total foot forces) were analyzed with a repeated measures ANOVA. For the standing weight and peak force analysis, the fixed factors include rotation rate (upright, 23 RPM, 30 RPM), gender (male or female), group (A or B), and resistance (0, 10, 25% body weight). In the knee-angle-specific analysis, the fixed factors are the same as the previous list with squat direction (ascent, descent), and knee angle (15..90 degrees) added. Subject was the blocking factor and was considered a random variable.

“Standing Weight”

The foot reaction force of the subject prior to beginning each set of squat exercises was expressed as a percentage of the subject’s 1-G upright body weight (Figure 62). Not surprisingly, we found that the force of the subject against the foot plates increased with

resistance ($p < 0.0005$). The “standing weight” of the subject was the least at 23 RPM, and we did not find any difference between Upright and 23 RPM. We also found a significant interaction between the rotation rate and gender. During 23 and 30 RPM centrifugation, the females tended to have higher “standing weights” than the males. It should be noted that the standing weight in the Upright, 0% resistance condition is slightly greater than 100% (Figure 62 and Figure 63). This is the result of the upright back-slider not being perfectly counterbalanced. Therefore, the subject had to carry a small fraction of the weight of the upright backslider when exercising.

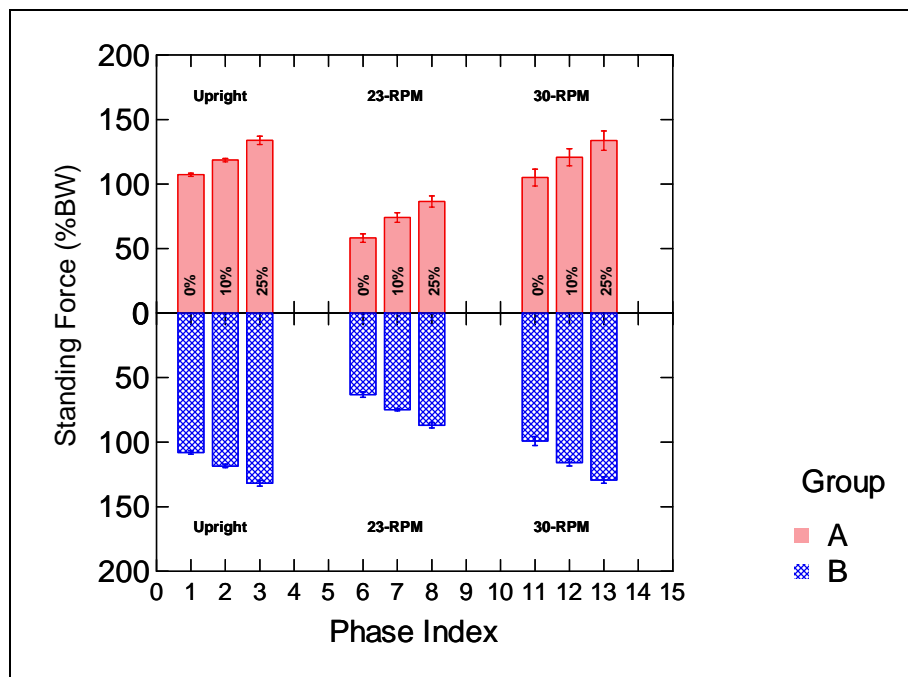


Figure 62. "Standing Weight" of the subject as a percentage of their 1-G upright weight. Group A deflections are shown sequentially in the Phase Index. Group B phases are re-arranged so that they are plotted against the similar experimental conditions in Group A. Data for 12 of the 13 subjects. Mean +/- SEM.

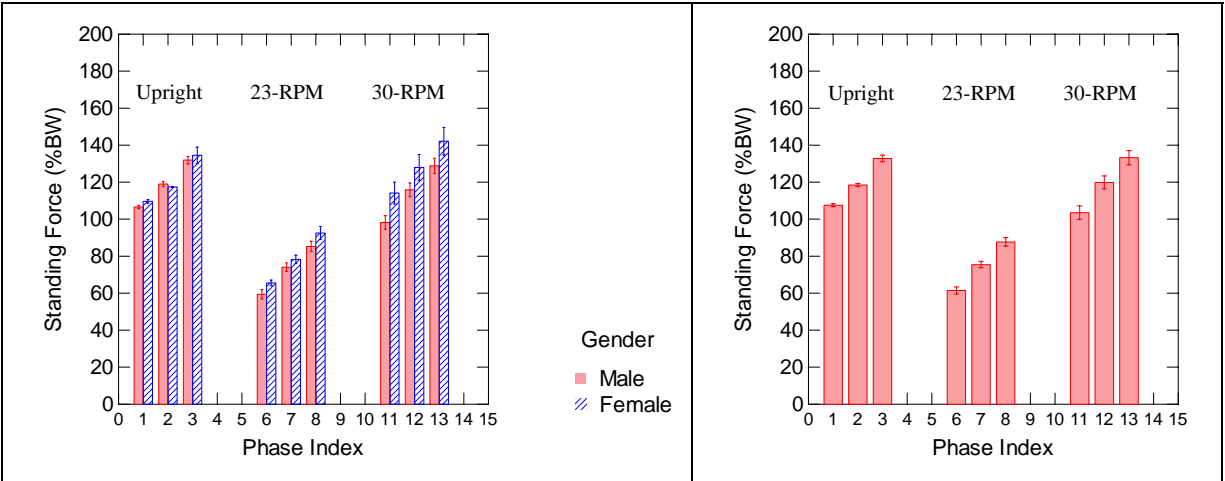


Figure 63. Left: “Standing weight” of the subject as a percentage of their 1-G upright weight for males and females. We see the interaction between rotation rate and gender in Phase Indices 6 thru 13. Data for 12 of the 13 subjects is shown. Mean +/- SEM. Right: “Standing weight” of the subject as a percentage of their 1-G upright weight. Both groups averaged together. Data for 12 of the 13 subjects is shown. Mean +/- SEM.

We made several comparisons between conditions to determine those that resulted in similar “standing weights” to determine parameters for designing AG squat exercise protocols. Table 9 shows that standing at 30 RPM results in an apparent weight that is similar to standing upright on Earth. Similarly, Upright plus X% resistance is similar to 30 RPM plus X% resistance, where X, in our case, is 10% or 25% body weight resistance.

Table 9. Comparison of mean standing foot reaction forces across conditions. The conditions where the mean standing foot reaction forces are not significantly different from one another are highlighted, with p-values shown.

		Centrifuge					
		23-RPM			30-RPM		
		0%	10%	25%	0%	10%	25%
Upright	0%	Up: 107.6 23: 60.5	Up: 107.6 23: 74.4	Up: 107.6 23: 86.7	Up: 107.6 30: 102.3 p = 0.163	Up: 107.6 30: 118.4	Up: 107.6 30: 131.6
	10%	Up: 118.5 23: 60.5	Up: 118.5 23: 74.4	Up: 118.5 23: 86.7	Up: 118.5 30: 102.3	Up: 118.5 30: 118.4 p = 0.986	Up: 118.5 30: 131.6
	25%	Up: 132.8 23: 60.5	Up: 132.8 23: 74.4	Up: 132.8 23: 86.7	Up: 132.8 30: 102.3	Up: 132.8 30: 118.4	Up: 132.8 30: 131.6 p = 0.781

Peak Foot Reaction Forces

The peak foot reaction force during each repetition was expressed as a percentage of the subject's 1-G standing bodyweight (Figure 64). Peak forces were smallest during the 23 RPM squats, greater during the Upright exercises, and the 30 RPM squats had the highest foot reaction forces ($p < 0.0005$). Similar to the standing force, we found that the peak forces increased with increasing resistance ($p < 0.0005$).

We also found a significant interaction between the rotation rate and assigned group. Group A subjects had higher peak foot reaction forces during 30-RPM squats, but smaller forces than Group B's during the Upright and 23 RPM squats. This effect, albeit small was statistically significant and surprising because the subjects in each group were balanced, approximately, for gender, height, and weight. There was also an interaction between the rotation rate and level of additional resistance. The difference in peak foot reaction forces between levels of resistance decreased as rotation rate increased. This effect was due to the larger increase in weight from centripetal acceleration compared with the constant force spring resistance.

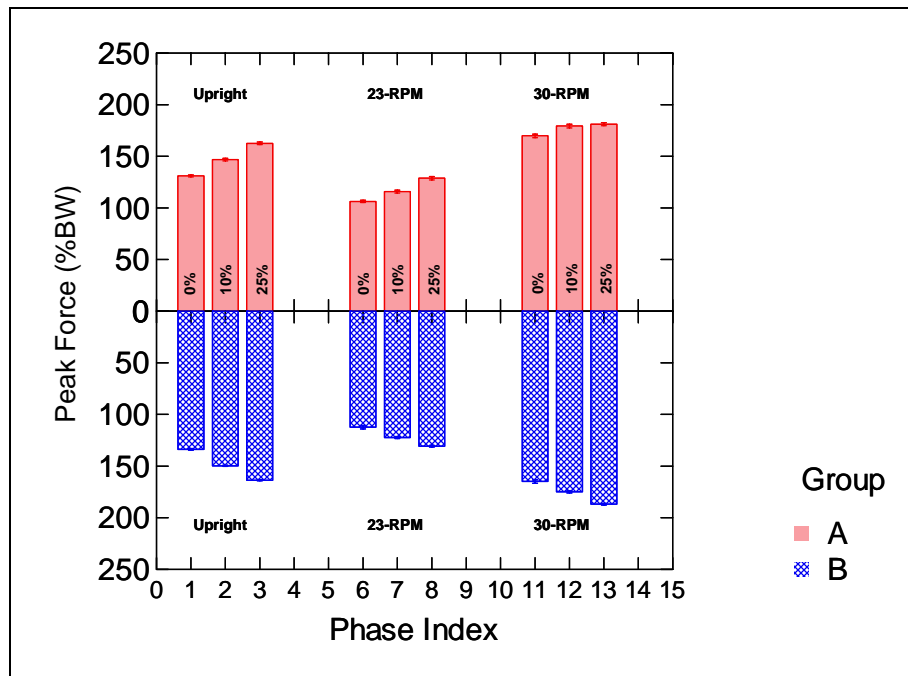


Figure 64. Peak foot reaction forces (percentage of 1-G upright standing weight). Group A deflections are shown sequentially in the Phase Index. Group B phases are re-arranged so that they are plotted against the similar experimental conditions in Group A. Within each cluster of three Phases, the additional resistance is zero (left bar), 10% body weight (middle bar), and 25% body weight (right bar). Data from 12 of 13 subjects is shown. Mean +/- SEM.

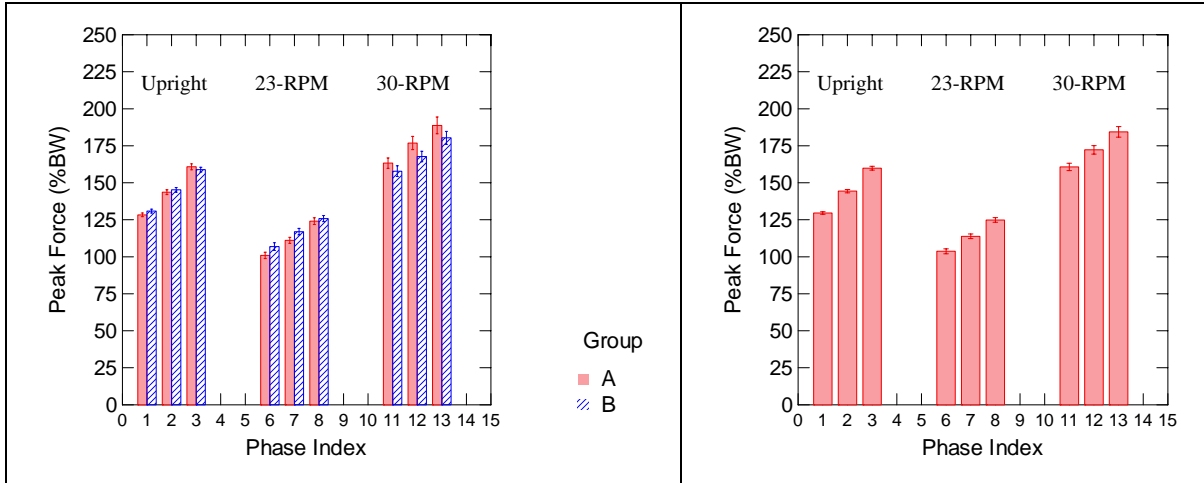


Figure 65. Left: Peak force as a percentage of 1-G upright weight during each repetition for subjects in Group A and B. We see the RPM * Group effect in Phase Indices 11 thru 13. Data for 12 of the 13 subjects is shown. Mean +/- SEM. Right: Peak force as a percentage of 1-G upright weight. Both groups averaged together. Data for 12 of the 13 subjects is shown. Mean +/- SEM.

Table 10 shows a comparison of peak foot reaction forces between the experimental conditions (Rotation Rate and Resistance). Unlike the “standing weights,” there were only two pairs of conditions that resulted in similar peak forces. These comparisons are a bit more difficult to interpret intuitively because they depend on factors such as height, weight, exercise cadence, and the depth of the squat. Nonetheless, it gave us a starting point for designing squat exercise protocols based on peak foot forces.

Table 10. Comparison of mean peak foot reaction forces (% body weight) during the exercise repetitions across conditions. The conditions where the mean peak foot reaction forces appear similar to one another are highlighted, with p-values shown.

		Centrifuge					
		23-RPM			30-RPM		
		0%	10%	25%	0%	10%	25%
Upright	0%	Up: 132.4 23: 109.1	Up: 132.4 23: 118.7	Up: 132.4 23: 129.6 p = 0.016	Up: 132.4 30: 167.5	Up: 132.4 30: 177.2	Up: 132.4 30: 184.4
	10%	Up: 148.2 23: 109.1	Up: 148.2 23: 118.7	Up: 148.2 23: 129.6	Up: 148.2 30: 167.5	Up: 148.2 30: 177.2	Up: 148.2 30: 184.4
	25%	Up: 163.1 23: 109.1	Up: 163.1 23: 118.7	Up: 163.1 23: 129.6	Up: 163.1 30: 167.5 p = 0.002	Up: 163.1 30: 177.2	Up: 163.1 30: 184.4

Individual Foot Force as a Function of Knee Angle

From the kinematics and synchronized foot force measures, we retrieved the foot force data as a function of knee angle. We used the same definition of knee angle as in Experiment 1. In Figure 66, the ratio of left foot force divided by right foot force minus one is plotted at each knee angle. Upon first inspection, we see trends in the foot force ratio during rotation are similar to Experiment 1. Within each level of rotation rate and resistance, we averaged the eight repetitions across knee angles to make the data set manageable for a repeated measures analysis.

As expected, from the direction of the Coriolis forces and from the results in Experiment 1, the left to right foot force ratio was greater during knee flexion (descent) than knee extension (ascent) ($p = 0.001$). Because of this asymmetry, the ratio during centrifugation (23- and 30-RPM) was greater than when upright ($p = 0.019$). When we add additional resistance, particularly during 23- or 30 RPM rotation, the ratio minus 1.0 moved closer to zero, particularly at 25% body weight resistance, indicating a reduction in the left to right foot asymmetry ($p < 0.0005$). Lastly, the ratio has the largest magnitude at the mid-flexion/extension angles compared with full extension or flexion ($p < 0.0005$).

We also found four significant interactions between dependent variables, some of which are apparent in Figure 66. First, we identified an interaction between rotation rate and resistance ($p = 0.018$). This was evident from the delineation in the ratio across levels of resistance during the centrifugation conditions, whereas there was no apparent difference between levels of resistance when exercising upright. Second, there was an interaction between rotation rate and squat direction ($p < 0.0005$). This was the result of an apparent 180-degree phase shift in the left to right force ratio between upright and centrifugation conditions. That is, when exercising upright subjects put more weight on their right foot during descent and more weight on their left foot during ascent. On the centrifuge, the opposite occurred – more weight on the left foot during descent and more weight on the right foot during descent. The third interaction was between the squat direction (ascent/descent) and the levels of resistance ($p = 0.019$). During centrifugation there is a greater separation in the magnitude of the foot force ratio with additional resistance during squat descent (knee flexion) than during ascent (knee extension). The fourth, and last, interaction was between squat direction (ascent/descent) and knee angle ($p < 0.0005$). The difference between ascent (knee flexion) and descent (extension) was greater at mid-flexion/extension angles than it was at full flexion/extension.

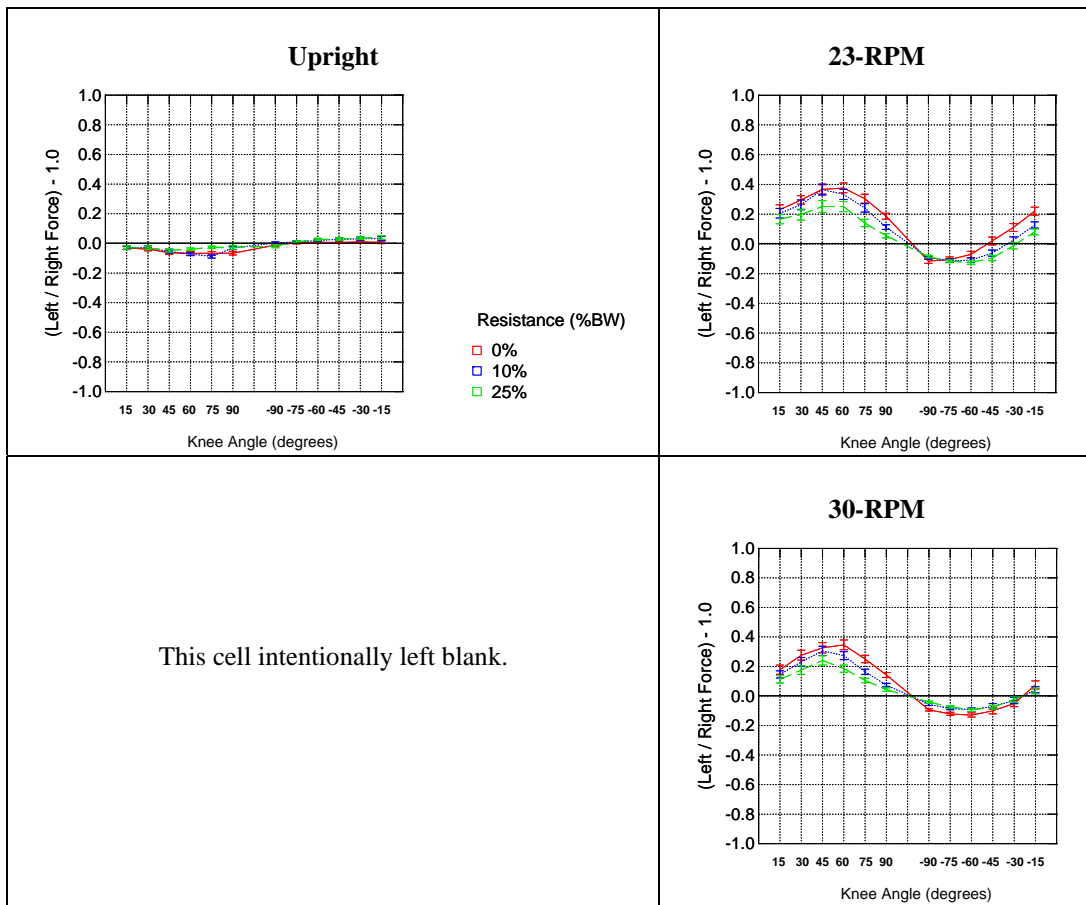


Figure 66. Ratio of left foot force to right foot force minus one as a function of knee excursion angle. Data from 12 of the 13 subjects are shown. Mean +/- SEM.

Total Foot Force as a Function of Knee Angle

The foot force sum is presented as a percentage of each subject's 1-G upright standing weight (Figure 67). It is shown clearly that the total foot reaction force increased with constant force spring resistance, that there was a difference between upright and centrifugation, and that the forces were slightly greater during knee extension compared with flexion.

Our analysis found that, on average, the total foot force while exercising upright was greater than 23 RPM ($p < 0.0005$) and that 30 RPM foot forces were greater than upright ($p = 0.004$). The foot forces also increased with resistance ($p < 0.0005$). Also, as expected, the inertial contribution to foot reaction forces resulted in greater force during squat ascent (inertia and gravity add) than during descent ($p < 0.0005$). Because of the centripetal acceleration and

gravity gradient on-board the centrifuge, the foot forces get greater as the torso moves away from the center of rotation ($p < 0.0005$).

There were four significant interactions among the dependent variables. The first was between rotation rate and squat direction (ascent/descent) ($p < 0.0005$). This was a relatively small effect. The difference between ascent and descent was greater when exercising upright than when performing supine squats at either 23- or 30 RPM. The second interaction, between rotation rate and knee angle, reflects the qualitative difference in the trend of foot force vs. knee angle (Figure 68) ($p < 0.0005$). The foot forces were nearly sinusoidal between ascent and descent when exercising upright, but when the centrifuge was rotating, the total foot reaction force continued to increase with knee angle. Third, the interaction between resistance and rotation rate, which was rather small, was due to the smaller difference in foot force smaller difference between upright and 30 RPM without any resistance than between any other conditions ($p < 0.0005$). Lastly, we found that the difference in total foot force between ascent and descent at large knee angles was greater than at smaller knee angles ($p < 0.0005$).

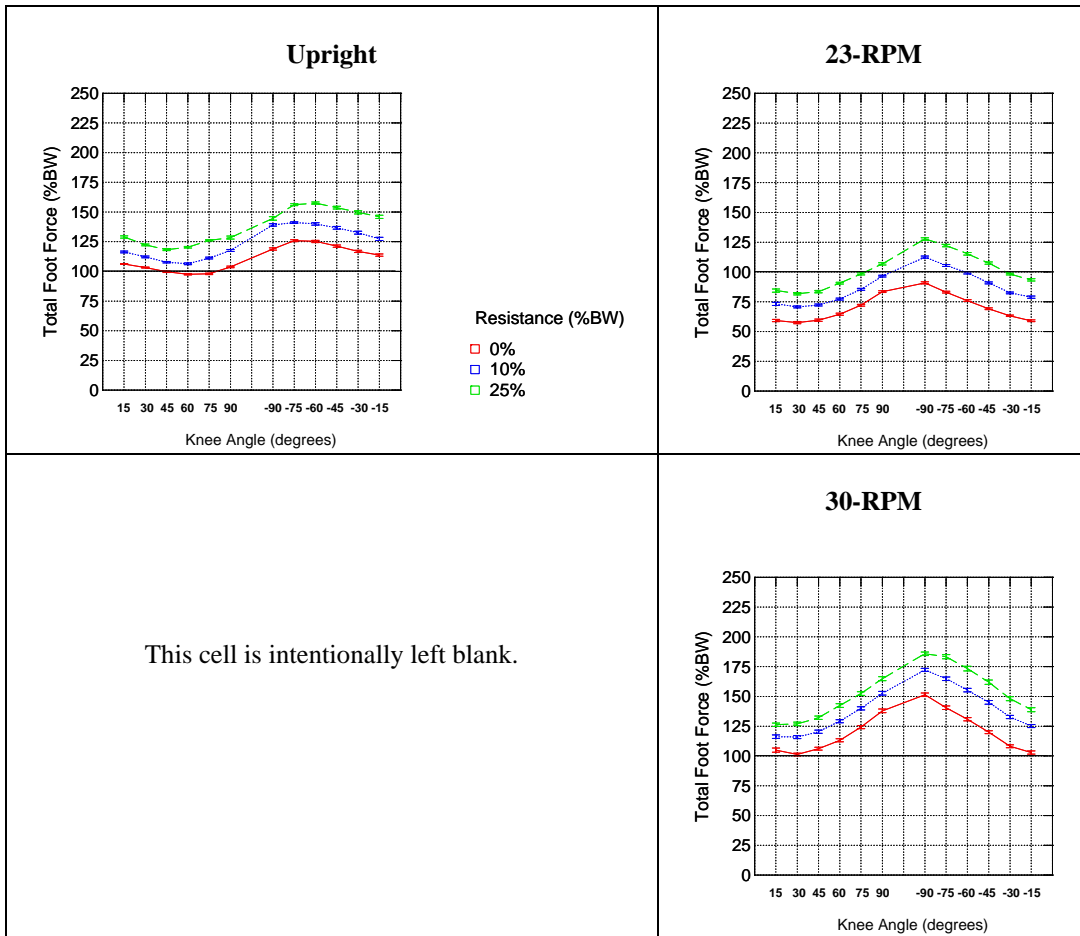


Figure 67. Total foot reaction force (percentage of 1-G upright body weight) as a function of knee angle. Data from 12 of the 13 subjects are shown. Mean +/- SEM.

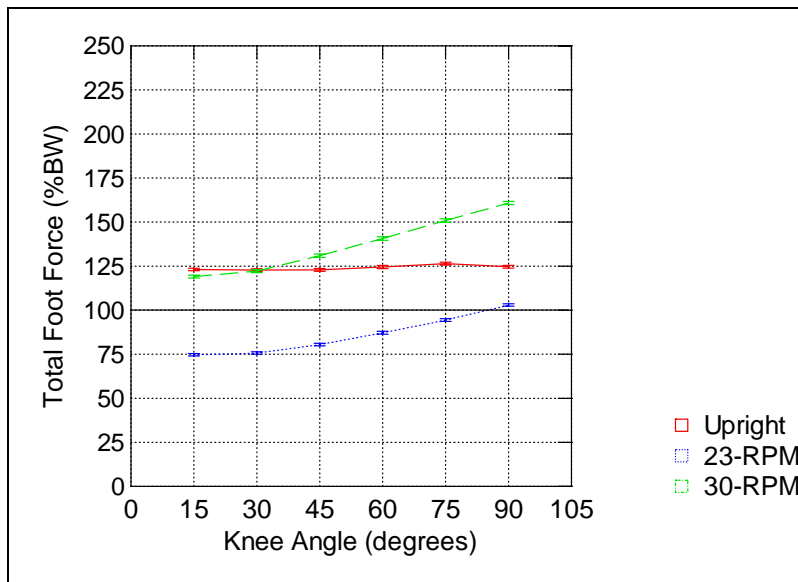


Figure 68. Total foot reaction force as a function of knee angle. The knee angles during flexion and extension are averaged together. Data from 12 of 13 subjects is shown. Mean +/- SEM.

Surface Electromyography

We recorded muscle activity from the same seven muscle groups as in Experiment 1, and the data was again expressed as a percentage of maximum voluntary isometric contraction (%MVIC) collected before starting the experiment in the same procedure previously outlined. Due to the differences in the left and right legs (dominant vs. non-dominant leg) during MVIC testing, we analyzed the muscle activity for the left and right leg separately (Figure 69 thru Figure 75). Statistical analyses included a hierarchical mixed regression (HMR) on the left and right leg %MVIC separately to identify conditions between upright and centrifuge supine that produce similar responses. The asymmetry between the left and right legs was not addressed in this analysis.

Soleus

We investigated the soleus muscle activity as a function of knee angle under three rotation rates (upright, 23 RPM, and 30 RPM) and three levels of additional resistance (0, 10, 25% body weight) (Figure 69). The left and right soleus was relatively inactive during the squat descent, reached its peak at large knee extension angles, and then decreased during the ascent ($p < 0.0005$). Over the majority of knee angles, the activity generally increased with increasing

resistance ($p < 0.0005$). Similar to the foot reaction forces, the upright activity was greater than 23 RPM and the 30 RPM soleus activity was greater than upright.

Lateral Gastrocnemius

The lateral head of the gastrocnemius, in either the right or left leg, was fairly inactive during either the upright or AG squat (Figure 70). We found that the ascent phase resulted in slightly greater activation than the descent phase ($p < 0.0005$). The 23 RPM squats produced less activity than upright, and 30 RPM squats resulted in more activity than upright ($p < 0.0005$) (Figure 70). Muscle activity also increased with resistance ($p < 0.0005$). These effects are similar in trend to both the foot reaction forces and the soleus muscle activity.

Medial Gastrocnemius

The medial head of the gastrocnemius, which is normally very active during free squats, did not show a large amount of activity during these experiments (Figure 71). There was a small asymmetry between the left and right legs (Figure 71). When upright, the left leg %MVIC was greater than when spinning at 23 RPM ($p = 0.001$), but the right leg upright %MVIC is less than 23 RPM ($p = 0.008$). Additionally, the muscle activity in the left leg between no resistance and 10% body weight resistance were not significantly different from one another ($p = 0.606$). However, in the right leg, no resistance resulted in less activity than 10% body weight resistance ($p = 0.012$). These effects, although different from the findings in the previously discussed muscle groups, are rather small in a muscle group that was not very active in these exercises.

Tibialis Anterior

When performing upright or AG supine squats, the tibialis anterior was not active except at large knee angles (Figure 72). Even so, this activity rarely exceeded 20 %MVIC. The trends in the left leg reflected what we would expect to see: 23 RPM < Upright < 30 RPM ($p < 0.0005$), 0% < 10% < 25% body weight resistance ($p < 0.039$), and ascent > descent ($p < 0.0005$) (Figure 72). The right leg, in large part, showed these same trends except the fact that no-resistance and 10% body weight resistance were not significantly different. The relatively small activity in this muscle group and the inactivity over a large range of knee angles likely resulted in this similarity.

Vastus Lateralis

Qualitatively, the vastus lateralis showed similar trends in activity across knee angles between the upright and centrifuge supine squats (Figure 73). Unlike the previous muscles, there was a clear increase in muscle activity with additional resistance ($p < 0.0005$). The muscle activity increased with increasing gravitational load: 23 RPM < Upright < 30 RPM ($p < 0.0005$), and the ascent (concentric contraction) was greater than the descent phase (eccentric contraction) ($p < 0.0005$) (Figure 73).

Vastus Medialis

The vastus medialis showed a near identical response to that of the vastus lateralis (Figure 74), including the magnitude of the muscle activity. There was also a relatively clear increase in muscle activity with additional resistance ($p < 0.0005$), and gravitational load: 23 RPM < Upright < 30 RPM ($p < 0.0005$) (Figure 74).

Rectus Femoris

This muscle showed a trend of increased muscle activity at larger knee flexion and extension angles (Figure 75), which was expected based on previous literature [78]. At these larger knee angles, the increase in muscle activity with additional resistance became quite evident ($p < 0.0005$). The statistical analyses of this muscle showed a trend that was similar to the vastus medialis, vastus lateralis, and soleus (Figure 75). However, the muscle activity during the upright squats are greater than 30-RPM ($p < 0.012$). This could be explained from a fundamental difference between the upright squats and supine leg presses, previously reported in the literature – supine leg presses do not work the rectus femoris as much as an upright squat [78].

Muscle Activity Plots

In this section, we plot the %MVIC activity as a function of knee angle for each muscle group: soleus, lateral gastrocnemius, medial gastrocnemius, tibialis anterior, vastus lateralis, vastus medialis, and rectus femoris.

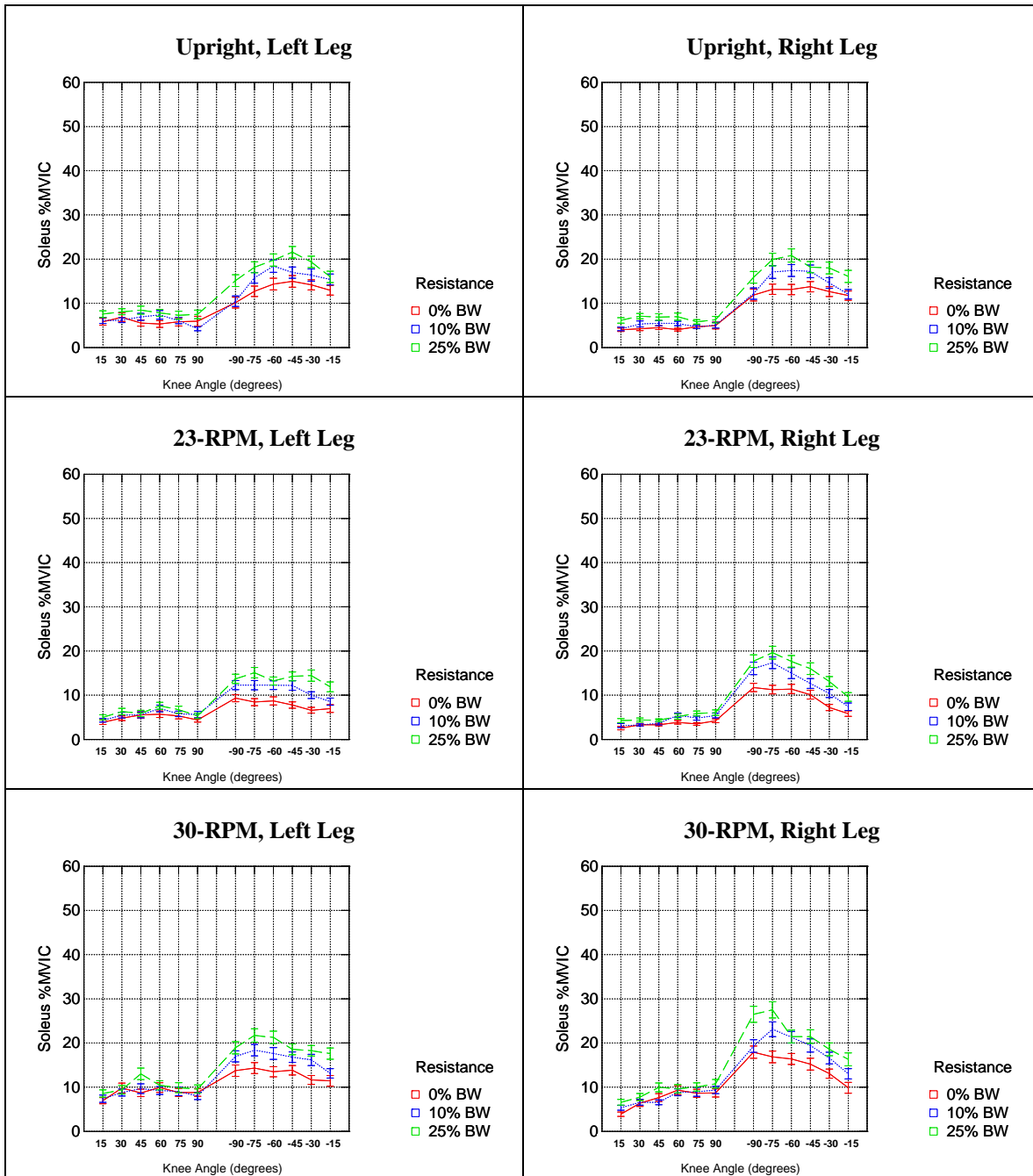


Figure 69. Soleus muscle activity (%MVIC) plotted as a function of knee angle. Mean +/- SEM.

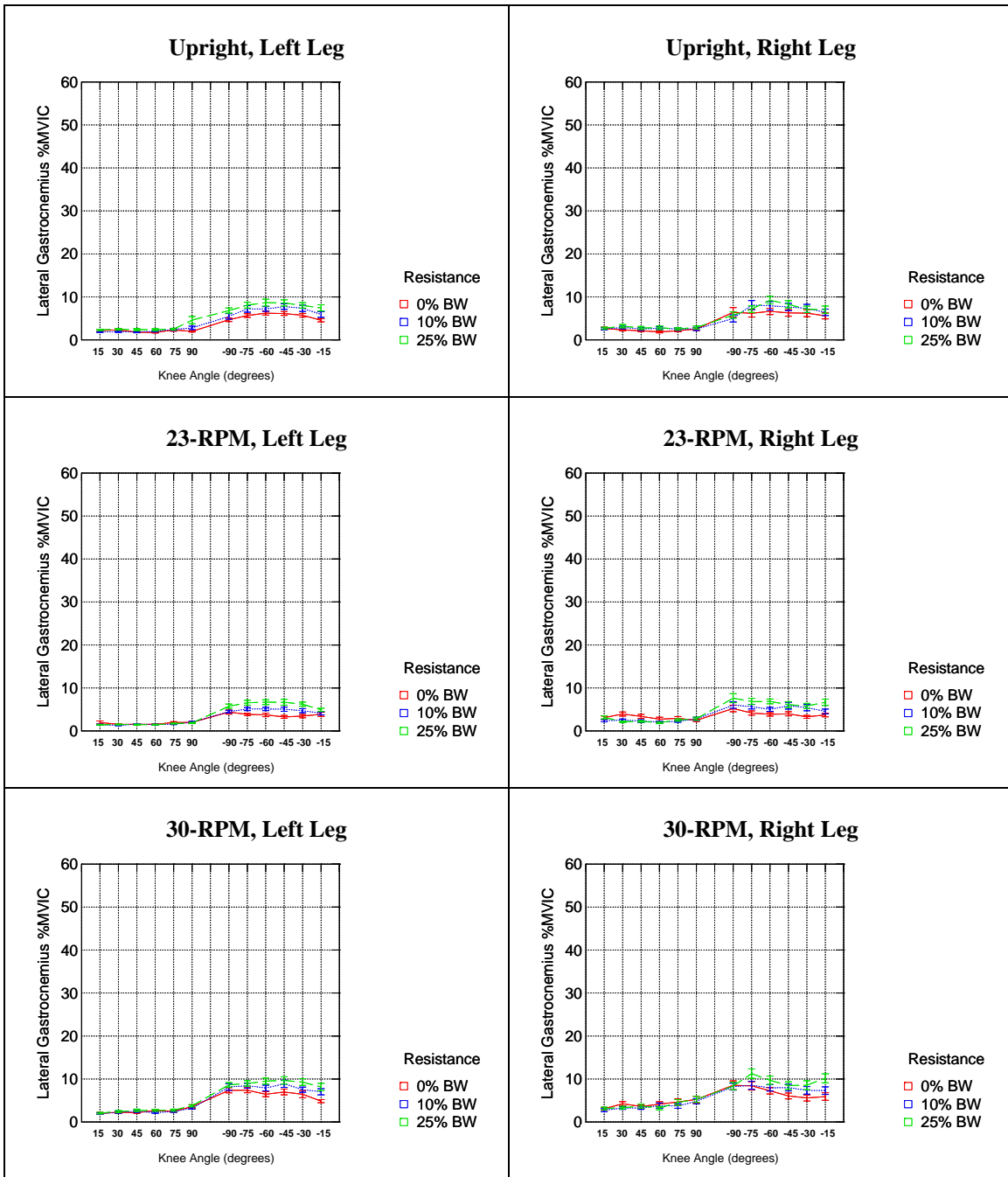


Figure 70. Lateral gastrocnemius muscle activity (%MVIC) plotted as a function of knee angle. Mean +/- SEM.

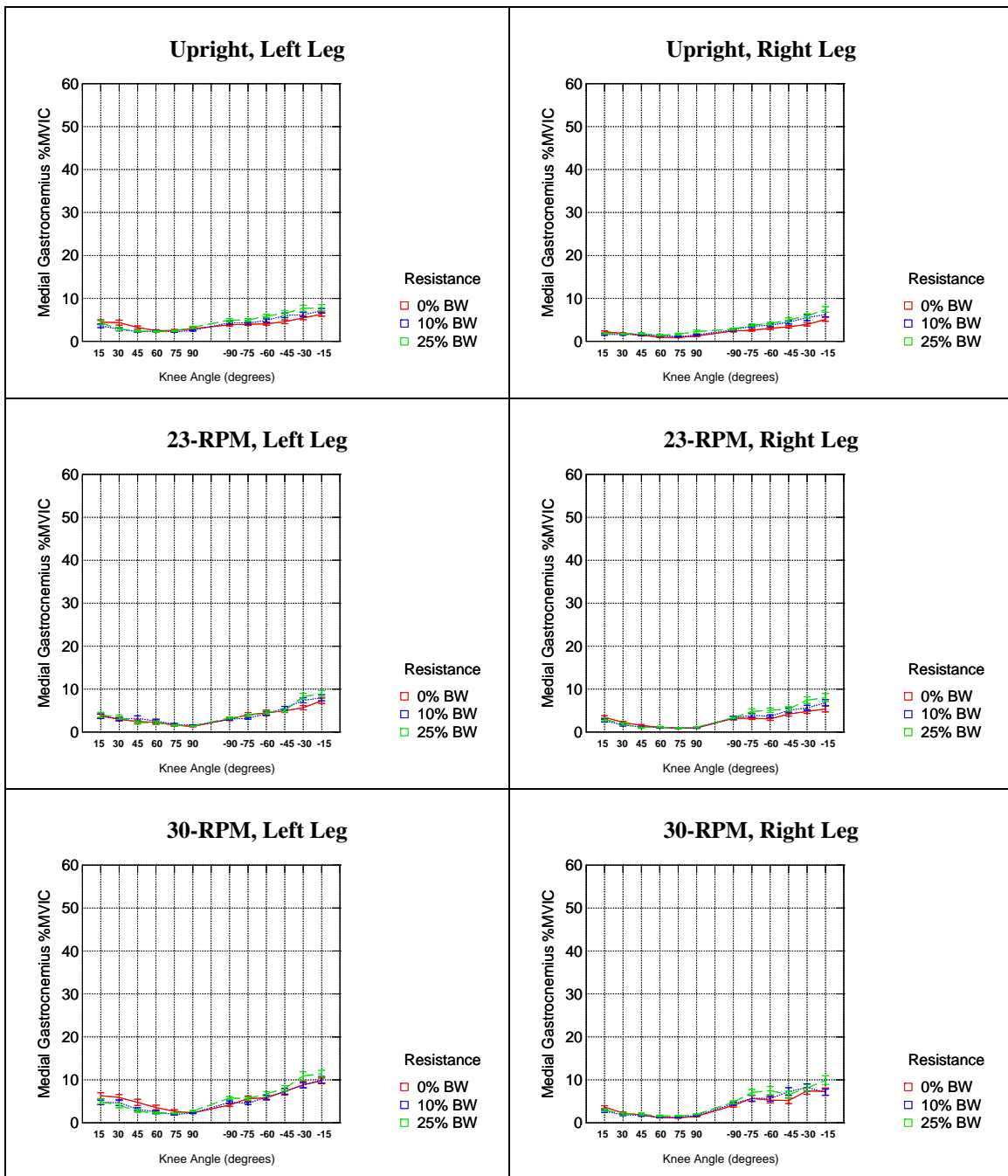


Figure 71. Medial gastrocnemius muscle activity (%MVIC) plotted as a function of knee angle. Mean +/- SEM.

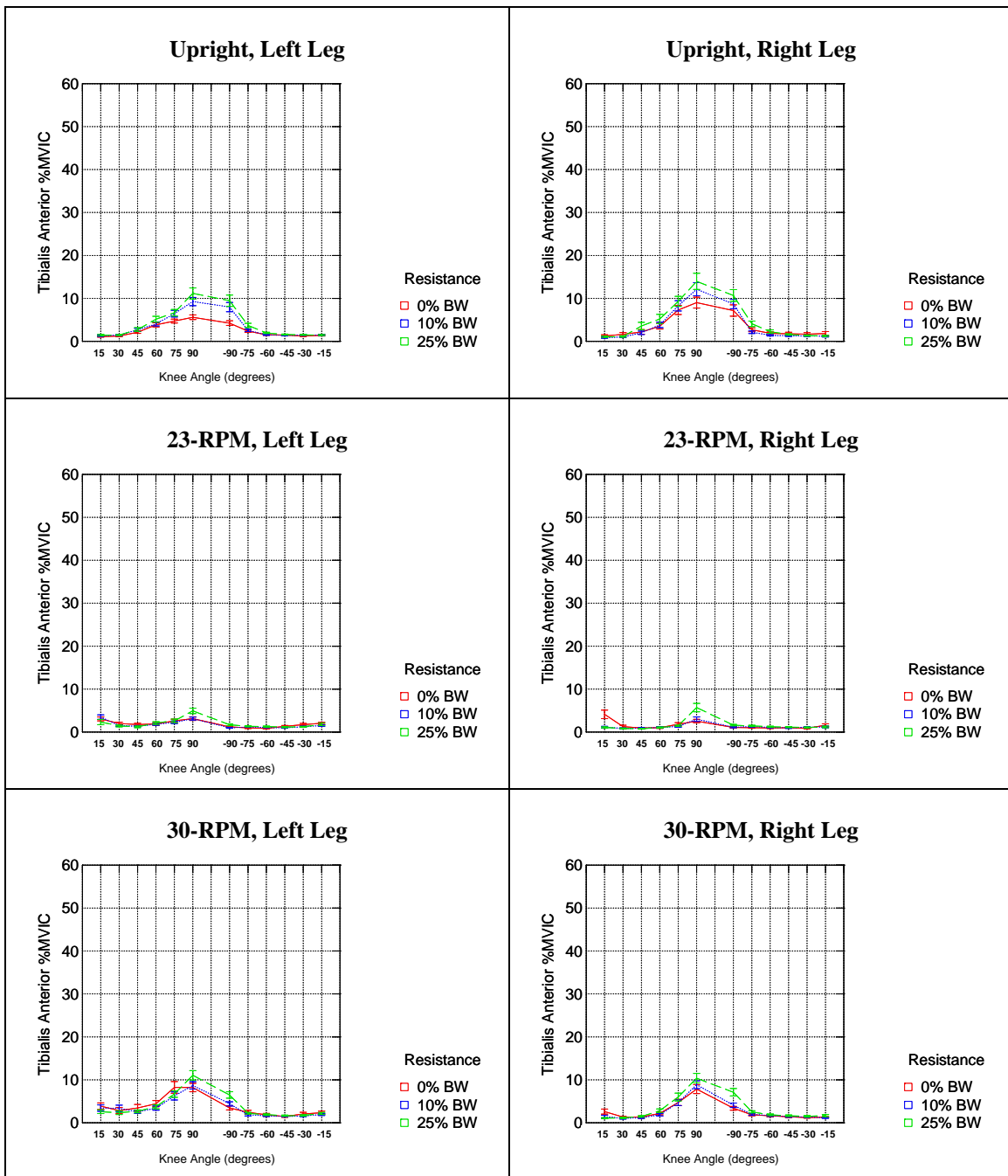


Figure 72. Tibialis anterior muscle activity (%MVIC) plotted as a function of knee angle. Mean +/- SEM.

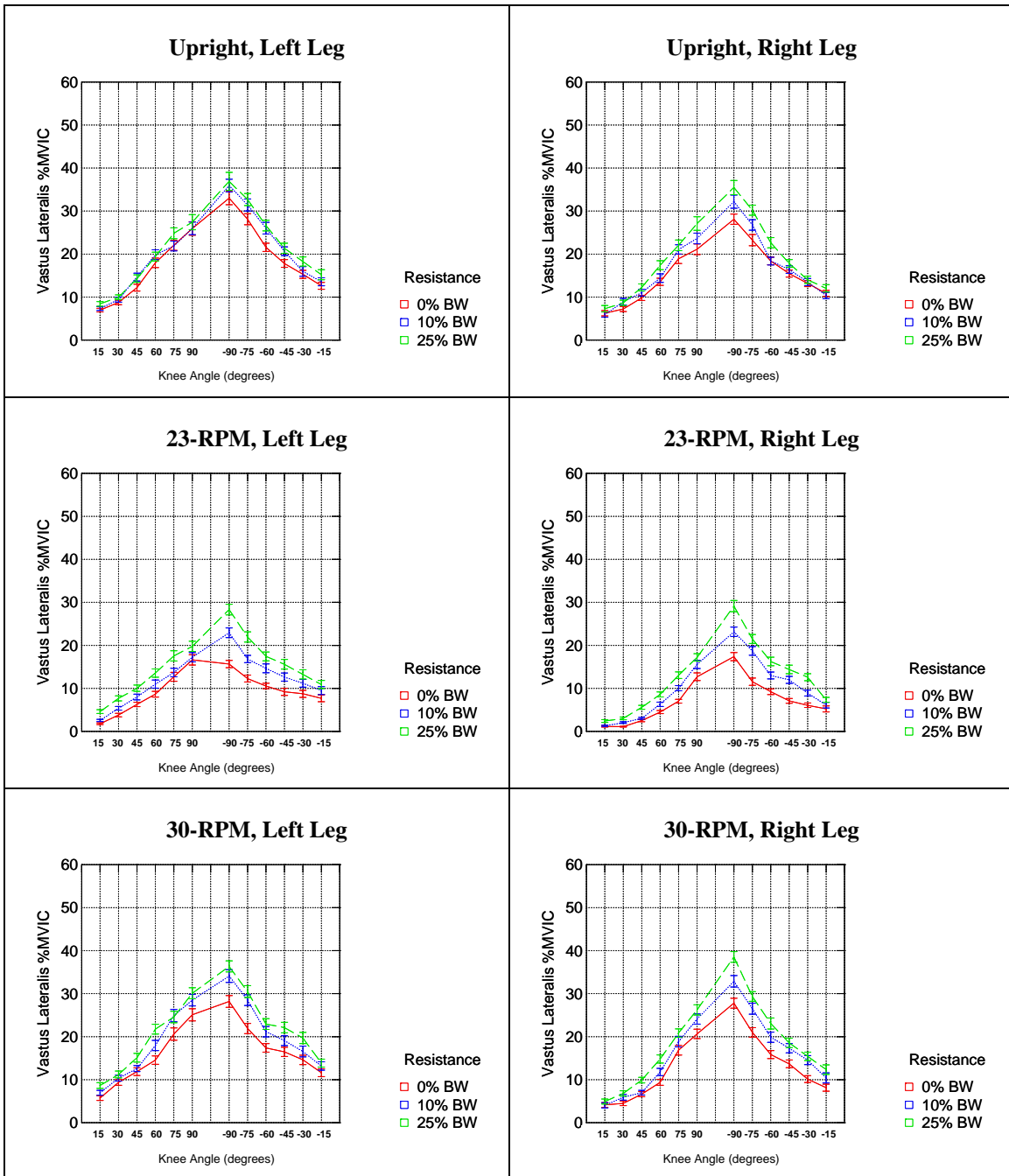


Figure 73. Vastus lateralis muscle activity (%MVIC) plotted as a function of knee angle. Mean +/- SEM.

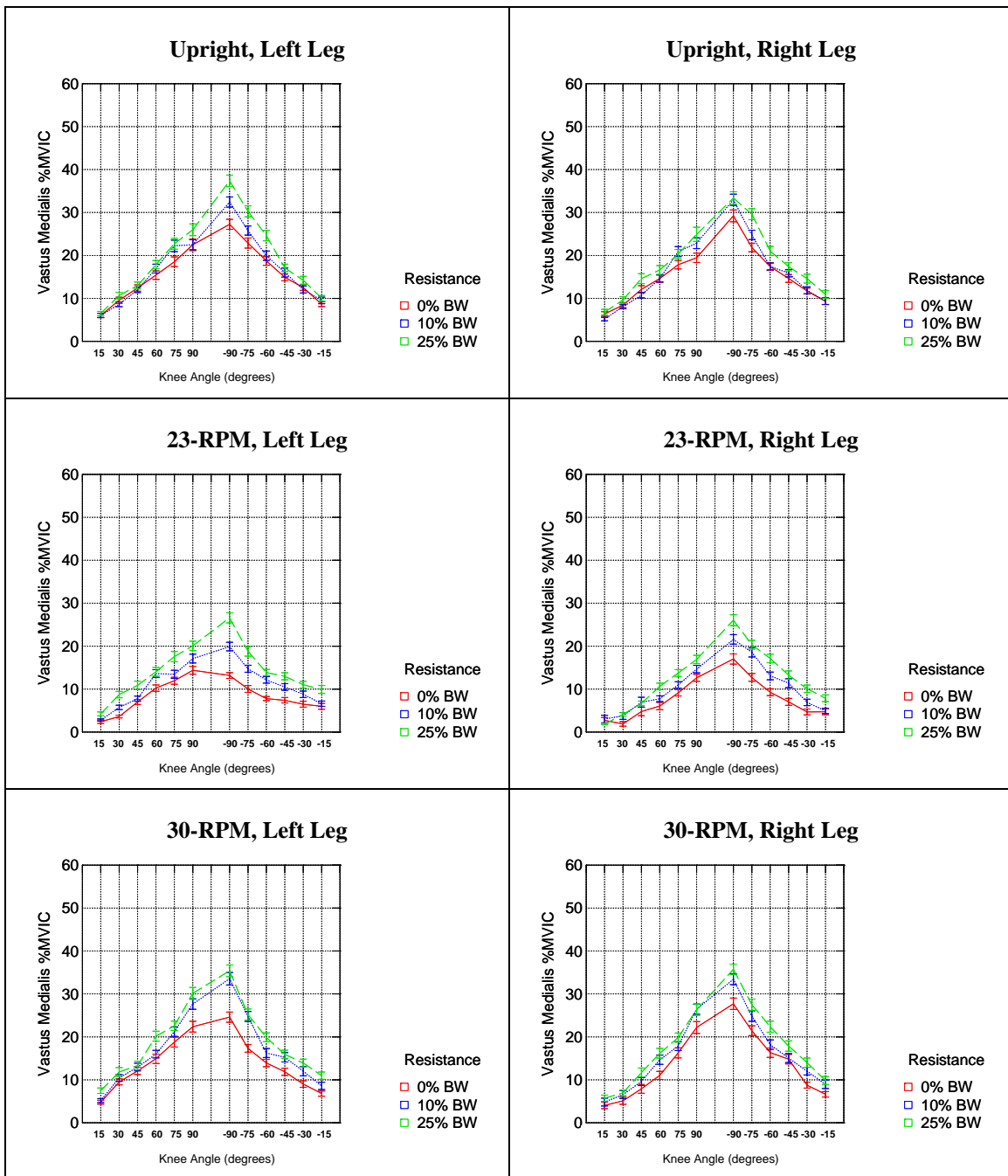


Figure 74. Vastus medialis muscle activity (%MVIC) plotted as a function of knee angle. Mean +/- SEM.

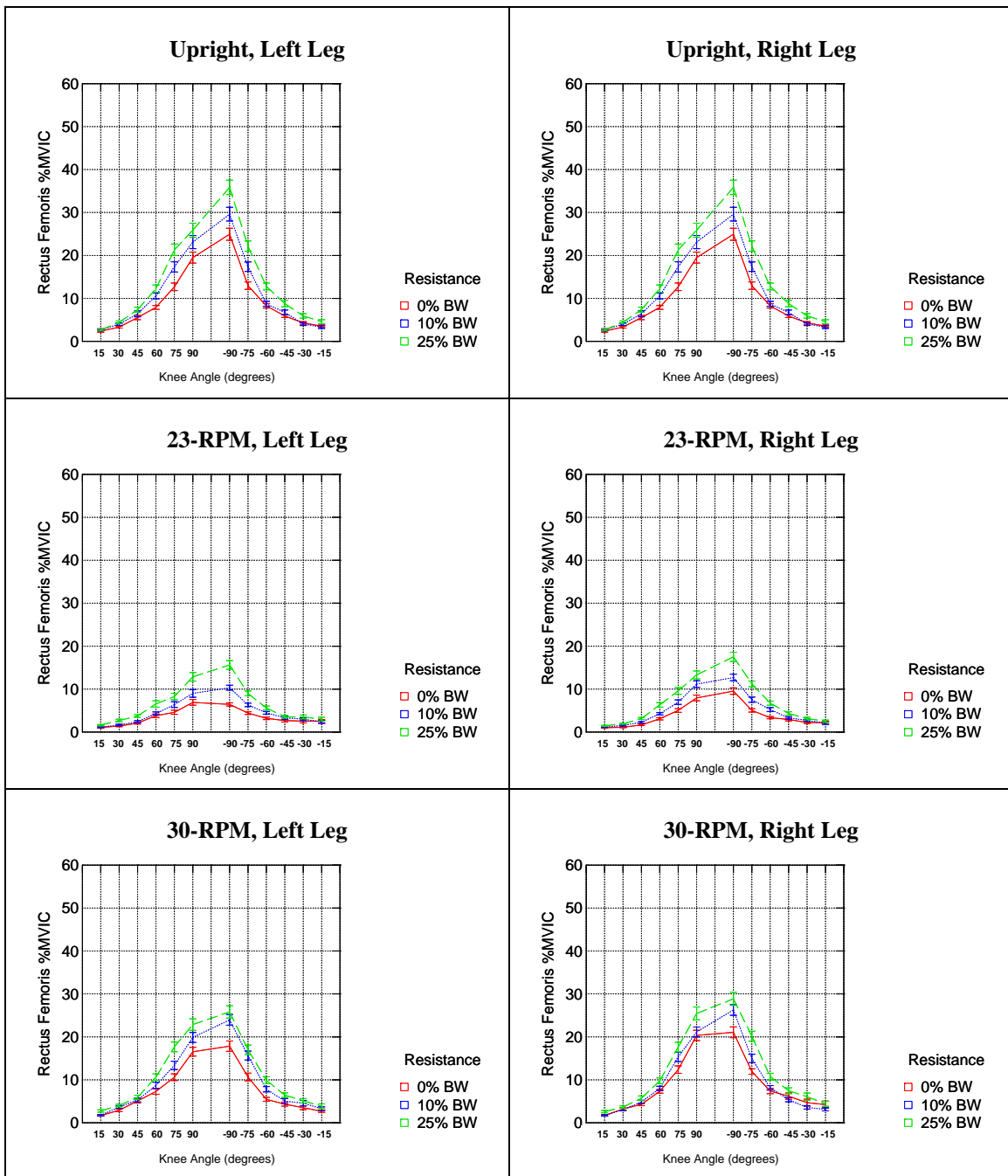


Figure 75. Rectus femoris muscle activity (%MVIC) plotted as a function of knee angle. Mean +/- SEM.

Borg Rating of Perceived Physical Exertion

After completing each set of squats, the subjects were asked to rate their perceived physical exertion on the Borg (6 – 20) scale (Figure 76). This data was also analyzed with a repeated measures ANOVA. The fixed factors included rotation rate (upright, 23 RPM, 30 RPM), resistance (0, 10, 25% body weight), gender (male or female), and group (A or B). As with the previous analysis, subjects were a random variable in the statistical model. We found, as we expected, that perceived effort increased with resistance: no resistance was less than 10% body weight resistance ($p = 0.002$) and 10% was less than 25% ($p < 0.0005$). Similar to the foot reaction forces, perceived effort when squatting upright was greater than at 23 RPM ($p = 0.060$) and 30 RPM was greater than upright ($p = 0.031$).

We found two significant interactions. The 30 RPM Borg scores were greater in the group of subjects who took part in the 23 RPM squats before the 30 RPM squats (Group A) than those who took part in the 30 RPM squats before the 23 RPM squats (Group B). This resulted in a cross effect between rotation rate and group ($p = 0.005$). There was also an interaction between resistance and group ($p = 0.017$). Here, the differences between Group A and B Borg scores were greater at 30 RPM than at 23 RPM or while exercising upright.

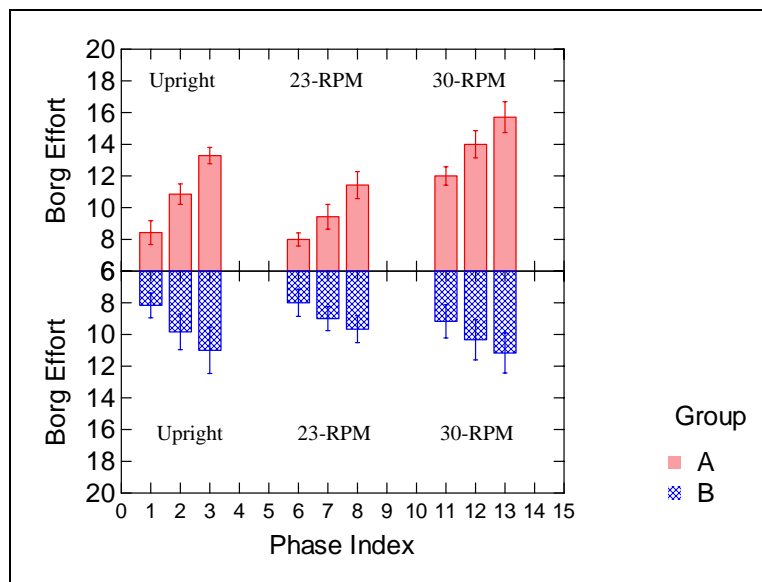


Figure 76. Borg rating of perceived physical exertion. Groups A and B are plotted separately. Within each cluster of three phases (Upright, 23 RPM, and 30 RPM), there are increasing levels of resistance (0-, 10-, and 25% of 1-G upright body weight). Data for all 13 subjects is shown. Mean +/- SEM.

Motion Sickness

Subjective motion sickness (0 – 20 scale) was recorded in all conditions after each set of eight squat repetitions. A histogram of the reports during rotation is shown in Figure 77. The greatest motion sickness report was 5 out of 20, which occurred once at 30 RPM and 25% body weight resistance (Phase 13). Two subjects (one naïve, one experienced) reported motion sickness in Phase 14 after the rotation had stopped. We used a non-parametric Kruskal-Wallis test to analyze the data. We found that motion sickness was significantly greater when spinning than when not ($p < 0.0005$), but was not significantly different between 23 and 30 RPM.

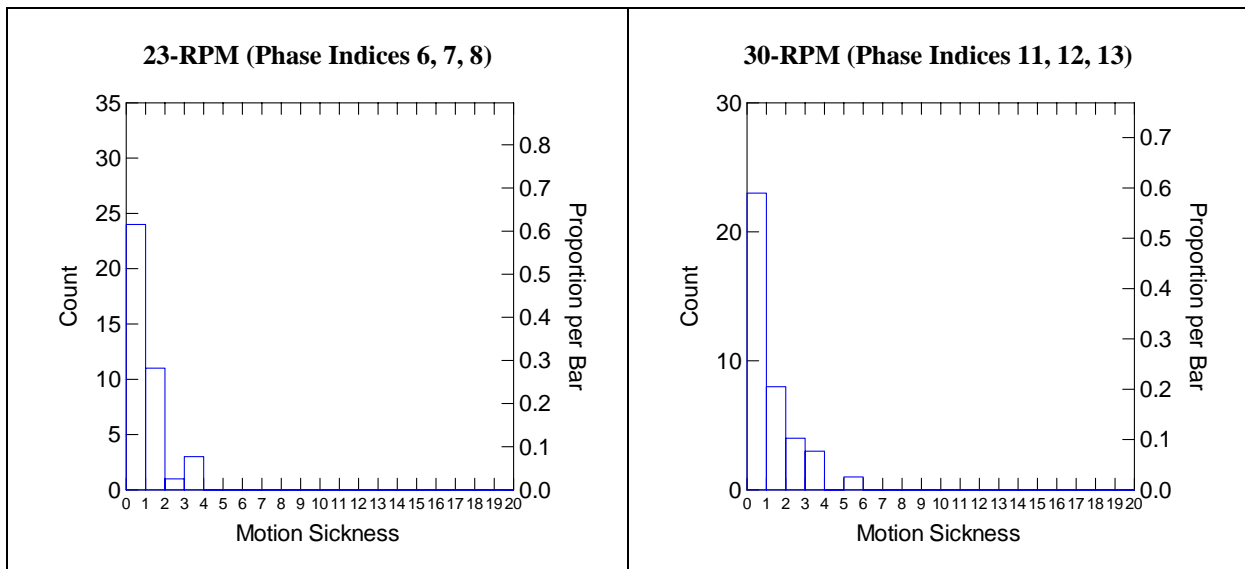


Figure 77. Histogram of the subjective reports of motion sickness at 23-RPM (Left; Phase Indices 6, 7, 8) and 30-RPM (Right; Phase Indices 11, 12, 13). Data for all 13 subjects.

Tabulation of Experiment 2 Statistical Results

In this section, we tabulate the dependent and independent variables in our statistical analyses. These analyses summarize the statistical claims in the presentation of Experiment 1 results. Significant and non-significant results are listed. The statistically significant results have the p-values highlighted.

Table 11. Statistical analyses results for Experiment 2: Knee Kinematics, Foot Forces, Borg Effort. [p < 0.05]

Dependent variable	Independent Variable	Parameter	DOF	Value	p-Value
Maximum M-L knee travel	RPM (Up, 23-RPM, 30-RPM)	F	2,18	9.57	0.001
	Repetition (1..8)	F	7, 63	3.09	0.007
	Leg (Left, Right)	F	1, 7	0.024	0.880
	Group (A, B)	F	1, 7	0.166	0.693
	Gender (Male, Female)	F	1, 7	0.049	0.832
	Experience (Experienced, Naïve)	F	1, 7	0.272	0.618
	Resistance (0, 10, 25% BW)	F	2, 18	1.802	0.193
	RPM * Resistance	F	4, 36	2.963	0.033
Standing weight	RPM (Up, 23-RPM, 30-RPM)	F	2, 18	42.92	< 0.0005
	Gender (Male, Female)	F	1, 9	4.328	0.067
	Group (A, B)	F	1, 9	0.784	0.399
	Resistance (0, 10, 25% BW)	F	2, 18	102.12	< 0.0005
	RPM * Gender	F	2, 18	4.096	0.034
Peak foot force	RPM (Up, 23-RPM, 30-RPM)	F	2, 18	425.6	< 0.0005
	Resistance (0, 10, 25% BW)	F	2, 18	142.2	< 0.0005
	Gender (Male, Female)	F	1, 9	1.659	0.230
	Group (A, B)	F	1, 9	0.004	0.953
	RPM * Group	F	2, 18	3.72	0.044
	RPM * Resistance	F	4, 36	8.27	< 0.0005
Individual foot forces as a function of knee angle	Gender (Male, Female)	F	1, 8	3.339	0.105
	Group (A, B)	F	1, 8	2.926	0.126
	Squat direction (Ascent, Descent)	F	1, 11	18.27	0.001
	RPM (Up, 23-RPM, 30-RPM)	F	2, 22	4.47	0.019
	Resistance (0, 10, 25% BW)	F	2, 22	12.67	< 0.0005
	Knee Angle (15..90)	F	5, 55	6.53	< 0.0005
	RPM * Resistance	F	4, 44	4.09	0.018
	RPM * Squat Direction	F	2, 22	20.41	< 0.0005
	Resistance * Squat Direction	F	2, 22	6.19	0.019
	Squat direction * Knee Angle	F	5, 55	14.42	< 0.0005
Total foot force as function of knee angle	RPM (Up, 23-RPM, 30-RPM)	F	2, 22	376.8	< 0.0005
	Resistance (0, 10, 25% BW)	F	2, 22	150.8	< 0.0005
	Squat Direction (Ascent, Descent)	F	1, 11	393.1	< 0.0005
	Knee Angle (15..90)	F	5, 55	53.2	< 0.0005
	Gender (Male, Female)	F	1, 11	3.084	0.113
	Group (A, B)	F	1, 11	0.451	0.519
	RPM * Squat Direction	F	2, 22	18.52	< 0.0005
	RPM * Knee Angle	F	10, 110	5.54	< 0.0005
	Resistance * Squat Direction	F	2, 22	47.03	< 0.0005
	Squat Direction * Knee Angle	F	5, 55	30.28	< 0.0005
	Borg effort	RPM (Up, 23-RPM, 30-RPM)	F	2, 20	21.38
Resistance (0, 10, 25% BW)		F	2, 20	48.50	< 0.0005
Gender (Male, Female)		F	1, 10	0.292	0.601
Group (A, B)		F	1, 10	3.823	0.079
Resistance * Group		F	2, 20	5.008	0.017
RPM * Group		F	2, 20	6.963	0.005

Table 12. Statistical analyses results for Experiment 2: HMR Muscle Activity.

Muscle Group	Independent Variable	Left Leg	Right Leg
Soleus	RPM (Up, 23-RPM, 30-RPM)	Main effect: $p < 0.0005$ Upright > 23-RPM ($p < 0.0005$) 30-RPM > Upright ($p < 0.0005$)	Main effect: $p < 0.0005$ Upright > 23-RPM ($p < 0.0005$) 30-RPM > Upright ($p < 0.0005$)
	Resistance (0, 10, 25% BW)	Main effect: $p < 0.0005$ 0 < 10%BW ($p < 0.0005$) 10 < 25%BW ($p < 0.0005$)	Main effect: $p < 0.0005$ 0 < 10%BW ($p < 0.0005$) 10 < 25%BW ($p < 0.0005$)
	Squat Direction (Ascent, Descent)	Ascent > Descent ($p < 0.0005$)	Ascent > Descent ($p < 0.0005$)
	Knee Angle (15..90)	$p < 0.0005$	$p < 0.0005$
Lateral Gastrocnemius	RPM (Up, 23-RPM, 30-RPM)	Main effect: $p = 0.090$ Upright > 23-RPM ($p < 0.0005$) 30-RPM > Upright ($p < 0.0005$)	Main effect: $p < 0.0005$ Upright > 23-RPM ($p < 0.0005$) 30-RPM > Upright ($p < 0.0005$)
	Resistance (0, 10, 25% BW)	Main effect: $p < 0.0005$ 0 < 10%BW ($p < 0.0005$) 10 < 25%BW ($p < 0.0005$)	Main effect: $p < 0.0005$ 0 < 10%BW ($p < 0.0005$) 10 < 25%BW ($p < 0.0005$)
	Squat Direction (Ascent, Descent)	Ascent > Descent ($p < 0.0005$)	Ascent > Descent ($p < 0.0005$)
	Knee Angle (15..90)	$p < 0.0005$	$p < 0.0005$
Medial Gastrocnemius	RPM (Up, 23-RPM, 30-RPM)	Main effect: $p < 0.0005$ Upright > 23-RPM ($p = 0.001$) 30-RPM > Upright ($p = 0.001$)	Main effect: $p < 0.0005$ Upright < 23-RPM ($p = 0.008$) 30-RPM > Upright ($p < 0.0005$)
	Resistance (0, 10, 25% BW)	Main effect: $p < 0.0005$ 0 = 10%BW ($p = 0.606$) 10 < 25%BW ($p = 0.001$)	Main effect: $p < 0.0005$ 0 < 10%BW ($p = 0.012$) 10 < 25%BW ($p < 0.0005$)
	Squat Direction (Ascent, Descent)	Ascent > Descent ($p < 0.0005$)	Ascent > Descent ($p < 0.0005$)
	Knee Angle (15..90)	$p < 0.0005$	$p < 0.0005$
Tibialis Anterior	RPM (Up, 23-RPM, 30-RPM)	Main effect: $p < 0.001$ Upright > 23-RPM ($p < 0.0005$) 30-RPM > Upright ($p < 0.0005$)	Main effect: $p < 0.0005$ Upright > 23-RPM ($p < 0.0005$) 30-RPM > Upright ($p < 0.0005$)
	Resistance (0, 10, 25% BW)	Main effect: $p = 0.305$ 0 < 10% BW ($p = 0.039$) 10 < 25% BW ($p = 0.003$)	Main effect: $p < 0.0005$ 0 = 10%BW ($p = 0.639$) 10 < 25%BW ($p < 0.0005$)
	Squat Direction (Ascent, Descent)	Ascent > Descent ($p < 0.001$)	Ascent > Descent ($p < 0.0005$)
	Knee Angle (15..90)	$p < 0.001$	$p < 0.0005$
Vastus Lateralis	RPM (Up, 23-RPM, 30-RPM)	Main effect: $p < 0.0005$ Upright > 23-RPM ($p < 0.0005$) 30-RPM > Upright ($p < 0.0005$)	Main effect: $p < 0.0005$ Upright > 23-RPM ($p < 0.0005$) 30-RPM > Upright ($p < 0.0005$)
	Resistance (0, 10, 25% BW)	Main effect: $p < 0.0005$ 0 < 10%BW ($p < 0.0005$) 10 < 25%BW ($p < 0.0005$)	Main effect: $p < 0.0005$ 0 < 10%BW ($p < 0.0005$) 10 < 25%BW ($p < 0.0005$)
	Squat Direction (Ascent, Descent)	Ascent > Descent ($p < 0.0005$)	Ascent > Descent ($p < 0.0005$)
	Knee Angle (15..90)	$p < 0.0005$	$p < 0.0005$
Vastus Medialis	RPM (Up, 23-RPM, 30-RPM)	Main effect: $p < 0.0005$ Upright > 23-RPM ($p < 0.0005$) 30-RPM > Upright ($p < 0.0005$)	Main effect: $p = 0.550$ Upright > 23-RPM ($p < 0.0005$) 30-RPM > Upright ($p < 0.0005$)
	Resistance (0, 10, 25% BW)	Main effect: $p < 0.0005$ 0 < 10%BW ($p < 0.0005$) 10 < 25%BW ($p < 0.0005$)	Main effect: $p < 0.0005$ 0 < 10%BW ($p < 0.0005$) 10 < 25%BW ($p < 0.0005$)
	Squat Direction (Ascent, Descent)	Ascent > Descent ($p < 0.0005$)	Ascent > Descent ($p < 0.0005$)
	Knee Angle (15..90)	$p < 0.0005$	$p < 0.0005$
Rectus Femoris	RPM (Up, 23-RPM, 30-RPM)	Main effect: $p < 0.0005$ Upright > 23-RPM ($p < 0.0005$) Upright > 30-RPM ($p < 0.0005$)	Main effect: $p < 0.0005$ Upright > 23-RPM ($p < 0.0005$) Upright > 30-RPM ($p = 0.012$)
	Resistance (0, 10, 25% BW)	Main effect: $p < 0.0005$ 0 < 10%BW ($p < 0.0005$) 10 < 25%BW ($p < 0.0005$)	Main effect: $p < 0.0005$ 0 < 10%BW ($p < 0.0005$) 10 < 25%BW ($p < 0.0005$)
	Squat Direction (Ascent, Descent)	Ascent > Descent ($p < 0.0005$)	Ascent > Descent ($p < 0.0005$)
	Knee Angle (15..90)	$p < 0.0005$	$p < 0.0005$

Chapter 7: Discussion



“When the numbers acquire the significance of language, they acquire the power to do all things which language can do: to become fiction and drama and poetry.”

Bill James

We conducted two separate experiments and biomechanical modeling to understand the kinetics and kinematics of supine squats while rotating on a short-radius centrifuge. The motion of our legs is affected by several factors that are specific to artificial gravity exercise. These include Coriolis accelerations, as well as the centripetal acceleration and its gradient. In this section, we discuss how these factors may have affected our kinetics, kinematics, and muscle activity during the squat exercise. The modeling work is also discussed in terms of the safety of the artificial gravity squat and uses for designing exercise programs for various radius centrifuges. The results of the comparison between upright and centrifuge supine squats are summarized in terms of designing strength training exercise programs. Potential similarities and differences between our results on AG squats and other researchers’ work on AG cycle ergometry is also presented.

Kinematics

Both experiments were designed to investigate the effects of Coriolis accelerations on our exercise kinematics during 0.5 Hz cadence (two second repetition) squats while upright and while lying supine on the centrifuge. In Experiment 1, we were interested in how our mediolateral knee motion may be affected by a forty repetition (five sets of eight repetitions) protocol at two angular velocities (23 and 30 RPM). The pre- and post-rotation squats provided insights into post-rotatory effects from adaptation to the Coriolis accelerations, since previous research on human movement during centrifugation indicates appropriate per-rotation compensation and inappropriate post-rotation compensation for these Coriolis-induced limb

perturbations [11, 96]³⁶. The data from our second experiment, Experiment 2, allowed us to directly compare upright squats with centrifuge supine squats. Additional constant force resistance was added to the squat to investigate whether or not it would reduce the mediolateral knee motion during centrifuge supine squats. It also allowed us to broaden the exercise parameter space (rotation rate, radius, resistance, etc.) for protocol design.

Coriolis-induced Medial-Lateral Perturbations

As we hypothesized, the mediolateral knee travel during supine squats was significantly greater during rotation compared with either no-rotation (Experiment 1) or upright squats (Experiment 2) (Figure 38 and Figure 59). In Experiment 1, the mediolateral travel of the knees during centrifugation was, on average, 0.5 to 1.0 centimeters greater than while exercising supine (no-rotation) with body weight resistance. The conditions in Experiment 2 reveal 1.0 to 2.0 centimeter greater medial-lateral travel during AG squats compared with upright. We also found trends in the mediolateral travel as a function of time (Figure 39). The greater deflection during the very first squat was expected, but what we did not expect was the longer-term temporal trends. At 23 RPM, the subjects quickly responded to reducing the mediolateral travel after the first few repetitions, and then continued to have a near-constant magnitude of mediolateral travel for the remainder of the protocol. When the rotation was increased to 30 RPM, we did not see the initial large deflection likely because of an order effect. The 30 RPM squats always followed those at 23 RPM. At 30-RPM, there was a different longer-term trend – the deflections continued to increase with repetition. This finding points to fatigue. As the protocol progressed, the subjects were concentrating more effort on completing the repetitions rather than correcting for the Coriolis accelerations.

The approximate two-dimensional motion of the thigh and shin during the centrifuge supine squat produced Coriolis accelerations in the frontal plane perpendicular to the longitudinal axis of the body (i.e., +/- body y-axis). The thigh accelerations were between 0.25 and 0.32 G, and between 0.05 and 0.07 G on the shin, for a median-sized male squatting at a 0.5 Hz cadence while rotating between 23 and 30 RPM. These accelerations were enough to cause the

³⁶ We also conducted similar pointing studies in our laboratory with a visiting researcher, Michele Tagliabue, Ph.D., from the Politecnico di Milano. His research was supported by the Roberto Rocca Project within the MIT-Italy Program.

significant increase in mediolateral travel of the knee during the supine squats. Although we only report the maximum acceleration, it should be noted that these are not impulses. The acceleration profile follows the motion of the body, which is typically close to sinusoidal (e.g., Figure 19). A single (or few) occurrences of this deflection may not cause any problems to the mechanics of the body joints. However, as we will later discuss, repetitive motions may lead to musculo-tendon injuries.

Post-Rotatory Effects

Post-rotatory effects on human movement are well known and well documented [11, 96]. However, we did not find any evidence of increased medial-lateral travel of the knee after repeated centrifuge supine squats – rejecting our hypothesis on sensory-motor after-effects. The differences between closed vs. open kinetic chain exercise and the pre- and post-rotation squat motion that differs from per-rotation squats may have masked any significant effects.

The previous work on adaptation and after-effects from human movement in rotating environments focuses on open kinetic chain movements, primarily finger pointing. The squat, however, is a closed kinetic chain exercise because the distal element is opposed by a resistance. In both types of movement, Coriolis accelerations perturb a portion of the limb, but the control strategies are different. The finger pointing is a goal-directed task with proprioceptive error feedback, whereas in the squat exercise the foremost goal was to complete the repetition and not to compensate for the Coriolis accelerations. Nonetheless, some subjects did comment on trying to compensate for the medial and lateral perturbations, but they did not have a target for proprioceptive error feedback, which likely limited the adaptation process.

Our experiment and hardware design did not allow us to perform identical motions before, during, and after rotation. If we were to apply a resistive load to the subject post-rotation, they would have to perform the squat motion to connect the constant force springs. Since this first motion is often the most indicative of the after-effects, we decided to use a pre- and post-rotation motion that was different from per-rotation – a no-resistance supine squat. The subject is supine and uses, primarily, their tibialis anterior and biceps femoris (hamstrings) to pull the torso towards the feet. When full knee flexion is reached, the quadriceps and triceps surae (soleus and gastrocnemius) push the torso away from the feet. This is an almost-effortless task since the

back slider is on near-frictionless linear rails, which makes this motion quite different from the “weighted” AG squats. As a result, the subject must use different muscle activation and sensory-motor control to complete the repetitions, which may have also contributed to the lack of increased post-rotatory mediolateral knee travel.

Supine vs. Upright Squats

The difference in magnitude of the mediolateral knee deflections between pre-centrifuge supine/upright and those during rotation seem to imply that our experimental comparisons may have underestimated the magnitude of the difference in Experiment 1. However, there is a fundamental difference in the maximum mediolateral travel in the knee between upright and supine under the same loading condition (Figure 60). Mediolateral knee travel was greater when supine with body weight resistance (4.3 cm) compared with upright squats against their body weight (3.7 cm) (Experiment 2). The direction of gravity with respect to the subject’s body may have contributed to this difference. When upright, the subjects may have felt as though they needed to keep their knees underneath and close to their center of gravity for stability. Whereas, when supine, postural control was not a factor and they could have greater freedom in the mediolateral movement of their knees while still completing the squat exercise.

Additional Resistance

We had hypothesized that we could reduce the magnitude of the medial-lateral travel of the knee by adding resistance to the artificial gravity squat. We did not find any evidence to support this hypothesis. A close look at the data may indicate that this was in fact the case during 23 RPM squats, but at 30 RPM the medial-lateral travel of the knee seemed to increase with resistance (cross effect between rotation rate and resistance) (Figure 58).

The lack of a significant difference in the medial-lateral knee travel between the 23- and 30 RPM conditions in Experiment 1 also points to this interaction. During each of the rotation rates, the exercise cadence was kept constant and therefore the Coriolis accelerations increased at 30-RPM, but the mediolateral travel did not (Figure 38). At these higher rotation rates, the centripetal acceleration and its gradient that the subject is exercising in is greater, which results in an increased “weight” of the squat. We may have been able to find an effect of resistance on the medial-lateral knee travel if we used higher resistance at the lower rotation rates. At higher

rotation rates, there may be an opposite effect. Fatigue (mental and physical) may increase the mediolateral knee travel.

Cycle Ergometry Comparison

Other modes of exercise, such as cycle ergometry or stair stepping, will also be susceptible to these types of perturbations in our legs. The high cadence, low resistance exercises will be most susceptible since the conditions of their movement are approaching an open kinetic chain exercise. Our estimates of Coriolis accelerations during 30 RPM AG cycling reveal that at a 40 RPM pedal cadence they may be as high as 0.21 G on the thigh and 0.05 G on the shin, but when the pedal cadence approaches 120 RPM, the Coriolis accelerations exceed 0.60 G on the thigh and 0.12 G on the shin³⁷. The majority of the previous AG exercise work has focused on these types of exercise, but none have mentioned the biomechanical effects of movement in a rotating environment [6-9, 98, 100]. These studies certainly resulted in measurable deflections in the knees because of the supine body orientation and the leg kinematics from cycling, but were not reported. One Earth-based device might not be as susceptible to these perturbations. On Earth, the body orientation SpaceCycle™ is not perpendicular to the centrifuge angular velocity vector because of the pendulous arm, but in microgravity we would have situation where the subject is perpendicular to the axis of rotation. This will reduce the magnitude of the medial-lateral accelerations proportional to the pendulous swing: up to 30% at a 45 degree angle. However, using this device on the ground must always be done in hypergravity, which itself may work to prevent the Coriolis-induced deflections.

Kinetics

We were only interested in the foot forces when the subject was in a “weighted” condition. That is, when they were standing upright, supine with body weight resistance, or during centrifugation. From our synchronized foot force and body position measures, we were also able to extract the foot reaction forces as a function of knee angle, which provided some very interesting results regarding an asymmetry between the left and right foot force that varies with

³⁷ We applied the two-dimensional model developed in this thesis (presented in Chapter 4 and Appendix) to predict the Coriolis accelerations during cycle ergometry. Assumptions include the same median-sized male subject as in Chapter 4, a pedal rotation diameter of 41 cm (16 in.), and the leg at full extension at the “bottom” of the power stroke.

the squat cycle. The comparison of the upright and centrifuge supine conditions in Experiment 2 allowed us to determine AG exercise parameters (rotation and resistance) that produce foot forces similar to upright. We also discuss the magnitude of the induced joint torques and how those during AG cycling may differ from AG squats.

“Standing Weight”

In our study, the artificial gravity weight of the subject is the sum of the AG weight of the subjects themselves plus the AG weight of the back-slider since it is not counterbalanced (in the upright conditions, the backslider is approximately 95% counterbalanced).

In Experiment 1, we found that the 23 RPM standing weight was less than supine with body weight resistance, and that 30 RPM was greater than supine with body weight resistance. Due to our constant force spring assembly, it was frequently the case that the “standing weight” while supine with body weight resistance was slightly less than the subject’s body weight. On average, the constant force springs, when configured for 100% body weight resistance provided 93% of body weight resistance. This was simply an error in the spring settings and calibration, and was complicated by a small change in spring resistance over time. For our subjects, this was a resistive force approximately eight to fourteen pounds less than their actual body weight.

The comparison of standing weight between upright and centrifuge supine in Experiment 2 resulted in slightly different results from Experiment 1. We still found the 23 RPM standing weight to be less than upright, but the 30 RPM and upright conditions were not significantly different. The differing result between Experiments is due to, in part, the non-zero counterbalancing of the upright backslider. On average, when upright the subject was standing against 108% of their body weight, which was not significantly different from 30 RPM. The different results between Experiment 1 and 2 could also be attributed to the subject demographics. In Experiment 1, we had a greater fraction of females (7 males, 8 females) than in Experiment 2 (9 males, 4 females). Females, which tend to be smaller than males and have a lower center of gravity, have a greater foot reaction force than males at a particular rotation rate.

Peak Foot Forces

The peak foot reaction forces result from a combination of gravitational and inertial acceleration acting on the body segments. We were interested in the peak foot reaction forces because of their high magnitude and (relatively) low frequency of occurrence, and their role in the maintenance of bone mineral density [46, 47, 49]. This is one of the reasons astronauts spend a great deal of time exercising with the iRED and running on the treadmill in space.

Performing the artificial gravity squats with your feet fixed with respect to the centrifuge and your torso moving away from- and towards- the center of rotation provides a unique gravitational setting for exercise. Because of the gravity gradient on the short-radius centrifuge, the subject is actually heavier in the full squat compared to “standing.” In our conditions, we were able to provide peak reaction forces that were approaching 200% of body weight (Figure 64). This is still less than the approximately 280% body weight reaction forces experienced when running on Earth (Figure 78), but more than the 160% body weight from the bungee resistance when running on the ISS treadmill [58]. For comparison, the maximum loading of the iRED is roughly 380 pounds [43], which is approximately 210% of body weight for a 800 N (180 pound) person.

The constant force resistance we used in these experiments was very conservative. The maximum we tested was 25% of body weight, and for our largest subject this was 222 N (50 pounds). For a young healthy individual performing a traditional squat exercise in the gym, this is a very light resistive load. However, because of the gravity gradient and concerns of fatigue we opted to keep this resistive force relatively low. In an artificial gravity strength maintenance and training program, resistance much greater than 25% body weight, perhaps as high as 75% of one-repetition maximum (1 RM) and would result in foot reaction forces near those of jogging. The American College of Sports Medicine (ACSM), for example, recommends at least three sets of eight to twelve repetitions at a high intensity, such that the last repetition in each set is to “approximate momentary muscular fatigue.” In a twelve repetitions strength training protocol, quadriceps muscle activity reached 80% MVIC, which indicates that our loading conditions were less than those in the strength training protocol [45, 113].

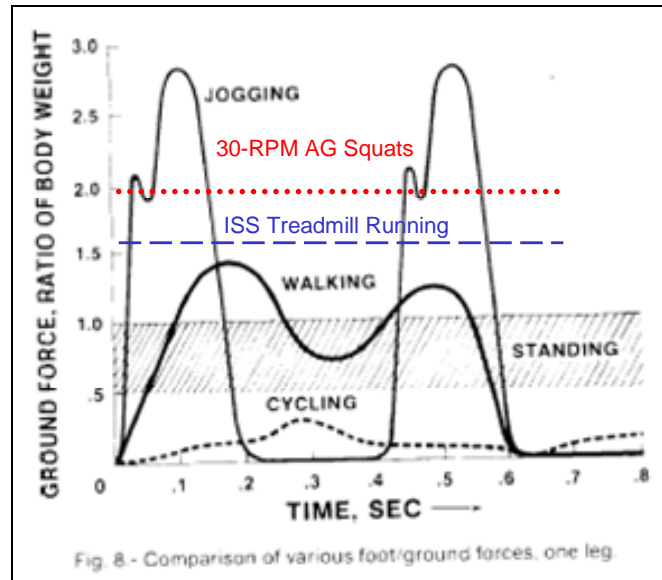


Figure 78. Ground reaction force as a ratio of body weight for various terrestrial, centrifuge, and space-based activities. ISS Treadmill Running and 30-RPM AG Squats depict the peak forces and not the time-course of the ground reaction force, as with the other illustrated activities. Figure modified from [114].

In weightlessness, the peak foot forces are a combination of the bungee resistance and the inertial acceleration of the body segments. As a result, the foot reaction forces are both qualitatively and quantitatively different from Earth-based exercise equipment [65, 67]. Centrifugation provides a loading profile that is more natural and similar to Earth. Although our resistance device did not provide any inertial contribution to the foot reaction forces (i.e., we used springs and not “free-weights”), the motion of the body on the centrifuge was sufficient to provide loading profiles that could be equated to Earth upright exercise force profiles.

The mechanics of the leg also allow us to estimate the internal compressive forces on the tibia and femur [115]. During a 30 RPM squat, where the total foot reaction force approaches twice body weight, the internal compressive force on each tibia exceeds 670 N (150 lbs.) for an 800 N (180 lb.) person. The compressive force on the femur may be approximately 90-lbs when in the full squat and increases during knee extension. From the estimated bending moments and tibia geometry, the surface strains will be between 3,500 and 4,500 microstrain, and for the femur between 2,000 and 3,000 microstrain. These strains are of the same order of magnitude previously reported for maintenance of bone mineral density in turkey bone using low-frequency high impact daily loading [49].

Foot Force vs. Knee Angle

In addition to the quantitative differences in standing weight between upright and centrifugation, there were also qualitative differences in the time-course of the foot reaction forces throughout the squat cycle. When upright (or on the centrifuge) the net acceleration during knee flexion is the gravitational (or centripetal) acceleration minus the inertial acceleration and during knee extension the accelerations add. This causes lesser foot reaction forces during descent and a greater foot reaction force during ascent, which is illustrated nicely in the upright foot reaction force profiles (Figure 67). The position of the torso follows an approximate sinusoid, and differentiation of this position twice leads to a sinusoidal acceleration profile. Hence, a sinusoidal force profile. On the centrifuge, however, we do not see a sinusoidal trend in the foot reaction forces. It is more of an inverted V-shape. Even though the subjects were performing the centrifuge supine squats at the same cadence, and therefore same inertial acceleration, the foot force profiles are qualitatively different from upright because of the centripetal acceleration. Primarily because of the increase in gravity as the subject moves away from the center of rotation.

Additionally, we see that the inertial contribution to the foot reaction force differs between upright and centrifuge supine (Figure 79). In Figure 79, we plot the ratio of the inertial acceleration to gravitational (or centripetal) acceleration. The ratio in the first half of the cycle is negative because inertia and gravitational acceleration have opposite signs and tend to cancel in the descent phase, whereas they add when ascending in the squat (second half of the cycle). At 23 RPM (lesser centripetal acceleration), inertia contributes up to 15% of the total foot reaction forces, whereas the inertial contribution during upright and 30 RPM squats is, at most, 13%. This finding is due to the lesser “gravitational” acceleration at 23 RPM compared to the other conditions, and illustrates the complex nature of exercising within a gravity gradient.

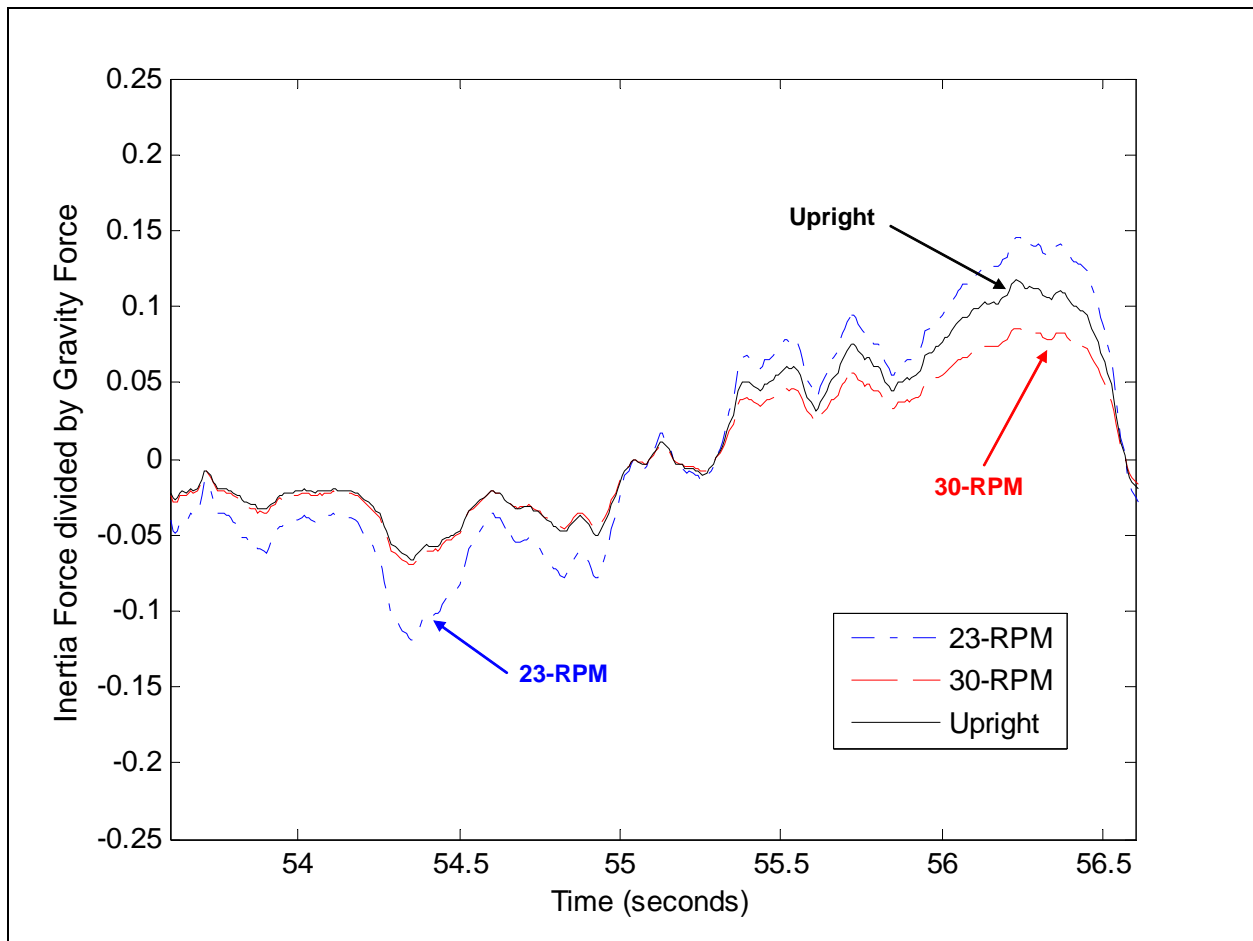


Figure 79. Inertial and gravity/centripetal contributions to foot reaction forces. Kinematic data recorded from the supine squats was used to plot the ratio of the inertial force to gravity/centripetal force throughout one squat cycle.

Designing exercise protocols that match knee-angle-specific foot reaction forces during AG squats to those during upright squats is a challenging task. It is possible to match foot reaction forces at a few knee angles, but that does not allow for matching the forces at the other angles. In Figure 80, the conditions that produced either similar “standing” or peak foot forces between upright and centrifuge supine are compared over several knee angles.

Matching the forces across the entire squat cycle is not feasible with the experimental equipment used in this experiment. It could be accomplished with a counterbalancing system that “offloads” some weight when the subject descends in the squat. Such devices could include a moveable mass on an opposing centrifuge arm, or a non-linear spring balancing system.

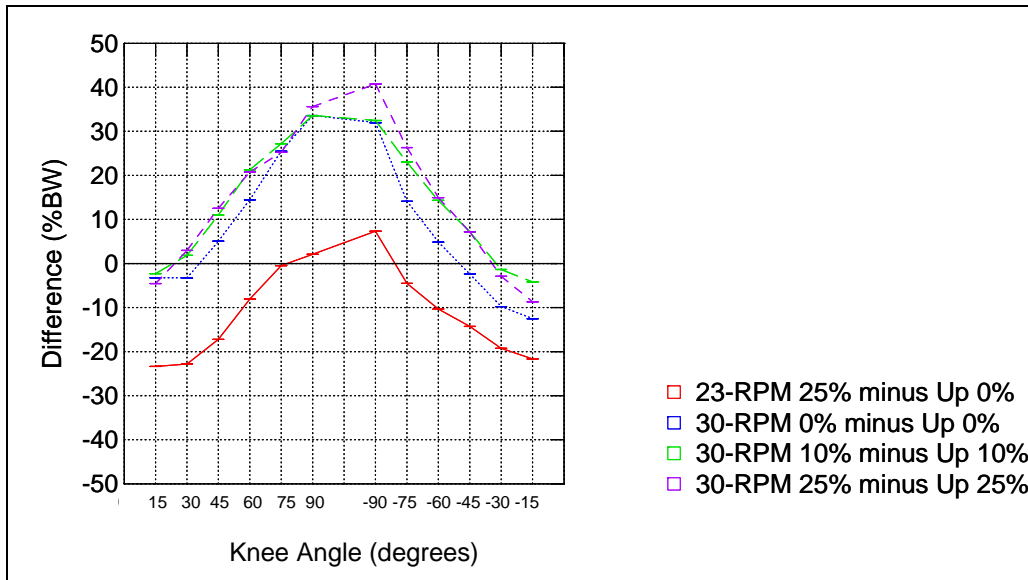


Figure 80. Difference in mean total foot reaction forces (% body weight) at each of the flexion angles. Multiple conditions are shown where the foot reaction forces were thought to be similar. Data from 12 of 13 subjects is shown. Mean +/- SEM.

Left-Right Foot Asymmetry

We identified an asymmetry between the left and right foot during the squat cycle (Figure 43 and Figure 66). Our hypothesis is that this is a postural correction in the frontal-plane for the inter-aural Coriolis accelerations. These accelerations are perceived not only by the sensory-motor alterations in the legs, but by the tactile sensations between the subject’s back and the back-slider and the otoliths organs of the vestibular system.

In the descent phase of the squat (knee flexion) while lying supine and spinning clockwise, the Coriolis acceleration acts to push the body to the left. The postural correction in this situation is to apply greater force to the left leg in an attempt to “re-center” the body upright. Conversely, in the ascent phase of the squat (knee extension) the Coriolis acceleration acts to push the body to the right and we apply greater force with our right leg to “re-center” our body. We say “re-center” in quotations because the body does not move in the frontal plane, but the tactile and vestibular systems sense an acceleration suggesting that it does. If the centrifuge were to spin counterclockwise, we would have mirror-image result: greater force on right foot during descent, and greater force on left foot during ascent.

We also notice that the asymmetry is not perfectly sinusoidal; the ascent magnitude is less than the descent magnitude. From full knee flexion, the subject could not ascend in the squat while appropriately compensating for the Coriolis-induced postural correction solely on the right leg. A greater contribution from the left leg was necessary to ascend the body while maintaining a 0.5 Hz cadence.

Since this asymmetry is hypothesized to be, at least partly, a perceptually mediated phenomenon, we expect to see some change in the response over time (Figure 44). Interestingly, these changes are not in a direction to reduce the asymmetry. They are in the direction of increasing asymmetry during descent and decreasing asymmetry during ascent. This might reflect right leg fatigue. A fatigued right leg would result in greater eccentric loading on the left leg during the descent phase, and increased concentric loading on the left leg during the ascent phase, which is what we see. In other words, the subject is compensating more with the left leg to reduce the workload on the right leg. This may also explain why there is a significant gender effect that follows this adaptation trend. The females may have fatigued earlier and were compensating to a greater extent than the males with their left leg.

There is one artifact in our data that, although it does not distort the interpretation of our results, it is a finding that is not easily explained. In Figure 43 when the subjects are supine with body weight resistance, there is a left foot dominance throughout the entire squat cycle. This effect is specific to this particular condition, and is exhibited by all subjects. When the subject is upright using the same force plates and resistive equipment, there is no dominance of either the left or right foot (Figure 66). We can identify no obvious factors that could have contributed to this. Measurement of the location of the foot holds shows that the left foot hold is approximately 6 mm (0.25 in.) closer to the center of rotation than the right foot hold. This is a relatively small offset and would likely not account for the full magnitude of the asymmetry. If it were an error in the force sensor calibration, we would also see this offset when exercising upright. Similarly, if the subjects were compensating by putting more pressure on their left shoulder than their right because of discomfort in the shoulder harness assembly we would see this in the upright exercises (the same shoulder harness was used on the centrifuge back slider and the upright back

slider). The centrifuge structure and back slider are level to the local Earth horizontal, which could rule out any perceptual effects from feeling tilted while lying supine.

Joint Torques

Involuntary joint torque that is result of novel and unexpected external forces specific to an environment we are working in is a serious concern. For the Coriolis torques, we must consider the peak magnitude as well as its change in magnitude over time. As we estimated, the acceleration and the torque are relatively low magnitude and time-varying. If these Coriolis accelerations and resultant torques were a high impact event, there should be more cause for concern.

From our predictions of the Coriolis accelerations, the induced joint torque in the frontal plane from these squat motions will be on the order of 50 N m at the hip and about 0.5 N m at the knee for a median-sized male. In comparison, the same medium-sized male might experience a frontal plane knee torque on the order of 34 N m when exercising upright due to an 8 centimeter lateral deflection of a knee (approximately 15 N m for the 3 centimeter lateral deflections measured in Experiment 2, Figure 24). At this extreme condition, Coriolis accelerations contribute less than 2% of the total frontal plane knee torque, but they are in a potentially harmful direction. Even though the torque at the knee may not exceed 34 N m, this translates to a strain on the lateral and medial collateral ligaments (LCL and MCL). The danger in these Coriolis-induced deflections is that they are unexpected and enter the system as a perturbation in our biomechanics that may or may not be actively (or consciously) resisted. Even though our two-dimensional mechanics estimate 640 N of tensile force on this ligament, we do not account for the muscular co-contraction to stabilize the knee, nor do we account for the forces absorbed in the cartilage. In these experiments, we demonstrated that the musculo-tendon units provided enough reaction force to stabilize the knee and safely accomplish the squat during these brief exercise protocols. What we do need to be concerned with is the potential for repetitive motion injuries.

Cycle Ergometry Comparison

Peak foot reaction forces vary with exercise. For stair-stepping or cycling, they do not exceed body weight [114, 116], and therefore the bone loading is less than that during the squat exercise.

However, the frontal plane knee torque still exists, and may be significantly larger than during the squat. It may be as high as 30 Nm from the cycling biomechanics alone [107], and Coriolis-induced torques may approach 2 Nm in this same plane (120 RPM pedal cadence at 30 RPM centrifugation). Although the forces between a squat and cycling are significantly different, the magnitude of the torque in the frontal plane at the knee joint is similar. Anecdotal evidence suggests that a once per pedal revolution of the knee torque may be responsible for repetitive motion injuries in the knee during cycling, especially with the feet rigidly attached to the pedals. The use of swivel toe-clips helps to reduce this mechanically-induced torque, and would be highly recommended for supine cycling on a centrifuge.

Muscle Activity

The surface EMG data provided us with a great deal of information regarding muscular activity during artificial gravity exercise. In Experiment 1 we were primarily interested in the asymmetry (or symmetry) in the same muscle between the right and left leg. This was motivated by our findings of the asymmetry in the right and left foot reaction forces. The EMG data from Experiment 2 was used to characterize the muscle activity over various knee angles. It was used to define artificial gravity exercise parameters based on similar upright responses.

Percent MVIC Normalization

One of the challenges of surface EMG testing, in addition to skin preparation and electrode placement, is the normalization process. We asked the subject to perform a series of maximum voluntary isometric contractions (MVICs) before starting the experiment to record the activity in the muscle during maximum volitional work. Even though the subjects were healthy and trained on how to perform the task, we found a difference in the muscle activity between the dominant and non-dominant leg. This is why in Experiment 1, we compared the %MVIC ratio between the left and right leg over time. A difference in left and right leg %MVIC would appear as a bias in the ratio and not as a significant difference between the legs. In Experiment 2, we compared the muscle activity in a single leg across the various conditions to avoid this issue.

Left-Right Leg Asymmetry

We looked at the ratio of the %MVIC activity in the left leg to the %MVIC in the right leg for each of the seven muscles (soleus, medial and lateral gastrocnemius, tibialis anterior, vastus

medialis and lateralis, and rectus femoris) we tested. Of these seven muscles, only three (soleus, vastus lateralis, and vastus lateralis) showed the same asymmetry as the foot reaction forces during centrifugation.

The soleus, an antigravity muscle that is composed mainly of type I fibers, controls anterior-posterior posture and aids in plantar flexion of the foot. The postural correction for the Coriolis accelerations, as well as the foot placement, was likely responsible for this asymmetry. Since the feet were close together and only slightly elevated relative to the frontal plane, the subject coordinated a postural correction by plantar flexing with more pressure on the ball of the foot.

We also saw the left-right leg asymmetry in the vastus lateralis and vastus medialis. These muscles are approximately a 50-50 mix of type I and type II fibers and are primarily responsible for knee extension. In the descent phase of the squat there was a greater eccentric loading on the left leg and during the ascent phase there is a greater concentric loading on the right leg, which was the origin of this asymmetry. We found no asymmetry in the rectus femoris between the right and left leg. The rectus femoris was relatively inactive over the knee angles (30- to 75-degrees) where the greatest Coriolis acceleration was generated (Figure 75).

The medial and lateral head of the gastrocnemius, as well as the tibialis anterior did not show any asymmetry. These muscle groups were relatively inactive ($< 15\%$ MVIC) throughout the entire range of motion during either the upright or centrifuge supine squats (Figure 70 thru Figure 72). Even if there was an asymmetry, it would be difficult to isolate and confirm within these inactive muscles. The foot placement during these squats resulted in knee and hip flexion over the entire squat cycle. This puts the gastrocnemius and rectus femoris, the “two-joint” muscles, at a mechanical disadvantage, and that may explain the lack of activity and asymmetry in these muscle groups.

Comparison between Upright and AG Supine Squats

Experiment 2 was designed to identify centrifuge supine exercise parameters that give similar responses to upright squats. We tested the same seven muscle groups in the left and right legs. However, we were not interested in the asymmetry between legs, but rather the differences between experimental conditions (rotation rate and resistance) within a leg. The muscles that

were the most active during the upright and centrifuge supine squats are the same as those during Experiment 1 (soleus, vastus lateralis, vastus medialis, rectus femoris). The other three muscles (tibialis, medial and lateral gastrocnemius) were active, but their activity rarely exceeded 15% MVIC.

In the majority of our conditions, we found a greater %MVIC during ascent than during descent, because of the greater contractile force. There was not a clear delineation of the muscle activity between levels of additional resistance, as seen with the foot forces (Figure 67), for at least two reasons. First, the muscles that were not active without any resistance continued to be inactive when additional resistance was added. Secondly, the resistive loads used worked the low end of the subject's exercise capability: small weight increases resulted in small %MVIC increases.

Despite these relatively low levels of activity, we proceeded to contrast the muscle activity at each knee angle across conditions (e.g., soleus muscle: Upright, 0% resistance vs. 23-RPM, 25% resistance, see Figure 81) (full tabulation of the contrasts is in the Appendix). We noticed that there were often several conditions that resulted in similar muscle activity. This made it particularly difficult to identify a set of artificial gravity supine squat parameters that produced similar muscle activity at each of the knee angles when upright. However, there were often sets of conditions that produced similar muscle activity over a majority of the knee angles. We explored twelve knee angles (six ascent, six descent). A criterion for matching AG and upright conditions for exercise programs could be similar activity at nine of the twelve knee angles (75% similar). Table 13 shows the number of knee angles where the soleus %MVIC data are not significantly different from one another at the various conditions.

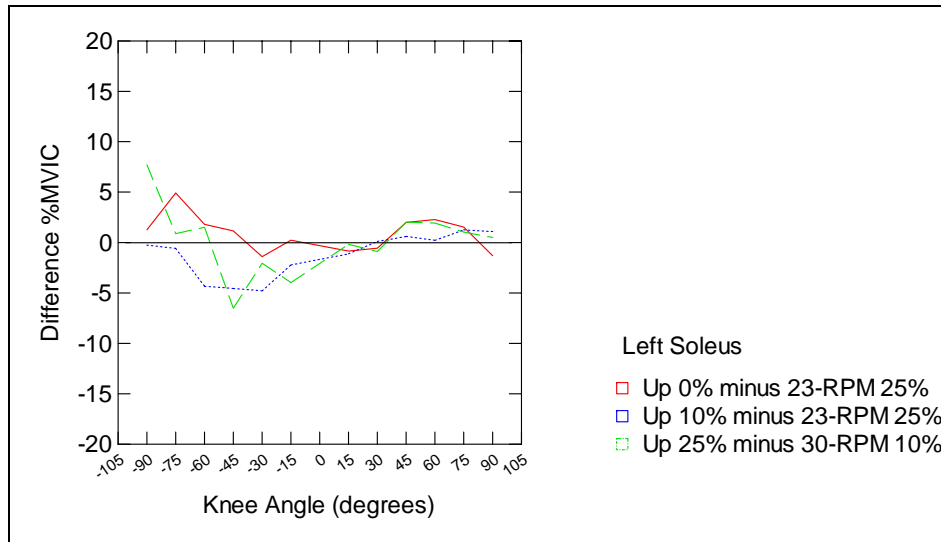


Figure 81. Difference in %MVIC between experimental conditions of the left soleus at various knee angles.

Table 13. Contrast table for the soleus %MVIC data. Out of the 12 knee angles we tested, the number of knee angles that are not significantly different between the conditions compared. The matching conditions where at least nine of the twelve knee angles produce similar activity are highlighted.

	Upright	23-RPM			30-RPM		
		0%	10%	25%	0%	10%	25%
Left Soleus	0%	6	10	11	7	6	1
	10%	5	6	12	7	7	3
	25%	1	4	8	9	10	7
Right Soleus	0%	6	8	8	3	0	0
	10%	2	5	11	7	3	0
	25%	0	4	5	4	8	0

The resistive force in these experiments, as we previously mentioned, was often at the low end of each subject’s capability. We believe this since the muscle activity only reached as high as 50% MVIC in the vastus lateralis, vastus medialis, and rectus femoris. Subjective reports of effort and visual observation of their performance showed that the rotation rate and resistance used, for a majority of the subjects, was not a particularly challenging protocol. By increasing the resistive load to 80% of 1-RM, as that suggested for many strength training protocols, we may achieve muscle activity in the quadriceps muscles as high as 80% MVIC during a 12-RM protocol (Figure 82).

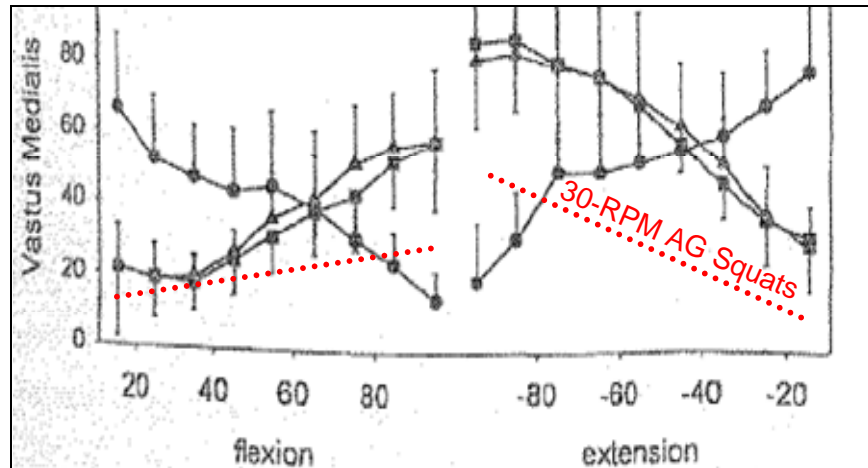


Figure 82. Vastus medialis %MVIC (triangles) as a function of knee angle (degrees). Muscle activity is from a 12-RM strength training protocol. Modified from [78].

Stabilization of the Knee

There are two ways to think about stabilization of the knee: internal stabilization of the joint, and stabilization of the knee in space. The co-contraction of the quadriceps and hamstrings works to internally stabilize the knee joint and reduce the loading on the ligaments [117]. Because of the mechanical torque from the mediolateral position of the knee and the Coriolis-induced knee torque, we might expect to see an asymmetry between the vastus lateralis and vastus medialis activity within each leg working to reduce the ligament loading. However, we did not find any evidence of this in our data.

During the AG supine squats, when Coriolis forces are deflecting the knee medially and laterally, within each leg we also might expect to see the hip abductors and adductors working to stabilize the knee in space. We did not record surface EMG from any of these muscles, so we cannot confirm this speculation.

Cycle Ergometry Comparison

The level of muscular activity between upright cycle ergometry [107, 118] and the centrifuge supine squats is likely quite similar. The greatest level of muscular activity reported during cycling occurred in the vastus lateralis and vastus medialis (~50% MVIC) as well as the soleus (~35% MVIC), which is nearly exactly what we found during the 30-RPM squats. The medial and lateral gastrocnemius were more active during cycling than during our experiments. Despite producing larger Coriolis acceleration (and torques) and resulting in lesser foot reaction forces,

cycle ergometry appears to be a potential exercise for the maintenance of muscular strength and endurance.

Motion Sickness and Perceived Effort

Subjective reports of motion sickness (0 – 20 scale) are often used to quantify an overall physiological adaptation to the nauseating stimulus of turning your head when on a fast-rotating centrifuge. We were not interested in these adaptation parameters, *per se*, but whether the AG supine squat stimulus makes you sick. The subjects reported their level of motion sickness after each set of eight repetitions in both Experiment 1 and 2. In Experiment 2, we had some objective measures of how hard the subjects were working (e.g., EMG, foot forces), but we wanted a subjective measure to confirm those results. We asked the subjects to rate how hard they were working on the Borg rating of perceived physical exertion (6 – 20 scale) after each set.

Motion Sickness

In these experiments, where the subject was instructed not to turn their head during the squat motions, we did not expect to see large reports (> 10 / 20) of motion sickness. However, because of the radial motion of the head, there were inter-aural Coriolis accelerations and dorsal-ventral inertial and centripetal accelerations acting on the otoliths. Gravity remained constant in the nasal-occipital direction. These accelerations created complex and oscillating (direction and magnitude) linear accelerations that “swing” the GIF vector in the sagittal and transverse planes. These accelerations can be approximated with the assumption that the subject’s head is at the center of rotation and they are performing a 0.5 Hz squat with 0.5 meter slider amplitude (Figure 83).

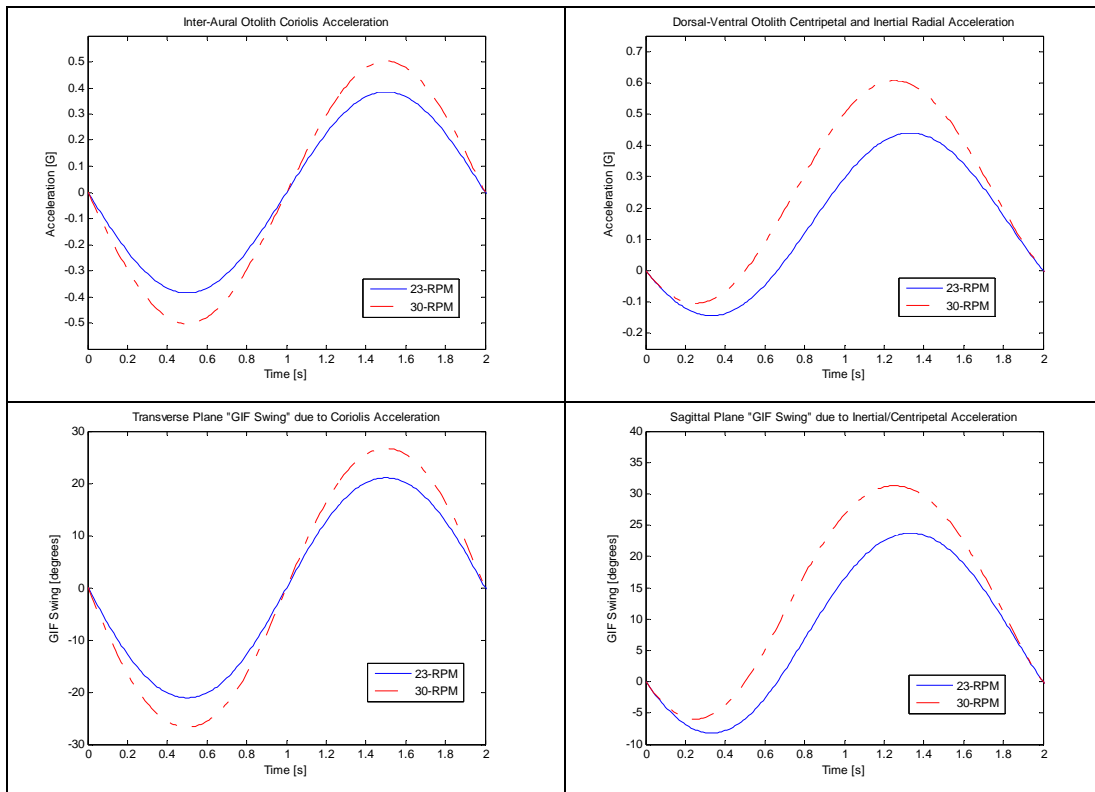


Figure 83. Accelerations on the otoliths organs from a 0.5 Hz squat with 0.5 m amplitude. Earth gravity is constant in the nasal-occipital direction. **Top left:** Inter-aural Coriolis accelerations. **Top right:** Dorsal-ventral inertial and centripetal accelerations. **Bottom left:** Coriolis-induced swing of the GIF vector in the transverse plane. **Bottom right:** Inertial/centripetal-induced swing of the GIF in the sagittal plane.

In these experiments, the largest subjective report of motion sickness was 5 / 20 and none of the subjects terminated the experiment because of sickness. This is encouraging since these induced accelerations are well-known to cause motion sickness [119]. Prior to starting Experiment 2, there was concern that the large number of centrifuge angular accelerations and decelerations (“spin-ups and spin-downs”) may have increased the motion sickness reports, but that was not the case.

Perceived Effort

The Borg rating of perceived physical exertion was used as a subjective measure for confirming the foot force and muscle activity data. This measure also gives us insights into the fatiguing nature of the protocols used: Group A vs. B in Experiment 2. We found that when the 30 RPM squats followed the 23 RPM squats, the Borg ratings increased with time, yet when the 23 RPM squats followed the 30 RPM squats, the Borg ratings were approximately constant (cross effect

between rotation rate and group). From a subject effort point of view, this suggests that if a multi-RPM protocol is to be used the higher rotation speed should precede the lower.

AG Squat Exercise Protocol Design

Based on the results of this work, there are many factors that need to be taken into account when designing centrifuge-based squat exercise protocols. The direct comparison of AG supine and upright squats has given us a great insight into the designing protocols that account for these factors. Briefly, we must consider the rotation rate, the magnitude of the resistive force (if any), movement of the torso along the centrifuge radius vs. movement of the feet, and body orientation (supine vs. shoulder down). We must also consider how these factors would be affected if you are exercising on a centrifuge in an orbiting laboratory.

Rotation Rate and Resistance

The angular velocity of the centrifuge and the additional resistance are probably the two most important parameters involved in designing centrifuge squat exercise programs. These parameters contribute to the magnitude of the Coriolis accelerations, the static loading of the subject, the peak foot forces during each repetition, and the magnitude of the muscle activity. The Coriolis accelerations affect our performance both directly, by deflecting the knees medially and laterally and inducing frontal plane joint torques when exercising supine, and indirectly by creating illusions of body tilt that are reflected in the foot forces. We can reduce or eliminate the effects of these Coriolis accelerations by spinning the centrifuge slower (23 RPM or less), choosing an appropriate foot position and foot external rotation, or change the direction of the Coriolis acceleration vector by putting the subject on their side.

The “standing weight” of the subject is important for the tonic loading of the musculoskeletal system, but it is the low frequency, high impact loads from the squat motion itself that are important for the maintenance of bone mineral density. It was easier to match artificial gravity “standing weights” with 1-G body weights by varying rotation rate and resistance, but more difficult to match peak foot reaction forces with only a single exercise cadence. Our ability to successfully predict foot reaction forces from the kinematic data could be used for designing exercise protocols at other cadences, rotation rates, and levels of resistance. This estimation is

gravity-independent, which would make it an ideal method for evaluating current space-flight exercise hardware designs as well as designing future ones.

Muscle activity during AG squats, on the other hand, was often surprisingly similar to upright over several rotation rates and levels of resistance. It was even possible to match the muscle activity over a large number of knee angles within a set of conditions, unlike the foot reaction forces. Although, the large number of similar conditions may have resulted from the small increment increase in muscle activity with additional resistance.

An ideal approach would: 1) include a rotation rate (and centrifuge radius) that would result in a standing foot reaction force equivalent to body weight, 2) squat exercise equipment that when used replicates upright exercise foot reaction forces and muscle activity in a manner for maintaining or developing strength and endurance, 3) provides both high frequency, low magnitude and low frequency, high magnitude foot reaction forces [49, 120], 4) provide sufficient stress to maintain cardiovascular function, and 5) reduces neurovestibular and sensory-motor disturbances.

Body Orientations

If the subjects were to be supine on the centrifuge and performed squats by moving their torso along the radius of the centrifuge, we would have to deal with the Coriolis accelerations continually deflecting our limbs and the left-right force/muscle activity asymmetry. The centrifuge would have to be spun in both directions to balance the muscular and skeletal consequences of asymmetric foot loading, which is less than ideal from a neurovestibular adaptation point of view.

An appropriate selection of body orientation could help eliminate these problems. A subject on their side so that either their face or back were “into the wind” during rotation would place the Coriolis accelerations in the anterior-posterior direction. Therefore, we would not have any Coriolis-induced medial-lateral deflection of the knee, or a side-to-side perception of tilt. On Earth, however, this would not be comfortable because of the necessary hip abduction to resist the gravity torque on the upper leg. It would work nicely in weightlessness. The Coriolis accelerations in this orientation, however, may induce an illusion of postural instability in the

anterior-posterior direction. This would need to be overcome by adequate support, training, and/or harnessing, especially if the squat motions were to be performed in darkness.

While remaining supine, it is possible to adjust the foot positioning for reducing the magnitude of the Coriolis acceleration in the +/- body y-axis by 1) elevating the feet above the torso, and 2) external rotation of the feet. A proper foot placement, which may not be comfortable for exercise, will only reduce the Coriolis accelerations by a small magnitude. However, by choosing a body orientation, other than supine, along with proper foot placement it may be possible to eliminate the Coriolis accelerations.

Torso vs. Foot Motion

In addition to manipulating the body orientation, we may also provide the resistive force to the legs by fixing the feet and moving the torso along the radius of the centrifuge (as we did in these experiments) or by fixing the torso and allowing the feet to move. Each of these options (“torso motion” and “foot motion”) has their advantages and disadvantages.

Torso motion provides the “inertial feel” to the squat exercise motions. The lack of this has been cited as possible causes for the ineffectiveness of the iRED in preventing musculoskeletal deconditioning in ISS astronauts and cosmonauts [65-67]. It has also been a motivator for the development of the advanced resistive exercise device (ARED) [68]. On the other hand, the linear movement of the large torso mass results in Coriolis-induced hip and knee torques in the frontal plane (when supine) and sagittal plane (when shoulder down).

Providing sufficient resistive force with foot motion may require tremendous, carefully counterbalanced, mass system or a bungee/spring resistance assembly. If we consider the spring resistance, this would not provide the inertial feel which has been a shortfall of previously designed spaceflight exercise devices. However, it would reduce the large Coriolis torques at the hip (knee torques would still exist).

Future Work

This research program has provided us with a great deal of information regarding the operational and safety issues associated with artificial gravity resistive exercises. It has also sparked new

scientific questions regarding exercise during short-radius centrifugation. We present a few topics and questions that should be considered in future studies:

- Explore clockwise and counterclockwise rotation, and body orientations (if practical).
- Are sensory-motor after-effects seen in other post-centrifugation movements? Long-term sensory-motor consequences from AG motions?
- Investigate the differences in squat biomechanics between “foot motion” and “torso motion.”
- What are the long-term strength training effects and benefits from working out on-board centrifuges (short, medium, or large radius)?
- What is the optimum strength training protocol in an environment that allows you to set the G-level and gravity gradient?
- How might the joint torques and injury risk be affected by physiological de-conditioning?
- Implement multi-axis foot force sensors to determine the Coriolis-induced loading at the feet for developing a higher-fidelity biomechanical model.
- What are the cardiovascular responses to AG squats? How do they differ from cycle ergometry, or other exercises?

Chapter 8: Conclusions and Recommendations



“The Earth is the cradle of humanity, but mankind cannot stay in the cradle forever.”
Konstantin Tsiolkovsky

Two experiments, along with modeling efforts, investigated the effects that a rotating environment and gravity gradient has on our squat biomechanics. We recorded the three-dimensional position of the left and right knee, one-dimensional foot reaction forces, and muscle activity while performing squats upright and while lying supine on a clockwise rotating short-radius centrifuge. These experiments investigated the effects Coriolis forces have on the mediolateral position of our knees as well as the sensory-motor adaptation to these forces at several rotation rates and levels of additional resistive force at a single exercise cadence. The biomechanical data collected during the upright squats was compared and contrasted with the artificial gravity supine squats to define centrifuge exercise parameters.

These findings are important for developing and implementing safe and effective artificial gravity exercise protocols. Although artificial gravity research has been conducted for over forty years, results and conclusions on efficacy of the operating parameters are just beginning to emerge. Recent literature on AG exercise has focused on cardiovascular de-conditioning, primarily cycle ergometry, with little or no mention of strength training or biomechanics. Musculoskeletal and cardiovascular exercises will likely be added to a centrifuge on a Mars-transit spacecraft to achieve a time- and cost-efficient and safe comprehensive countermeasure.

The main conclusions of these two experiments are:

- Coriolis accelerations induced significant mediolateral perturbations in our knees while performing 0.5 Hz cadence supine squats. Total mediolateral travel of the knees during centrifugation was 1.0 cm greater than non-rotating supine squats (body weight resistance) and 2.0 cm greater than upright squats (Figure 84).

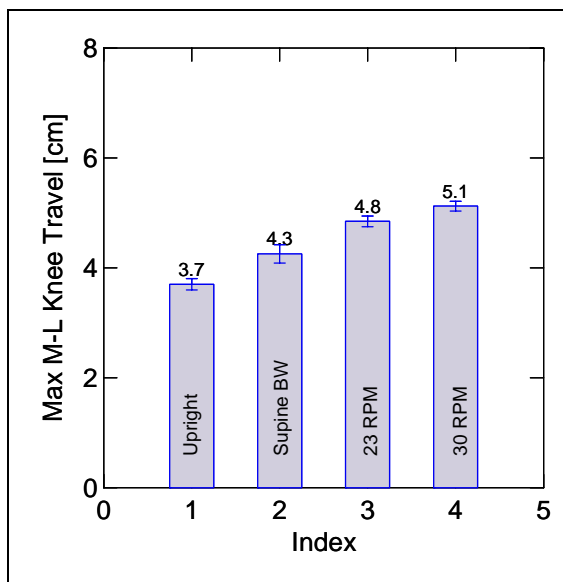


Figure 84. Maximum average mediolateral knee travel while upright, supine, and while rotating at 23 and 30 RPM. Data from Experiment 2. All levels of resistance averaged together while upright and while rotating. Mean +/- SEM.

- the magnitude of the Coriolis accelerations on the thigh (0.32 G) and shin (0.07 G) at 30-RPM centrifugation induce frontal plane knee torque of up to 0.6 Nm. For comparison: a 120 RPM cycling cadence at 30 RPM centrifugation will result in thigh accelerations of 0.6 G and 0.12 G on the shin (2 Nm frontal plane knee torque). A single, or low-frequency (~100 to 200 squat repetitions per week), occurrence of this knee torque is unlikely to cause repetitive stress knee injuries. Longer-duration and higher frequency, such as the thousands of repetitions in a single cycling workout (~ 1 hour) could result in repetitive stress injuries in the knee.
- mediolateral knee travel did not increase with rotation rate, and was unaffected by adding additional resistive force to the squat.
- there was no evidence of sensory-motor after-effects from a forty repetition (5 sets of 8 repetitions) protocol at either 23 or 30 RPM (Figure 85).

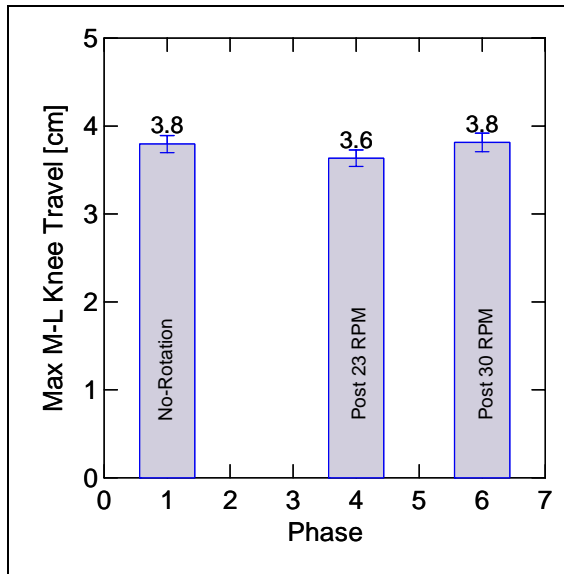


Figure 85. Maximum average mediolateral knee travel without rotation and after a forty repetition artificial gravity squat protocol at 23 and 30 RPM. Mean +/- SEM.

- the ratio of left to right foot reaction force was non-constant and concordant with a postural correction for the lateral Coriolis accelerations.

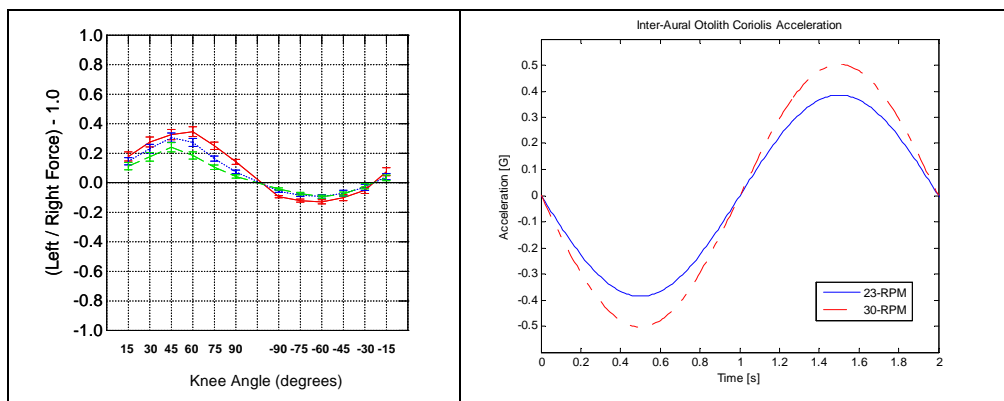


Figure 86. Left: Left-to-right foot force ratio minus 1.0 during 30 RPM squats. Mean +/- SEM. Right: Inter-aural Coriolis acceleration during 0.5 Hz squats. This figure illustrates the fact that the foot force compensation is 180 degrees out of phase with the Coriolis accelerations. Although the abscissas of the graphs are different units (degrees vs. time), both plots represent one cycle of the squat.

- the rectus femoris, vastus lateralis, and vastus medialis muscles had the greatest muscle activity (up to 50% MVIC) during either the upright or 30 RPM centrifuge supine squats. The soleus was active up to 40% MVIC. The ratio of the left to right leg vastus lateralis, vastus medialis, and soleus muscle activity showed the same non-constant asymmetry as the foot forces.

- foot reaction forces and muscle activity during the 30 RPM squats were more similar to upright than 23 RPM forces and muscle activity, which were less than upright (Figure 87). Peak foot forces approached 200% body weight during 30 RPM squats with 25% body weight resistance.

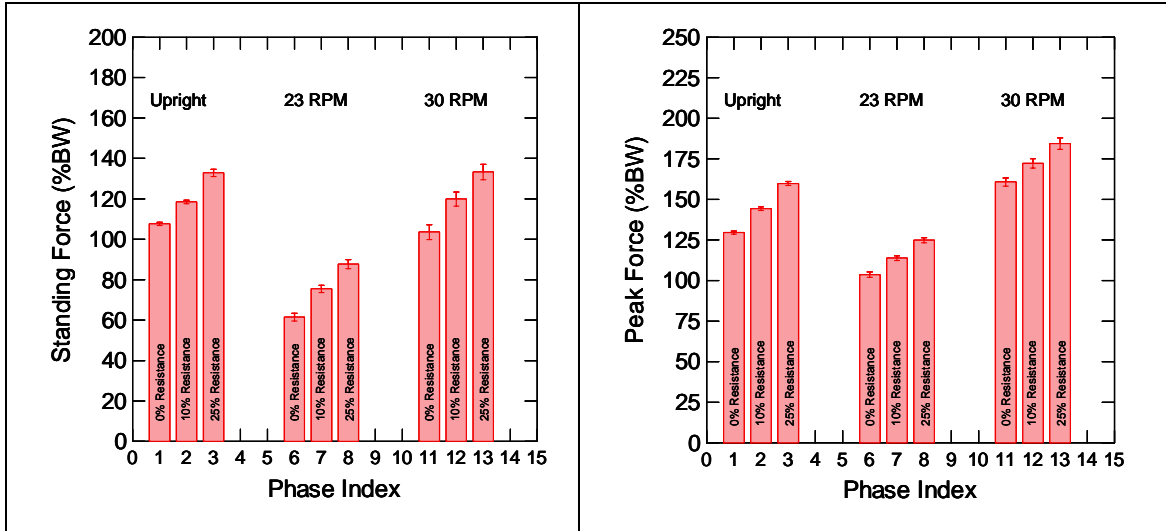


Figure 87. Left: Standing force as a percentage of body weight while standing upright, and lying supine at 23 and 30 RPM squats (Experiment 2). N = 12. Mean +/- SEM. Right: Peak force as a percentage of body weight during upright squats, and AG supine squats at 23 and 30 RPM (Experiment 2). N = 12. Mean +/- SEM.

- the greatest motion sickness report was 5 out of 20 despite the +/- 0.5 G inter-aural Coriolis and -0.15 to +0.60 dorsal-ventral inertial/centripetal oscillating accelerations.

The results and conclusions from this research program have led to several recommendations for the design and implementation of future artificial gravity exercise protocols. We recommend:

- orient the subject's body so that they are left or right shoulder down to minimize (or reduce) the medial-lateral Coriolis accelerations. If earth supine, spin the centrifuge in both directions to balance left-to-right foot force asymmetry (or alternate supine / prone postures).
- increase the rotation rate and/or resistance for muscular training programs. It is recommended by the ACSM to train at a high intensity until momentary muscular fatigue. The squat protocol should have at least three sets of 8 to 12 repetitions (80% 1-RM) three times per week plus warm-up and cool down.

- increase the rotation rate, resistance, or add “impactors” to the feet for maintenance of bone mineral density. Impactors should be designed to engage when the subjects is at near full knee extension (~15 degrees) in the ascent phase. Peak foot reaction forces were, on average, 2.0 times body weight. We would like them at least 2.6 times body weight (earth jogging).
- use the biomechanical model developed to in this work to design squat exercise protocols for future centrifuges: short-, medium-, or large-radius. Choose appropriate exercise parameters based on the centrifuge radius, rotation rate, and exercise cadence.
- consider foot motion rather than torso motion if the resistive load and “inertial feel” can be replicated to eliminate the “swinging GIF” at the head.
- implementing AG exercise as a countermeasure on an interplanetary (Mars-transit) spacecraft. Squats on a short-radius centrifuge can provide sufficient stress to the musculo-skeletal system. Consider mounting a “multi-gym” on the centrifuge to save space within the vehicle and time during exercise countermeasure prescription.

References

- [1] NSBRI. (cited 2006) Research Areas: National Space Biomedical Research Institute. Available from: <http://www.nsbri.org/Research/index.html>.
- [2] NASA/SP-2004-6113. (2004) Bioastronautics Roadmap: A Risk Reduction Strategy for Human Space Exploration. p. 1-164.
- [3] Davis, J.R. (1999) Medical issues for a mission to Mars. Aviation, Space, and Environmental Medicine. 70(2): p. 162-8.
- [4] Diamandis, P.H. (1988) The Artificial Gravity Sleeper: A Deconditioning Countermeasure for Long Duration Space Habitation, S.M. Thesis in Aeronautics and Astronautics. Massachusetts Institute of Technology: Cambridge, MA.
- [5] Paloski, W.H. and L.R. Young. (1999) NASA/NSBRI Artificial Gravity Workshop: Proceedings and Recommendations. p.
- [6] Caiozzo, V.J., et al. (2004) Hemodynamic and metabolic responses to hypergravity on a human-powered centrifuge. Aviation, Space, and Environmental Medicine. 75(2): p. 101-8.
- [7] Iwase, S. (2004) Effectiveness of centrifuge-induced artificial gravity with ergometric exercise as a countermeasure during simulated microgravity exposure in humans. in Proceedings of the 55th International Astronautical Congress 2004. Vancouver, Canada.
- [8] Iwase, S., et al. (2003) Effects of Simultaneous Load of Centrifuge-Induced Artificial Gravity and Ergometer Exercise as the Countermeasures for Space Deconditioning on Human Cardiovascular Function. Journal of Gravitational Physiology. 10(1): p. P-101-104.
- [9] Katayama, K., et al. (2004) Acceleration with Exercise During Head-Down Bed Rest Preserves Upright Exercise Responses. Aviation, Space, and Environmental Medicine. 75: p. 1029-35.
- [10] Edmonds, J. (2005) Exercise in Artificial Gravity, SM in Aeronautics and Astronautics. Massachusetts Institute of Technology: Cambridge, MA.
- [11] DiZio, P. and J.R. Lackner. (2002) Sensorimotor aspects of high-speed artificial gravity: III. Sensorimotor adaptation. Journal of Vestibular Research. 12(5-6): p. 291-9.
- [12] Nicogossian, A., C.F. Sawin, and C.L. Huntoon. (1994) Chapter 11: Physiologic adaptation to space flight, in Space Physiology and Medicine, A. Nicogossian, C.L. Huntoon, and S.L. Pool, Editors. Lea & Fibiger: Philadelphia.

- [13] Jennings, R.T., J.R. Davis, and P.A. Santy. (1988) Comparison of aerobic fitness and space motion sickness during the shuttle program. *Aviation, Space, and Environmental Medicine*. 59: p. 448-451.
- [14] Buckey, J.C., Jr. (2006) Space Physiology. New York: Oxford University Press.
- [15] Oman, C.M. (2003) Chapter 19: Human Visual Orientation in Weightlessness, in Levels of Perception, L.R. Harris and M. Jenkin, Editors. Springer-Verlag: New York. p. 375-395.
- [16] Paloski, W.H., et al. (1999) Recovery of Postural Equilibrium Control Following Space Flight (DSO 605), in Extended duration orbiter medical project final report 1989-1995. NASA SP-1999-534, C.F. Sawin, G.R. Taylor, and W.L. Smith, Editors. p. 5.4-1 - 5.4-16.
- [17] Bloomberg, J.J. and A.P. Mulavara. (2003) Changes in Walking Strategies after Spaceflight. *IEEE Engineering in Medicine and Biology Magazine*. (March/April): p. 58-62.
- [18] Bloomberg, J.J., et al. (2001) Locomotion after long-duration spaceflight: Adaptive modulation of a full-body head and gaze stabilization system. in *Proceedings of the Bioastronautics Investigators' Workshop*. Galveston, Texas.
- [19] Astrand, P.-O., et al. eds. (2003) *Textbook of Work Physiology: Physiological Bases of Exercise, 4th Edition*. Human Kinetics: Champaign, IL.
- [20] Heldt, T. (2004) Computational Models of Cardiovascular Response to Orthostatic Stress, Doctor of Philosophy in Medical Physics in Harvard - MIT Division of Health Sciences and Technology. Massachusetts Institute of Technology: Cambridge, MA.
- [21] Thornton, W.E., G.W. Hoffler, and J.A. Rummel. (1977) Chapter 32: Anthropometric Changes and Fluid Shifts, in Biomedical Results from Skylab (NASA SP-377), R.S. Johnston and L.F. Dietlein, Editors. p. 330-338.
- [22] Guyton, A.C. and J.E. Hall. (2000) Textbook of Medical Physiology. Tenth ed: W.B. Saunders Company.
- [23] Convertino, V.A. (1996) Exercise as a countermeasure for physiological adaptation to prolonged spaceflight. *Medicine and Science in Sports and Exercise*. 28(8): p. 999-1014.
- [24] Fritsch-Yelle, J.M., et al. (1996) Subnormal norepinephrine release relates to presyncope in astronauts after spaceflight. *Journal of Applied Physiology*. 81(5): p. 2134-41.
- [25] Greenisen, M.C., J.C. Hayes, and S.F. Siconolfi. (1999) Functional Performance Evaluation, in Extended duration orbiter medical project final report 1989-1995. NASA SP-1999-534, C.F. Sawin, G.R. Taylor, and W.L. Smith, Editors. p. 3-1 - 3-24.

- [26] Levine, B.D., et al. (1996) Maximal exercise performance after adaptation to microgravity. *Journal of Applied Physiology*. 81(2): p. 686-94.
- [27] Newman, D.J. and D.K. Jackson. (2000) Chapter 20: Altered Astronaut Performance Following Spaceflight: Control and Modeling Insights, in Biomechanics and Neural Control of Posture and Movement, J. Winters and P. Crago, Editors. Springer-Verlag. p. 282-291.
- [28] Edgerton, V.R. and R.R. Roy. (1993) Neuromuscular Adaptations to Actual and Simulated Spaceflight (Manuscript), in APS Handbook of Physiology, Section 4, Adaptation to the Environment, M.J. Fregly and C.M. Blatteis, Editors. Oxford University Press.
- [29] LeBlanc, A., et al. (1995) Regional muscle loss after short duration spaceflight. *Aviation, Space, and Environmental Medicine*. 66(12): p. 1151-4.
- [30] LeBlanc, A., et al. (2000) Muscle volume, MRI relaxation times (T2), and body composition after spaceflight. *Journal of Applied Physiology*. 89(6): p. 2158-64.
- [31] Smith, M.C., Jr., et al. (1977) Chapter 20: Bone Mineral Measurement -- Experiment M078, in Biomedical Results from Skylab (NASA SP-377), R.S. Johnston and L.F. Dietlein, Editors. NASA Scientific and Technical Information Office: Washington, D.C. p. 183-190.
- [32] Miyamoto, A., et al. (1998) Medical baseline data collection on bone and muscle change with space flight. *Bone*. 22(5 Suppl): p. 79S-82S.
- [33] LeBlanc, A., et al. (2000) Bone mineral and lean tissue loss after long duration space flight. *J Musculoskelet Neuronal Interact*. 1(2): p. 157-60.
- [34] Oganov, V. and V.S. Schneider. (1996) Skeletal system, in Space Biology and Medicine, A. Nicogossian and O.G. Gzenko, Editors. American Institute of Aeronautics and Astronautics: Reston, VA. p. 247-266.
- [35] Shackelford, L.C., et al. (2004) Resistance exercise as a countermeasure to disuse-induced bone loss. *Journal of Applied Physiology*. 97(1): p. 119-29.
- [36] Linenger, J.M. (2000) Off the Planet. New York: McGraw-Hill.
- [37] Sibonga, J.D. (2005) What happens to bone health during and after spaceflight? in Proceedings of the Bone Loss During Spaceflight. Cleveland, OH.
- [38] Zerwekh, J. (2005) What is the risk of renal stones during spaceflight? in Proceedings of the Bone Loss During Spaceflight. Cleveland, OH.

- [39] Schaffner, G. (1999) Assessment of hip fracture risk in astronauts exposed to long-term weightlessness, Doctor of Philosophy in Medical Engineering in Aeronautics and Astronautics. Massachusetts Institute of Technology: Cambridge, MA.
- [40] Beyene, N.M. (2004) The Art of Space Flight Exercise Hardware: Design and Implementation. in Proceedings of the Space 2004 Conference and Exhibit. San Diego, California.
- [41] Coolahan, J.E., A.B. Feldman, and S.P. Murphy. (2004) Integrated Physiological Simulation of an Astronaut Exercise Protocol. in Proceedings of the 55th International Astronautical Congress. Vancouver, Canada.
- [42] Williams, D.R. (2003) The Biomedical Challenges of Space Flight. Annual Reviews of Medicine. 54: p. 245-256.
- [43] Lu, E. (cited 2005) Working Out. Available from: http://spaceflight.nasa.gov/station/crew/exp7/luletters/lu_letter7.html.
- [44] Bloomberg, J.J., et al. (2005) Development of an inflight countermeasure to mitigate postflight gait dysfunction. in Proceedings of the Bioastronautics Investigators' Workshop. Galveston, TX.
- [45] Whaley, M.H., P.H. Brubaker, and R.M. Otto. eds. (2006) *American College of Sports Medicine's Guidelines for Exercise Testing and Prescription*. Lippincott Williams & Wilkins: Philadelphia. 1-366.
- [46] Turner, C.H. (1998) Three Rules for Bone Adaptation to Mechanical Stimuli. Bone. 23(5): p. 399-407.
- [47] Turner, C.H. and A.G. Robling. (2003) Designing exercise regimens to increase bone strength. Exerc Sport Sci Rev. 31(1): p. 45-50.
- [48] Rubin, C.T. and L.E. Lanyon. (1984) Regulation of bone formation by applied dynamic loads. J Bone Joint Surg Am. 66(3): p. 397-402.
- [49] Qin, Y.X., C.T. Rubin, and K.J. McLeod. (1998) Nonlinear dependence of loading intensity and cycle number in the maintenance of bone mass and morphology. Journal of Orthopaedic Research. 16(4): p. 482-9.
- [50] Rubin, C., et al. (2004) Prevention of Postmenopausal Bone Loss by a Low-Magnitude, High-Frequency Mechanical Stimuli: A Clinical Trial Assessing Compliance, Efficacy, and Safety. Journal of Bone and Mineral Research. 19(3): p. 343-351.
- [51] Greenleaf, J.E., et al. (1989) Work capacity during 30 days of bed rest with isotonic and isokinetic exercise training. Journal of Applied Physiology. 67(5): p. 1820-6.

- [52] Greenleaf, J.E., et al. (1992) Effect of leg exercise training on vascular volumes during 30 days of 6-degrees head-down bed rest. *Journal of Applied Physiology*. 72(5): p. 1887-1894.
- [53] Akima, H., et al. (2005) Intensive cycle training with artificial gravity maintains muscle size during bed rest. *Aviation, Space, and Environmental Medicine*. 76(10): p. 923-9.
- [54] Webster, B. (2006) Low magnitude high frequency vibrations applied to the foot through the pedal of a human powered artificial gravity (HPAG) cycle, S.M. in *Aeronautics and Astronautics*. Massachusetts Institute of Technology: Cambridge, MA.
- [55] Nicogossian, A., S. Pool, and C. Sawin. (1995) Status and efficacy of countermeasures to physiological deconditioning from space flight. *Acta Astronautica*. 36(7): p. 393-8.
- [56] CCF. (cited 2006) The Cleveland Clinic Center for Space Medicine. Available from: <http://www.lerner.ccf.org/csm/>.
- [57] Cavanagh, P.R. (cited 2006) Foot/Ground Reaction Forces During Space Flight (Foot). Available from: <http://exploration.nasa.gov/programs/station/Foot.html>.
- [58] Cavanagh, P.R., et al. (2005) Foot Reaction Forces During Simulated ISS Exercise Countermeasures. in *Proceedings of the Bioastronautics Investigators' Workshop*. Galveston, TX.
- [59] Schaffner, G., et al. (2005) Effect of load levels of subject loading device on gait, ground reaction force, and kinematics during human treadmill locomotion in a weightless environment (NASA/TP-2005-213169). NASA Johnson Space Center p. 1-40.
- [60] Convertino, V.A. (1991) Neuromuscular aspects in development of exercise countermeasures. *Physiologist*. 34(1 Suppl): p. S125-8.
- [61] Bembien, D.A., et al. (2000) Musculoskeletal responses to high- and low-intensity resistance training in early postmenopausal women. *Medicine and Science in Sports and Exercise*. 32(11): p. 1949-57.
- [62] Layne, J.E. and M.E. Nelson. (1999) The effects of progressive resistance training on bone density: a review. *Medicine and Science in Sports and Exercise*. 31(1): p. 25-30.
- [63] Baldwin, K.M., et al. (1996) Musculoskeletal adaptations to weightlessness and development of effective countermeasures. *Medicine and Science in Sports and Exercise*. 28(10): p. 1247-53.
- [64] Tesch, P.A. and H.E. Berg. (1997) Resistance Training in Space. *International Journal of Sports Medicine*. 18(Supplement 4): p. s322-324.

- [65] Lee, S.M., et al. (2004) Foot-ground reaction force during resistive exercise in parabolic flight. Aviation, Space, and Environmental Medicine. 75(5): p. 405-12.
- [66] Schneider, S.M., et al. (2003) Training with the International Space Station interim resistive exercise device. Medicine and Science in Sports and Exercise. 35(11): p. 1935-45.
- [67] Amonette, W.E., et al. (2004) Ground Reaction Force and Mechanical Differences Between the Interim Resistive Exercise Device (iRED) and Smith Machine While Performing a Squat. Lyndon B. Johnson Space Center (NASA/TP-2004-212063). p. 1-39.
- [68] Bentley, J.R., et al. (2006) Advanced Resistive Exercise Device (ARED) Man-in-the-Loop Test (MILT). Lyndon B. Johnson Space Center -- Wyle Laboratories (NASA/TP-2006-213717). p. 31.
- [69] Bamman, M.M., et al. (1998) Impact of resistance exercise during bed rest on skeletal muscle sarcopenia and myosin isoform distribution. Journal of Applied Physiology. 84(1): p. 157-63.
- [70] Gallagher, P., et al. (2005) Effects of 84-days of bedrest and resistance training on single muscle fibre myosin heavy chain distribution in human vastus lateralis and soleus muscles. Acta Physiol Scand. 185(1): p. 61-9.
- [71] Alkner, B.A. and P.A. Tesch. (2004) Efficacy of a gravity-independent resistance exercise device as a countermeasure to muscle atrophy during 29-day bed rest. Acta Physiol Scand. 181(3): p. 345-57.
- [72] Hueser, D., et al. (2004) The Fly Wheel Exercise Device (FWED): A countermeasure against Bone Loss and Muscle Atrophy. in Proceedings of the 55th International Astronautical Congress 2004. Vancouver, Canada.
- [73] Greenleaf, J.E., et al. (1994) Isokinetic strength and endurance during 30-day 6 degrees head-down bed rest with isotonic and isokinetic exercise training. Aviation, Space, and Environmental Medicine. 65(1): p. 45-50.
- [74] Greenleaf, J.E., et al. (1983) Handgrip and general muscular strength and endurance during prolonged bedrest with isometric and isotonic leg exercise training. Aviation, Space, and Environmental Medicine. 54(8): p. 696-700.
- [75] Morrissey, M.C., E.A. Harman, and M.J. Johnson. (1995) Resistance training modes: specificity and effectiveness. Medicine and Science in Sports and Exercise. 27(5): p. 648-60.
- [76] Bloomberg, J., et al. (2006) Development of In-Flight Countermeasures with Multimodal Effects - Muscle Strength and Balance Function. in Proceedings of the The Seventh

Symposium on the Role of the Vestibular Organs in Space Exploration. Noordwijk, the Netherlands.

- [77] Bloomberg, J. (cited 2006) Promoting Sensorimotor Response Generalizability: A Countermeasure to Mitigate Locomotor Dysfunction After Long-Duration Space Flight (Mobility). Available from: <http://exploration.nasa.gov/programs/station/Mobility.html>.
- [78] Escamilla, R.F., et al. (1998) Biomechanics of the knee during closed kinetic chain and open kinetic chain exercises. *Medicine and Science in Sports and Exercise*. 30(4): p. 556-69.
- [79] Escamilla, R.F., et al. (2001) A three-dimensional biomechanical analysis of the squat during varying stance widths. *Medicine and Science in Sports and Exercise*. 33(6): p. 984-98.
- [80] Escamilla, R.F., et al. (1997) The effects of technique variations on knee biomechanics during the squat and leg press. *Medicine and Science in Sports and Exercise*. 29(5): p. S156.
- [81] Abelbeck, K.G. (2002) Biomechanical model and evaluation of a linear motion squat type exercise. *Journal of Strength and Conditioning Research*. 16(4): p. 516-24.
- [82] McLaughlin, T.M., T.J. Lardner, and C.J. Dillman. (1978) Kinetics of the parallel squat. *Res Q*. 49(2): p. 175-89.
- [83] Klein, K.K. (1961) The deep squat exercise as utilized in weight training for athletes and its effects on the ligaments of the knee. *JAPMR*. 15(1): p. 6-11.
- [84] Woo, S.L., et al. (1991) Tensile properties of the human femur-anterior cruciate ligament-tibia complex. The effects of specimen age and orientation. *American Journal of Sports Medicine*. 19(3): p. 217-25.
- [85] Pandy, M.G. and K. Sasaki. (1998) A Three-Dimensional Musculoskeletal Model of the Human Knee Joint. Part 2: Analysis of Ligament Function. *Computational Methods in Biomechanics and Biomedical Engineering*. 1(4): p. 265-283.
- [86] Pandy, M.G., K. Sasaki, and S. Kim. (1998) A Three-Dimensional Musculoskeletal Model of the Human Knee Joint. Part 1: Theoretical Construct. *Computational Methods in Biomechanics and Biomedical Engineering*. 1(2): p. 87-108.
- [87] Shelburne, K.B. and M.G. Pandy. (1997) A musculoskeletal model of the knee for evaluating ligament forces during isometric contractions. *Journal of Biomechanics*. 30(2): p. 163-76.
- [88] Shelburne, K.B., et al. (2004) Pattern of anterior cruciate ligament force in normal walking. *Journal of Biomechanics*. 37(6): p. 797-805.

- [89] Escamilla, R.F. (2001) Knee biomechanics of the dynamic squat exercise. *Medicine and Science in Sports and Exercise*. 33(1): p. 127-41.
- [90] Tsiolkovsky, K.E. (1911) Exploration of global space with jets., in Collected Works (1954, in Russia): Nauka, Moscow. p. 100-139.
- [91] Young, L.R. (1999) Artificial gravity considerations for a mars exploration mission. *Annals of the New York Academies of Sciences*. 871: p. 367-378.
- [92] Hill, P.R. and E. Schnitzer. (1962) Rotating Manned Space Stations. *Astronautics*. 7(9): p. 14-18.
- [93] Graybiel, A., et al. (1965) Effects Of Exposure To A Rotating Environment (10 Rpm) On Four Aviators For A Period Of Twelve Days. *Aerospace Medicine*. 36: p. 733-54.
- [94] Brown, E.L., H. Hecht, and L.R. Young. (2002) Sensorimotor aspects of high-speed artificial gravity: I. Sensory conflict in vestibular adaptation. *Journal of Vestibular Research*. 12(5-6): p. 271-82.
- [95] Elias, P.Z. (2006) Incremental Adaptation to Yaw Head Movements During 30 RPM Centrifugation, S.M. in *Aeronautics and Astronautics*. Massachusetts Institute of Technology: Cambridge, MA.
- [96] DiZio, P. and J.R. Lackner. (1997) Deviations and rapid adaptation of leg movements perturbed by Coriolis forces in a rotating room. *Society for Neuroscience Abstracts*. 23: p. 1562.
- [97] Hoche, J. and A. Graybiel. (1973) The value of exercise at one-half earth gravity in preventing adaptation to simulated weightlessness. *Naval Aerospace Medical Research Laboratory* p.
- [98] Greenleaf, J.E., et al. (1997) Cycle-Powered Short Radius (1.9m) Centrifuge: Effect of Exercise Versus Passive Acceleration on Heart Rate in Humans. NASA Ames Research Center (NASA Technical Memorandum 110433). p. 1-13.
- [99] Kreitenberg, A., et al. (1998) The "Space Cycle" self powered human centrifuge: a proposed countermeasure for prolonged human spaceflight. *Aviation, Space, and Environmental Medicine*. 69(1): p. 66-72.
- [100] Kreitenberg, A., J.B. Witmer, and J. Spiegel. (2000) Space Cycle - Ground-Based Prototype Development. AIAA. 2000-5207: p. 1-10.
- [101] Watenpugh, D.E., et al. (1994) Dynamic leg exercise improves tolerance to lower body negative pressure. *Aviation, Space, and Environmental Medicine*. 65(5): p. 412-8.

- [102] Cardus, D. (1994) Artificial gravity in space and in medical research. Journal of Gravitational Physiology. 1(1): p. P19-22.
- [103] Davis, B.L., P.R. Cavanagh, and J.E. Perry. (1994) Locomotion in a rotating space station: a synthesis of new data with established concepts. Gait & Posture. 2: p. 157-65.
- [104] Yeadon, M.R. (1990) The simulation of aerial movement--II. A mathematical inertia model of the human body. Journal of Biomechanics. 23(1): p. 67-74.
- [105] Robinson, J.R., A.M. Bull, and A.A. Amis. (2005) Structural properties of the medial collateral ligament complex of the human knee. Journal of Biomechanics. 38(5): p. 1067-74.
- [106] van Dommelen, J.A.W., et al. (2005) Characterization of the Rate-Dependent Mechanical Properties and Failure of Human Knee Ligaments. SAE International. (2005-01-0293).
- [107] Ericson, M. (1986) On the Biomechanics of Cycling. Scandanavian Journal of Rehabilitation in Medicine Supplement. 16: p. 1-43.
- [108] Asplund, C. and P. St. Pierre. (2004) Knee Pain and Bicycling. The Physician and Sports Medicine. 32(4): p. 1-12.
- [109] Hecht, H., et al. (2001) Orientation illusions and heart-rate changes during short-radius centrifugation. Journal of Vestibular Research. 11(2): p. 115-27.
- [110] Basmanjian, J.V., R. Blumenstein, and M. Dismatsek. (1980) Electrode Placement in EMG Biofeedback. Baltimore, MD: The Williams and Wilkins Company.
- [111] Basmajian, J.V., R. Blumenstein, and M. Dismatsek. (1980) Electrode Placement in EMG Biofeedback. Baltimore, MD: The Williams and Wilkins Company.
- [112] Konrad, P. (2005) The ABC of EMG: A Practical Introduction to Kinesiological Electromyography. Scottsdale, AZ: Noraxon, Inc. 1-60.
- [113] Fleck, S.J. and W.J. Kraemer. (1987) Designing Resistance Training Programs. Second ed. Champaign, IL: Human Kinetics. pp. 1-275.
- [114] Thornton, W.E. (1986) Work, Exercise, and Space Flight II. Modification of Adaptation by Exercise (Exercise Prescription). in Proceedings of the Workshop on Exercise Prescription for Long-Duration Space Flight. Houston, TX: NASA CP-3051.
- [115] Cowin, S.C. ed. (1989) *Bone Mechanics*. CRC Press: Boca Raton, FL.
- [116] Edmonds, J., T. Jarchow, and L.R. Young. (forthcoming) A stair-stepper for exercising on a short-radius centrifuge [Accepted]. Aviation, Space, and Environmental Medicine.

- [117] Lloyd, D.G., T.S. Buchanan, and T.F. Besier. (2005) Neuromuscular biomechanical modeling to understand knee ligament loading. *Medicine and Science in Sports and Exercise*. 37(11): p. 1939-47.
- [118] Hull, M.L. and M. Jorge. (1985) A method for biomechanical analysis of bicycle pedalling. *Journal of Biomechanics*. 18(9): p. 631-44.
- [119] Money, K.E. (1970) Motion Sickness. *Physiological Reviews*. 50(1): p. 1-39.
- [120] Rubin, C., et al. (2001) Anabolism. Low mechanical signals strengthen long bones. *Nature*. 412(6847): p. 603-4.

Appendix A: Biographical Sketch

Kevin Ronald Duda

Department of Aeronautics and Astronautics
Massachusetts Institute of Technology
77 Massachusetts Avenue, Building 37-219
Cambridge, MA 02139
Voice: (617) 253-7509
Fax: (617) 253-8111
duda@mit.edu



Personal Data: Born October 11, 1979 in Greenfield, Massachusetts, but considers Whately, Massachusetts to be his hometown. He enjoys flying (private pilot with instrument rating), playing soccer, baseball, and golf, riding his motorcycle, and is an avid Red Sox fan.

Education: Graduated valedictorian from Frontier Regional High School, South Deerfield, Massachusetts, in 1997. He received a Bachelor of Science (Magna Cum Laude) in Aerospace Engineering from Embry-Riddle Aeronautical University (Daytona Beach campus) in 2001, and a Masters of Science in Aeronautics and Astronautics from the Massachusetts Institute of Technology in 2004. He recently defended his doctoral thesis and will receive a Doctor of Philosophy in the Department of Aeronautics and Astronautics at MIT in February 2007.

Research: While at ERAU, he participated in NASA's Reduced Gravity Student Flight Opportunities Program in 1998 and 2001. The research projects involved investigating fluid transport in a microgravity environment (1998) and the development and performance of a new EVA ratchet tool concept (2001). His master's research involved investigating the human perception of illusory self-motion as part of the Visuomotor and Orientation Investigations in Long-duration Astronauts (VOILA) ISS experiment (Advisor: Charles M. Oman, Ph.D.). Sensory- and visuo-motor research was conducted on earth and in parabolic flight. His doctoral dissertation research is focused on the biomechanics and physiological responses to exercise during short-radius centrifugation as a comprehensive countermeasure to the physiological deconditioning that results from long-duration spaceflight (Advisor: Laurence R. Young, Sc.D.). This research is in support of the International Multi-Disciplinary Artificial Gravity project, led by the NASA Johnson Space Center. He is also involved in a research collaboration between the MIT Man-Vehicle Laboratory and the Laboratory for Biomedical Technologies at the Politecnico di Milano (Milan, Italy) investigating motor control strategies in different gravito-inertial environments. All graduate research has been conducted in the MIT Man-Vehicle Laboratory.

Relevant Work Experience: He was an intern at Hamilton-Sundstrand Space Systems International (Windsor Locks, CT), summer 1999 and 2000. His responsibilities included obtaining and documenting operational and technical information on the Russian EVA System, the Orlan-M. He was also responsible for coordinating and publishing the latest revision of the

EMU Data Book for NASA. While at Embry-Riddle he held numerous positions within the academic departments (aerospace engineering, physical sciences, and mathematics) as a teaching assistant. As a Resident Advisor, he was responsible for counseling and advising numerous students, disciplinary action, and providing on-call services and crisis intervention.

Awards and Honors: The awards he has received include the “Outstanding Professional Development Award” from the Embry-Riddle Aeronautical University Aerospace Engineering Department, High School Valedictorian, Omicron Delta Kappa National Leadership Honor Society, Sigma Gamma Tau National Aerospace Engineering Honor Society, Sigma Gamma Tau National Undergraduate Award, Who’s Who Among Students, National Collegiate Engineering Award, and All-American Scholar.

Activities: Activities include Team Captain, 2000 NASA Reduced Gravity Student Flight Opportunities Program; Team Member, 1998 NASA Reduced Gravity Student Flight Opportunities Program; Treasurer, Omicron Delta Kappa National Leadership Honor Society; Secretary, Sigma Gamma Tau – National Honor Society in Aerospace Engineering; Embry-Riddle Aeronautical University Resident Advisor; Member, American Institute of Aeronautics and Astronautics (AIAA); Member, Society of Aerospace Engineers (SAE); Team Member, ERAU Varsity Soccer; Athletics Committee Chair, MIT Sidney-Pacific Graduate Residence; Treasurer, MIT Graduate Association of Aeronautics and Astronautics.

December 2006

Appendix B: MVL Centrifuge Technical Description

Centrifuge Structure

The horizontal platform of the centrifuge is 3.04-m long, 92-cm wide and 8.3-cm thick. The platform is an aluminum honeycomb sandwich (panels: 0.3175-cm thick 6061-T6, honeycomb: 7.62-cm thick, 0.953-cm cell size with 57.67 kg/m³ (3.6 lb/ft³) density). Additional structures are attached to the top and bottom surface of the platform to increase the rigidity of the honeycomb sandwich and to take up longitudinal bending moments. The top of the platform has two aluminum L-struts (7.6-cm x 7.6-cm) that run the full length, while the underside has four aluminum U-struts (7.6-cm base x 3.8-cm flanges), which are attached to the flange surrounding the rotation axis and extend radially outward. The underside U-struts are attached by means of 10.2-cm x 25.4-cm x 2.2-cm aluminum plates bolted to the honeycomb.

The axis of rotation divides the length of the bed into a long and a short arm. The long arm, on which the subject is positioned, is 2.13-m, and the short arm, which is above the head of the subject on the other side of the axis of rotation, is 91-cm. The rotation axis assembly is a tube-within-a-tube, with two large radial ball bearings (New Departures, Inc.) supporting and separating the tubes. A steel flange (17.8-cm radius, 1.9-cm thickness) welded to the top of the inner tube is attached to the underside of the bed via an aluminum flange inlaid in the honeycomb structure. Attached to the inner tube is the cogwheel that drives the rotation of the bed and the tube fits into the two sets of radial ball bearings held within the outer steel tube. The outer tube is threaded to a steel flange, which is welded to a 91 x 122-cm steel plate. The steel plate is bolted to the concrete floor of the laboratory in ten locations for additional rigidity. Four steel brackets connect the outer tube and the steel plate to support and stabilize the rotation axis assembly, which is adjusted to remain vertical within 0.1 degree during operation.

Drive Motor

A DC motor (1.0 HP, Browning) drives the rotating platform and is controlled by a DC motor controller (Browning LWS Series LW second generation). The rotation rate of the centrifuge is controlled either manually or via a PC. The controller allows for a maximal angular acceleration of 0.17°/s² until a constant angular velocity is reached. This motor controller is not equipped to dissipate the amount of energy stored in the rotating mass of the spinning centrifuge when breaking. The rotational kinetic energy of the centrifuge at 30-RPM is dependent on the mass-distribution along the rotating arms and is on the order of 10³ Joules. To achieve an adequate breaking performance six 100-Watt light bulbs are added in parallel with the motor. This additional load allows breaking at maximally 0.17°/s² (0.002 rad/sec²).

A 1:10-wormgear reducer (Browning) at the output shaft of the motor drives a cogwheel (2 x 15.2-cm, 40 teeth) and a shaft encoder (256-pulses, HP HEDS-7500). A belt around the motor side cogwheel drives the rotation axis cogwheel (2 x 36.6-cm, 96 teeth). This leads to a total 1:24 reduction of the motor RPM. The 256 pulses per revolution of the shaft encoder are converted to a voltage (ML2907M-8) and used to record centrifuge rotation rate. Redundantly, a read switch is triggered once per revolution by the rotation axis cogwheel and used to derive rotation rate.

Electronics

On-board power supply

Power on board is provided by two 24-Volt uninterrupted power supplies (UPS) (SF-6030, 300Wh) and two 12-Volt sealed lead batteries (12V 35Ah, UB12350, Universal Battery) arranged in series. The different voltages driving various kinds measurement equipment is delivered by a switched ATX computer power supply running off 24Volts (Orion, 300DX/24). The two UPS-units and a power converter (S300-124, Go Power! Electric, Inc.) provide 120-Volt 60-Hz AC power on-board the centrifuge.

On-board DAQ

The on-board PC is controlled remotely by the experiment operator through a wireless internet connection running PC-Anywhere (Version 11.5, Symantec). The PC is set up to record up to 32 analog (16-bit) and up to 96 digital signals from equipment on board (PCI-6229, National Instruments, Inc.) and additionally a 16-channel eletromyography (Bagnoli-16, DelSys, Inc., PCI-6034E, National Instruments, Inc.) Data acquisition rate is usually 1.0-kHz, but depends on the specific application and may be set accordingly. Data is saved to the hard disk of the on-board PC and downloaded for analysis after the experiment has been completed. Due to the switching power supply frequency of 68-kHz each of the data acquisition channels have to be low pass filtered using a simple resistor-capacitor (R-C) circuit with a cutoff frequency of 32-kHz.

Slip ring

A 25-channel slip ring (Poly-Scientific, P/N #1444) within the rotation axis assembly also allows for the transmission of data between the experiment operator's computer(s) and the on-board data acquisition equipment. This data may include centrifuge velocity, emergency stop button, and the surveillance camera. Each of the slip ring channels are buffered by unity gain operational amplifiers.

Head Position Helmet

A mountaineering-style helmet (Petzl, Inc.) mounted to a custom made pivot and mounting pole is used to accurately control and monitor the position of the subject's head. Single axis head rotation is recorded by means of a precision potentiometer attached to the rotation axis. The mounting pole is attached to the top surface of the centrifuge and is aligned with the centrifuge axis of rotation, and the pivot system is aligned with the longitudinal axis of the centrifuge. The helmet pivot allows for 360-degree rotary motion about a single axis. It also has servo-controlled locking pins to discretely position the head every 10-degrees for 90-degree head yaws of a supine subject from nose-up vertical, in either direction. Typically, when the subject's head is securely fastened within the helmet, the vestibular system has little radial deviation from the centrifuge axis of rotation.

Back Slider

The centrifuge is equipped with a moveable cushioned backrest in order to accommodate artificial gravity exercise, as well as understanding the neurovestibular adaptation effects when the vestibular system is radially displaced from the axis of rotation. The backslider is a welded Unistrut® frame with a foam-covered sheet. It can be locked in a fixed position or move linearly along the radius of the centrifuge. Four linear pillow-block bearings (Thomson Industries, Inc.,

P/N: SSUPB012) allow for 61-cm of travel along two precision linear rails (McMaster-Carr, P/N: 6039K34), which are rigidly attached to the centrifuge platform. The ends of the precision rails have end-stop collars (McMaster-Carr, P/N: 5375K13) to prevent the backslider from becoming detached. The backslider also allows for the attachment of resistive cables and cushioned shoulder pads to accommodate resistive-type exercises, such as a hack squat.

Foot Plate

At the most distant point along the radius of the centrifuge is an aluminum plate mounted vertically, and perpendicular to the radius. The footplate acts as a “floor” for the subject when they are either lying supine or on their shoulder. It is a 6.35-mm aluminum plate with steel angle brackets. The footplate can be moved linearly along the radius of the centrifuge bed surface and can be locked in position (2.54-cm increments) by four removable pins. There are safety stoppers at the end of the centrifuge to prevent the footplate from sliding off should the pins fail. Attached to the footplate are a stair stepper for cardiovascular exercise and constant-force spring assembly for resistive exercise.

Exercise Equipment

The centrifuge is equipped with a stair stepper (Kettler Vario Mini Stepper) for cardiovascular exercise and an array of constant force spring for resistive exercise. The stair stepper includes a passive mechanical linkage between the two footholds and a passive damping system. It is rigidly mounted to the surface of the footplate using four U-bolts. To exercise with this device, it requires that the lie supine on the backslider. This exercise is easier to perform when the centrifuge is rotating due to the “gravity assist” in depressing the footholds. The subject’s feet are snugly strapped into the footholds for safety and to keep the subject’s feet in contact with the stepper.

To perform resistive squat exercises, the stepper must be locked in a fixed position so that the footholds are symmetrically aligned. An array of constant force springs is attached to the backside of the footplate. Parallel connection of the springs can provide up to 108.8-kg (240-lbs) of resistive force in 2.3-kg (5-lb) increments. The springs are connected to the backslider frame via two steel cables and a pulley system. Load-rated carabiners allow for the adjustment of the length of cable connection between the springs and the backslider. During the squat exercise, the feet are strapped into the footholds on the stair stepper for safety. The resistive force is applied to the subject at the shoulders through a shoulder pad assembly attached to the backslider (similar to a hack squat).

Safety

A safety restraint, centrifuge side rails, and emergency stop buttons are provided to ensure the safety of the subject. The restraint belt is a seatbelt-type harness that is connected to the backslider frame. It is one strap that is fastened over the subject’s torso and adjusted for a snug fit. Additional straps hold the subject’s feet into the footholds of the stair stepper. The side rails are on either side of the centrifuge and run the length of the subject. They stand 30.5-cm above the surface of the centrifuge and span 137-cm along the radius of the horizontal platform. One of the two emergency stop buttons is located on-board the centrifuge. When depressed by the subject, it immediately disengages the electric drive motor and the centrifuge slowly stops rotating. The system is not equipped with an emergency breaking mechanism. An additional

emergency stop button is located at the experimenter's console and works identically to the on-board button. The subject is monitored at all times through an on-board video camera that is capable of imaging in darkness. The video signal is transferred through the slip rings to the experimenter's console.

Measurements

The MIT centrifuge is equipped with measurement capabilities for monitoring the centrifuge mechanical performance and human physiological responses to artificial gravity. The physiological measurements are aimed at understanding the neurovestibular adaptation to short-radius centrifugation, the biomechanical and neuromuscular responses to limb movements within a rotating environment, and the effects of centrifugation on our cardio-respiratory system. Additional measurements could include those related to body orientation perception. The analog measures are digitized and stored either electronically by the on-board computer, transmitted via the slip ring to the experimenter's computer, or securely sent over a wireless internet connection to a remote computer.

Centrifuge Performance

Many of the experiments are performed at a specified angular velocity as opposed to a specific centripetal acceleration. The advantage being that angular velocity is constant along the radius, whereas centripetal acceleration varies linearly with the radius. It is therefore that we carefully control and monitor the centrifuge angular velocity. The DC motor controller provides a voltage proportional to the angular velocity to the drive motor. The input voltage to the drive motor, the tachometer voltage and the once-per-revolution read switch on the drive motor cogwheel are integrated and are used to estimate angular velocity.

Eye Movement Recording

Horizontal and vertical eye movements are recorded at 60-Hz through infrared video cameras (Model RK-761PCI, ISCAN®) attached to a pair of goggles worn by the subject. All eye movements are recorded in complete darkness. A 360-degree free-turning potentiometer attached to the pivot of the helmet allows for head yaw angle measurement.

Sensory-Motor and Biomechanical Recording

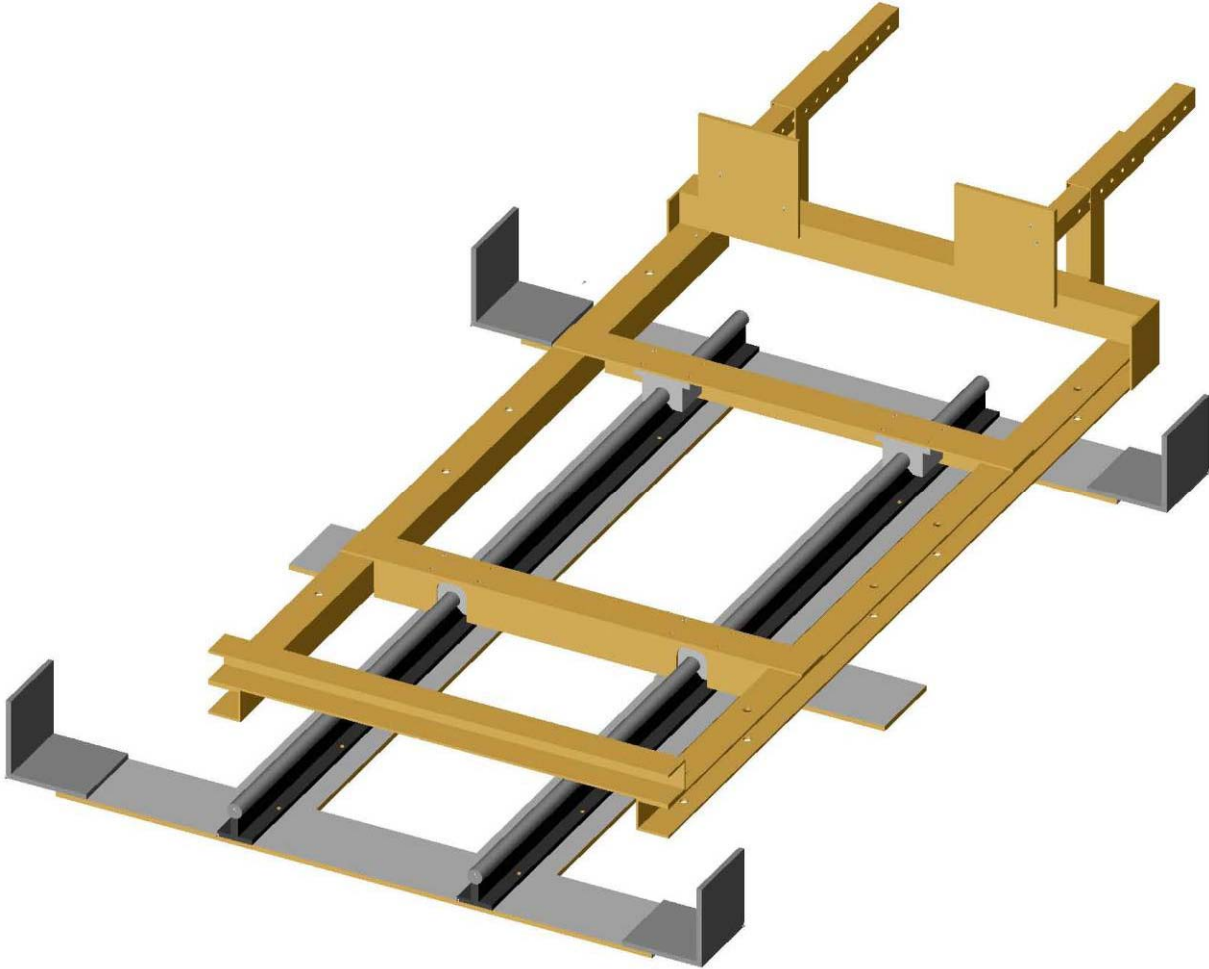
Reflective markers are placed on each of the limbs that we are interested in tracking. A series of infrared optical position tracking cameras (FLEX3, OptiTrack, Inc.) are rigidly attached to the centrifuge to determine the three-dimensional position of the interested limb segments while making movements in the darkness.

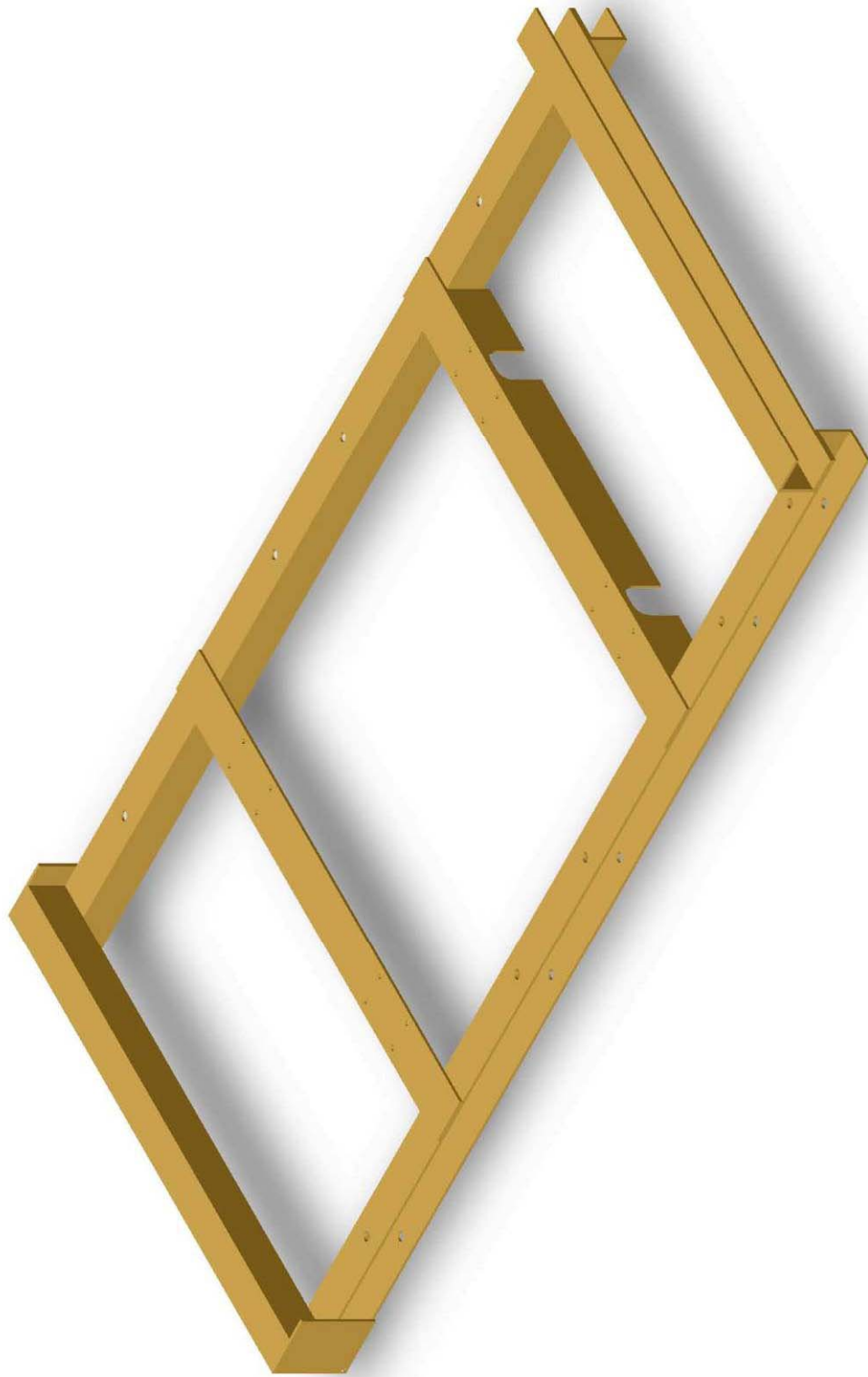
The centrifuge also has the capability to record other biomechanical-related parameters. A 16-channel surface electromyography (Bagnoli-16, DelSys, Inc.) is used to record muscle activity during exercise. Custom built and calibrated strain gauges mounted to the foot holds on the stair stepper are used to record foot reaction forces during "standing," stepping, or squatting. The linear potentiometer (Model LX-PA-30, UniMeasure, Inc.) attached to the backslider also provides information related to the radial movement of the torso during exercise.

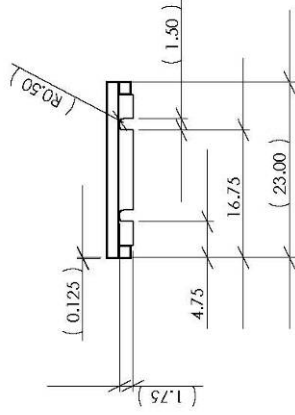
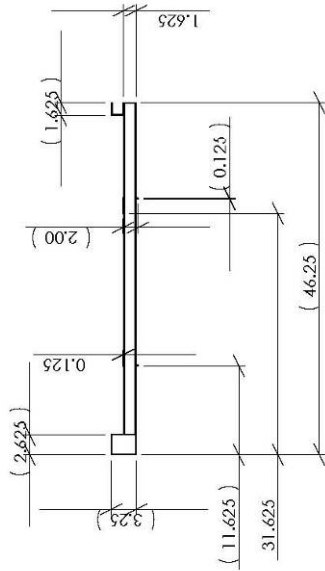
Cardiovascular and Exercise Performance Measures

To monitor parameters related to cardiovascular function, the centrifuge is equipped with an electrocardiogram (ECG) for determining heart rate and cardiac rhythms, and a pulse oximeter for monitoring blood oxygen saturation (Model 504-US, Criticare, Inc.). When supine, the centripetal acceleration results in a shift in body fluid from the thoracic cavity to the legs – an effect similar to standing up after lying down. Eight liquid metal strain gauges (Hokanson, Inc.) may be positioned around the circumference of the legs and the cumulative interpretation of their length changes indicates a volume change in the legs. There are also provisions for measuring and recording blood pressure and respiration rate during rotation, with and without exercise.

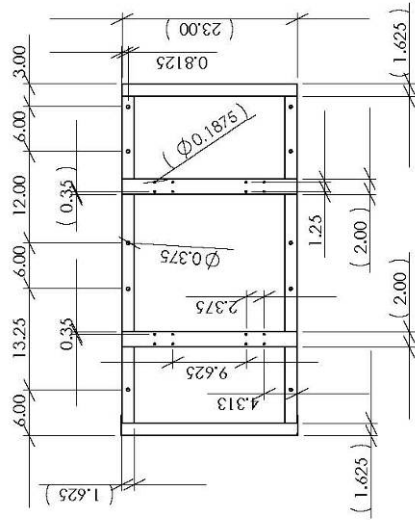
Appendix C: AG Exercise Device Drawings





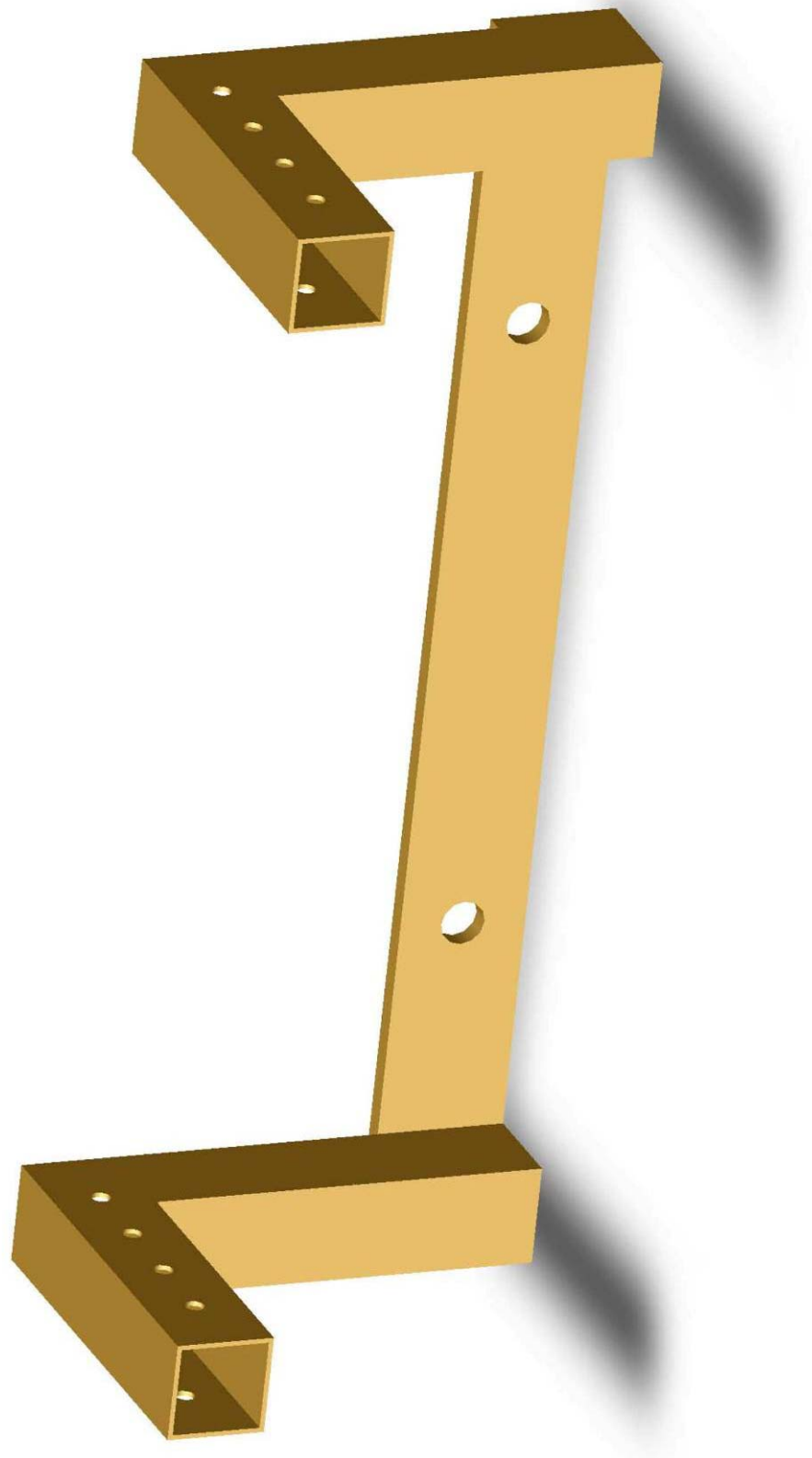


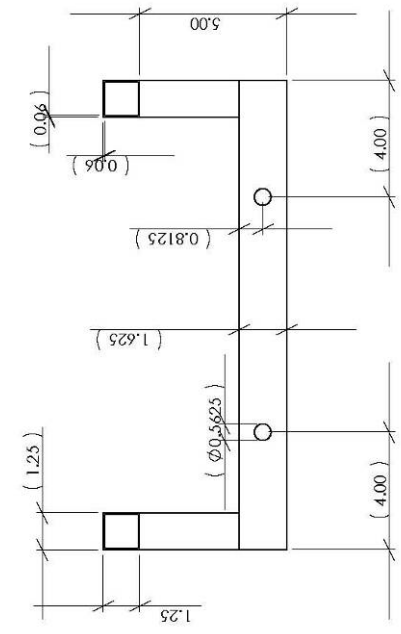
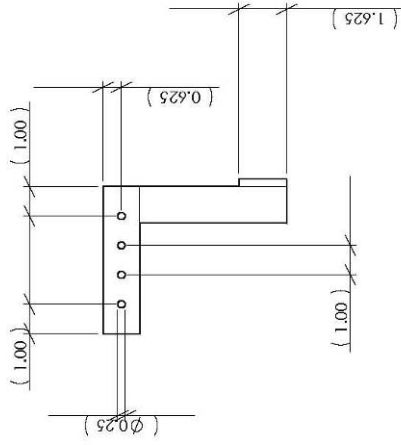
Unistrut 1-5/8" channel, facing "outwards"
 2" base, 1/8" L-bracket
 All joints welded.



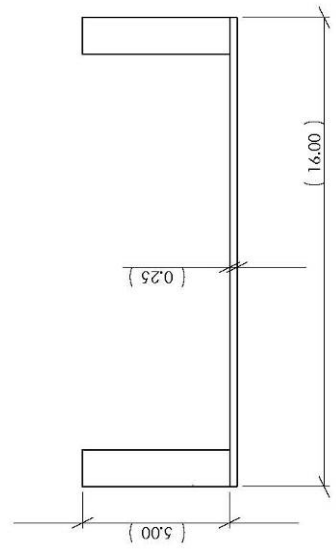
DIMENSIONS ARE IN INCHES		DRAWN		DATE	
TOLERANCES:		CHECKED			
FRACTIONAL ±		ENG APPR			
ANGULAR: MACH ±		MFG APPR			
TWO PLACE DECIMAL ±		Q.A.			
THREE PLACE DECIMAL ±		COMMENTS:			
MATERIAL		FINISH		SIZE DWG. NO.	
				A	
				SCALE: 1:20	
				REV.	
				SHEET 1 OF 1	

Backslider Frame Assembly
 Kevin R. Duda
 MIT Man-Vehicle Laboratory
 November 3, 2005





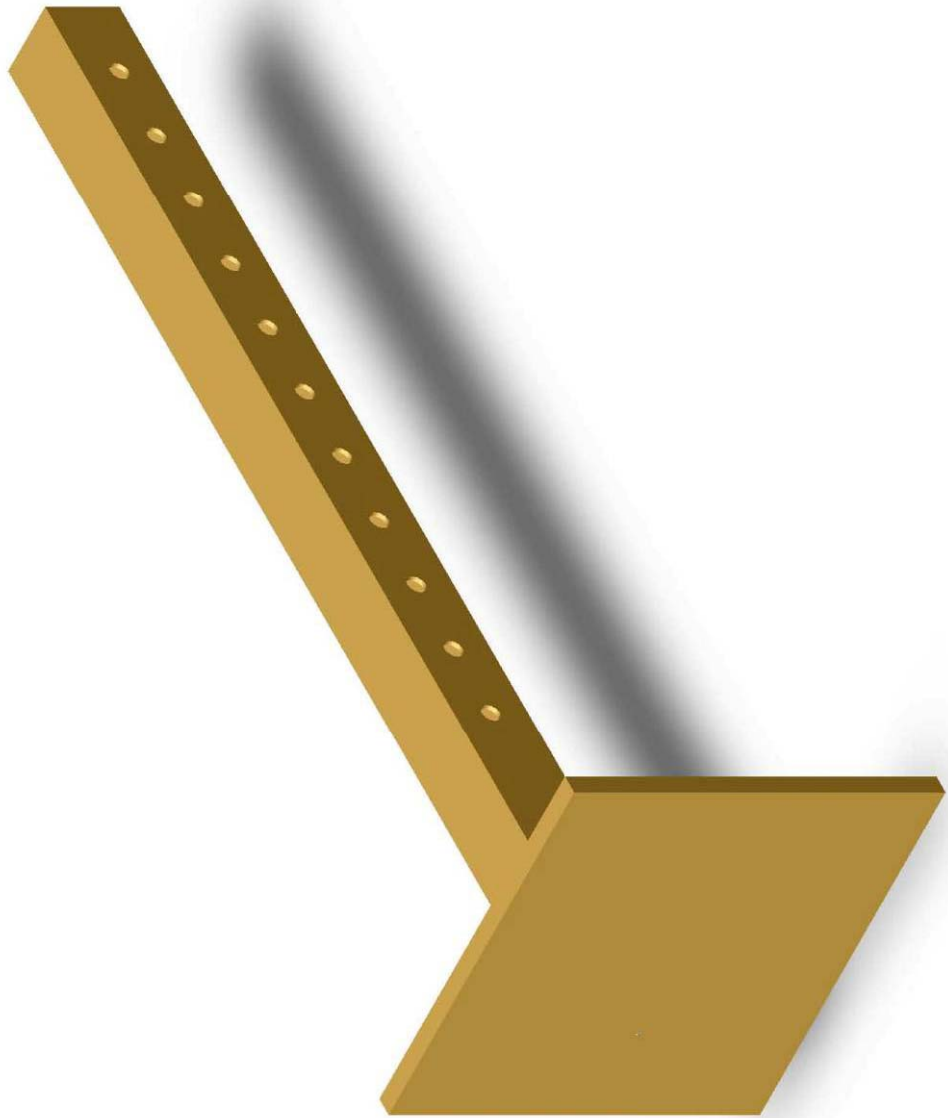
1.25" steel tubing
 0.060" wall thickness
 All joints welded.

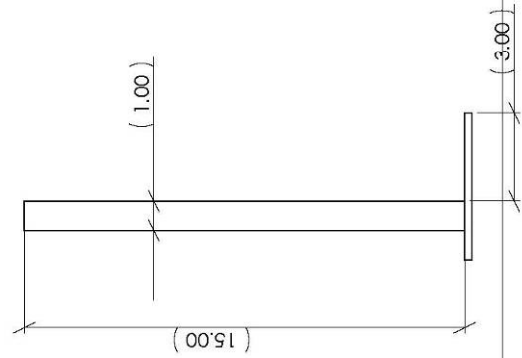
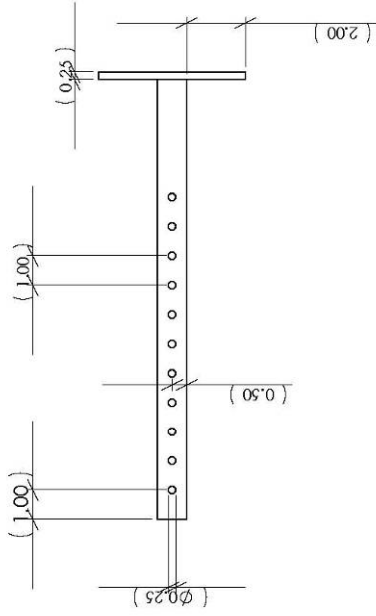
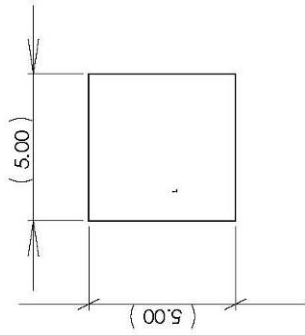


DIMENSIONS ARE IN INCHES		NAME	DATE
TOLERANCES:		DRAWN	
FRACTIONAL:		CHECKED	
ANGULAR: MACH ±	BEND ±	ENG APPR	
TWO PLACE DECIMAL ±		MFG APPR	
THREE PLACE DECIMAL ±		O.A.	
MATERIAL		COMMENTS:	
FINISH			
NEXT ASSY	USED ON		
APPLICATION		DO NOT SCALE DRAWING	
		SIZE	DWG. NO.
		A	
		SCALE: 1/16"	WEIGHT:
			REV.
			SHEET 1 OF 1

Shoulder Harness Assembly

Kevin R. Duda
 MIT Man-Vehicle Laboratory
 November 2, 2005



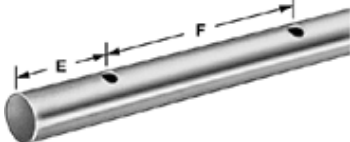
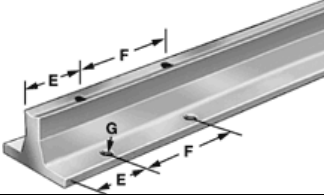




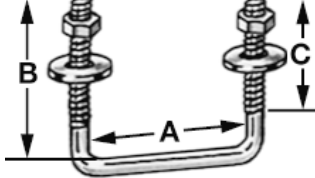
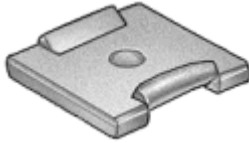
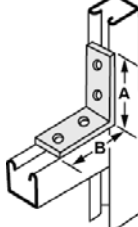



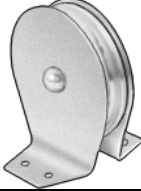

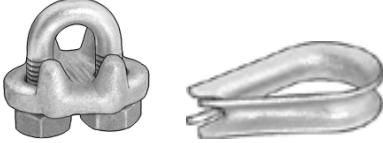
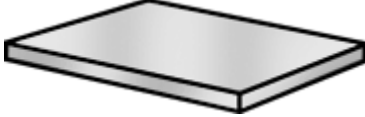


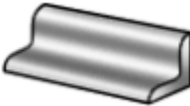

1-inch steel tubing
 0.060" wall thickness
 All joints welded.

NEXT ASSY		USED ON	APPLICATION		DO NOT SCALE	DRAWING	
NAME		DATE	DRAWN		DIMENSIONS ARE IN INCHES		COMMENTS:
Shoulder Pad Assembly			CHECKED		TOLERANCES:		
			ENG APPR		FRACTIONAL ±		
			MFG APPR		ANGULAR: MACH ±		
			O.A.		BEND ±		
					TWO PLACE DECIMAL ±		
					THREE PLACE DECIMAL ±		
					MATERIAL		
					FINISH		
					DO NOT SCALE		
					DRAWING		

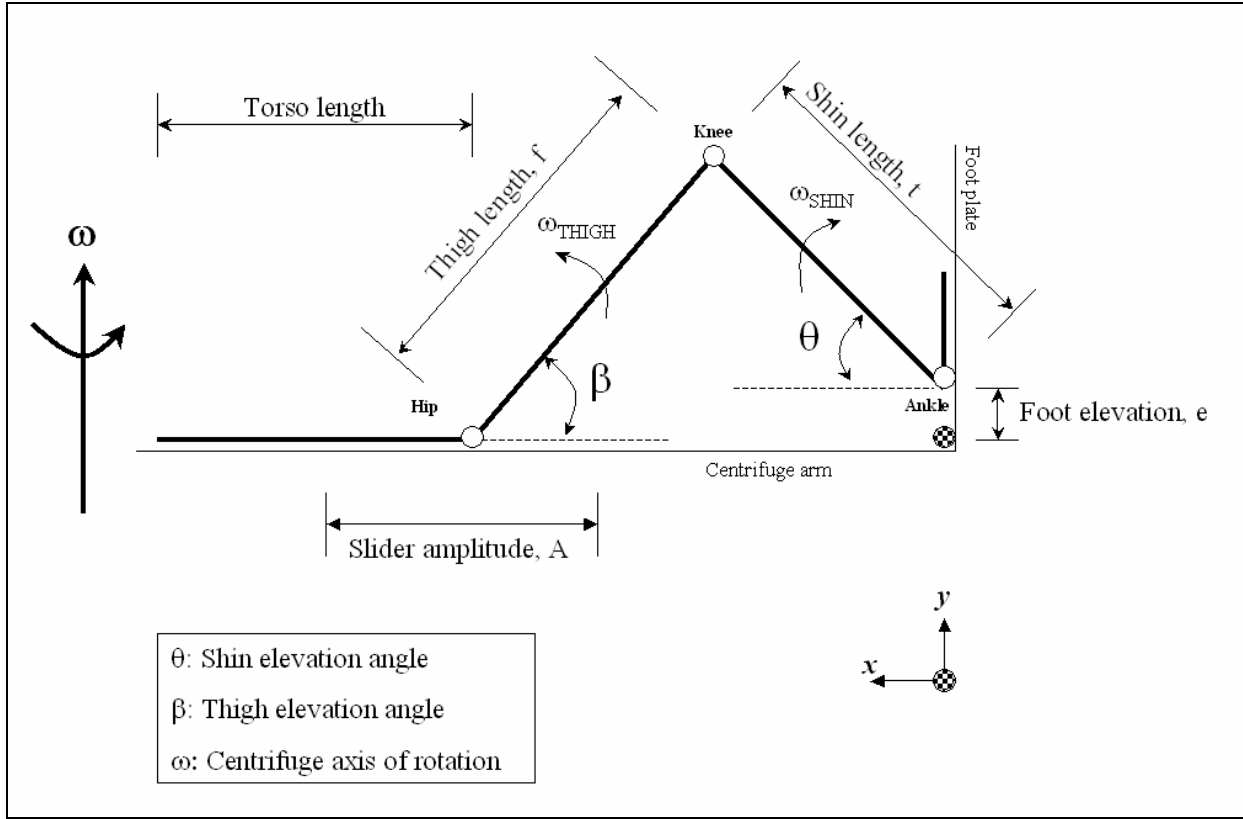
SIZE	DWG. NO.	REV.
A		
SCALE: 1/16"	WEIGHT:	SHEET 1 OF 1

Linear Back Slider and Constant Force Spring Assembly Part List. All components ordered from McMaster-Carr's online store <<http://www.mcmaster.com/>>

Image	P/N and Description	Cost
	Drilled and tapped hardened precision shaft. 440C stainless steel. 3/4" OD, 48" P/N: 6526K74 \$162.44 each, 2 units	\$324.88
	Drilled support rail. 48", for 3/4" shaft OD P/N: 6039K34 \$158.20 each, 2 units	\$316.40
	End-stop clamp-on collar. 3/4" bore. Stainless steel. P/N: 5375K13 \$21.06 each, 4 units	\$84.24
	Aluminum pillow-block self-aligning linear ball bearings (open bearings), 3/4" bearing ID P/N: 6255K26 \$78.41 each, 4 units	\$313.64
	Unistrut spring-backed nuts, 1 5/8" x 1 5/8" strut, 1/2" -13 thread size. P/N: 3259T15 \$6.19 per pack of 5, 2 packs	\$12.38
	T-handle quick release pins, 1/4" diameter, 1 3/4" usable length P/N: 90293A139 \$15.92 each, 4 units	\$63.68
	Square bend U-bolt. Stainless steel. 8" width (A), 3" thread length (C), 3/8" diameter P/N: 3060T81 \$13.81 each, 3 units	\$41.43
	Square steel unistrut grip washer. Fits 3/8" P/N: 3585T12 \$0.74 each, 6 units	\$4.44
	Unistrut corner brace. 4 1/8" x 3 1/2" galvanized steel P/N: 33125T34 \$2.38 each, 2 units	\$4.76

	Unistrut channel. Galvanized steel. 1 5/8" x 1 5/8", 10' length. P/N: 3310T2 \$27.79 each, 1 unit	\$27.79
	Mounted block pulley for wire rope, single sheave. Rope diameter 3/8", sheave 3 1/2" OD P/N: 3099T4 \$15.73 each, 2 units	\$31.46
	Coated wire rope. 1/8" (bare) – 5/32" (coated), 1,700 lbs. P/N: 8939T12 \$0.94 per foot, 20 feet	\$18.80
	Wire rope clip and thimble. Forged steel for 3/16" rope diameter. P/N: 3372T22 \$4.88 per unit, 4 units	\$19.52
	High density polyethylene. 48" x 24" x 1/2" P/N: 8619K475 \$46.00 per unit, 1 unit	\$46.00
	Constant force springs. 4,000 cycle life 40-lb., 4 units, \$25.80 each (9293K14) 25-lb., 2 units, \$17.50 each (9293K13) 10-lb., 4 units, \$9.81 each (9293K12) 5-lb., 3 units, \$7.85 each (9293K56)	\$200.99
	Ultra high molecular weight (UHMW) Polyethylene. For constant force spring bushings. 1" thick, 6" width P/N: 8702K129 \$16.09 per foot, 3 feet	\$48.37
	Aluminum L-bracket, 4" base, 0.25" thick, rounded corner to mate with centrifuge rail. 48" length, P/N: 8982K64 \$46.73 per unit, 1 unit	\$46.73
	Aluminum sheet, 1/4" thick, 4" wide, 6' long. For backslider support base. P/N: 8975K29 \$44.08 per unit, 3 units	\$132.24
	Total	\$1,737.75

Appendix D: Biomechanical Model Calculations



Two dimensional squat biomechanics diagram. All parameters (lengths, angles, and coordinate systems) are shown.

We start with the equations of relative motion for the ankle, knee, and hip:

$$\vec{v}_{HIP} = \vec{v}_{KNEE} + \vec{v}_{HIP/KNEE} \quad \rightarrow \quad \vec{v}_{HIP} = \vec{v}_{KNEE} + \vec{\omega}_{THIGH} \times \vec{r}_{HIP/KNEE} \quad (1)$$

$$\vec{v}_{ANKLE} = \vec{v}_{KNEE} + \vec{v}_{ANKLE/KNEE} \quad \rightarrow \quad \vec{v}_{ANKLE} = \vec{v}_{KNEE} + \vec{\omega}_{SHIN} \times \vec{r}_{ANKLE/KNEE} \quad (2)$$

Solving for the velocity of the knee in equation (2) and substituting into equation (1), and setting $\vec{v}_{ANKLE} = 0$, we have the following relationship:

$$\vec{v}_{HIP} = \vec{\omega}_{THIGH} \times \vec{r}_{HIP/KNEE} - \vec{\omega}_{SHIN} \times \vec{r}_{ANKLE/KNEE} \quad (3)$$

We first assume that the motion for each leg is two-dimensional, with all motion occurring in the x-y plane. Therefore, rotation rates of the thigh and shin are in the z-direction. This allows us to formulate equation (3) in terms of x- and y-components. If we then equate those components:

$$x: v_{HIP} = \omega_{THIGH} f \sin \beta + \omega_{SHIN} t \sin \theta \quad (4)$$

$$y: 0 = -\omega_{THIGH} f \cos \beta + \omega_{SHIN} t \cos \theta \quad (5)$$

Equations (4) and (5) yield four unknowns: rotation rates and angles. The remaining two equations come from the geometry of the problem. From the relative position relationships:

$$\bar{r}_{HIP} = \bar{r}_{KNEE} + \bar{r}_{HIP/KNEE} \quad (6)$$

$$\bar{r}_{ANKLE} = \bar{r}_{KNEE} + \bar{r}_{ANKLE/KNEE} \quad (7)$$

Solving equation (6) for the knee position and substituting into equation (7):

$$\bar{r}_{HIP} = \bar{r}_{ANKLE} - \bar{r}_{ANKLE/KNEE} + \bar{r}_{HIP/KNEE} \quad (8)$$

Again, if we assume two-dimensional motion, then equating y-components in equation (8) yields the following:

$$0 = e + t \sin \theta - f \sin \beta \quad (9)$$

We now have three equations, but still have four unknowns. The last equation also comes from the two-dimensional geometry. The distance of the hip from the coordinate system origin is constrained by the dimensions of the body:

$$r_{HIP} = f \cos \beta + t \cos \theta \quad (10)$$

To summarize, the four equations defining the leg press biomechanics in two-dimensions are:

$$v_{HIP} = \omega_{THIGH} f \sin \beta + \omega_{SHIN} t \sin \theta \quad (11)$$

$$0 = -\omega_{THIGH} f \cos \beta + \omega_{SHIN} t \cos \theta$$

$$0 = e + t \sin \theta - f \sin \beta$$

$$r_{HIP} = f \cos \beta + t \cos \theta$$

Solving the four equations in (11), assuming both v_{HIP} and r_{HIP} are known, results in the two-dimensional biomechanics of the leg press. Once we know the velocity of the hip and the rotation rates of both the thigh and shin, we are able to calculate the Coriolis accelerations at any point on the leg. Coriolis accelerations are defined by the following relationship:

$$\bar{a}_{CORIOLIS} = 2(\bar{\omega}_{CENTRIFUGE} \times \bar{v}_{VELOCITY_OF_LIMB}) \quad (12)$$

Appendix E: COUHES Informed Consent

CONSENT TO PARTICIPATE IN BIOMEDICAL RESEARCH

Biomechanics and Physiological Responses to Exercise During Short-Radius Centrifugation

You are asked to participate in a research study conducted by Professor Laurence Young, Sc.D., Thomas Jarchow, Ph.D., and Kevin R. Duda, from the Department of Aeronautics and Astronautics Man-Vehicle Laboratory at the Massachusetts Institute of Technology (M.I.T). The results of this study may be published in a student thesis or scientific journal. You have been asked to participate in this study because you have volunteered and meet the minimum health and physical requirements for our study. You should read the information below, and ask questions about anything you do not understand, before deciding whether or not to participate.

• PARTICIPATION AND WITHDRAWAL

Your participation in this research is completely voluntary. If you choose to participate you may subsequently withdraw from the study at any time without penalty or consequences of any kind. The investigator may withdraw you from this research if circumstances arise which warrant doing so. Such circumstances include evidence that you do not meet the minimum health and physical requirements, or that during the study it becomes clear to the experimenter that you are becoming drowsy, unalert, or uncooperative. If you choose not to participate, it will not affect your relationship with M.I.T. or your right to health care or other services to which you are otherwise entitled.

You should not participate in this study if you have any medical heart conditions, respiratory conditions, medical conditions which would be triggered if you develop motion sickness, are under the influence of alcohol, anti-depressants, or sedatives, have suffered in the past from a serious head injury (concussion), or if there is any possibility that you may be pregnant. In addition, you should not participate if you have any musculoskeletal, spinal, or other injury that prevents you from participating in resistance exercises, such as a squat or leg press. The experimenter will check to see if you meet these requirements.

• PURPOSE OF THE STUDY

The purpose of this study is to 1) investigate the biomechanics and cardiovascular response to exercises on-board the Man-Vehicle Laboratory short-radius centrifuge, 2) compare those biomechanics and cardiovascular responses to upright exercises in the laboratory, and 3) investigate the biomechanics and coordination during combined exercises and finger pointing. Short-radius centrifugation is currently being investigated as a countermeasure to the deleterious effects of long-duration weightlessness. Exercise during centrifugation has the potential to

increase the effectiveness artificial gravity as a countermeasure during spaceflight. We aim to use these results to define exercise protocols to be used on-board future centrifuge designs.

- **PROCEDURES**

If you volunteer to participate in this study, we would ask you to do the following things:

When you first arrive at the lab, you will be briefed on the background of short-radius centrifugation, disqualifying medical conditions, the experiment protocol, the upright exercise device, and the various components of the centrifuge, including the emergency stop button, restraining belt, exercise equipment, and the various data collection devices. The data collection devices include a commercially available automatic blood pressure cuff, a electrocardiogram (ECG) with fingertip pulse oximeter, infrared motion analysis cameras with reflective markers, surface electromyography (EMG), backslider position measurement, a clickable event button, and force sensors on the footplates. After your initial briefing, you will be asked to fill out a questionnaire that asks basic questions about your health, and any history of prior injuries or current joint pain. Your height, weight, blood pressure, and heart rate may be recorded at this time. We will also take standard anthropometric measurements in order to estimate the inertial properties of each of your individual body segments.

As a participant in this experiment, you will be asked to exercise upright in the laboratory or while lying supine or on your side on the rotating centrifuge. The experimenter will inform you of the portion of the study in which you will be taking part. Before beginning either experiment, you will be instrumented with the surface EMG electrodes. Your skin will first be cleaned with rubbing alcohol and cotton pads. The electrodes will then be attached to your skin with two-sided adhesive. No shaving is required. The ECG electrodes will be attached to your chest and rib cage (or to your arms and leg) using medical-grade adhesive. The experimenter will show you on a diagram where they should be placed before affixing them to your skin. A pulse oximeter may be clipped to your finger to record your blood pressure and the oxygen content of your blood. Small infrared reflective markers will be attached to your hips, knees, and ankles using two-sided medical adhesive. You may also be asked to have a blood pressure cuff on your arm throughout the experiment.

Measures

Each session will begin with an initial warm-up sequence of 5-10 minutes of stretching and/or low aerobic exercises such as using a stair stepper. Once the EMG electrodes are satisfactorily attached, we will ask you to contract the muscles of your thigh, shin, and calf while you are sitting or standing still (maximum voluntary isometric contractions (MVICs)). The following is a brief description of how we will test each of the muscle groups (the experimenter will demonstrate the motions for you):

- Quadriceps. You will sit in a chair with your knees bent 90-degrees, the ball of your foot up against a wall, and you will contract your thigh muscles by trying to extend your leg. The chair will be anchored to the ground, and we may place a buckling safety belt across your legs to keep you firmly seated in the chair. During this test, we will ask you to slowly increase the contraction, reach your maximum voluntary effort after 3-5 seconds, hold that maximum contraction for about 3 seconds, and then slowly relax the contraction. This test

sequence will be repeated at least once, with at least 30-60 seconds between contractions. Your legs may be tested one at a time, or both at the same time.

- Triceps surae. Your calf muscle (gastrocnemius) will be tested while you are seated in the same chair, this time with your legs fully extended and feet against the wall in front of you. We will ask you to perform a calf raise (i.e., raise your heel) with the same sequence of events as the thigh contraction (i.e., slowly increase contraction, and hold it for 3-seconds, ...). The other muscle in your lower leg (soleus) will also be tested while you are seated in the chair, with your knees bent 90-degrees. We will ask you to perform a calf raise (similar to what you just did for your calf muscle), against a padded bar that will be placed over your knees. The same sequence of events as the thigh contraction will also be used here. These muscles may be tested on one leg at a time or both legs simultaneously.

- Tibialis anterior. The muscle on the front of your shin (tibialis anterior) will be tested while you are standing upright. During the test, we will ask you to raise your toes by flexing your ankle against a padded bar placed over your foot. You will be allowed to hold onto a rigid fixture within the lab to help keep your balance. The same sequence of events as the thigh contraction will also be used here. These muscle groups will be tested one leg at a time.

Upright exercise

In the upright portion of the study, you will be asked to perform standard squat motions with our exercise hardware. You may also be asked to point to a target in front of you while performing the squat exercise. The exercise protocol will include several sets (not exceeding 10) of several repetitions (not exceeding 15) per session. The depth of the squat will be based on what is most comfortable for you. Additional resistance may be added by using constant force springs connected to the backslider of the exercise device. This additional resistive weight will be applied to you via shoulder pads (similar to a leg press and/or a hack squat machine in many fitness centers). The maximum additional resistance will not exceed 75% of your self-reported one-repetition maximum (1-RM) squat/leg press load. You will not be asked to exercise, for more than one-hour. During and after the exercises, you will be asked how much effort you perceive you are exerting on the Borg scale (explained on separate sheet), and any feelings of motion sickness (on a 0-20 scale). Most exercises will be done in the light with your eyes open, however, the lights may be turned off when asked to point to a target in front of you.

Centrifuge exercise

In the centrifuge portion of the study, you will lie supine or on your side on the padded slider on the centrifuge. The EMG and ECG electrodes, and the infrared reflective spheres will be attached before you get onto the centrifuge. Once you lie down on the padded backslider, the experimenter will ensure that you are comfortable. At this time, physiological measures (e.g., heart rate, blood pressure) will be recorded while the centrifuge is stationary, and you will have an opportunity to rest for approximately 10-minutes. After this rest period, and prior to centrifuge rotation, you will be asked to perform several sets of squat exercises while in the supine position. Similar to the upright study, you may be asked to point to a target in front of you while performing the squat exercise. Once again, additional resistance may be added, not to exceed 75% of your self-reported one-repetition maximum (1-RM) squat/leg press load.

Prior to starting the rotation of the centrifuge, the experimenter will ask you if you are ready to begin. Your rotation on the centrifuge will not exceed the following parameters:

- Acceleration no greater than 1 revolution per minute, per second.
- Rotation rate not exceeding 30 revolutions per minute.
- Time of rotation not exceeding 1-hour.

The supine squat exercise on the centrifuge may be in the dark and/or in the light. The depth of the squat will be self-determined. The exercise protocol will ask you to perform several sets (not exceeding 10) of several repetitions (not exceeding 15) per session. The experimenter may ask you to exercise at several speeds (i.e., how fast you do one repetition of the squat). The fastest speed will not exceed one repetition per second. During rotation and after the centrifuge has stopped, you will be asked to report your subjective experience (how you feel, your level of perceived effort on the Borg scale, and/or how you perceive exercise to be different from exercising in a upright orientation). You will also be asked to report your motion sickness during and after rotation. When the experiment is complete, the centrifuge will be stopped, and the experimenter may collect some additional data. The experimenter will help you to get off of the centrifuge.

Further participation

As a participant in these experimental trials, we ask that you tentatively agree to return for additional sessions (at most 5) as requested by the experimenter. You may or may not be assigned to a study group that performs similar tasks. Other than the time required for rotation (which is estimated to last approximately 45 minutes), the time commitment is 60 minutes for the first briefing and attachment of EMG and ECG electrodes, 60 minutes for the exercise conditions (upright or centrifuge), and 30 minutes for other procedures before and after rotation. The total time for participation in one day will be approximately 2.5 hours.

• POTENTIAL RISKS AND DISCOMFORTS

The MVIC tests may include muscle soreness or "pressure points" where the padded bar is pressed against your body. Muscle or tendon tear may occur in rare and extreme situations. The body positions (knee and ankle angles) used for this testing allow you to maximally contract your muscles as without producing maximum force. This minimizes your chances of tearing a muscle or tendon. Prior to take part in the experiment, you will be asked to complete a medical and exercise history questionnaire. Any history of current or previous injuries to the joints, bones, or muscles of the lower body may disqualify you from participation in this study. If you are permitted to take part in the study, you will be asked to warm up with light aerobic exercises (e.g., stair stepping.) and stretching prior to the MVIC testing. The experimenter will instruct and demonstrate to you how to safely perform the contractions. In the unlikely case that you feel any pain or discomfort while you are contracting your muscles, we ask that you immediately discontinue the exercise and release the contraction.

Repeated exercise against resistance that approaches 75% of a self-reported 1-RM may lead to feelings of post-exercise fatigue and muscle soreness. Should you feel extreme fatigue, or muscle or joint pain during the experiment, you will be asked to terminate the study. If this should occur when the centrifuge is rotating, it will be stopped immediately and you will be

assisted off the centrifuge by the experimenter. You may terminate the study at any point should you feel uncomfortable or have any noticeable pain.

During rotation you may develop a headache or feel pressure in your legs caused by a fluid shift from your thorax to your lower extremities due to centrifugation. You may also experience nausea or motion sickness and/or drowsiness. When exercising while the centrifuge is rotating, you may experience lateral forces on your knees. Your heart rate may increase due to the rotation speed, and it may increase more due to exercise on the centrifuge. For experiments with accelerations of more than 1.0-G at your feet, your heart rate will be continuously monitored. The experiment will be terminated if your heart rate goes above the value: (220 minus your age [in years]) or a maximum of 200 beats per minute.

You will be continuously monitored by at least one experimenter in the same room. The investigator can also see you through a video camera mounted on the centrifuge, and in this way determine your well-being and the nature of any problems that arise. You can also terminate rotation at any time for any reason by pressing the emergency stop button.

Serious injury could result from falling off the centrifuge while it is rotating. You will be restrained by a safety belt, which is to be worn around the waist/chest at all times while the centrifuge is rotating. The centrifuge is equipped with strong side railings similar to those on a hospital bed, which you may use these to stabilize yourself while you exercise if that is more comfortable for you.

The procedure may involve risks that are currently unforeseeable.

- **ANTICIPATED BENEFITS TO SUBJECTS**

You will receive no benefits from this research.

- **ANTICIPATED BENEFITS TO SOCIETY**

The potential benefits to science and society are a better understanding of how short radius centrifugation combined with exercise can enable long duration spaceflight.

- **PAYMENT FOR PARTICIPATION**

Eligible subjects will receive payment of \$10/hr for their participation. Checks will be mailed within 4-6 weeks of participation. Subjects not eligible for compensation include international students who work more than 20 hours per week, or volunteers from the MIT Man-Vehicle Laboratory.

- **PRIVACY AND CONFIDENTIALITY**

The only people who will know that you are a research subject are members of the research team. No information about you, or provided by you during the research will be disclosed to others without your written permission, except if necessary to protect your rights or welfare, or if required by law.

When the results of the research are published or discussed in conferences, no information will be included that would reveal your identity. The data may consist of measures of your foot pressure and heart rate, information from the computer on an exercise device, subjective ratings of motion sickness and illusions experienced during centrifugation, subjective descriptions of your experience during centrifugation, and subjective descriptions of your orientation in space.

During the experiment, the experimenter will monitor you through a video camera capable of imaging in darkness. You will be monitored to ensure your state of well-being and compliance with the experiment protocol. In some cases the video data will be recorded on VHS tapes. You have the right to review and edit the tape. Any recorded videotapes will be accessible only by members of the current Artificial Gravity research team. Videotapes will be erased in 5 years, at most.

Research data collected during the experiment will be stored in coded files that contain no personal information. The coding of the data will prevent linking your personal data to research data when it is analyzed or archived. Research data is stored in a database and/or ASCII files, and there is no certain date for destruction. The data is stored in the Man-Vehicle Lab computers that remain accessible only by Artificial Gravity team members. The investigator will retain a record of your participation so that you may be contacted in the future should your data be used for purposes other than those described here.

- **WITHDRAWAL OF PARTICIPATION BY THE INVESTIGATOR**

The investigator may withdraw you from participating in this research if circumstances arise which warrant doing so. If you experience abnormally high heart rate, very high motion sickness levels, or extreme drowsiness or dizziness, you may have to drop out, even if you would like to continue. The investigators, Prof. Laurence R. Young, Dr. Thomas Jarchow, and Kevin Duda, will make the decision and let you know if it is not possible for you to continue. The decision may be made either to protect your health and safety, or because it is part of the research plan that people who develop certain conditions may not continue to participate.

If you must drop out because the investigator asks you to (rather than because you have decided on your own to withdraw), you will be paid the hourly amount stated (\$10/hr) for the amount of time that you spent as a subject.

- **NEW FINDINGS**

During the course of the study, you will be informed of any significant new findings (either good or bad), such as changes in the risks or benefits resulting from participation in the research or new alternatives to participation, which might cause you to change your mind about continuing in the study. If new information is provided to you, your consent to continue participating in this study will be re-obtained.

- **EMERGENCY CARE AND COMPENSATION FOR INJURY**

“In the unlikely event of physical injury resulting from participation in this research you may receive medical treatment from the M.I.T. Medical Department, including emergency treatment and follow-up care as needed. Your insurance carrier may be billed for the cost of such treatment. M.I.T. does not provide any other form of compensation for injury. Moreover, in either providing or making such medical care available it does not imply the injury is the fault of the investigator. Further information may be obtained by calling the MIT Insurance and Legal Affairs Office at 1-617-253 2822.”

- **IDENTIFICATION OF INVESTIGATORS**

In the event of a research related injury or if you experience an adverse reaction, please immediately contact one of the investigators listed below. If you have any questions about the research, please feel free to contact:

Principal Investigator:
Prof. Laurence R. Young, Sc.D.
77 Massachusetts Avenue
37-219
Cambridge, MA 02139
(617) 253-7759

Co-Investigators:
Thomas Jarchow, Ph.D.
77 Massachusetts Avenue
37-219
Cambridge, MA 02139
(617) 253-0017

Kevin R. Duda
77 Massachusetts Avenue
37-219
Cambridge, MA 02139
(617) 253-7509

• **RIGHTS OF RESEARCH SUBJECTS**

You are not waiving any legal claims, rights or remedies because of your participation in this research study. If you feel you have been treated unfairly, or you have questions regarding your rights as a research subject, you may contact the Chairman of the Committee on the Use of Humans as Experimental Subjects, M.I.T., Room E32-335, 77 Massachusetts Ave, Cambridge, MA 02139, phone 1-617-253 6787.

SIGNATURE OF RESEARCH SUBJECT OR LEGAL REPRESENTATIVE

I have read (or someone has read to me) the information provided above. I have been given an opportunity to ask questions and all of my questions have been answered to my satisfaction. I have been given a copy of this form.

BY SIGNING THIS FORM, I WILLINGLY AGREE TO PARTICIPATE IN THE RESEARCH IT DESCRIBES.

Name of Subject

Signature of Subject or Legal Representative

Date

SIGNATURE OF INVESTIGATOR

I have explained the research to the subject or his/her legal representative, and answered all of his/her questions. I believe that he/she understands the information described in this document and freely consents to participate.

Name of Investigator

Signature of Investigator

Date (must be the same as subject's)

**Appendix F: Rating of Perceived Exertion Scale
(Borg Scale)**

Rating of Perceived Exertion Scale

(Overall Effort, Not Solely Leg Fatigue)

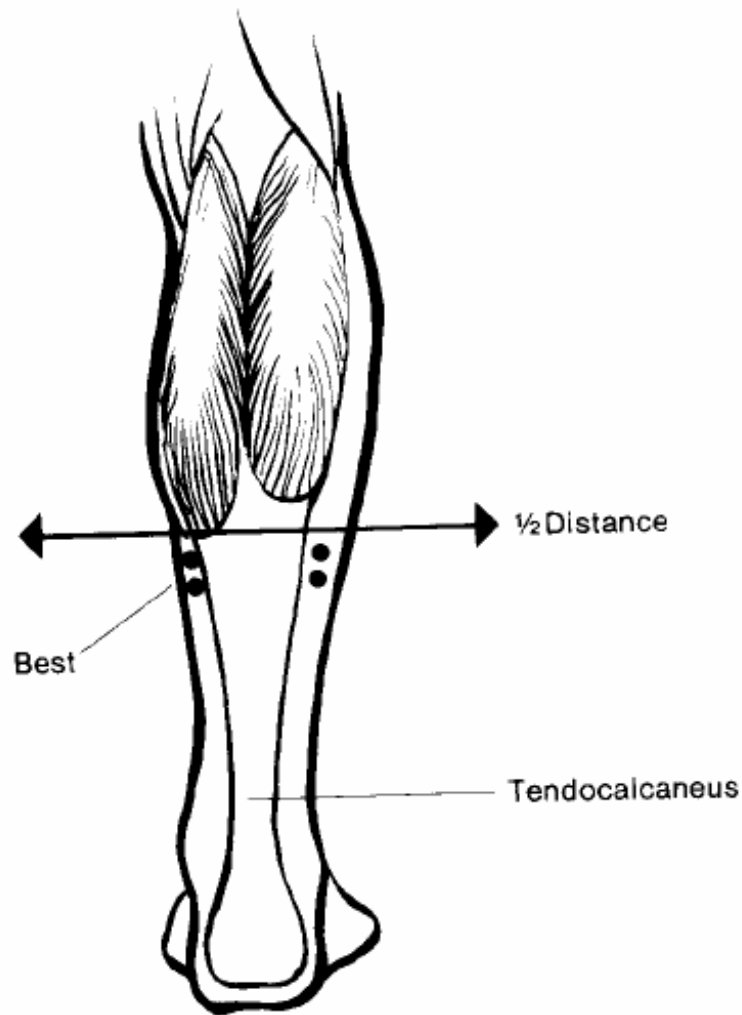
6	
7	Very, Very Light
8	
9	Very Light
10	
11	Fairly Light
12	
13	Somewhat Hard
14	
15	Hard
16	
17	Very Hard
18	
19	Very, Very Hard
20	

“During the exercise test we want you to pay close attention to how hard you feel the exercise work rate is. This feeling should reflect you total amount of exertion and fatigue, combining all sensations and feelings of physical stress, effort, and fatigue. Don’t concern yourself with any one factor such as leg pain, shortness of breath or exercise intensity, but try to concentrate on your total, inner feeling of exertion. Try not to underestimate or overestimate your feelings of exertion; be as accurate as you can.”

Appendix G: Surface EMG Electrode Placement

Specification of the surface electrode placement on the soleus, medial and lateral gastrocnemius, tibialis anterior, vastus lateralis and medialis, and rectus femoris.

Basmajian, J.V., R. Blumenstein, and M. Dismatsek. (1980) Electrode Placement in EMG Biofeedback. Baltimore, MD: The Williams and Wilkins Company.



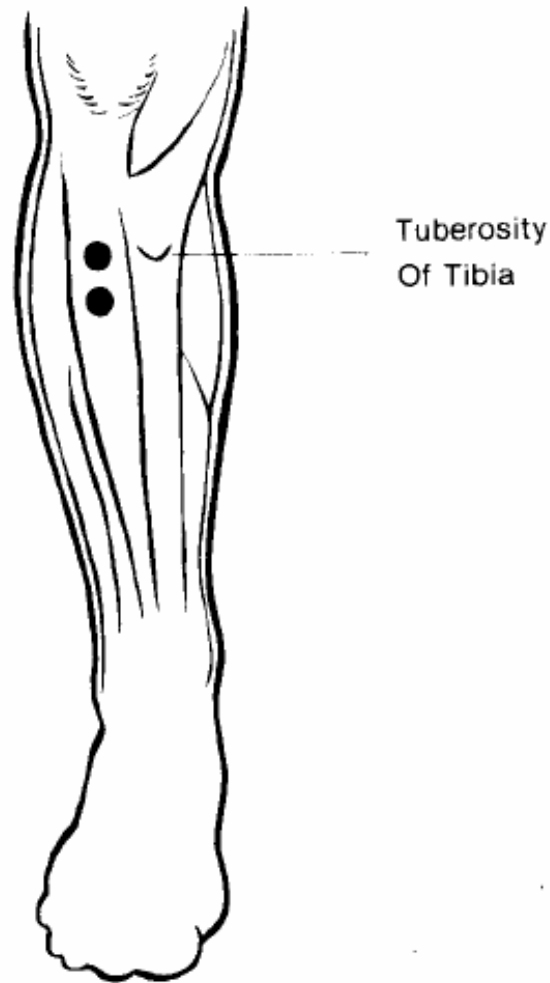
SOLEUS

Center the electrodes in a narrow oval area just medial to the edge of the tendon below the $\frac{1}{2}$ -way mark on back of leg. The lateral placement is usually less effective (but possible).



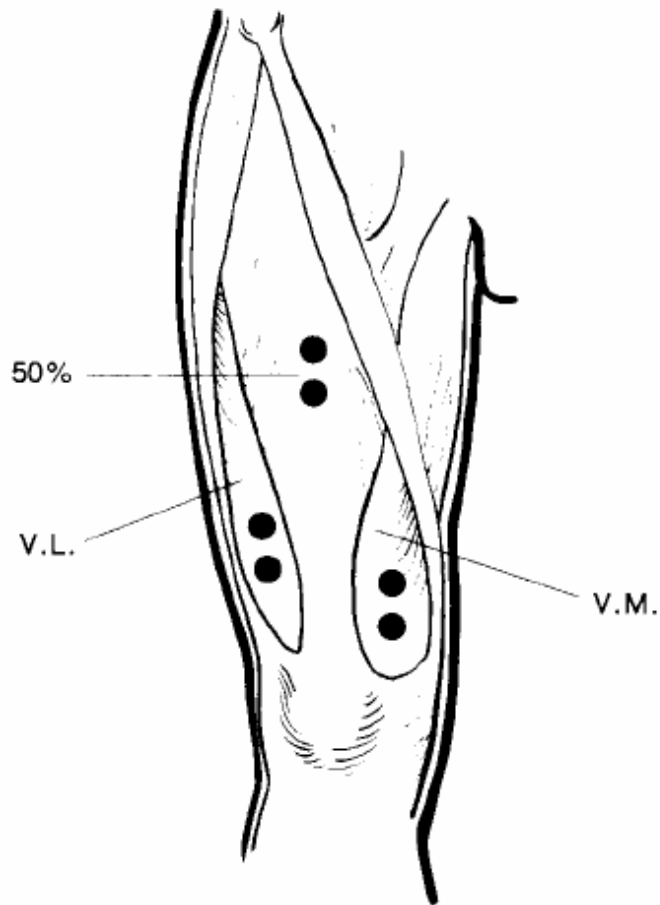
GASTROCNEMIUS [MEDIAL AND LATERAL HEADS]

Place the electrodes almost anywhere over the bulge of either head of gastrocnemius.



TIBIALIS ANTERIOR

Center the electrodes in a long narrow oval area whose upper part is 1 or 2 finger's breadths from the tuberosity of the tibia. It is possible to use placements considerably lower than the above (down to the mid-shaft of the tibia).



QUADRICEPS FEMORIS

For maximum pickup of the whole muscle mass, center the electrodes in the large oval area over rectus femoris, with the lower electrode being a minimum of 10cm. above the patella. For the vastus lateralis choose the area inferolateral to this. For the vastus medialis, the best area is the inferomedial oval, where the muscle is seen to bulge in a well muscled person.

Appendix H: Thesis Defense Slides

Squat Exercise Biomechanics During Short-Radius Centrifugation



Kevin R. Duda
Ph.D. Thesis Defense
December 13, 2006

1

Thesis Committee

Laurence R. Young, Sc.D. (Chair)

Jeffrey A. Hoffman, Ph.D.

Dava J. Newman, Ph.D.

Lars Oddsson, Dr.Med.Sci.

Charles M. Oman, Ph.D.

Faculty at Large

Thomas Jarchow, Ph.D.

William H. Paloski, Ph.D.

2

Motivation

- Physiological de-conditioning resulting from space flight (e.g., Buckey 2006)
- Combine exercise and short-radius centrifugation
- Target musculoskeletal de-conditioning (e.g., Fleck and Kraemer 1987)
- Evaluate safety
- Make recommendations for AG exercise prescription (e.g., ACSM)



3

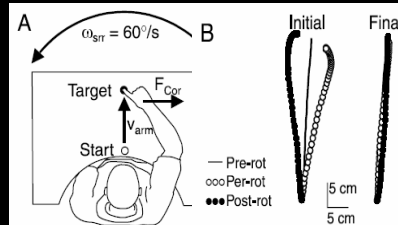
Background

- Previous AG exercise studies
 - Traditional cardiovascular exercises (e.g., Iwase et. al 2004, Caiozzo et. al 2004, Edmonds 2005)
 - → Biomechanics (Edmonds 2005)
 - → Exercise prescription (Caiozzo et. al 2004)
 - → No safety assessments



- Human movement during centrifugation
 - Sensory-motor adaptation
 - After-effects (e.g., DiZio and Lackner 2002)
 - → None predicted Coriolis forces

$$\vec{F}_{Coriolis} = -2m(\vec{\omega} \times \vec{v})$$



4

Background

- The squat exercise
 - Increase muscle strength and mass
(e.g., Fleck and Kraemer 1987)
 - Increase bone mineral density
(e.g., Layne and Nelson 1999, Shackelford et. al 2004)
 - Biomechanics are well documented
(e.g., Escamilla et. al 1998, Abelbeck 2002)
 - Core exercise on the ISS
(e.g., Lee et. al 2004)



5

Research Aims and Hypotheses

Before AG exercise can be certified safe and effective, we must first understand the effects a rotating environment and a gravity gradient have on our biomechanics, and how those biomechanics may differ from when we exercise upright on Earth.

- **Aim #1: Coriolis-induced knee deflections**
 - Hypothesis #1: *Medial-lateral knee deflections will increase with increasing rotation rate, while keeping exercise cadence constant. Additional resistance at a particular rotation rate and exercise cadence will reduce those deflections.*
- **Aim #2: Adaptation and post-rotatory effects**
 - Hypothesis #2: *Medial-lateral knee deflections will persist after rotation has stopped due to adaptation to the Coriolis forces.*
- **Aim #3: AG and upright squat comparison**
 - Recommendations for artificial gravity squat exercise design based on the comparison between upright and centrifuge supine squats.
- **Aim #4: Predicting Coriolis accelerations**
 - Joint torques and vestibular inputs

6

Research Aims and Hypotheses

Before AG exercise can be certified safe and effective, we must first understand the effects a rotating environment and a gravity gradient have on our biomechanics, and how those biomechanics may differ from when we exercise upright on Earth.

- **Aim #1: Coriolis-induced knee deflections**
 - Hypothesis #1: *Medial-lateral knee deflections will increase with increasing rotation rate, while keeping exercise cadence constant. Additional resistance at a particular rotation rate and exercise cadence will reduce those deflections.*
- **Aim #2: Adaptation and post-rotatory effects**
 - Hypothesis #2: *Medial-lateral knee deflections will persist after rotation has stopped due to adaptation to the Coriolis forces.*
- **Aim #3: AG and upright squat comparison**
 - Recommendations for artificial gravity squat exercise design based on the comparison between upright and centrifuge supine squats.
- **Aim #4: Predicting Coriolis accelerations**
 - Joint torques and vestibular inputs

7

Research Aims and Hypotheses

Before AG exercise can be certified safe and effective, we must first understand the effects a rotating environment and a gravity gradient have on our biomechanics, and how those biomechanics may differ from when we exercise upright on Earth.

- **Aim #1: Coriolis-induced knee deflections**
 - Hypothesis #1: *Medial-lateral knee deflections will increase with increasing rotation rate, while keeping exercise cadence constant. Additional resistance at a particular rotation rate and exercise cadence will reduce those deflections.*
- **Aim #2: Adaptation and post-rotatory effects**
 - Hypothesis #2: *Medial-lateral knee deflections will persist after rotation has stopped due to adaptation to the Coriolis forces.*
- **Aim #3: AG and upright squat comparison**
 - Recommendations for artificial gravity squat exercise design based on the comparison between upright and centrifuge supine squats.
- **Aim #4: Predicting Coriolis accelerations and foot forces**
 - Joint torques and vestibular inputs

8

Research Aims and Hypotheses

Before AG exercise can be certified safe and effective, we must first understand the effects a rotating environment and a gravity gradient have on our biomechanics, and how those biomechanics may differ from when we exercise upright on Earth.

- **Aim #1: Coriolis-induced knee deflections**
 - Hypothesis #1: *Medial-lateral knee deflections will increase with increasing rotation rate, while keeping exercise cadence constant. Additional resistance at a particular rotation rate and exercise cadence will reduce those deflections.*
- **Aim #2: Adaptation and post-rotatory effects**
 - Hypothesis #2: *Medial-lateral knee deflections will persist after rotation has stopped due to adaptation to the Coriolis forces.*
- **Aim #3: AG and upright squat comparison**
 - Recommendations for artificial gravity squat exercise design based on the comparison between upright and centrifuge supine squats.
- **Aim #4: Predicting Coriolis accelerations**
 - Joint torques and vestibular inputs

9

Research Aims and Hypotheses

Before AG exercise can be certified safe and effective, we must first understand the effects a rotating environment and a gravity gradient have on our biomechanics, and how those biomechanics may differ from when we exercise upright on Earth.

- **Aim #1: Coriolis-induced knee deflections**
 - Hypothesis #1: *Medial-lateral knee deflections will increase with increasing rotation rate, while keeping exercise cadence constant. Additional resistance at a particular rotation rate and exercise cadence will reduce those deflections.*
- **Aim #2: Adaptation and post-rotatory effects**
 - Hypothesis #2: *Medial-lateral knee deflections will persist after rotation has stopped due to adaptation to the Coriolis forces.*
- **Aim #3: AG and upright squat comparison**
 - Recommendations for artificial gravity squat exercise design based on the comparison between upright and centrifuge supine squats.
- **Aim #4: Predicting Coriolis accelerations**
 - Joint torques and initial safety assessment

10

Contributions

1. Quantified AG squat exercise biomechanics
(knee kinematics, foot forces, muscle activity)
2. Recommendations for AG squat protocol design
3. Model dynamics of the squat for predicting Coriolis forces and initial safety assessments
4. Resistive exercise equipment for the MVL centrifuge

11

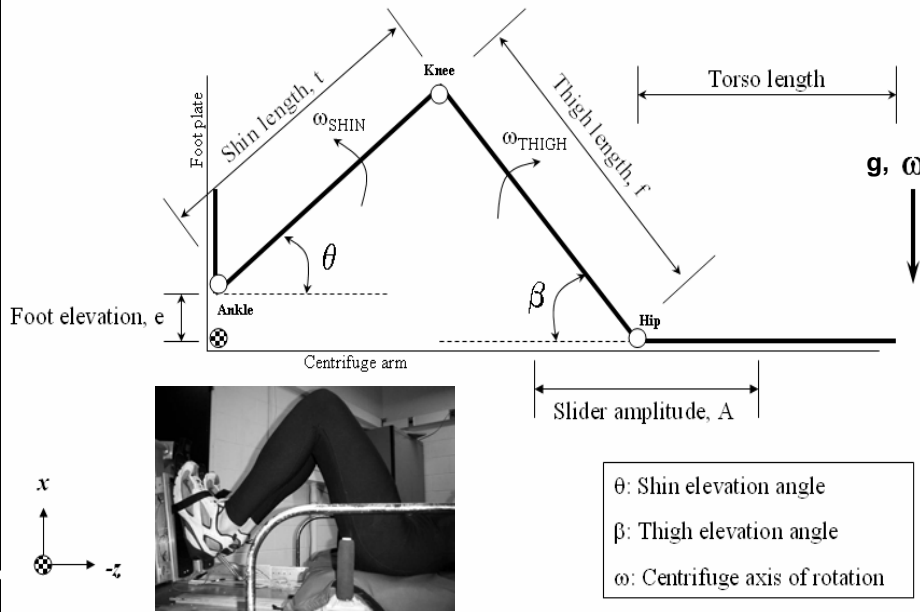
Squat Biomechanics Modeling

Coriolis Forces

Safety Assessment

12

Squat Biomechanics Modeling



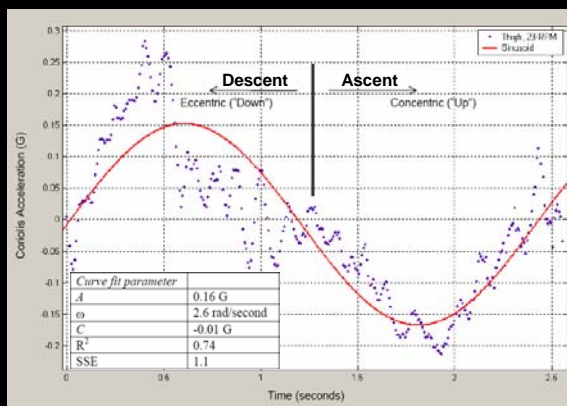
13

Predicting Coriolis Accelerations

- Linear movement of any object within a rotating environment creates a Coriolis acceleration

$$\vec{a}_{CORIOLIS} = -2(\vec{\omega}_{CENTRIFUGE} \times \vec{v}_{VELOCITY_OF_LIMB})$$

$$\vec{F}_{Coriolis} = -2m(\vec{\omega} \times \vec{v})$$

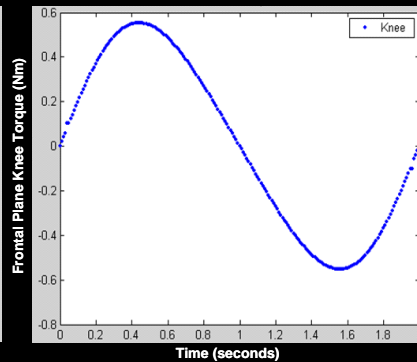
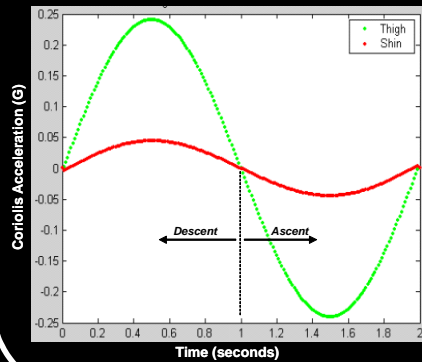


Representative data
 1 Subject, 1 Squat Cycle
 Crossbow CXL02LF3, 100-Hz
 MATLAB 6.5 Curve Fitting Toolbox

14

Predicting Knee Torque

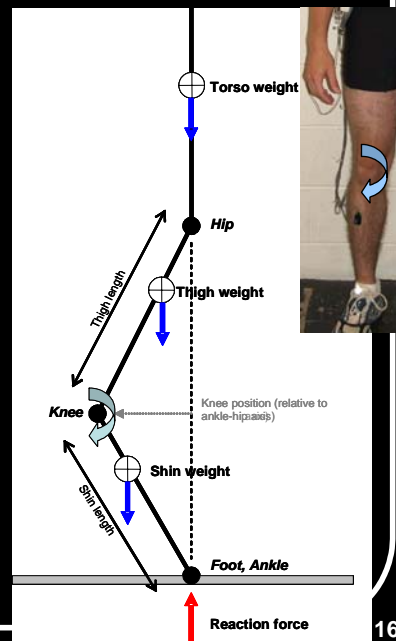
- The center of mass of the thigh and shin have different radial velocities during the squat cycle
- Each limb segment has a different mass
→ Knee torque



15

Predicting Knee Torque

- Mechanical torque
 - Lateral knee position due to Coriolis forces
 - → 30 N-m
- Coriolis torque
 - Exercise kinematics
 - → 0.6 N-m



16

Biomechanical Modeling Discussion

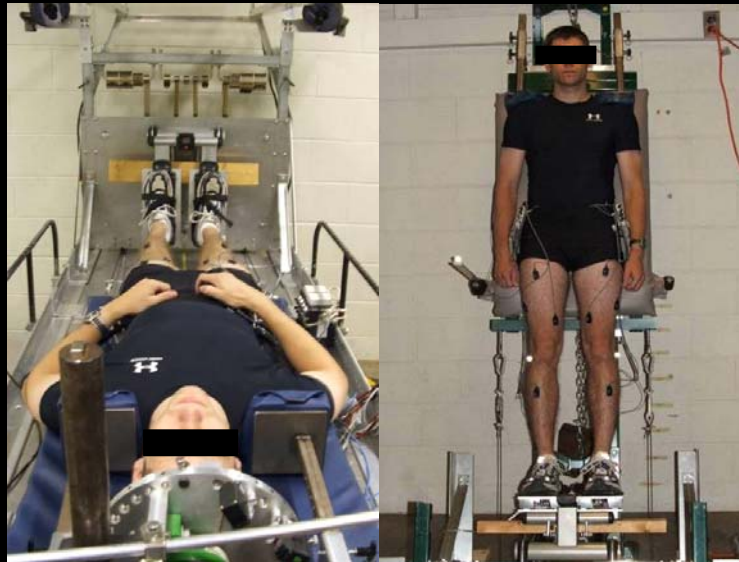
- Two-dimensional squat biomechanics model
 - Coriolis acceleration predictions
 - Frontal-plane knee torque
- Coriolis and mechanical knee torque
 - ~30 N-m
 - Cycling biomechanics ~ 30 N-m

(Hull and Jorge 1985, Ericson 1985, Gregor and Wheeler 1994)
- Repetitive Strain Injuries
 - Unlikely during AG squats
 - Cycling reps vs. Squat reps



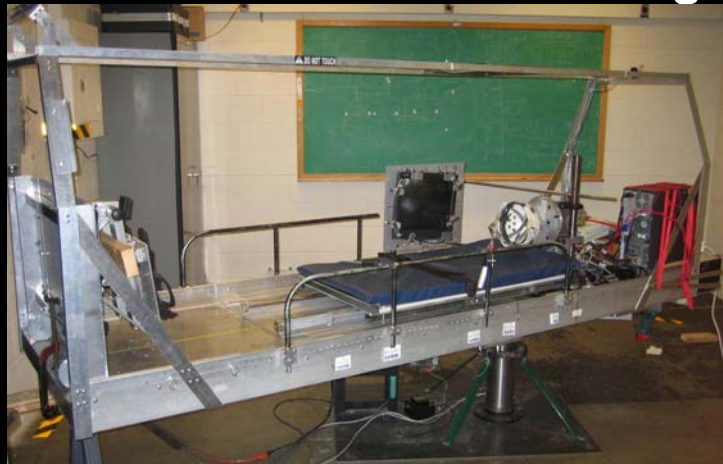
17

Squat Biomechanics Experiments



18

MVL Short-Radius Centrifuge



- 2.1 m subject rotation radius
- Horizontal rotation about an Earth-vertical axis
- Up to 30 RPM (180 degrees / second)

19

Resistive Exercise Device

- On-board MVL short-radius centrifuge
- Linear back slider with shoulder pads
- Constant force spring assembly
 - Up to 230-lbs in 5-lb increments
- Upright back slider that utilizes centrifuge components



20

Experiment 1: AG Squats

Research Aims

- Quantify mediolateral knee travel
 - No-rotation vs. AG
 - Hypothesis #1 (Aim #1)
 - No-rotation vs. post-rotation
 - Hypothesis #2 (Aim #2)

Experiment Overview

- N = 15 (7 male, 8 female)
- Ages 19-39, regular exercisers
- 0.5 Hz self-paced cadence
- All trials on-board centrifuge
 - Clockwise rotation
 - Supine

Experiment Protocol

Phase	1	2	3					4	5					6
Repetitions	8	8	8	8	8	8	8	8	8	8	8	8	8	8
Resistance (%BW)	0	100	0	0	0	0	0	0	0	0	0	0	0	0
RPM	0	0	23	23	23	23	23	0	30	30	30	30	30	0

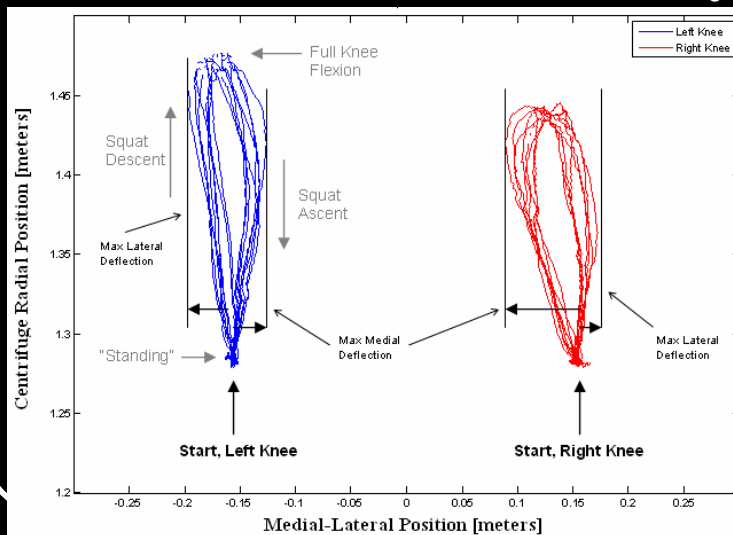
40 repetitions
(5 sets of 8 reps)

40 repetitions
(5 sets of 8 reps)

21

Mediolateral Knee Travel

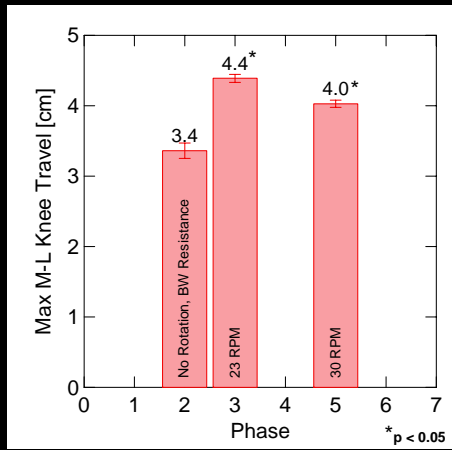
- Maximum Total Medial-Lateral Travel
 - Sum of max medial and max lateral deflection during each rep



Experiment 1
Subject #7
23 RPM
8 reps

22

Mediolateral Knee Travel



No rotation, BW < 23 RPM
(p = 0.004)

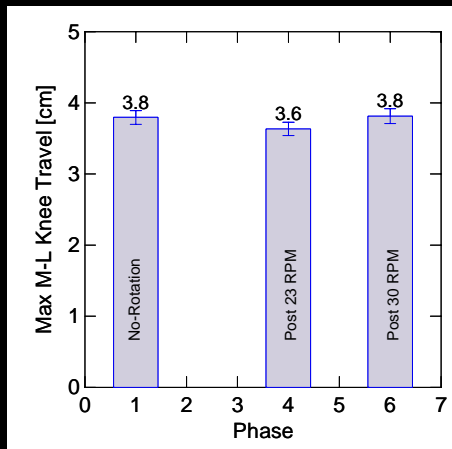
No Rotation, BW < 30 RPM
(p = 0.006)

No significant differences:
23 vs. 30 RPM
Left vs. Right Leg
Male vs. Female

N = 14
Mean +/- SEM
Repeated measures ANOVA

Phase	1	2	3					4	5					6
Repetitions	8	8	8	8	8	8	8	8	8	8	8	8	8	8
Resistance (%BW)	0	100	0	0	0	0	0	0	0	0	0	0	0	0
RPM	0	0	23	23	23	23	23	0	30	30	30	30	30	0

Mediolateral Knee Travel



No rotation vs. Post-23 (n.s.)
No rotation vs. Post-30 (n.s.)

→ No significant after-effects

N = 14
Mean +/- SEM
Repeated measures ANOVA

Phase	1	2	3					4	5					6
Repetitions	8	8	8	8	8	8	8	8	8	8	8	8	8	8
Resistance (%BW)	0	100	0	0	0	0	0	0	0	0	0	0	0	0
RPM	0	0	23	23	23	23	23	0	30	30	30	30	30	0

Experiment 2: AG + Upright Squats

Research Aims

- Quantify mediolateral knee travel
 - Effect of Additional Resistance
 - Hypothesis #1 (Aim #1)
- Upright vs. AG biomechanics
 - Aim #3

Experiment Overview

- N = 13 (9 male, 4 female)
 - 8 repeated from Experiment 1
- Ages 19-39
- 0.5 Hz cadence
- 2 Groups
- 0, 10, 25% body weight resistance

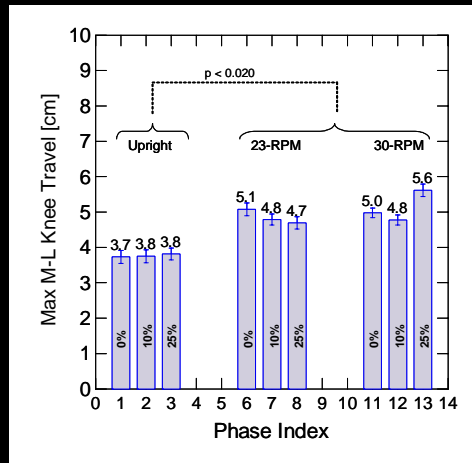
Experiment Protocol

Phase	1	2	3	4	5	6	7	8	9	10	11	12	13	14
Repetitions	8	8	8	8	8	8	8	8	8	8	8	8	8	8
Posture	Up	Up	Up	Su	Su	Su	Su	Su	Su	Su	Su	Su	Su	Su
Resistance (%BW)	0	10	25	0	100	0	10	25	0	0	0	10	25	0

Upright (Phases 1-5) Centrifuge Group A: 23 RPM (Phases 6-8) Group B: 30 RPM (Phases 9-10) Centrifuge Group A: 30 RPM (Phases 11-13) Group B: 23 RPM (Phases 12-13)

25

Mediolateral Knee Travel



No significant effect of resistance, group, leg, or gender

23 vs. 30 RPM (n.s.)

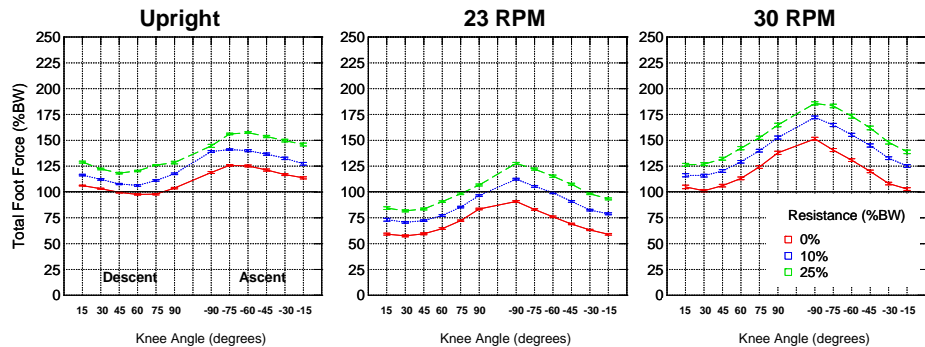
N = 11

Mean +/- SEM

Repeated measures ANOVA

Phase	1	2	3	4	5	6	7	8	9	10	11	12	13	14
Repetitions	8	8	8	8	8	8	8	8	8	8	8	8	8	8
Posture	Up	Up	Up	Su	Su	Su	Su	Su	Su	Su	Su	Su	Su	Su
Resistance (%BW)	0	10	25	0	100	0	10	25	0	0	0	10	25	0
RPM (Group A)	0	0	0	0	0	23	23	23	0	0	30	30	30	0
RPM (Group B)	0	0	0	0	0	30	30	30	0	0	23	23	23	0

Foot Reaction Forces

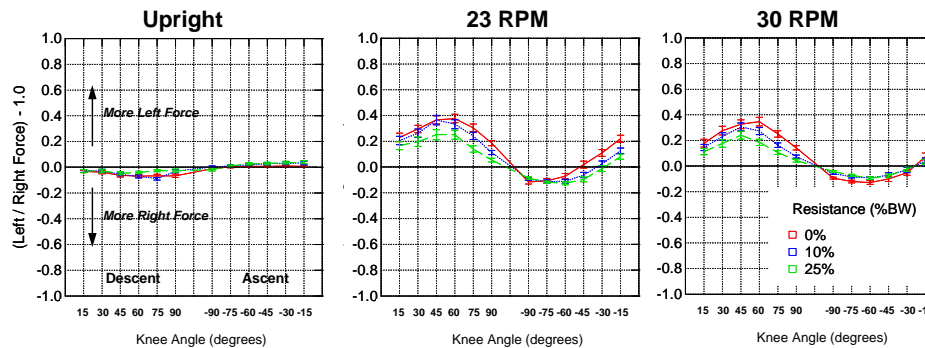


- Ascent > Descent ($p < 0.0005$)
- 23-RPM < Upright < 30-RPM ($p < 0.0005$)
- No significant differences between Gender or Group
- Qualitative differences between Upright and AG
 - Upright: approximately sinusoidal
 - Centrifuge: approximately parabolic

N = 11
Mean +/- SEM
Repeated Measures ANOVA

27

Foot Reaction Forces

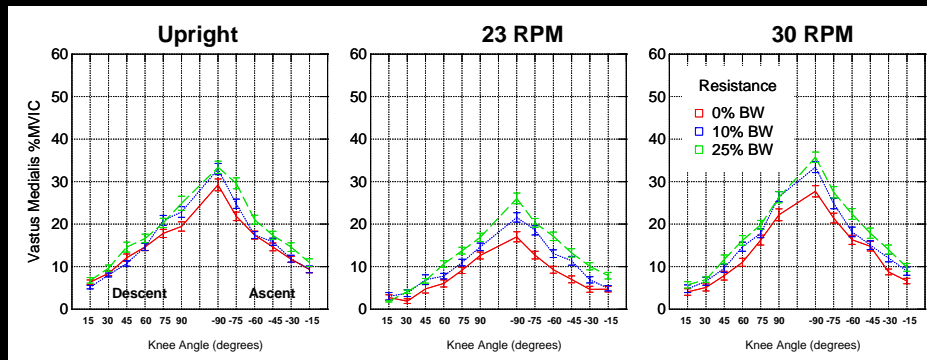


- Descent > Ascent ($p = 0.001$)
- 23, 30 RPM > Upright ($p = 0.019$)
- Ratio decreases with increasing resistance ($p < 0.0005$)
- No significant effects of Dominant Foot, Gender, or Group

N = 11
Mean +/- SEM

28

Muscle Activity



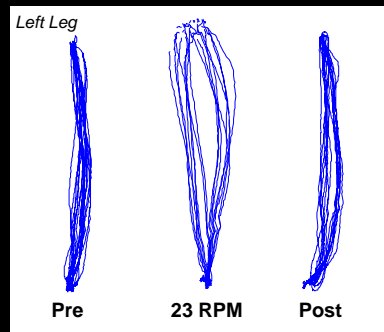
- 23-RPM < Upright < 30-RPM ($p < 0.0005$)
- %MVIC increases with resistance ($p < 0.0005$)
- Vastus medialis, vastus lateralis, and soleus showed similar left-to-right asymmetry as the foot forces

Right Vastus Medialis
N = 11
Mean +/- SEM

29

Discussion and Conclusions

1. Mediolateral knee travel
 - 1.0 to 2.0 cm greater during AG squats
 - No significant difference between genders or left/right leg
 - Unaffected by additional resistance
 - No significant after-effects
2. Two-dimensional squat model
 - Coriolis accelerations predictions
 - ~0.6 N-m knee torque from Coriolis forces
 - ~30 N-m knee torque from biomechanics
 - Repetitive stress injuries unlikely

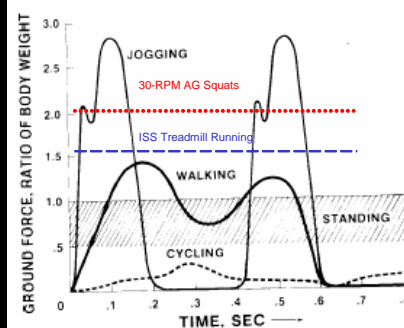


30

Discussion and Conclusions

3. Foot reaction forces

- 30 RPM > Upright > 23 RPM
- Peak forces less than jogging
(Thornton et. al 1986, Cavanagh 2005)
- Likely sufficient for bone maintenance
(Qin, Rubin, and McLeod 1998)
- Left/right asymmetry hypothesized as postural correction



4. Muscle Activity

- Quadriceps ~ 50% MVIC, Soleus ~ 40% MVIC
- Other muscles not very active (< 15% MVIC)
- 12 RM strength training protocol ~80% MVIC quadriceps
(Escamilla et. al 1998)
- Left-to-right asymmetry (not all muscle groups)

(Thornton et. al 1986)

31

Recommendations

1. In 0-G, exercise left or right shoulder “down” to minimize (or eliminate) M-L Coriolis accelerations. If Earth-supine, spin the centrifuge in both directions.
2. Increase the rotation rate and/or resistance for muscular training. The ACSM recommends at least 3 sets of 8 to 12 repetitions to “maximum momentary failure.”
3. Increase the rotation rate, resistance, or add “impactors” to the feet for maintaining bone mineral density. Peak foot forces of at least 260% body weight are desirable (e.g., Earth jogging).
4. Consider foot motion instead of torso motion if the resistive load and “inertial feel” can be replicated to eliminate vestibular Coriolis and inertial/centripetal accelerations.

32

Summary of Contributions

- Quantified the mediolateral knee travel during upright, supine, and artificial gravity squats
- Compared the biomechanics of upright and artificial gravity squats for exercise protocol design
- Developed and validated a two-dimensional model for predicting Coriolis accelerations
- Made initial assessments on the safety of AG exercises
- Designed and built squat exercise hardware for use on the MVL centrifuge

33

Acknowledgements

- Thesis Committee: Larry Young, Lars Oddsson, Chuck Oman, Dava Newman, Jeff Hoffman
- Thomas Jarchow and Pranay Sinha
- All my test subjects
- Supported by NASA Grant NNJ04HD64G and the MIT-Italy Program Progetto Roberto Rocca



34

Key References

- NSBRI. (cited 2006) Research Areas: National Space Biomedical Research Institute. Available from: <http://www.nsbri.org/Research/index.html>.
- Diamandis, P.H. (1988) The Artificial Gravity Sleeper: A Deconditioning Countermeasure for Long Duration Space Habitation. S.M. Thesis in Aeronautics and Astronautics, Massachusetts Institute of Technology: Cambridge, MA.
- Paloski, W.H. and L.R. Young. (1999) NASA/NSBRI Artificial Gravity Workshop: Proceedings and Recommendations.
- Caiozzo, V.J., et al. (2004) Hemodynamic and metabolic responses to hypergravity on a human-powered centrifuge. *Aviation, Space, and Environmental Medicine*, 75(2): p. 101-8.
- Iwase, S. (2004) Effectiveness of centrifuge-induced artificial gravity with ergometric exercise as a countermeasure during simulated microgravity exposure in humans. in Proceedings of the 55th International Astronautical Congress 2004, Vancouver, Canada.
- Edmonds, J. (2005) Exercise in Artificial Gravity, SM in Aeronautics and Astronautics, Massachusetts Institute of Technology: Cambridge, MA.
- DiZio, P. and J.R. Lackner. (2002) Sensorimotor aspects of high-speed artificial gravity. III. Sensorimotor adaptation. *Journal of Vestibular Research*, 12(5-6): p. 291-9.
- Buckley, J.C., Jr. (2006) Space Physiology. New York: Oxford University Press.
- Thornton, W.E., G.W. Hoffer, and J.A. Rummel. (1977) Chapter 32. Anthropometric Changes and Fluid Shifts, in Biomedical Results from Skylab (NASA SP-377). R.S. Johnston and L.F. Diellein, Editors. p. 330-338.
- Conventino, V.A. (1996) Exercise as a countermeasure for physiological adaptation to prolonged spaceflight. *Medicine and Science in Sports and Exercise*, 28(8): p. 999-1014.
- LeBlanc, A., et al. (1995) Regional muscle loss after short duration spaceflight. *Aviation, Space, and Environmental Medicine*, 66(12): p. 1151-4.
- Shackelford, L.C., et al. (2004) Resistance exercise as a countermeasure to disuse-induced bone loss. *Journal of Applied Physiology*, 97(1): p. 119-29.
- Turner, C.H. and A.G. Robling. (2003) Designing exercise regimens to increase bone strength. *Exerc Sport Sci Rev*, 31(1): p. 45-50.
- Qin, Y.X., C.T. Rubin, and K.J. McLeod. (1998) Nonlinear dependence of loading intensity and cycle number in the maintenance of bone mass and morphology. *Journal of Orthopaedic Research*, 16(4): p. 482-9.
- Schneider, S.M., et al. (2003) Training with the International Space Station interim resistive exercise device. *Medicine and Science in Sports and Exercise*, 35(11): p. 1935-45.
- Escamilla, R.F., et al. (1998) Biomechanics of the knee during closed kinetic chain and open kinetic chain exercises. *Medicine and Science in Sports and Exercise*, 30(4): p. 556-69.
- Young, L.R. (1999) Artificial gravity considerations for a mars exploration mission. *Annals of the New York Academies of Sciences*, 871: p. 367-378.
- Greentleaf, J.E., et al. (1997) Cycle-Powered Short Radius (1.9m) Centrifuge: Effect of Exercise Versus Passive Acceleration on Heart Rate in Humans. NASA Ames Research Center (NASA Technical Memorandum 110433), p. 1-13.
- Kreitenberg, A., et al. (1998) The "Space Cycle" self powered human centrifuge: a proposed countermeasure for prolonged human spaceflight. *Aviation, Space, and Environmental Medicine*, 69(1): p. 66-72.
- Yeadon, M.R. (1990) The simulation of aerial movement-II. A mathematical inertia model of the human body. *Journal of Biomechanics*, 23(1): p. 67-74.
- Ericson, M. (1986) On the Biomechanics of Cycling. *Scandinavian Journal of Rehabilitation in Medicine Supplement*, 16: p. 1-43.
- Asplund, C. and P. St. Pierre. (2004) Knee Pain and Bicycling. *The Physician and Sports Medicine*, 32(4): p. 1-12.
- Fleck, S.J. and W.J. Kraemer. (1987) Designing Resistance Training Programs. Second ed. Champaign, IL: Human Kinetics, pp. 1-275.
- Thornton, W.E. (1986) Work, Exercise, and Space Flight II. Modification of Adaptation by Exercise (Exercise Prescription). in Proceedings of the Workshop on Exercise Prescription for Long-Duration Space Flight. Houston, TX: NASA CP-3051.

Appendix I: Individual Data

In Appendix H, we list the subject demographics and raw (or partially reduced) data for each of the dependent measures analyzed. We first present the data for Experiment 1 and Experiment 2. For the data in Experiment 2, we also present tabulations of the comparisons between the rotation rates and levels of additional resistance.

Experiment 1

Subject Demographics and Anthropometrics

The demographics and anthropometrics of the subjects who took part in Experiment 1 are listed in the following tables. The subject number, gender (male or female), age (in years), and footedness (left or right dominant foot) are listed in the left-most column. The anthropometrics are in the following columns. We present the mass and length of nine body segments. The center of mass (CoM) is measured from the proximal end of each segment, and we also show the center of mass of each segment relative to the top of the head. Total body mass is the sum of the torso and head plus twice the sum of the remaining segments (i.e., two upper arms, two lower arms, etc.)

		Mass [kg]	Length [m]	CoM [m]	CoM from Top of Head [m]
Subject 1 Male, 29 yrs., L footed	Torso and Head	39.93	0.90	0.54	0.54
	Upper Arm	2.00	0.26	0.12	0.55
	Lower Arm	0.99	0.21	0.09	0.78
	Palm	0.22	0.12	0.05	0.95
	Fingers	0.18	0.08	0.04	1.06
	Upper Leg	10.25	0.46	0.21	1.11
	Lower Leg	3.50	0.34	0.15	1.51
	Foot	0.53	0.15	0.06	1.70
	Toes	0.04	0.04	0.01	1.70
	Body Mass	75.36		Height	1.70

		Mass [kg]	Length [m]	CoM [m]	CoM from Top of Head [m]
Subject 2 Male, 27 yrs., R footed	Torso and Head	45.53	0.95	0.57	0.57
	Upper Arm	2.58	0.28	0.13	0.56
	Lower Arm	1.53	0.30	0.12	0.83
	Palm	0.22	0.12	0.05	1.06
	Fingers	0.18	0.08	0.04	1.17
	Upper Leg	11.14	0.51	0.23	1.18
	Lower Leg	3.72	0.39	0.17	1.63
	Foot	0.53	0.15	0.06	1.85
	Toes	0.04	0.04	0.01	1.85
	Body Mass	85.40		Height	1.85

Subject 3 Male 24 yrs., R footed		Mass [kg]	Length [m]	CoM [m]	CoM from Top of Head [m]
	Torso and Head	29.34	0.85	0.49	0.49
	Upper Arm	1.51	0.25	0.11	0.58
	Lower Arm	1.03	0.26	0.10	0.82
	Palm	0.22	0.12	0.05	1.03
	Fingers	0.18	0.08	0.04	1.14
	Upper Leg	9.08	0.51	0.24	1.09
	Lower Leg	3.43	0.36	0.16	1.52
	Foot	0.53	0.15	0.06	1.72
	Toes	0.04	0.04	0.01	1.72
Body Mass	61.38		Height	1.72	

Subject 4 Male, 29 yrs., R footed		Mass [kg]	Length [m]	CoM [m]	CoM from Top of Head [m]
	Torso and Head	42.37	0.91	0.54	0.54
	Upper Arm	3.20	0.31	0.14	0.58
	Lower Arm	1.45	0.28	0.11	0.86
	Palm	0.30	0.12	0.05	1.08
	Fingers	0.03	0.05	0.02	1.17
	Upper Leg	9.26	0.42	0.19	1.10
	Lower Leg	4.76	0.45	0.19	1.52
	Foot	1.52	0.28	0.12	1.78
	Toes	0.15	0.06	0.03	1.78
Body Mass	83.69		Height	1.78	

Subject 5 Female, 26 yrs., R footed		Mass [kg]	Length [m]	CoM [m]	CoM from Top of Head [m]
	Torso and Head	30.45	0.84	0.49	0.49
	Upper Arm	1.99	0.28	0.13	0.54
	Lower Arm	0.96	0.25	0.10	0.79
	Palm	0.28	0.12	0.05	0.99
	Fingers	0.05	0.05	0.03	1.09
	Upper Leg	11.18	0.52	0.24	1.08
	Lower Leg	4.33	0.41	0.18	1.54
	Foot	0.59	0.17	0.07	1.77
	Toes	0.04	0.04	0.01	1.77
Body Mass	69.27		Height	1.77	

Subject 6 Female, 19 yrs., L footed		Mass [kg]	Length [m]	CoM [m]	CoM from Top of Head [m]
	Torso and Head	34.47	0.84	0.50	0.50
	Upper Arm	1.76	0.26	0.12	0.54
	Lower Arm	0.95	0.26	0.10	0.78
	Palm	0.20	0.12	0.05	0.99
	Fingers	0.18	0.08	0.04	1.10
	Upper Leg	9.17	0.44	0.20	1.04
	Lower Leg	3.67	0.35	0.15	1.43
	Foot	0.53	0.15	0.06	1.63
	Toes	0.04	0.04	0.01	1.63
Body Mass	67.47		Height	1.63	

Subject 7 Male, 27 yrs., L footed		Mass [kg]	Length [m]	CoM [m]	CoM from Top of Head [m]
	Torso and Head	33.72	0.85	0.51	0.51
	Upper Arm	1.63	0.24	0.11	0.55
	Lower Arm	1.04	0.26	0.10	0.78
	Palm	0.22	0.12	0.05	0.99
	Fingers	0.18	0.08	0.04	1.10
	Upper Leg	8.65	0.50	0.23	1.08
	Lower Leg	3.10	0.37	0.16	1.51
	Foot	0.52	0.15	0.06	1.72
	Toes	0.04	0.04	0.01	1.72
	Body Mass	64.48		Height	1.72

Subject 8 Female, 28 yrs., L footed		Mass [kg]	Length [m]	CoM [m]	CoM from Top of Head [m]
	Torso and Head	33.61	0.90	0.53	0.53
	Upper Arm	1.83	0.27	0.12	0.59
	Lower Arm	0.94	0.25	0.10	0.84
	Palm	0.20	0.12	0.05	1.04
	Fingers	0.18	0.08	0.04	1.15
	Upper Leg	11.77	0.54	0.25	1.15
	Lower Leg	3.57	0.40	0.17	1.61
	Foot	0.53	0.15	0.06	1.84
	Toes	0.04	0.04	0.01	1.84
	Body Mass	71.71		Height	1.84

Subject 9 Female, 25 yrs., L footed		Mass [kg]	Length [m]	CoM [m]	CoM from Top of Head [m]
	Torso and Head	29.69	0.82	0.48	0.48
	Upper Arm	1.48	0.25	0.12	0.54
	Lower Arm	0.76	0.26	0.09	0.76
	Palm	0.16	0.12	0.06	0.99
	Fingers	0.18	0.08	0.04	1.09
	Upper Leg	8.86	0.48	0.21	1.03
	Lower Leg	2.81	0.37	0.16	1.46
	Foot	0.52	0.15	0.06	1.67
	Toes	0.04	0.04	0.01	1.67
	Body Mass	59.29		Height	1.67

Subject 10 Female, 39 yrs., R footed		Mass [kg]	Length [m]	CoM [m]	CoM from Top of Head [m]
	Torso and Head	34.09	0.83	0.50	0.50
	Upper Arm	1.67	0.24	0.11	0.52
	Lower Arm	0.89	0.26	0.09	0.74
	Palm	0.17	0.12	0.06	0.97
	Fingers	0.18	0.08	0.04	1.07
	Upper Leg	9.27	0.48	0.22	1.05
	Lower Leg	3.85	0.42	0.18	1.49
	Foot	0.53	0.15	0.06	1.73
	Toes	0.04	0.04	0.01	1.73
	Body Mass	67.28		Height	1.73

Subject 11 Female, 34 yrs., R footed		Mass [kg]	Length [m]	CoM [m]	CoM from Top of Head [m]
	Torso and Head	32.59	0.83	0.49	0.49
	Upper Arm	2.03	0.26	0.12	0.58
	Lower Arm	0.85	0.24	0.09	0.81
	Palm	0.19	0.12	0.06	1.02
	Fingers	0.18	0.08	0.04	1.12
	Upper Leg	10.30	0.49	0.22	1.05
	Lower Leg	3.83	0.37	0.16	1.48
	Foot	0.53	0.15	0.06	1.69
	Toes	0.04	0.04	0.01	1.69
	Body Mass	68.46		Height	1.69

Subject 12 Female, 19 yrs., R footed		Mass [kg]	Length [m]	CoM [m]	CoM from Top of Head [m]
	Torso and Head	28.18	0.82	0.48	0.48
	Upper Arm	1.45	0.25	0.11	0.53
	Lower Arm	0.80	0.26	0.09	0.76
	Palm	0.17	0.12	0.06	0.99
	Fingers	0.18	0.08	0.04	1.09
	Upper Leg	8.96	0.46	0.21	1.03
	Lower Leg	2.83	0.35	0.15	1.43
	Foot	0.52	0.15	0.06	1.63
	Toes	0.04	0.04	0.01	1.63
	Body Mass	58.11		Height	1.63

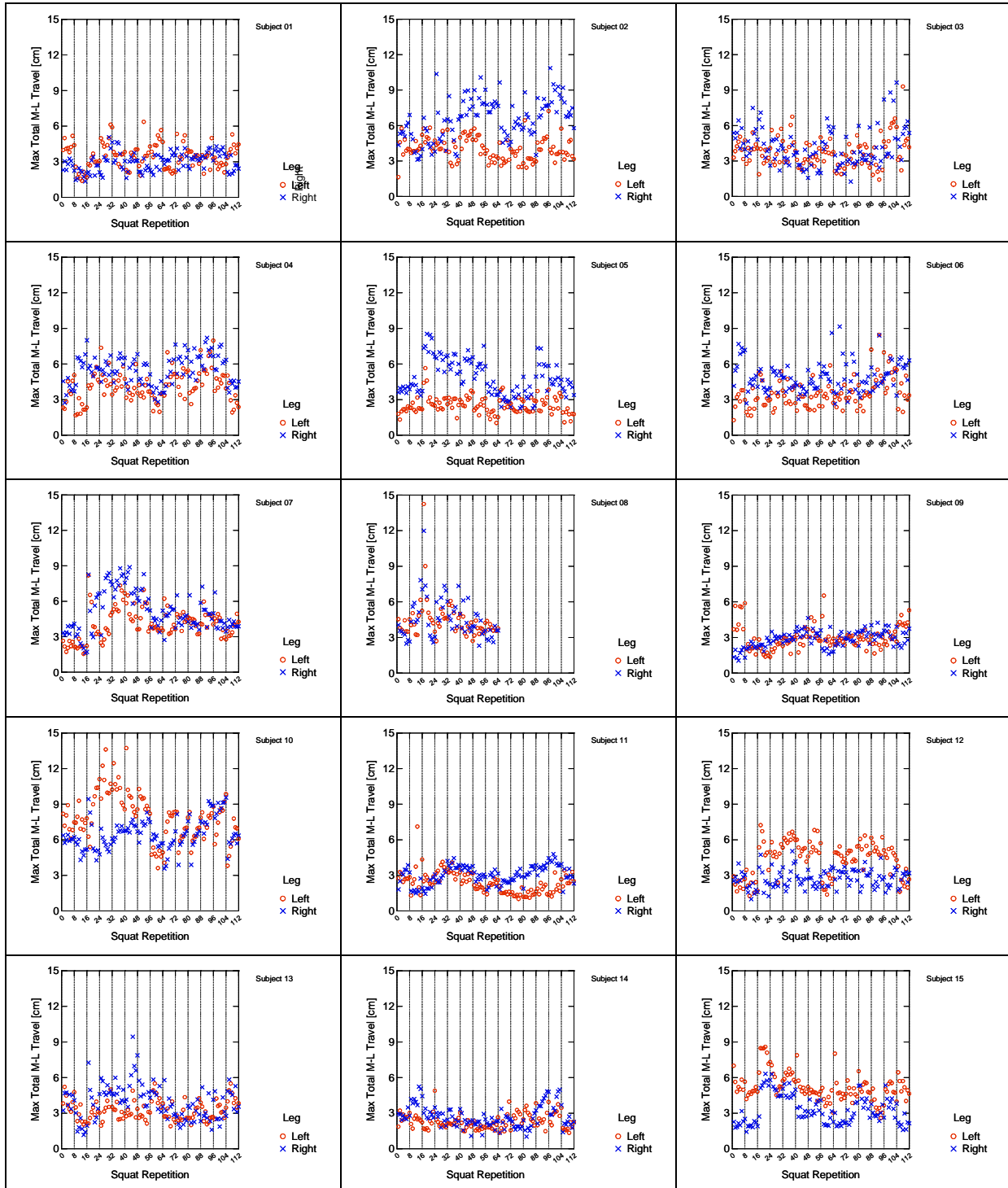
Subject 13 Male, 32 yrs., R footed		Mass [kg]	Length [m]	CoM [m]	CoM from Top of Head [m]
	Torso and Head	40.35	0.94	0.56	0.56
	Upper Arm	2.34	0.29	0.13	0.59
	Lower Arm	1.40	0.29	0.11	0.86
	Palm	0.21	0.12	0.05	1.09
	Fingers	0.18	0.08	0.04	1.20
	Upper Leg	10.10	0.47	0.21	1.15
	Lower Leg	3.30	0.39	0.16	1.57
	Foot	0.52	0.15	0.06	1.80
	Toes	0.04	0.04	0.01	1.80
	Body Mass	76.50		Height	1.80

Subject 14 Female, 27 yrs., R footed		Mass [kg]	Length [m]	CoM [m]	CoM from Top of Head [m]
	Torso and Head	24.06	0.77	0.44	0.44
	Upper Arm	1.32	0.25	0.11	0.49
	Lower Arm	0.59	0.24	0.08	0.71
	Palm	0.15	0.12	0.06	0.93
	Fingers	0.18	0.08	0.04	1.03
	Upper Leg	9.11	0.49	0.22	0.99
	Lower Leg	2.37	0.35	0.14	1.40
	Foot	0.51	0.15	0.06	1.61
	Toes	0.04	0.04	0.01	1.61
	Body Mass	52.57		Height	1.61

Subject 15 Male, 24 yrs., R footed		Mass [kg]	Length [m]	CoM [m]	CoM from Top of Head [m]
	Torso and Head	29.92	0.85	0.50	0.50
	Upper Arm	1.42	0.25	0.12	0.53
	Lower Arm	1.27	0.30	0.12	0.78
	Palm	0.22	0.12	0.05	1.01
	Fingers	0.18	0.08	0.04	1.12
	Upper Leg	9.60	0.45	0.21	1.06
	Lower Leg	3.43	0.36	0.15	1.45
	Foot	0.53	0.15	0.06	1.66
	Toes	0.04	0.04	0.01	1.66
	Body Mass	63.32		Height	1.66

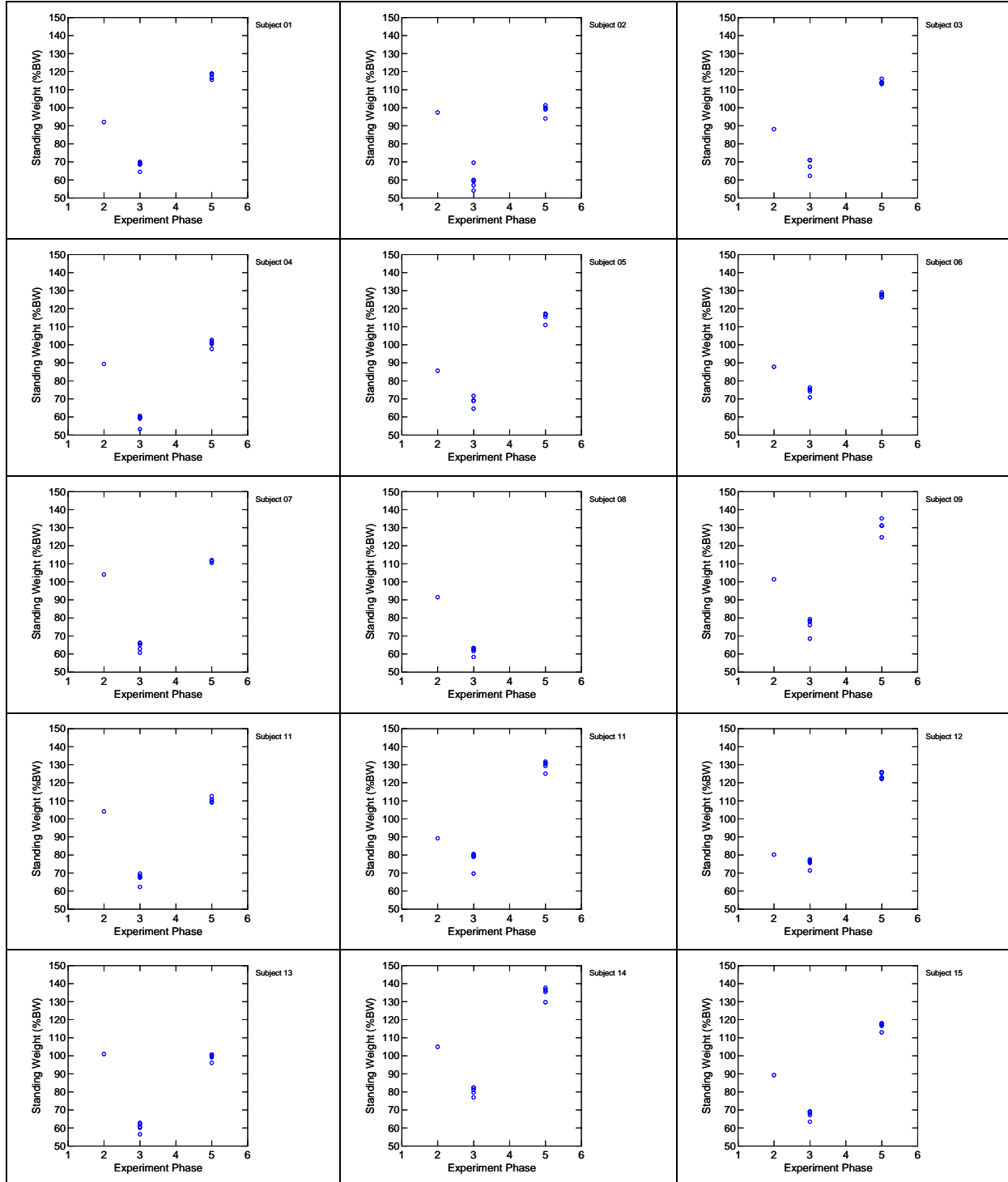
Maximum Medial-Lateral Knee Travel

The maximum medial-lateral knee travel in centimeters is shown for the left and right leg throughout all repetitions in Experiment 1. The repetitions are blocked sequentially by the experimental phases in groups of eight. Eight repetitions in Phases 1, 2, 4, and 6, and forty repetitions in Phases 3 and 5.



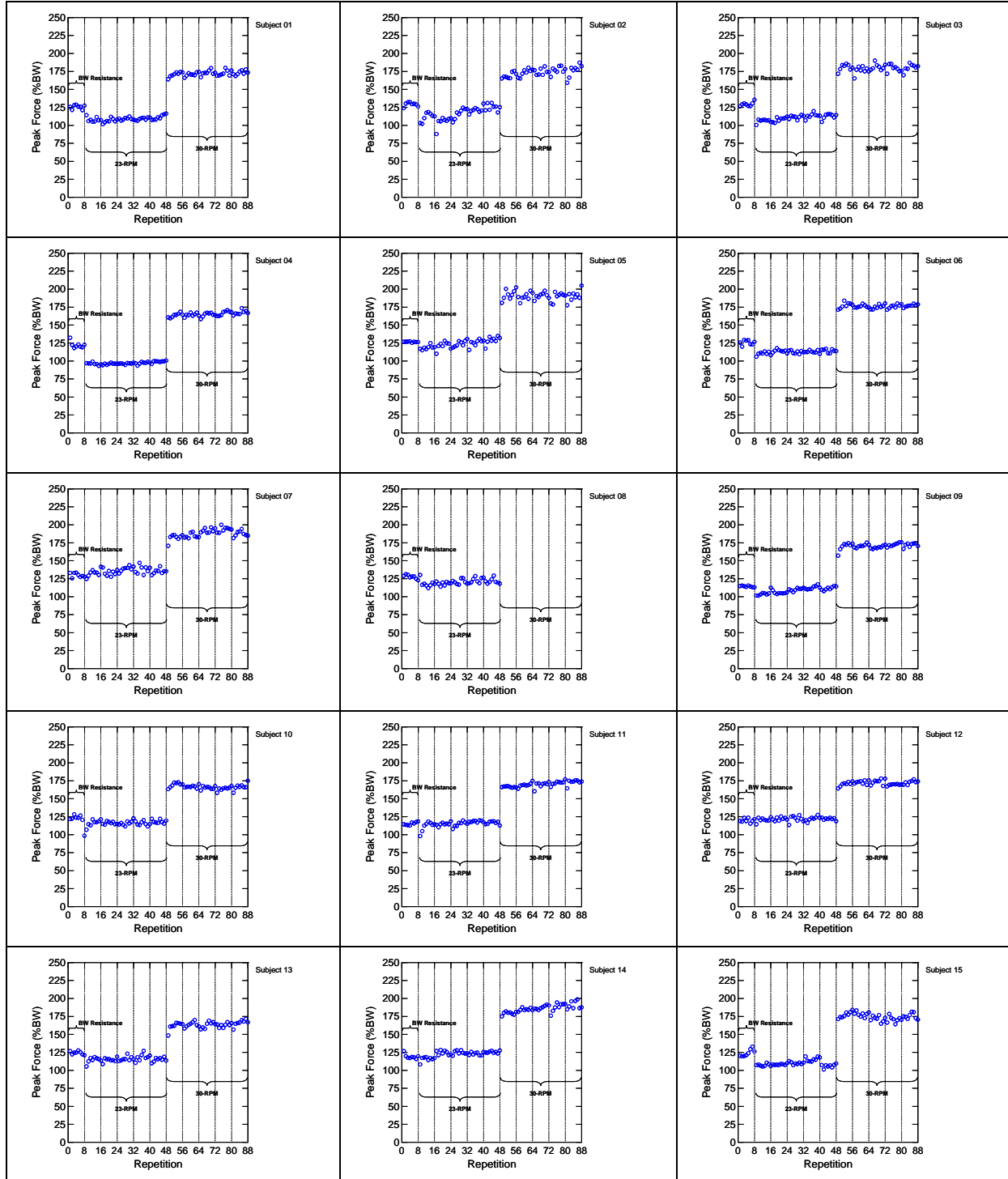
Standing Force

The standing force, expressed as a percentage of body weight, is shown for the three “weighted” phases: Phase 2, 3, and 5. There is one repetition in Phase 2, and five repetitions each in Phases 3 and 5 (one measurement before each set of eight squats).



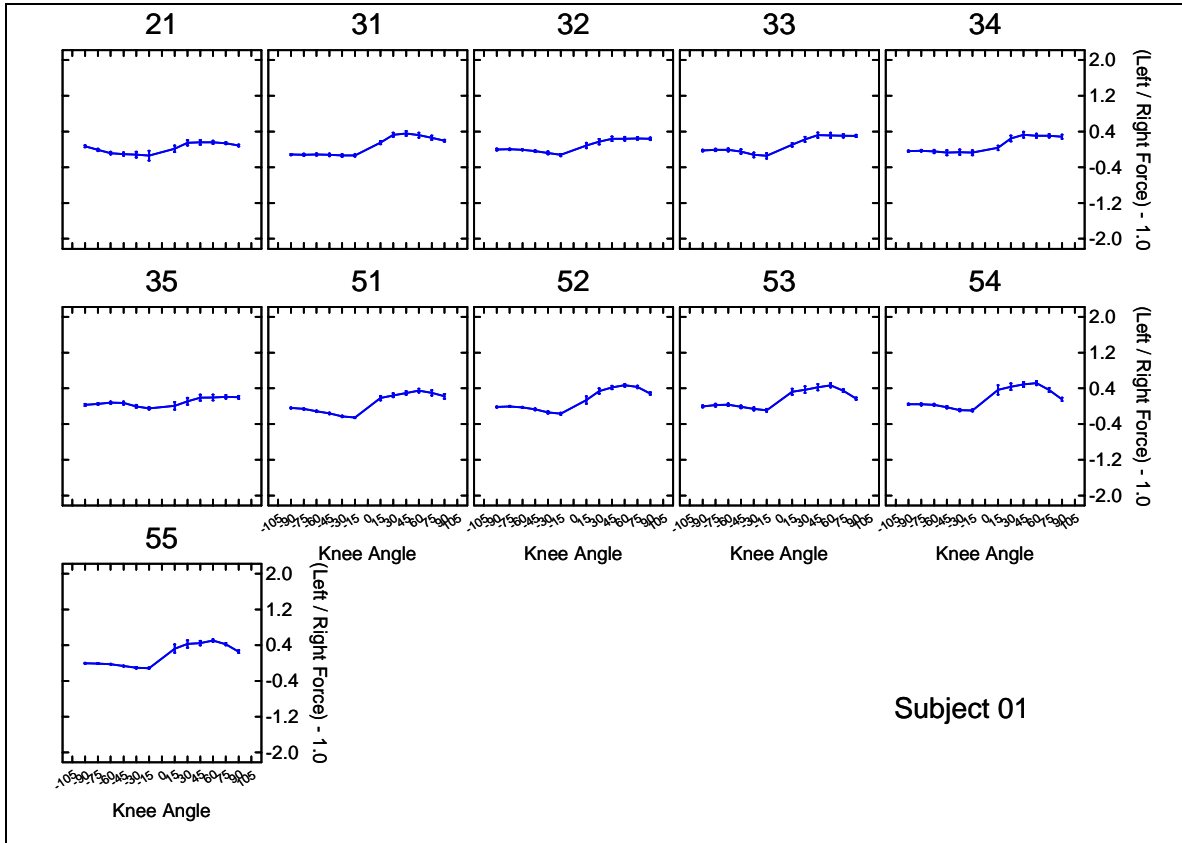
Peak Force

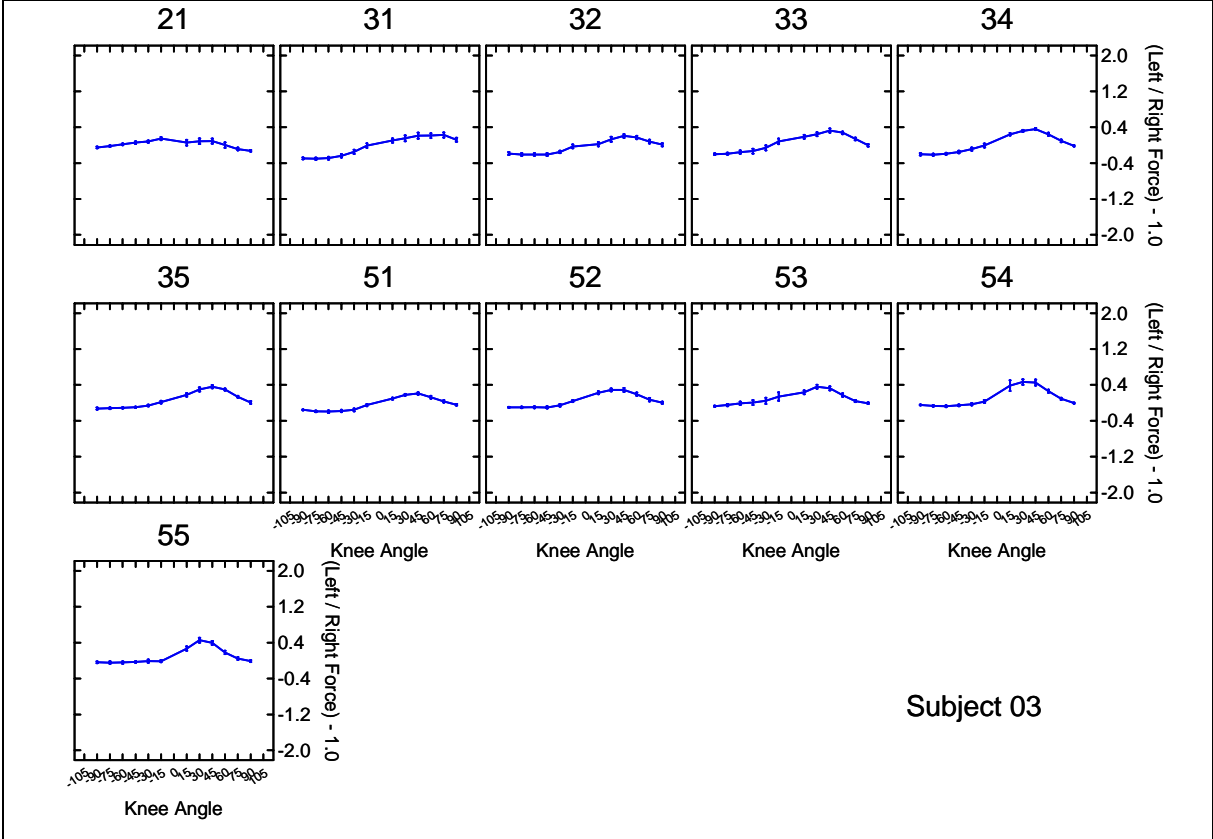
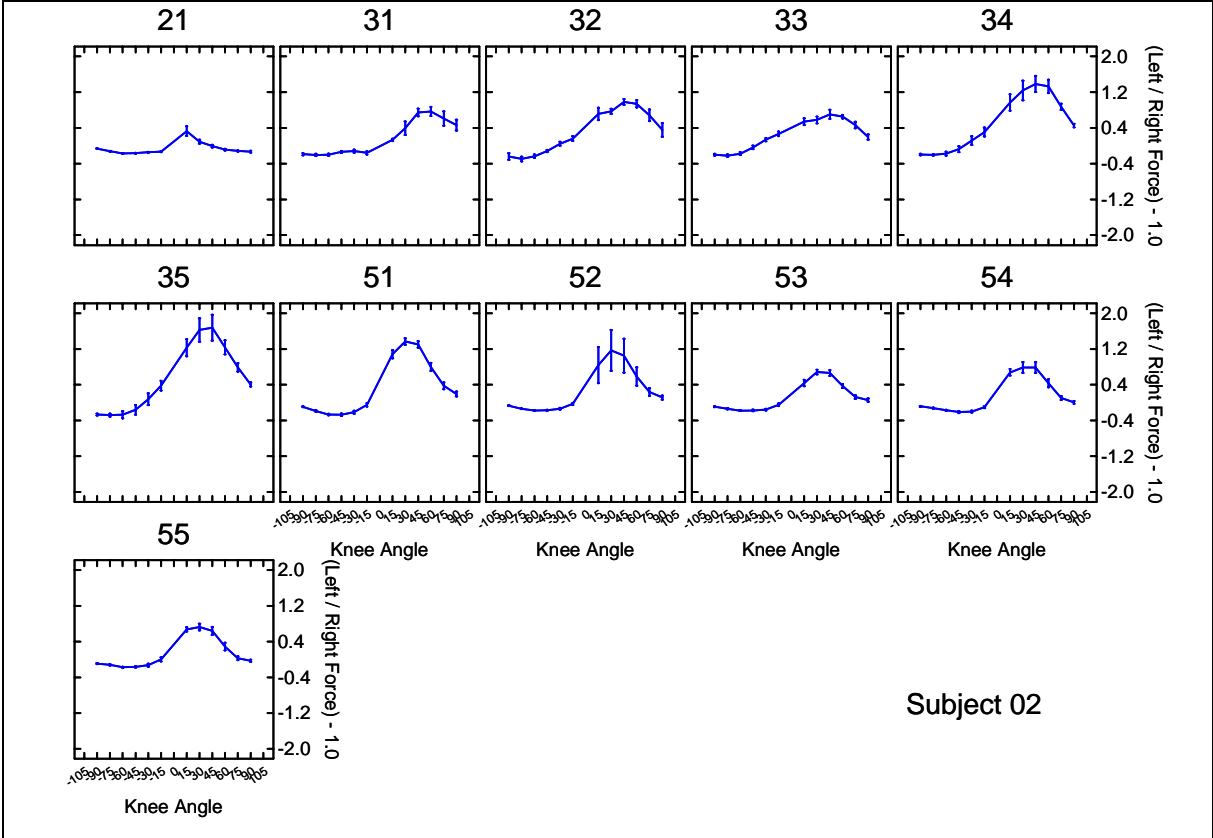
The peak force, expressed as a percentage of body weight, is shown for the three “weighted” phases: Phase 2, 3, and 5. Each of the repetitions is plotted sequentially for eight repetitions in Phase 2 and the forty repetitions in Phase 3 and 5.

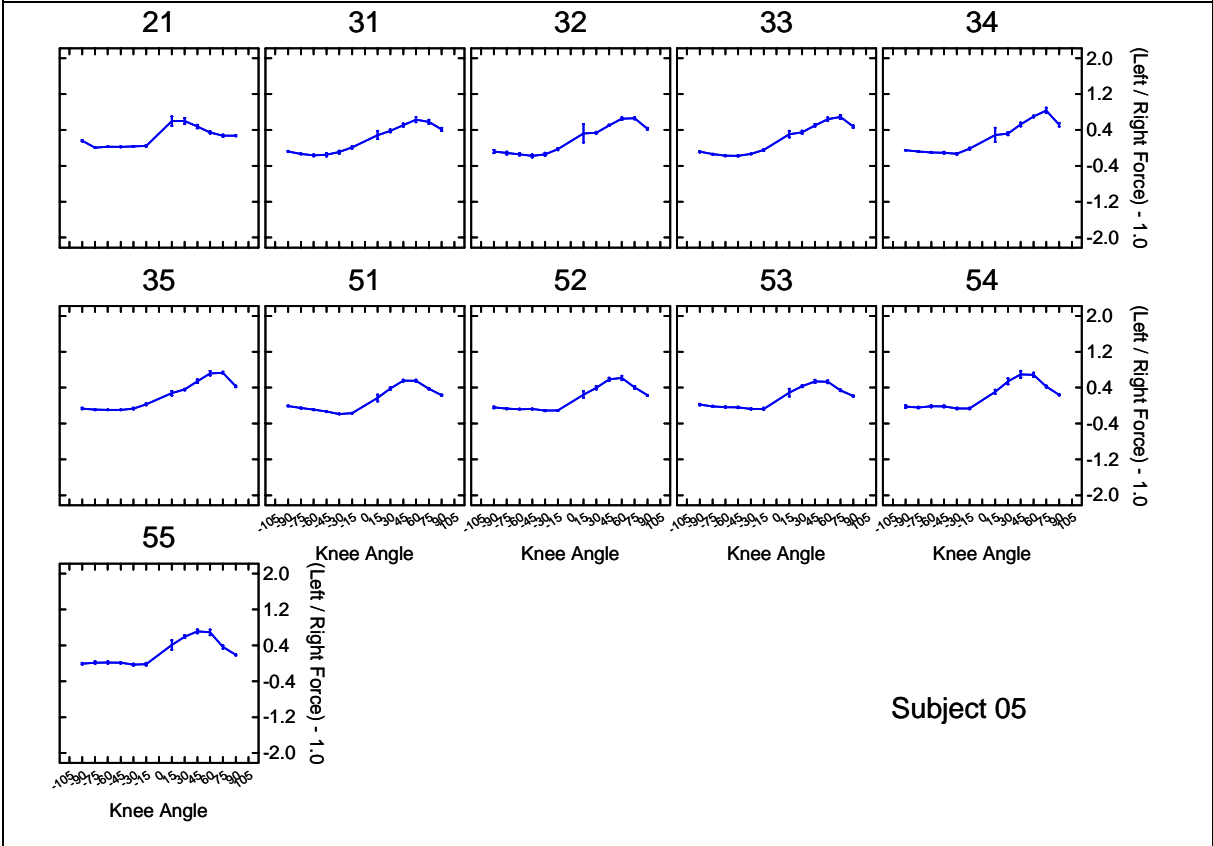
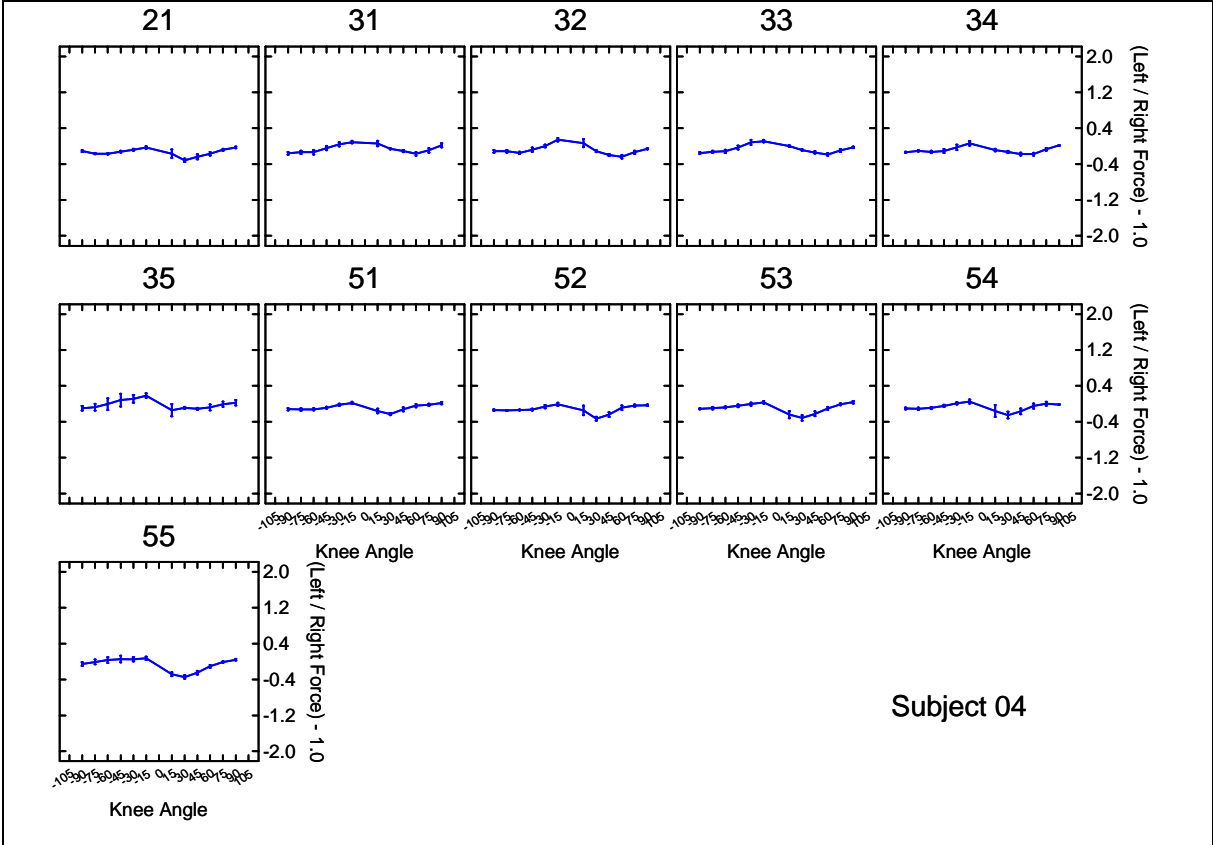


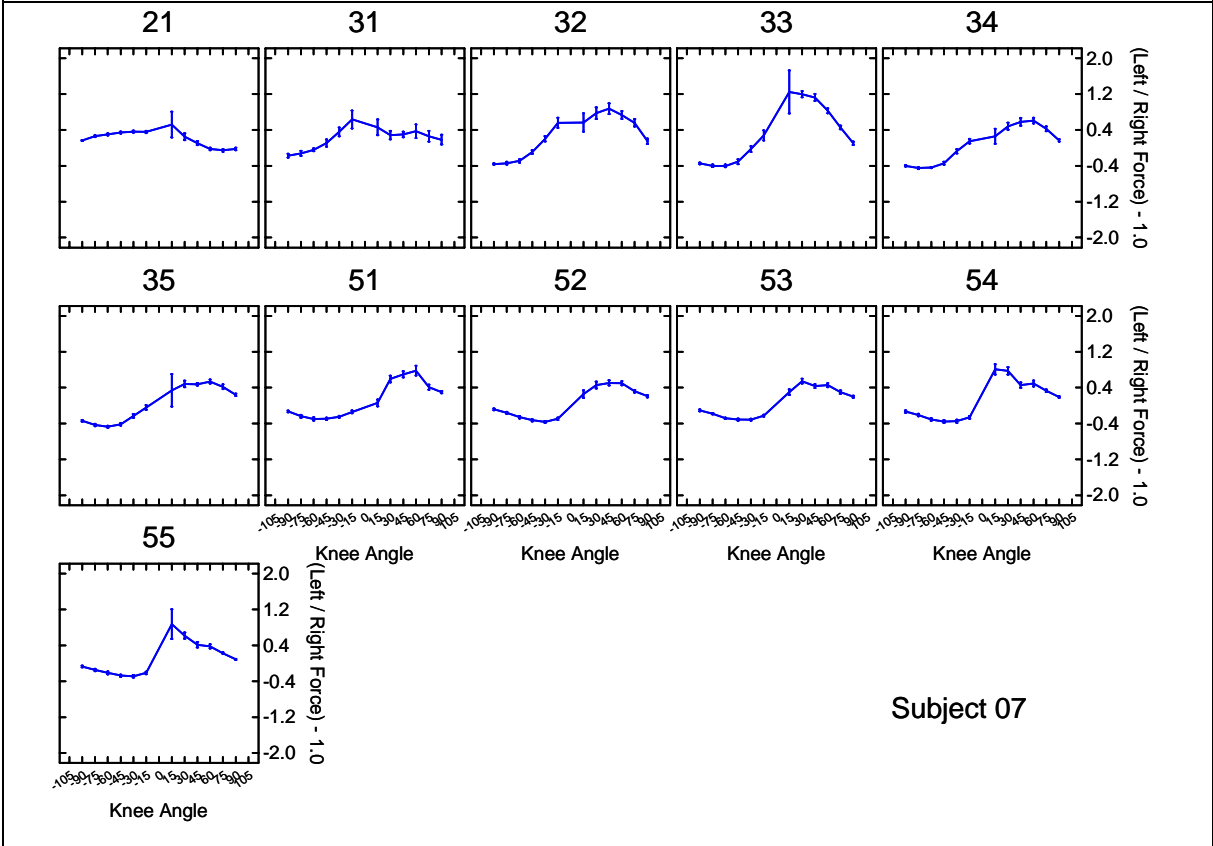
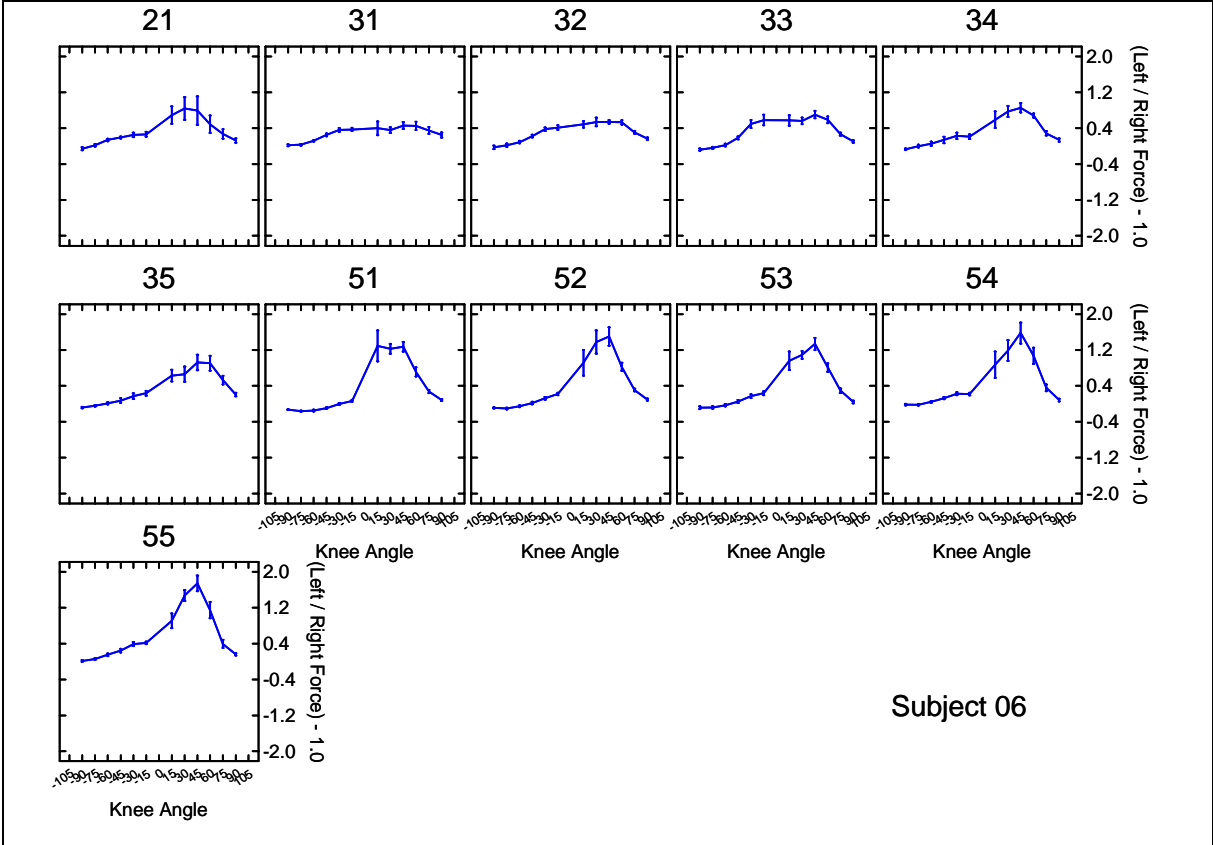
Left-Right Foot Force Asymmetry

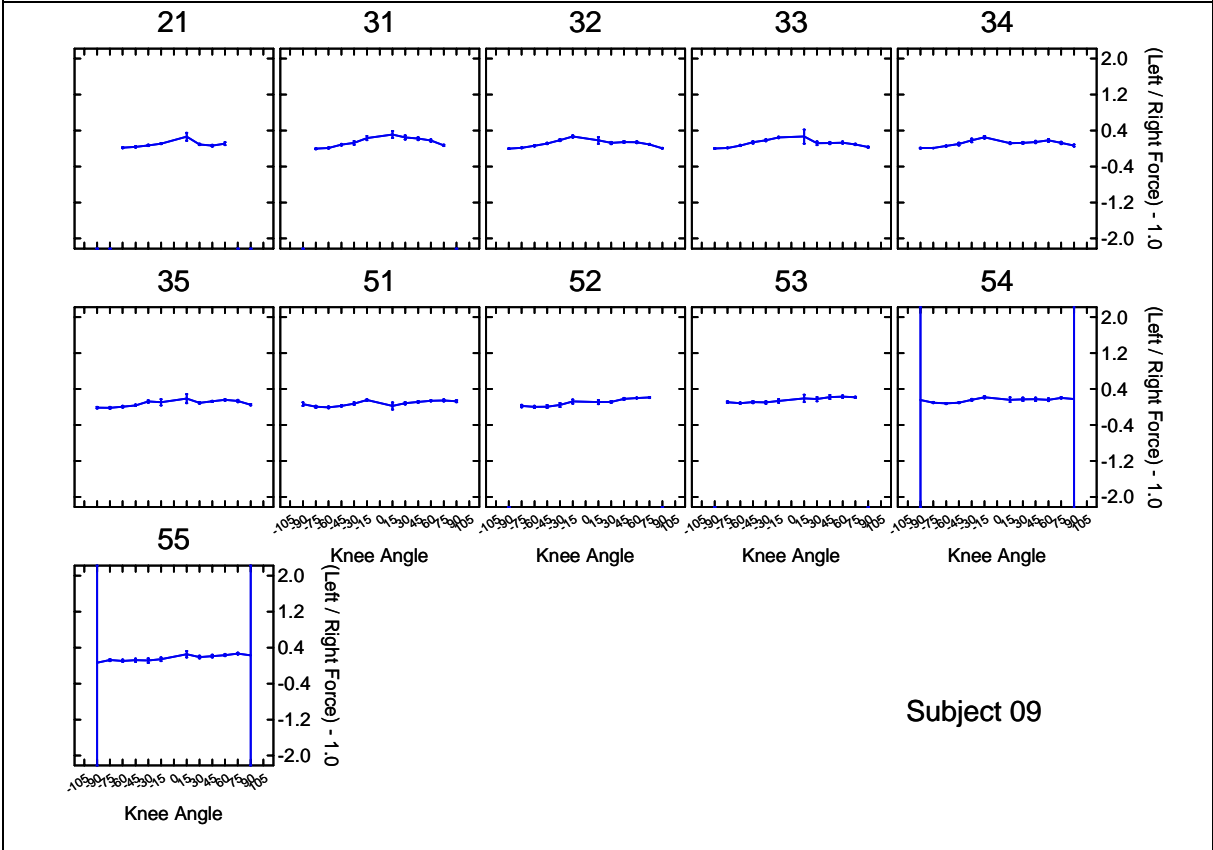
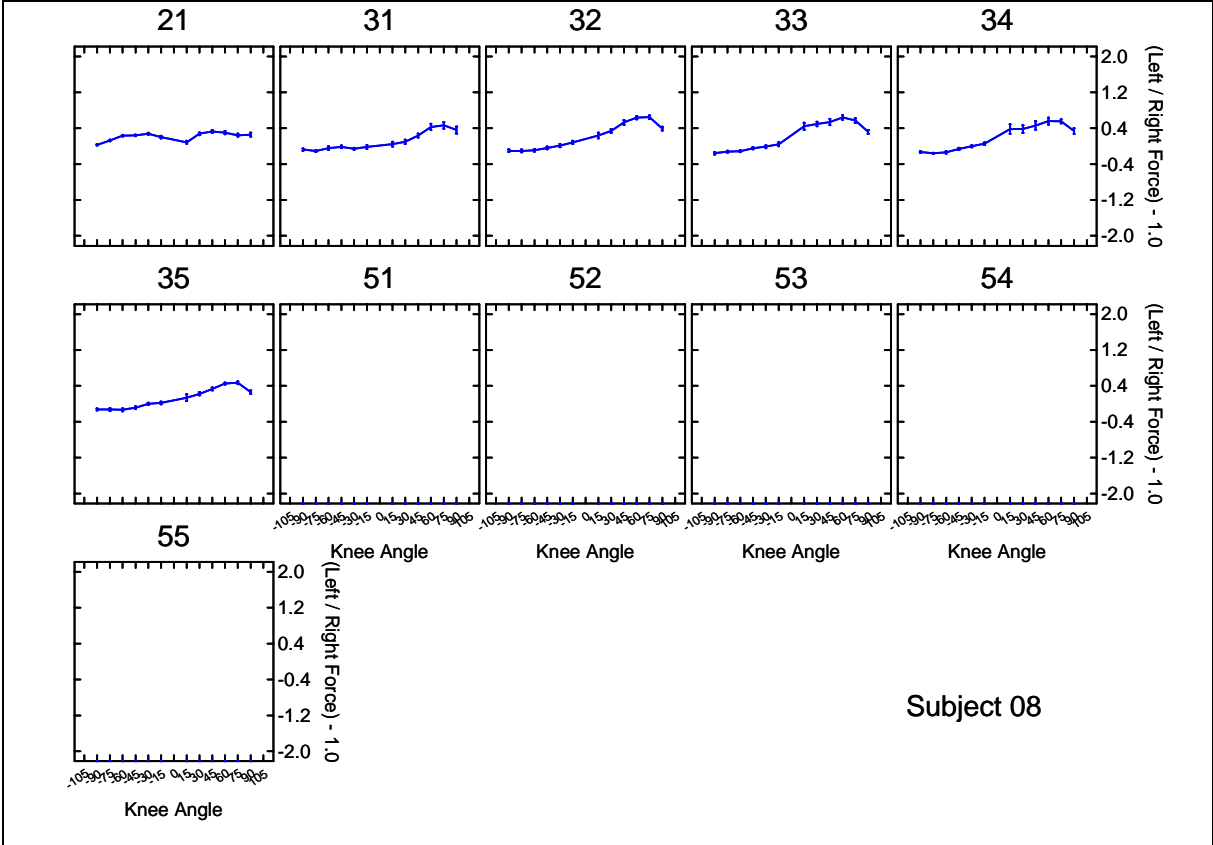
The left divided by right foot force minus one ($\text{Left} / \text{Right} - 1.0$) at several knee angles for each subject. The numbers on the top of the boxes are the Phase and Set. For example, 31 is Phase 3 (23-RPM), first set of eight repetitions. The eight repetitions within each set are averaged together. Mean \pm SEM. Note: The knee angles are the same as in the body of this thesis, however, the ordering of them is slightly different: 0-degree knee angle is in the middle of the graph and full extension (i.e., 90-degrees) is at the edges.

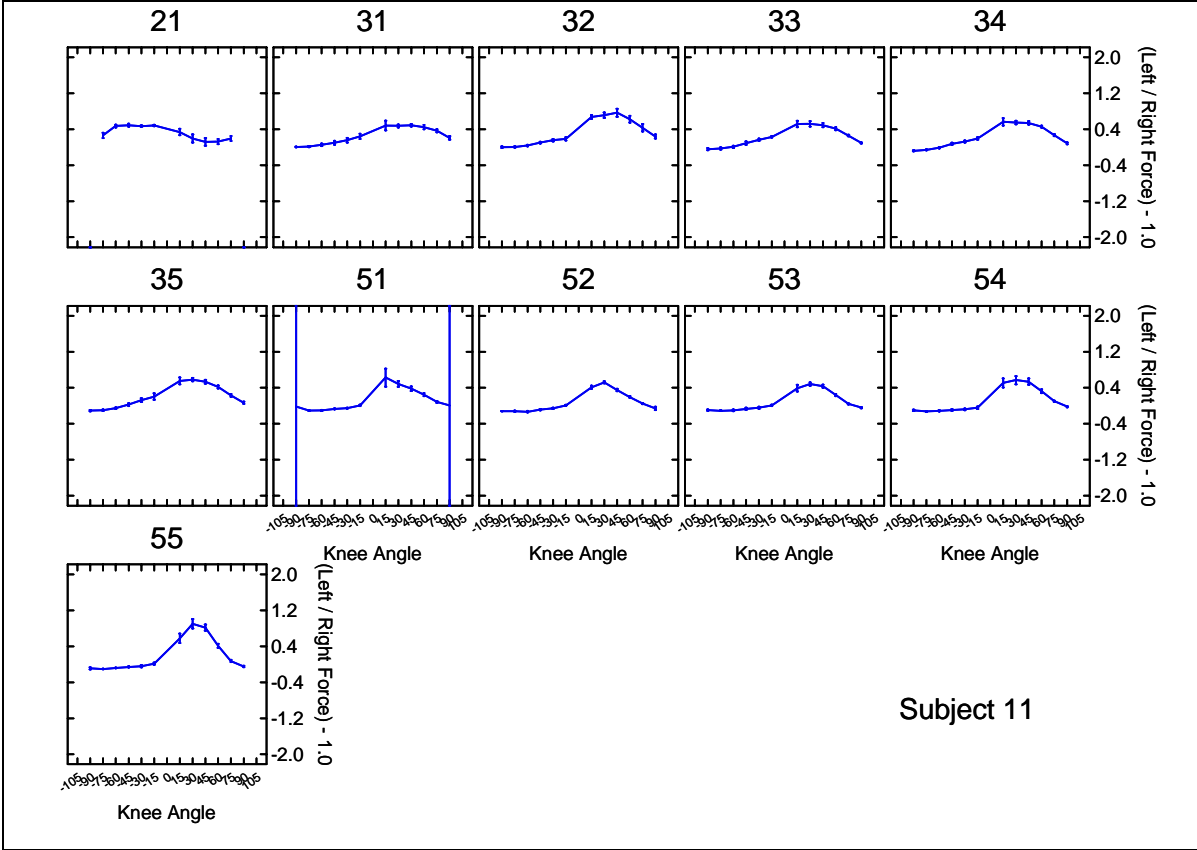
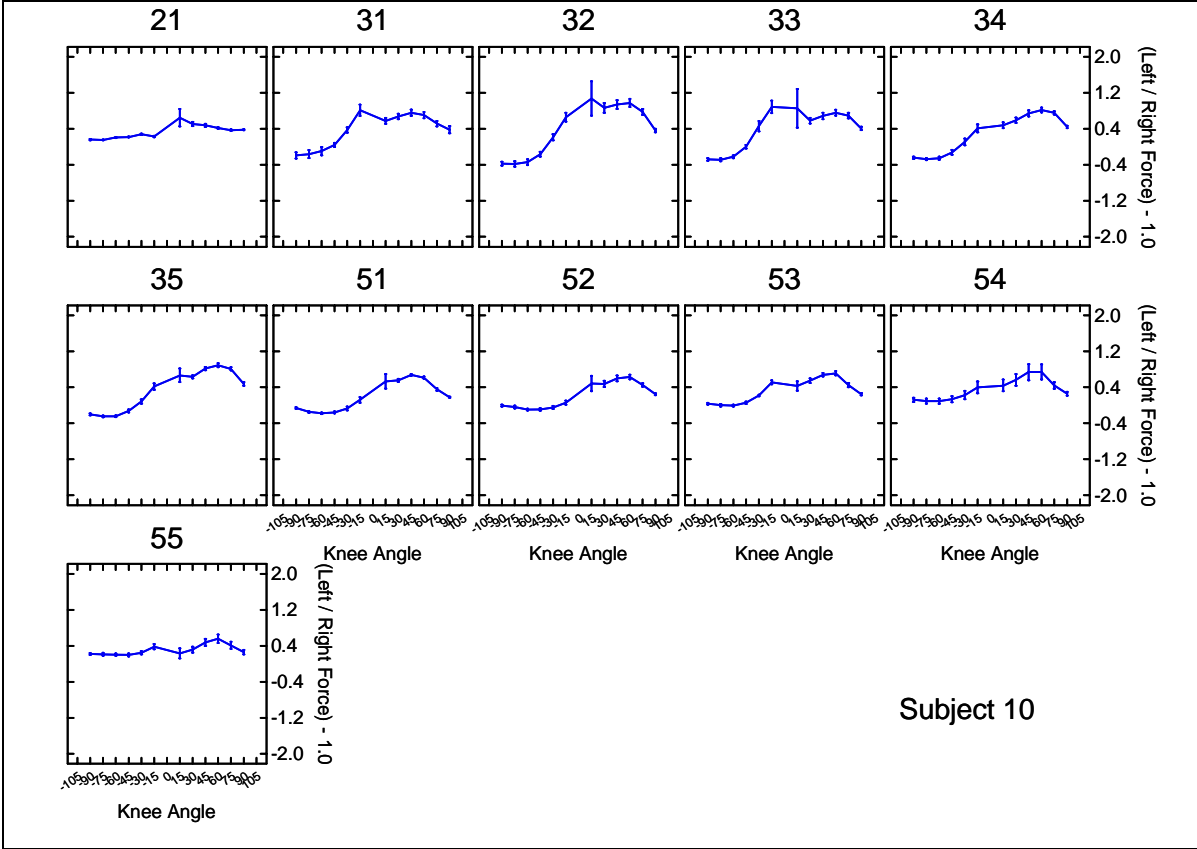


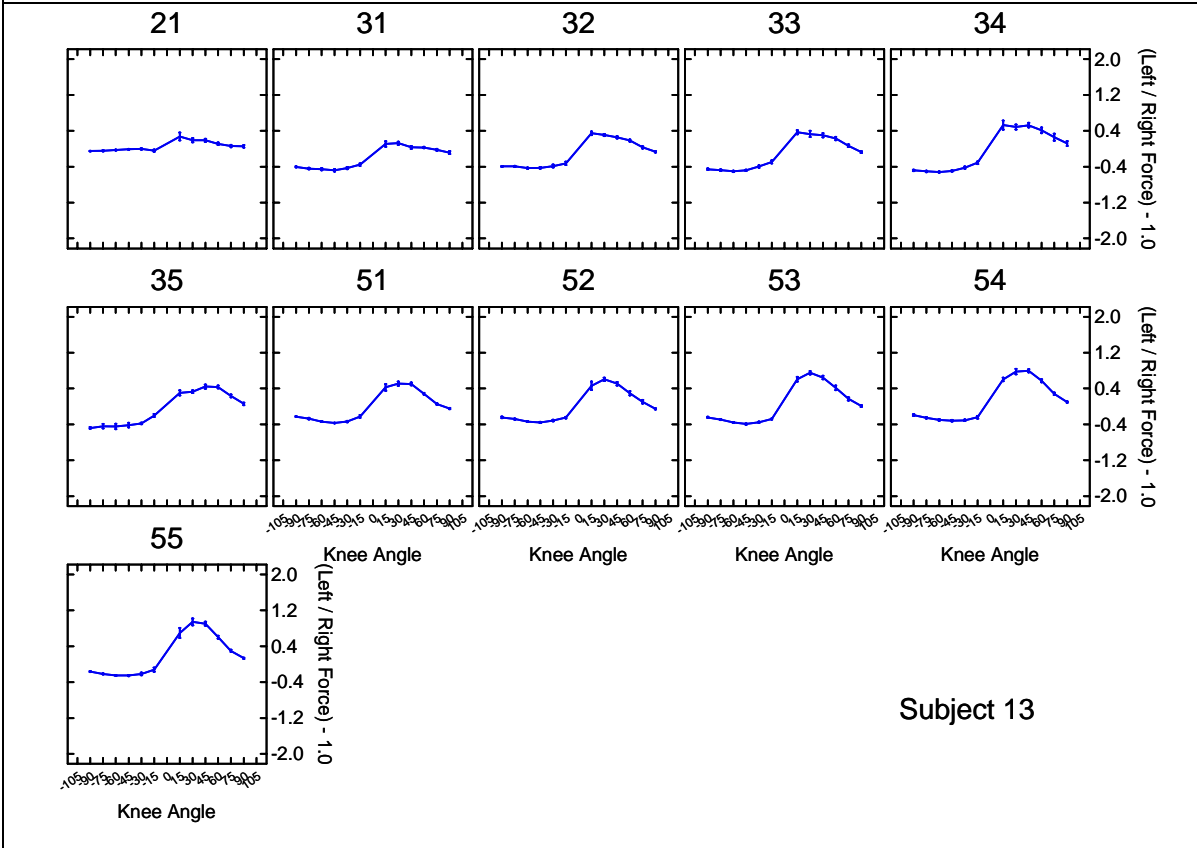
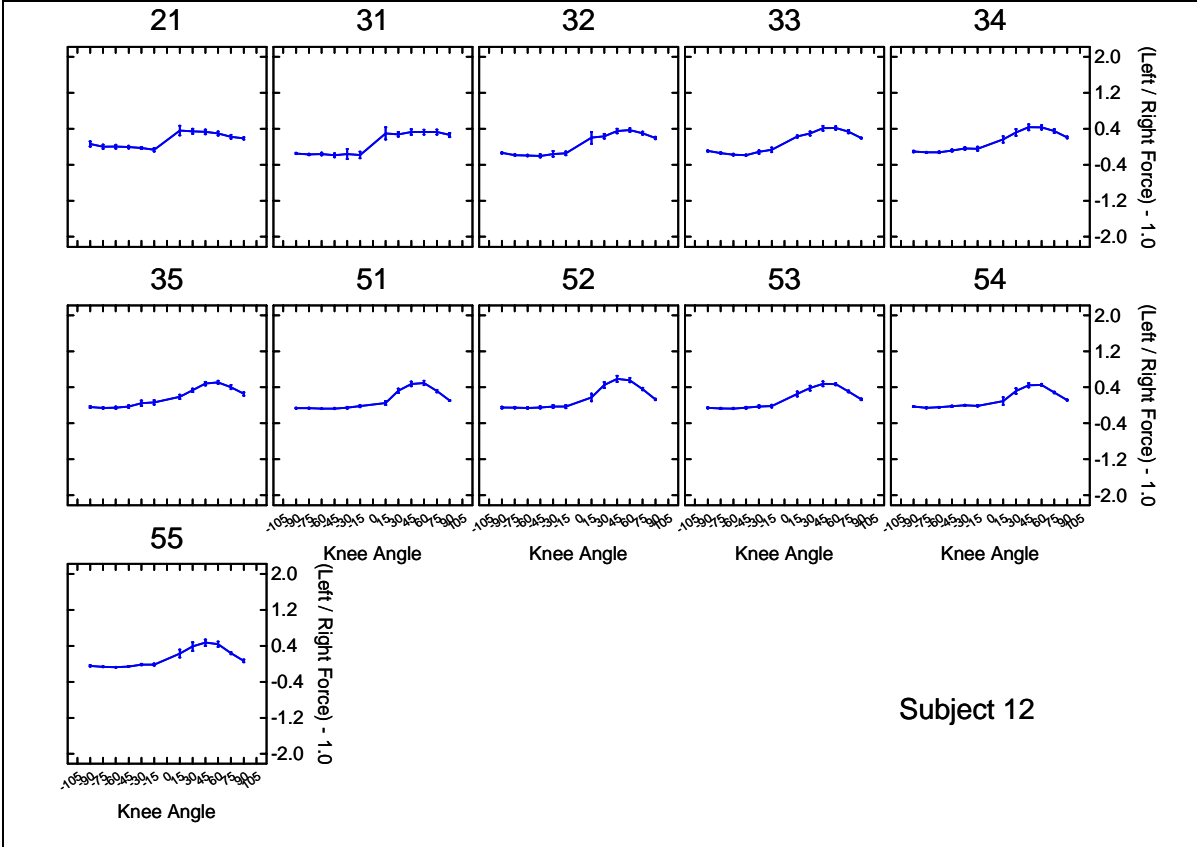


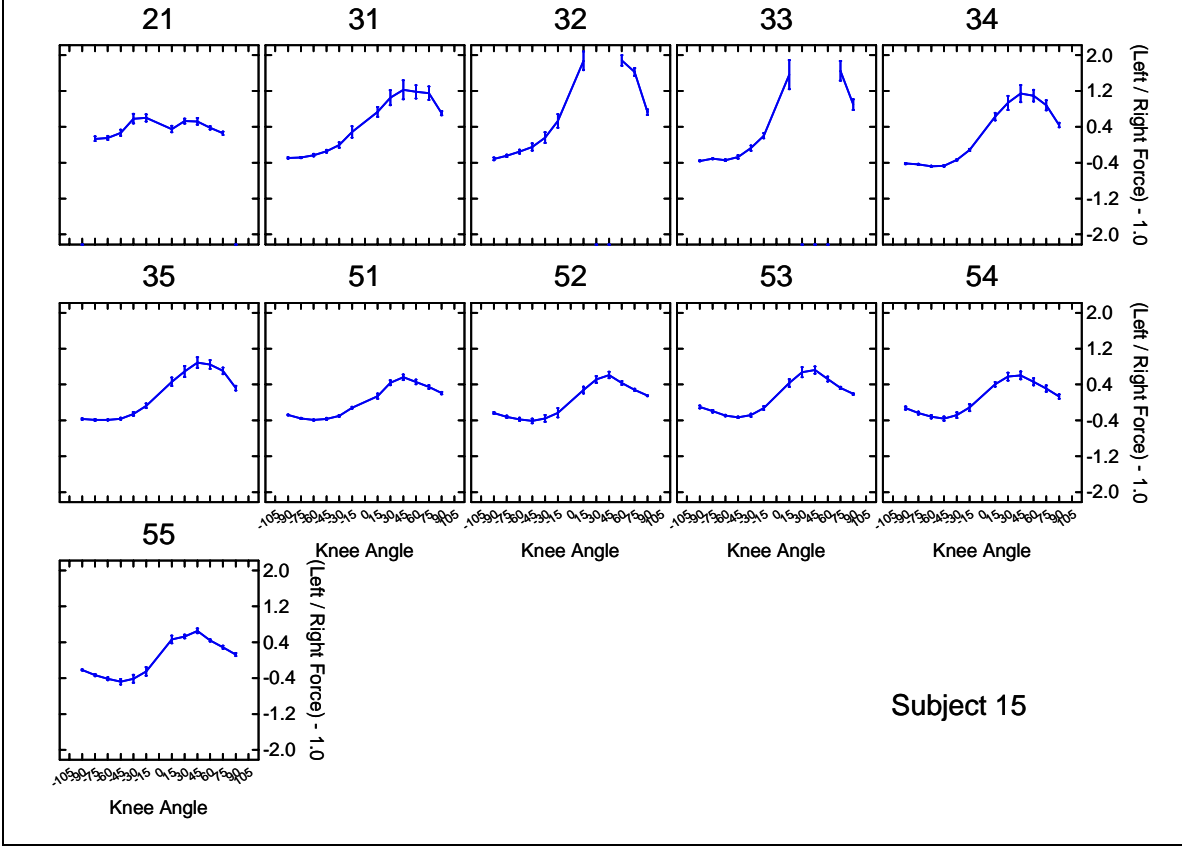
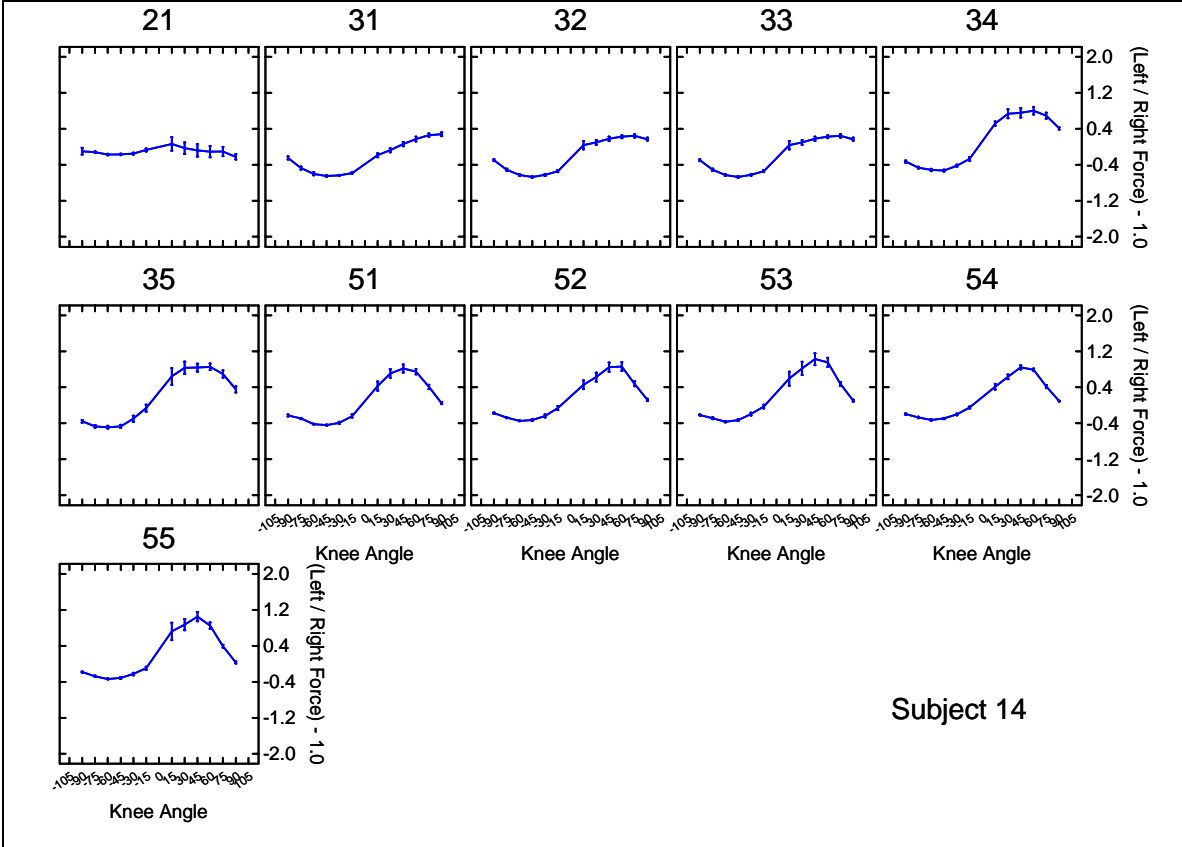






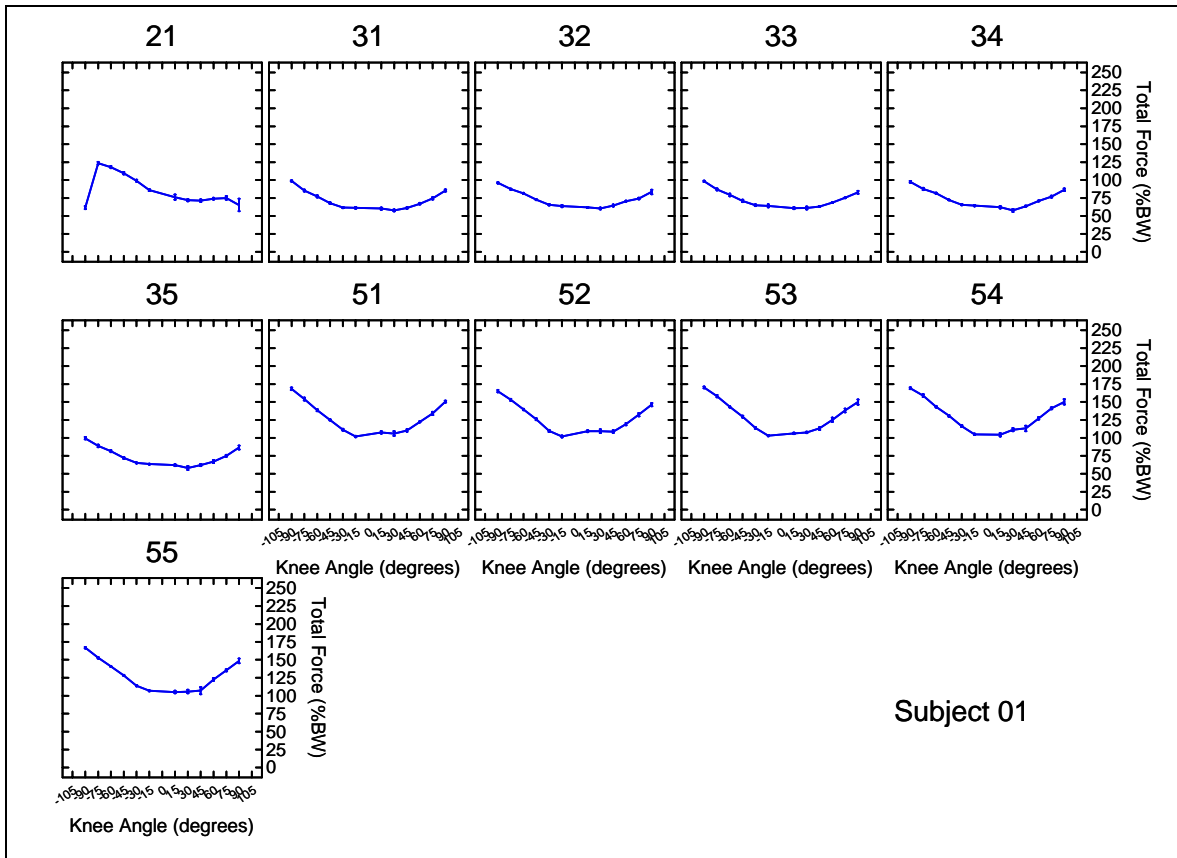


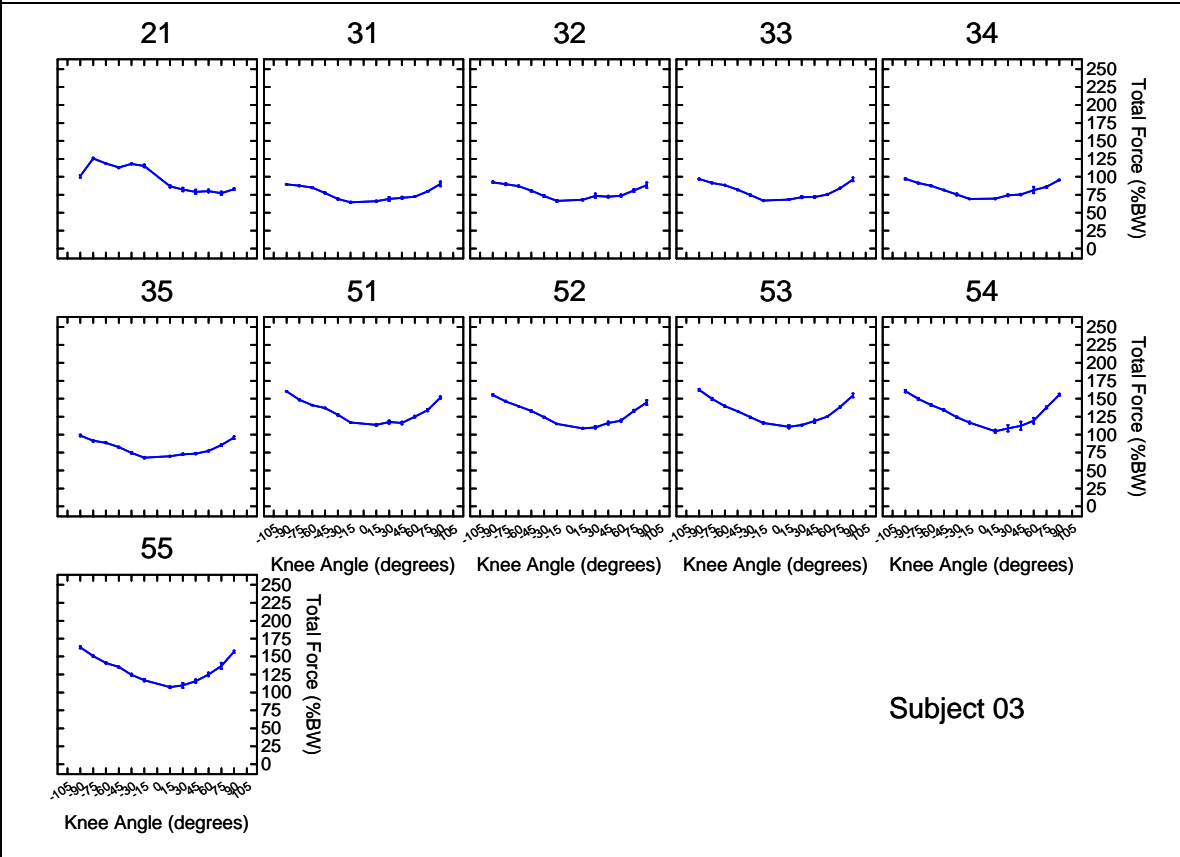
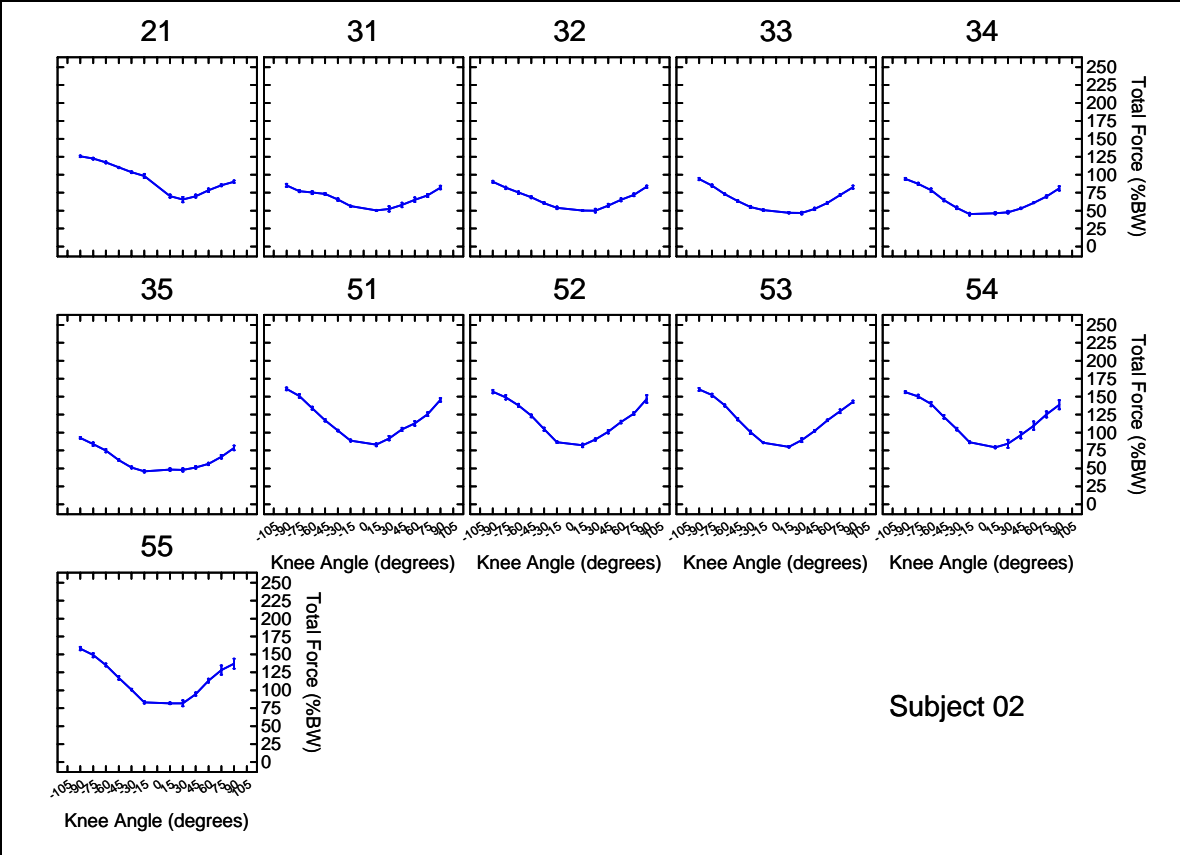


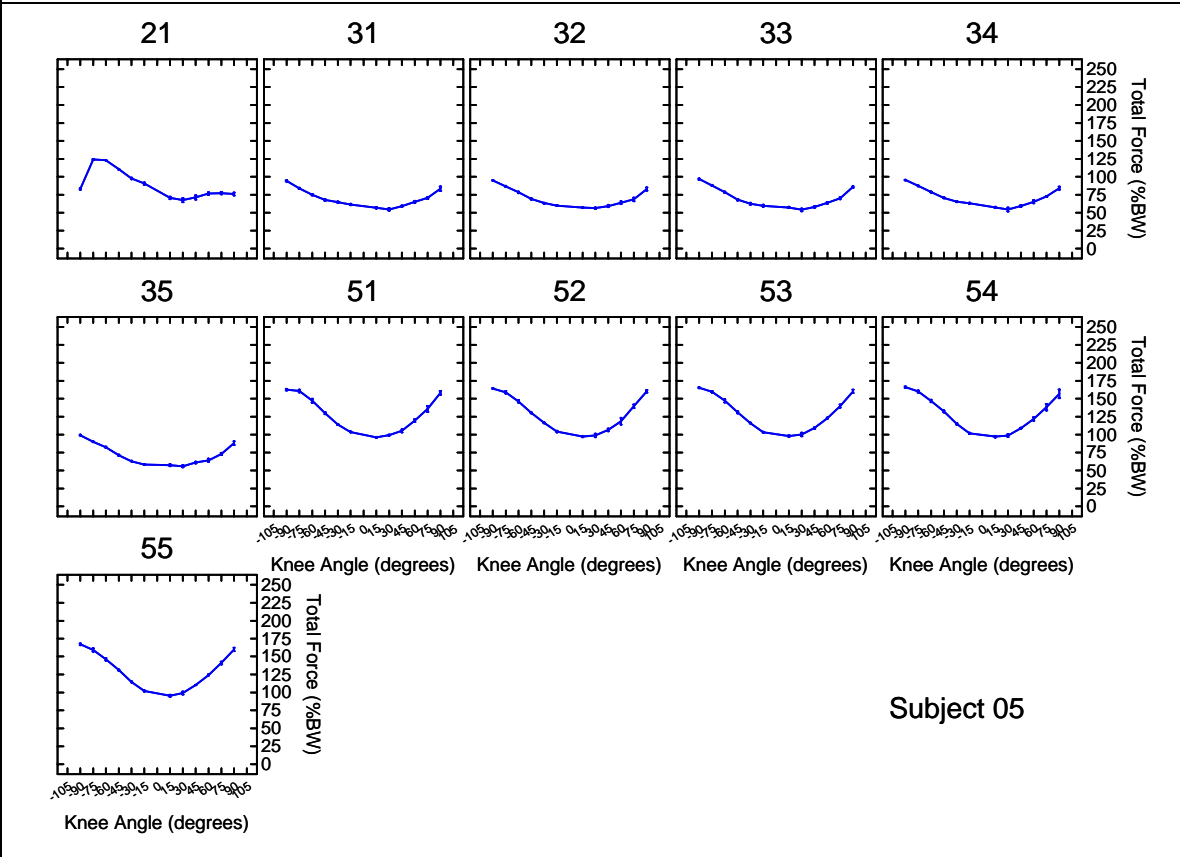
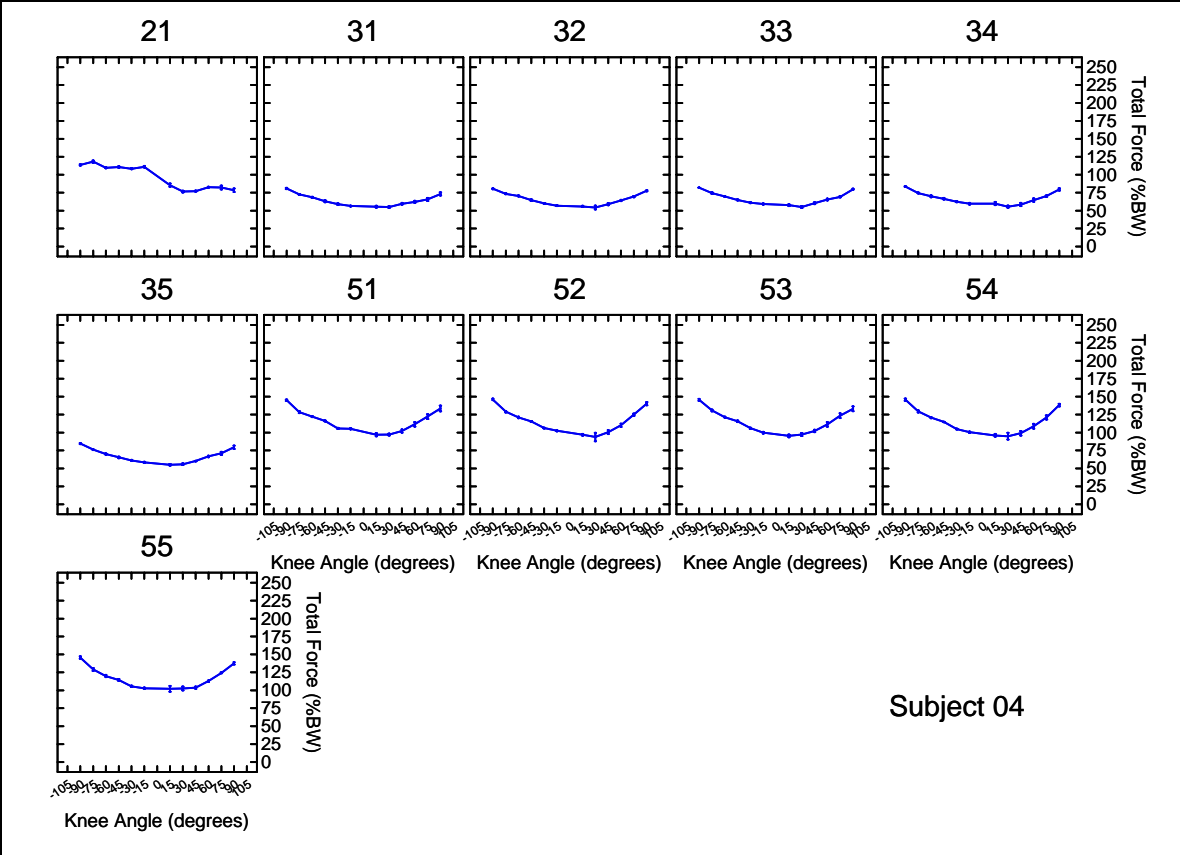


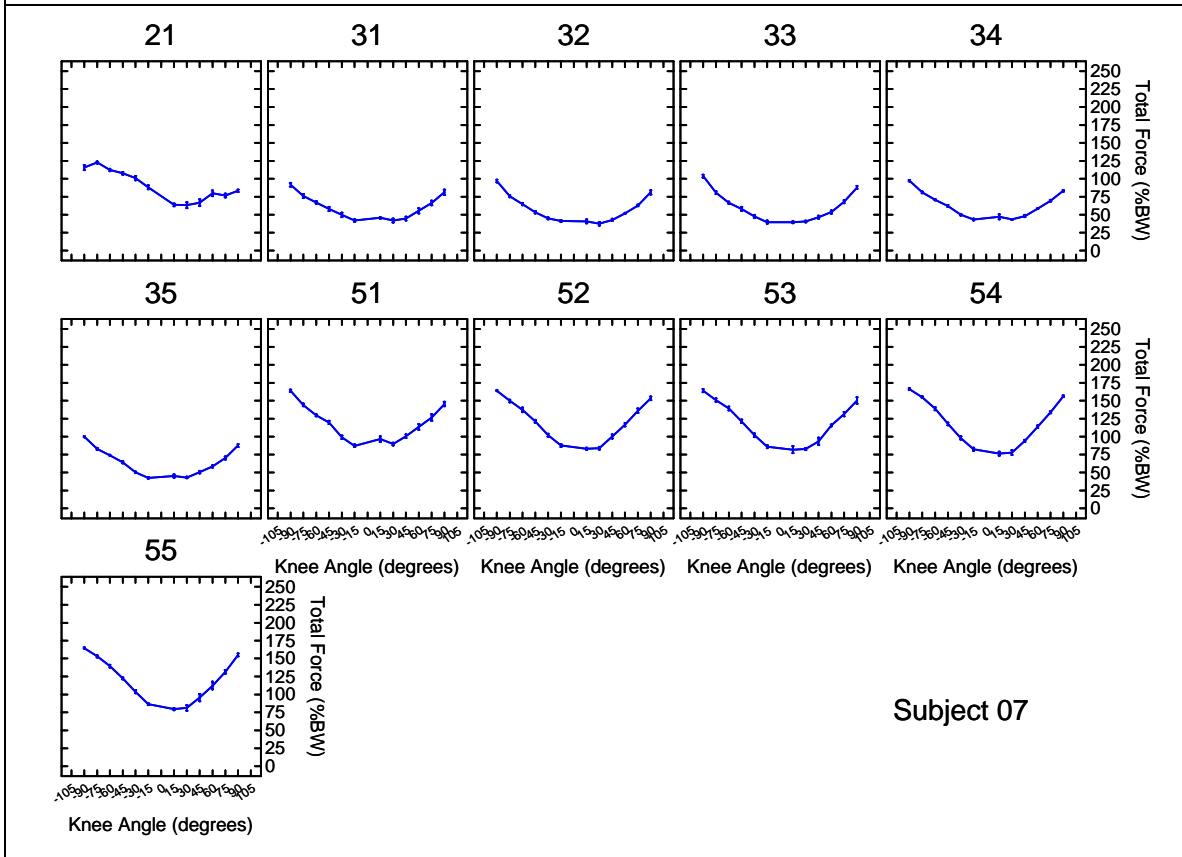
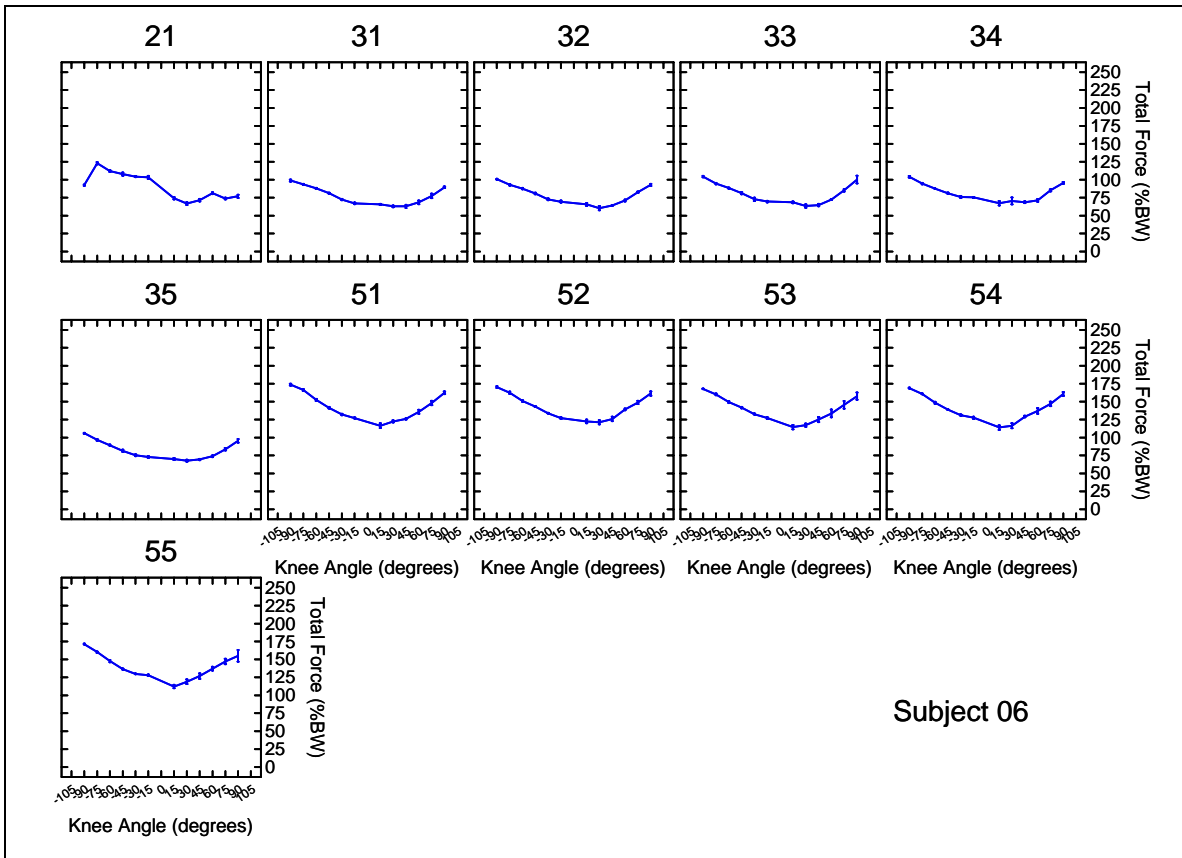
Total Foot Force

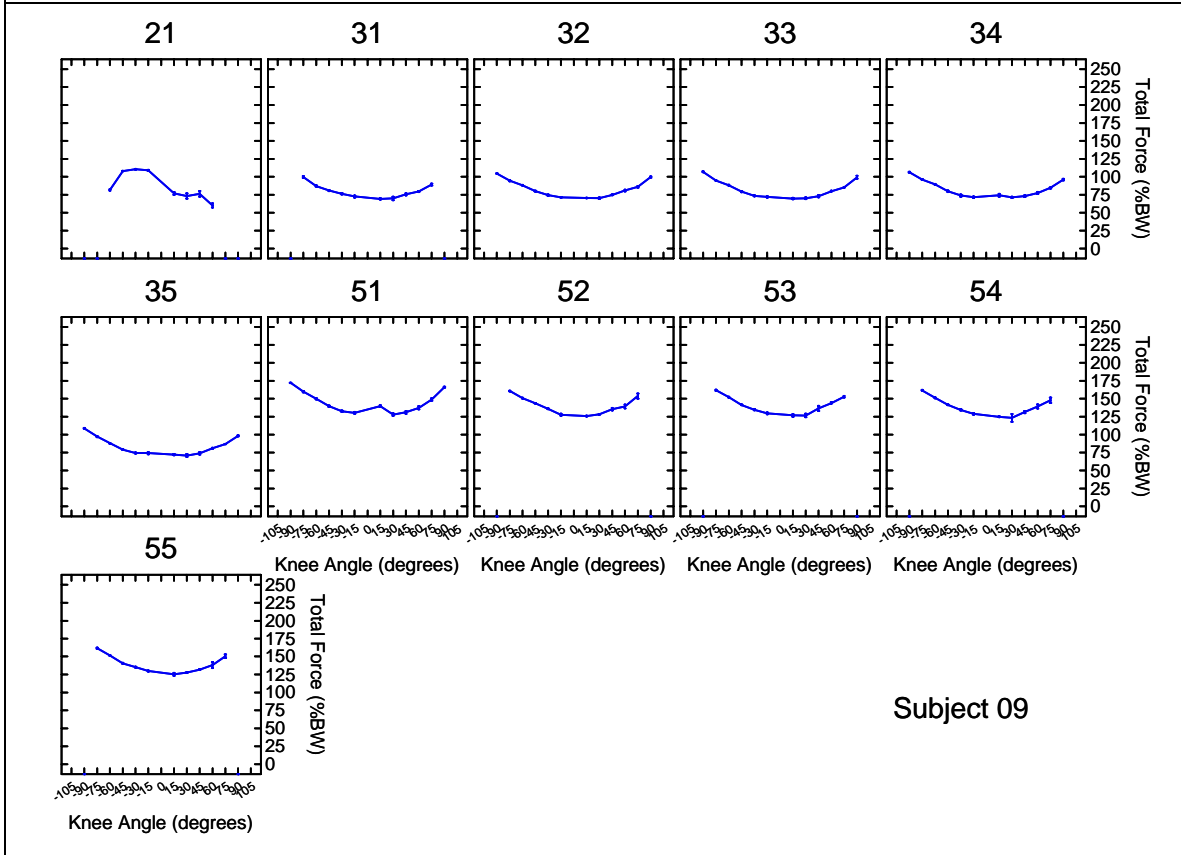
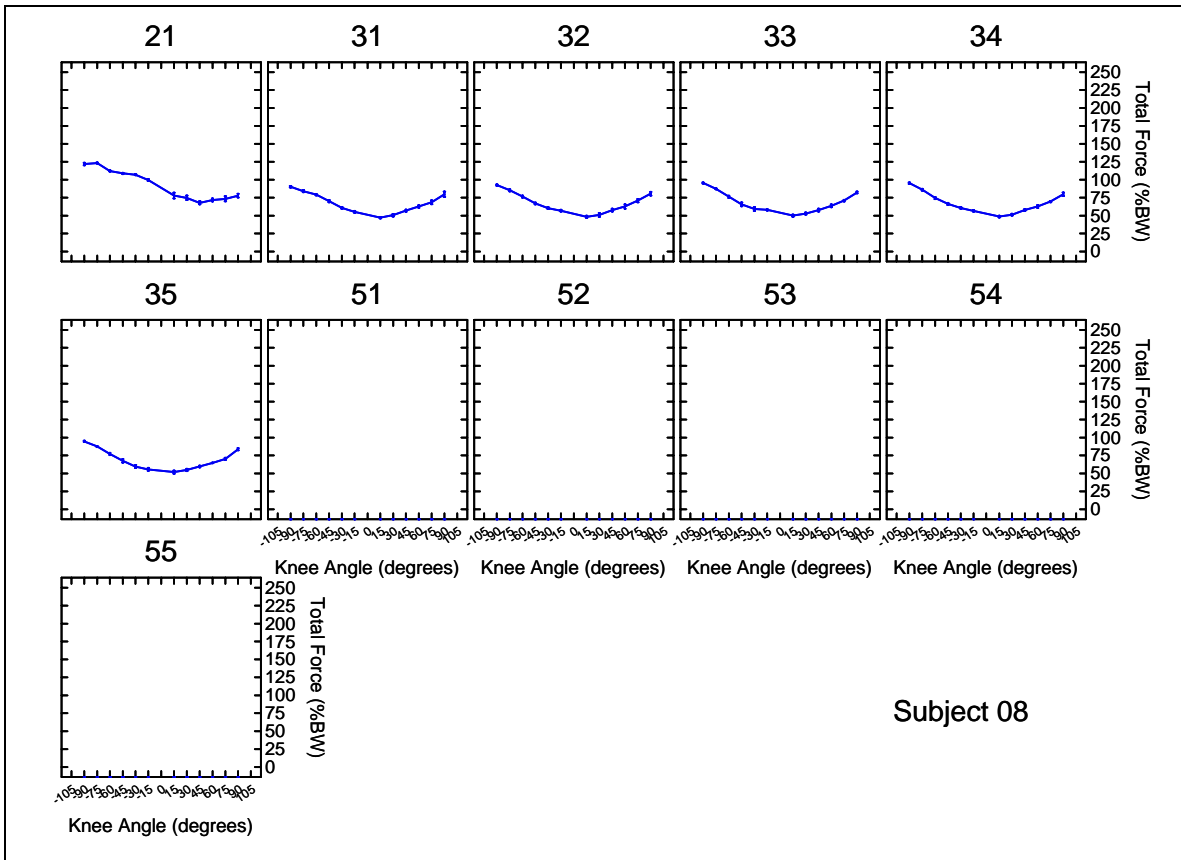
The sum of the left and right foot force, expressed as a percentage of body weight, at several knee angles. The numbers on the top of the boxes are the Phase and Set. For example, 31 is Phase 3 (23-RPM), first set of eight repetitions. The eight repetitions within each set are averaged together. Mean +/- SEM. Note: The knee angles are the same as in the body of this thesis, however, the ordering of them is slightly different: 0-degree knee angle is in the middle of the graph and full extension (i.e., 90-degrees) is at the edges.

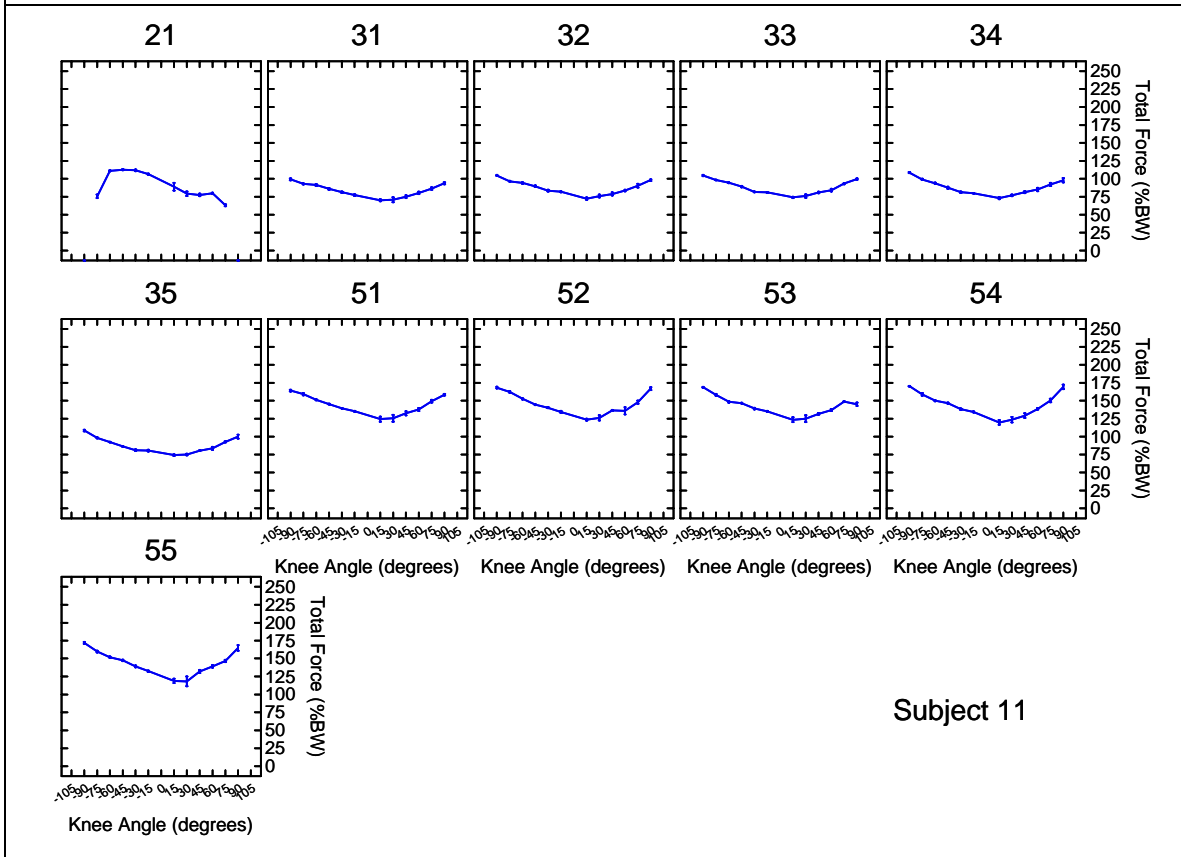
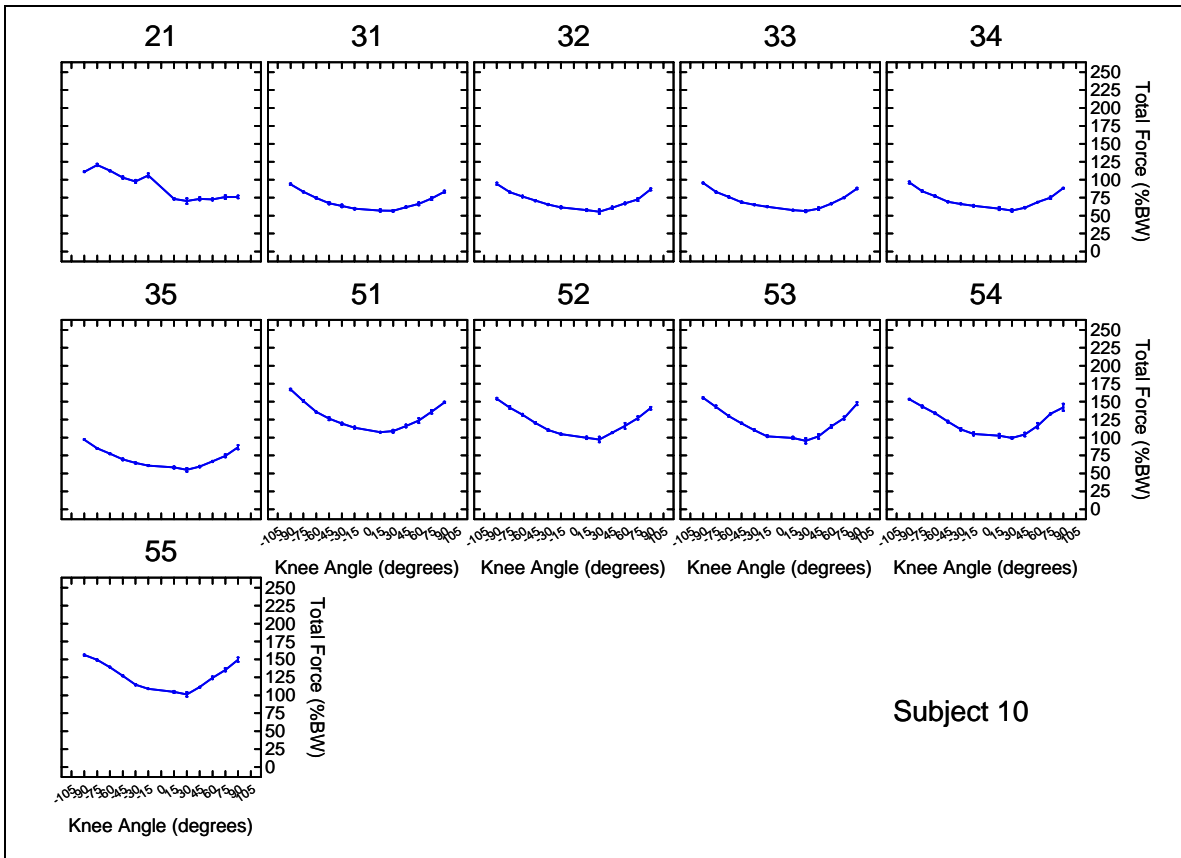


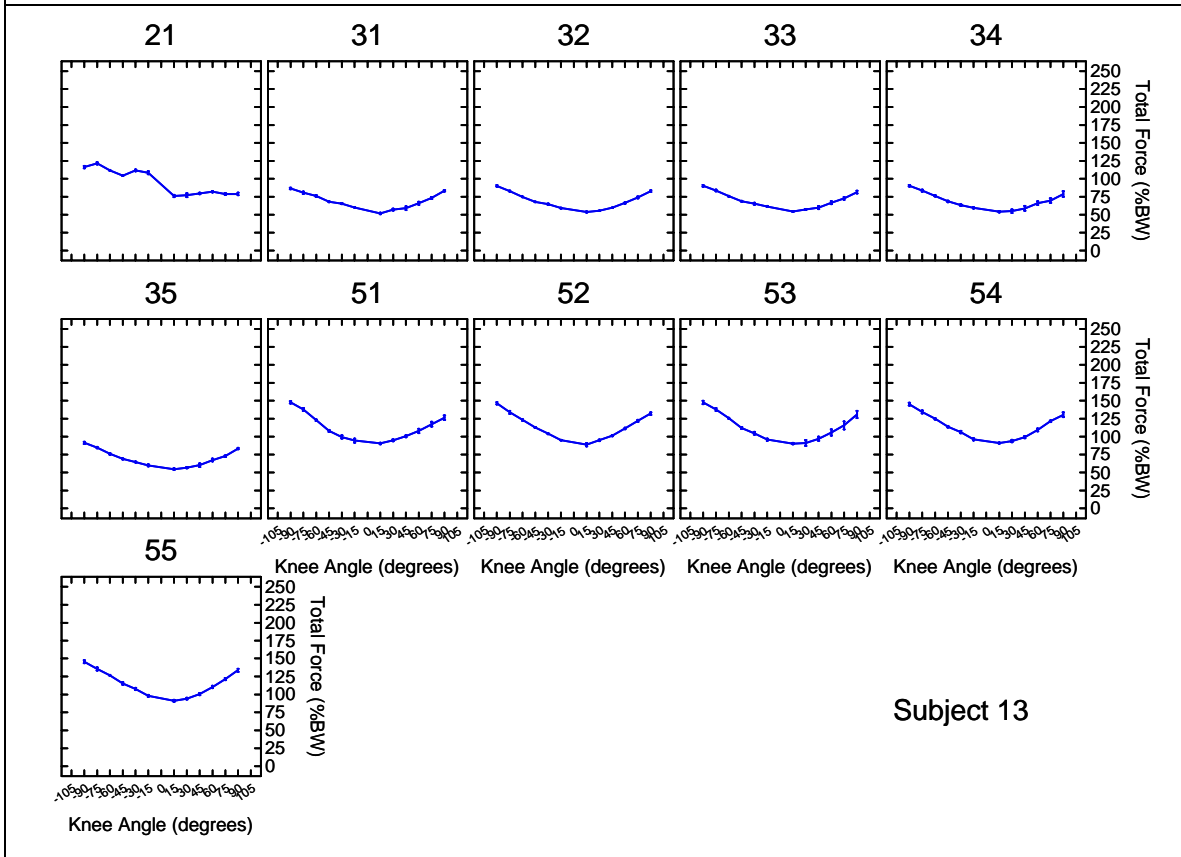
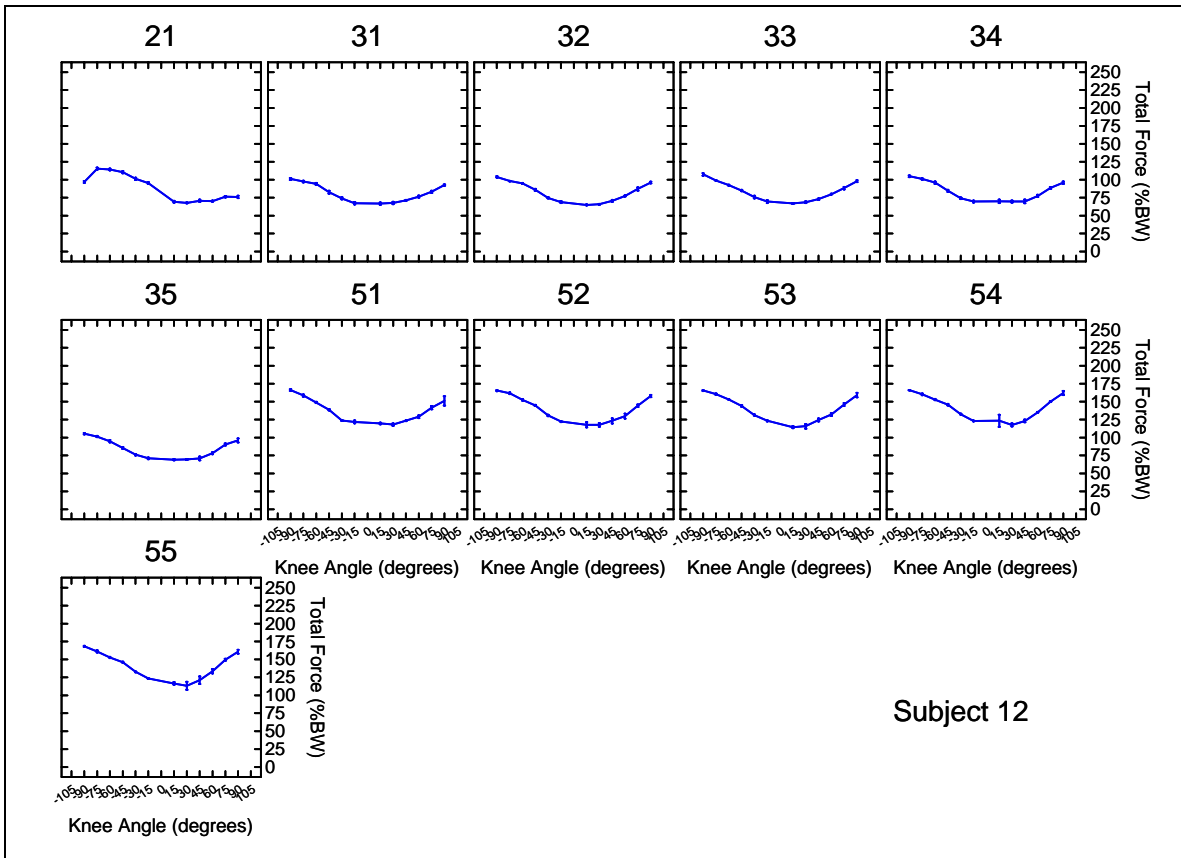


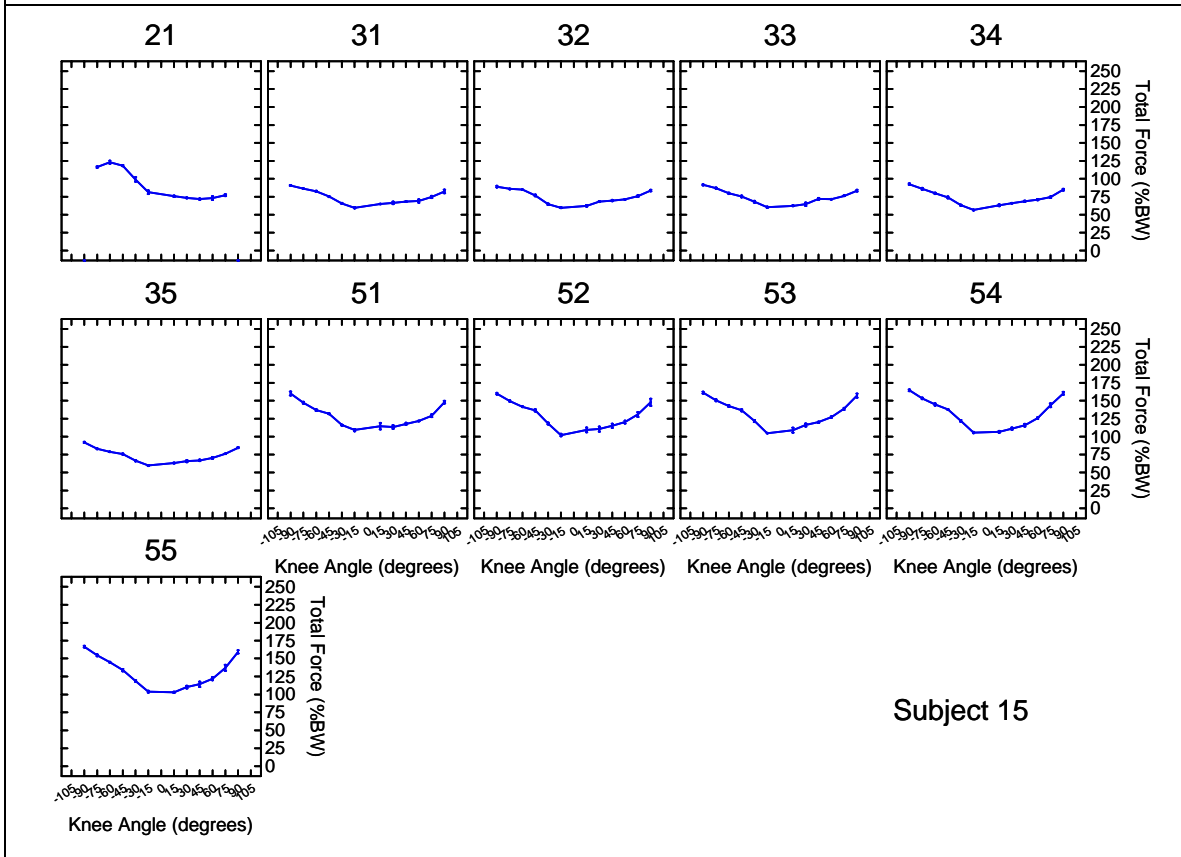
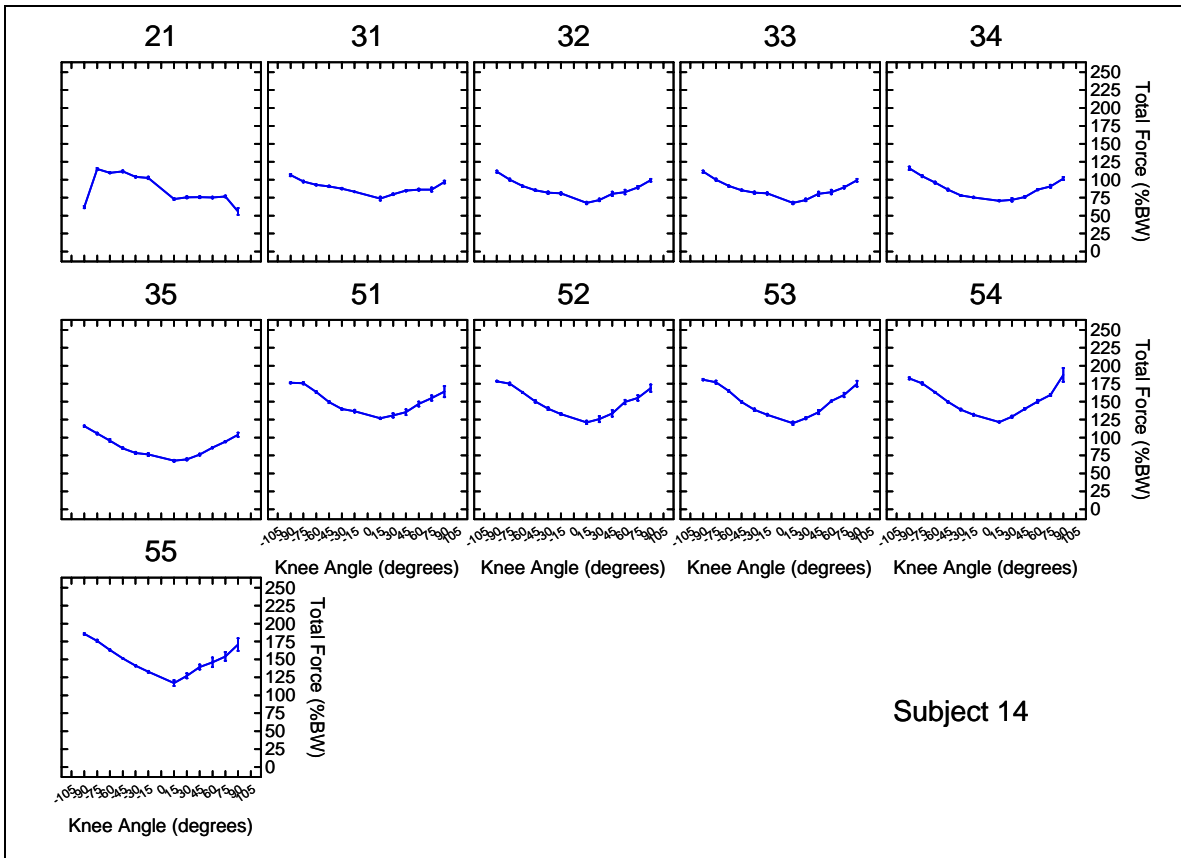






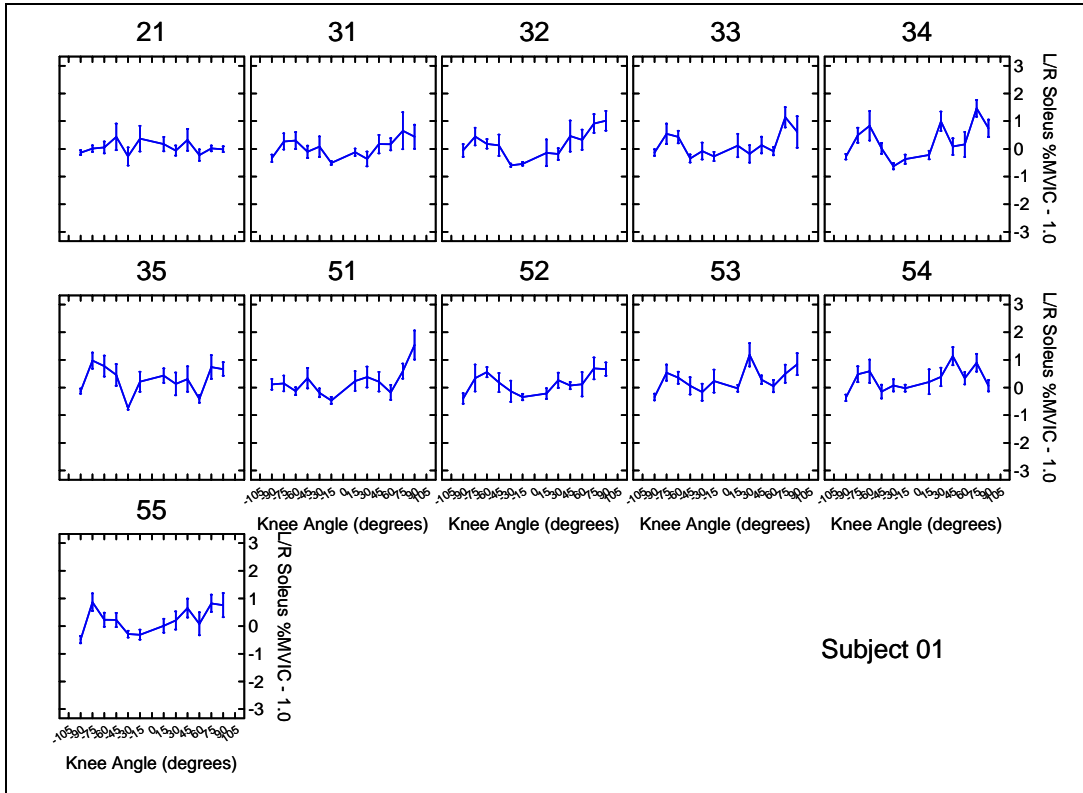


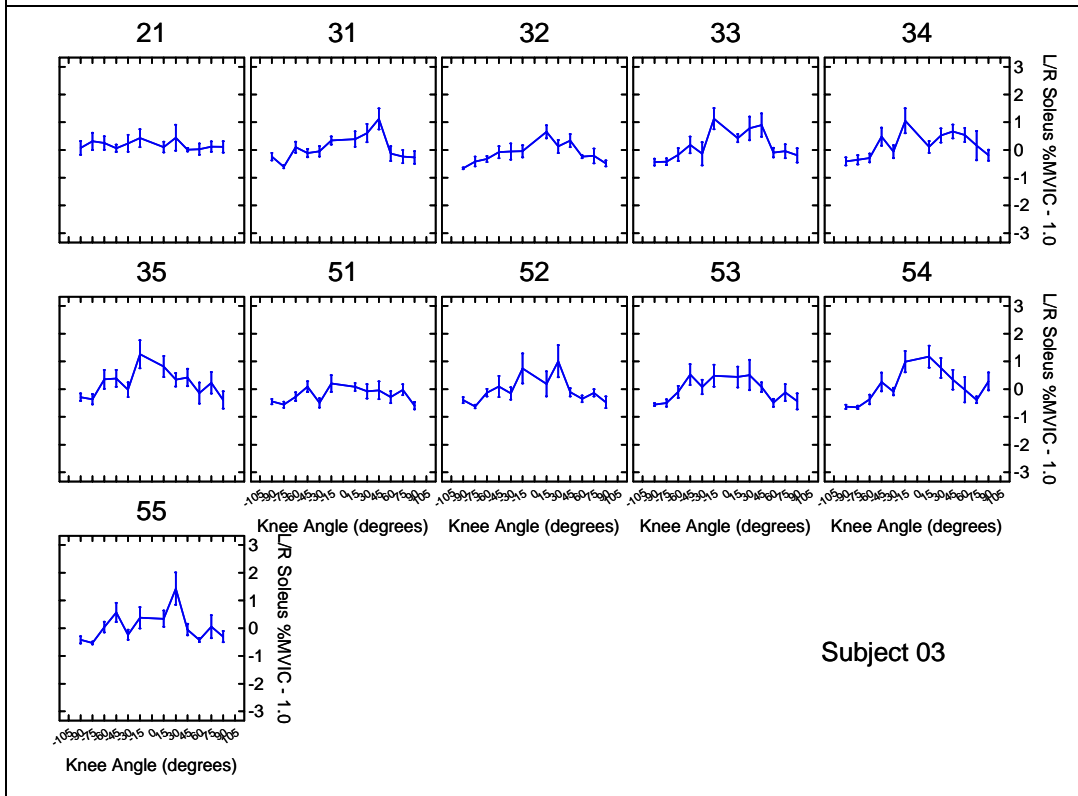
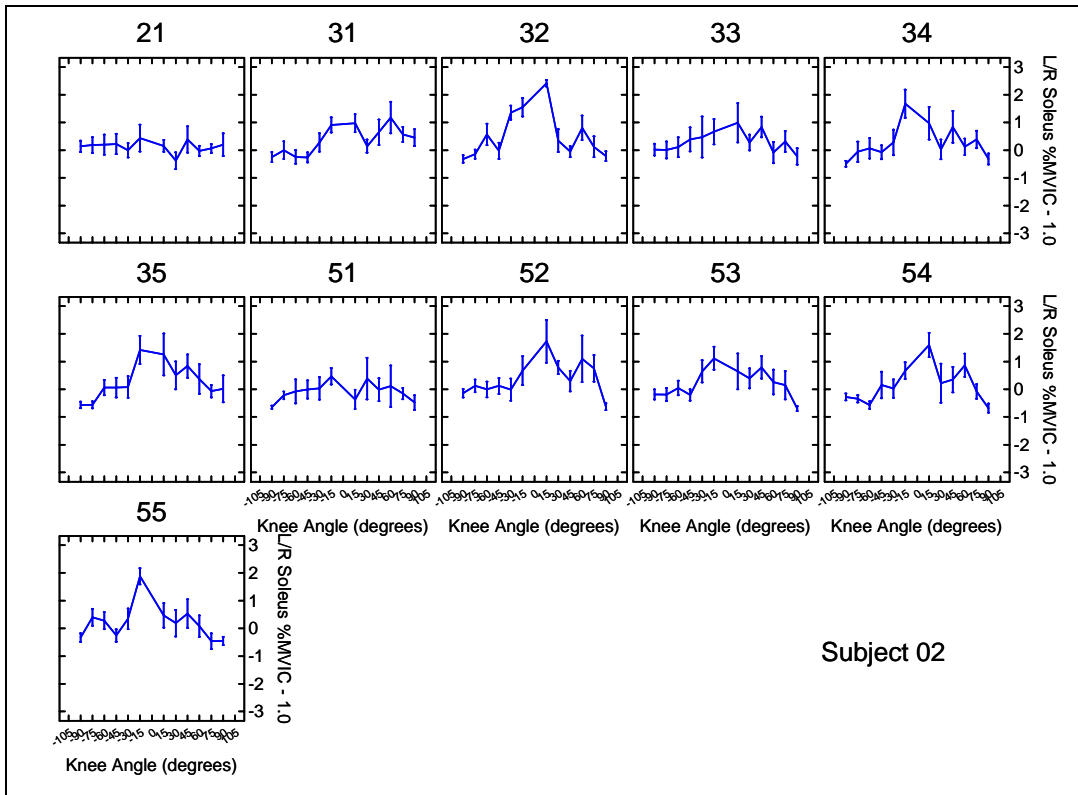


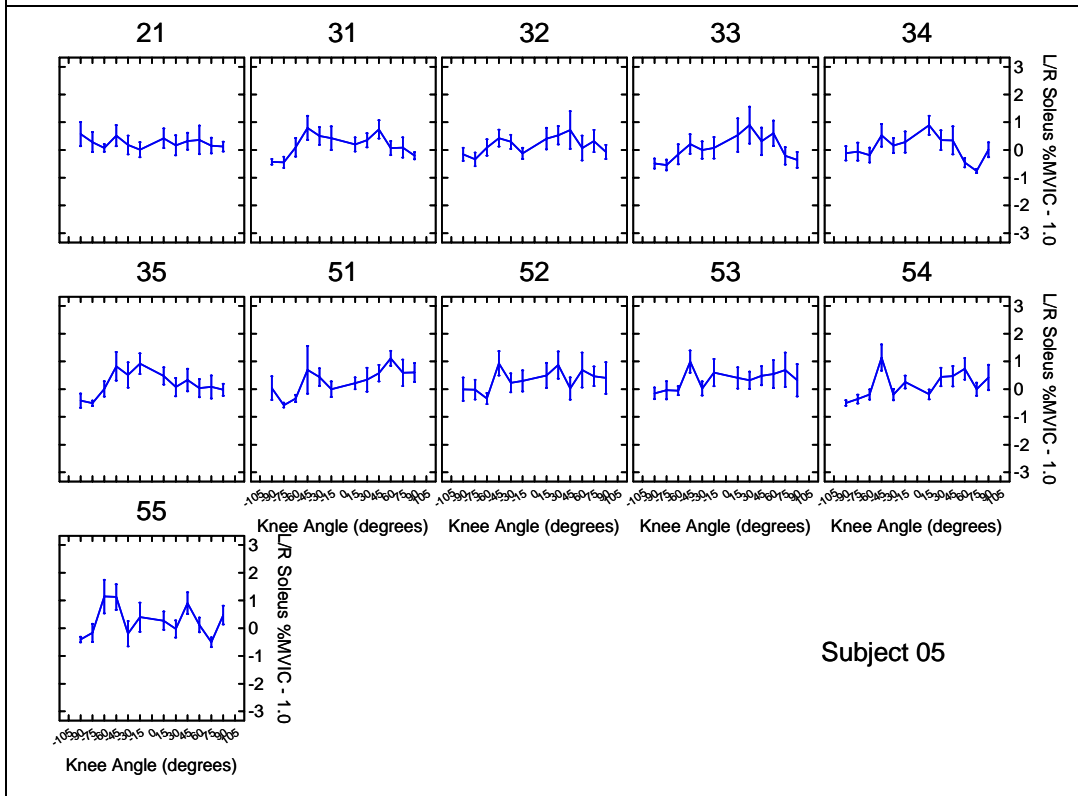
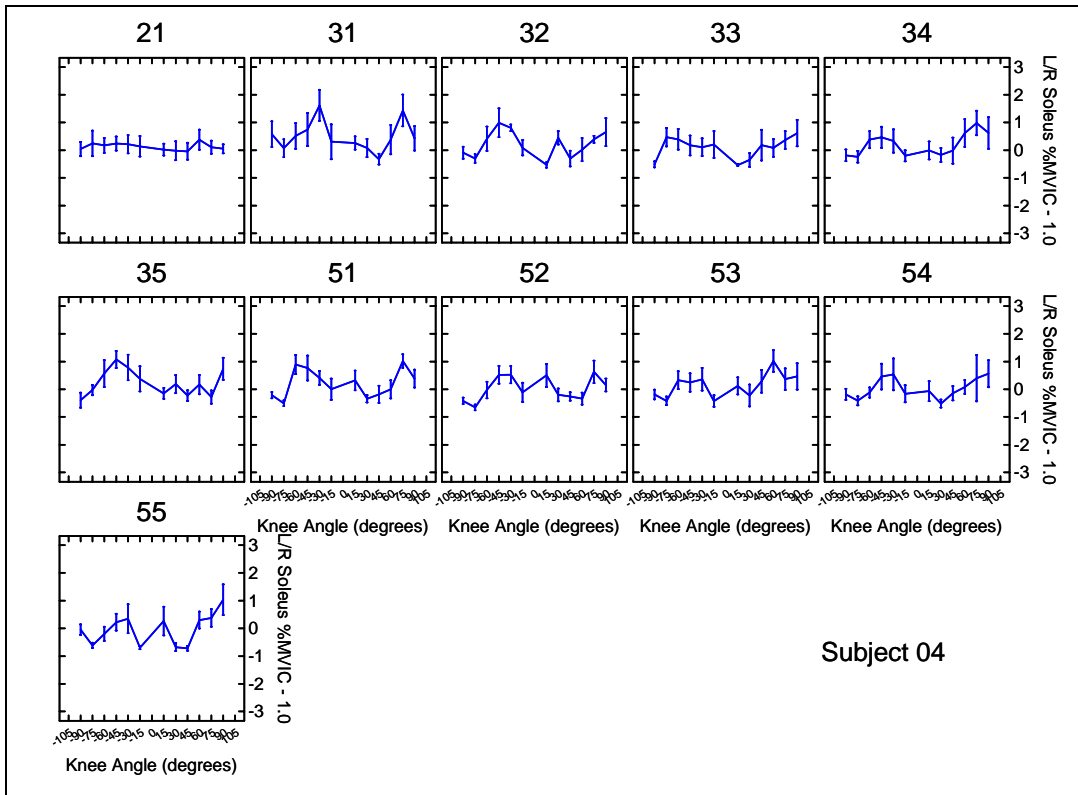


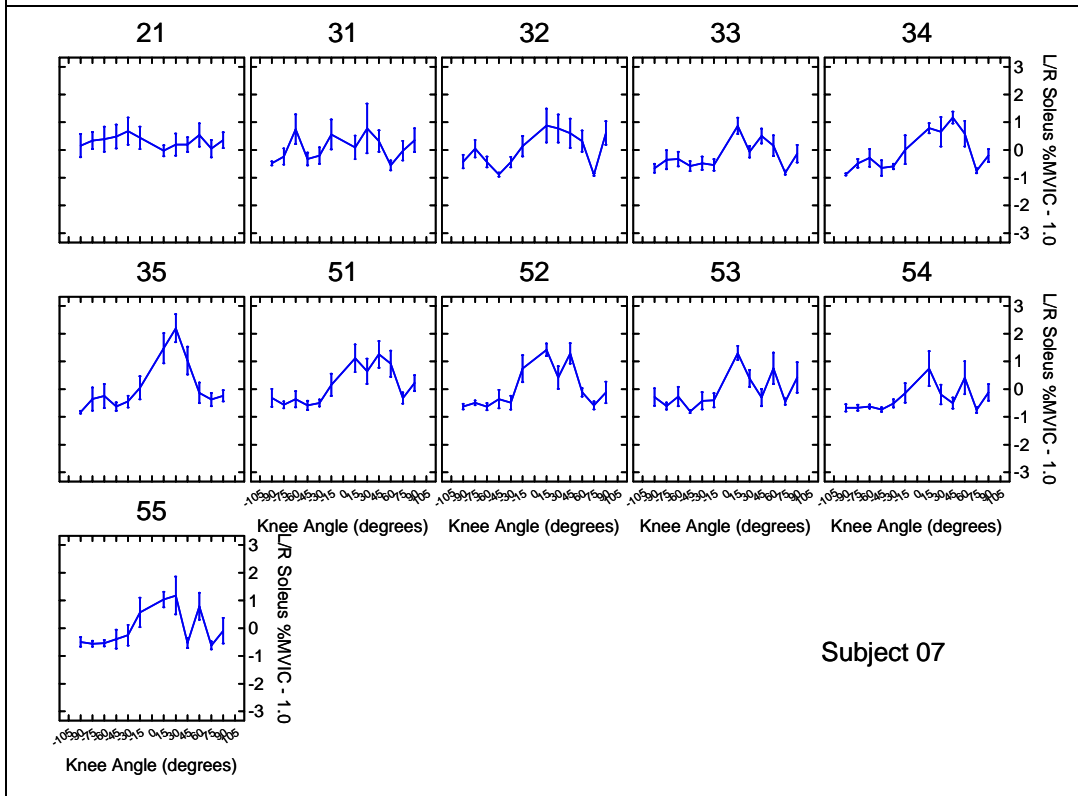
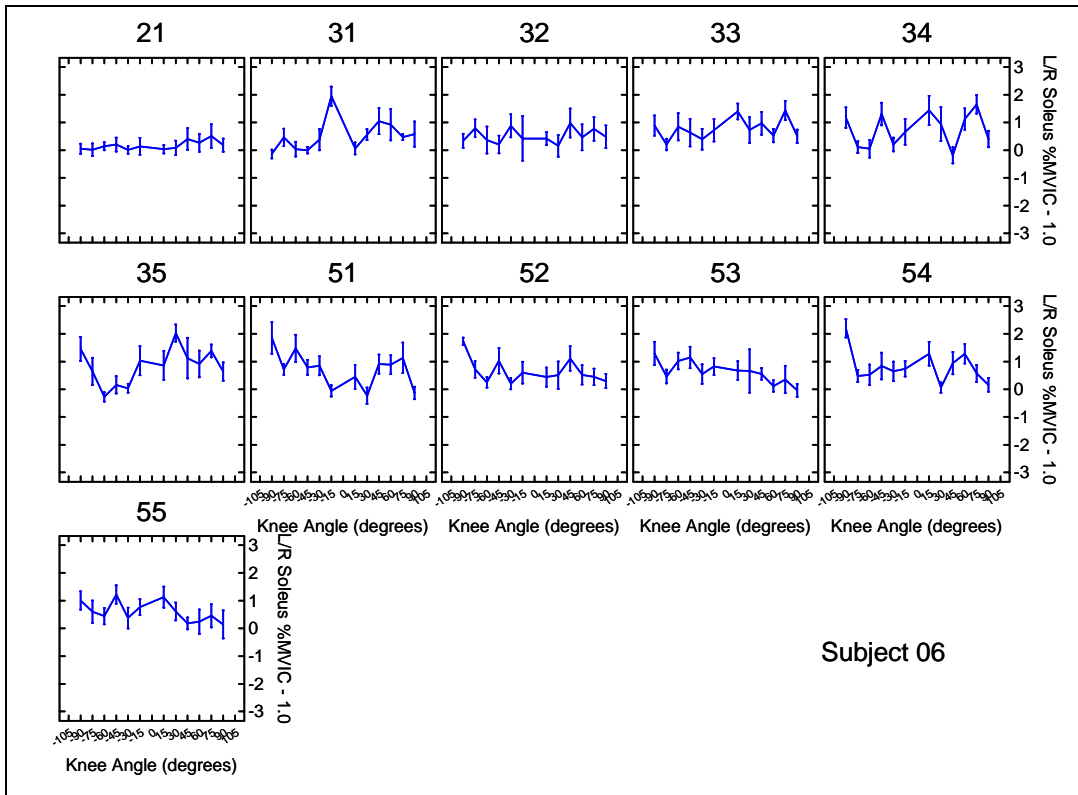
Soleus EMG

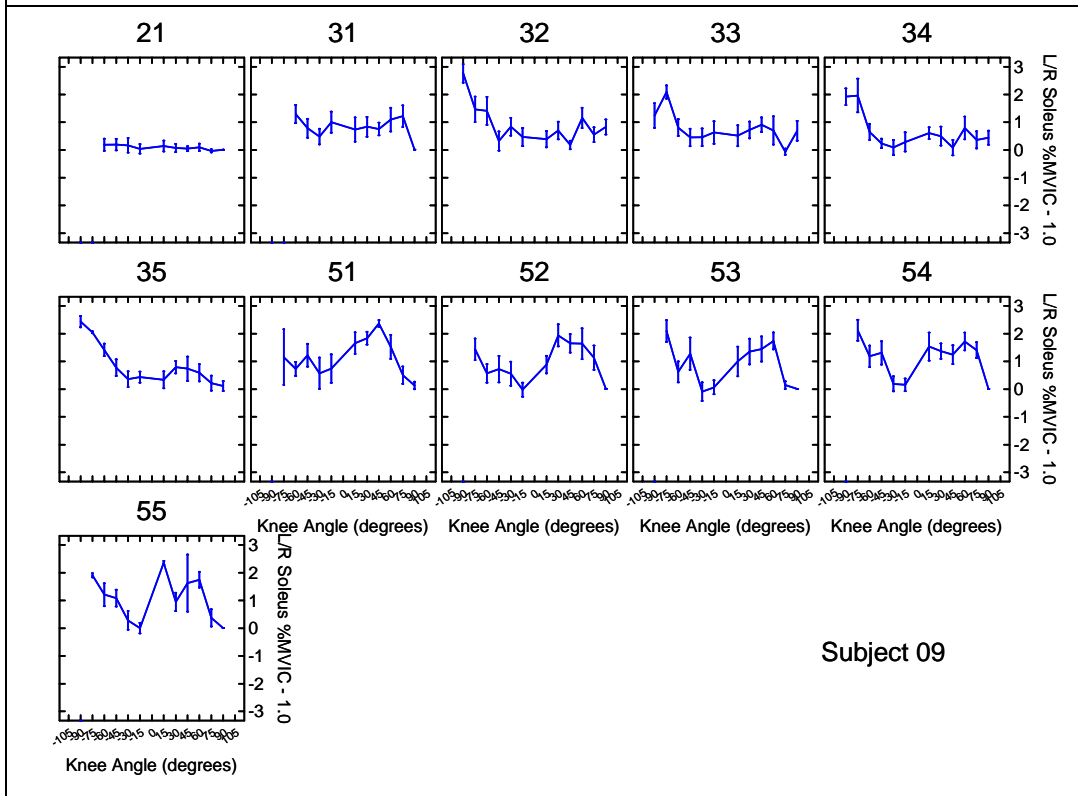
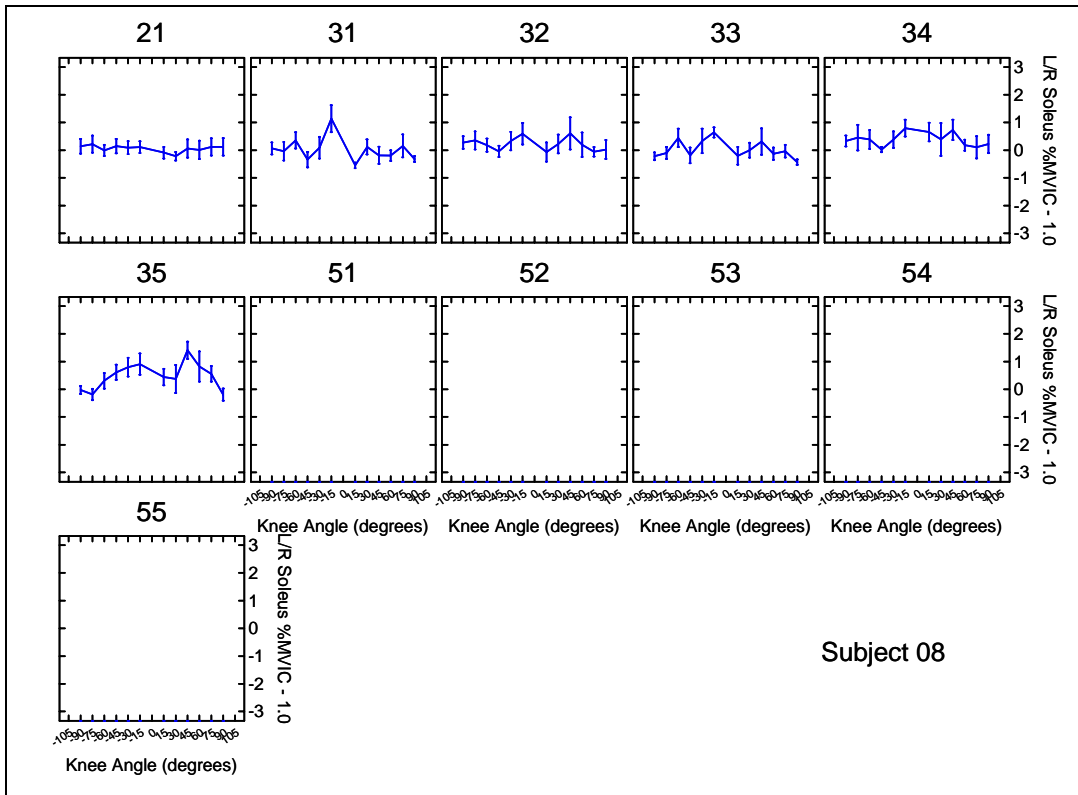
The left divided by right soleus %MVIC muscle activity minus one (Left / Right – 1.0) at several knee angles for each subject. The numbers on the top of the boxes are the Phase and Set. For example, 31 is Phase 3 (23-RPM), first set of eight repetitions. The eight repetitions within each set are averaged together. Mean +/- SEM. Note: The knee angles are the same as in the body of this thesis, however, the ordering of them is slightly different: 0-degree knee angle is in the middle of the graph and full extension (i.e., 90-degrees) is at the edges.

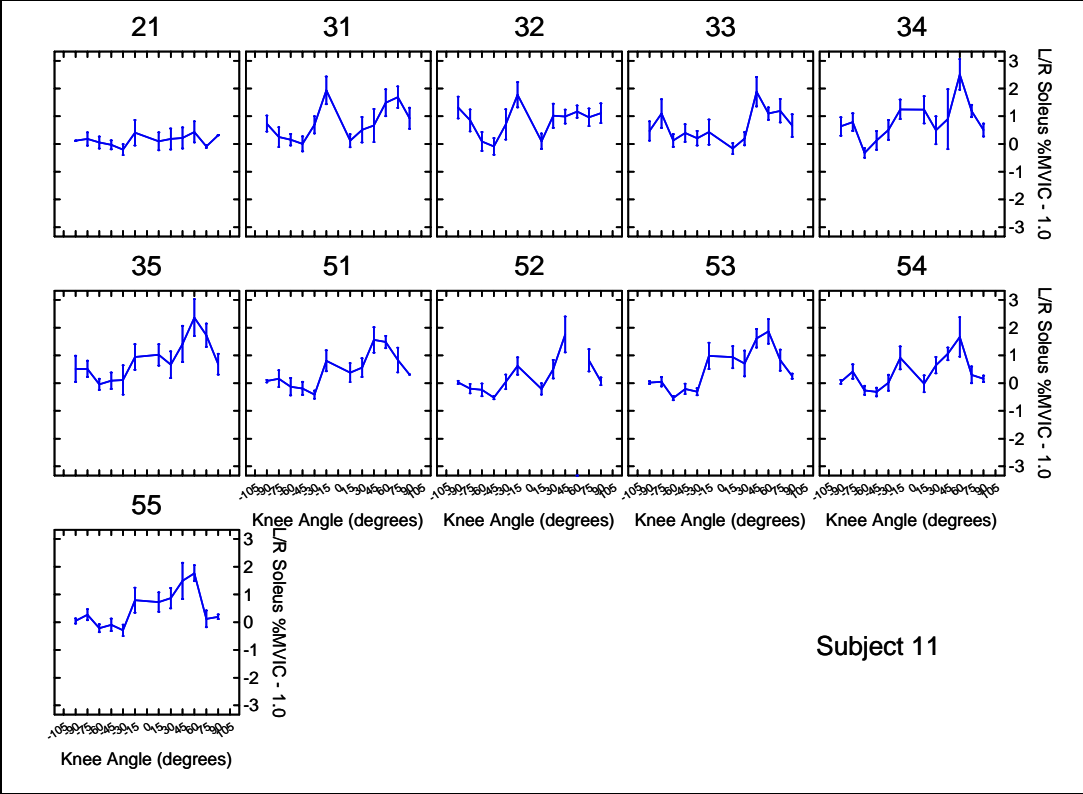
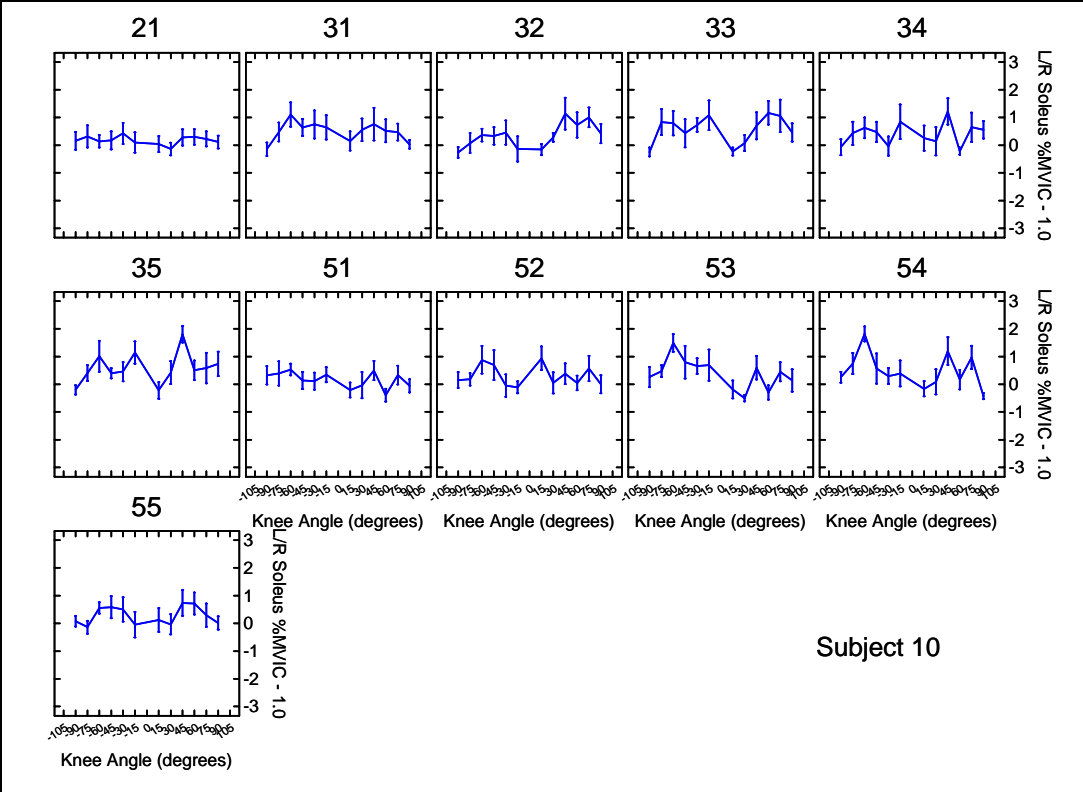


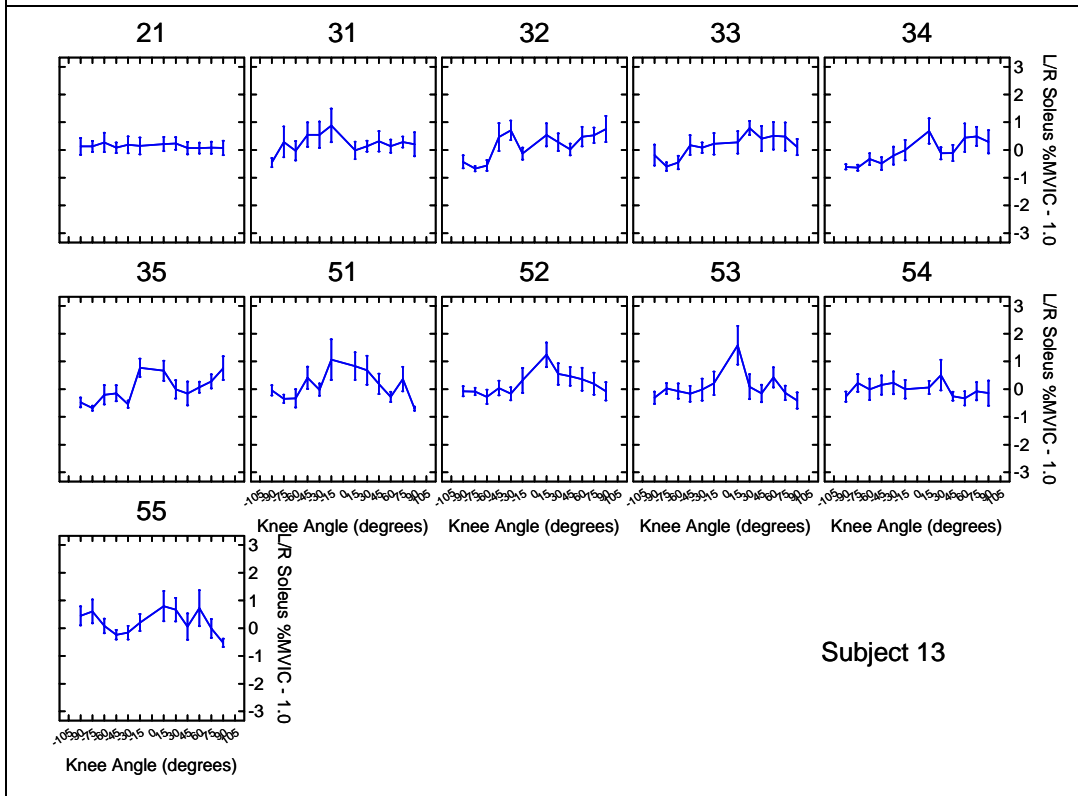
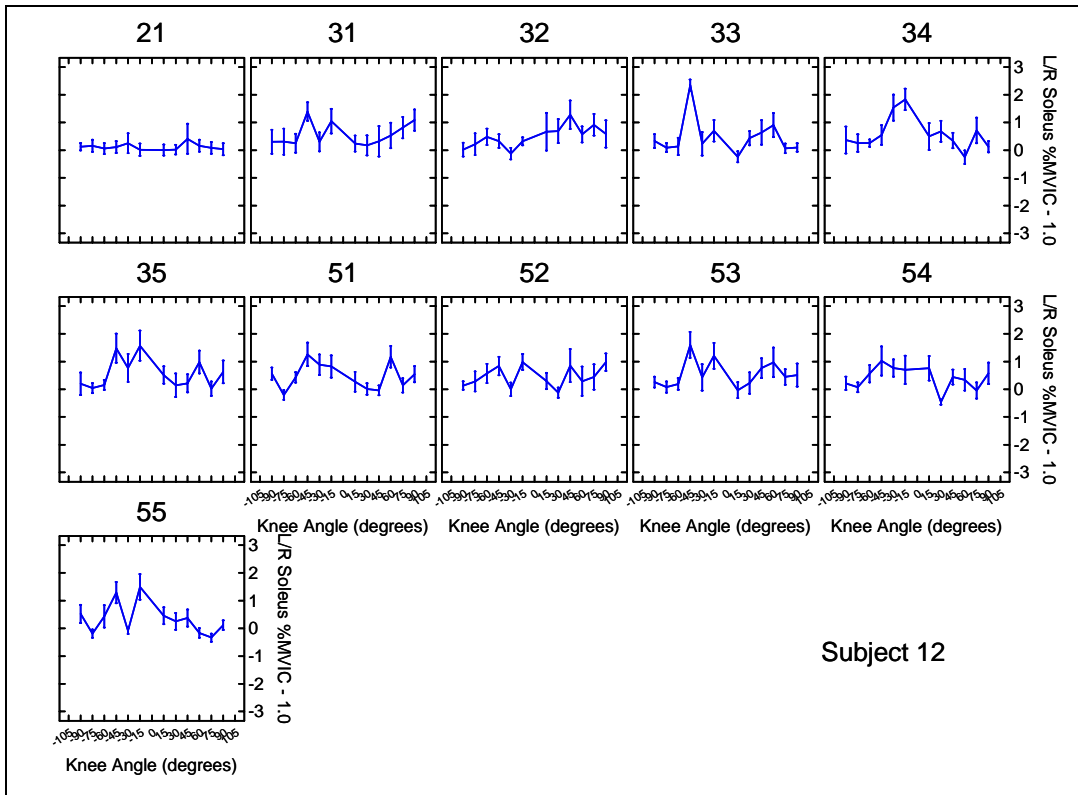






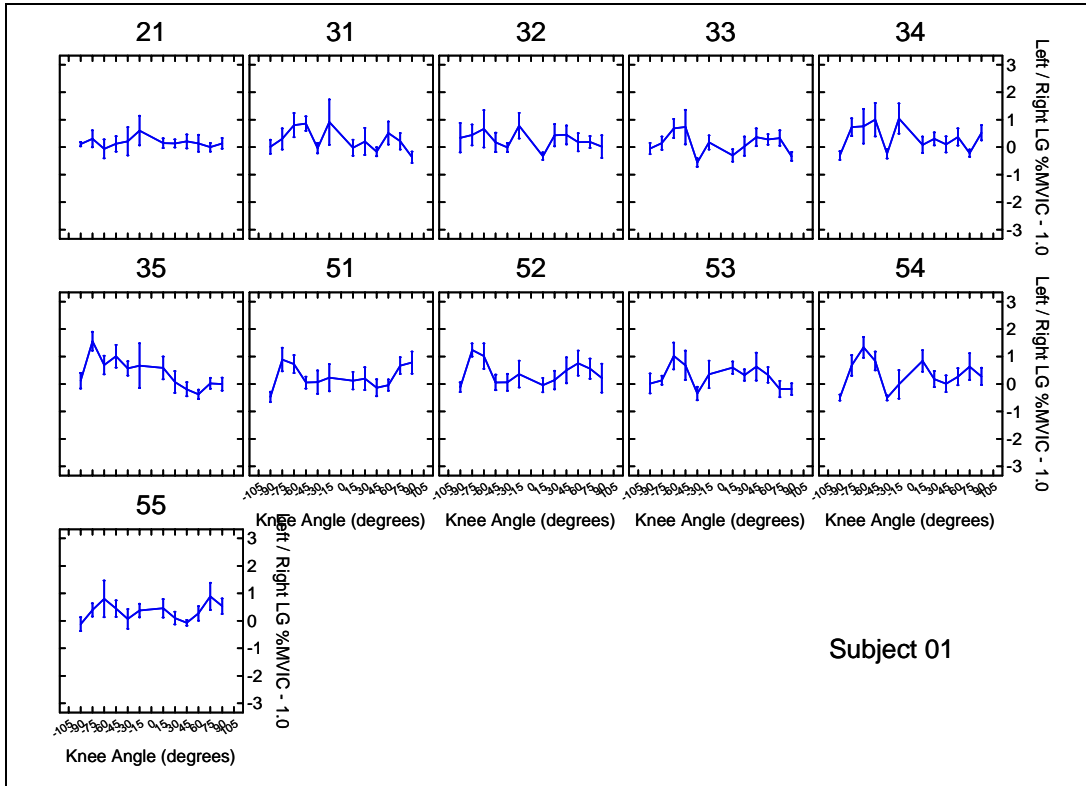


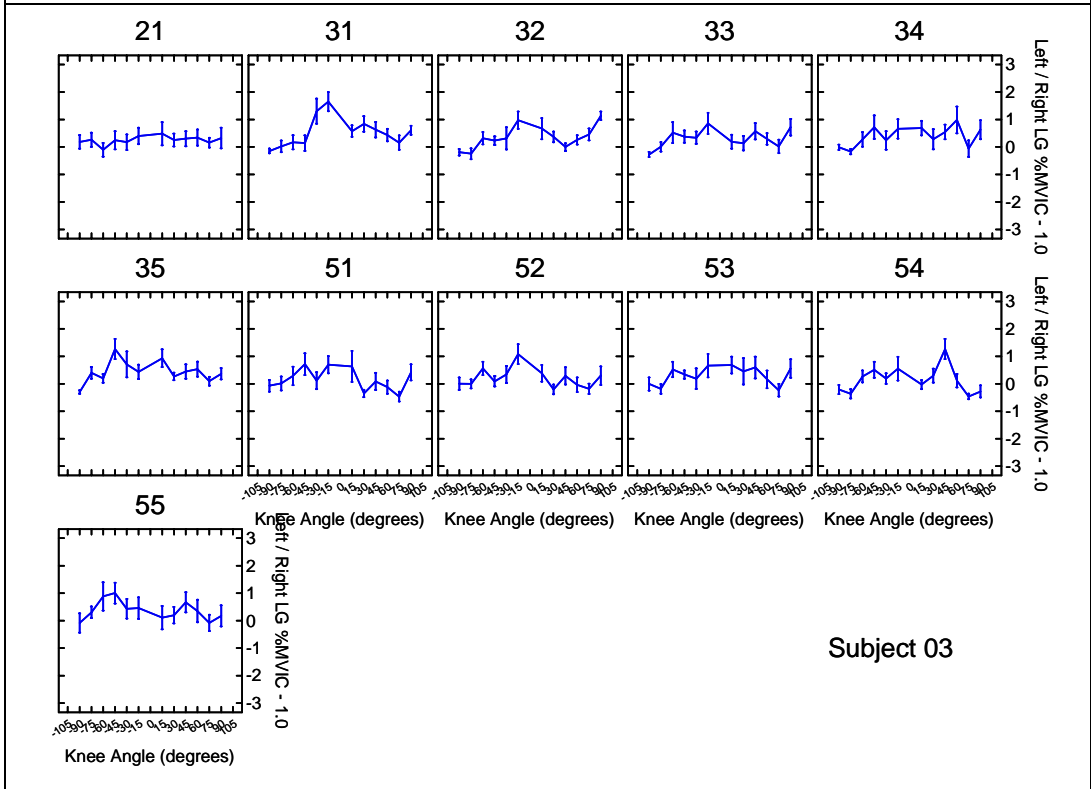
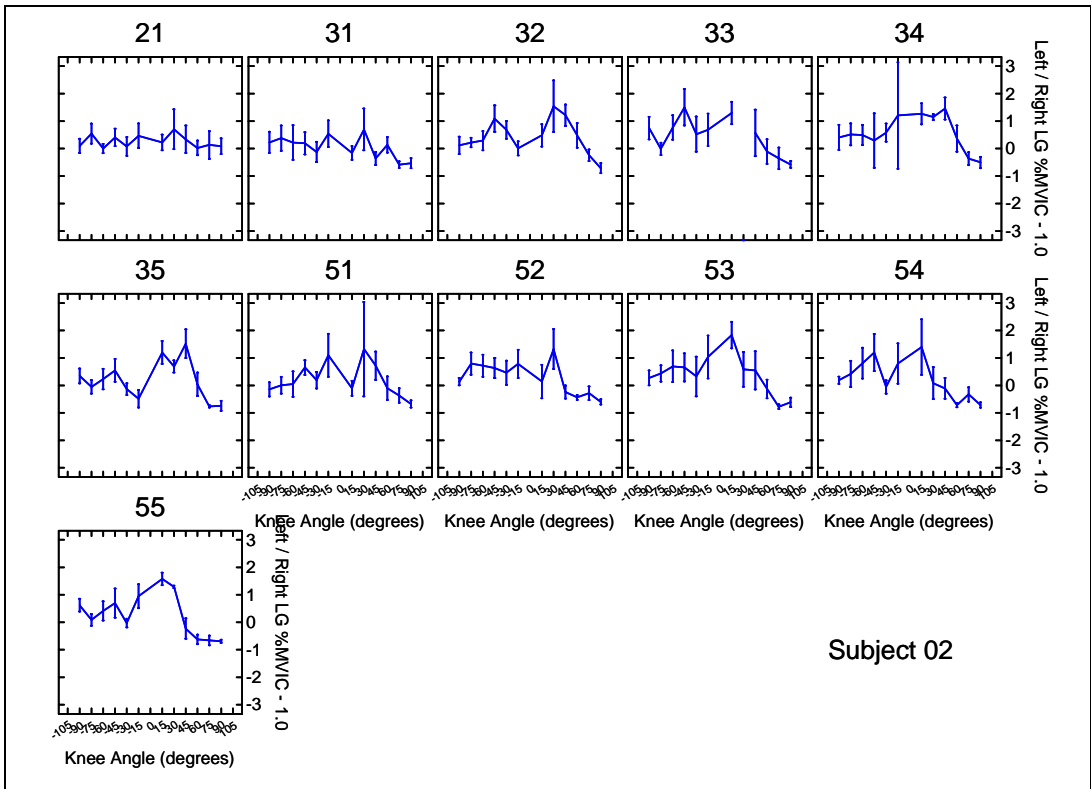


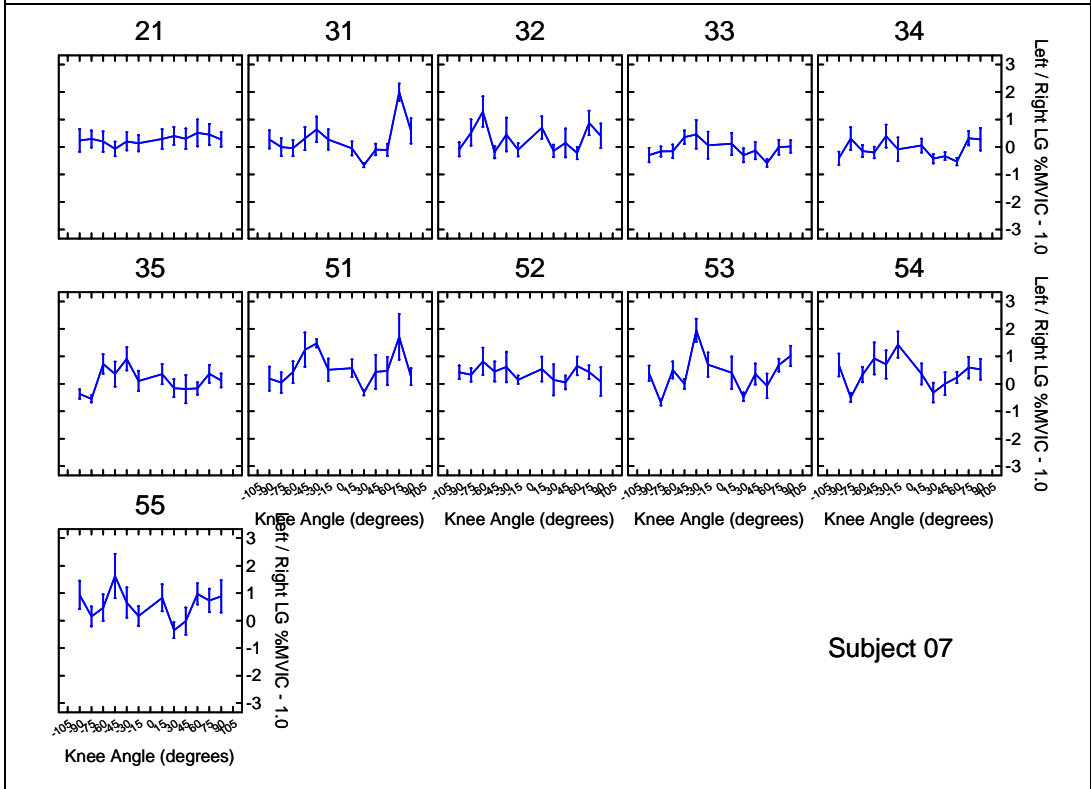
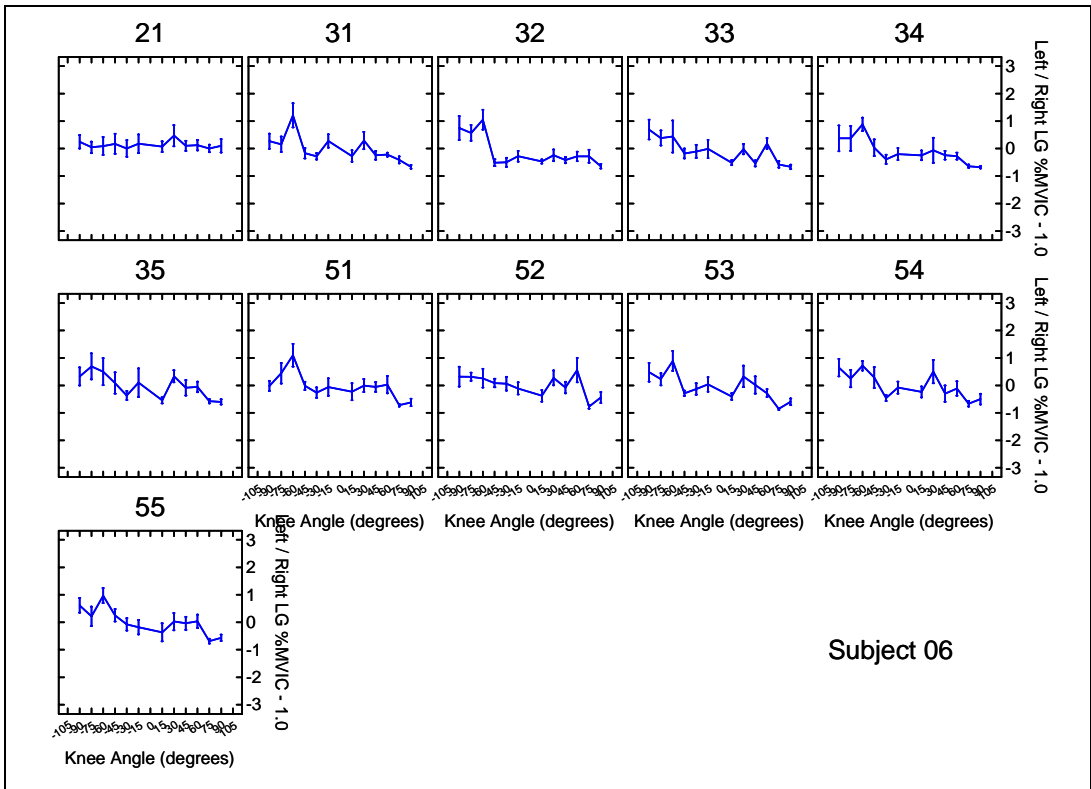


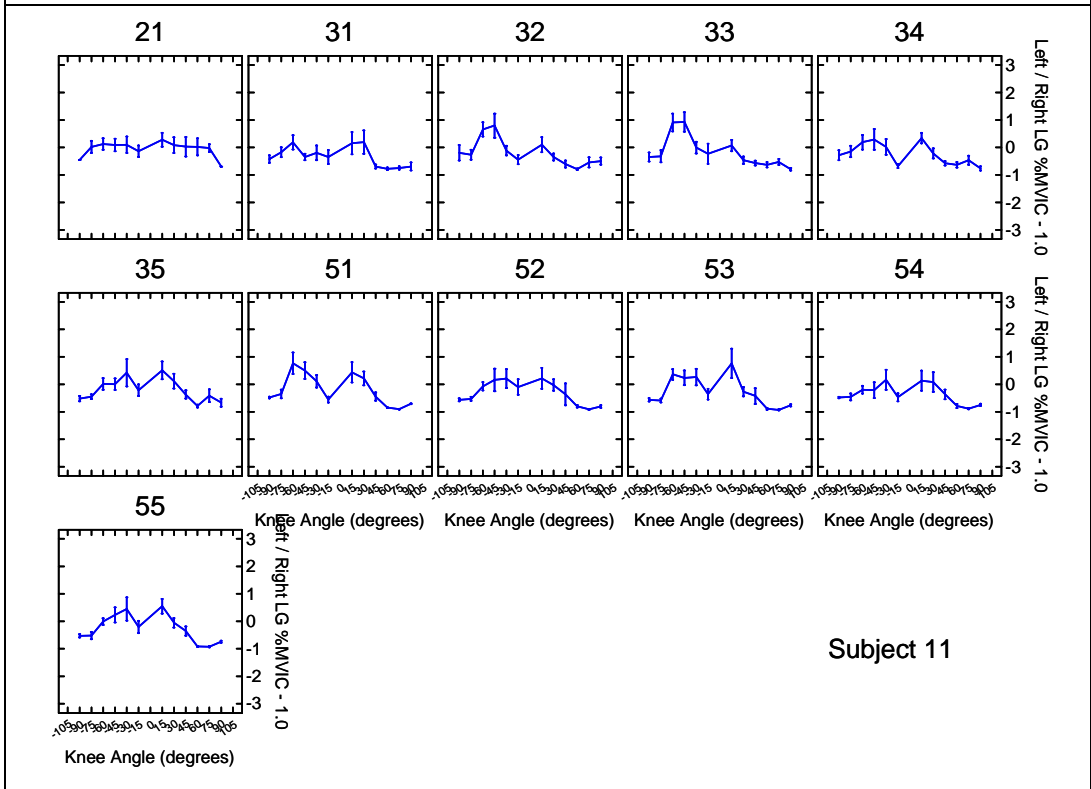
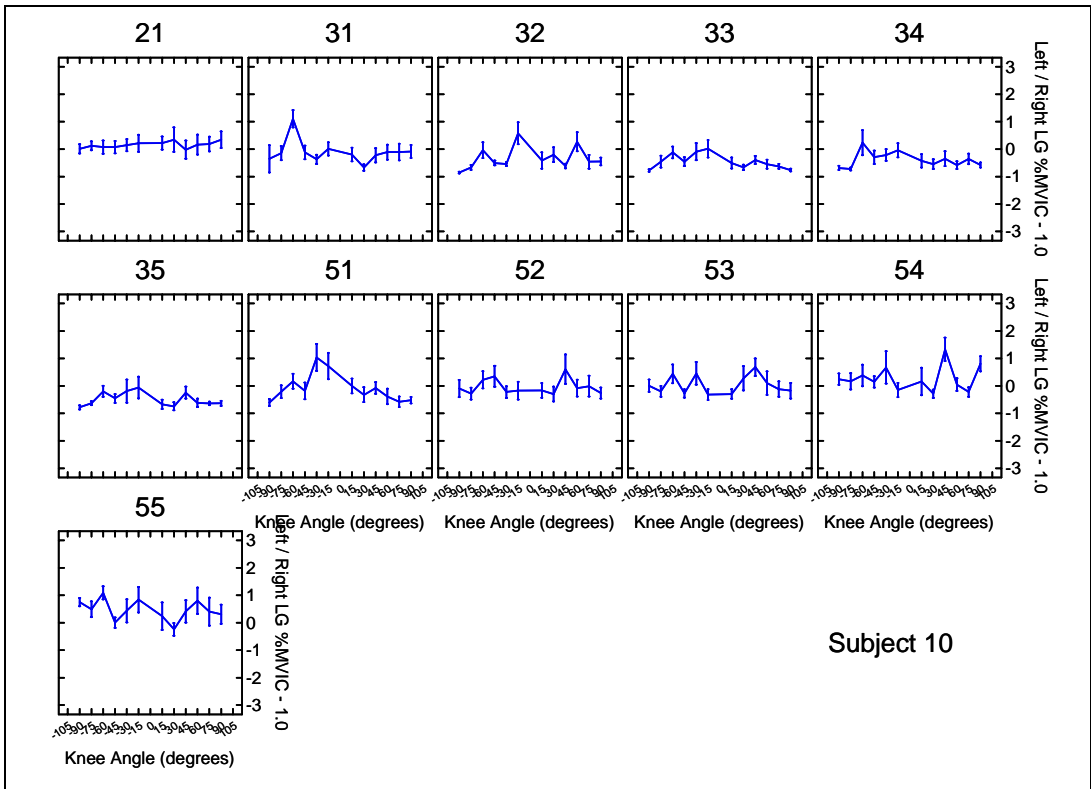
Lateral Gastrocnemius EMG

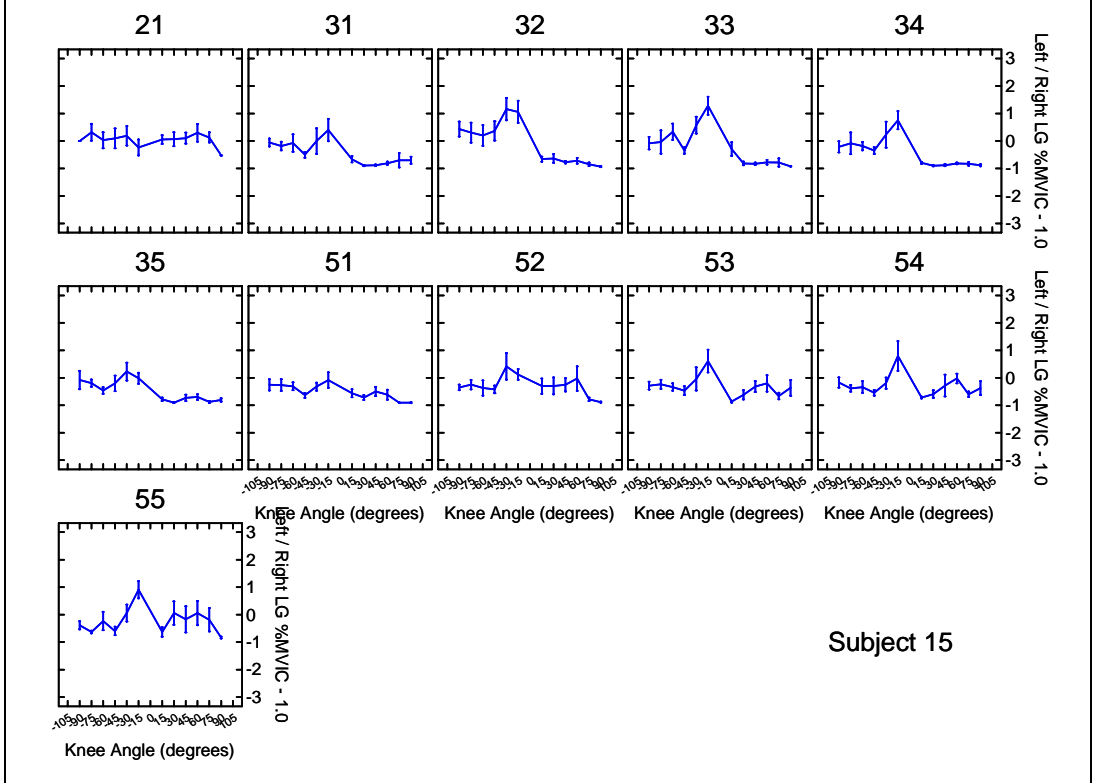
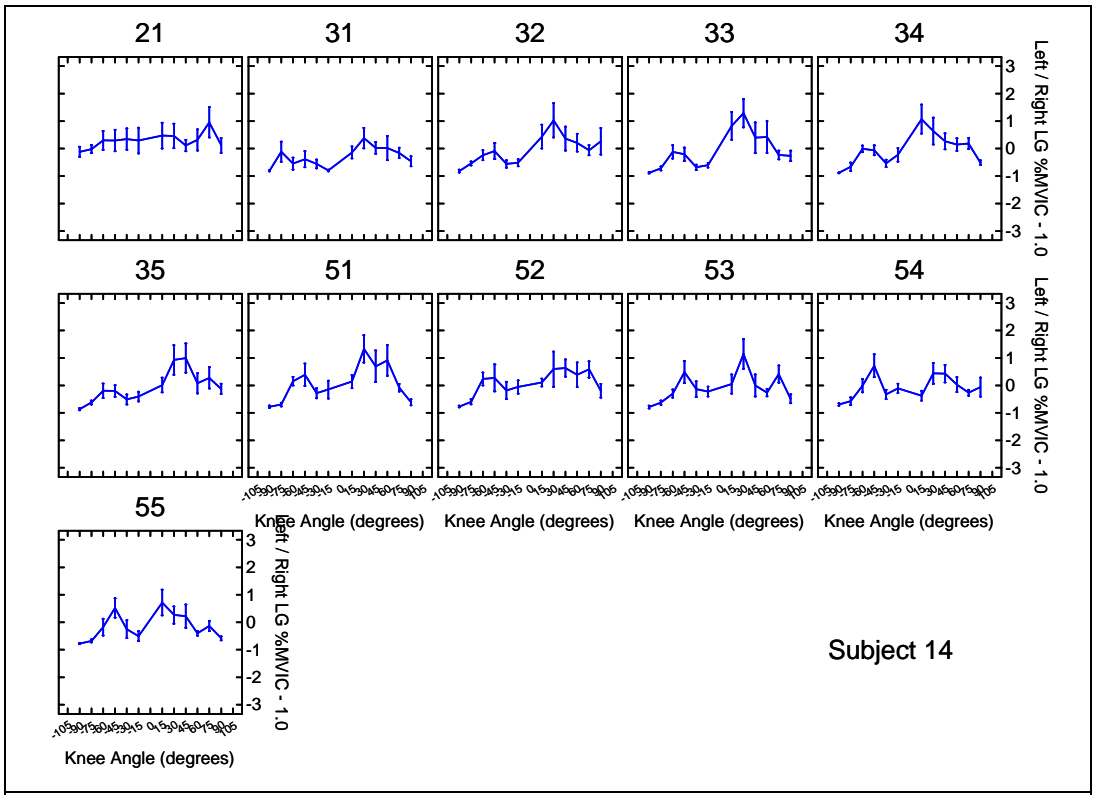
The left divided by right lateral gastrocnemius %MVIC muscle activity minus one (Left / Right – 1.0) at several knee angles for each subject. The numbers on the top of the boxes are the Phase and Set. For example, 31 is Phase 3 (23-RPM), first set of eight repetitions. The eight repetitions within each set are averaged together. Mean +/- SEM. Note: The knee angles are the same as in the body of this thesis, however, the ordering of them is slightly different: 0-degree knee angle is in the middle of the graph and full extension (i.e., 90-degrees) is at the edges.





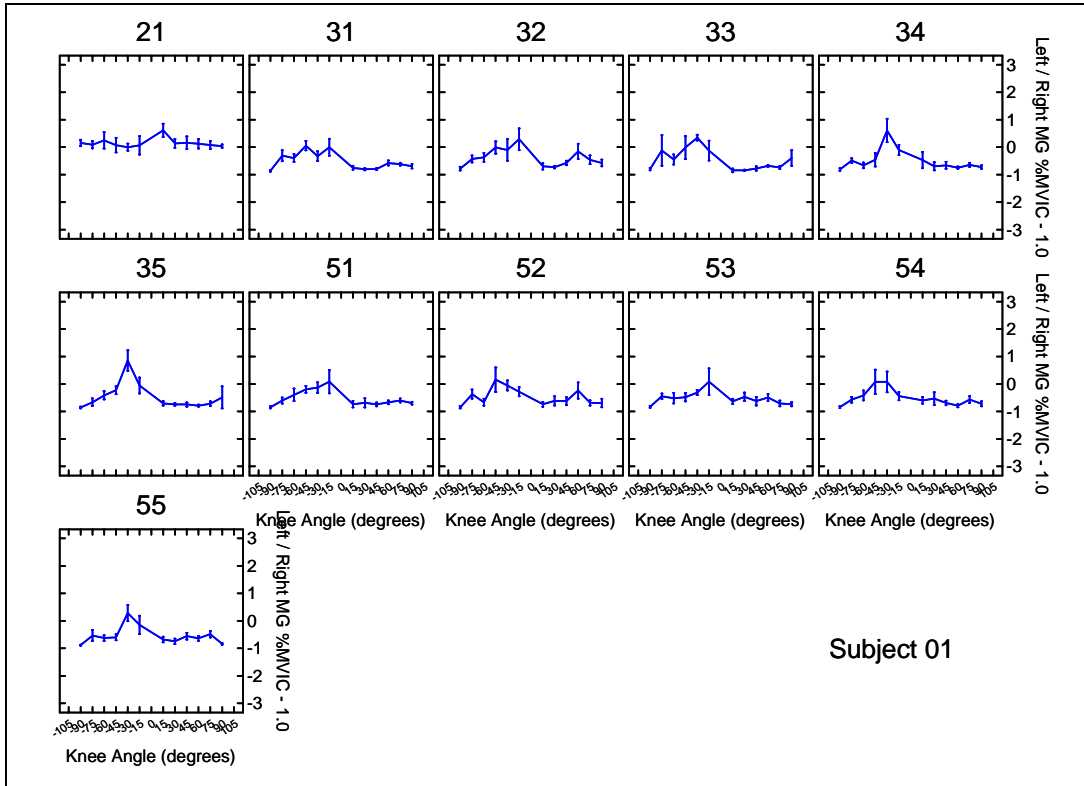


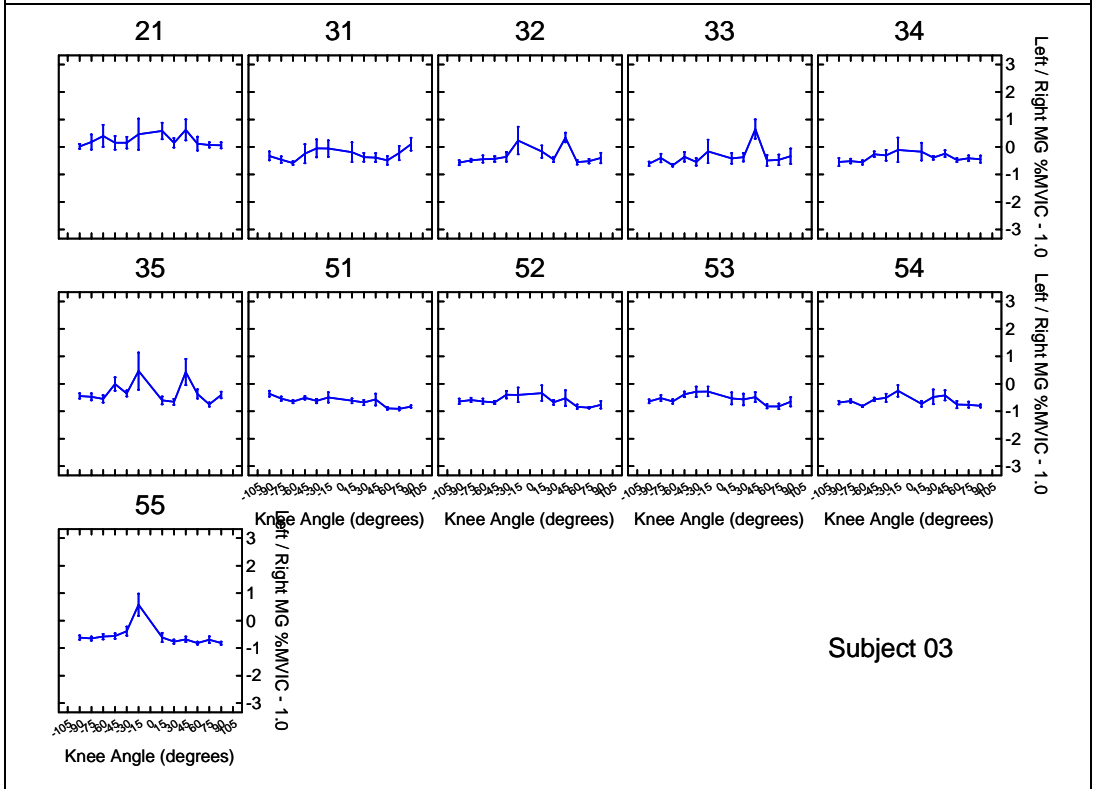
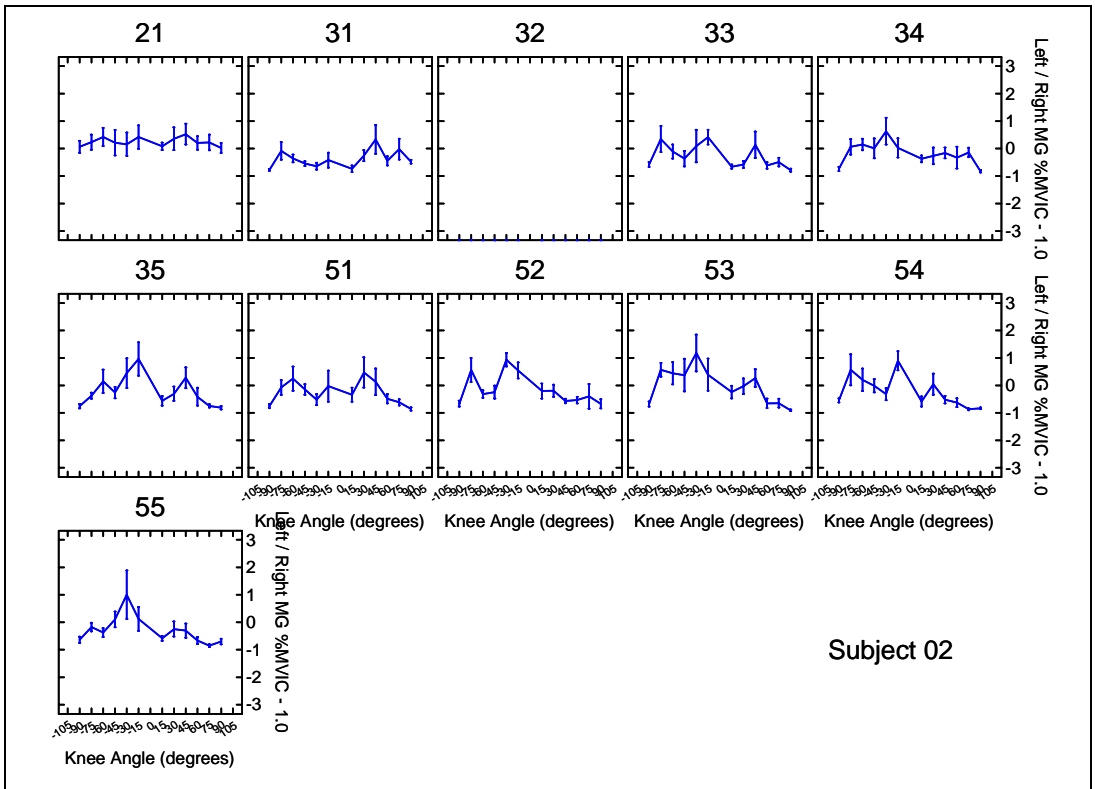


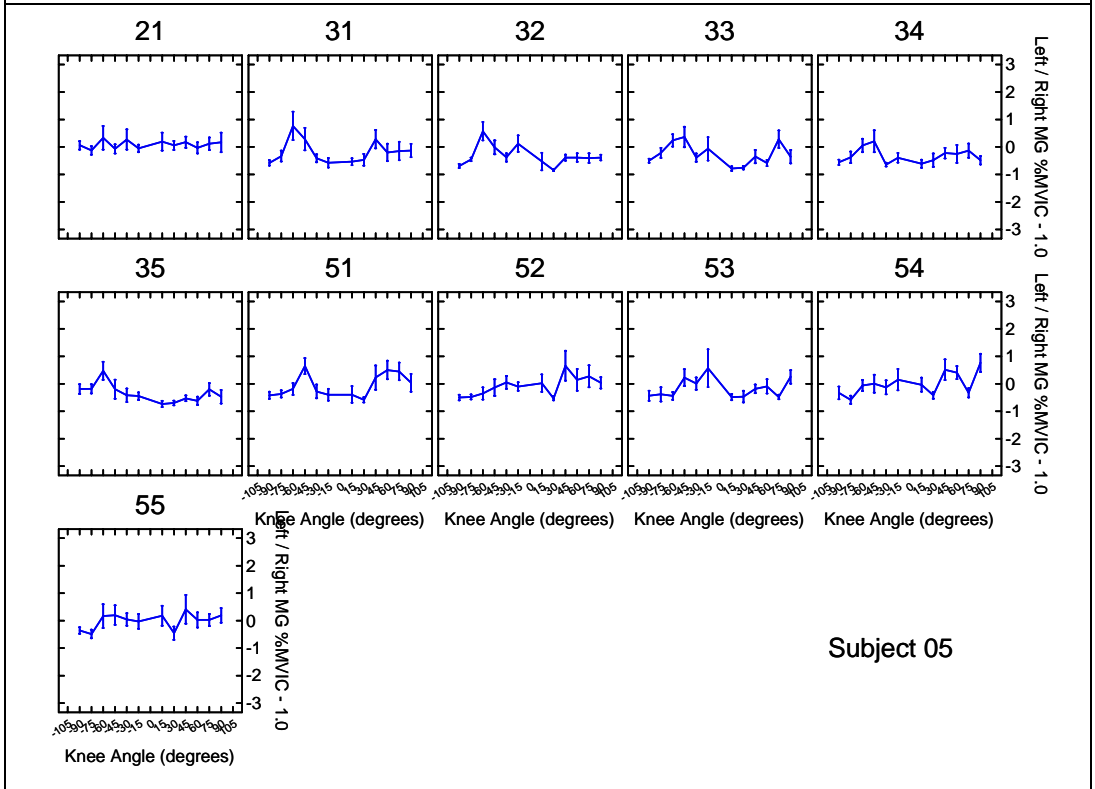
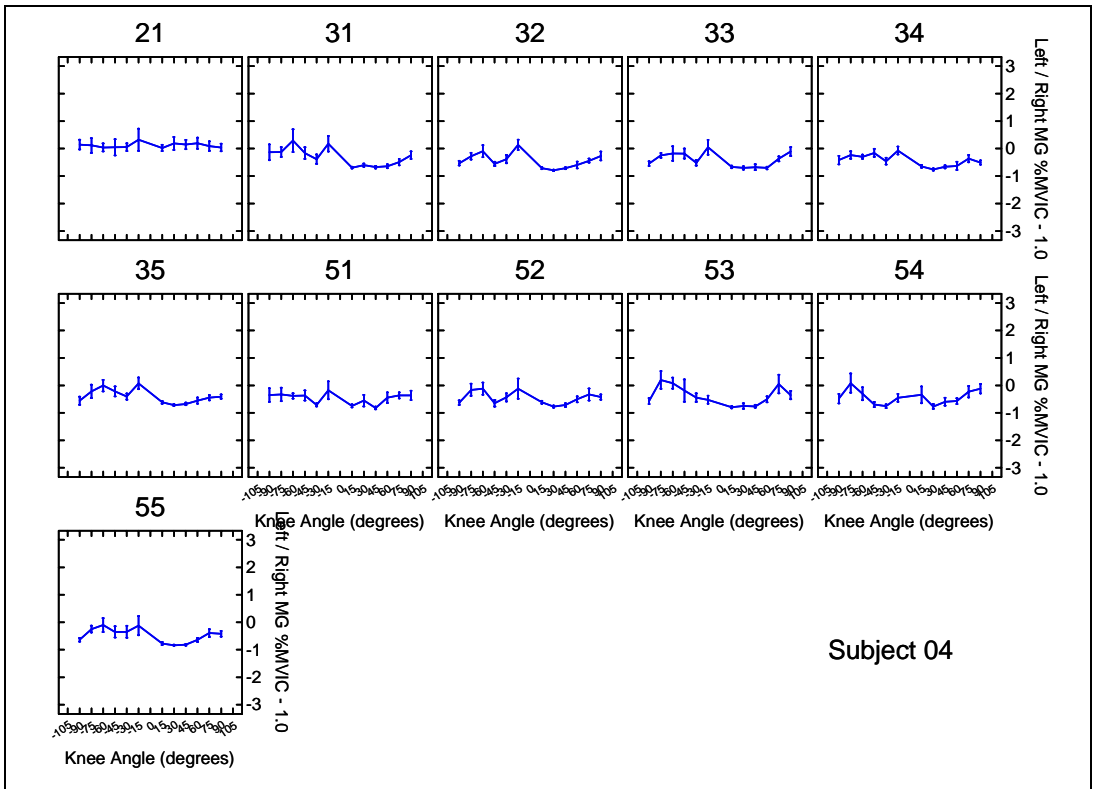


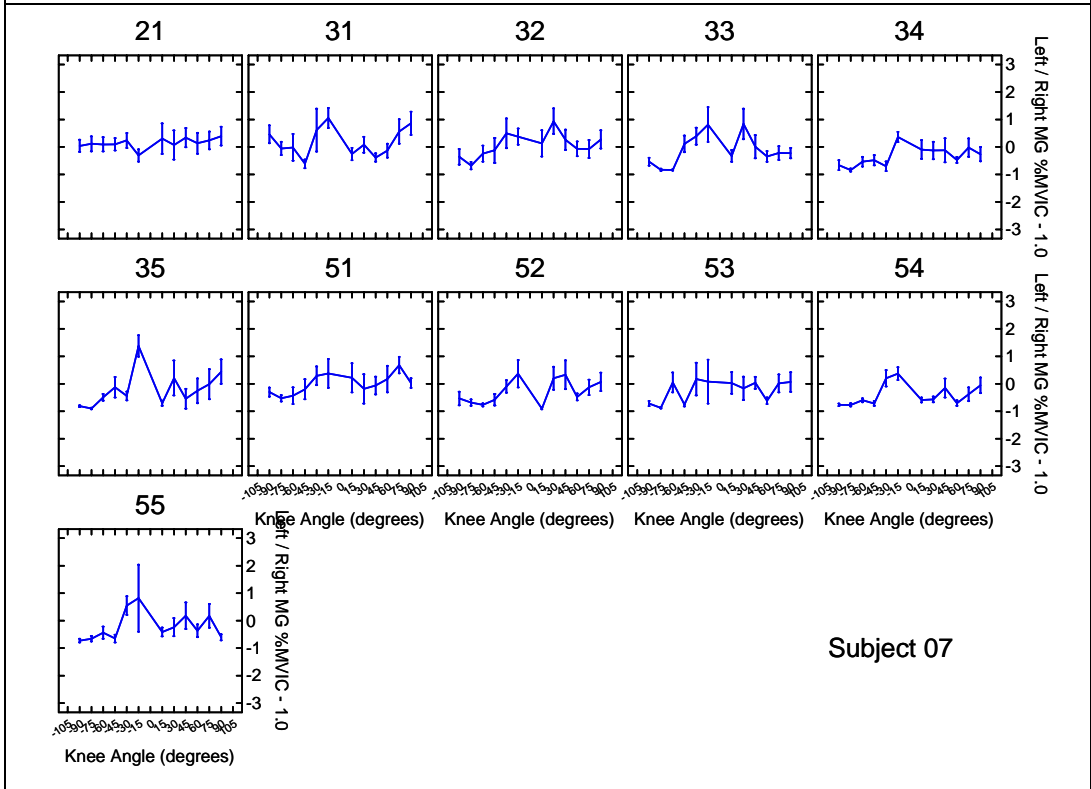
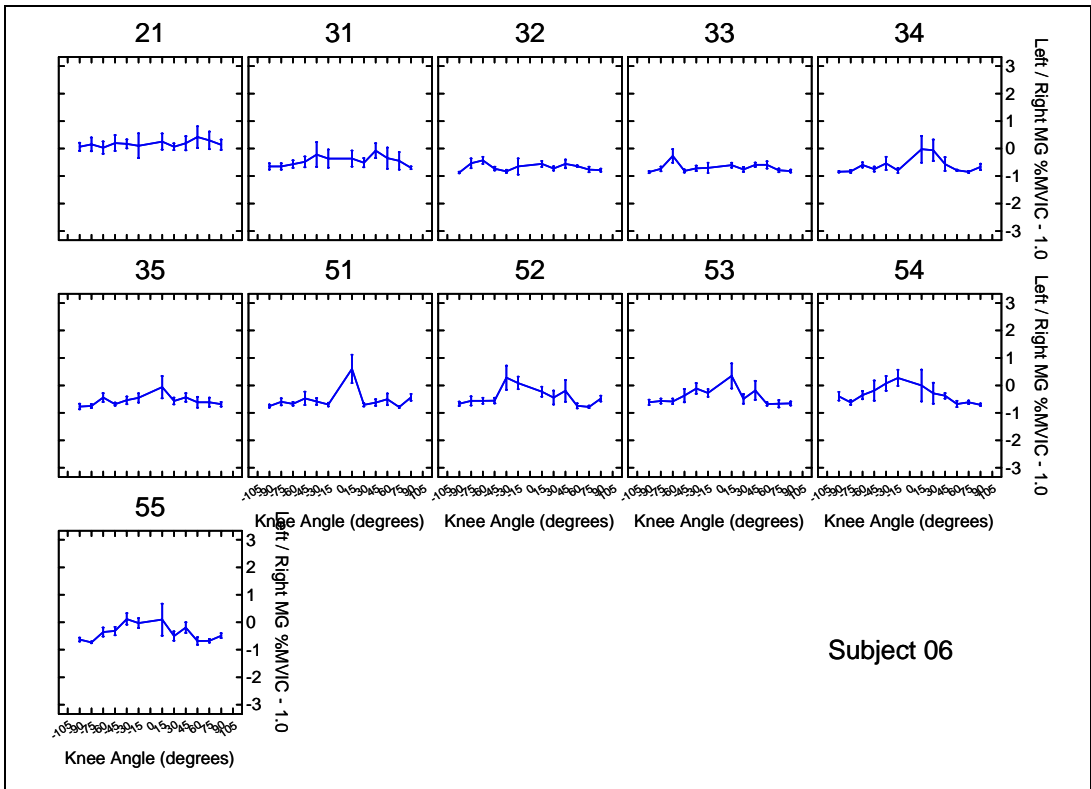
Medial Gastrocnemius EMG

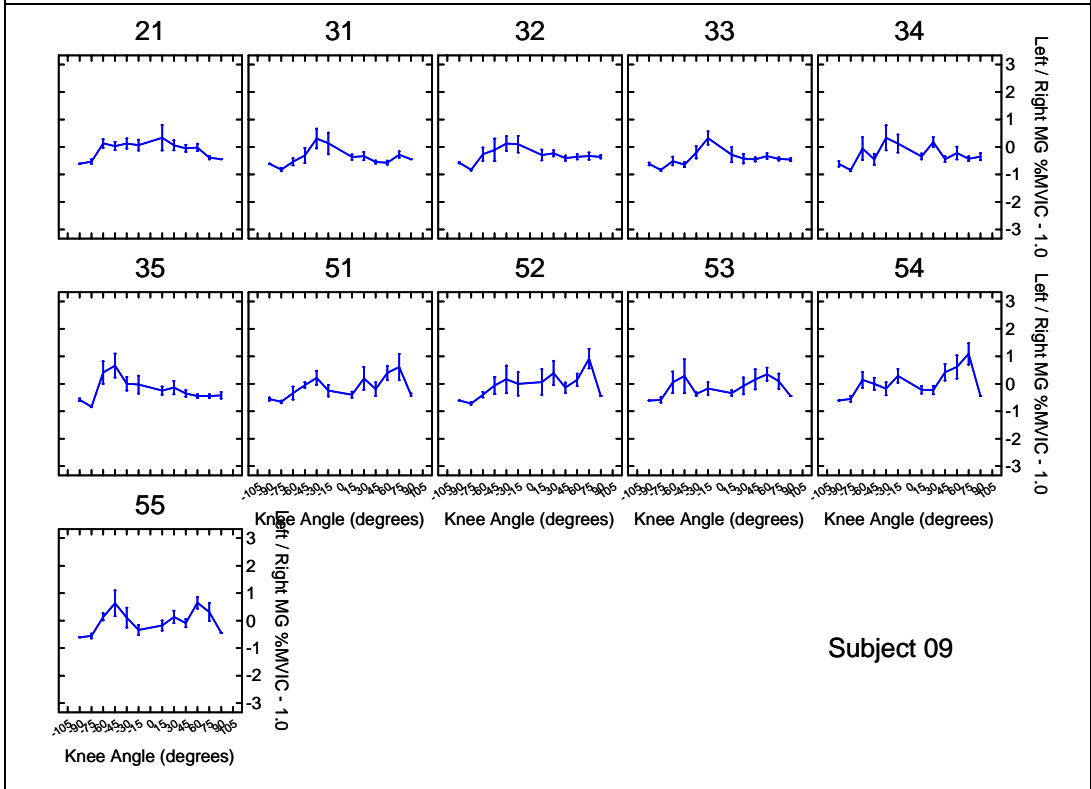
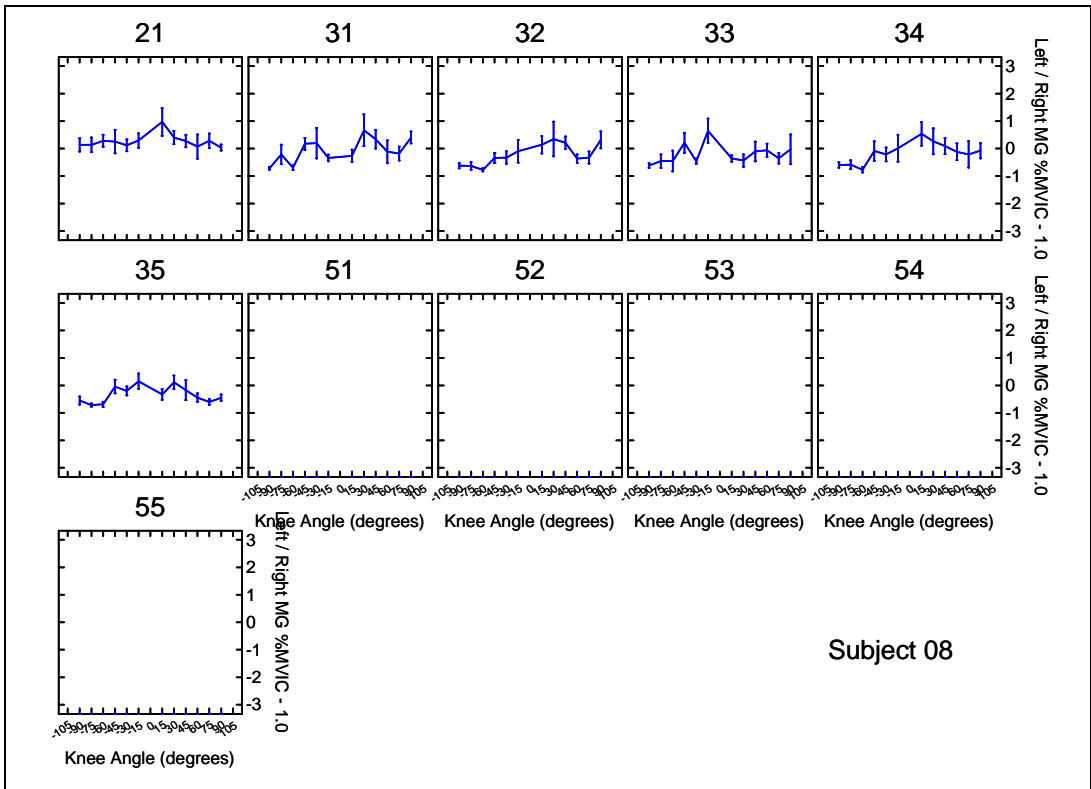
The left divided by right medial gastrocnemius %MVIC muscle activity minus one (Left / Right – 1.0) at several knee angles for each subject. The numbers on the top of the boxes are the Phase and Set. For example, 31 is Phase 3 (23-RPM), first set of eight repetitions. The eight repetitions within each set are averaged together. Mean +/- SEM. Note: The knee angles are the same as in the body of this thesis, however, the ordering of them is slightly different: 0-degree knee angle is in the middle of the graph and full extension (i.e., 90-degrees) is at the edges.

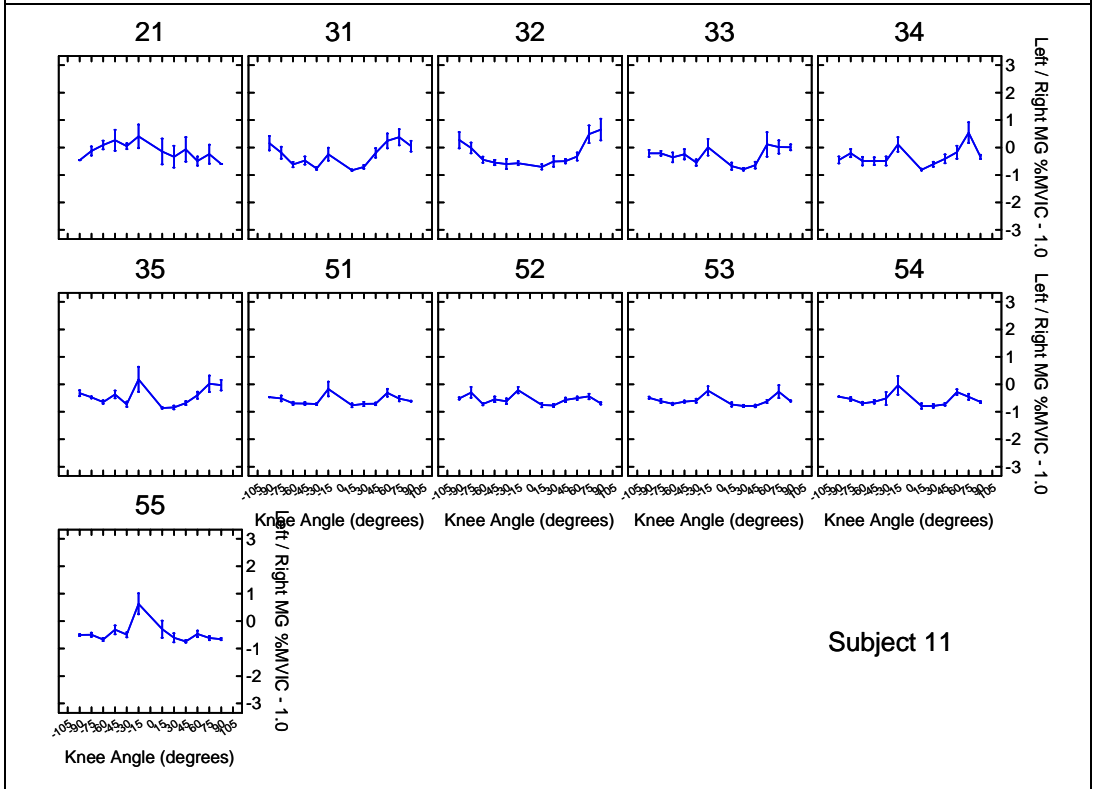
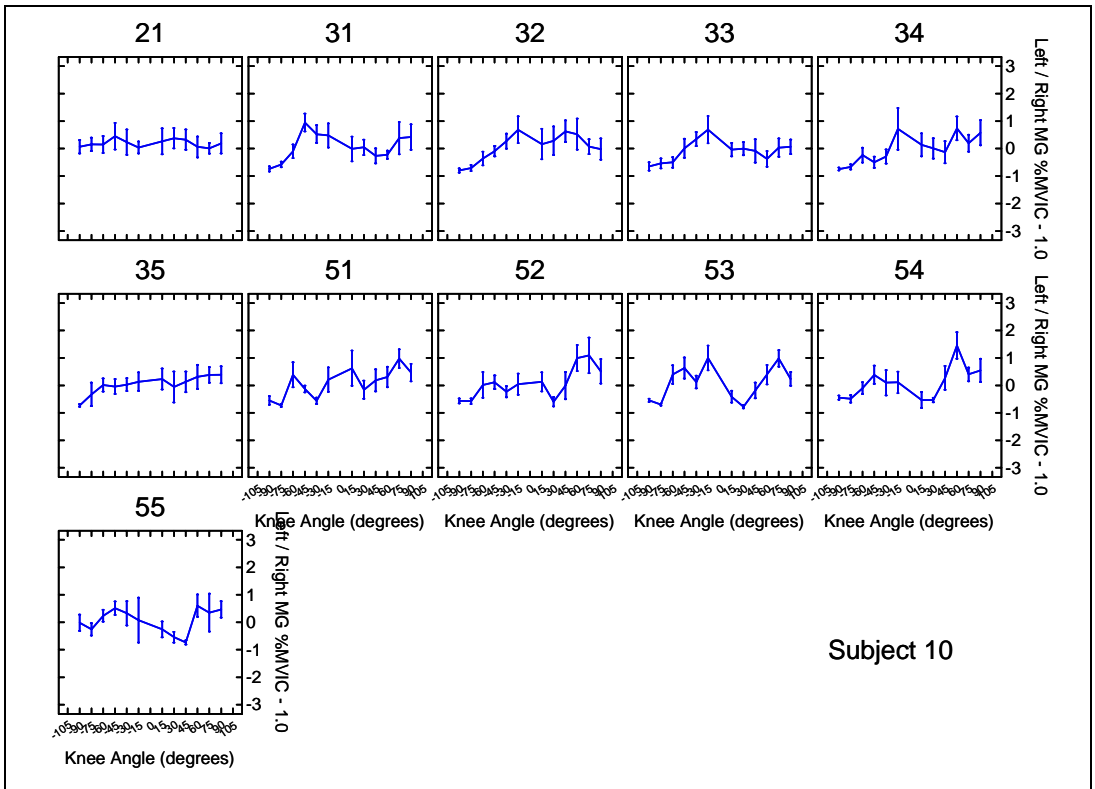


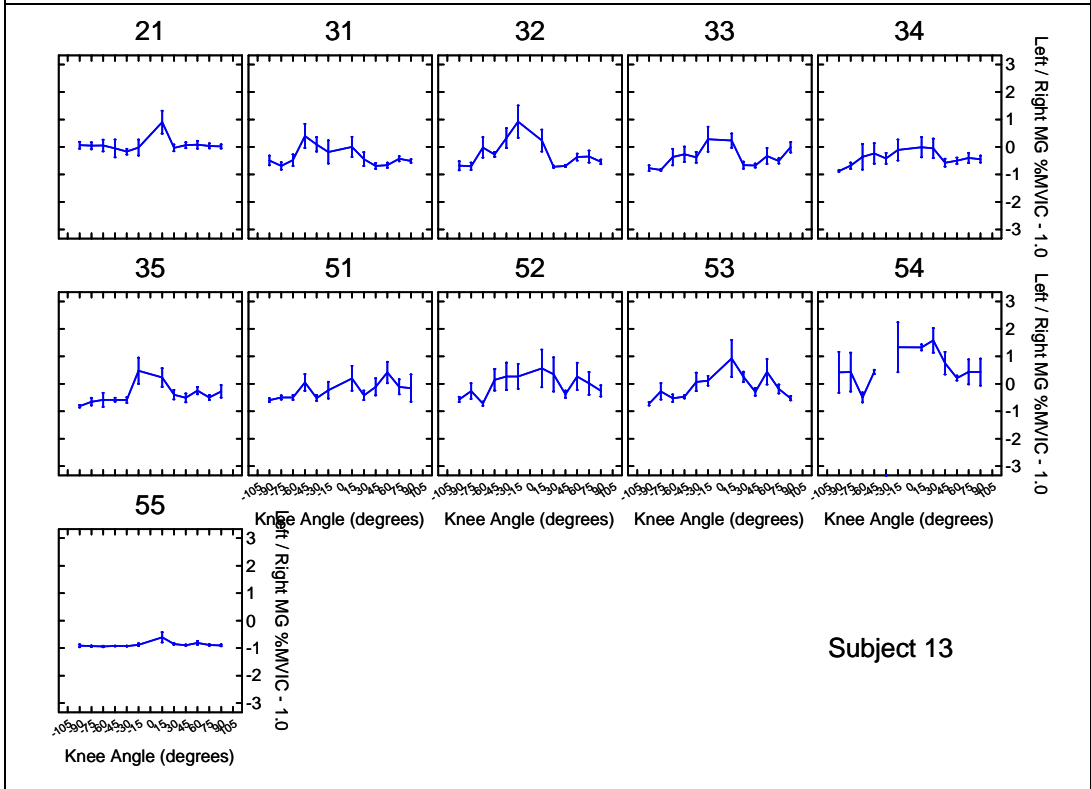
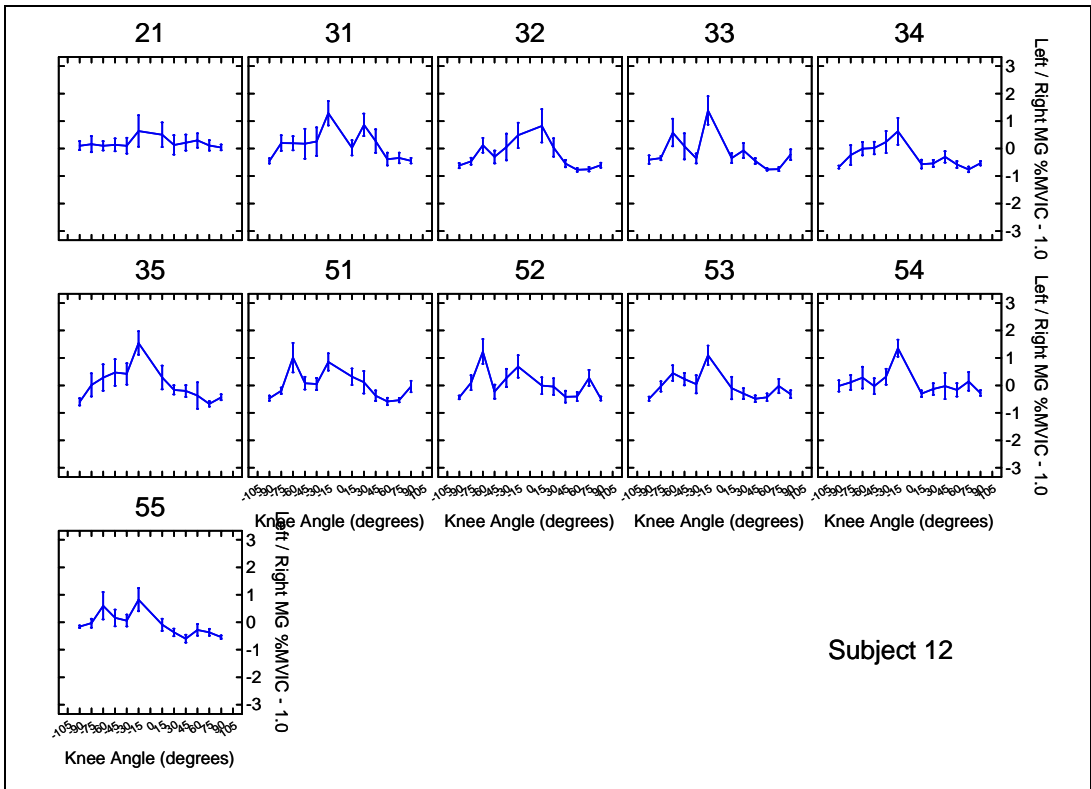


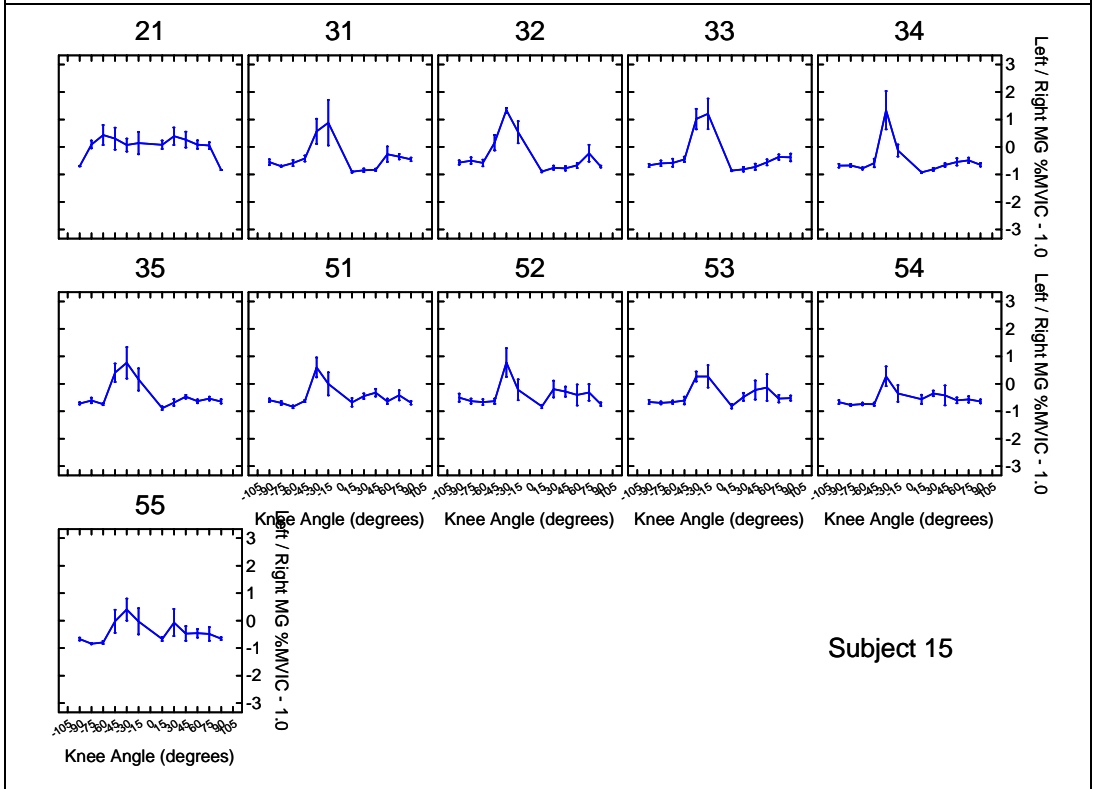
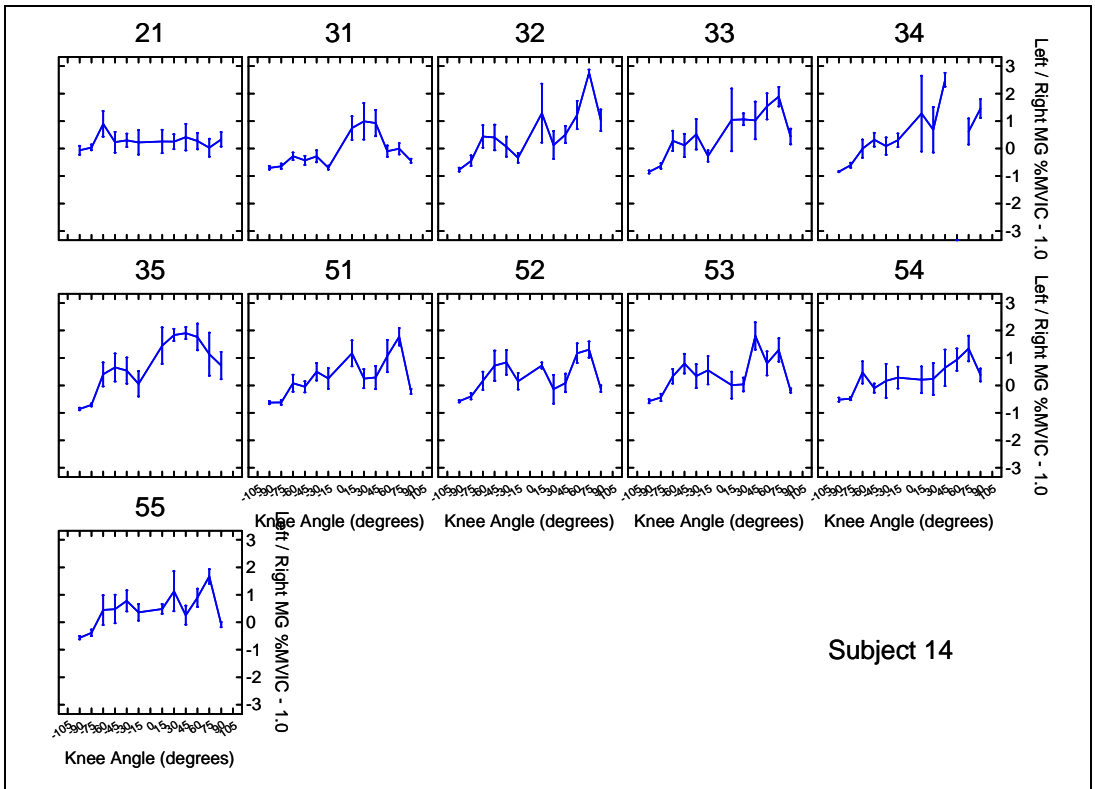






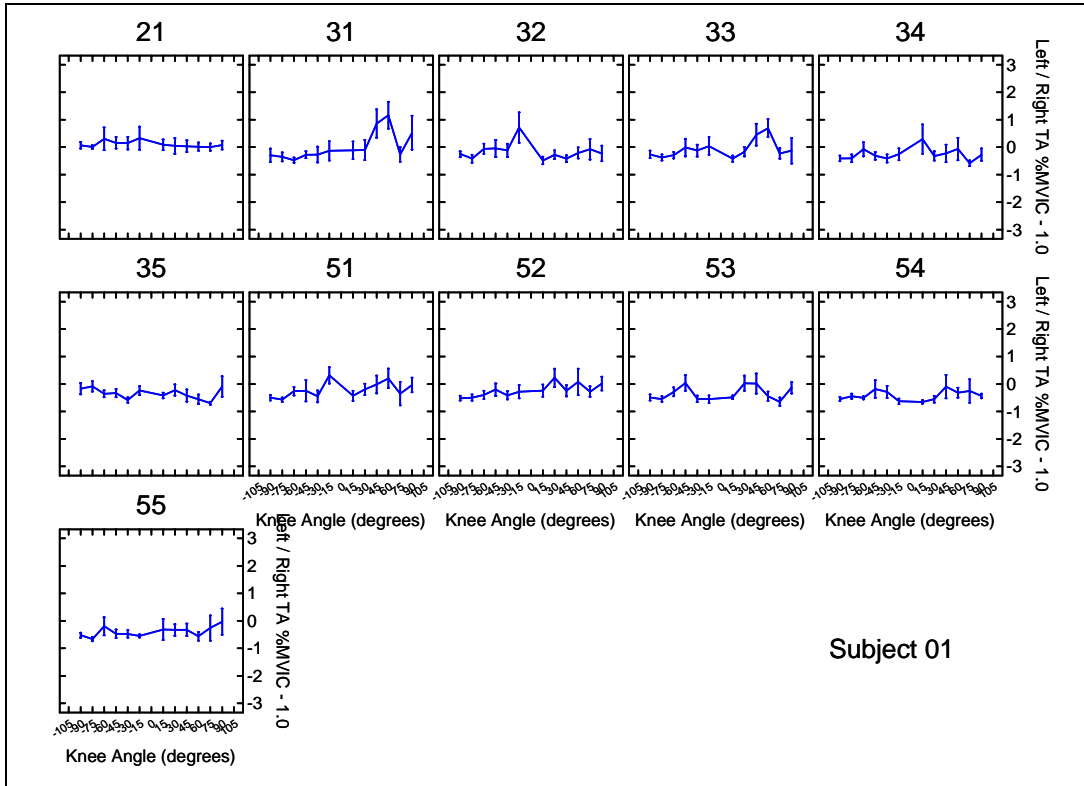


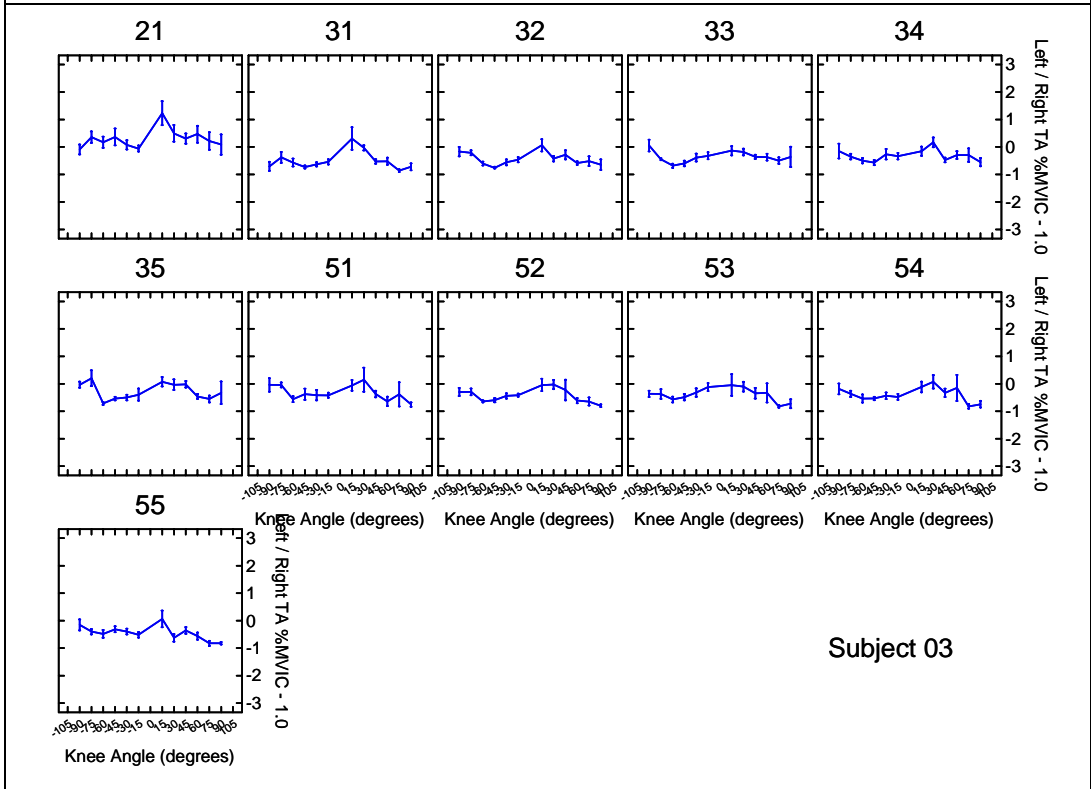
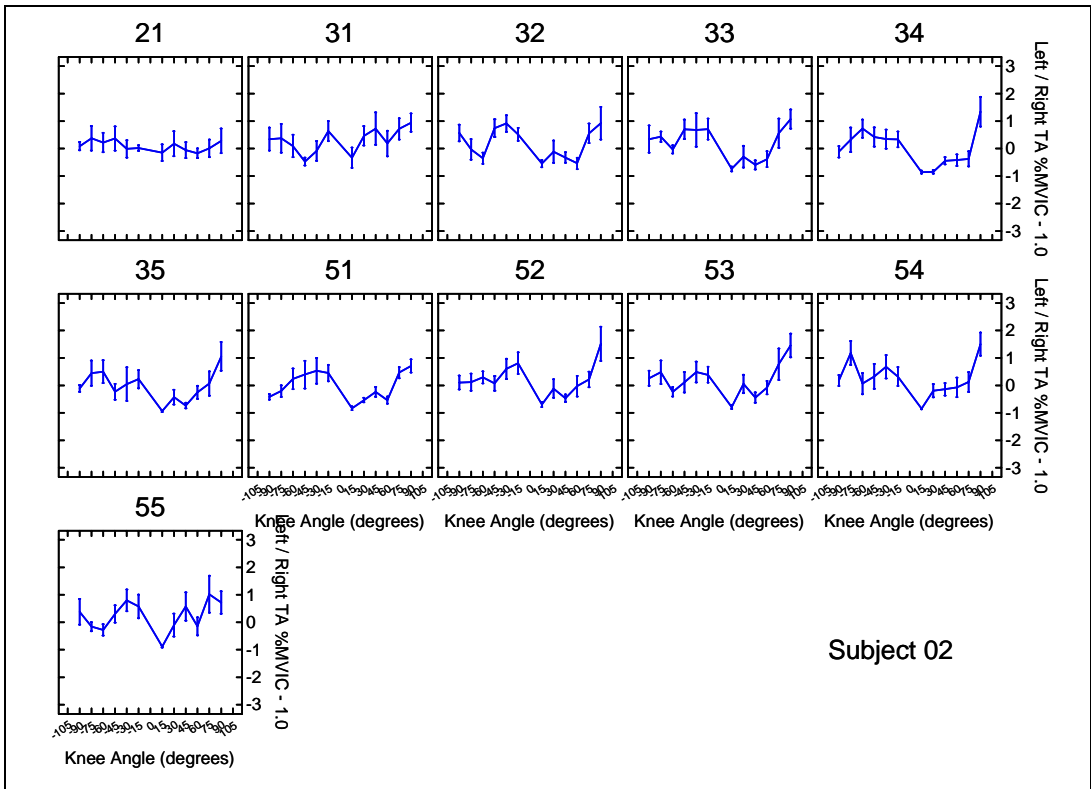


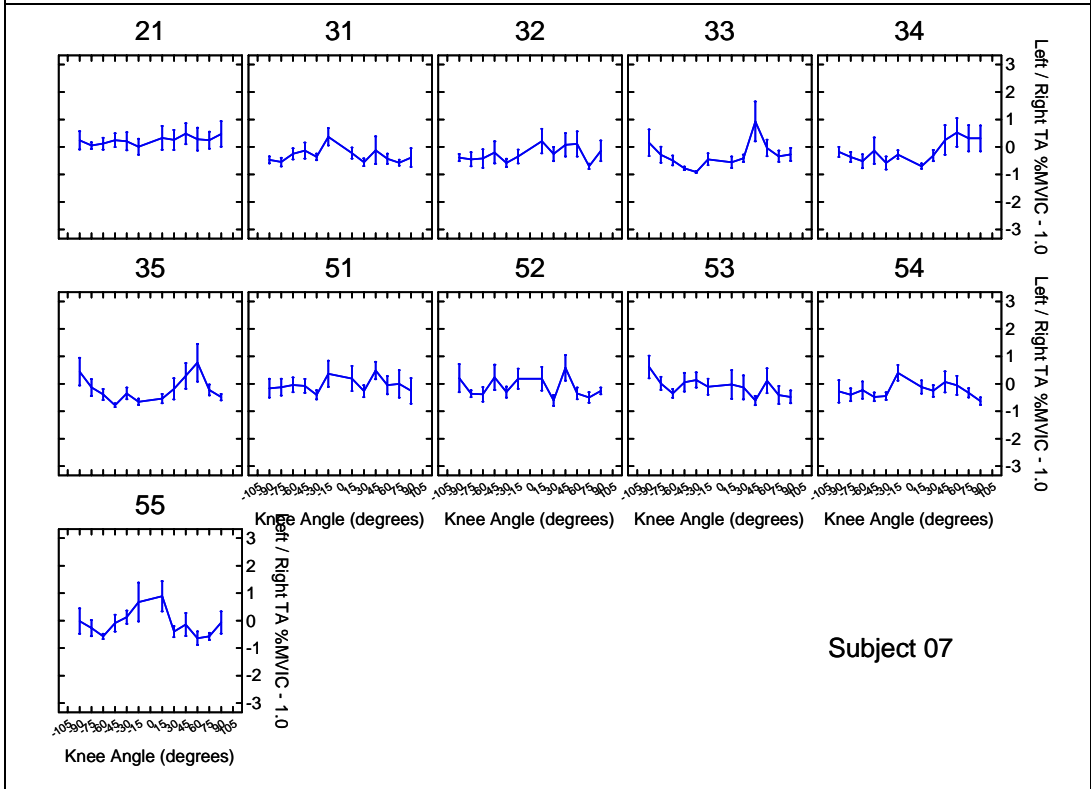
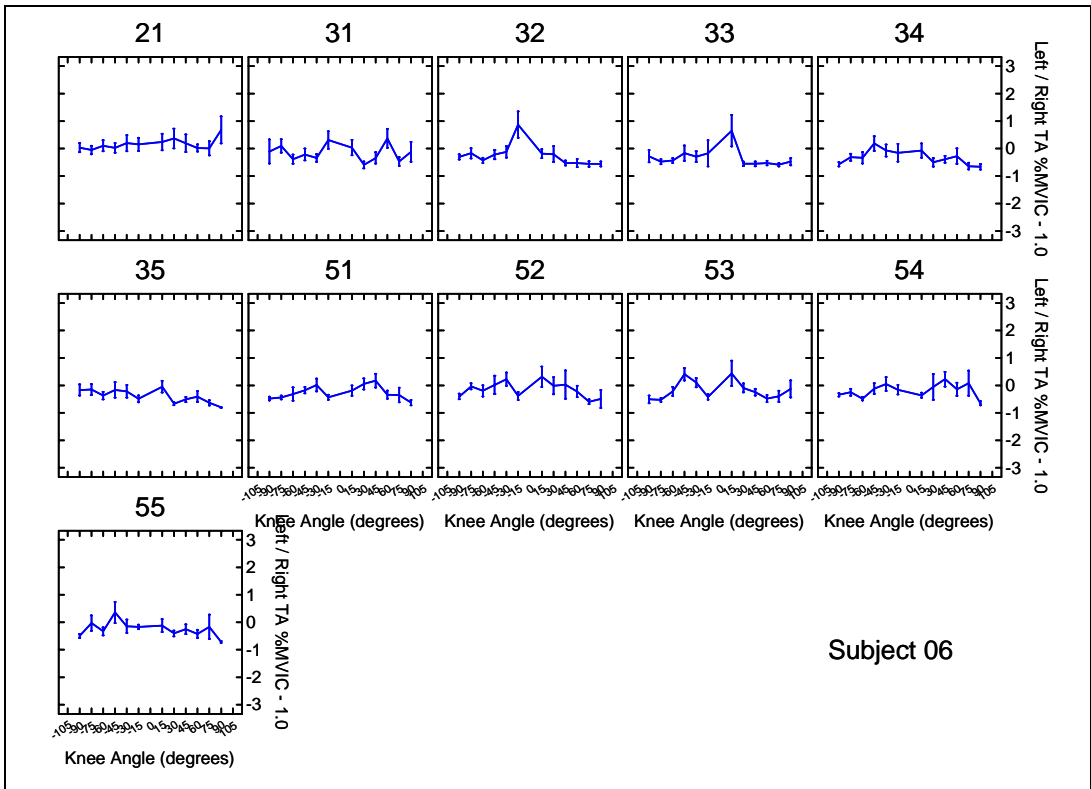


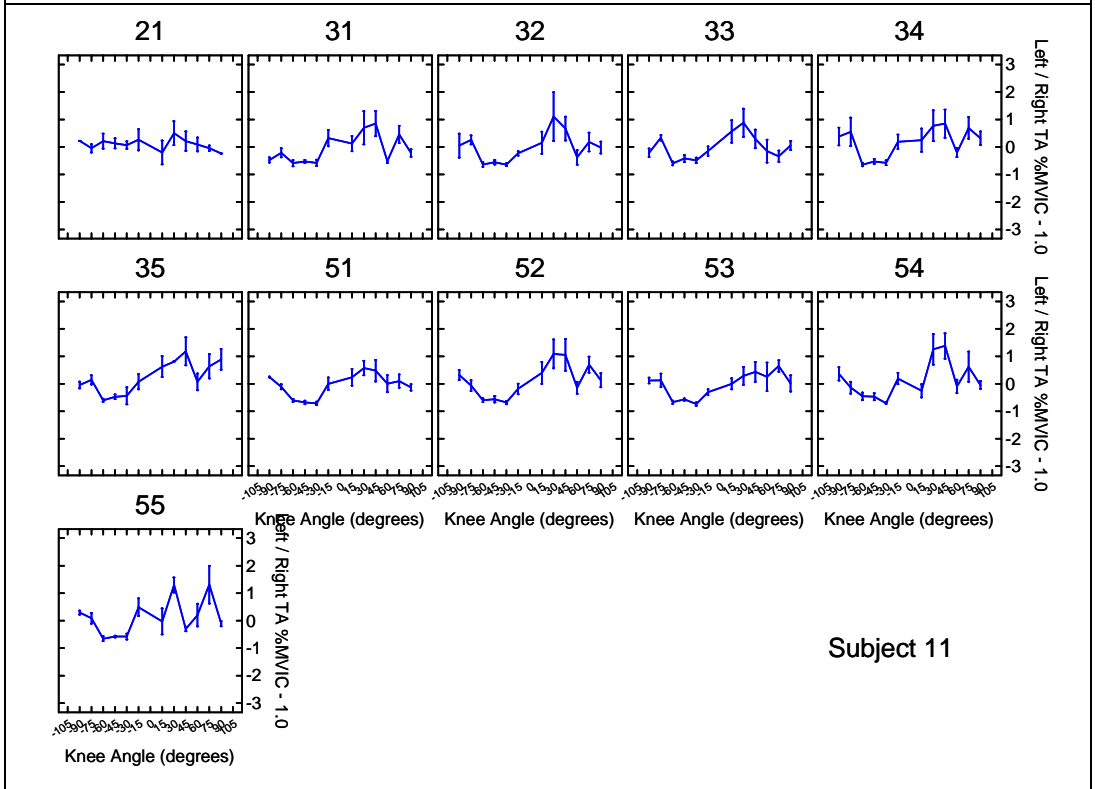
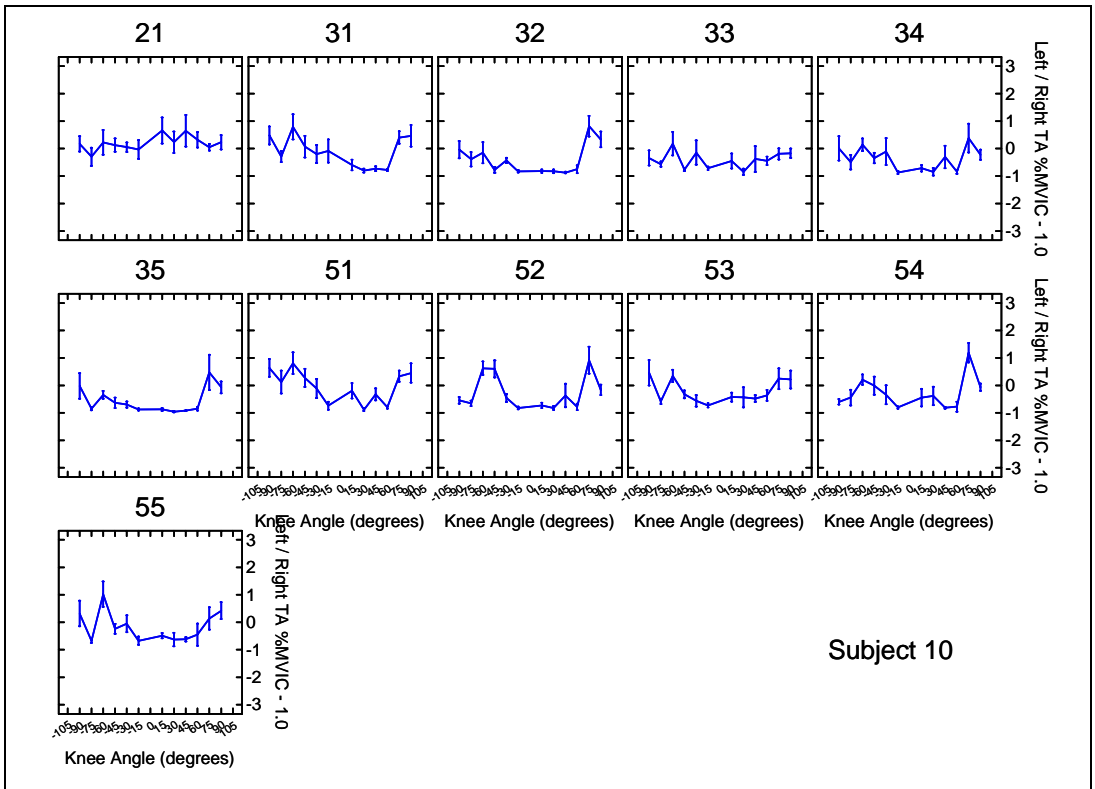
Tibialis Anterior EMG

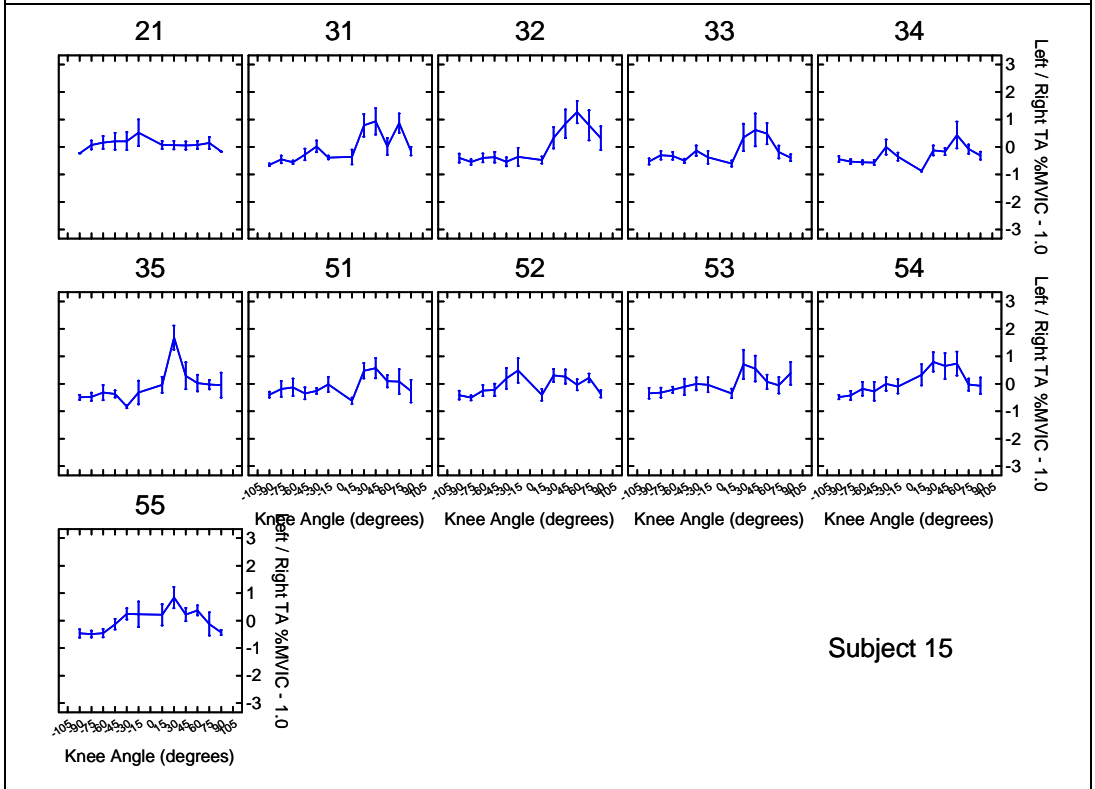
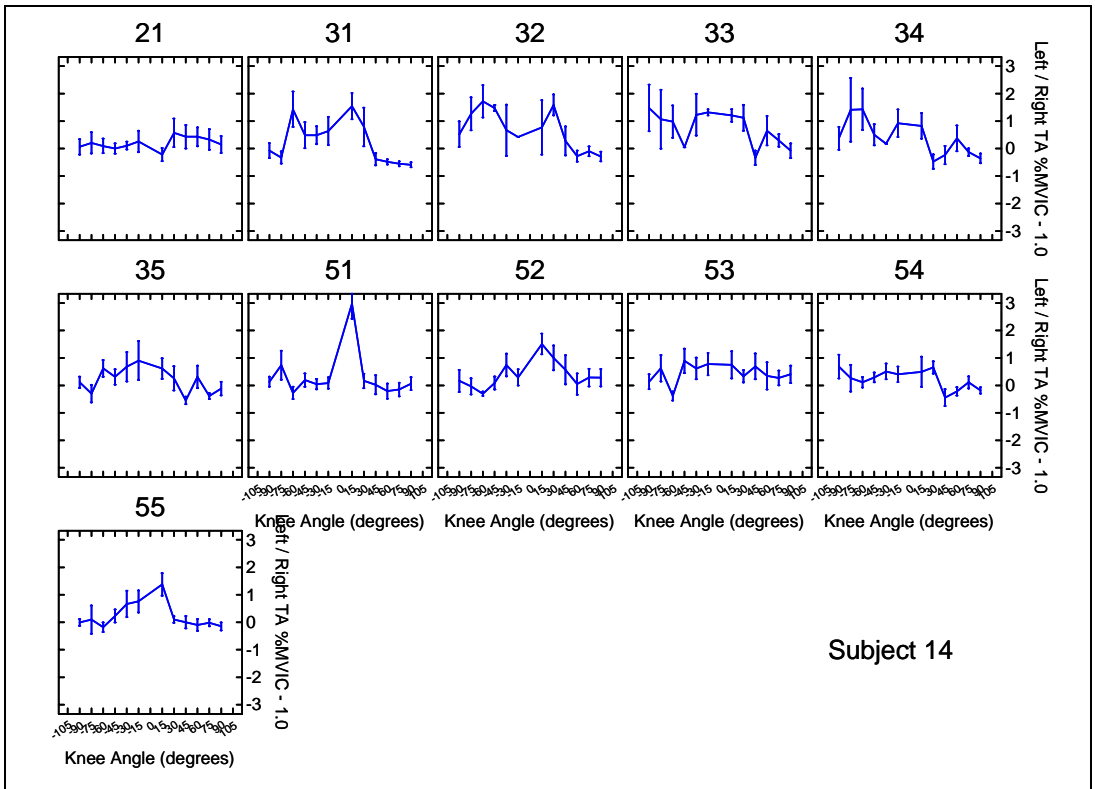
The left divided by right tibialis anterior %MVIC muscle activity minus one (Left / Right – 1.0) at several knee angles for each subject. The numbers on the top of the boxes are the Phase and Set. For example, 31 is Phase 3 (23-RPM), first set of eight repetitions. The eight repetitions within each set are averaged together. Mean +/- SEM. Note: The knee angles are the same as in the body of this thesis, however, the ordering of them is slightly different: 0-degree knee angle is in the middle of the graph and full extension (i.e., 90-degrees) is at the edges.





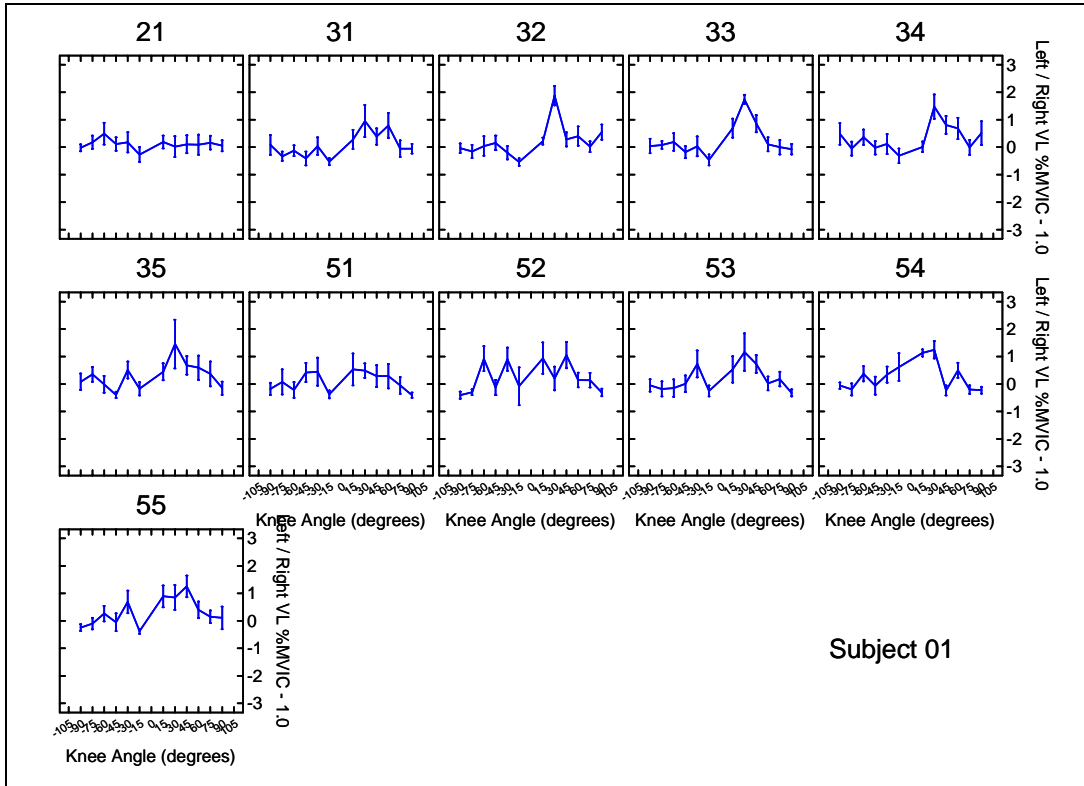


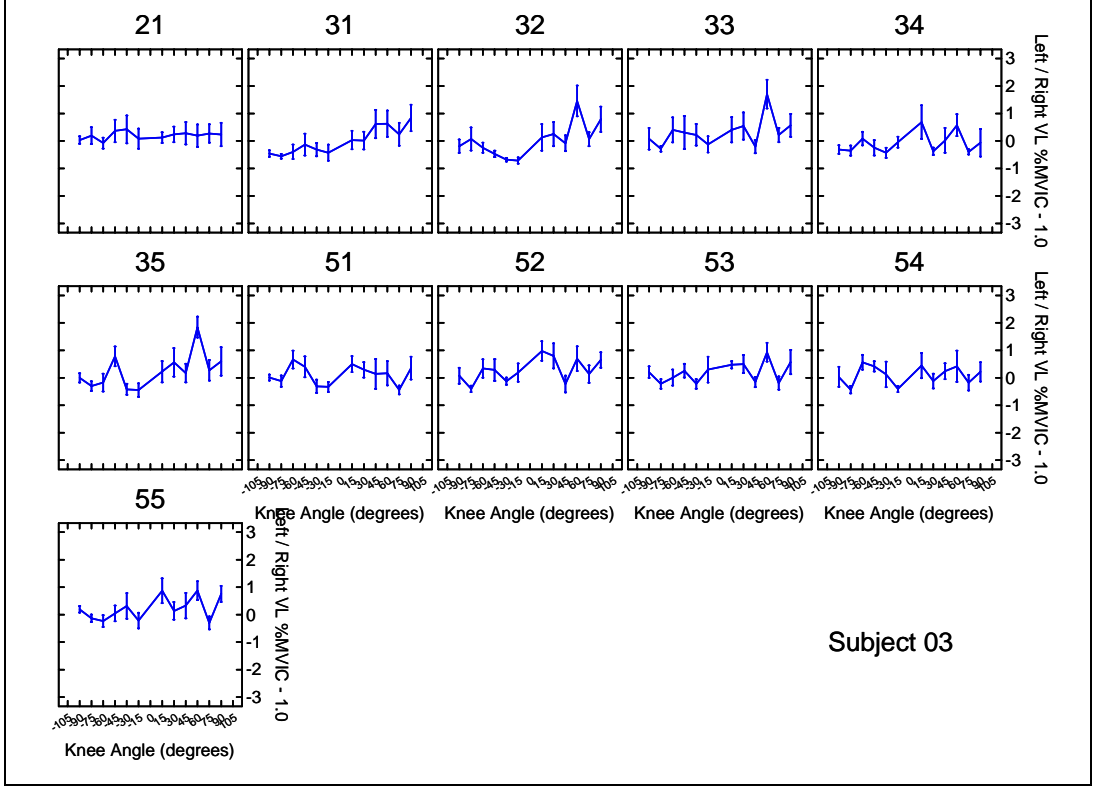
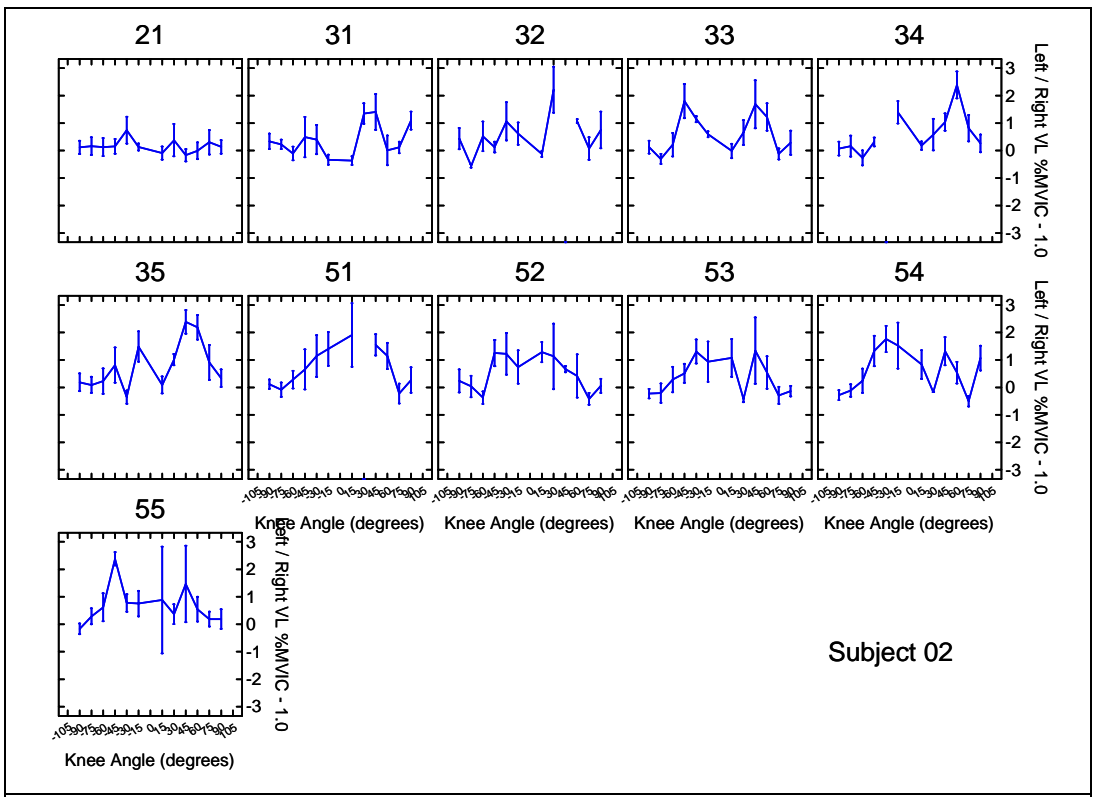


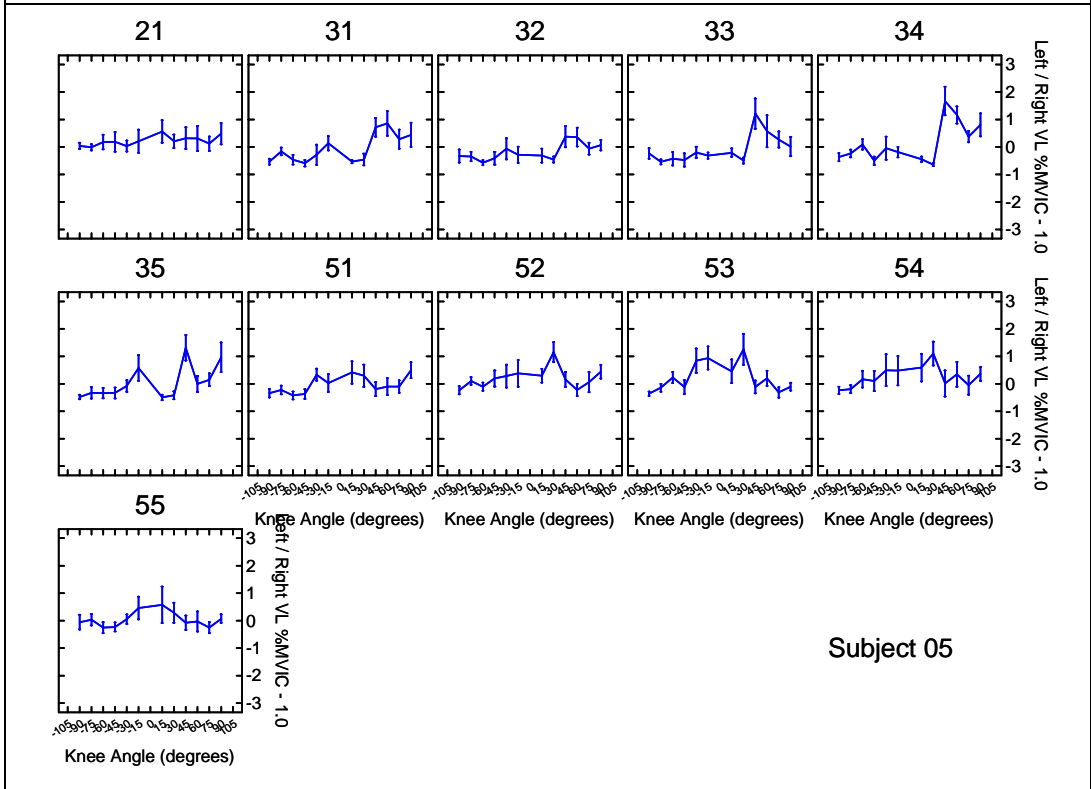
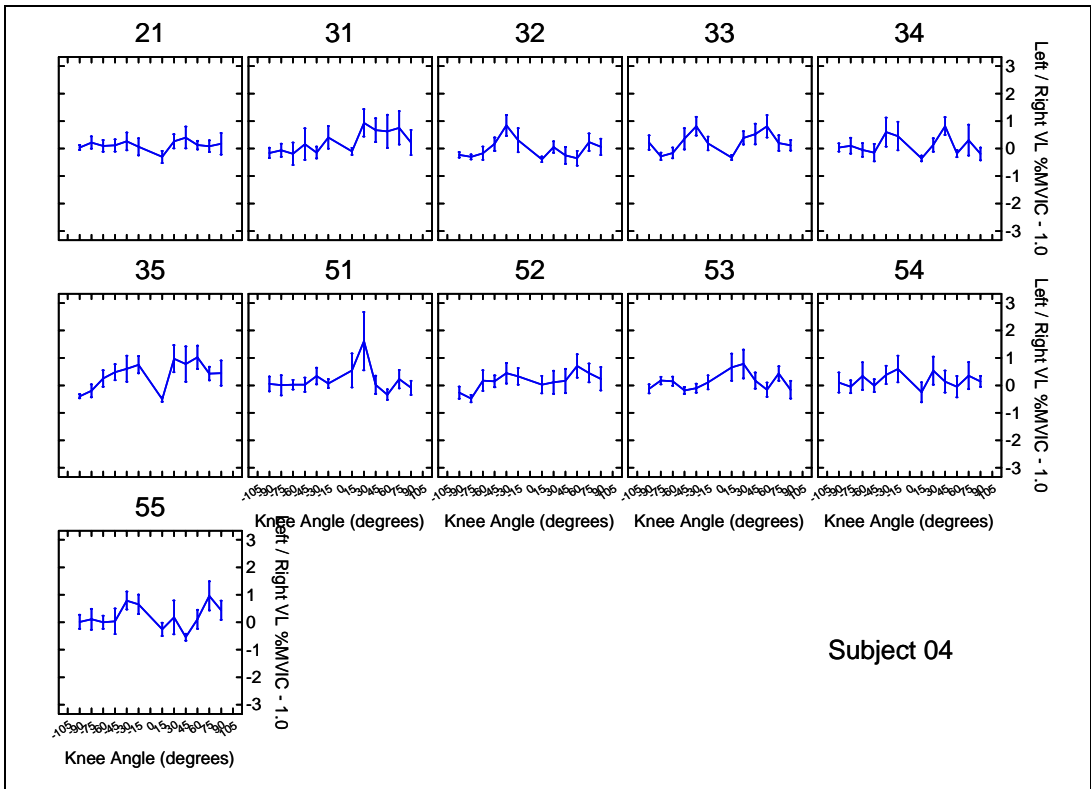


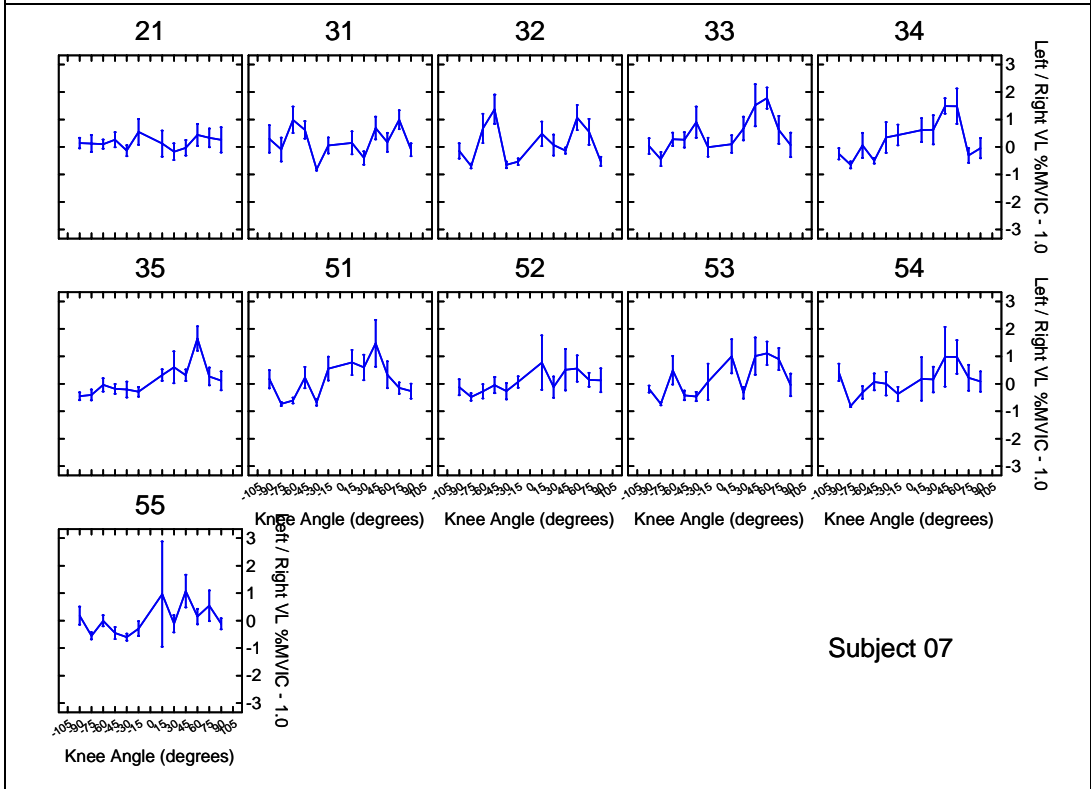
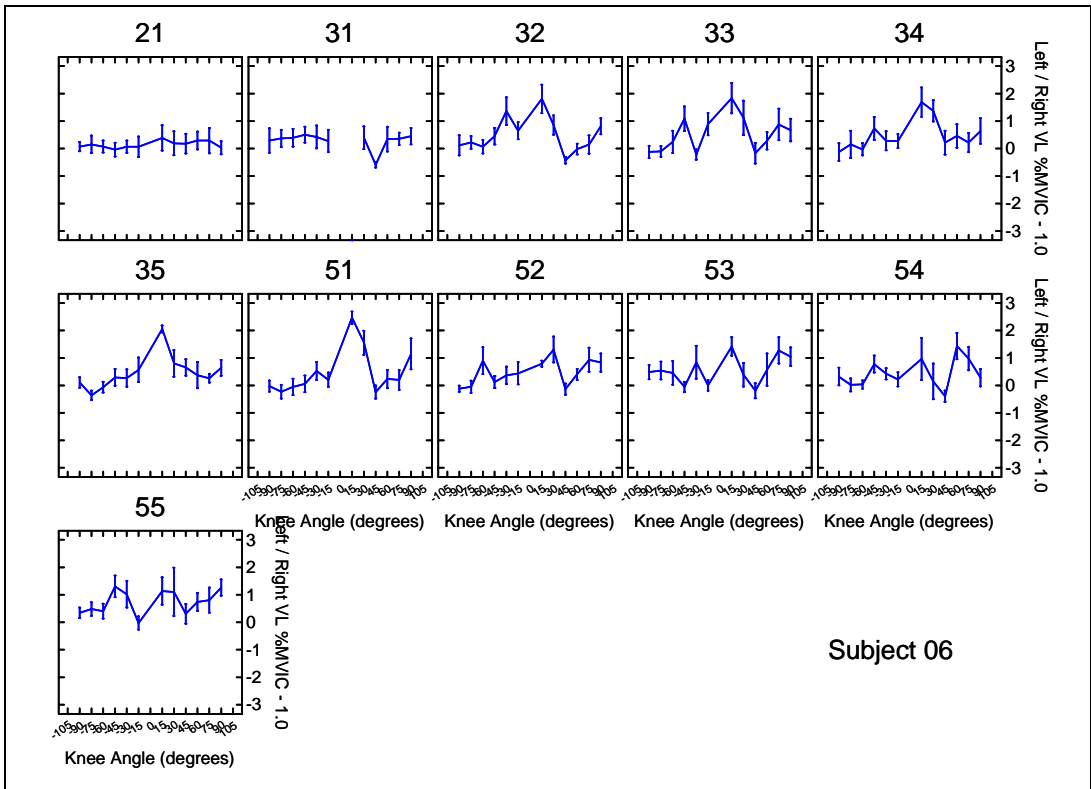
Vastus Lateralis EMG

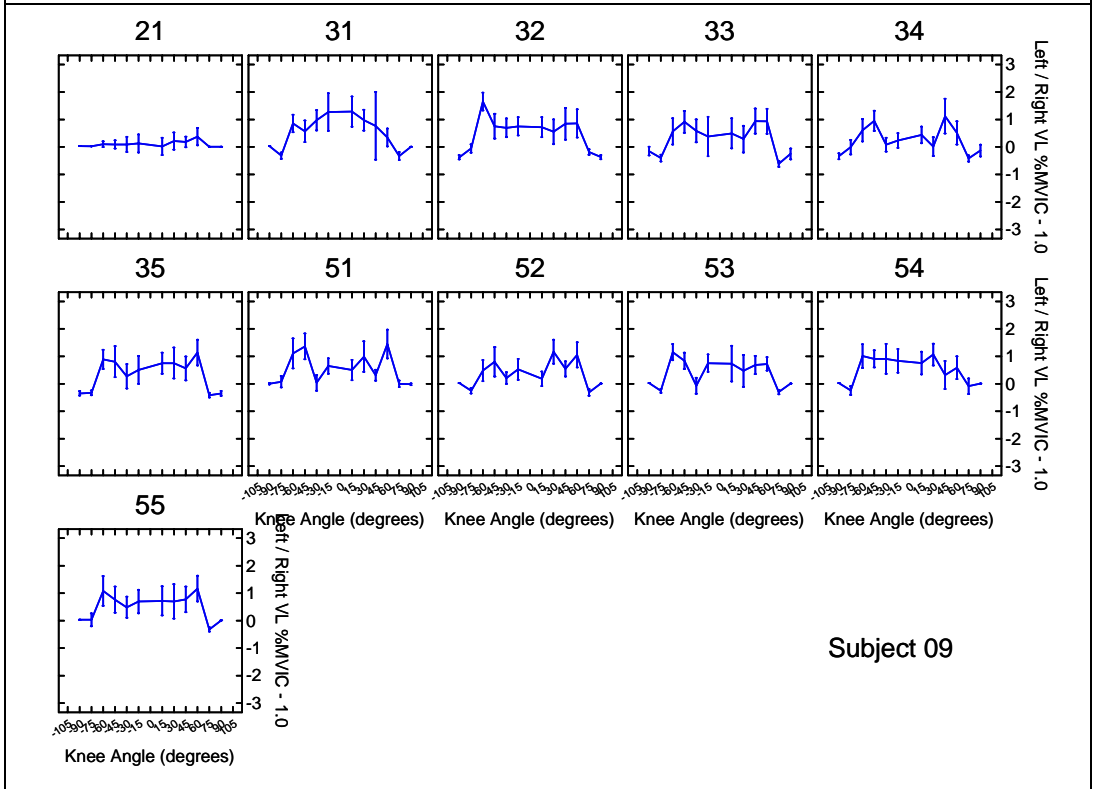
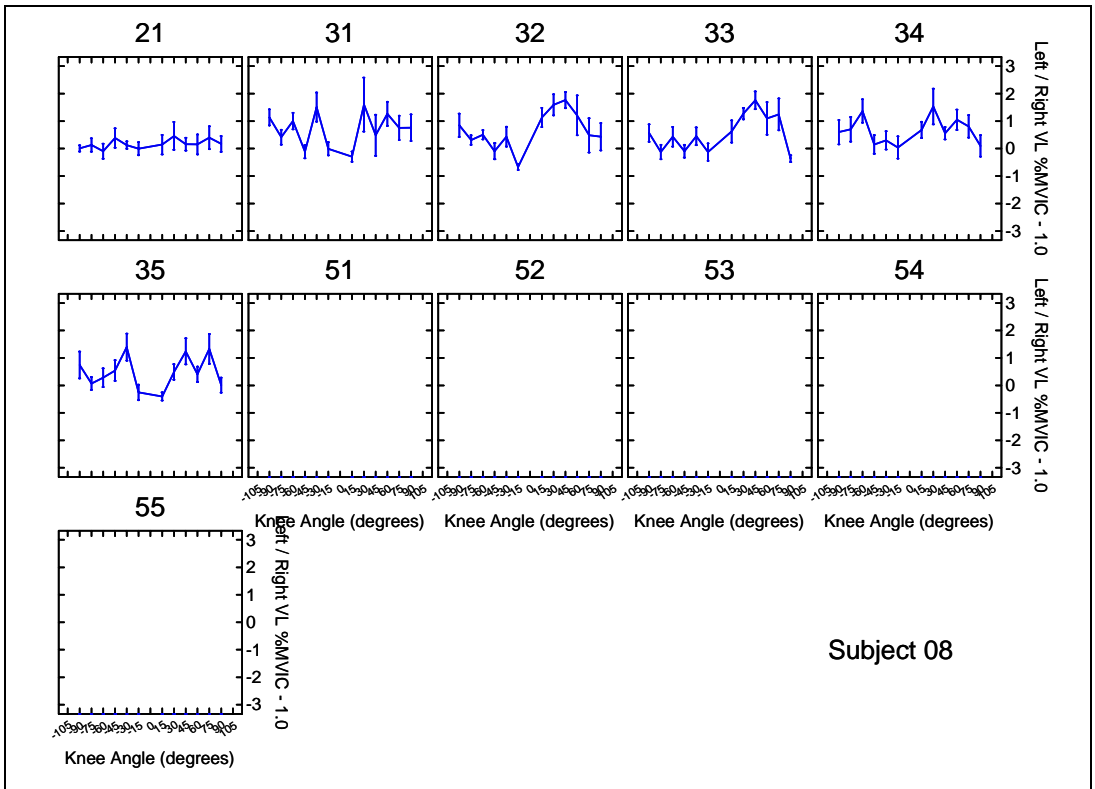
The left divided by right vastus lateralis %MVIC muscle activity minus one (Left / Right - 1.0) at several knee angles for each subject. The numbers on the top of the boxes are the Phase and Set. For example, 31 is Phase 3 (23-RPM), first set of eight repetitions. The eight repetitions within each set are averaged together. Mean +/- SEM. Note: The knee angles are the same as in the body of this thesis, however, the ordering of them is slightly different: 0-degree knee angle is in the middle of the graph and full extension (i.e., 90-degrees) is at the edges.

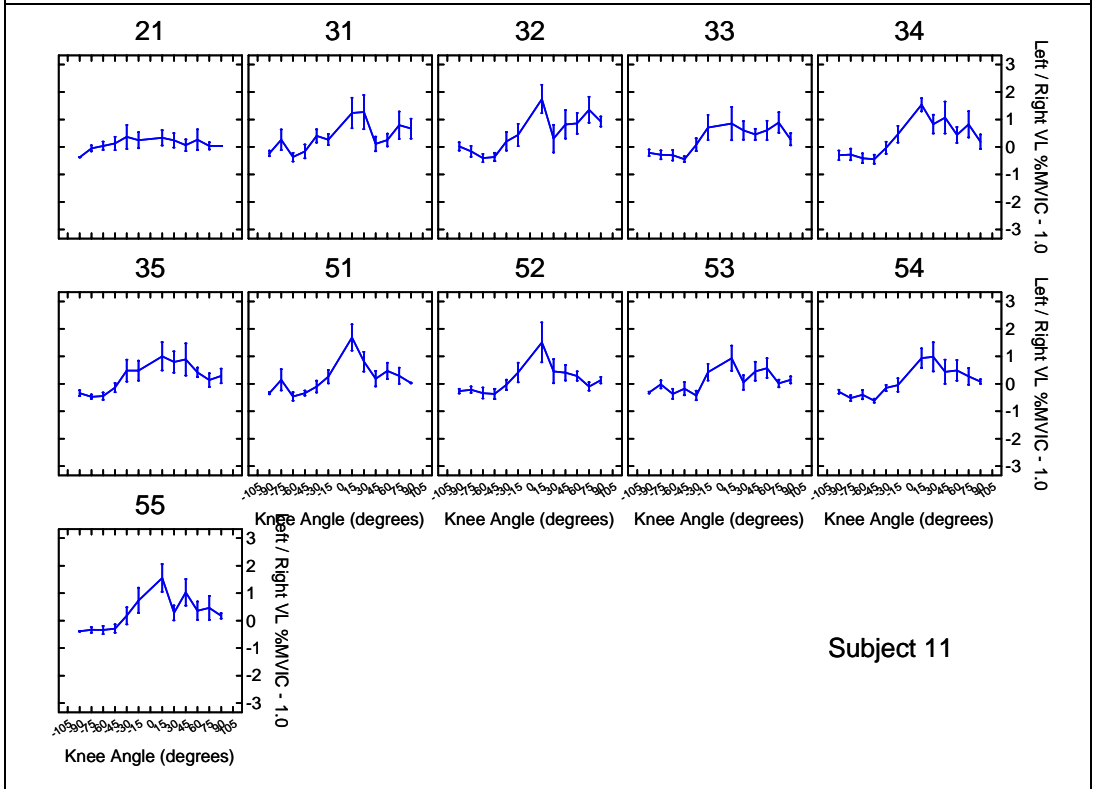
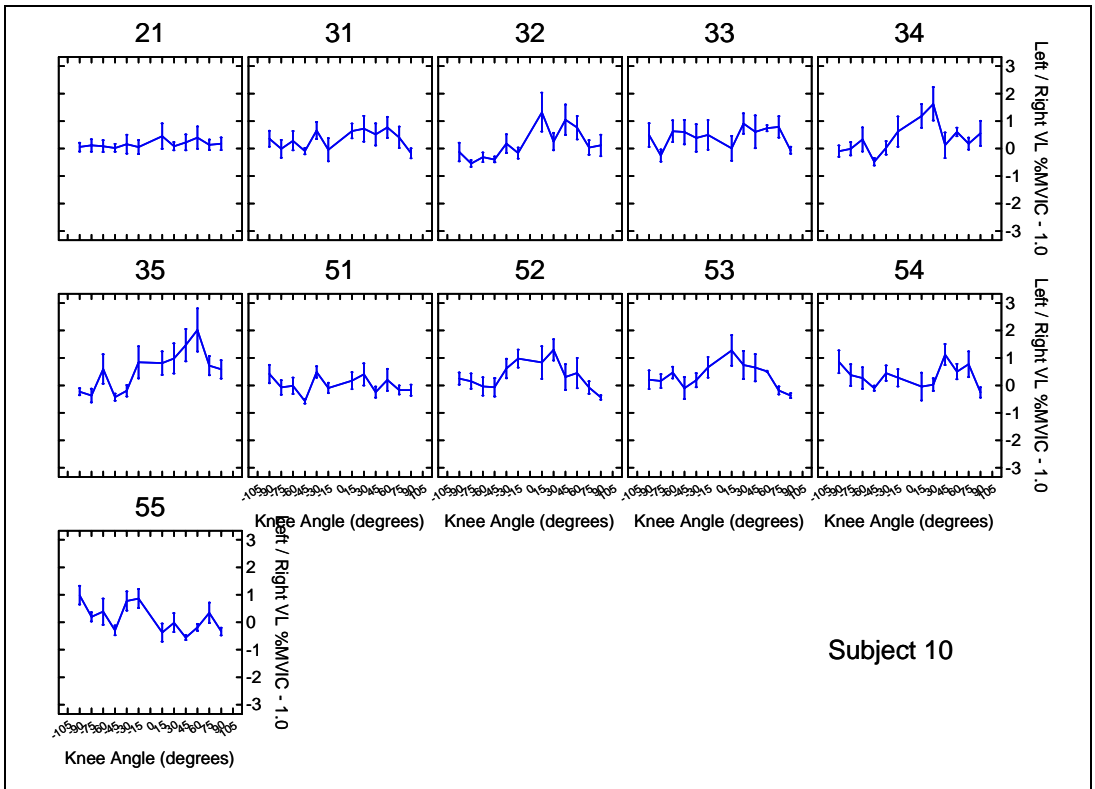


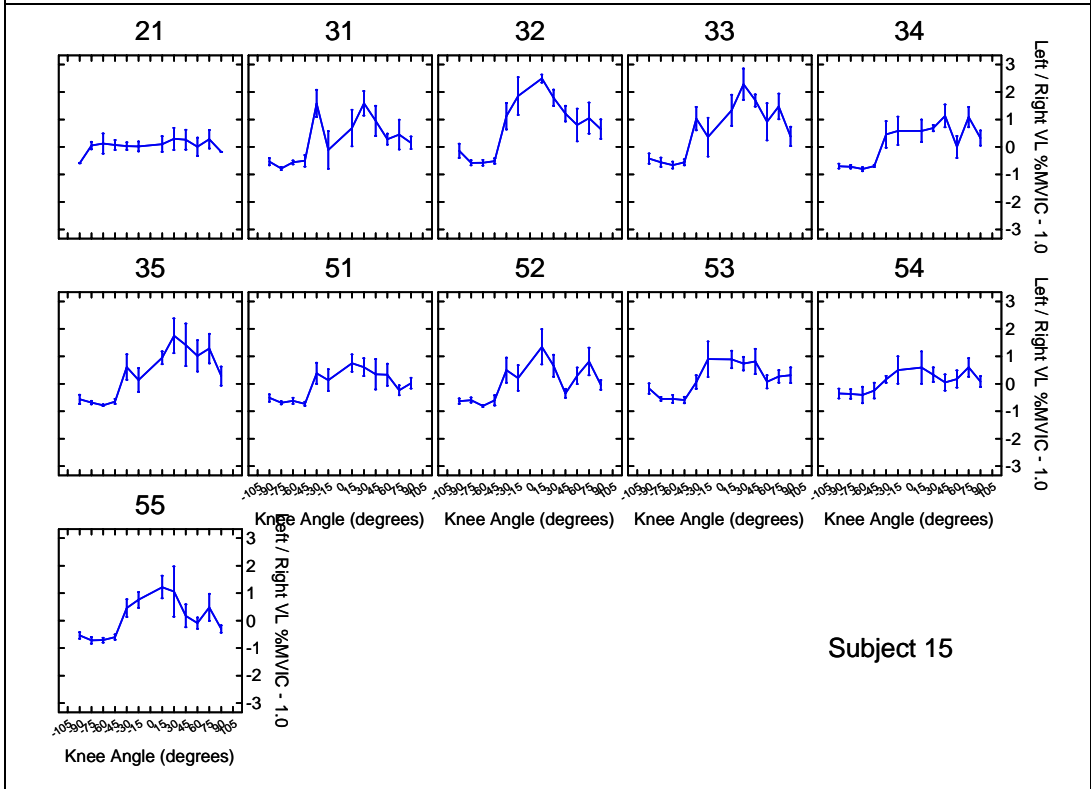
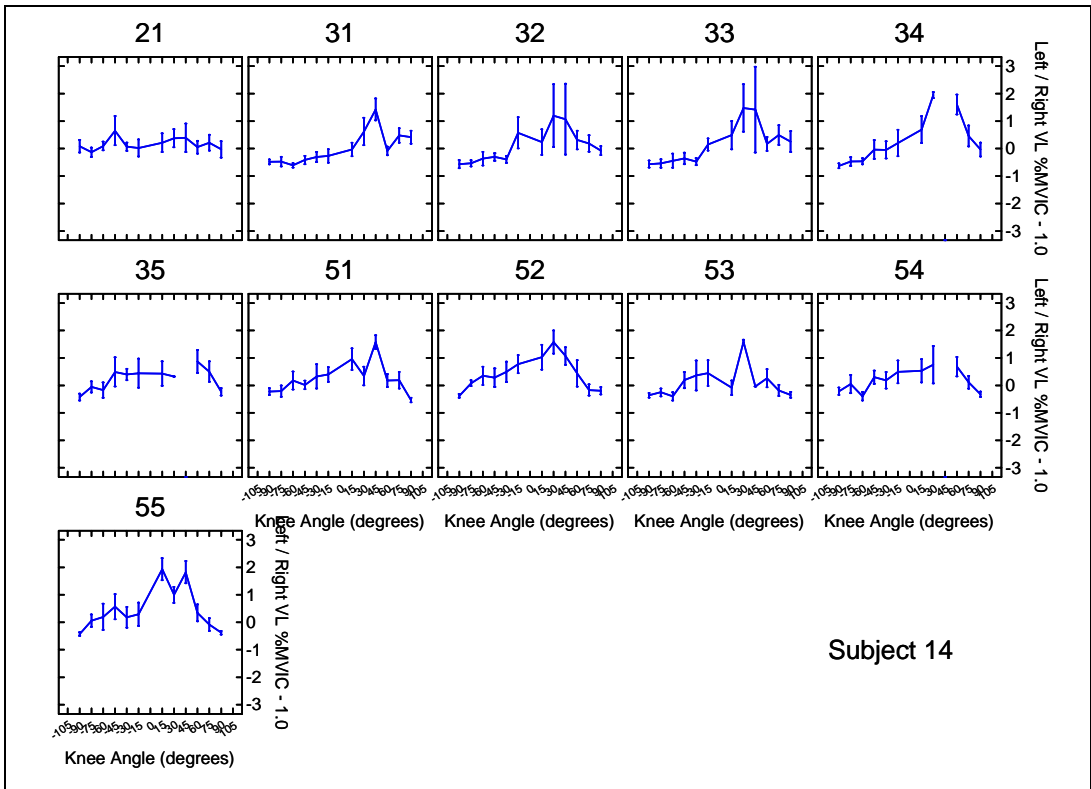






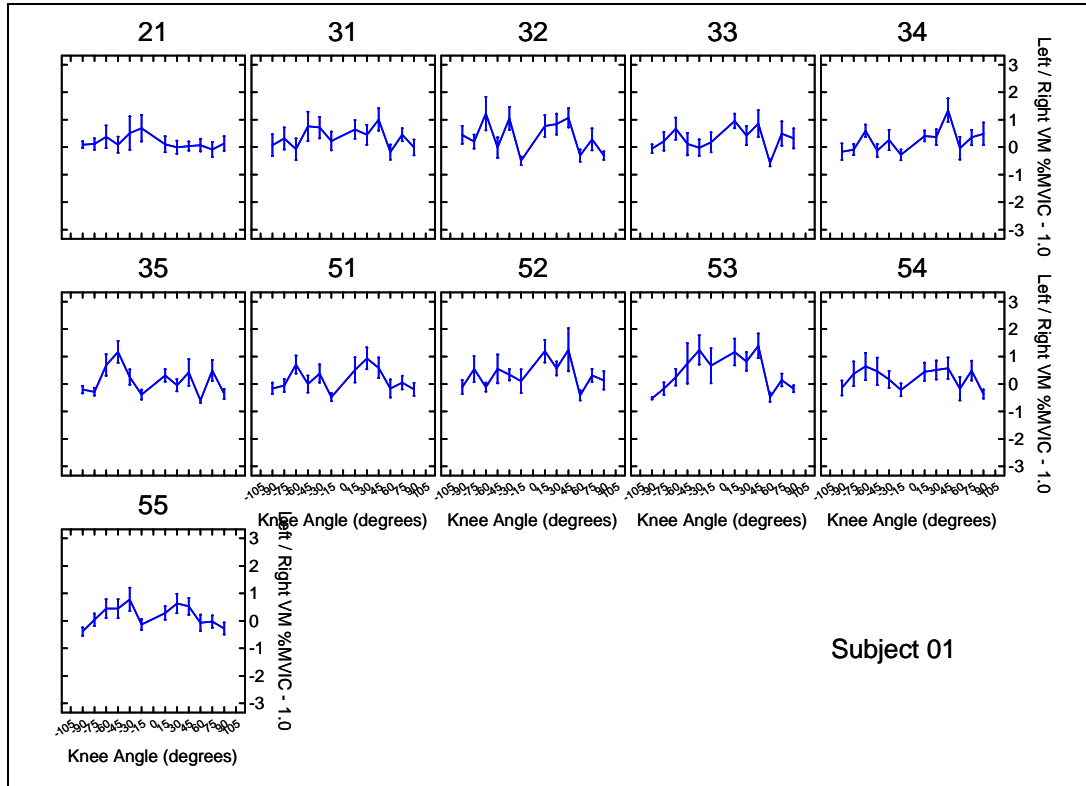


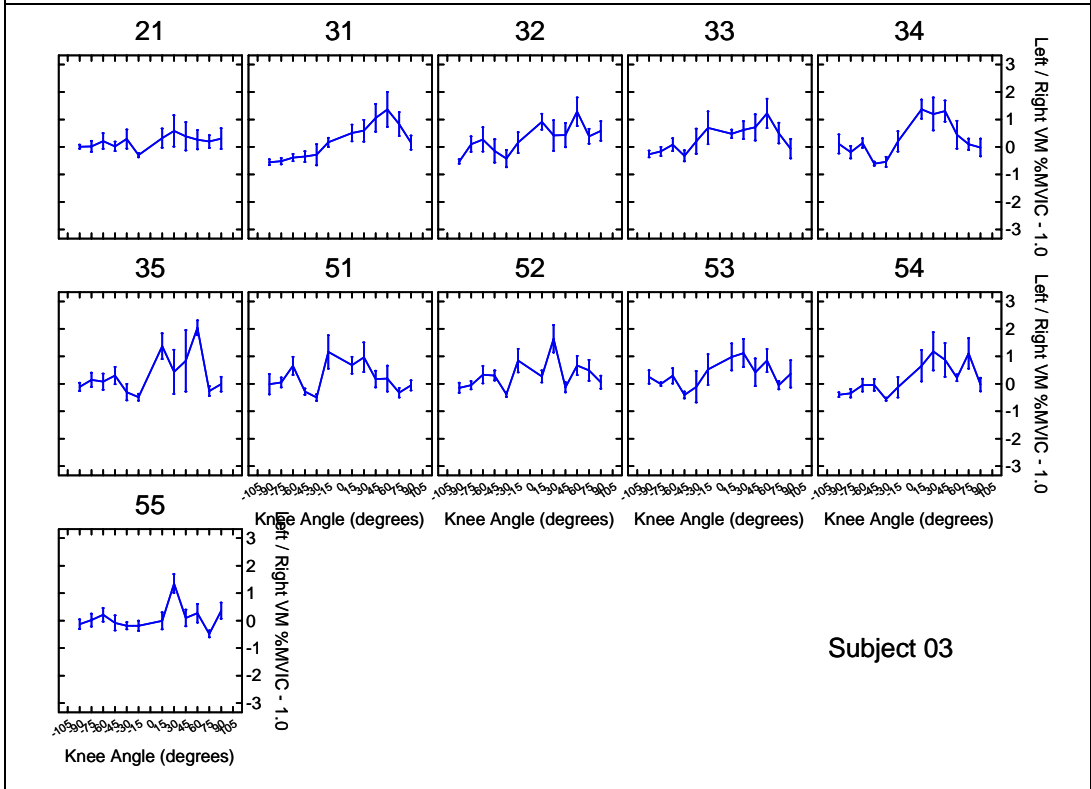
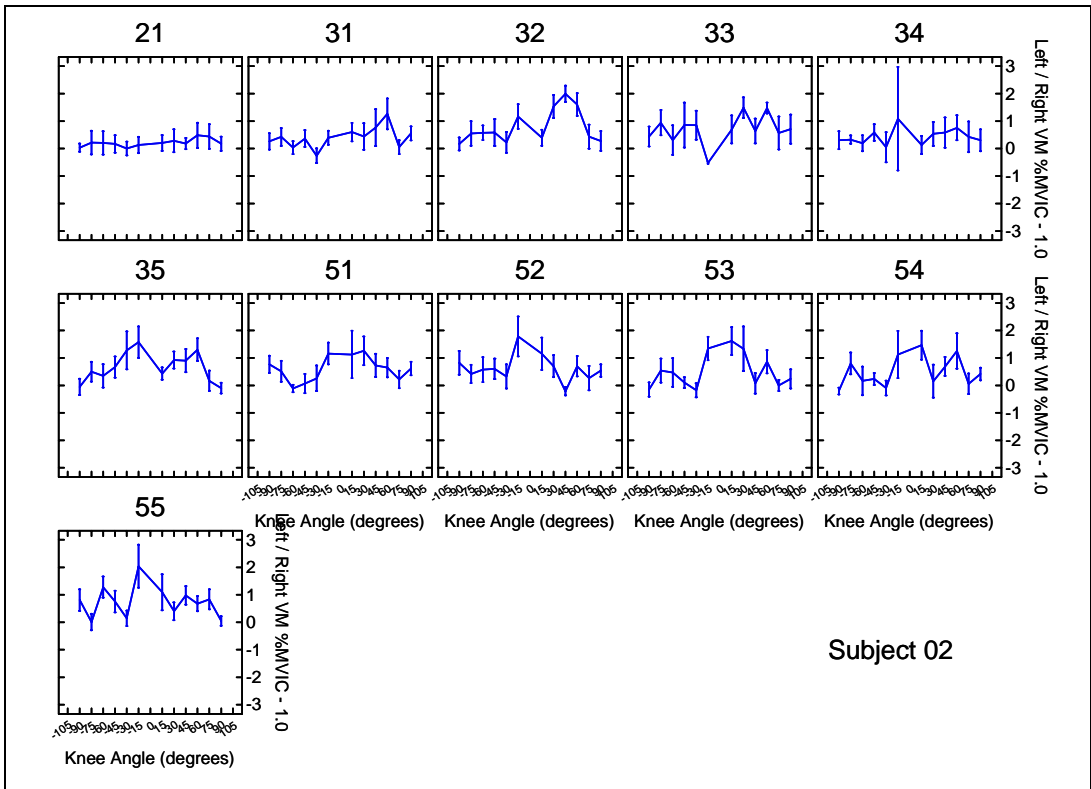


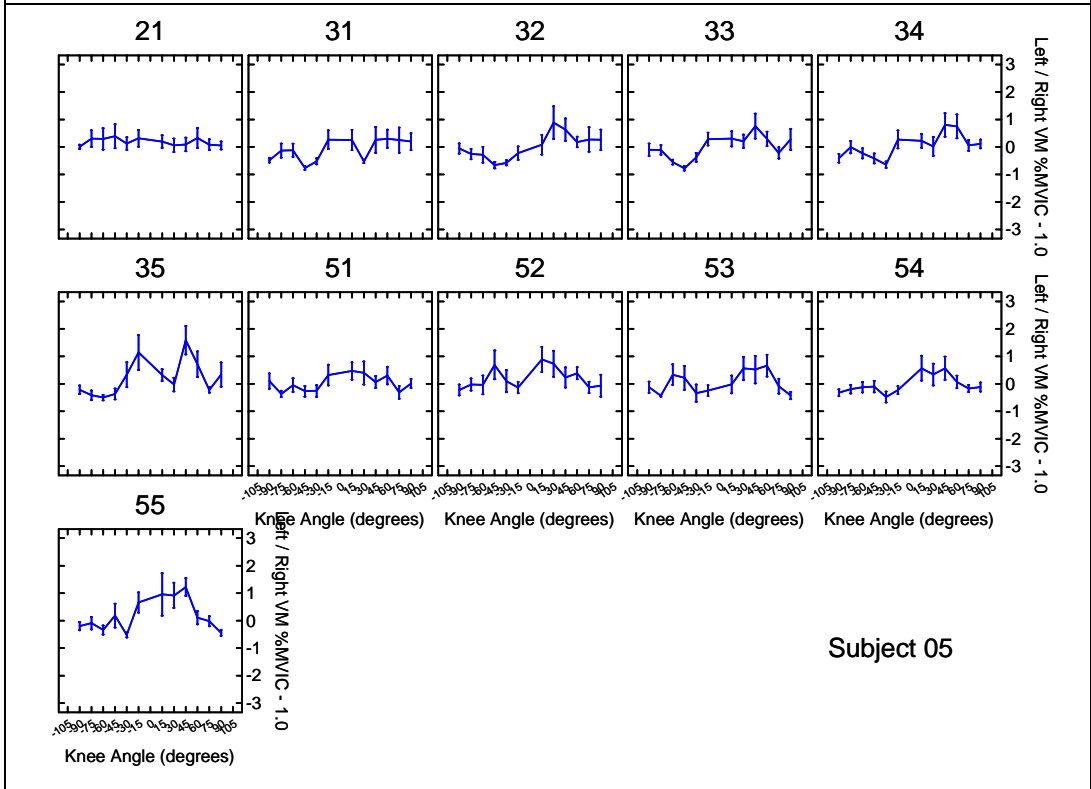
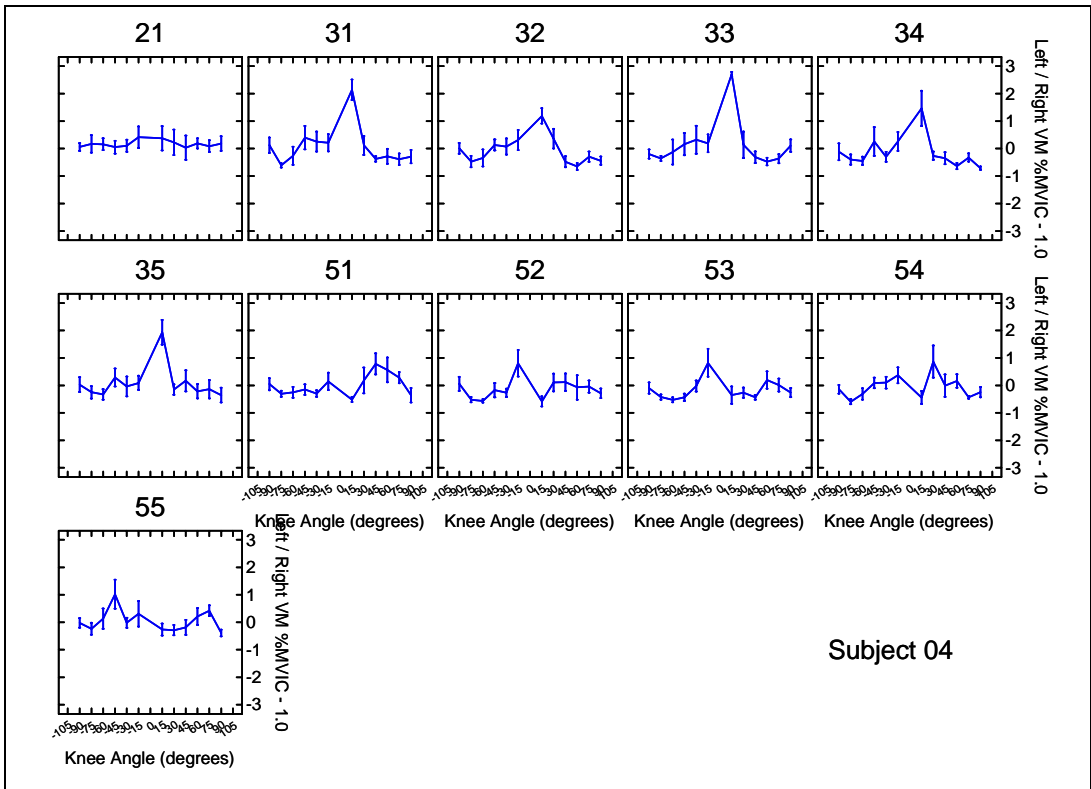


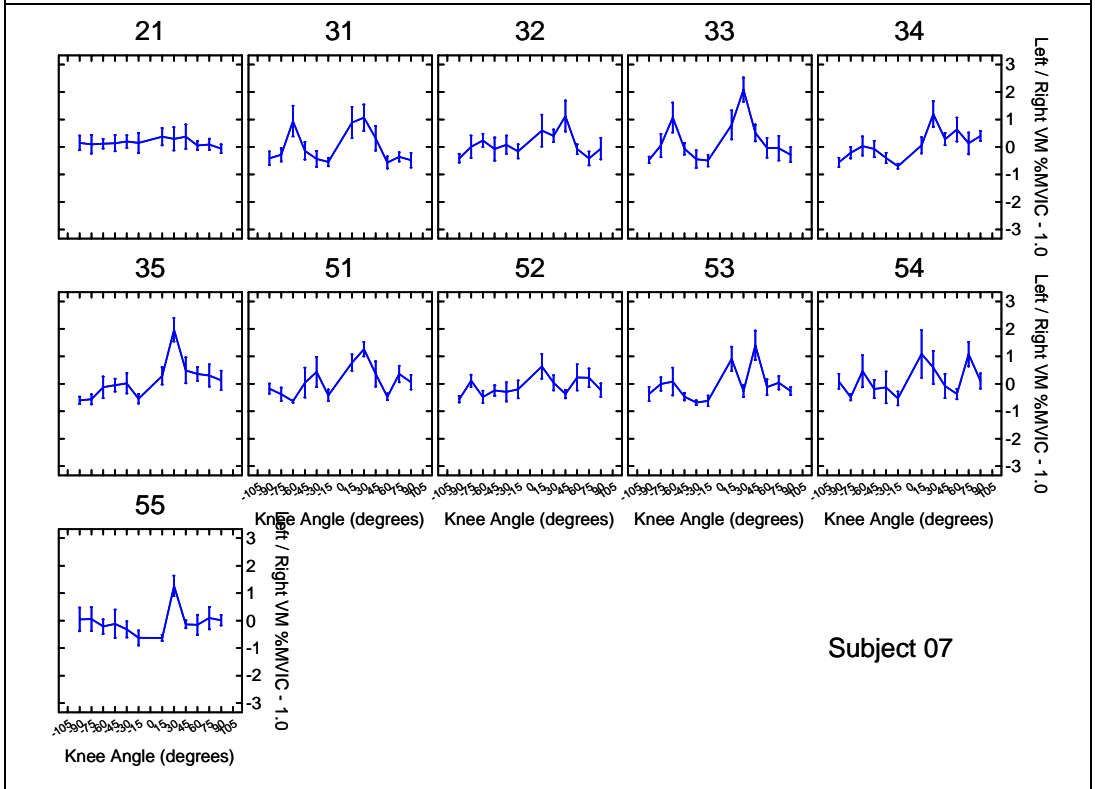
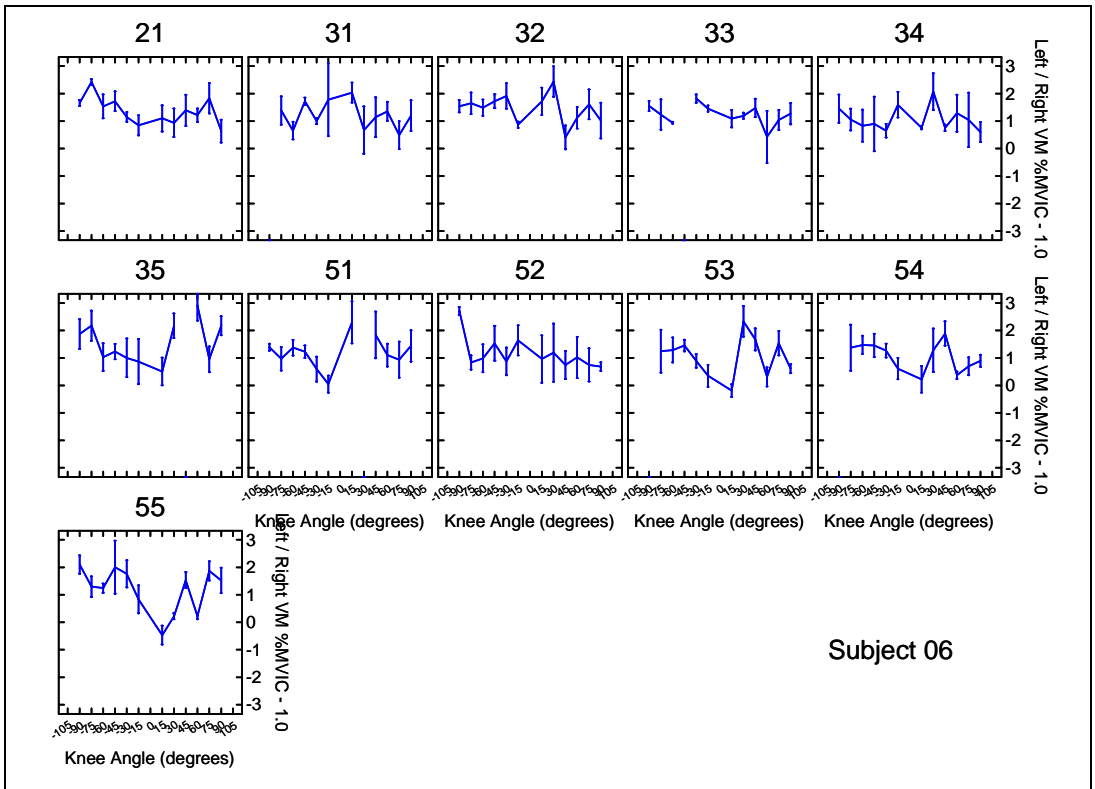
Vastus Medialis EMG

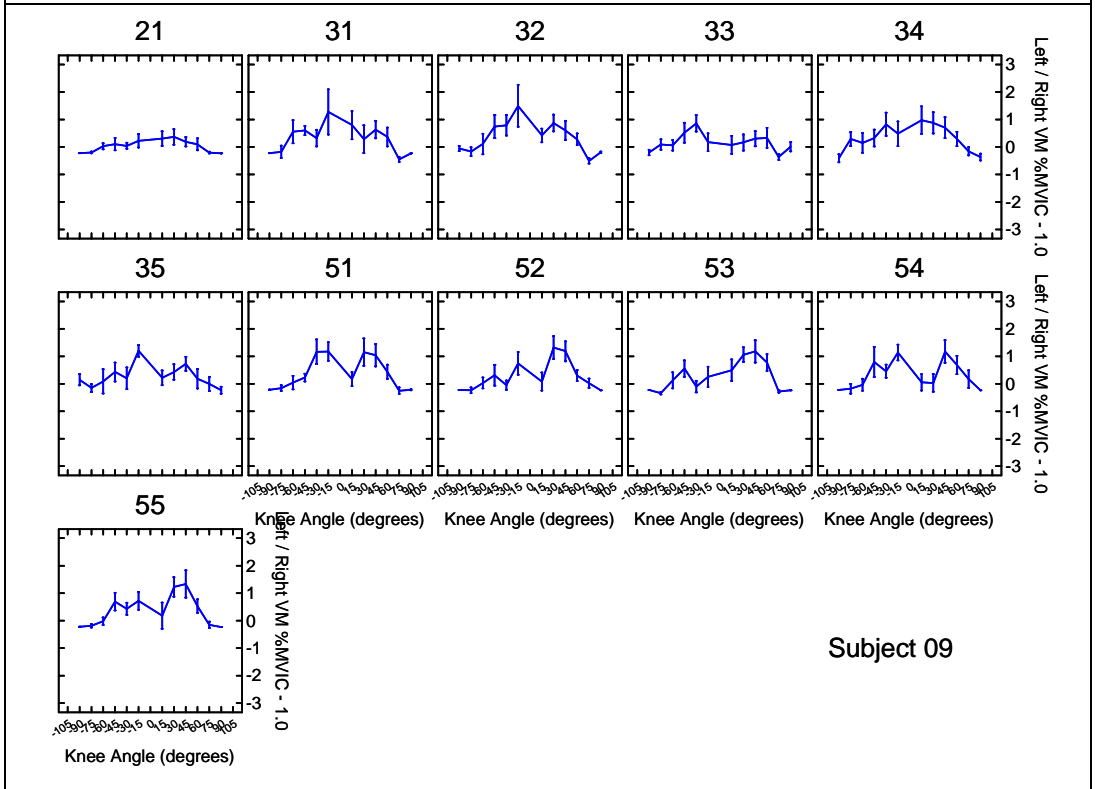
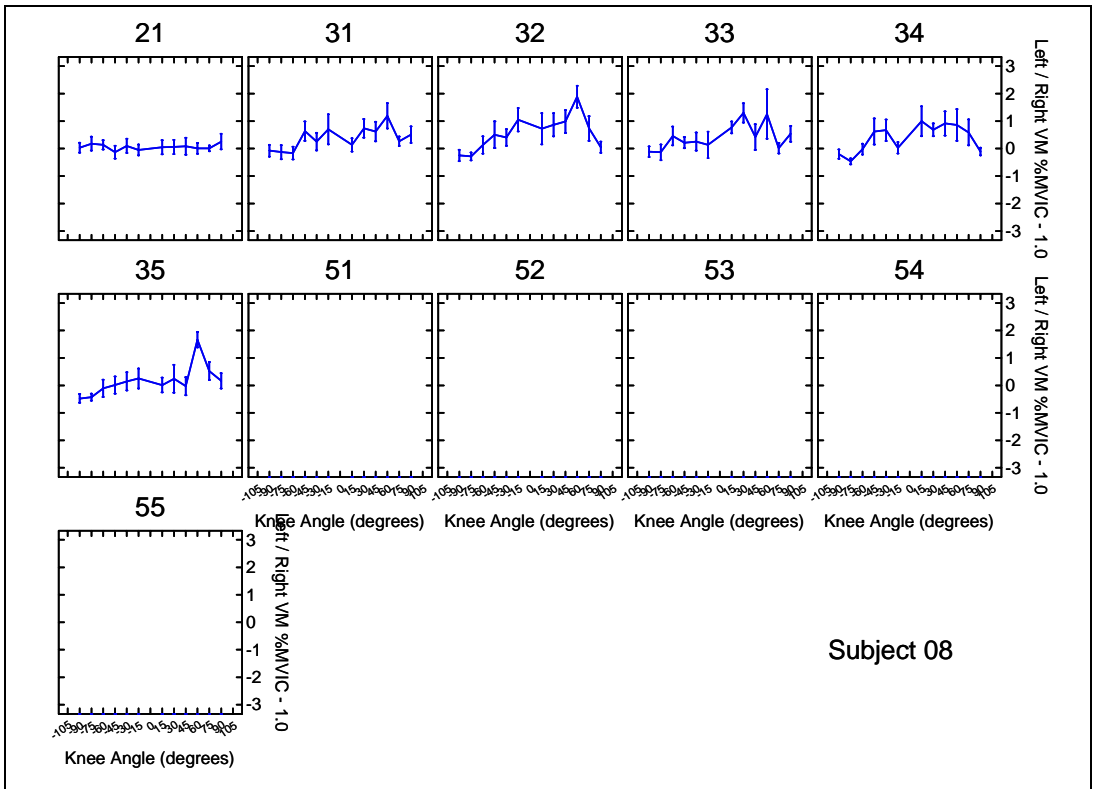
The left divided by right vastus medialis %MVIC muscle activity minus one (Left / Right – 1.0) at several knee angles for each subject. The numbers on the top of the boxes are the Phase and Set. For example, 31 is Phase 3 (23-RPM), first set of eight repetitions. The eight repetitions within each set are averaged together. Mean +/- SEM. Note: The knee angles are the same as in the body of this thesis, however, the ordering of them is slightly different: 0-degree knee angle is in the middle of the graph and full extension (i.e., 90-degrees) is at the edges.

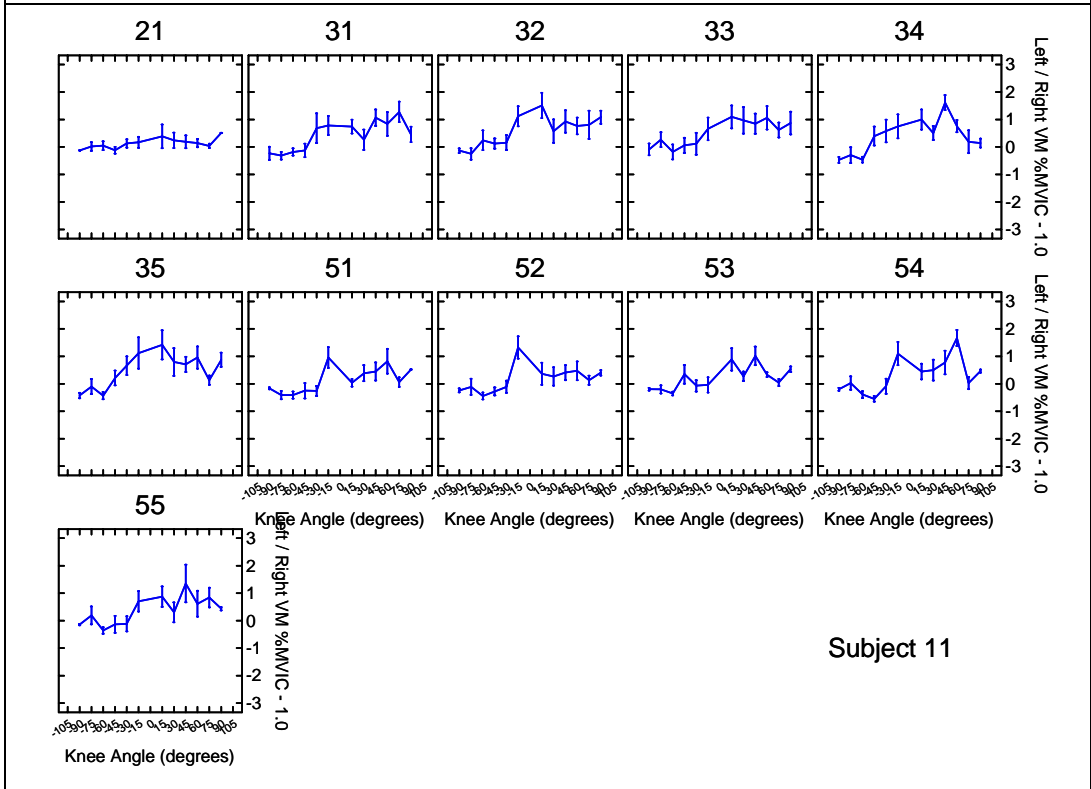
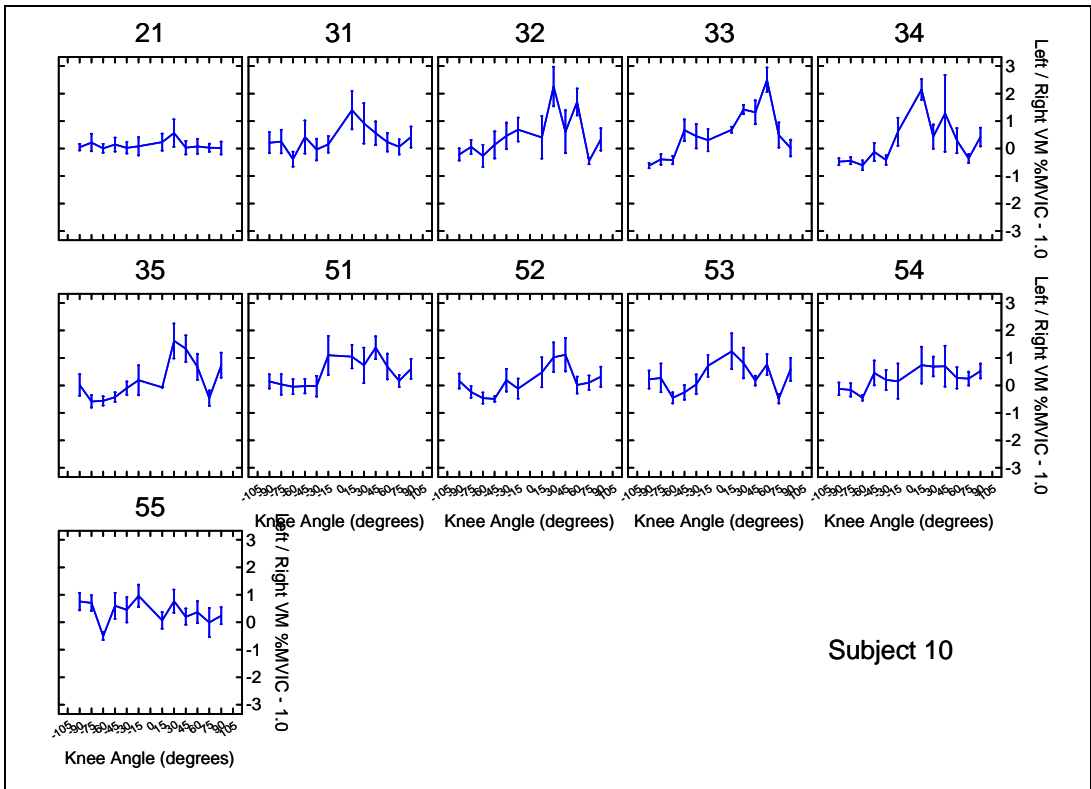


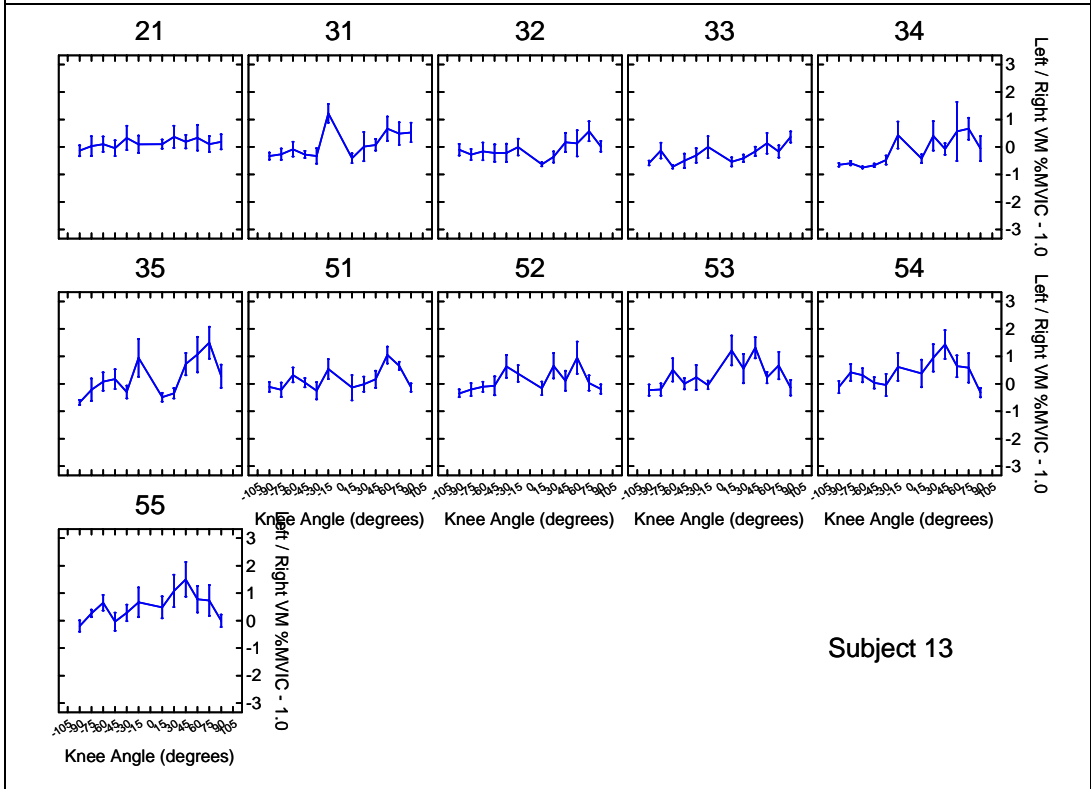
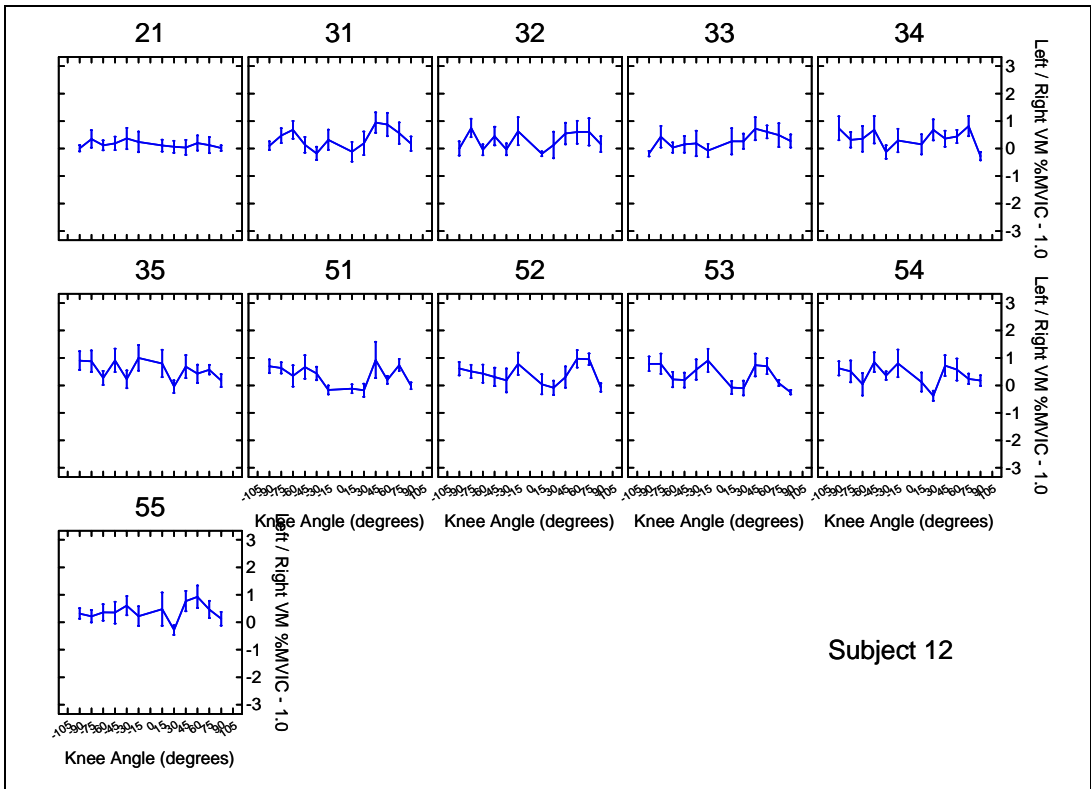


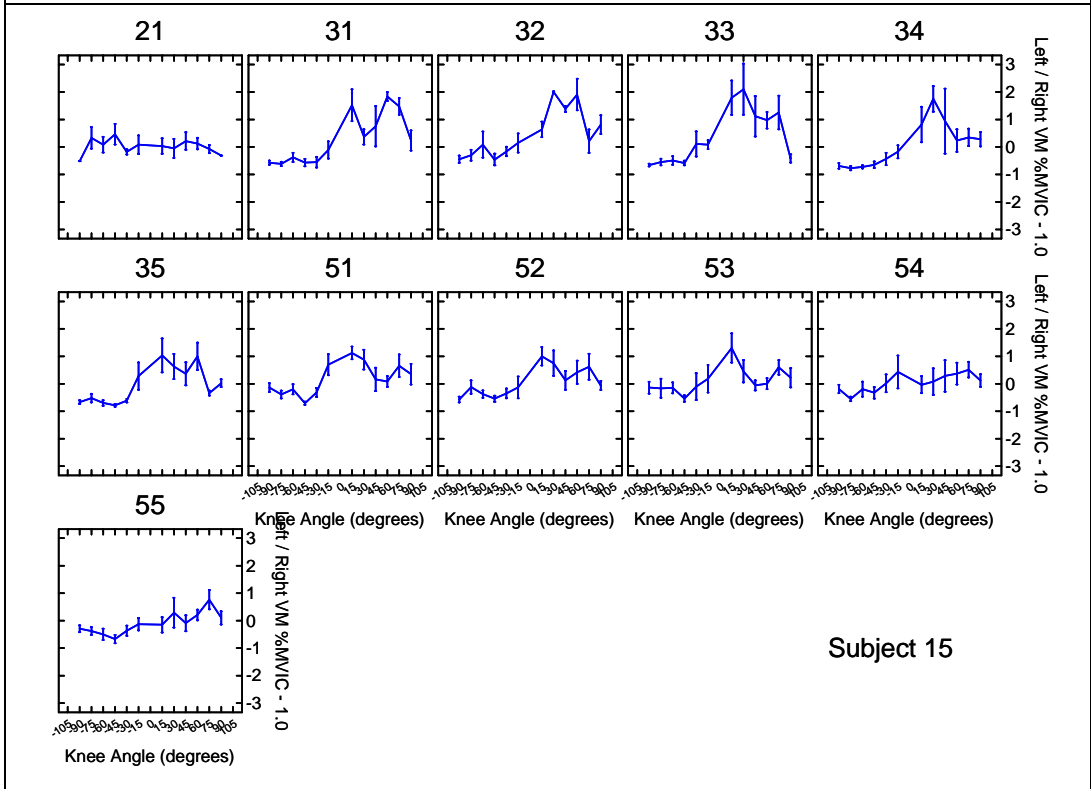
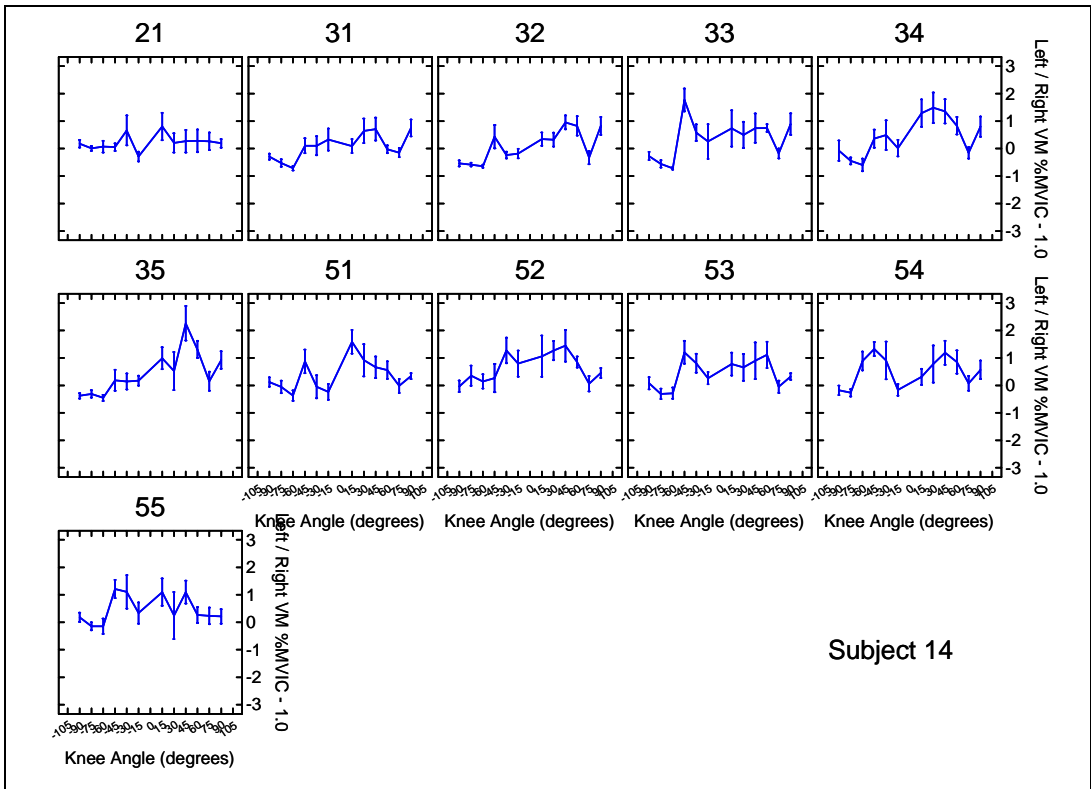






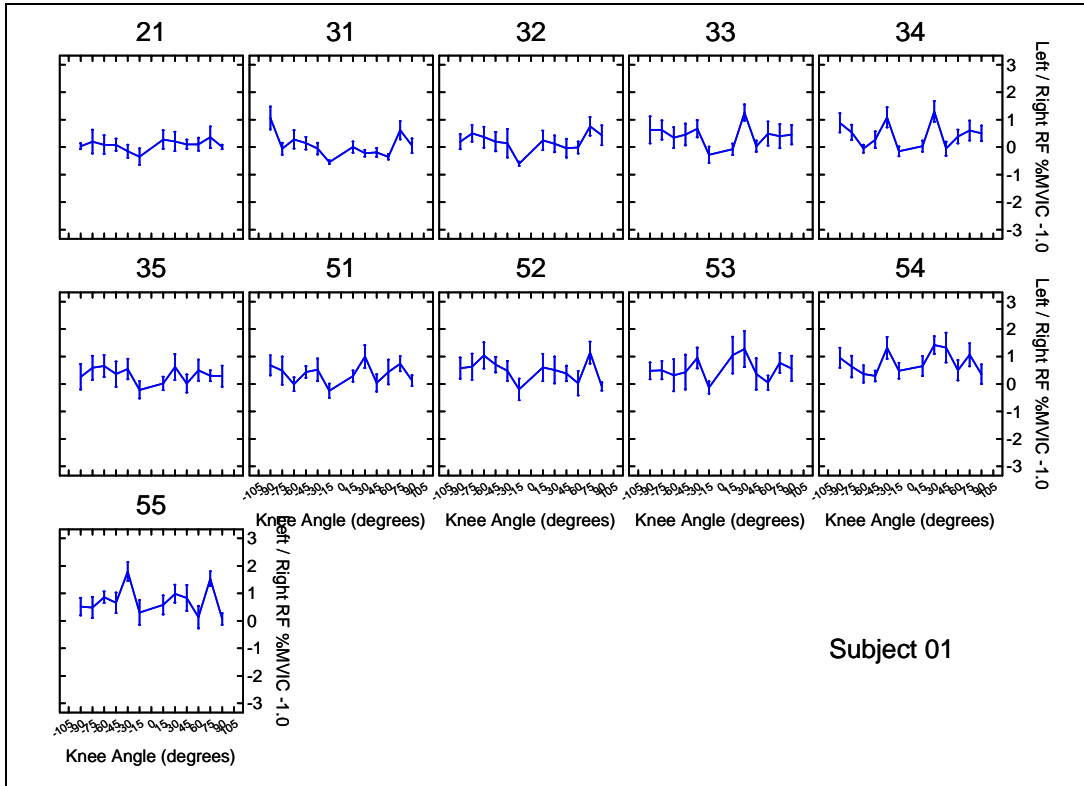


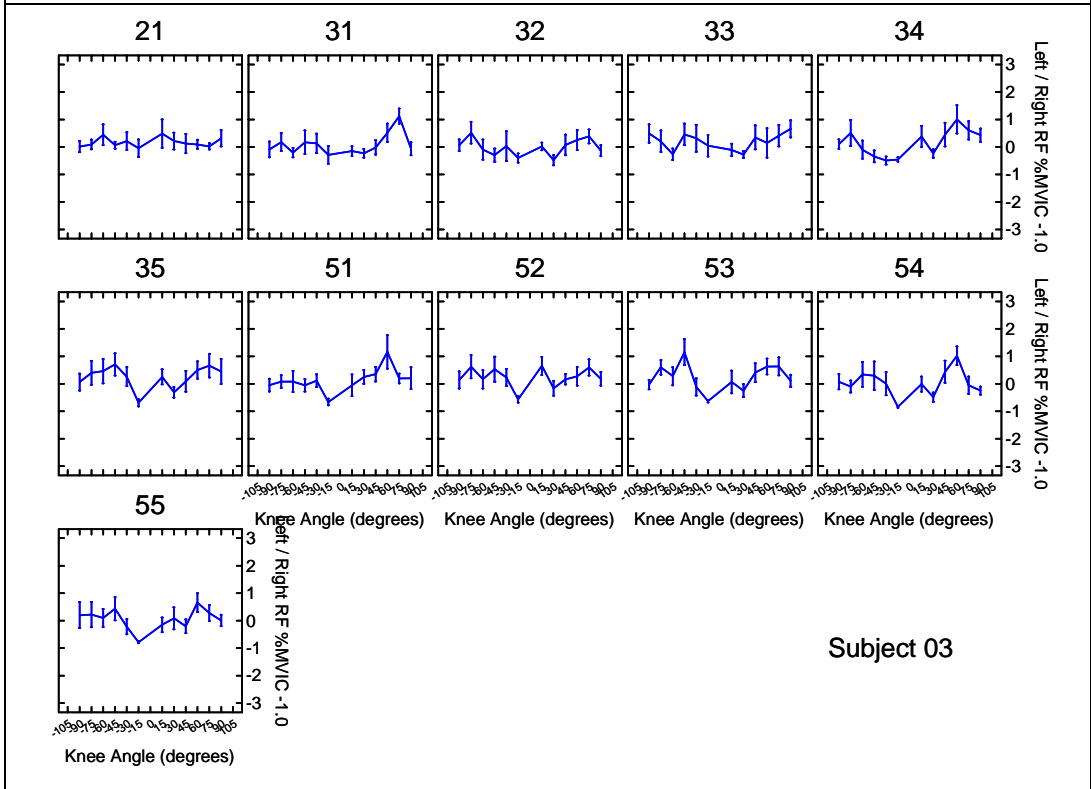
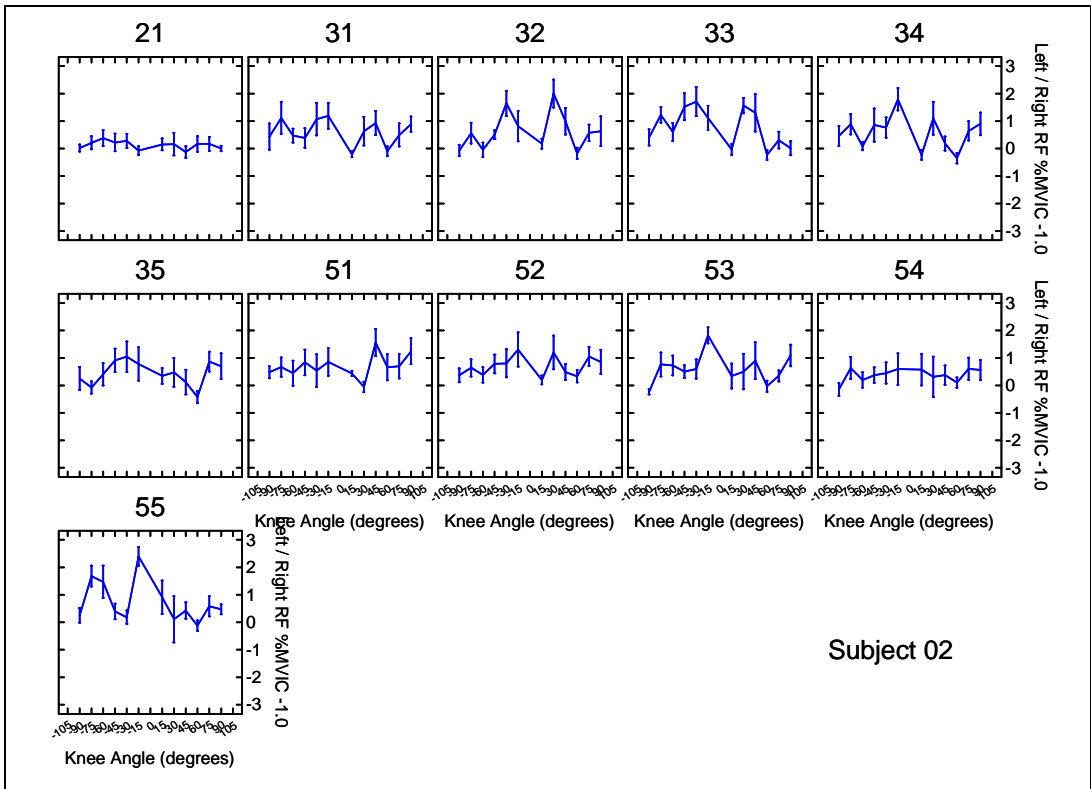


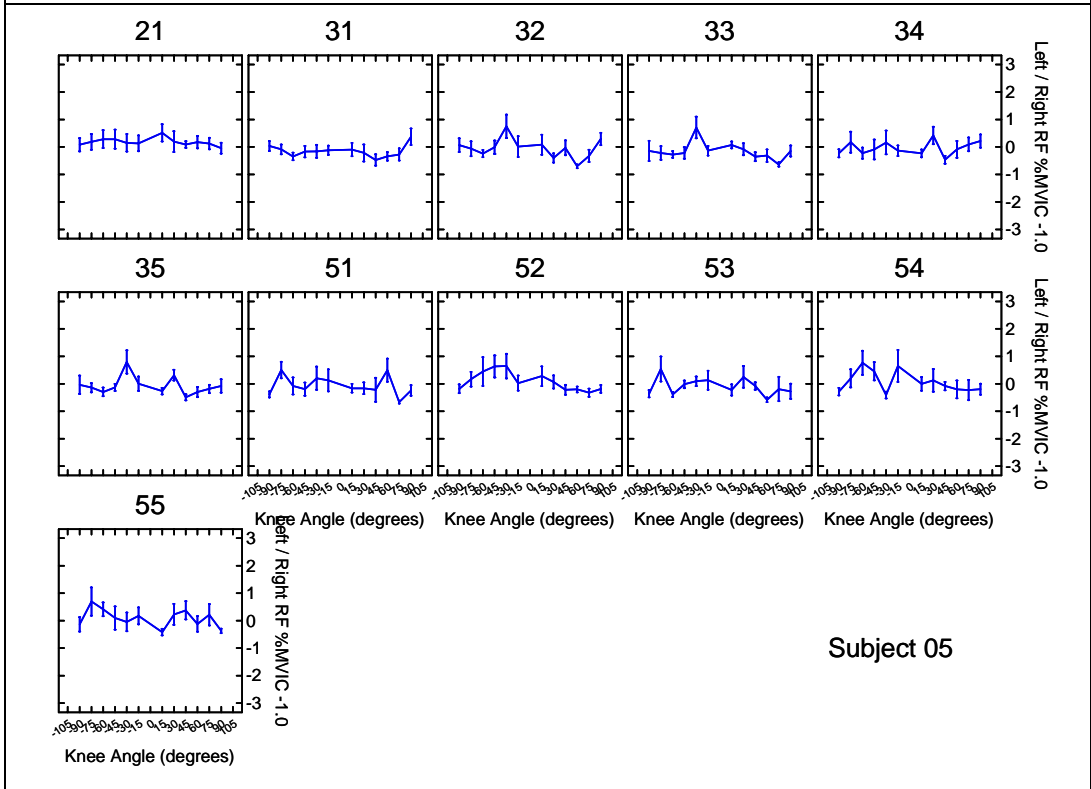
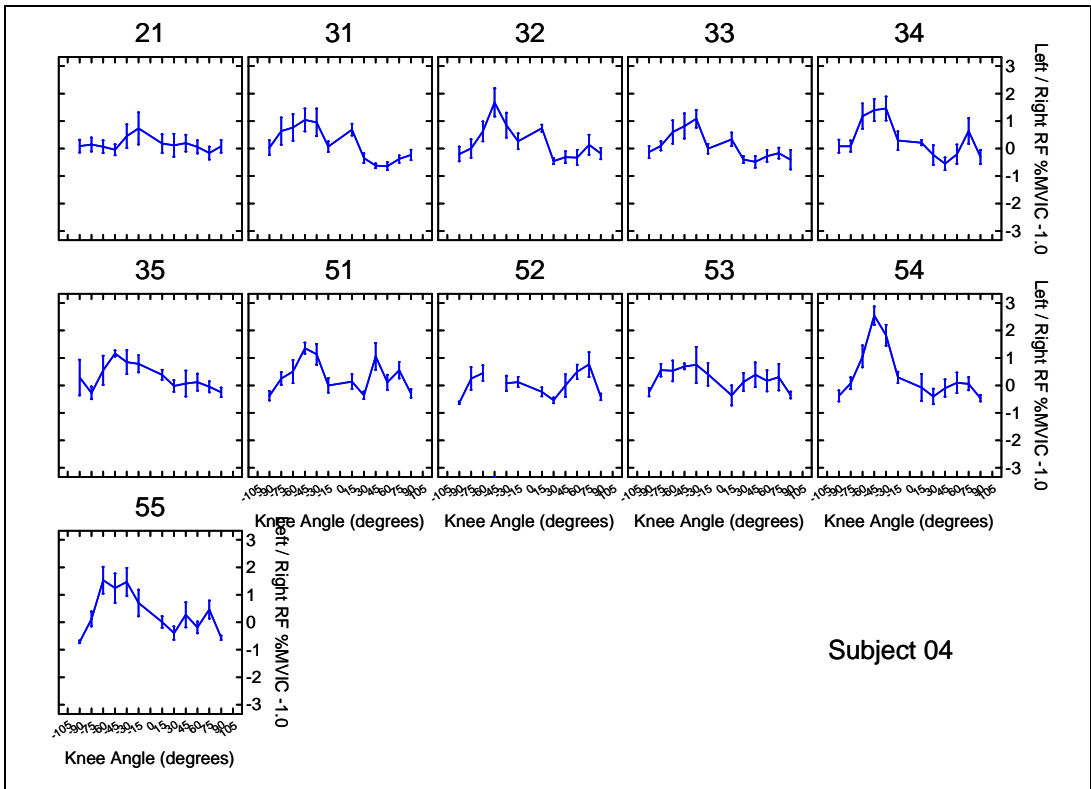


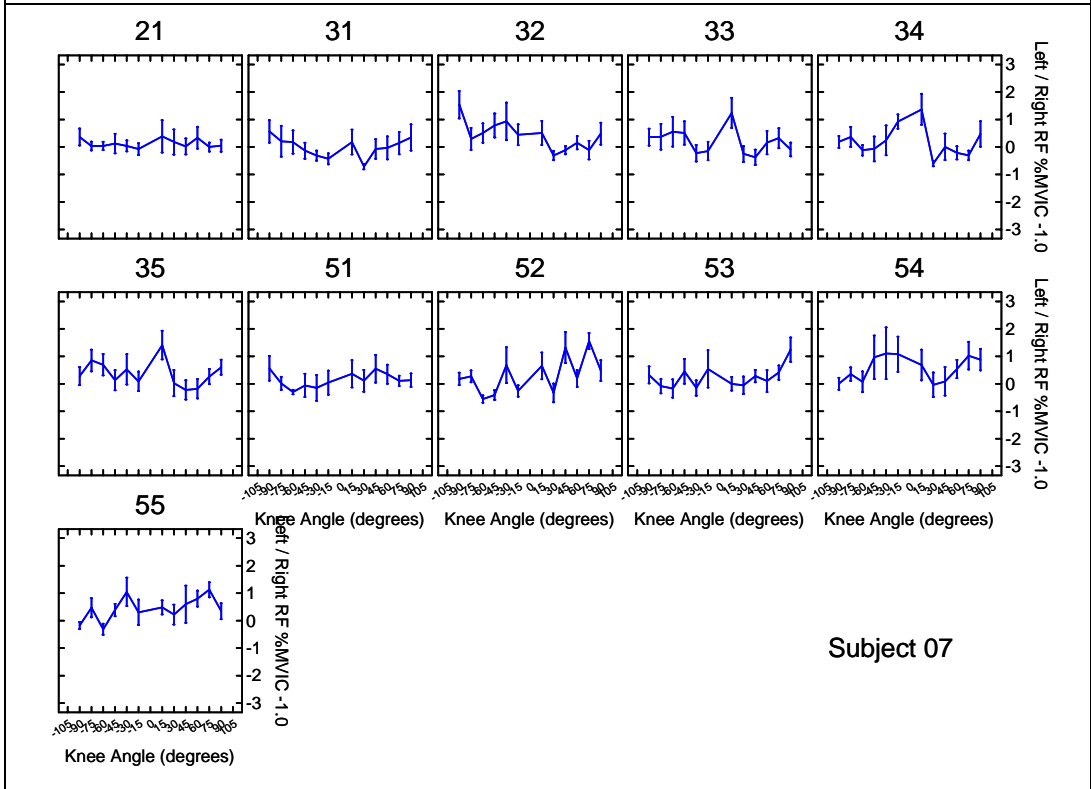
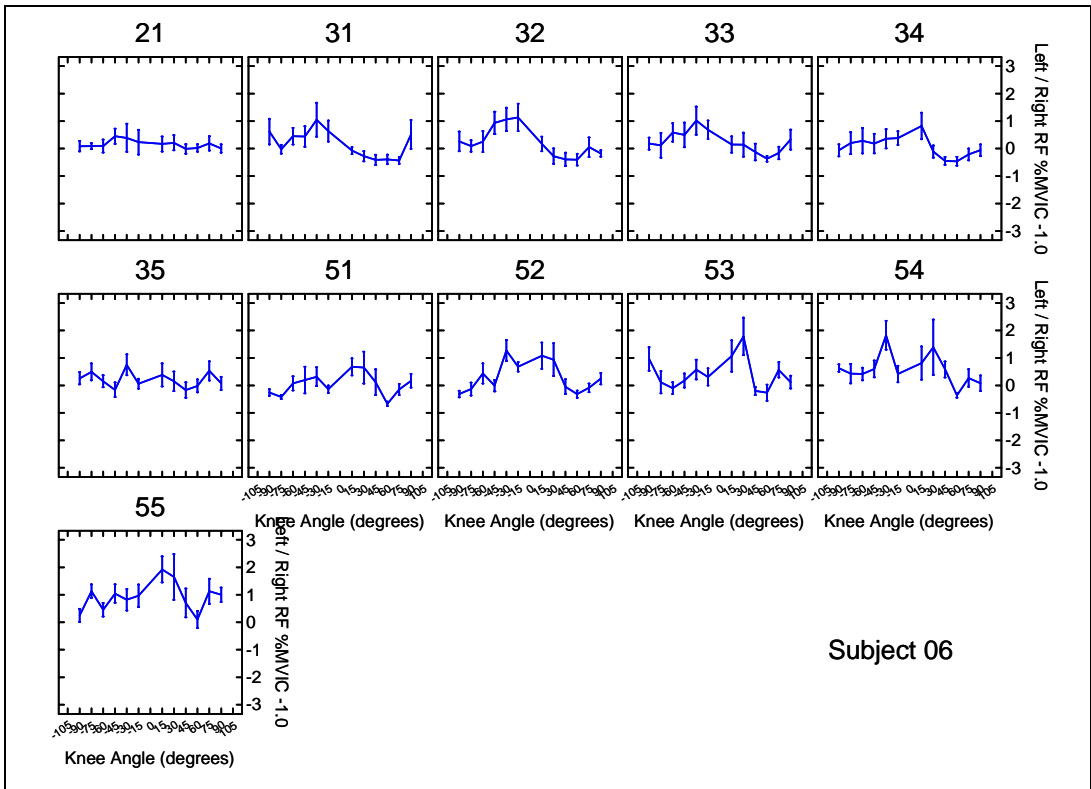
Rectus Femoris EMG

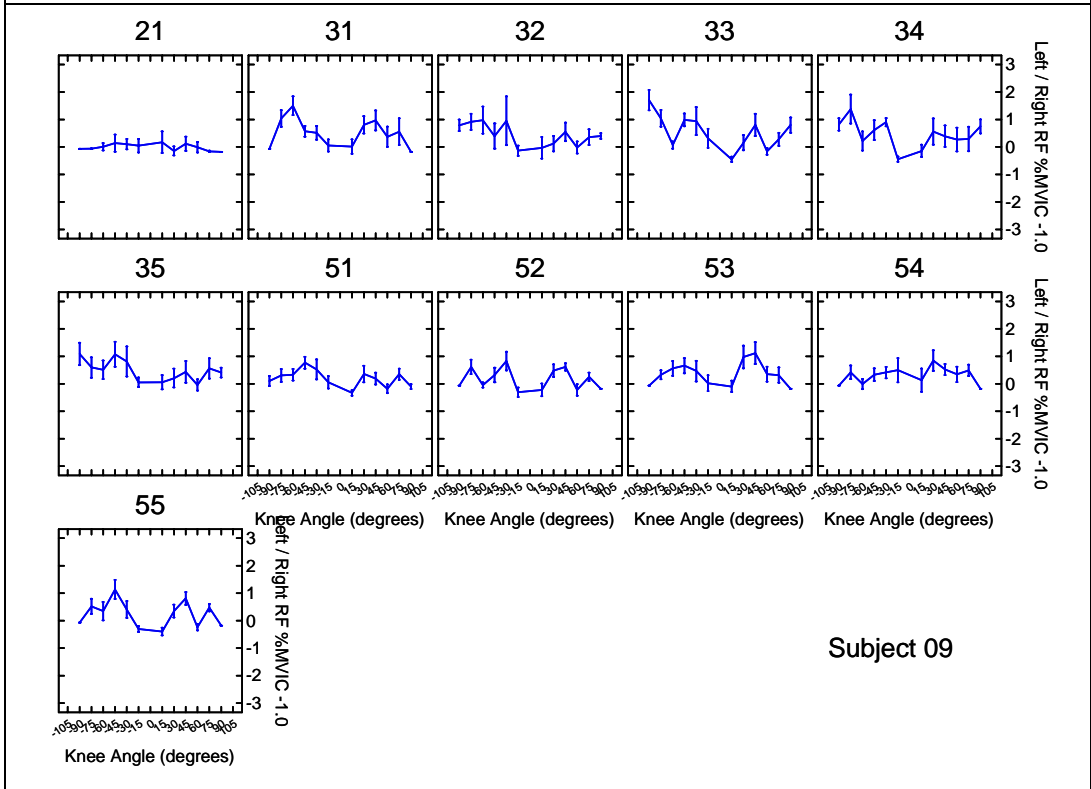
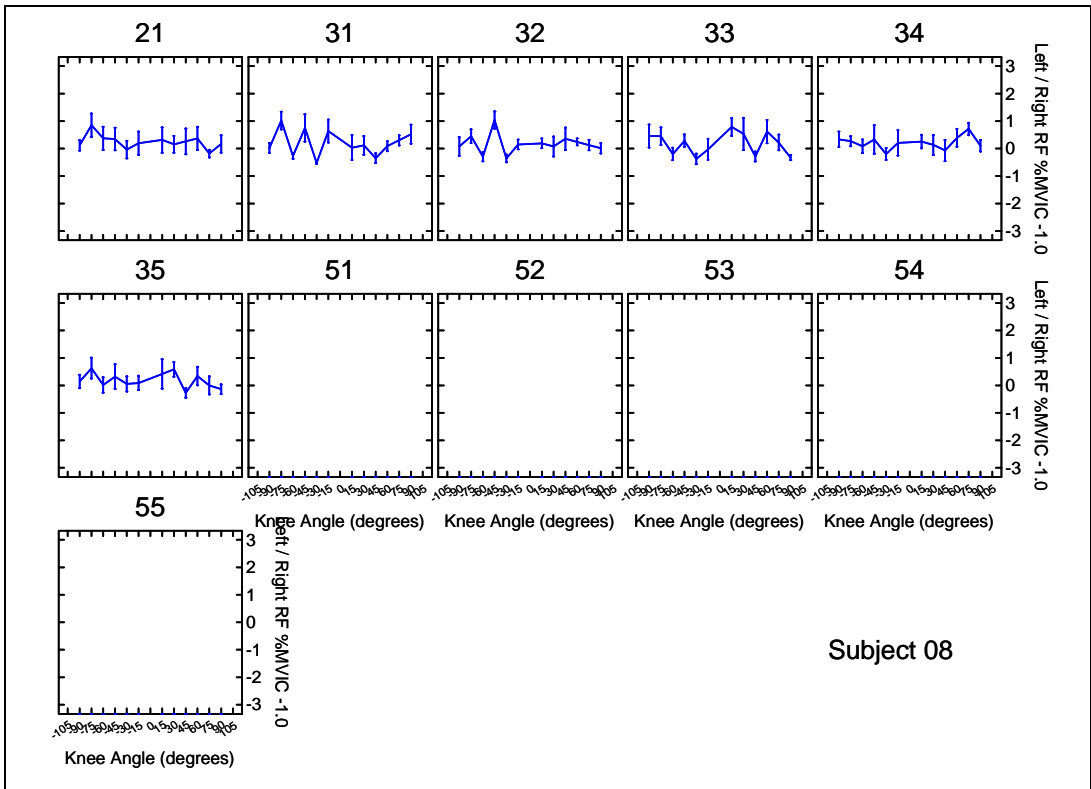
The left divided by right rectus femoris %MVIC muscle activity minus one (Left / Right – 1.0) at several knee angles for each subject. The numbers on the top of the boxes are the Phase and Set. For example, 31 is Phase 3 (23-RPM), first set of eight repetitions. The eight repetitions within each set are averaged together. Mean +/- SEM. Note: The knee angles are the same as in the body of this thesis, however, the ordering of them is slightly different: 0-degree knee angle is in the middle of the graph and full extension (i.e., 90-degrees) is at the edges.

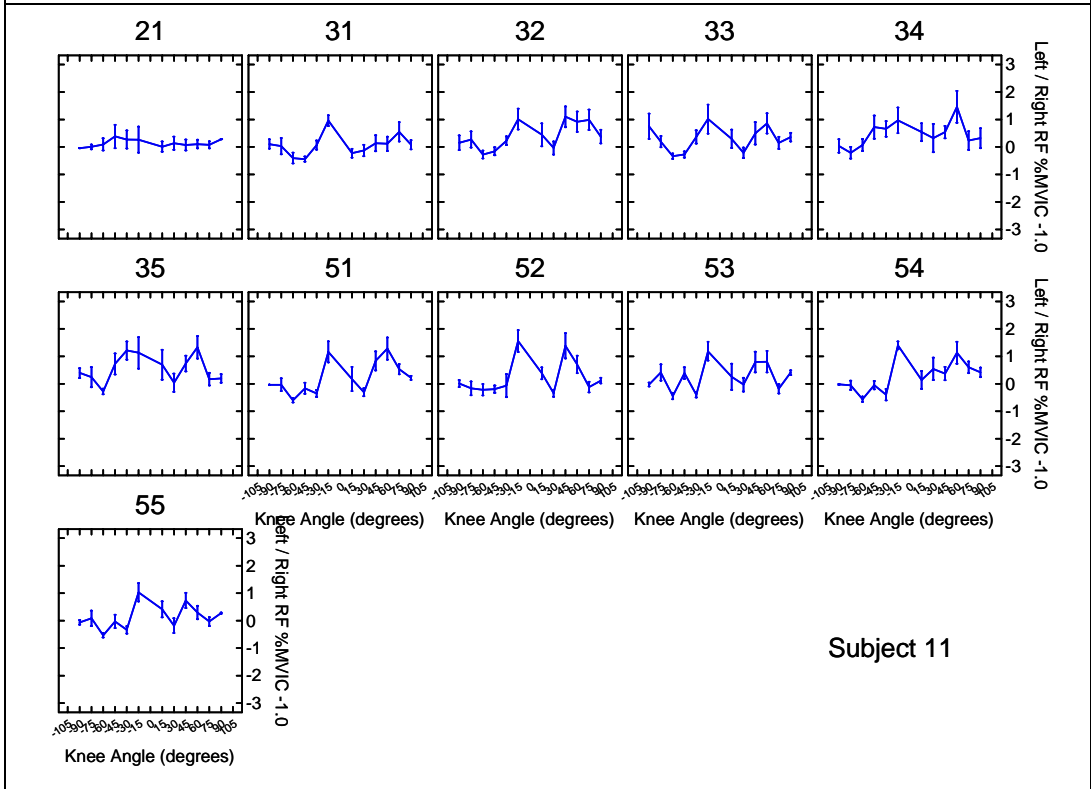
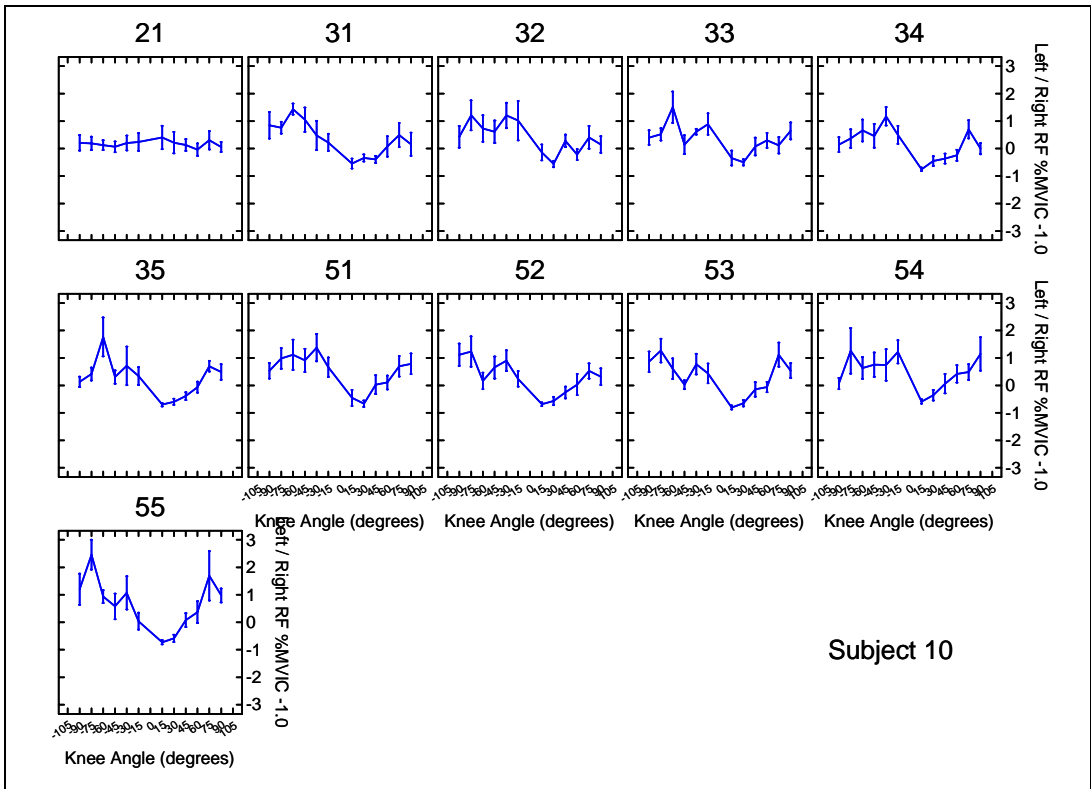


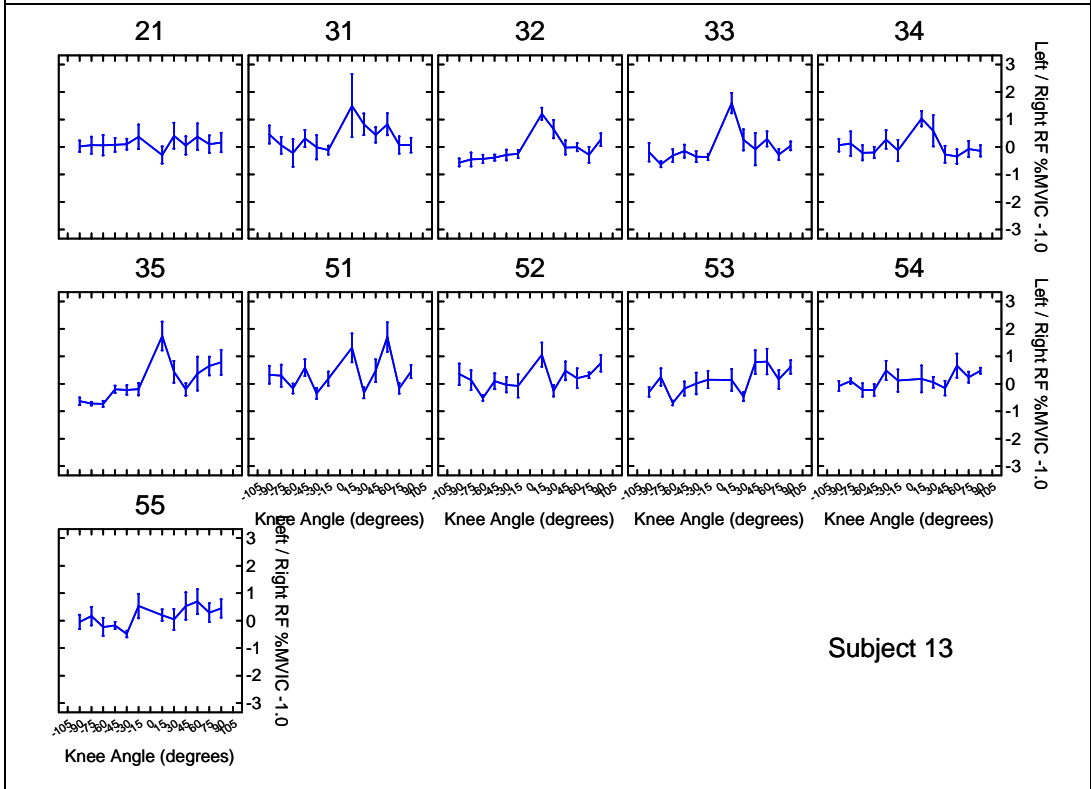
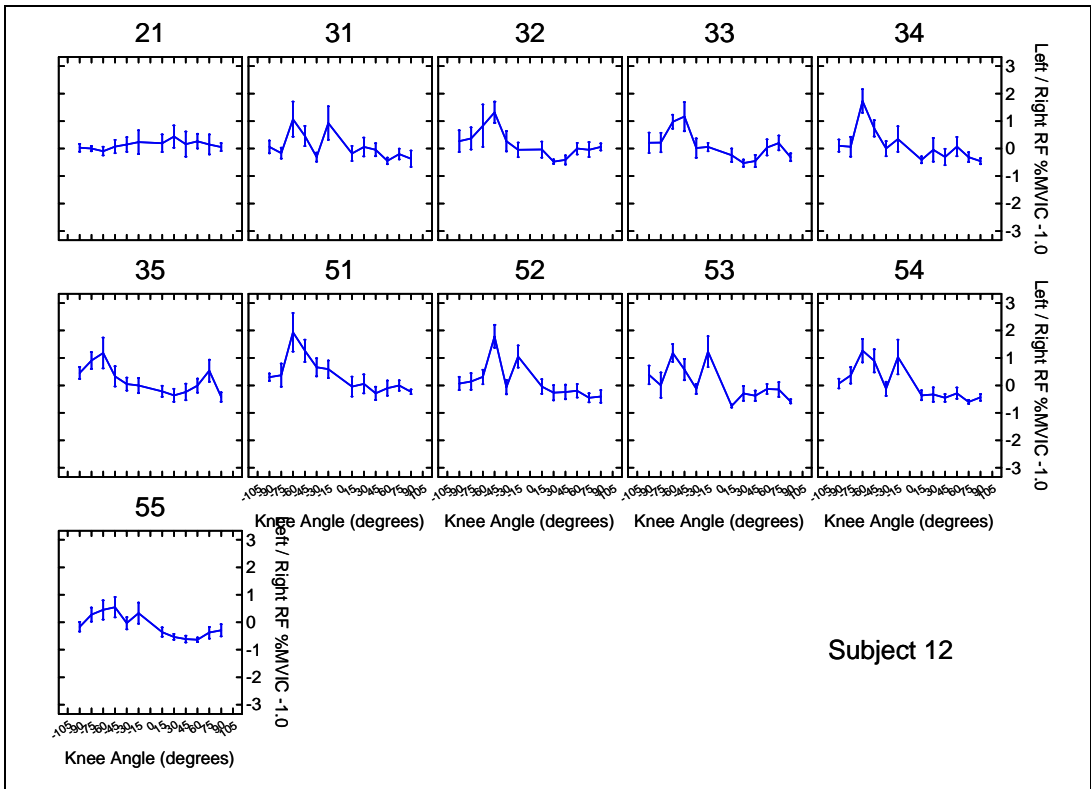


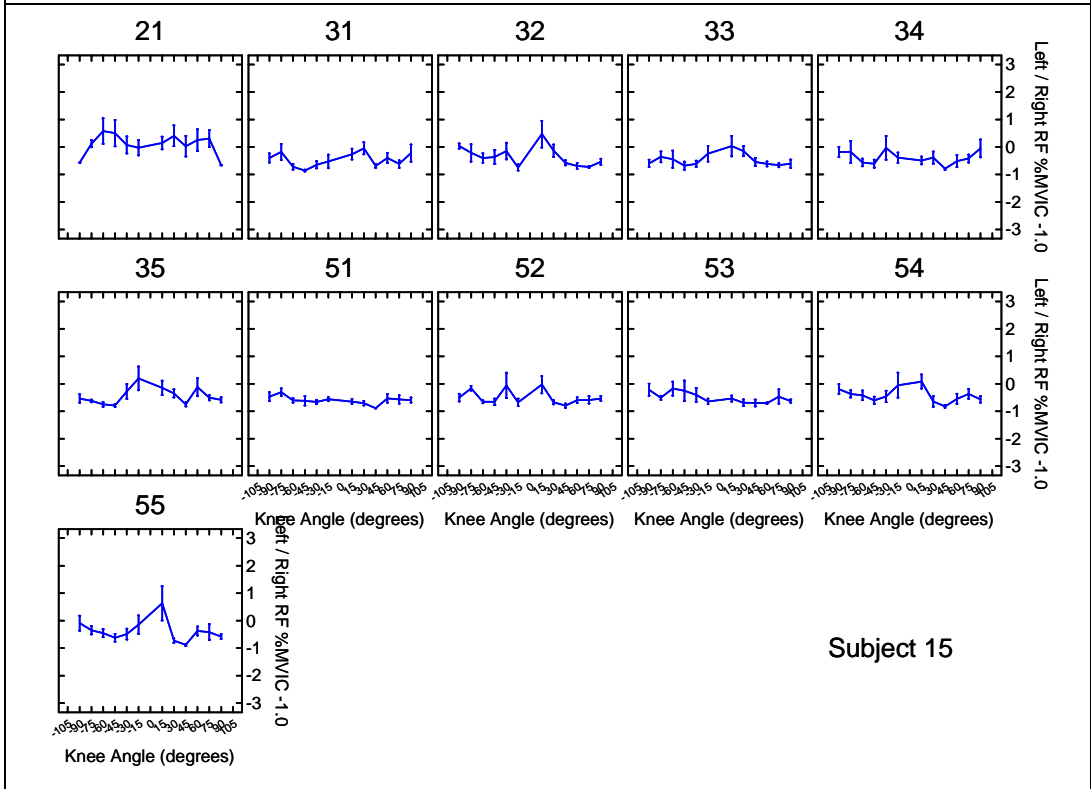
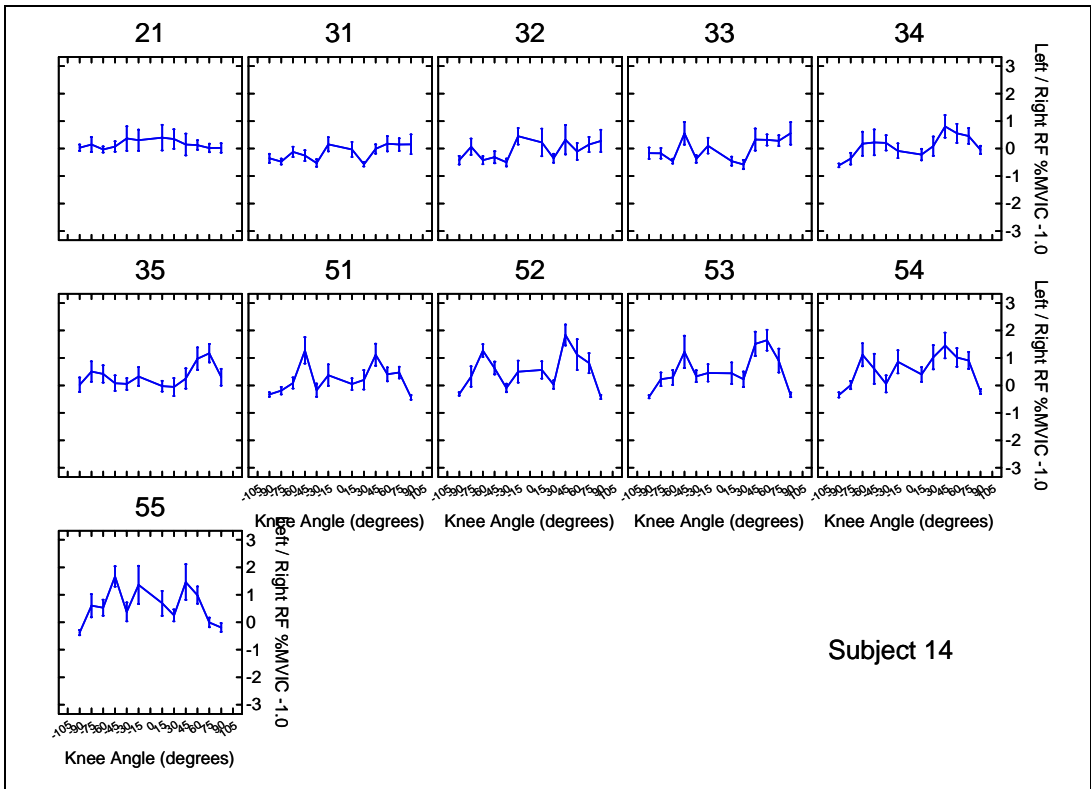






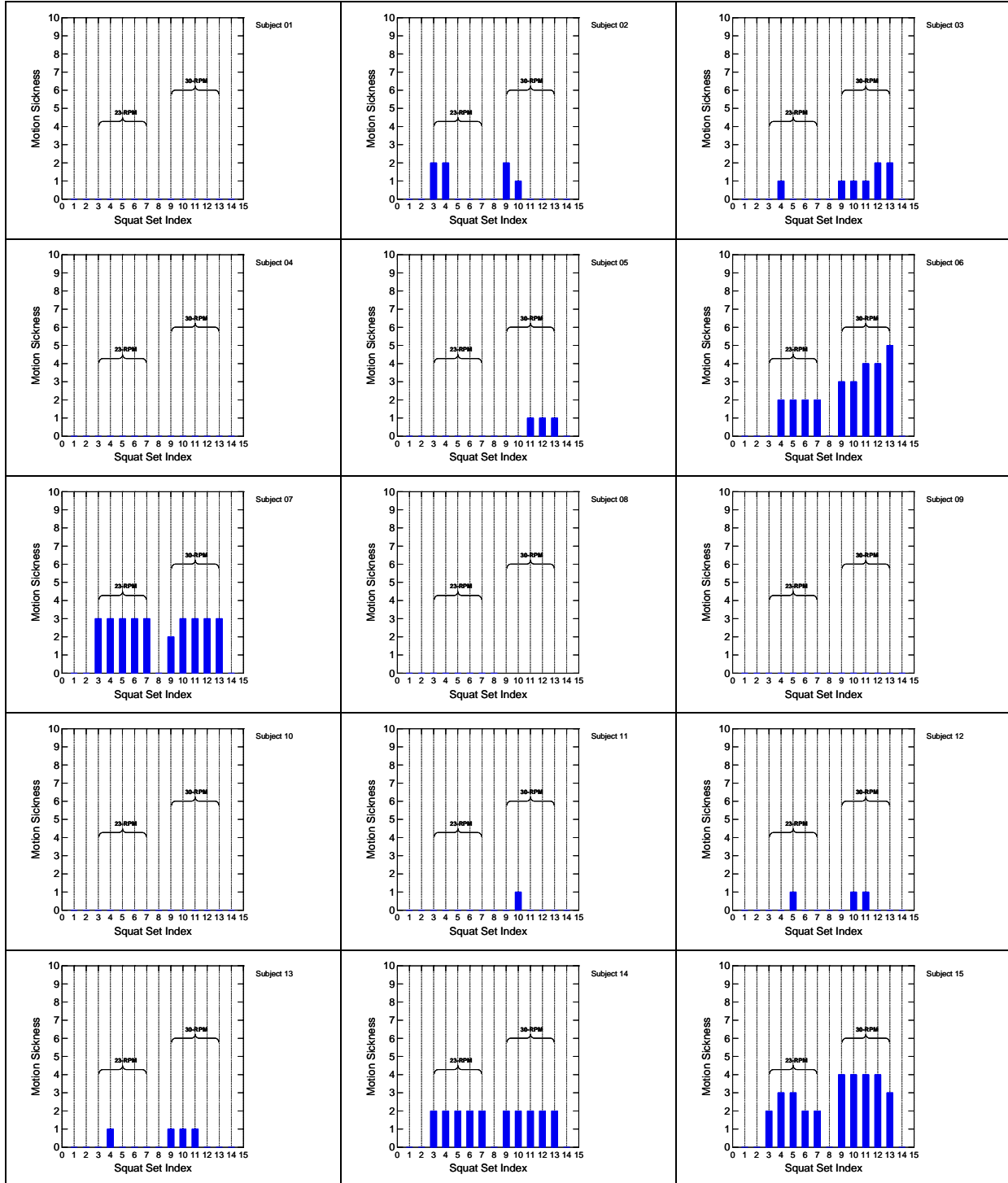






Motion Sickness

Motion sickness reports (0 – 20) scale at the end of each set of eight repetitions. We use the “Squat Set Index” to indicate the sequential set of eight repetitions. For example, Phase 1 is Squat Set Index 1, and the 23-RPM conditions (Phase 3, which has five sets of eight repetitions) is Squat Set Index 3 thru 7.



Experiment 2

Subject Demographics and Anthropometrics

The demographics and anthropometrics of the subjects who took part in Experiment 2 are listed in the following tables. The subject number, gender (male or female), age (in years), and footedness (left or right dominant foot) are listed in the left-most column. The anthropometrics are in the following columns. We present the mass and length of nine body segments. The center of mass (CoM) is measured from the proximal end of each segment, and we also show the center of mass of each segment relative to the top of the head. Total body mass is the sum of the torso and head plus twice the sum of the remaining segments (i.e., two upper arms, two lower arms, etc.)

Subject 1 – Group A Female, 19 yrs., L footed		Mass [kg]	Length [m]	CoM [m]	CoM from Top of Head [m]
	Torso and Head	34.47	0.84	0.50	0.50
	Upper Arm	1.76	0.26	0.12	0.54
	Lower Arm	0.95	0.26	0.10	0.78
	Palm	0.20	0.12	0.05	0.99
	Fingers	0.18	0.08	0.04	1.10
	Upper Leg	9.17	0.44	0.20	1.04
	Lower Leg	3.67	0.35	0.15	1.43
	Foot	0.53	0.15	0.06	1.63
	Toes	0.04	0.04	0.01	1.63
	Body Mass	67.47		Height	1.63

Subject 2 – Group B Female, 26 yrs., R footed		Mass [kg]	Length [m]	CoM [m]	CoM from Top of Head [m]
	Torso and Head	30.45	0.84	0.49	0.49
	Upper Arm	1.99	0.28	0.13	0.54
	Lower Arm	0.96	0.25	0.10	0.79
	Palm	0.28	0.12	0.05	0.99
	Fingers	0.05	0.05	0.03	1.09
	Upper Leg	11.18	0.52	0.24	1.08
	Lower Leg	4.33	0.41	0.18	1.54
	Foot	0.59	0.17	0.07	1.77
	Toes	0.04	0.04	0.01	1.77
	Body Mass	69.27		Height	1.77

Subject 3 – Group A Male 22 yrs., R footed		Mass [kg]	Length [m]	CoM [m]	CoM from Top of Head [m]
	Torso and Head	47.92	0.99	0.60	0.60
	Upper Arm	2.52	0.27	0.12	0.61
	Lower Arm	1.73	0.30	0.12	0.88
	Palm	0.24	0.12	0.05	1.11
	Fingers	0.18	0.08	0.04	1.22
	Upper Leg	14.60	0.54	0.25	1.24
	Lower Leg	4.79	0.44	0.19	1.72
	Foot	0.53	0.15	0.06	1.97
	Toes	0.04	0.04	0.01	1.97
	Body Mass	97.18		Height	1.97

Subject 4 – Group A Male, 27 yrs., R footed		Mass [kg]	Length [m]	CoM [m]	CoM from Top of Head [m]
	Torso and Head	45.53	0.95	0.57	0.57
	Upper Arm	2.58	0.28	0.13	0.56
	Lower Arm	1.53	0.30	0.12	0.83
	Palm	0.22	0.12	0.05	1.06
	Fingers	0.18	0.08	0.04	1.17
	Upper Leg	11.14	0.51	0.23	1.18
	Lower Leg	3.72	0.39	0.17	1.63
	Foot	0.53	0.15	0.06	1.85
	Toes	0.04	0.04	0.01	1.85
	Body Mass	85.40		Height	1.85

Subject 5 – Group B Male, 24 yrs., R footed		Mass [kg]	Length [m]	CoM [m]	CoM from Top of Head [m]
	Torso and Head	29.34	0.85	0.49	0.49
	Upper Arm	1.51	0.25	0.11	0.58
	Lower Arm	1.03	0.26	0.10	0.82
	Palm	0.22	0.12	0.05	1.03
	Fingers	0.18	0.08	0.04	1.14
	Upper Leg	9.08	0.51	0.24	1.09
	Lower Leg	3.43	0.36	0.16	1.52
	Foot	0.53	0.15	0.06	1.72
	Toes	0.04	0.04	0.01	1.72
	Body Mass	61.38		Height	1.72

Subject 6 – Group B Female, 39 yrs., R footed		Mass [kg]	Length [m]	CoM [m]	CoM from Top of Head [m]
	Torso and Head	34.09	0.83	0.50	0.50
	Upper Arm	1.67	0.24	0.11	0.52
	Lower Arm	0.89	0.26	0.09	0.74
	Palm	0.17	0.12	0.06	0.97
	Fingers	0.18	0.08	0.04	1.07
	Upper Leg	9.27	0.48	0.22	1.05
	Lower Leg	3.85	0.42	0.18	1.49
	Foot	0.53	0.15	0.06	1.73
	Toes	0.04	0.04	0.01	1.73
	Body Mass	67.28		Height	1.73

Subject 7 – Group B Male, 27 yrs., R footed		Mass [kg]	Length [m]	CoM [m]	CoM from Top of Head [m]
	Torso and Head	38.59	0.82	0.50	0.50
	Upper Arm	1.97	0.25	0.12	0.54
	Lower Arm	1.52	0.29	0.11	0.78
	Palm	0.22	0.12	0.05	1.01
	Fingers	0.18	0.08	0.04	1.12
	Upper Leg	14.25	0.54	0.25	1.07
	Lower Leg	4.78	0.40	0.17	1.53
	Foot	0.54	0.15	0.06	1.76
	Toes	0.04	0.04	0.01	1.76
	Body Mass	85.61		Height	1.76

Subject 8 – Group A Female, 19 yrs., R footed		Mass [kg]	Length [m]	CoM [m]	CoM from Top of Head [m]
	Torso and Head	28.18	0.82	0.48	0.48
	Upper Arm	1.45	0.25	0.11	0.53
	Lower Arm	0.80	0.26	0.09	0.76
	Palm	0.17	0.12	0.06	0.99
	Fingers	0.18	0.08	0.04	1.09
	Upper Leg	8.96	0.46	0.21	1.03
	Lower Leg	2.83	0.35	0.15	1.43
	Foot	0.52	0.15	0.06	1.63
	Toes	0.04	0.04	0.01	1.63
	Body Mass	58.11		Height	1.63

Subject 9 – Group B Male, 29 yrs., R footed		Mass [kg]	Length [m]	CoM [m]	CoM from Top of Head [m]
	Torso and Head	42.37	0.91	0.54	0.54
	Upper Arm	3.20	0.31	0.14	0.58
	Lower Arm	1.45	0.28	0.11	0.86
	Palm	0.30	0.12	0.05	1.08
	Fingers	0.03	0.05	0.02	1.17
	Upper Leg	9.26	0.42	0.19	1.10
	Lower Leg	4.76	0.45	0.19	1.52
	Foot	1.52	0.28	0.12	1.78
	Toes	0.15	0.06	0.03	1.78
	Body Mass	83.69		Height	1.78

Subject 10 – Group A Male, 33 yrs., L footed		Mass [kg]	Length [m]	CoM [m]	CoM from Top of Head [m]
	Torso and Head	28.06	0.76	0.44	0.44
	Upper Arm	1.72	0.26	0.12	0.51
	Lower Arm	1.02	0.28	0.10	0.75
	Palm	0.19	0.12	0.06	0.99
	Fingers	0.18	0.08	0.04	1.09
	Upper Leg	10.12	0.51	0.24	1.00
	Lower Leg	3.43	0.37	0.15	1.42
	Foot	0.52	0.15	0.06	1.64
	Toes	0.04	0.04	0.01	1.64
	Body Mass	62.50		Height	1.64

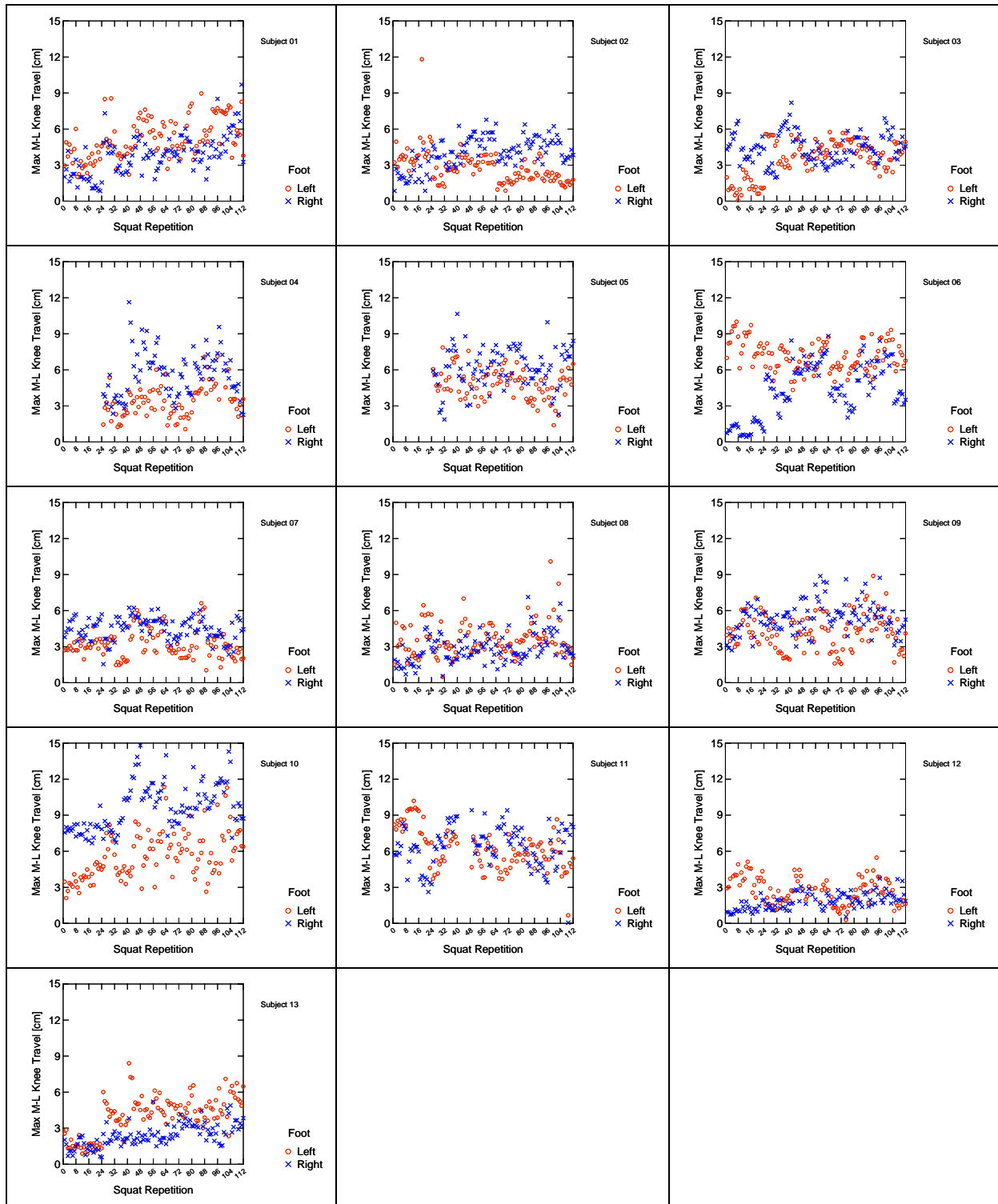
Subject 11 – Group A Male, 27 yrs., R footed		Mass [kg]	Length [m]	CoM [m]	CoM from Top of Head [m]
	Torso and Head	41.41	0.94	0.56	0.56
	Upper Arm	2.54	0.30	0.14	0.58
	Lower Arm	1.47	0.30	0.12	0.86
	Palm	0.22	0.12	0.05	1.09
	Fingers	0.18	0.08	0.04	1.20
	Upper Leg	10.84	0.47	0.21	1.15
	Lower Leg	4.68	0.44	0.19	1.60
	Foot	0.53	0.15	0.06	1.85
	Toes	0.04	0.04	0.01	1.85
	Body Mass	82.41		Height	1.85

Subject 12 – Group B Male, 27 yrs., R footed		Mass [kg]	Length [m]	CoM [m]	CoM from Top of Head [m]
	Torso and Head	34.17	0.90	0.51	0.51
	Upper Arm	2.04	0.29	0.13	0.54
	Lower Arm	0.99	0.27	0.10	0.80
	Palm	0.19	0.12	0.06	1.03
	Fingers	0.18	0.08	0.04	1.13
	Upper Leg	9.23	0.47	0.21	1.11
	Lower Leg	3.84	0.40	0.18	1.55
	Foot	0.53	0.15	0.06	1.77
	Toes	0.04	0.04	0.01	1.77
	Body Mass	68.26		Height	1.77

Subject 13 – Group A Male, 24 yrs., R footed		Mass [kg]	Length [m]	CoM [m]	CoM from Top of Head [m]
	Torso and Head	29.92	0.85	0.50	0.50
	Upper Arm	1.42	0.25	0.12	0.53
	Lower Arm	1.27	0.30	0.12	0.78
	Palm	0.22	0.12	0.05	1.01
	Fingers	0.18	0.08	0.04	1.12
	Upper Leg	9.60	0.45	0.21	1.06
	Lower Leg	3.43	0.36	0.15	1.45
	Foot	0.53	0.15	0.06	1.66
	Toes	0.04	0.04	0.01	1.66
	Body Mass	63.32		Height	1.66

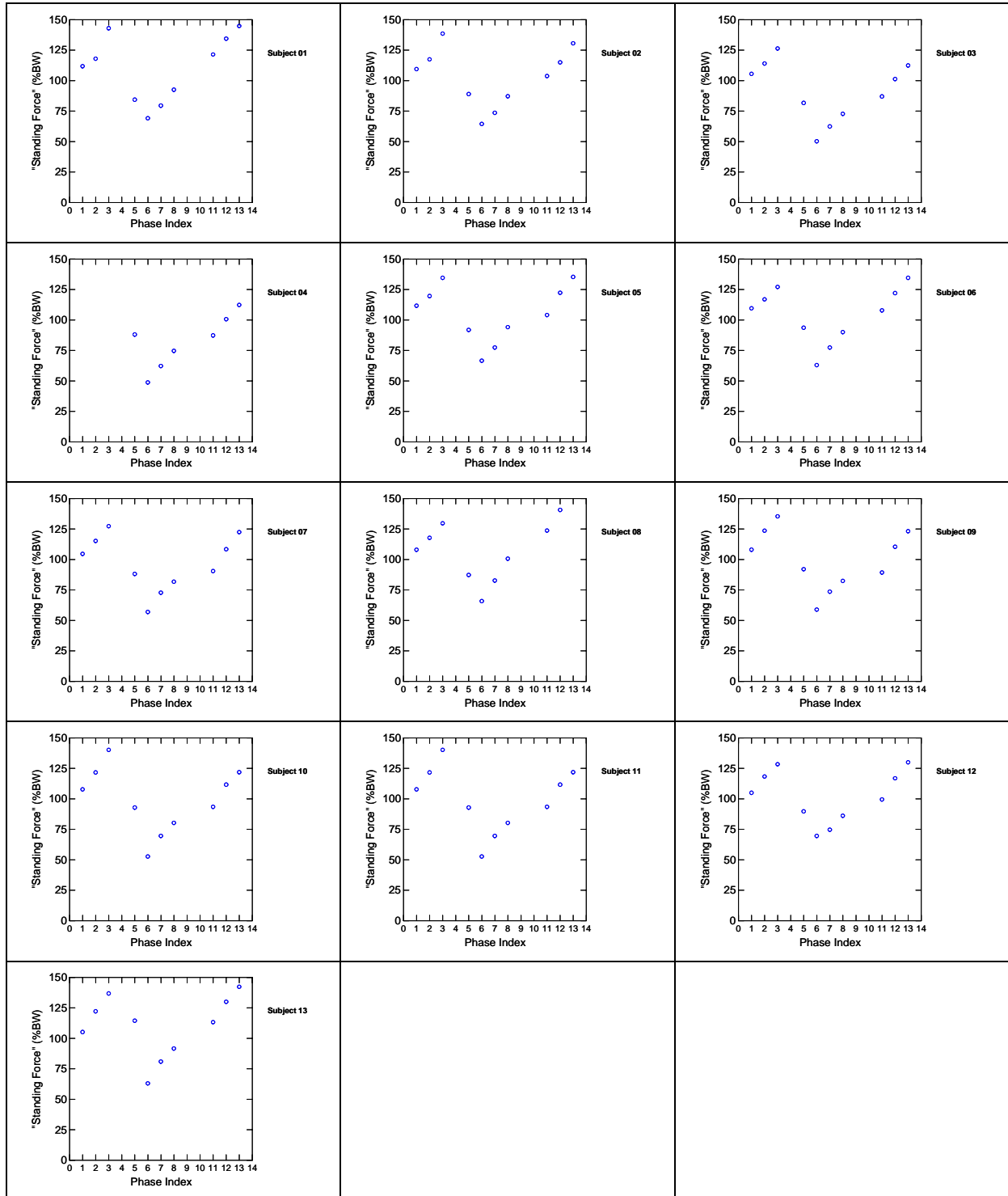
Maximum Medial-Lateral Knee Travel

The maximum medial-lateral knee travel in centimeters is shown for the left and right leg throughout all repetitions in Experiment 2. The repetitions are blocked sequentially by the experimental phases in groups of eight.



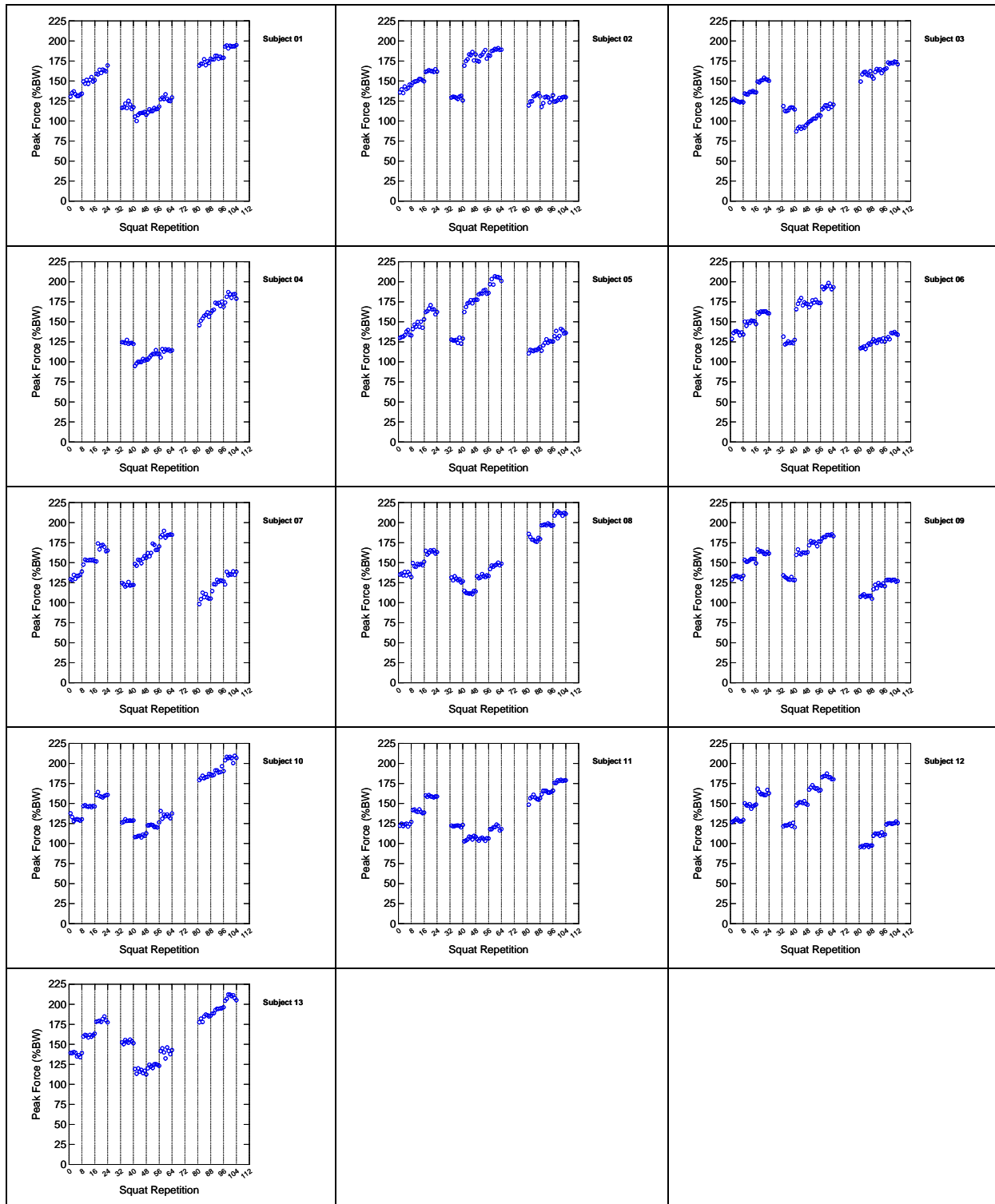
Standing Force

The standing force, expressed as a percentage of body weight, is shown for the three “weighted” phases: Phase 1, 2, 3, 5, 6, 7, 8, 11, 12, 13.



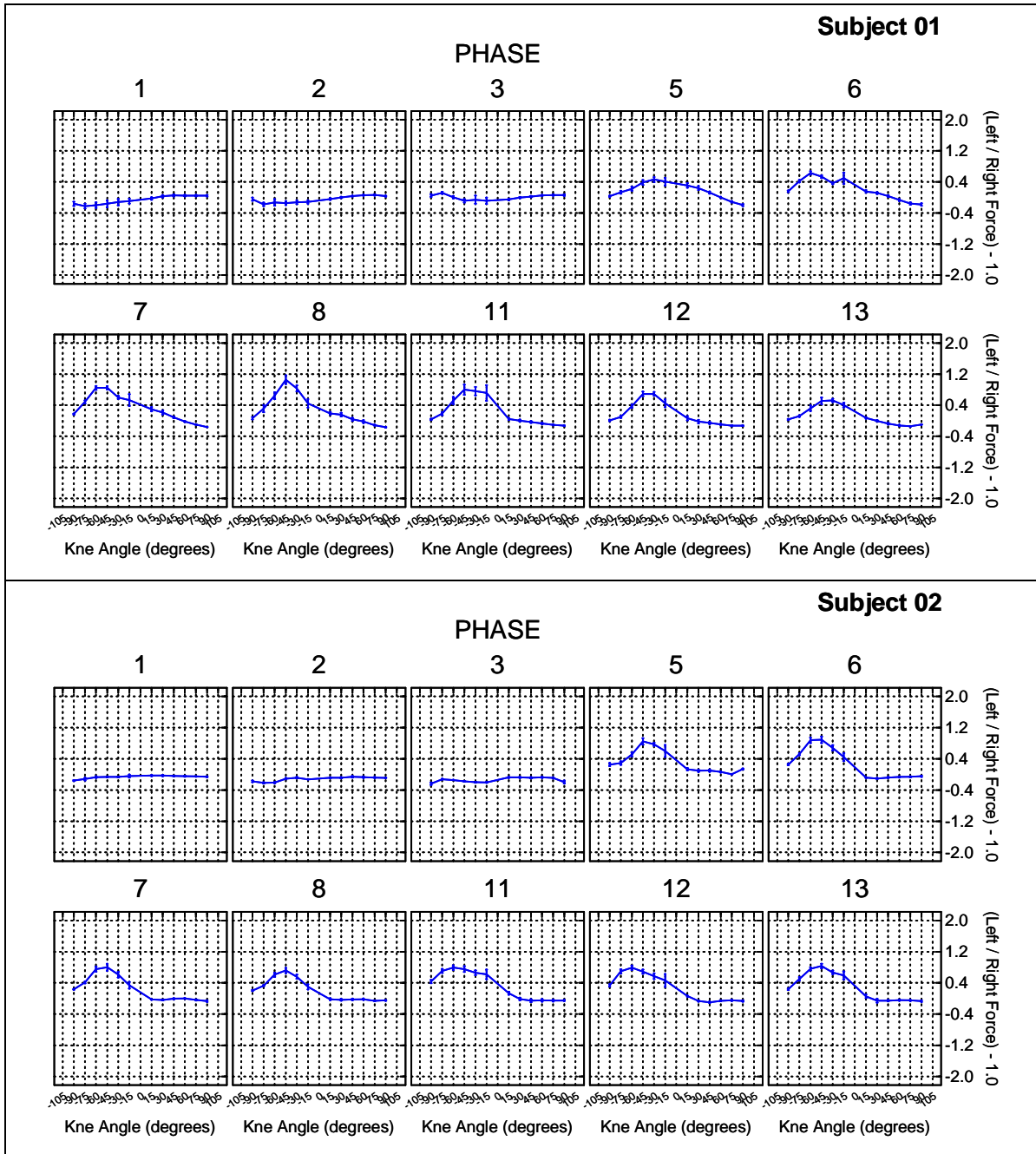
Peak Force

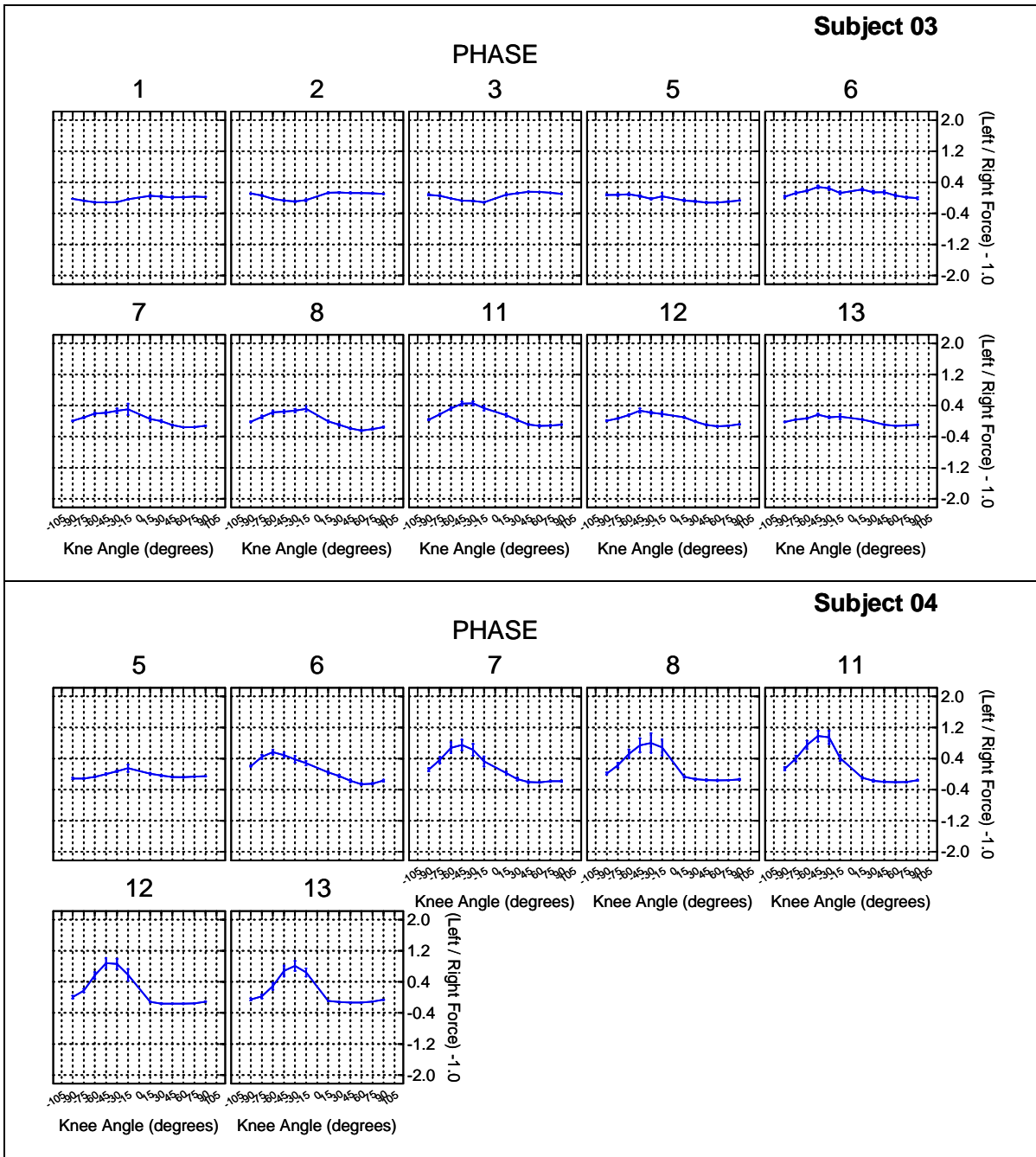
The peak force, expressed as a percentage of body weight, is shown for the “weighted” phases: Phase 1, 2, 3, 5, 6, 7, 8, 11, 12, 13. Each of the repetitions is plotted sequentially for eight repetitions in each phase.

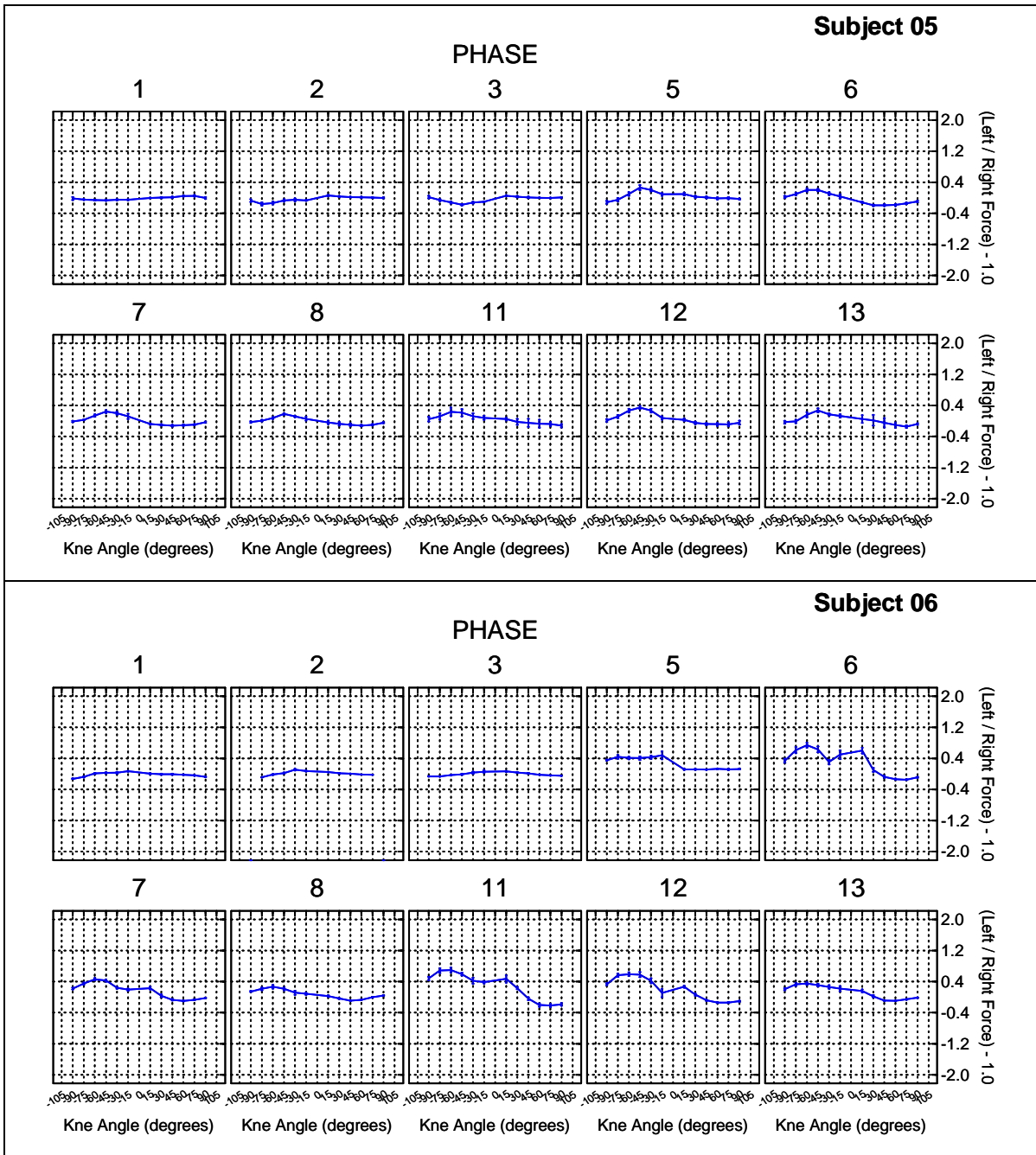


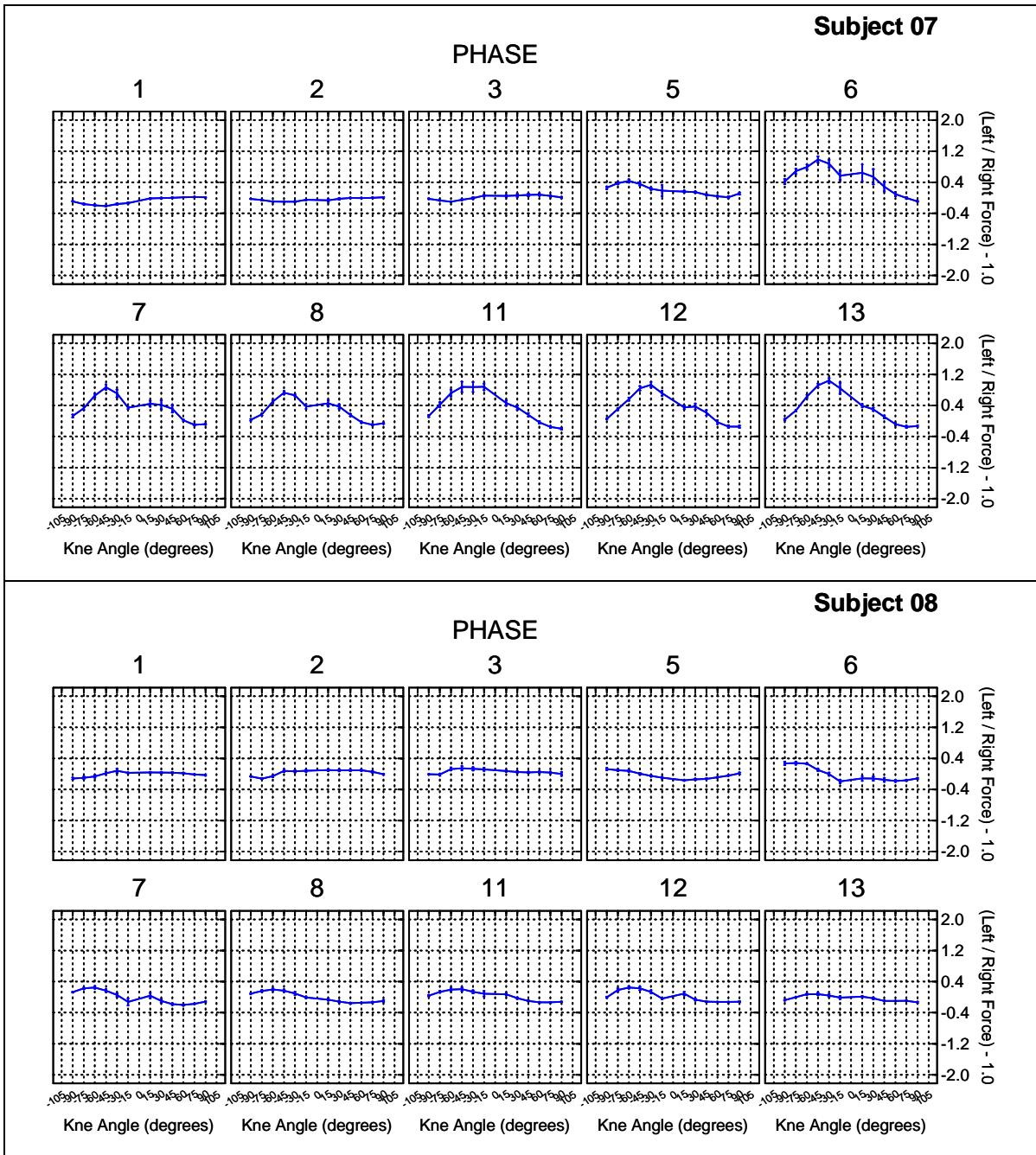
Left-Right Foot Force Asymmetry

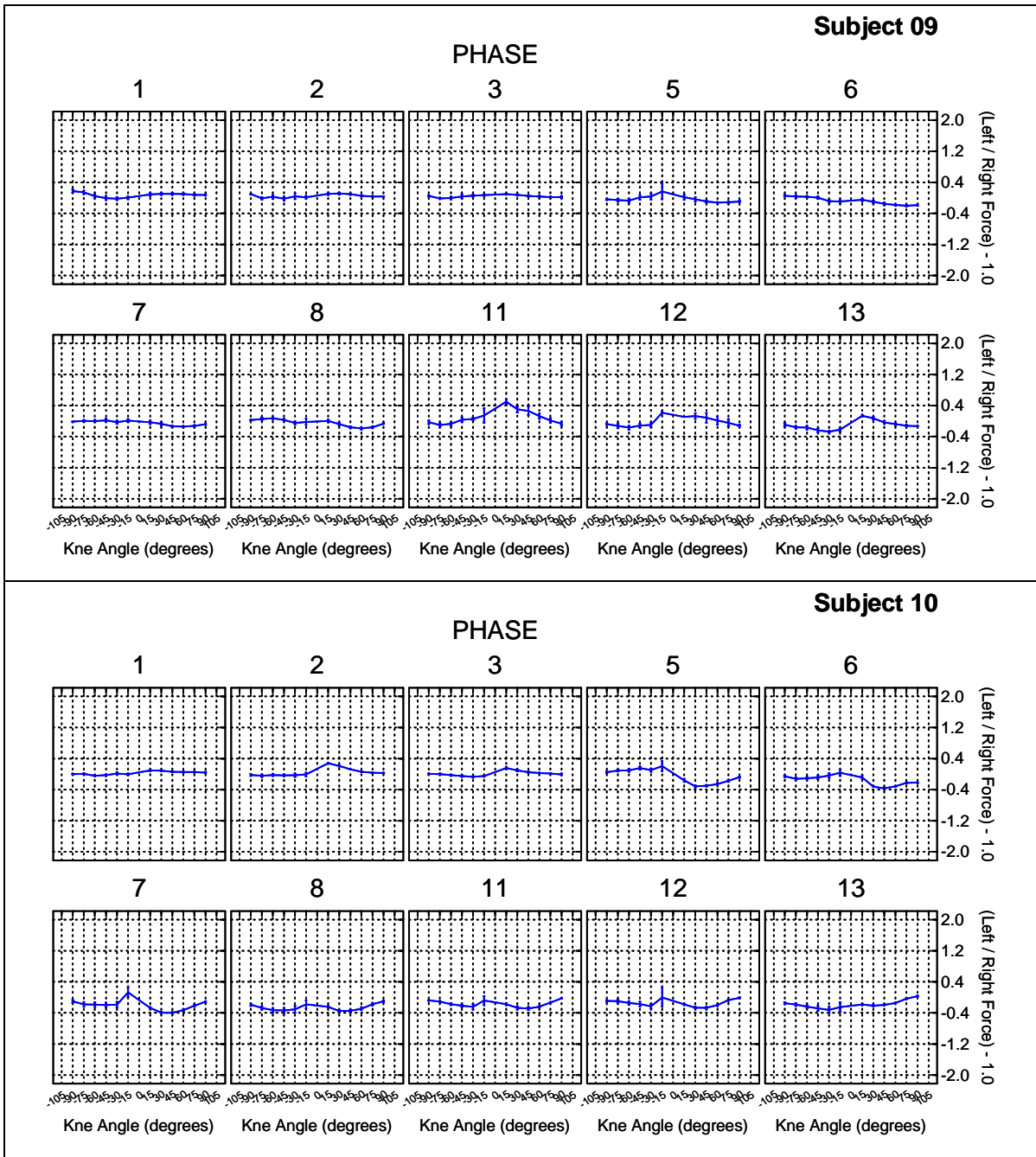
The left divided by right foot force minus one (Left / Right – 1.0) at several knee angles for each subject. The numbers on the top of the boxes is the Experiment Phase. The eight repetitions within each set are averaged together. Mean +/- SEM. Note: The knee angles are the same as in the body of this thesis, however, the ordering of them is slightly different: 0-degree knee angle is in the middle of the graph and full extension (i.e., 90-degrees) is at the edges.

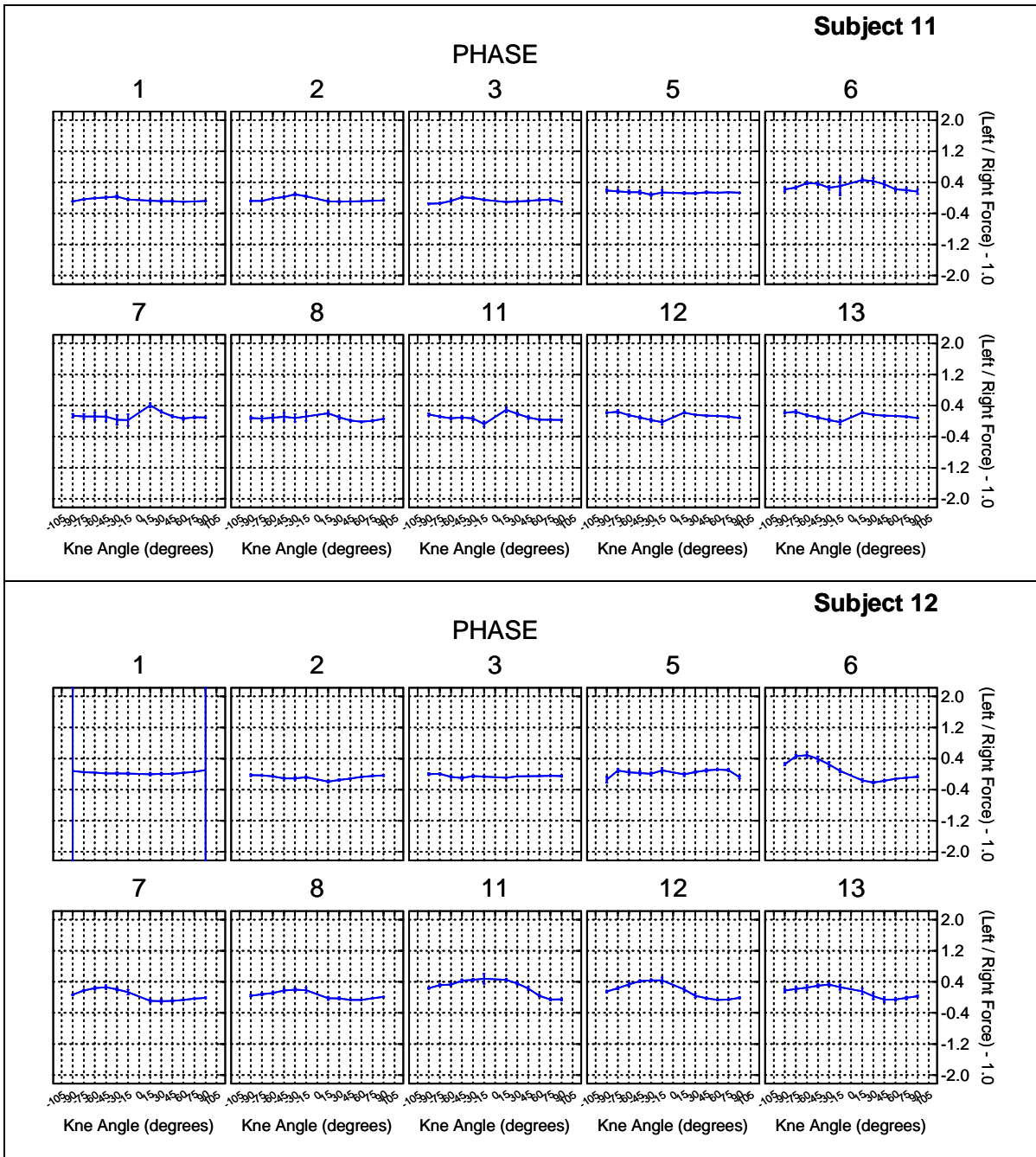


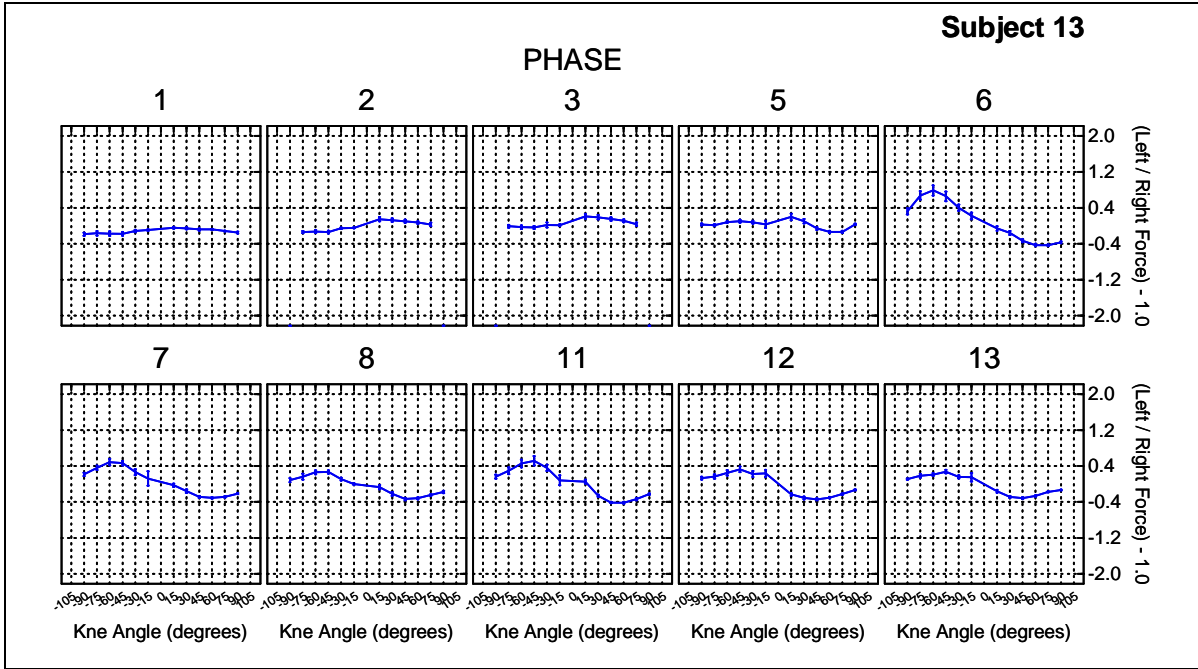






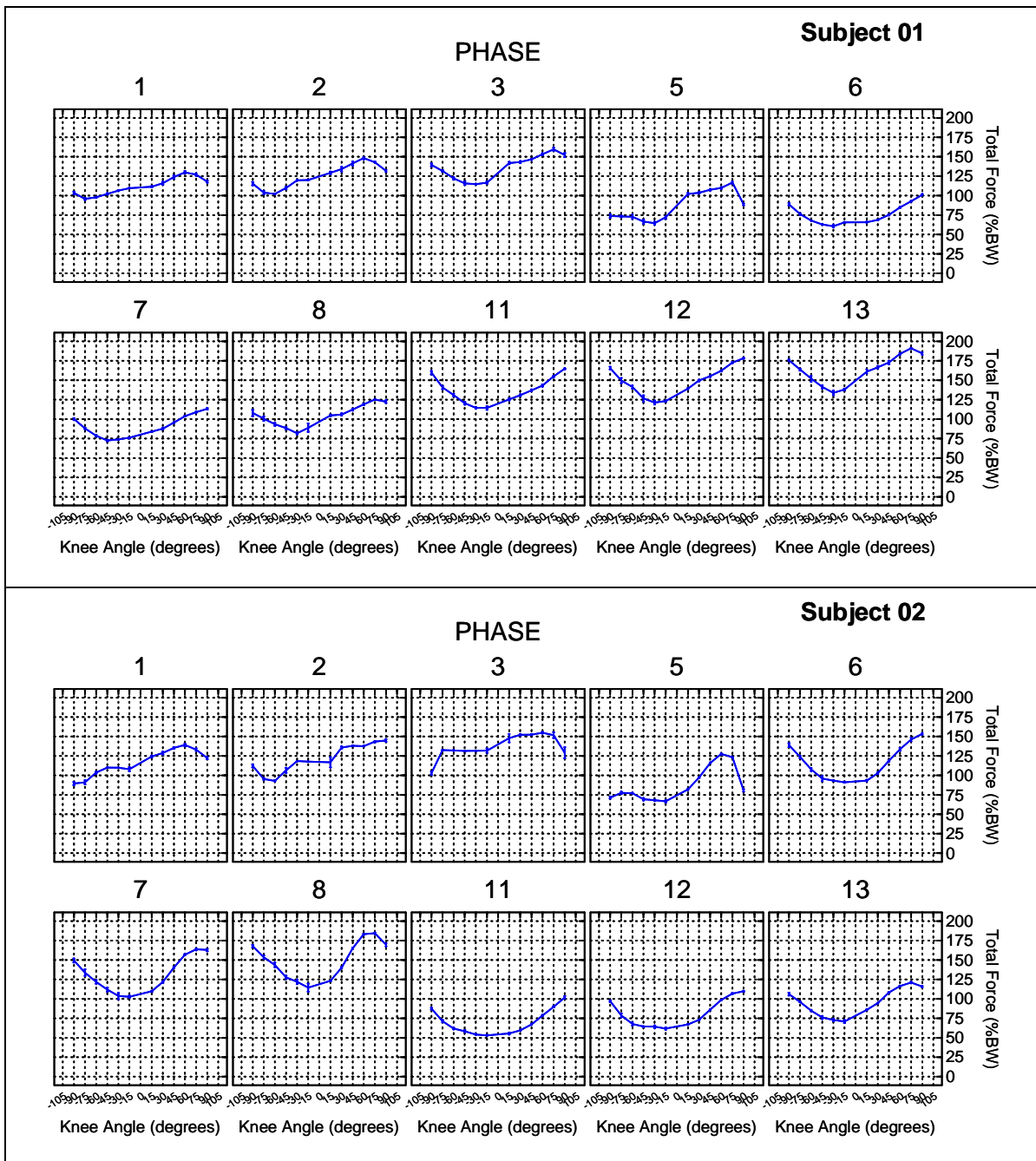


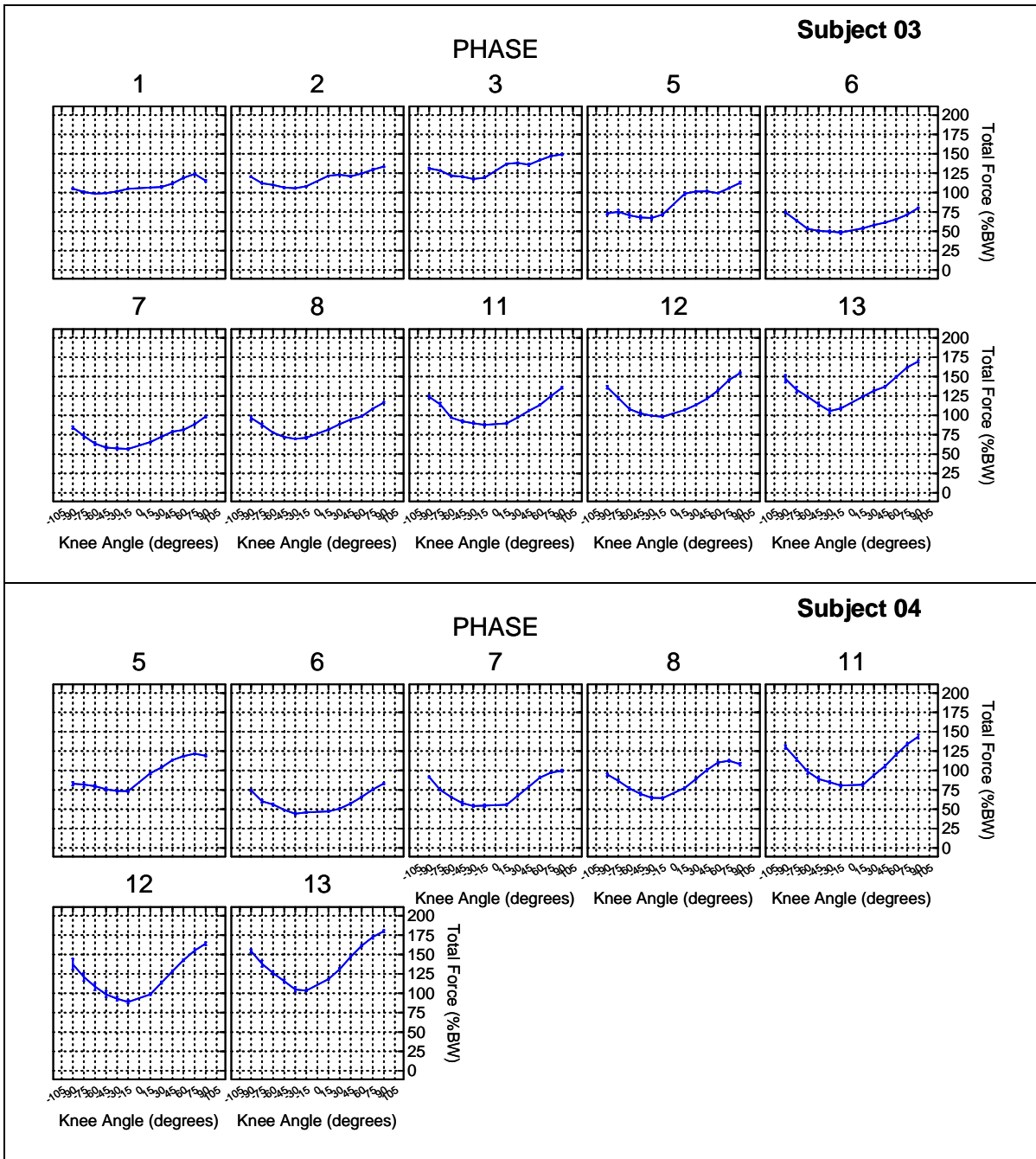


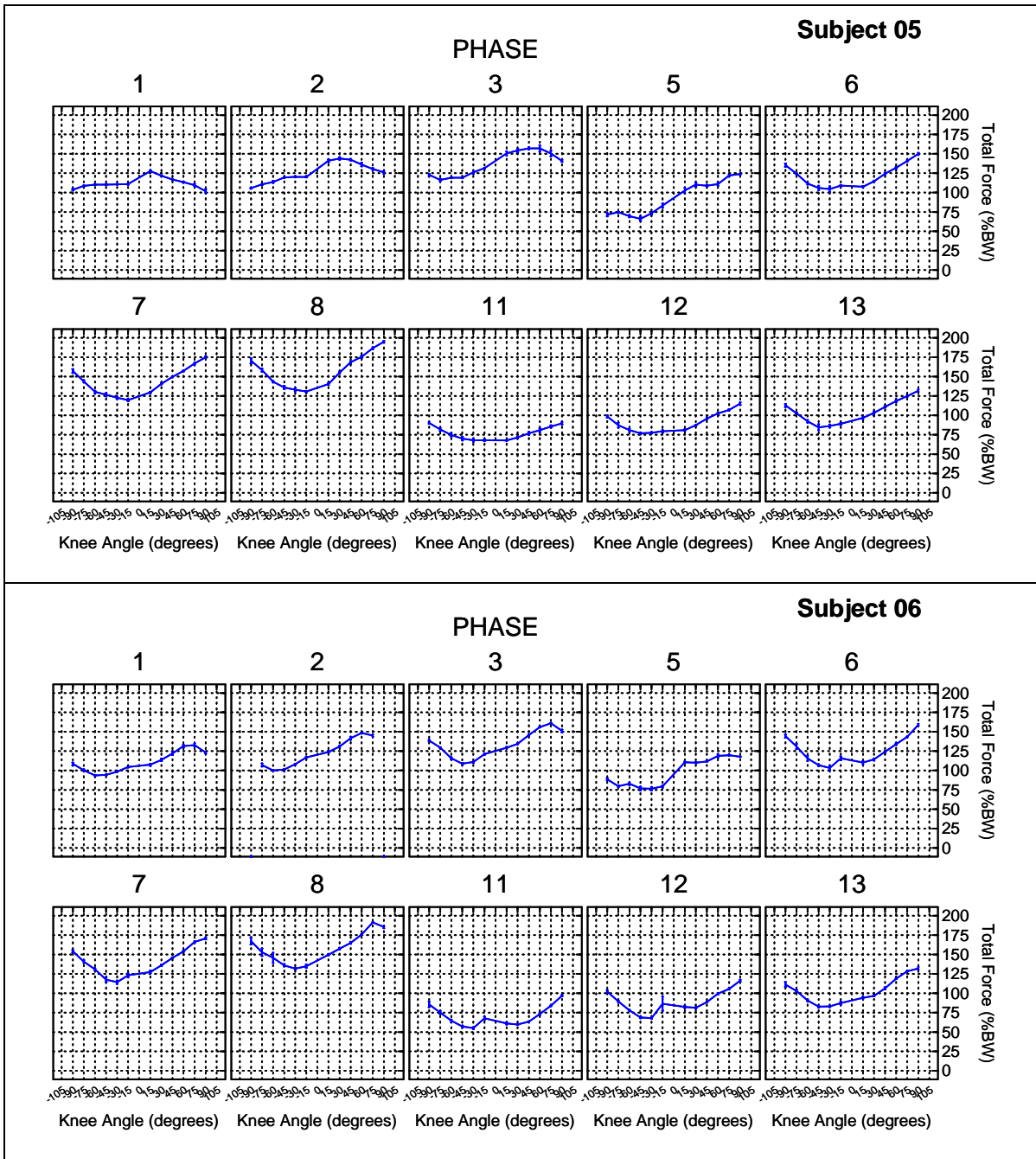


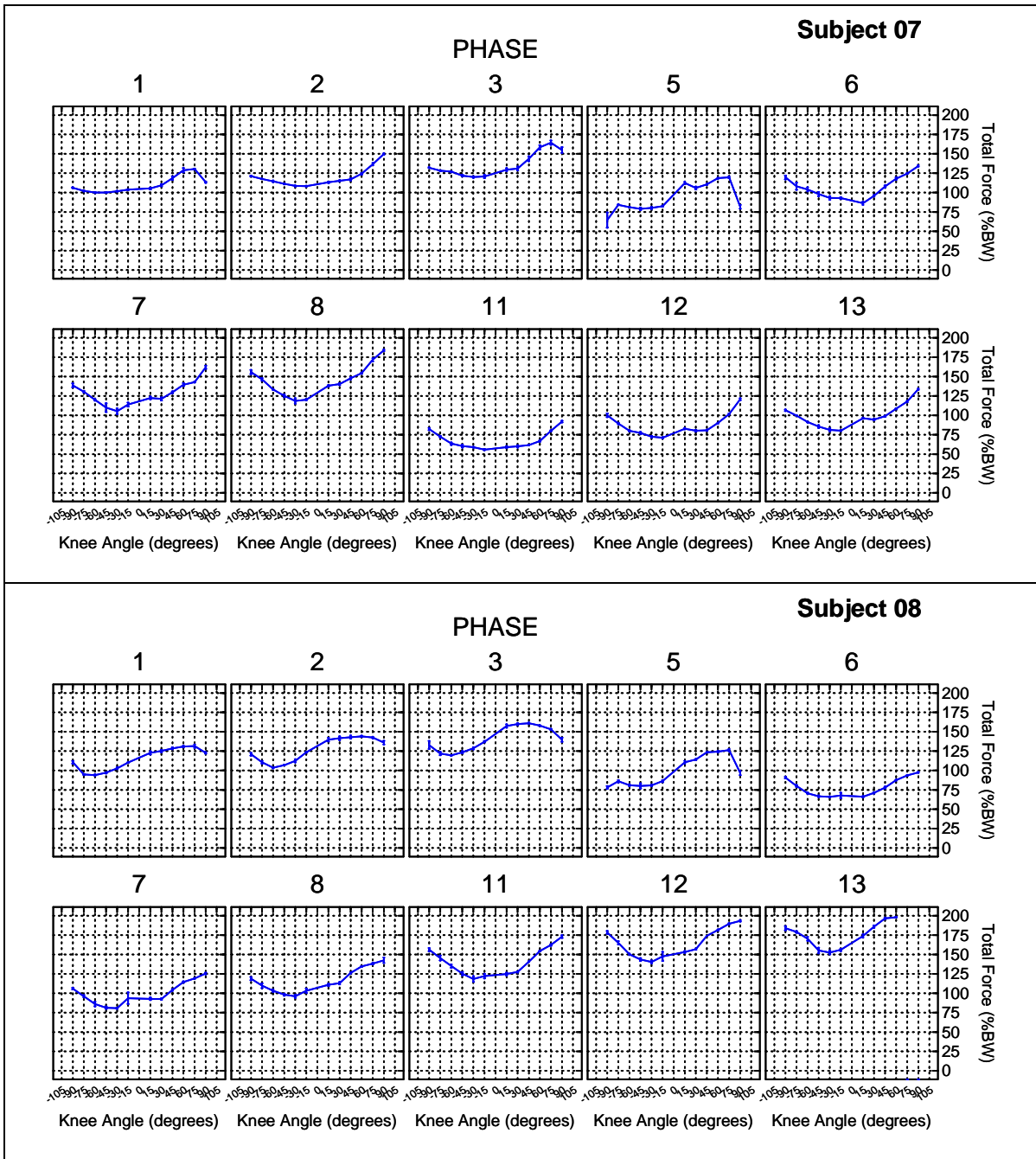
Total Foot Force

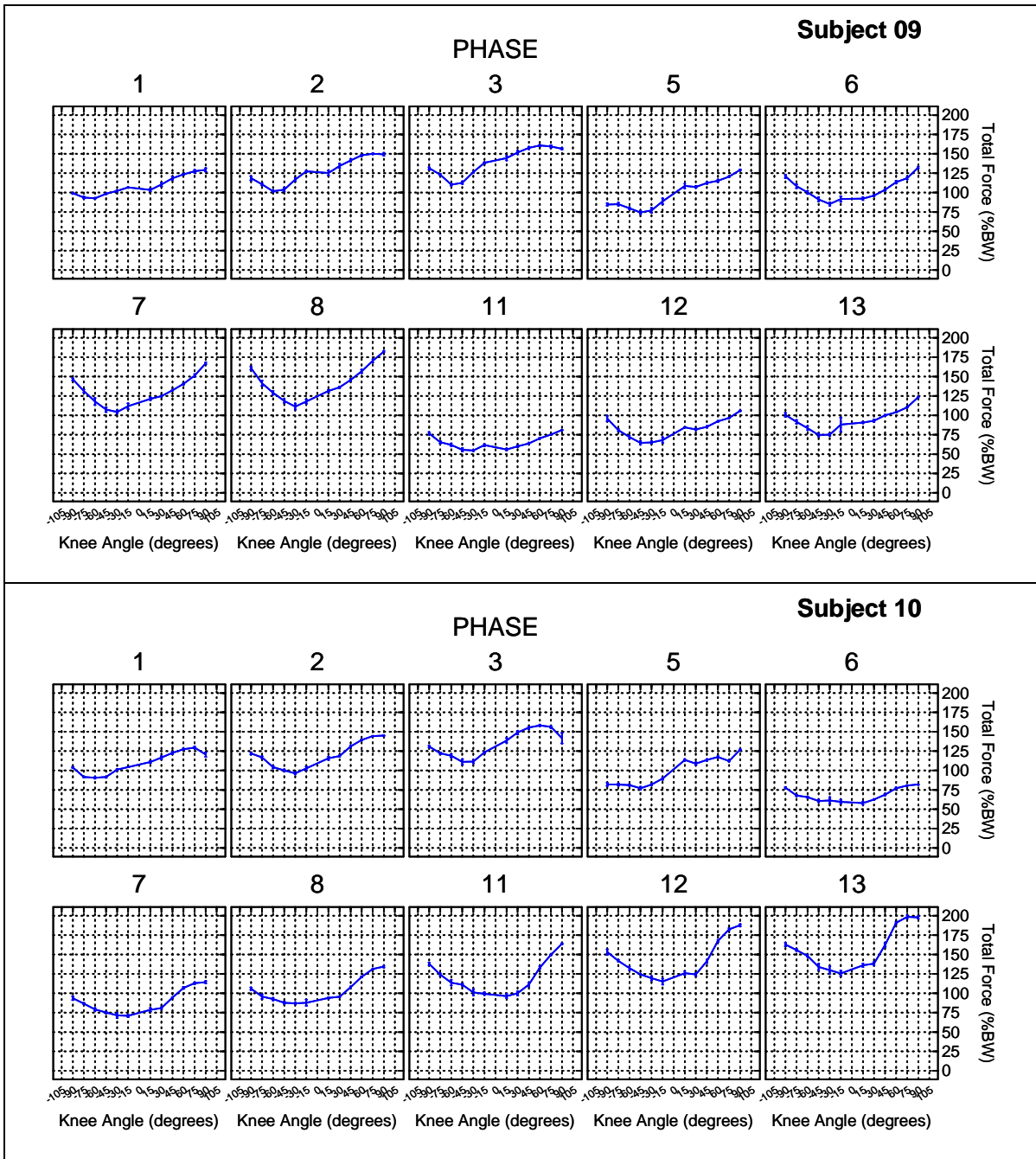
The sum of the left and right foot force, expressed as a percentage of body weight, at several knee angles. The numbers on the top of the boxes is the Experiment Phase. The eight repetitions within each set are averaged together. Mean \pm SEM. Note: The knee angles are the same as in the body of this thesis, however, the ordering of them is slightly different: 0-degree knee angle is in the middle of the graph and full extension (i.e., 90-degrees) is at the edges.

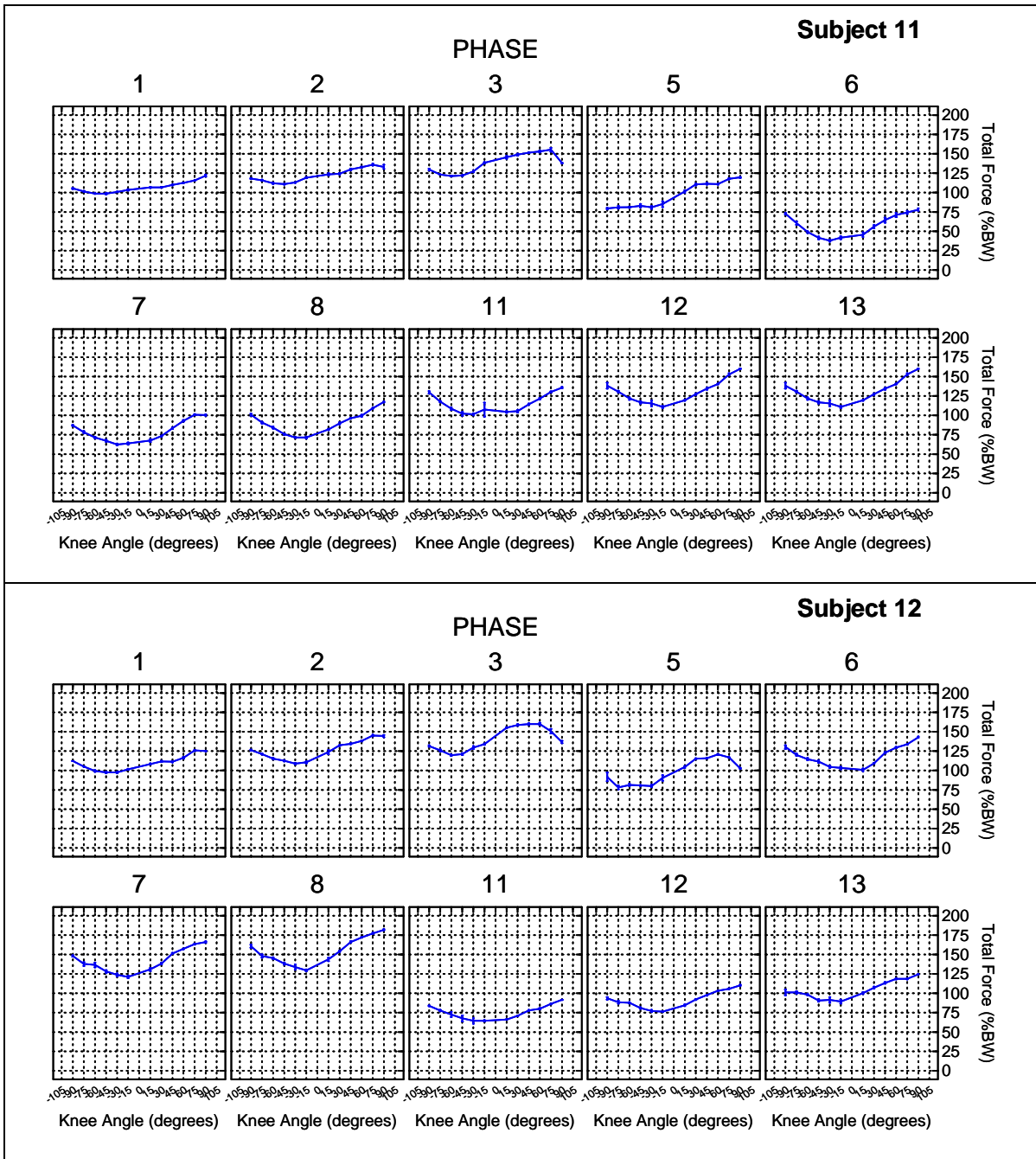


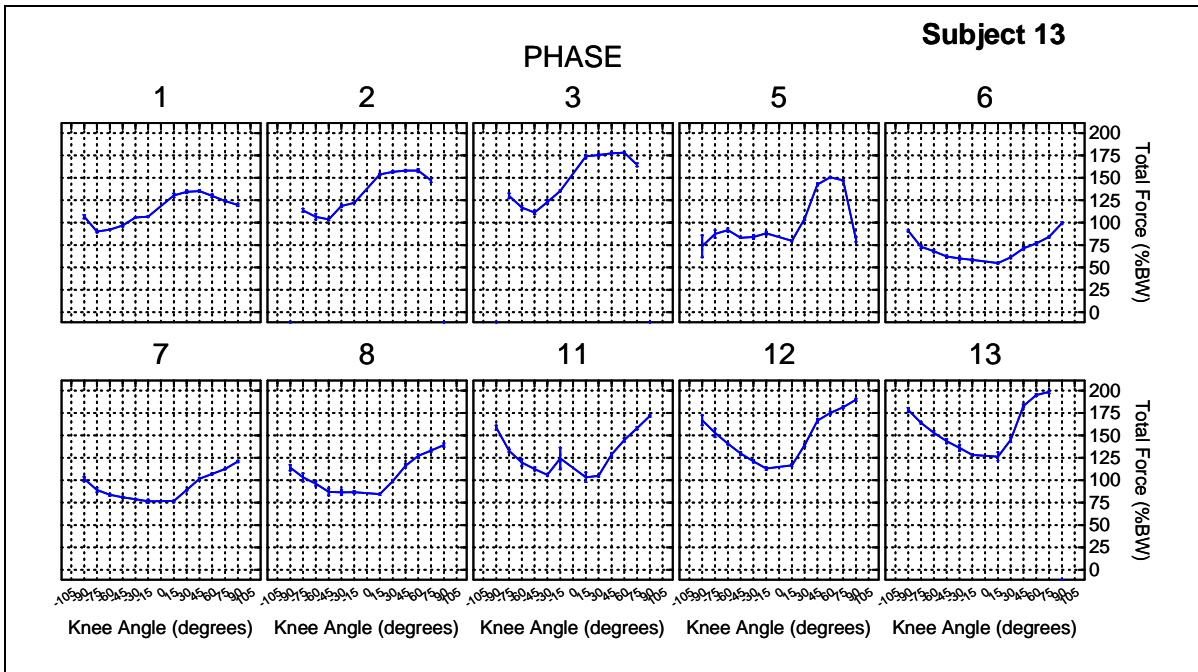












Foot Reaction Force Summary

The foot reaction force data (total force % body weight) is presented at each of the knee angles across upright, 23 RPM, and 30 RPM squats with the three levels of additional resistance. Mean +/- SEM. We contrasted the differences between the various conditions in order to define a set of artificial gravity exercise parameters that have similar foot reaction forces to those when exercising Earth upright. The multiple contrasts were Bonferroni-corrected to account for the numerous comparisons.

Mean total foot reaction force, as a percentage of 1-G upright body weight, at each of the knee flexion angles. Data from all thirteen subjects is shown.

KneeAngle	Upright			23-RPM			30-RPM		
	0%	10%	25%	0%	10%	25%	0%	10%	25%
15	106.2	116.4	128.9	58.1	71.8	82.8	103.0	114.1	124.4
30	103.2	112.2	122.2	56.3	69.3	80.4	99.9	114.0	125.2
45	99.6	107.7	118.3	58.5	71.1	82.4	104.7	118.6	130.8
60	97.6	106.3	120.3	63.7	76.3	89.5	112.0	127.6	141.1
75	97.9	111.2	126.1	71.0	84.6	97.4	123.4	138.5	151.3
90	103.7	117.6	128.4	82.6	96.1	105.8	137.3	151.2	164.0
-90	118.8	139.1	144.6	90.3	111.5	126.1	150.8	171.6	185.3
-75	125.9	141.0	156.1	82.4	104.8	121.4	140.0	164.0	182.4
-60	125.2	139.9	157.4	75.2	98.6	114.9	130.0	154.3	172.4
-45	121.2	136.6	153.6	68.1	89.9	106.9	118.8	143.8	160.8
-30	116.8	132.5	149.7	62.2	81.3	97.5	107.0	131.2	146.8
-15	113.1	127.3	145.9	58.0	77.1	92.1	101.2	123.1	137.3

Differences in mean total foot force data during centrifugation compared to upright squats with no additional resistance as a function of knee angle. Differences were tested with t-Tests with Bonferroni correction for multiple contrasts.

Knee Angle	Upright 0%	23-RPM 0%	23-RPM 10%	23-RPM 25%	30-RPM 0%	30-RPM 10%	30-RPM 25%
15	106.2	-48.1*	-34.4*	-23.3*	-3.2 [#]	7.9*	18.2*
30	103.2	-46.8*	-33.8*	-22.8*	-3.2*	10.9*	22.0*
45	99.7	-41.2*	-28.5*	-17.2*	5.1*	19.0*	31.2*
60	97.6	-33.9*	-21.2*	-8.0*	14.5*	30.0*	43.5*
75	97.9	-26.9*	-13.3*	-0.5 [#]	25.5	40.6*	53.4*
90	103.7	-21.1*	-7.6*	2.1 [#]	33.6*	47.5*	60.4*
-90	118.9	-28.5*	-7.4*	7.3*	32.0*	52.7*	66.5*
-75	125.9	-43.4*	-21.1*	-4.5*	14.2*	38.2*	56.6*
-60	125.2	-50.0*	-26.5*	-10.3*	4.9*	29.1*	47.2*
-45	121.3	-53.1*	-31.3*	-14.3*	-2.4 [#]	22.6*	39.6*
-30	116.8	-54.6*	-35.5*	-19.2*	-9.7*	14.4*	30.0*
-15	113.7	-55.6*	-36.7*	-21.6*	-12.5*	9.4*	23.6*

* p < 0.05, # p > 0.05

Differences in mean total foot force data during centrifugation compared to upright squats with 10% body weight additional resistance as a function of knee angle. Differences were tested with t-Tests with Bonferroni correction for multiple contrasts.

Knee Angle	Upright 10%	23-RPM 0%	23-RPM 10%	23-RPM 25%	30-RPM 0%	30-RPM 10%	30-RPM 25%
15	116.4	-58.3*	-44.6*	-33.5*	-13.4*	-2.3 [#]	8.0*
30	112.2	-55.8*	-42.8*	-31.8*	-12.2*	1.9 [#]	13.0*
45	107.7	-49.2*	-36.5*	-25.3*	-2.9*	11.0*	23.2*
60	106.4	-42.7*	-30.0*	-16.8*	5.7*	21.2*	34.7*
75	111.3	-40.2*	-26.7*	-13.8*	12.2*	27.2*	40.0*
90	117.6	-35.0*	-21.5*	-11.8*	19.7*	33.6*	46.5*
-90	139.1	-48.8*	-27.6*	-13.0*	11.7*	32.5*	46.2*
-75	141.1	-58.6*	-36.3*	-19.7*	-1.0 [#]	23.0*	41.4*
-60	140.0	-64.8*	-41.3*	-25.1*	-9.9*	14.3*	32.4*
-45	136.7	-68.5*	-46.7*	-29.7*	-17.8*	7.2*	24.2*
-30	132.6	-70.4*	-51.2*	-35.0*	-25.5*	-1.3 [#]	14.2*
-15	127.3	-69.2*	-50.3*	-35.2*	-26.1*	-4.2*	10.0*

* p < 0.05, # p > 0.05

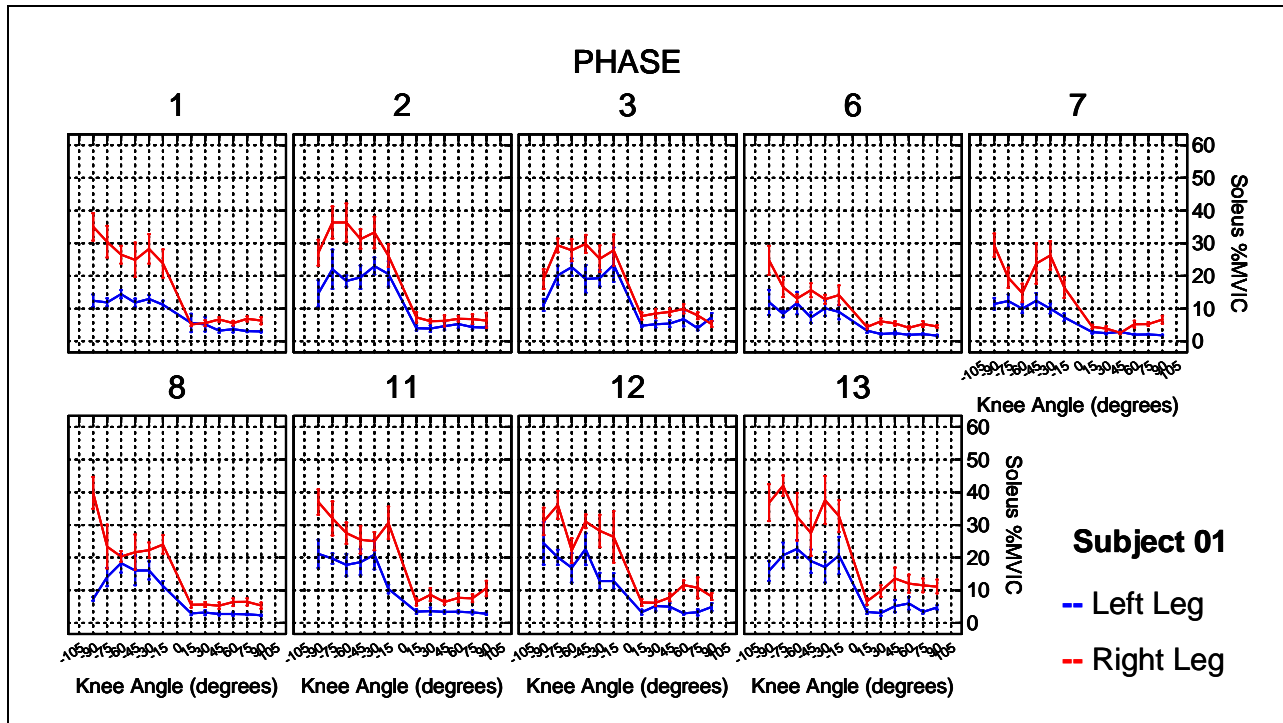
Differences in mean total foot force data during centrifugation compared to upright squats with 25% body weight additional resistance as a function of knee angle. Differences were tested with t-Tests with Bonferroni correction for multiple contrasts.

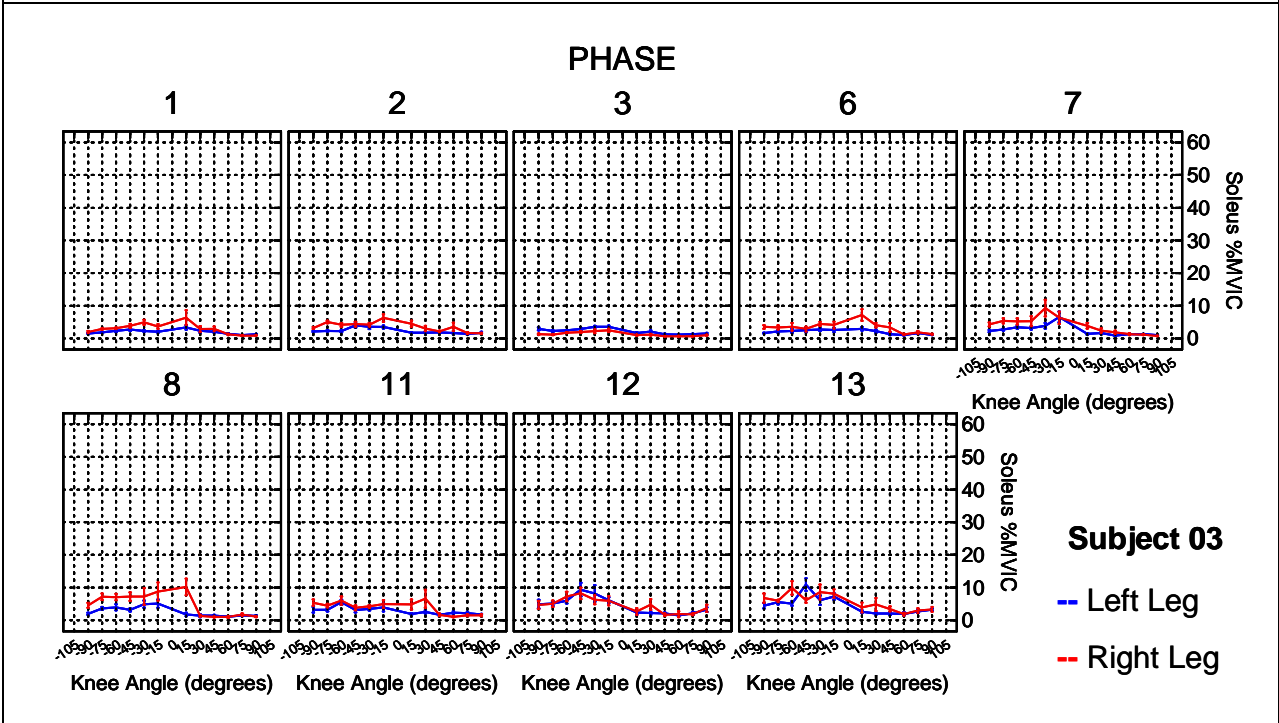
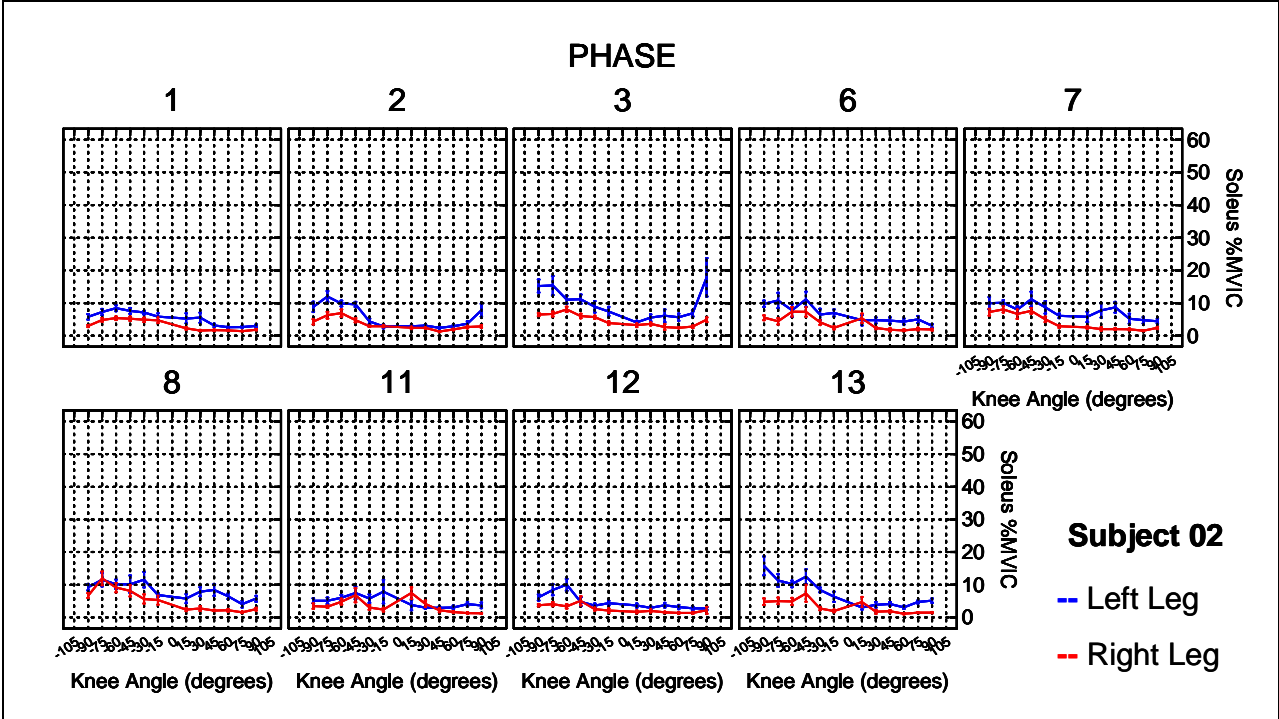
Knee Angle	Upright 25%	23-RPM 0%	23-RPM 10%	23-RPM 25%	30-RPM 0%	30-RPM 10%	30-RPM 25%
15	129.0	-70.9*	-57.2*	-46.1*	-26.0*	-14.9*	-4.6*
30	122.3	-65.9*	-52.9*	-41.8*	-22.3*	-8.2*	3.0 [#]
45	118.3	-59.8*	-47.2*	-35.9*	-13.6*	0.4 [#]	12.5*
60	120.3	-56.6*	-43.9*	-30.8*	-8.3*	7.3*	20.8*
75	126.1	-55.1*	-41.5*	-28.6*	-2.7 [#]	12.4*	25.2*
90	128.5	-45.8*	-32.3*	-22.6*	8.9*	22.7*	35.6*
-90	144.6	-54.2*	-33.1*	-18.4*	6.2*	27.0*	40.7*
-75	156.1	-73.7*	-51.3*	-34.7*	-16.1*	7.9*	26.3*
-60	157.5	-82.3*	-58.8*	-42.5*	-27.4*	-3.1 [#]	15.0*
-45	153.7	-85.5*	-63.7*	-46.7*	-34.8*	-9.9*	7.2*
-30	149.7	-87.5*	-68.4*	-52.1*	-42.6*	-18.5*	-2.9 [#]
-15	146.0	-87.9*	-68.9*	-53.8*	-44.7*	-22.8*	-8.6*

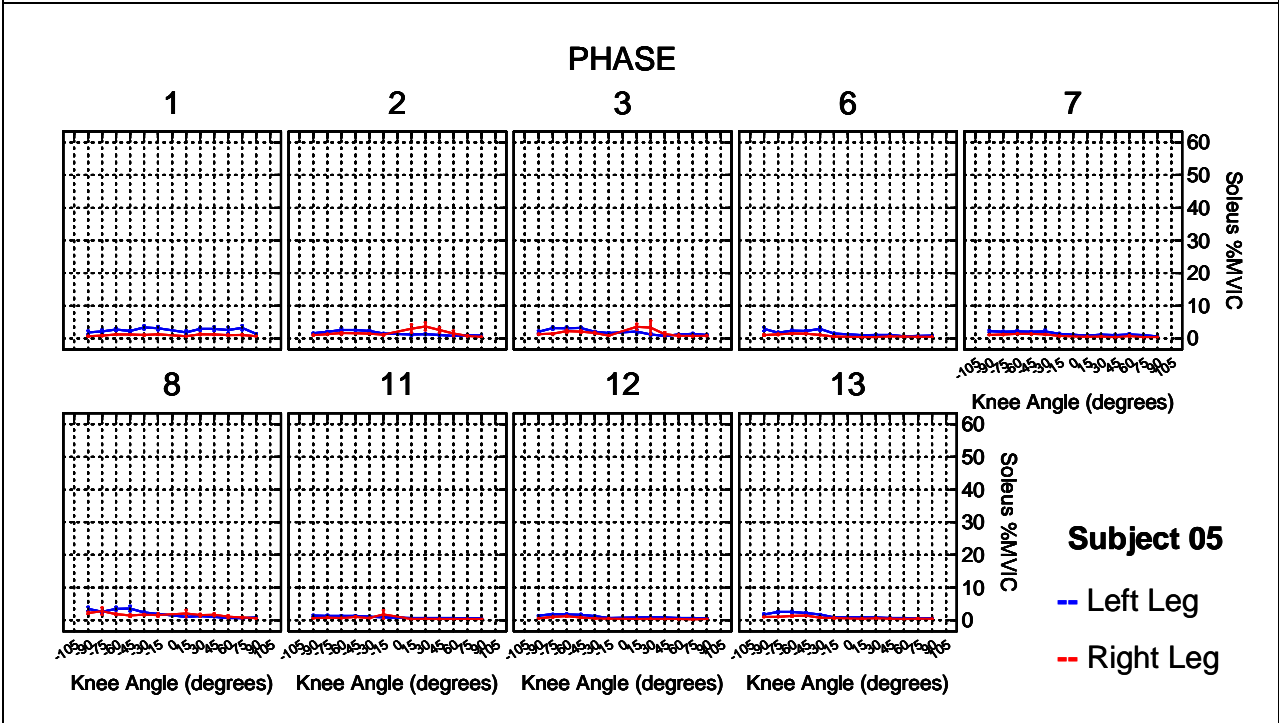
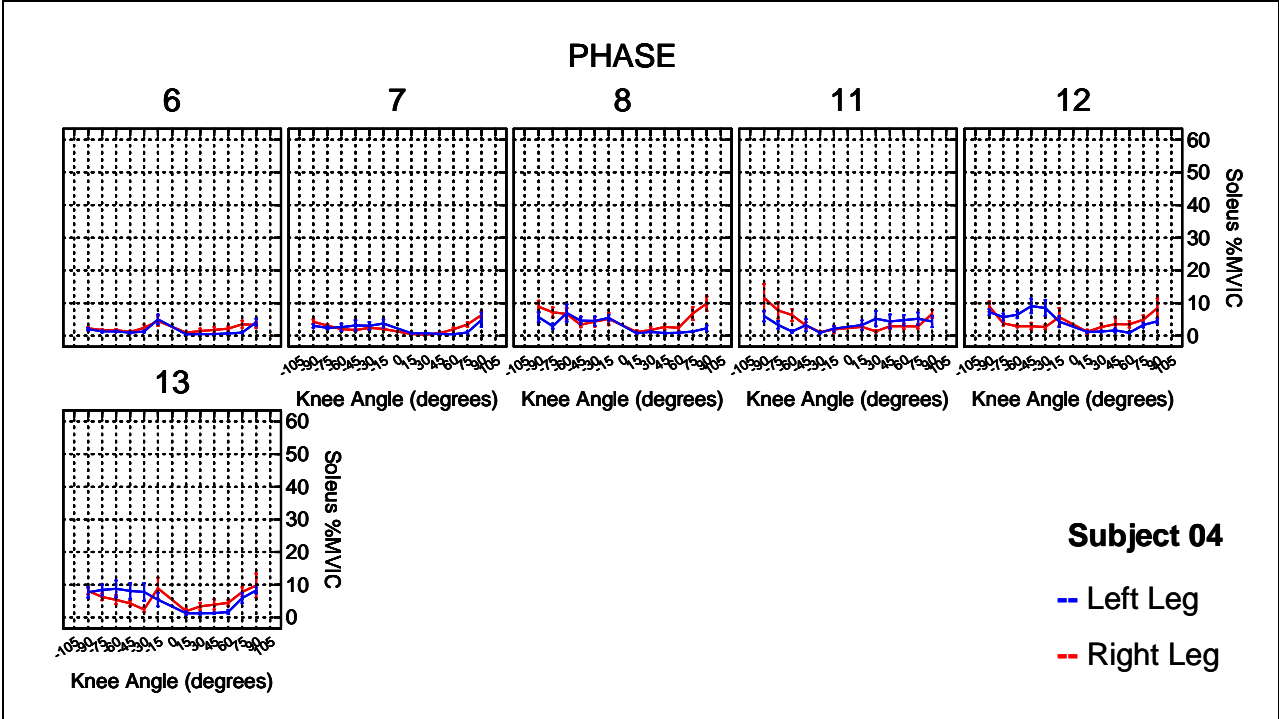
* p < 0.05, # p > 0.05

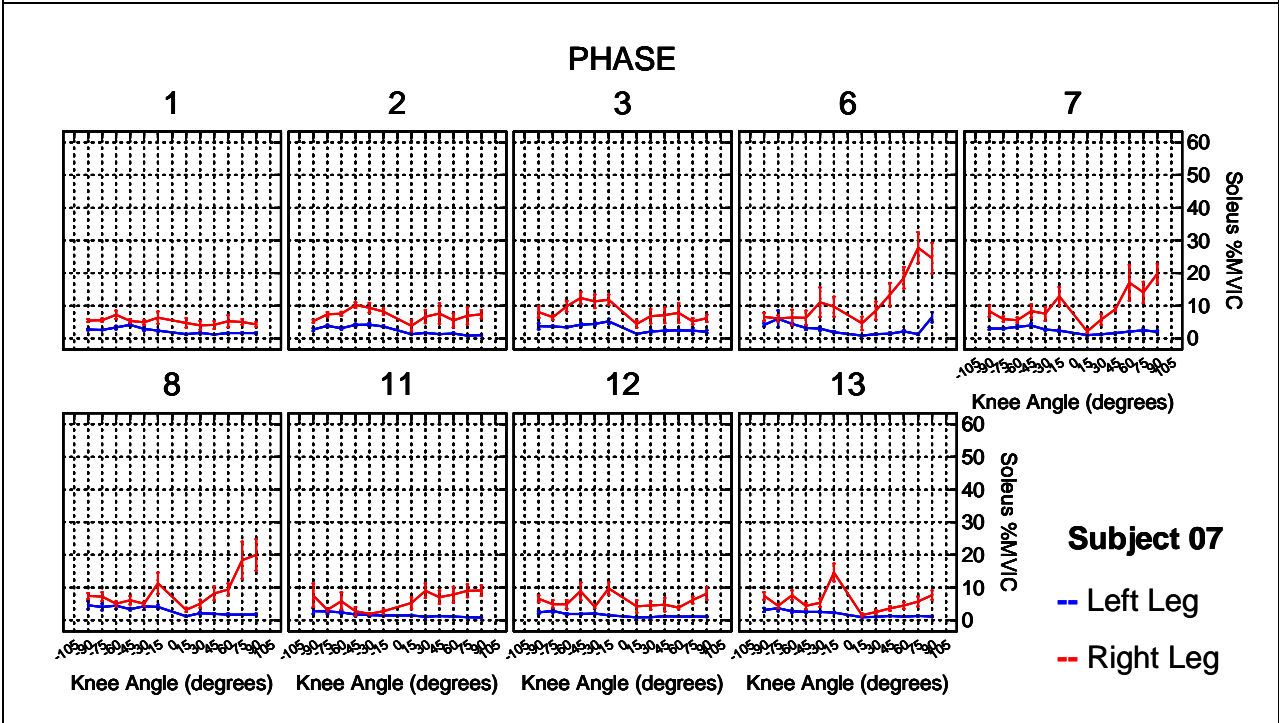
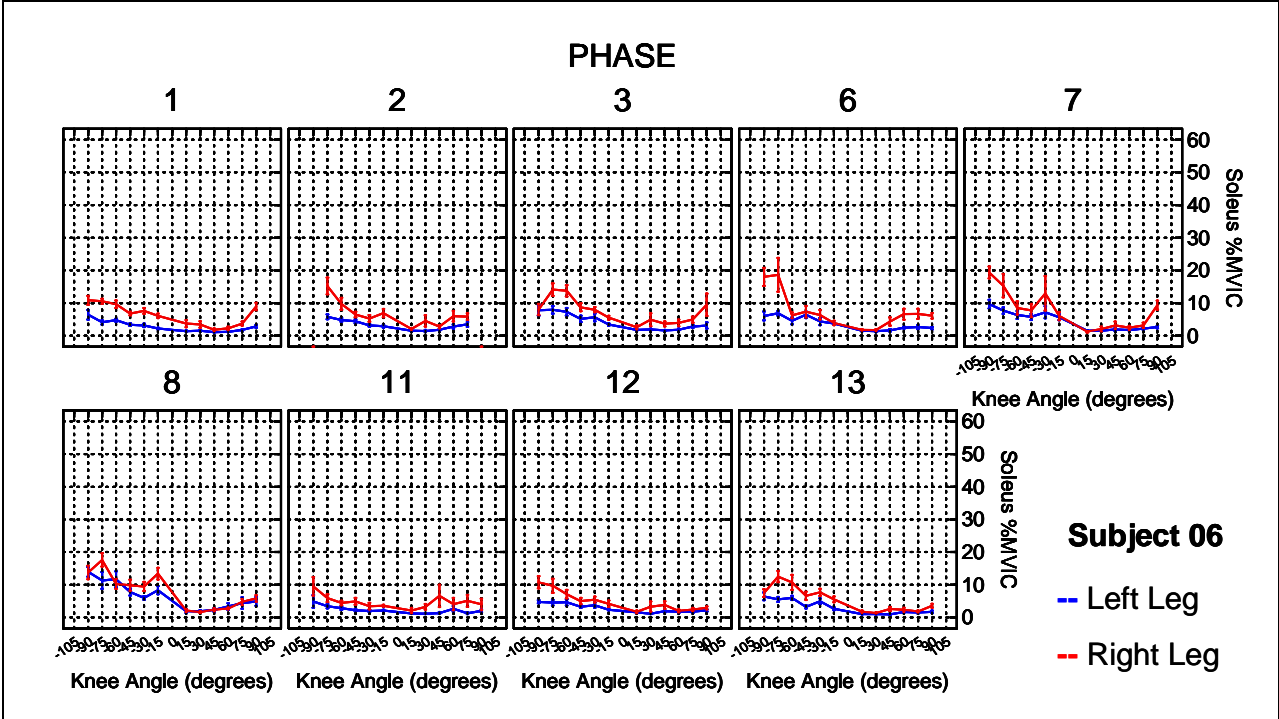
Muscle Activity

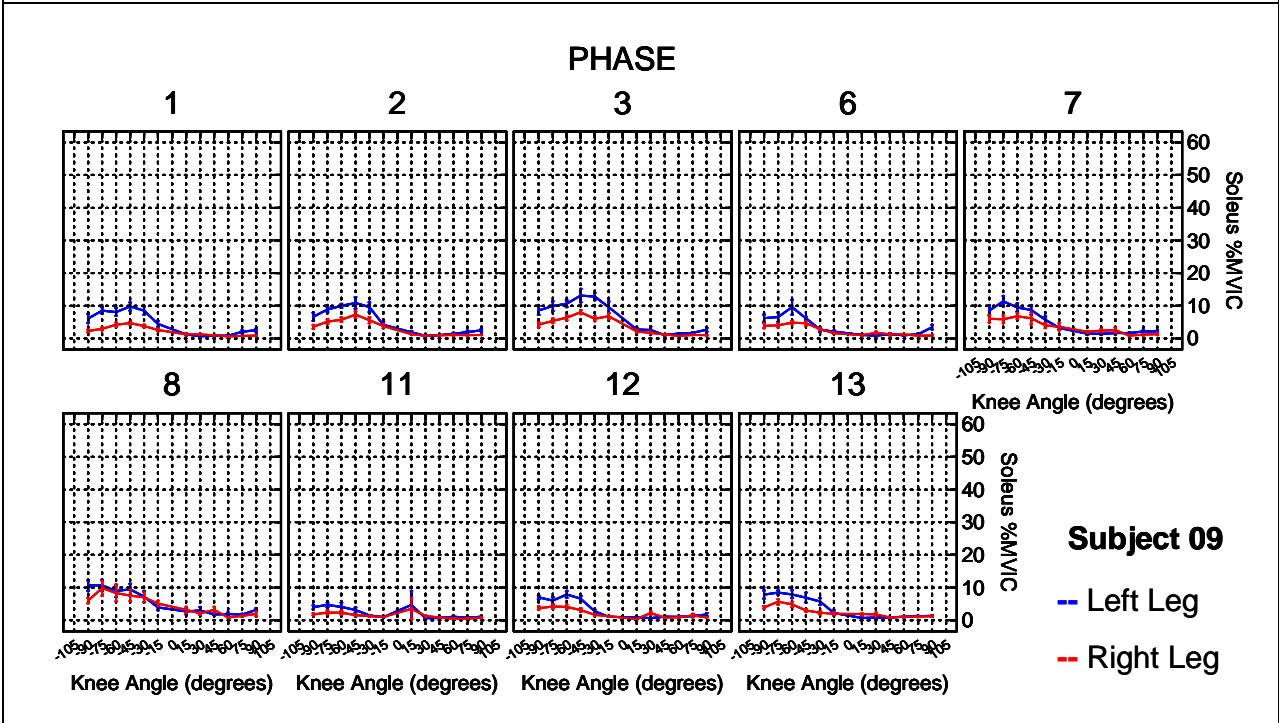
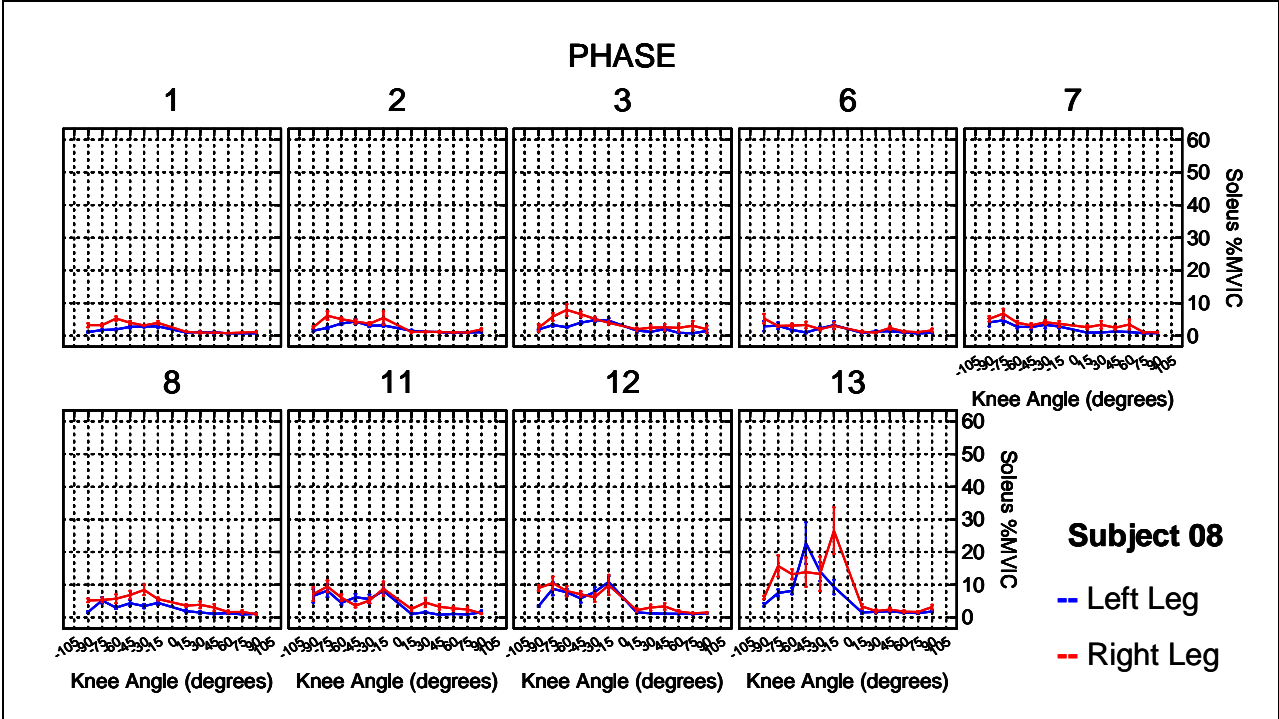
The muscle activity (%MVIC) in Experiment 2 is plotted for the right and left leg. Mean +/- SEM. The weighted phases, Phases 1-3, 6-8, and 11-13 are the only ones shown. To determine whether Phases 6-8 or 11-13 are at 23 or 30 RPM, check with the subject assignment group assignment at the beginning of this section with Experiment 2 data. At the end of the plots for each muscle group, the contrasts between conditions are presented. A p-value > 0.05 indicates that the conditions were not significantly different (these are the ones we're interested in for protocol design). All contrasts were Bonferroni-corrected for multiple comparisons.

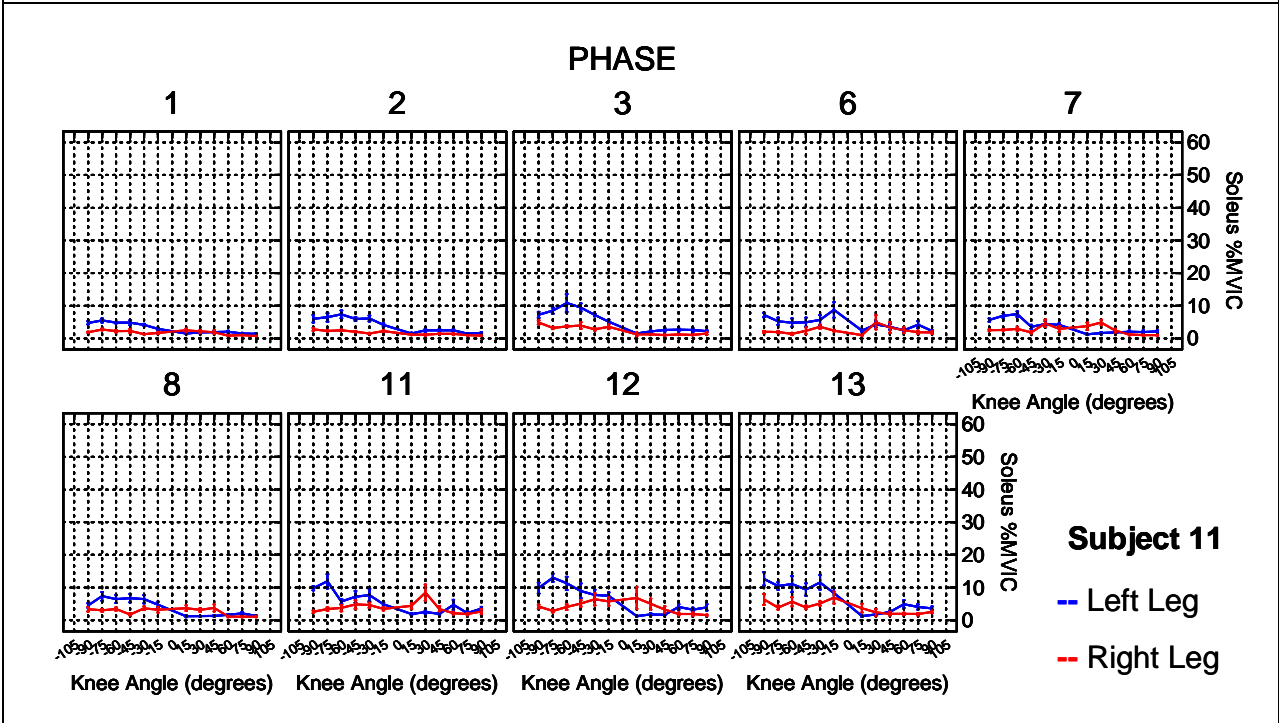
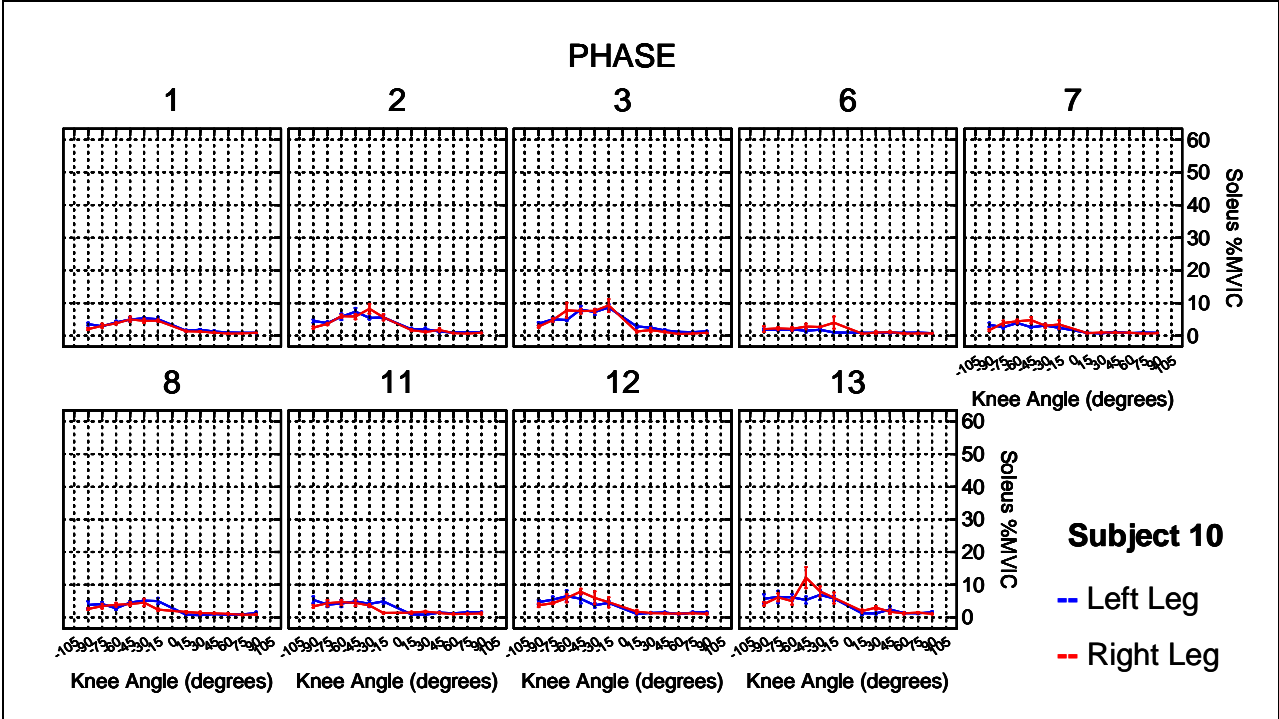


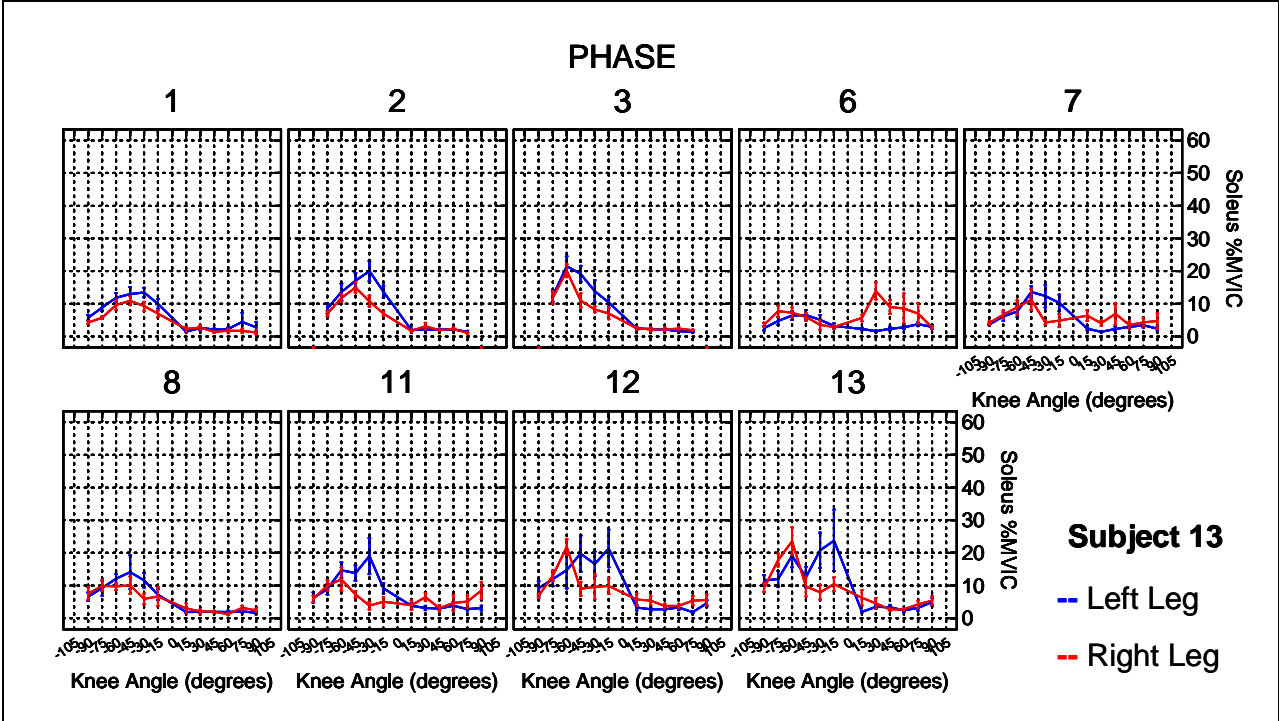
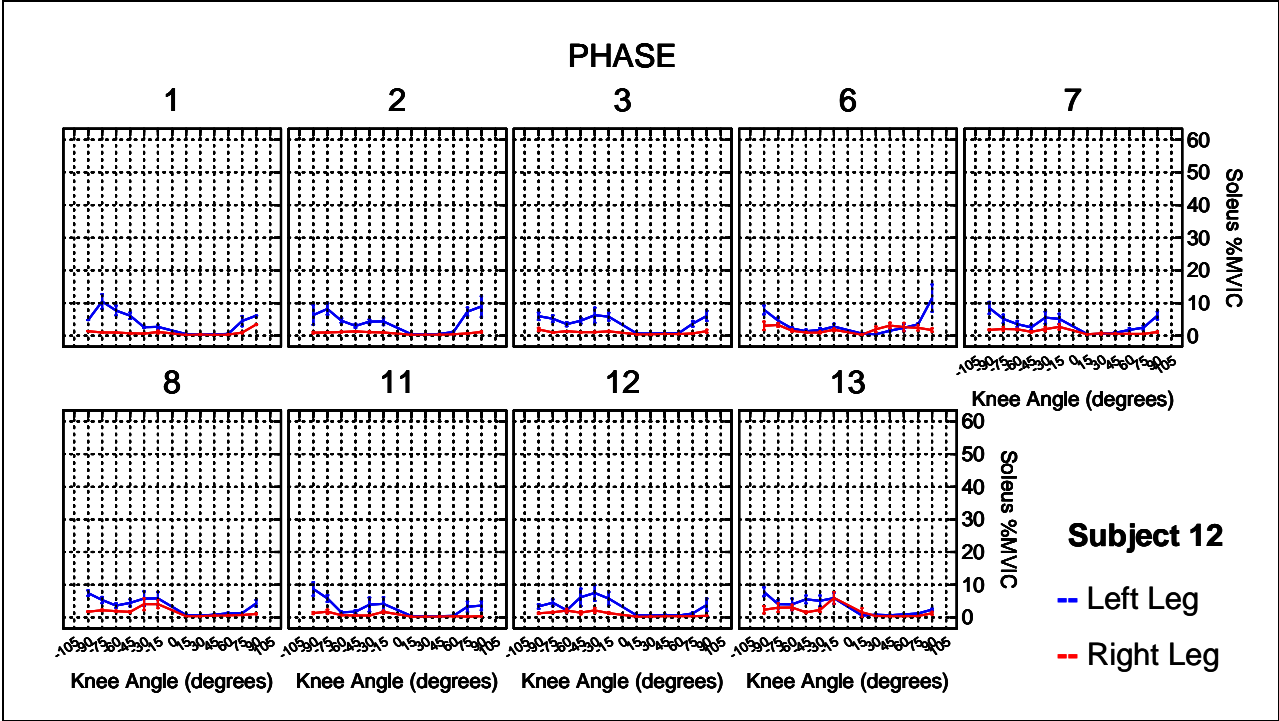












Left Soleus

Knee Angle	Up 0%	23-RPM 0%	23-RPM 10%	23-RPM 25%	30-RPM 0%	30-RPM 10%	30-RPM 25%
15	5.85	-1.95*	-1.52 [#]	-0.85 [#]	1.10 [#]	1.54 [#]	2.71*
30	6.87	-2.06 [#]	-1.37 [#]	-0.56 [#]	2.95*	1.92 [#]	5.43*
45	5.54	0.00 [#]	0.04 [#]	2.00 [#]	4.26*	6.79*	10.50*
60	5.33	0.92 [#]	1.66 [#]	2.28*	5.16*	4.45*	5.83*
75	5.81	-0.49 [#]	-0.02 [#]	1.53 [#]	4.22*	3.75*	4.78*
90	6.64	-1.67 [#]	-1.02 [#]	-1.30 [#]	2.76 [#]	1.35 [#]	2.94 [#]
-90	13.49	-3.65 [#]	0.25 [#]	1.27 [#]	7.58 [#]	9.36*	15.07*
-75	13.87	-4.80*	0.36 [#]	4.92 [#]	6.81*	9.63*	14.58*
-60	15.05	-5.38*	-1.13 [#]	1.80 [#]	5.15 [#]	8.75*	15.33*
-45	15.47	-6.33*	-1.95 [#]	1.16 [#]	2.21 [#]	4.28 [#]	11.97*
-30	16.48	-8.52*	-5.09*	-1.40 [#]	1.86 [#]	3.31 [#]	5.92*
-15	14.13	-7.13*	-5.58*	0.24 [#]	-1.01 [#]	1.59 [#]	6.51*

* p < 0.05, # p > 0.05

Knee Angle	Up 10%	23-RPM 0%	23-RPM 10%	23-RPM 25%	30-RPM 0%	30-RPM 10%	30-RPM 25%
15	6.11	-2.21*	-1.78*	-1.11 [#]	0.84 [#]	1.28 [#]	2.45*
30	6.20	-1.39 [#]	-0.70 [#]	0.11 [#]	3.62*	2.60*	6.10*
45	6.93	-1.40 [#]	-1.36 [#]	0.61 [#]	2.87 [#]	5.39*	9.11*
60	7.39	-1.14 [#]	-0.40 [#]	0.22 [#]	3.10*	2.39 [#]	3.77*
75	6.08	-0.76 [#]	-0.29 [#]	1.26 [#]	3.95*	3.48*	4.51*
90	4.24	0.72 [#]	1.37 [#]	1.09 [#]	5.15*	3.75*	5.34*
-90	15.02	-5.18*	-1.28 [#]	-0.26 [#]	6.05*	7.83*	13.55*
-75	19.37	-10.30*	-5.14*	-0.58 [#]	1.31 [#]	4.13 [#]	9.09*
-60	21.19	-11.52*	-7.27*	-4.34 [#]	-0.99 [#]	2.61 [#]	9.19*
-45	21.18	-12.05*	-7.66*	-4.56 [#]	-3.50 [#]	-1.43 [#]	6.26 [#]
-30	19.87	-11.92*	-8.49*	-4.79 [#]	-1.54 [#]	-0.09 [#]	2.52 [#]
-15	16.58	-9.59*	-8.04*	-2.22 [#]	-3.46 [#]	-0.87 [#]	4.06 [#]

* p < 0.05, # p > 0.05

Knee Angle	Up 25%	23-RPM 0%	23-RPM 10%	23-RPM 25%	30-RPM 0%	30-RPM 10%	30-RPM 25%
15	7.57	-3.67*	-3.24*	-2.57 [#]	-0.62 [#]	-0.18 [#]	0.99 [#]
30	9.68	-4.88*	-4.18*	-3.37 [#]	0.14 [#]	-0.89 [#]	2.62 [#]
45	10.30	-4.76*	-4.72*	-2.76 [#]	-0.49 [#]	2.03 [#]	5.74*
60	7.85	-1.60 [#]	-0.86 [#]	-0.24 [#]	2.64 [#]	1.93 [#]	3.31*
75	8.51	-3.19*	-2.73 [#]	-1.17 [#]	1.51 [#]	1.04 [#]	2.07 [#]
90	7.49	-2.53*	-1.88 [#]	-2.16 [#]	1.90 [#]	0.49 [#]	2.08 [#]
-90	15.14	-5.30*	-1.40 [#]	-0.38 [#]	5.93*	7.71*	13.43*
-75	22.61	-13.54*	-8.38*	-3.82 [#]	-1.94 [#]	0.89 [#]	5.84*
-60	22.28	-12.62*	-8.37*	-5.43*	-2.09 [#]	1.51 [#]	8.09*
-45	26.27	-17.13*	-12.75*	-9.64*	-8.59*	-6.52*	1.17 [#]
-30	21.83	-13.88*	-10.45*	-6.75*	-3.50 [#]	-2.05 [#]	0.56 [#]
-15	19.69	-12.69*	-11.14*	-5.33*	-6.57*	-3.97 [#]	0.95 [#]

* p < 0.05, # p > 0.05

Right Soleus

Knee Angle	Up 0%	23-RPM 0%	23-RPM 10%	23-RPM 25%	30-RPM 0%	30-RPM 10%	30-RPM 25%
15	4.02	-1.47*	-0.89 [#]	0.22 [#]	-0.13 [#]	1.31*	2.55*
30	4.24	-0.91 [#]	-0.95 [#]	0.17 [#]	2.13*	2.34*	3.52*
45	4.50	-1.18*	-0.87 [#]	-0.16 [#]	4.22*	2.64*	5.46*
60	4.05	-0.17 [#]	1.43*	1.13 [#]	6.46*	4.79*	5.58*
75	4.69	-1.18*	0.14 [#]	1.19 [#]	4.82*	4.26*	5.35*
90	4.99	-0.76 [#]	0.43 [#]	1.07 [#]	4.36*	4.37*	6.32*
-90	13.28	-0.30 [#]	4.23*	8.03*	9.19*	15.71*	20.36*
-75	13.82	-2.55 [#]	4.17*	7.57*	8.50*	15.17*	19.36*
-60	13.63	-2.22 [#]	1.83 [#]	5.13*	4.82*	12.71*	16.19*
-45	13.76	-3.07*	-0.51 [#]	5.74*	4.50*	8.05*	13.91*
-30	13.14	-5.91*	-2.75 [#]	0.70 [#]	1.17 [#]	6.52*	12.16*
-15	11.75	-5.91*	-3.84*	-0.93 [#]	-1.37 [#]	3.50*	9.09*

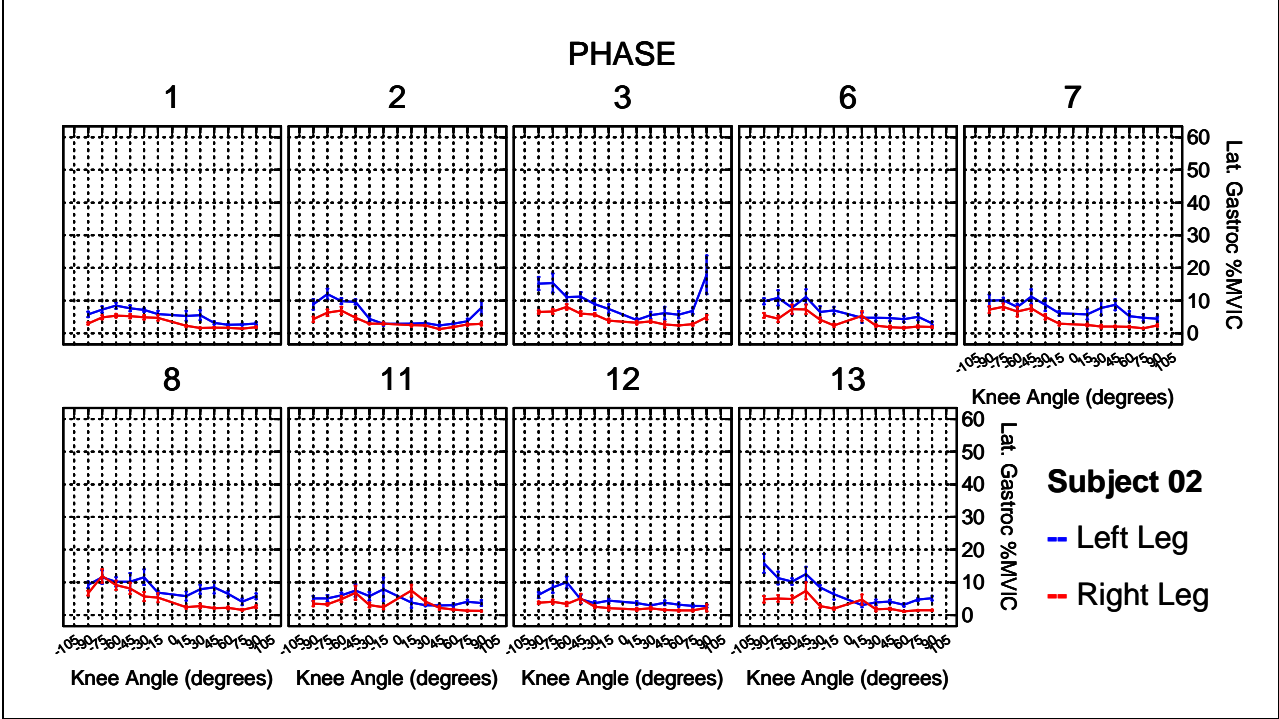
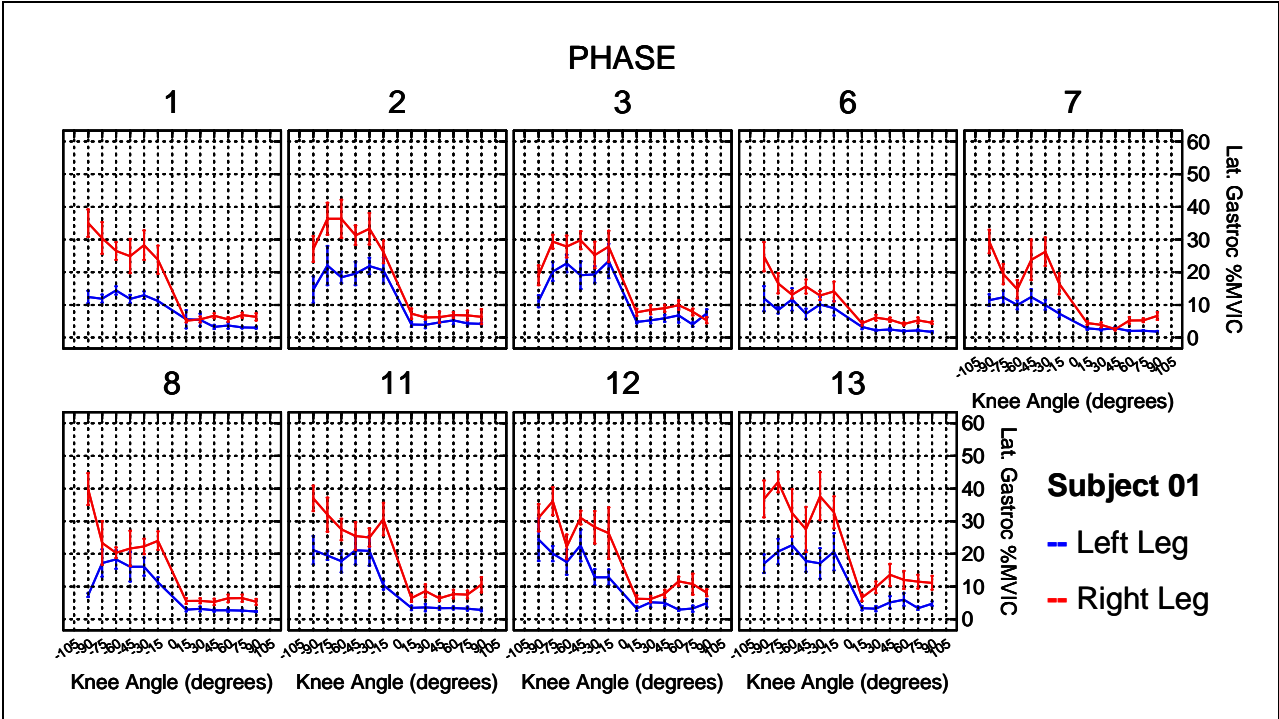
* p < 0.05, # p > 0.05

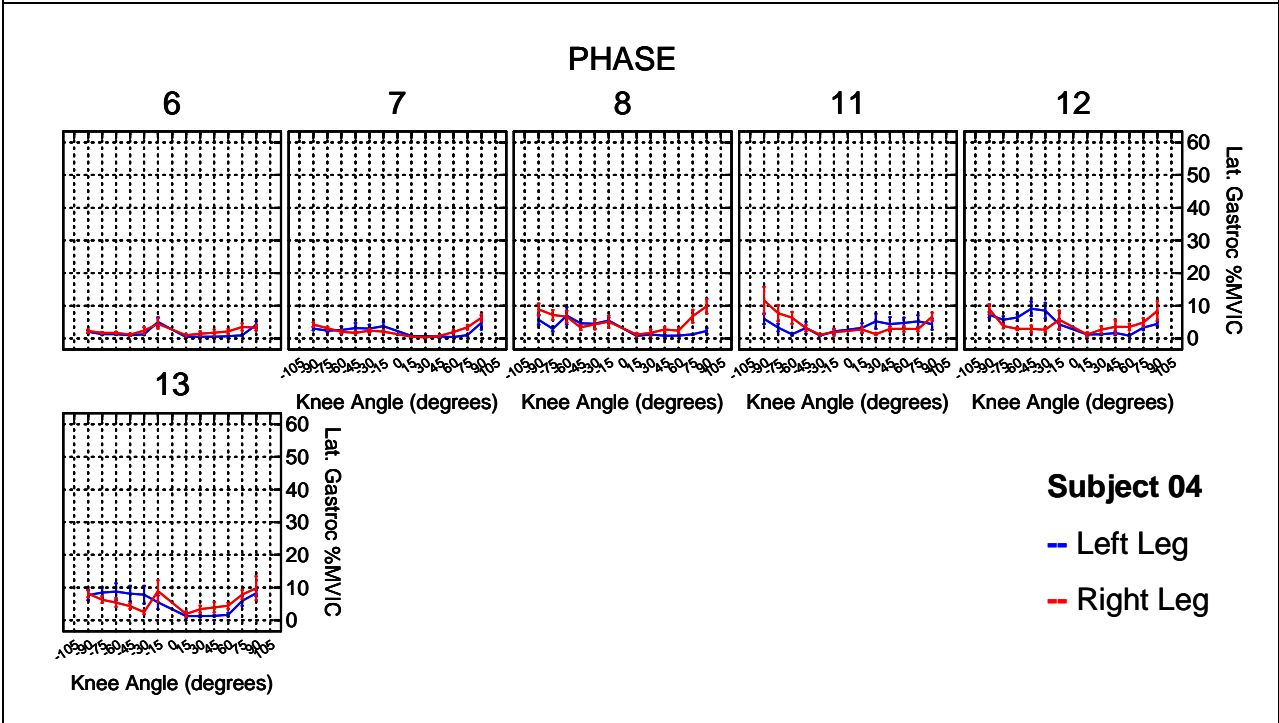
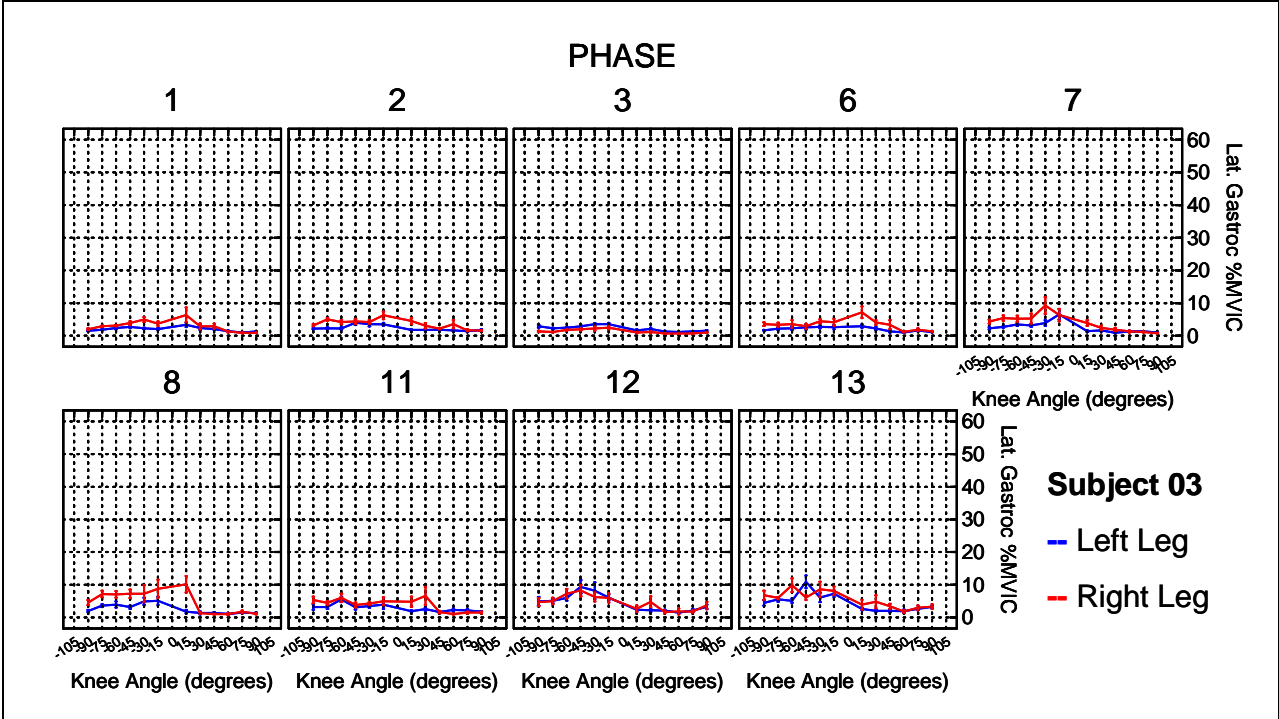
Knee Angle	Up 10%	23-RPM 0%	23-RPM 10%	23-RPM 25%	30-RPM 0%	30-RPM 10%	30-RPM 25%
15	4.21	-1.66*	-1.08 [#]	0.03 [#]	-0.32 [#]	1.12 [#]	2.36*
30	5.33	-2.00*	-2.04*	-0.92 [#]	1.04 [#]	1.25 [#]	2.43*
45	5.51	-2.18*	-1.88*	-1.16 [#]	3.22*	1.63 [#]	4.45*
60	5.43	-1.56*	0.05 [#]	-0.26 [#]	5.07*	3.41*	4.20*
75	4.67	-1.17*	0.15 [#]	1.20 [#]	4.83*	4.27*	5.37*
90	5.06	-0.83 [#]	0.36 [#]	1.00 [#]	4.30*	4.30*	6.25*
-90	12.91	0.07 [#]	4.60*	8.40*	9.56*	16.08*	20.73*
-75	18.27	-7.00*	-0.29 [#]	3.12 [#]	4.05 [#]	10.72*	14.91*
-60	18.52	-7.11*	-3.06*	0.24 [#]	-0.07 [#]	7.82*	11.30*
-45	18.20	-7.52*	-4.96*	1.29 [#]	0.06 [#]	3.61*	9.46*
-30	14.59	-7.37*	-4.20*	-0.75 [#]	-0.28 [#]	5.06*	10.71*
-15	12.05	-6.21*	-4.14*	-1.24 [#]	-1.67 [#]	3.20*	8.78*

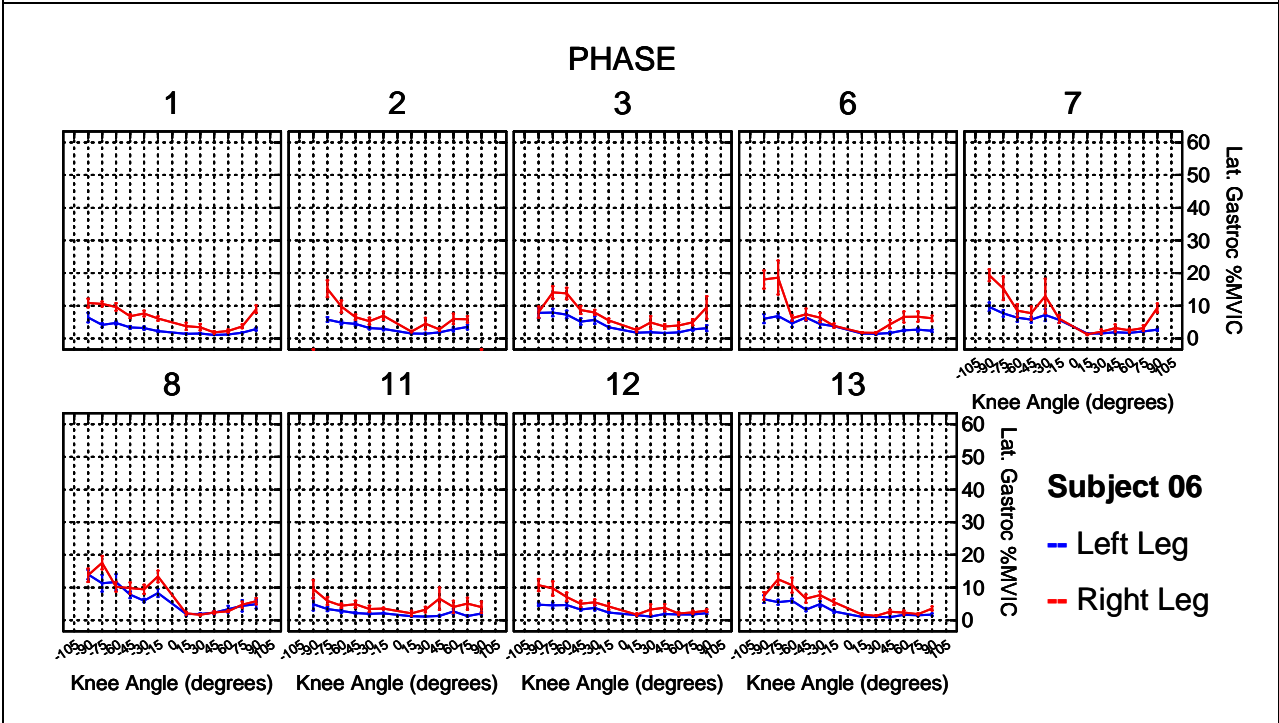
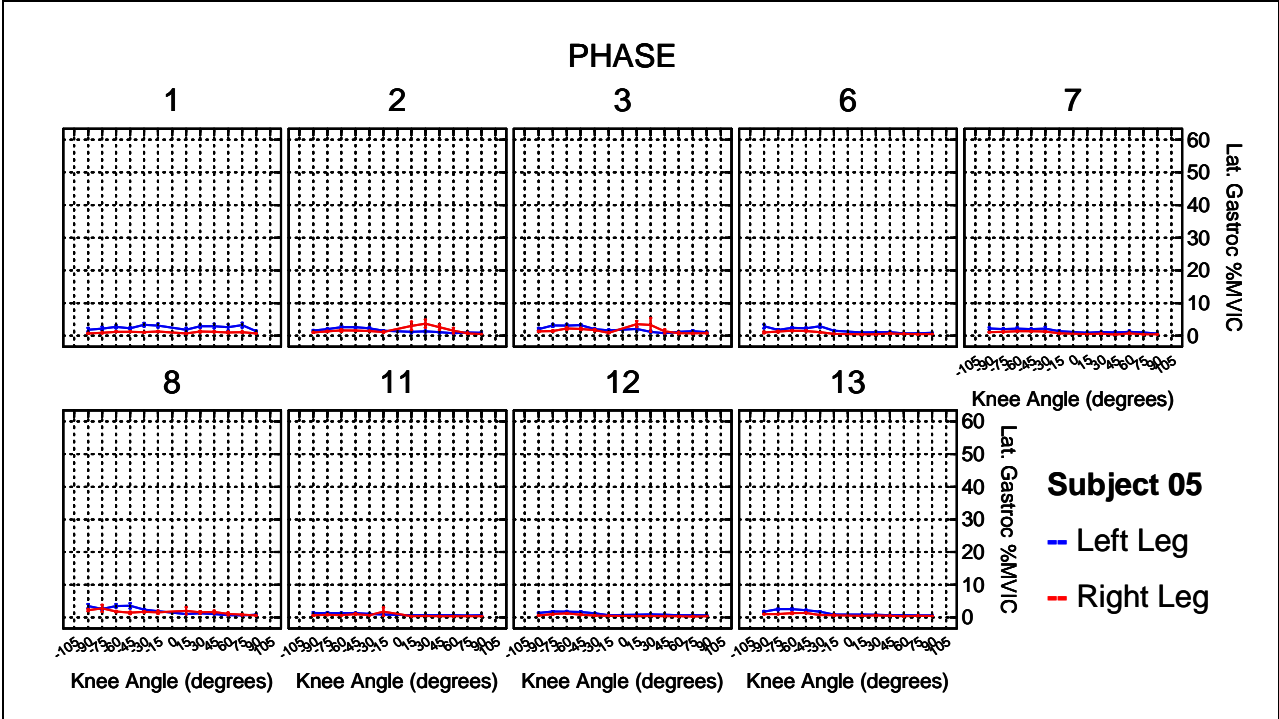
* p < 0.05, # p > 0.05

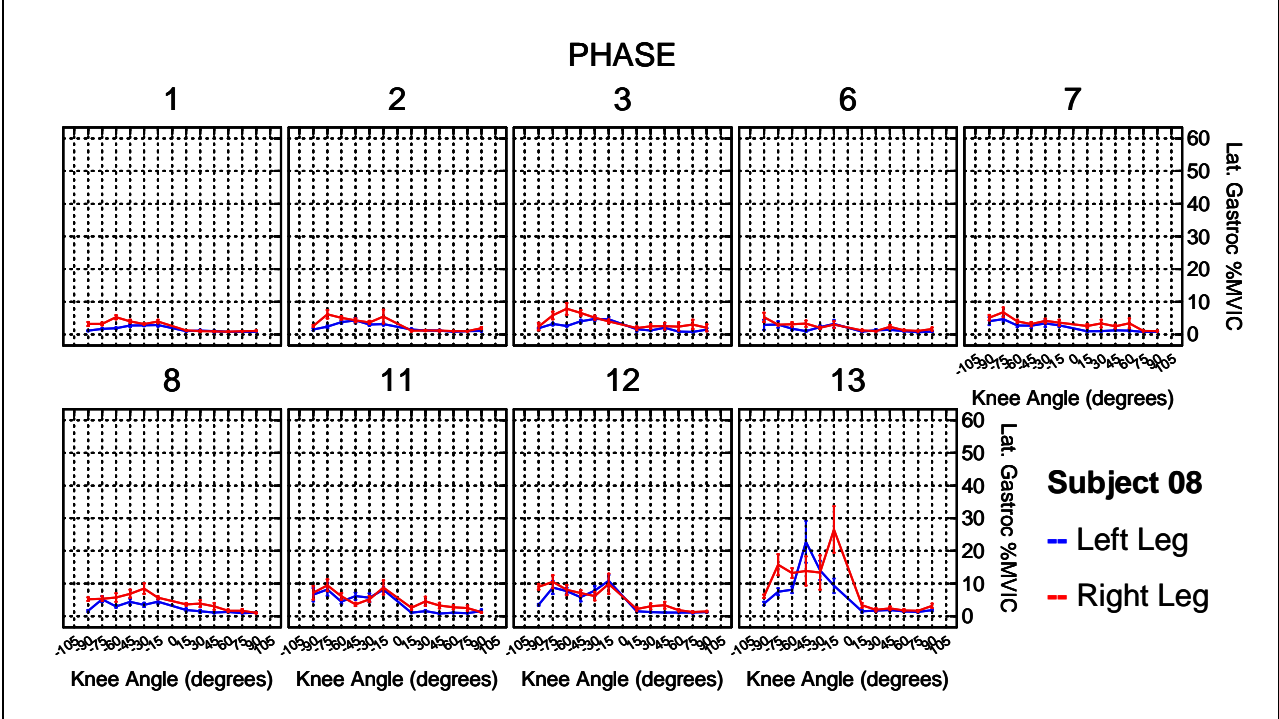
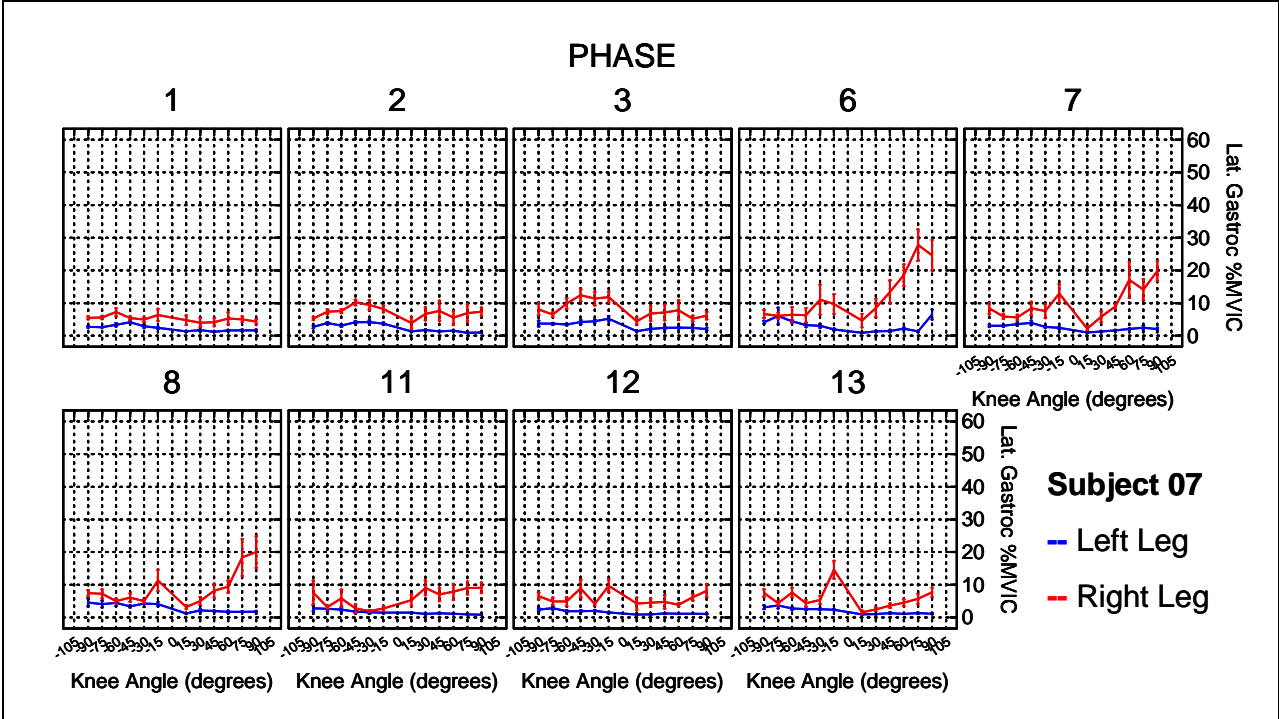
Knee Angle	Up 25%	23-RPM 0%	23-RPM 10%	23-RPM 25%	30-RPM 0%	30-RPM 10%	30-RPM 25%
15	6.14	-3.59*	-3.01*	-1.90*	-2.26*	-0.81 [#]	0.43 [#]
30	7.10	-3.78*	-3.82*	-2.70*	-0.73 [#]	-0.52 [#]	0.65 [#]
45	6.88	-3.56*	-3.25*	-2.54*	1.84 [#]	0.26 [#]	3.08*
60	6.99	-3.12*	-1.51 [#]	-1.81 [#]	3.52*	1.85 [#]	2.64*
75	5.80	-2.30*	-0.98 [#]	0.07 [#]	3.70*	3.14*	4.23*
90	6.30	-2.06*	-0.88 [#]	-0.24 [#]	3.06*	3.07*	5.01*
-90	15.87	-2.89*	1.64 [#]	5.44*	6.60*	13.12*	17.77*
-75	22.81	-11.54*	-4.83*	-1.42 [#]	-0.49 [#]	6.18*	10.37*
-60	23.45	-12.04*	-7.99*	-4.69*	-5.01*	2.88 [#]	6.37*
-45	21.09	-10.40*	-7.84*	-1.59 [#]	-2.83 [#]	0.73 [#]	6.58*
-30	19.52	-12.29*	-9.12*	-5.68*	-5.20*	0.14 [#]	5.78*
-15	17.65	-11.81*	-9.74*	-6.83*	-7.27*	-2.40 [#]	3.18*

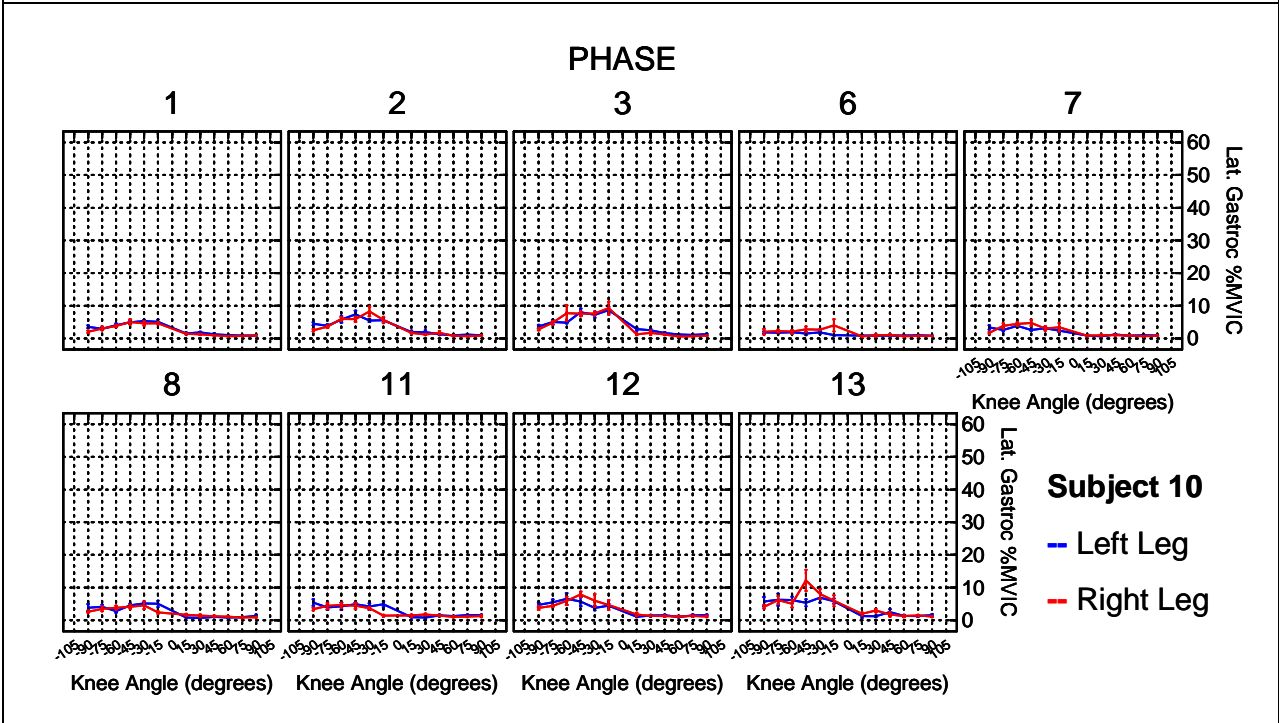
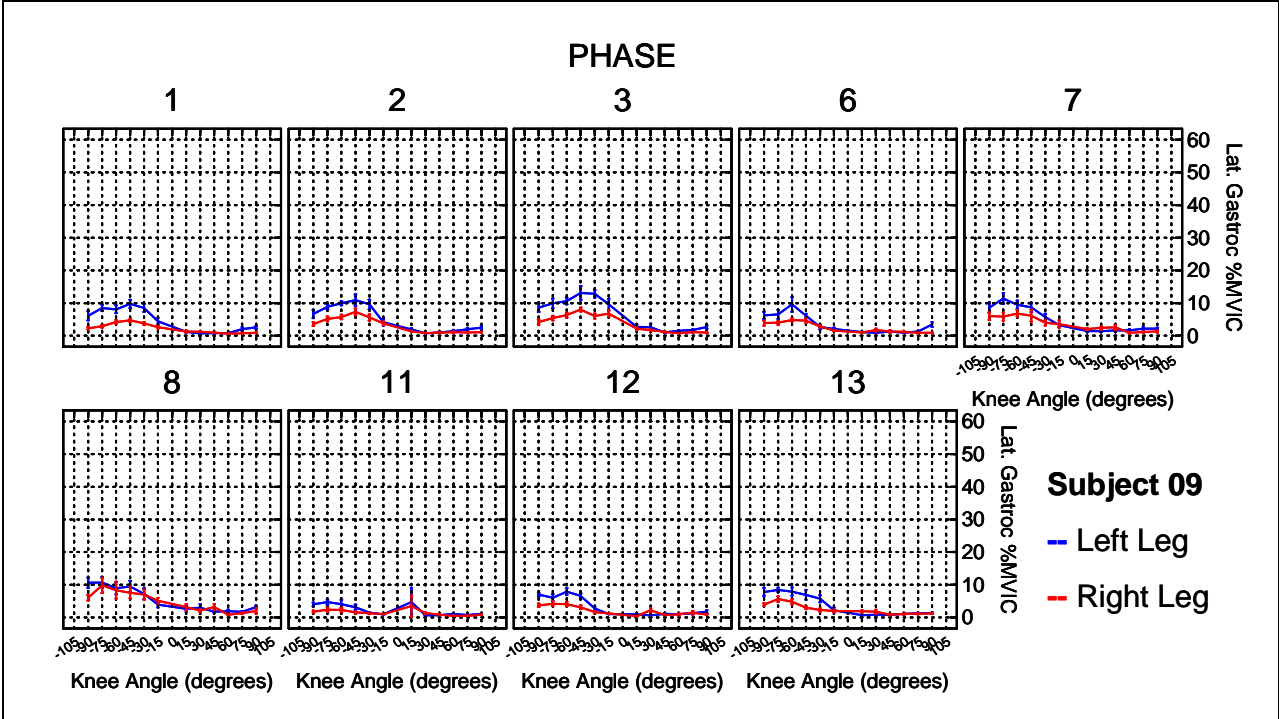
* p < 0.05, # p > 0.05

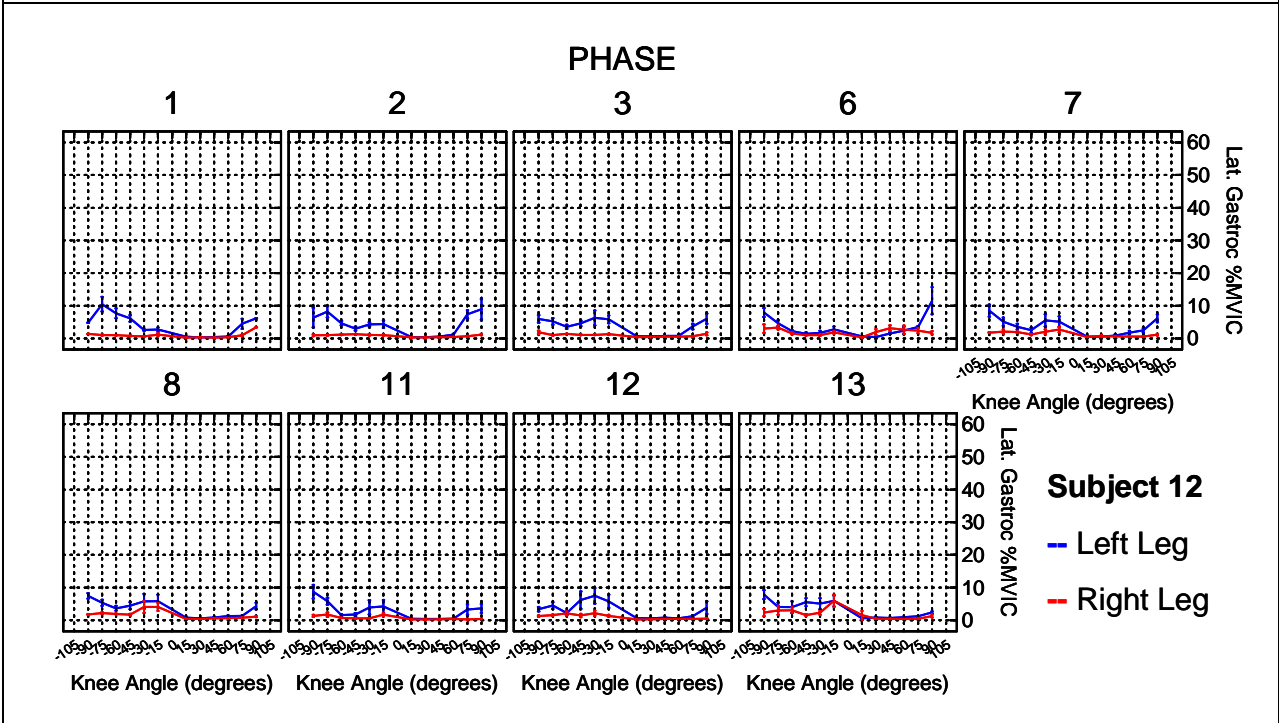
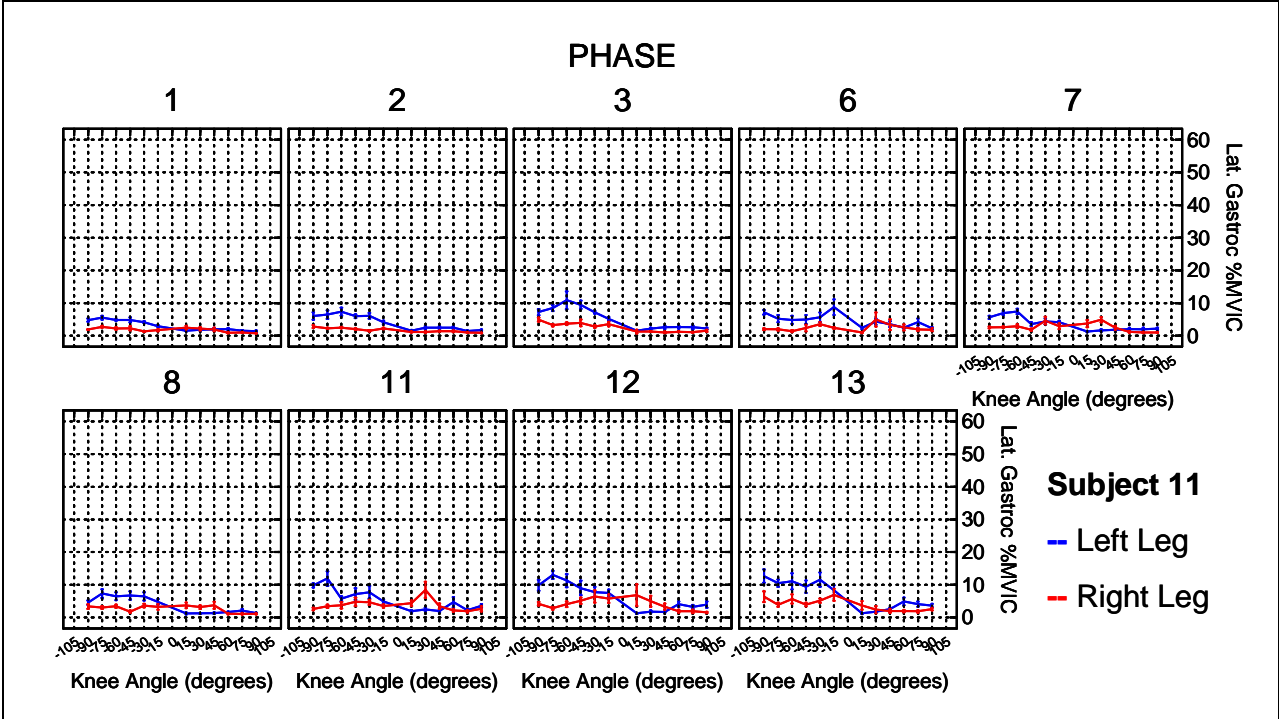


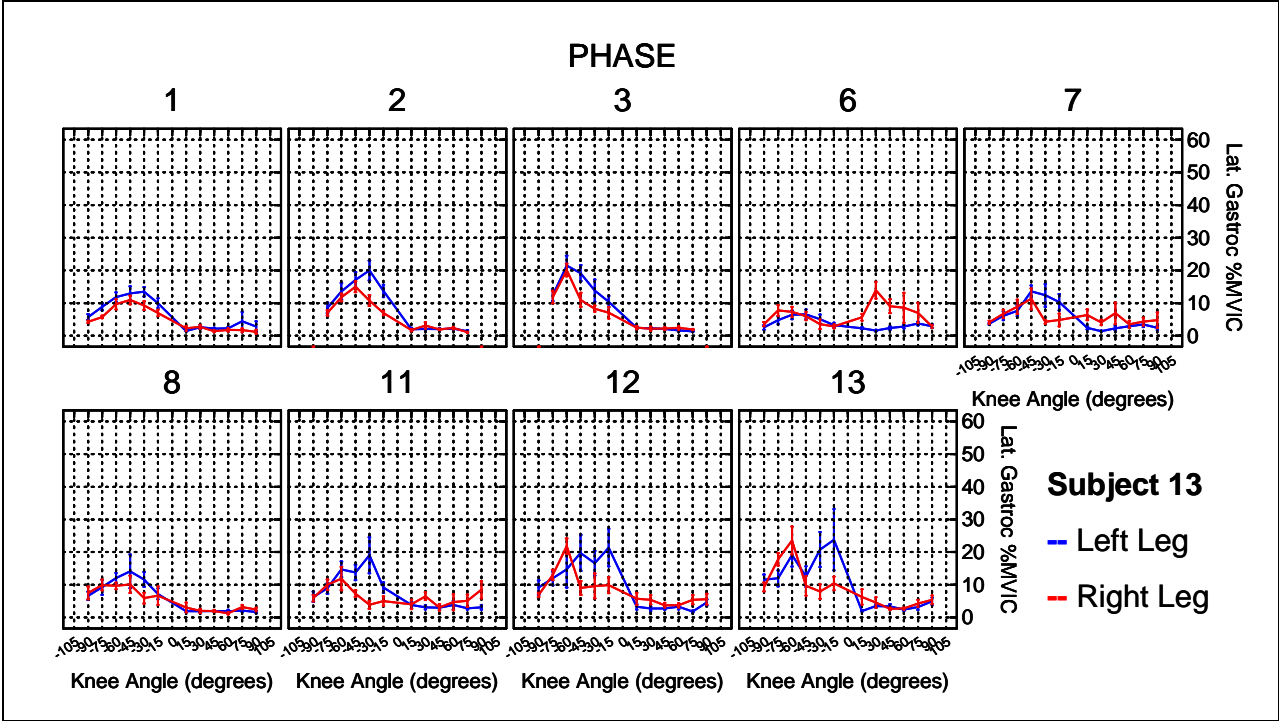












Left Lateral Gastrocnemius

Knee Angle	Up 0%	23-RPM 0%	23-RPM 10%	23-RPM 25%	30-RPM 0%	30-RPM 10%	30-RPM 25%
15	2.19	-0.23 [#]	-0.72 [*]	-0.75 [*]	-0.18 [#]	-0.02 [#]	-0.13 [#]
30	2.34	-0.78 [*]	-1.03 [*]	-0.82 [*]	-0.10 [#]	0.73 [#]	0.10 [#]
45	2.68	-1.14 [#]	-1.09 [#]	-1.21 [#]	-0.50 [#]	0.90 [#]	0.03 [#]
60	1.74	-0.19 [#]	-0.25 [#]	-0.27 [#]	0.91 [*]	0.65 [#]	0.98
75	2.32	-0.37 [#]	-0.73 [*]	-0.61 [#]	0.18 [#]	0.46 [#]	0.43 [#]
90	1.99	0.01 [#]	0.04 [#]	-0.13 [#]	1.61 [#]	1.24 [*]	1.80 [*]
-90	4.70	-0.30 [#]	-0.18 [#]	1.06 [#]	2.67 [*]	3.74 [*]	3.94 [*]
-75	5.68	-1.84 [*]	-0.57 [#]	0.89 [#]	1.72 [*]	4.61 [*]	3.30 [*]
-60	6.23	-2.48 [*]	-1.13 [#]	0.47 [#]	0.81 [#]	4.70 [*]	3.27 [*]
-45	6.14	-2.85 [*]	-1.08 [#]	0.54 [#]	0.85 [#]	5.62 [*]	3.54 [*]
-30	5.75	-2.29 [*]	-1.04 [#]	0.47 [#]	0.72 [#]	4.06 [*]	4.19 [*]
-15	4.59	-0.71 [#]	-0.49 [#]	0.32 [#]	0.27 [#]	3.16 [*]	5.24 [*]

* p < 0.05, # p > 0.05

Knee Angle	Up 10%	23-RPM 0%	23-RPM 10%	23-RPM 25%	30-RPM 0%	30-RPM 10%	30-RPM 25%
15	1.86	0.10 [#]	-0.39 [*]	-0.42 [*]	0.15 [#]	0.08 [#]	0.20 [#]
30	1.87	-0.32 [#]	-0.56 [*]	-0.35 [#]	0.36 [#]	0.42 [#]	0.56 [#]
45	1.82	-0.28 [#]	-0.23 [#]	-0.35 [#]	0.35 [#]	0.62 [#]	0.89 [*]
60	2.01	-0.46 [#]	-0.52 [*]	-0.54 [*]	0.64 [#]	0.19 [#]	0.71 [*]
75	2.45	-0.49 [#]	-0.86 [*]	-0.73 [*]	0.05 [#]	-0.03 [#]	0.30 [#]
90	2.80	-0.80 [#]	-0.78 [#]	-0.95 [*]	0.79 [*]	0.44 [#]	0.98 [*]
-90	5.48	-1.08 [#]	-0.96 [#]	0.28 [#]	1.89 [*]	2.66 [*]	3.16 [*]
-75	7.22	-3.38 [*]	-2.11 [*]	-0.65 [#]	0.18 [#]	1.23 [#]	1.76 [#]
-60	7.20	-3.45 [*]	-2.10 [*]	-0.50 [#]	-0.16 [#]	1.25 [#]	2.30 [*]
-45	7.77	-4.48 [*]	-2.71 [*]	-1.09 [#]	-0.78 [#]	1.14 [#]	1.91 [#]
-30	7.35	-3.90 [*]	-2.65 [*]	-1.13 [#]	-0.89 [#]	0.16 [#]	2.59 [#]
-15	6.67	-2.80 [*]	-2.58 [*]	-1.77 [#]	-1.82 [#]	0.37 [#]	3.15 [#]

* p < 0.05, # p > 0.05

Knee Angle	Up 25%	23-RPM 0%	23-RPM 10%	23-RPM 25%	30-RPM 0%	30-RPM 10%	30-RPM 25%
15	2.32	-0.36 [#]	-0.85 [*]	-0.88 [*]	-0.31 [#]	-0.38 [#]	-0.26 [#]
30	2.47	-0.92 [*]	-1.17 [*]	-0.96 [*]	-0.24 [#]	-0.19 [#]	-0.04 [#]
45	2.39	-0.85 [*]	-0.80 [*]	-0.92 [*]	-0.21 [#]	0.06 [#]	0.32 [#]
60	2.35	-0.80 [*]	-0.86 [*]	-0.88 [*]	0.30 [#]	-0.15 [#]	0.37 [#]
75	2.51	-0.56 [#]	-0.92 [*]	-0.80 [*]	-0.01 [#]	-0.09 [#]	0.24 [#]
90	4.60	-2.60 [*]	-2.57 [*]	-2.74 [*]	-1.01 [#]	-1.36 [#]	-0.81 [#]
-90	6.83	-2.42 [*]	-2.31 [*]	-1.06 [#]	0.54 [#]	1.31 [#]	1.81
-75	8.09	-4.25 [*]	-2.99 [*]	-1.53 [#]	-0.69 [#]	0.36 [#]	0.88 [#]
-60	9.23	-5.48 [*]	-4.12 [*]	-2.53 [*]	-2.19 [#]	-0.78 [#]	0.28 [#]
-45	9.20	-5.92 [*]	-4.15 [*]	-2.53 [*]	-2.21 [#]	-0.30 [#]	0.47 [#]
-30	8.03	-4.57 [*]	-3.32 [*]	-1.81 [*]	-1.56 [#]	-0.51 [#]	1.91 [#]
-15	7.44	-3.56 [*]	-3.34 [*]	-2.53 [*]	-2.58 [*]	-0.40 [#]	2.38 [#]

* p < 0.05, # p > 0.05

Right Lateral Gastrocnemius

Knee Angle	Up 0%	23-RPM 0%	23-RPM 10%	23-RPM 25%	30-RPM 0%	30-RPM 10%	30-RPM 25%
15	2.68	0.42 [#]	-0.27 [#]	0.48 [#]	0.41 [#]	-0.33 [#]	0.48 [#]
30	2.32	1.62 [*]	0.21 [#]	-0.18 [#]	1.92 [*]	-0.68 [#]	1.02 [*]
45	2.10	1.29 [*]	0.19 [#]	0.12 [#]	1.52 [*]	-0.11 [#]	1.59 [*]
60	1.87	0.87 [#]	0.19 [#]	0.06 [#]	2.28 [*]	1.06 [#]	1.97 [*]
75	2.12	0.82 [#]	0.13 [#]	0.41 [#]	3.57 [*]	0.79 [#]	2.43 [*]
90	2.54	-0.06 [#]	0.28 [#]	0.30 [#]	2.70 [*]	3.10 [*]	2.74 [*]
-90	6.42	-1.19 [#]	-0.39 [#]	1.21 [#]	2.12 [#]	4.14 [*]	3.43 [*]
-75	6.19	-2.02 [*]	-0.52 [#]	1.21 [#]	2.23 [#]	4.93 [*]	6.90 [*]
-60	6.63	-2.00 [*]	-1.62 [#]	0.24 [#]	0.63 [#]	3.31 [*]	4.33 [*]
-45	6.28	-2.29 [*]	-0.40 [#]	-0.16 [#]	0.58 [#]	4.02 [*]	2.79 [*]
-30	6.22	-2.93 [*]	-0.78 [#]	0.14 [#]	-0.05 [#]	5.19 [*]	3.53 [*]
-15	5.60	-1.88 [*]	-1.07 [#]	1.07 [#]	0.32 [#]	4.15 [*]	6.42 [*]

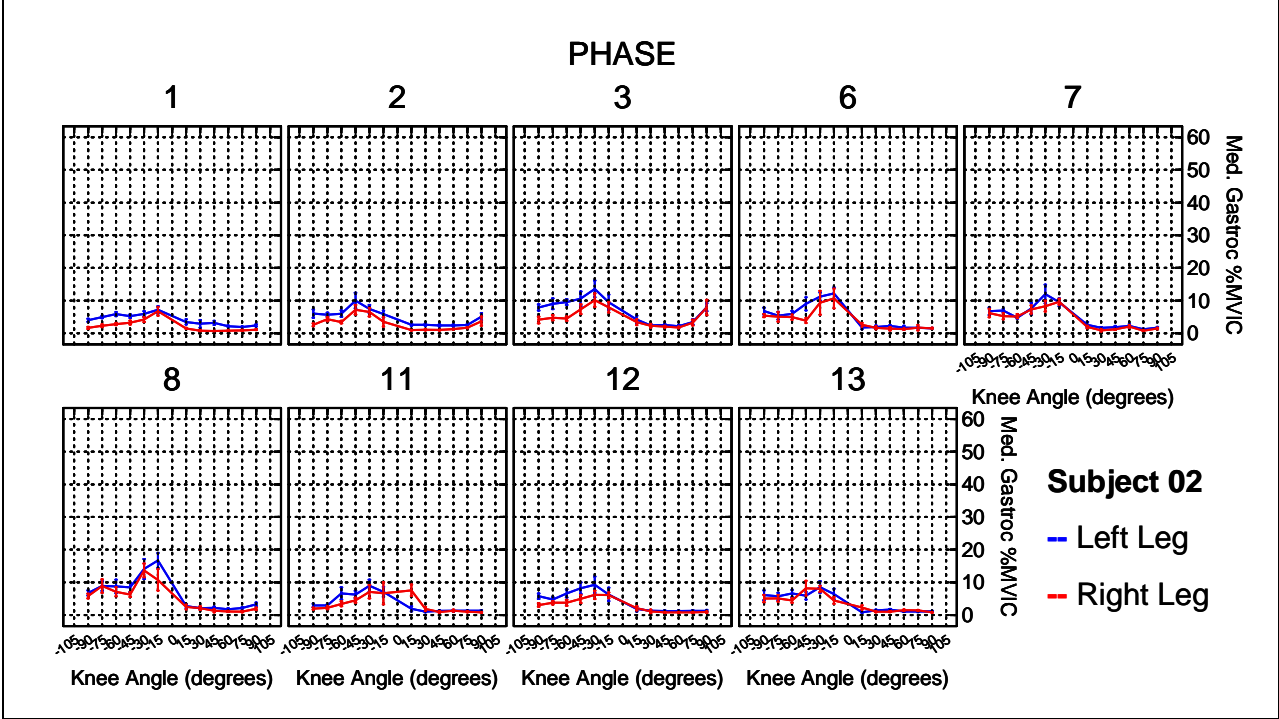
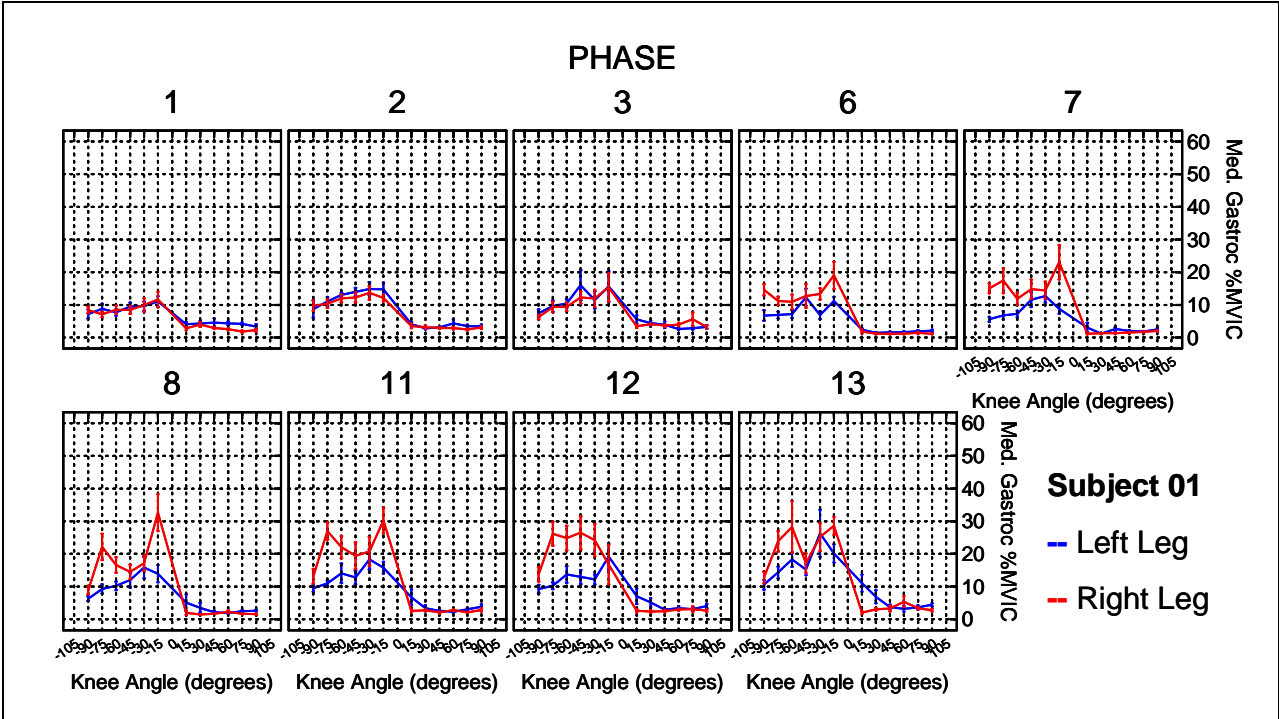
* p < 0.05, # p > 0.05

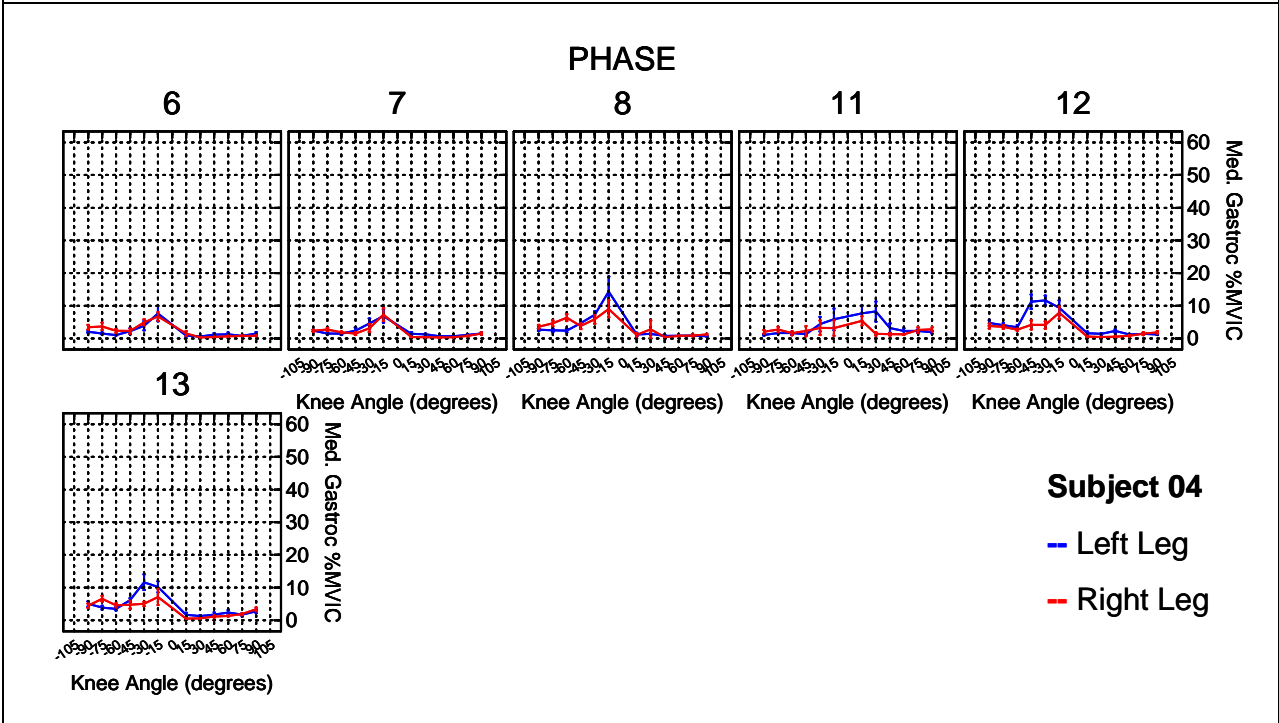
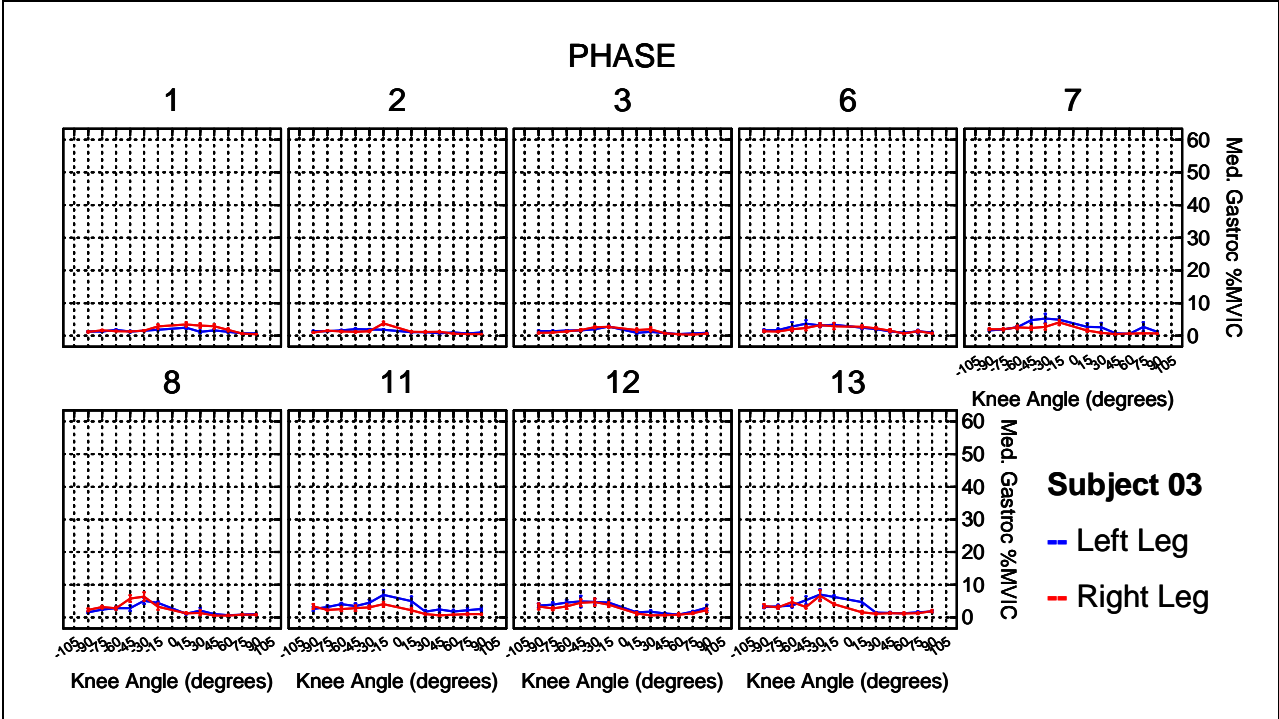
Knee Angle	Up 10%	23-RPM 0%	23-RPM 10%	23-RPM 25%	30-RPM 0%	30-RPM 10%	30-RPM 25%
15	2.57	0.52 [#]	-0.16 [#]	0.59 [#]	0.51 [#]	0.19 [#]	0.59 [#]
30	2.89	1.05 [#]	-0.36 [#]	-0.75 [#]	1.35 [*]	0.36 [#]	0.45 [#]
45	2.54	0.85 [#]	-0.25 [#]	-0.32 [#]	1.08 [*]	0.74 [#]	1.15 [*]
60	2.72	0.02 [#]	-0.66 [#]	-0.80 [#]	1.42 [#]	1.08 [#]	1.12 [#]
75	2.53	0.41 [#]	-0.28 [#]	0.00 [#]	3.16 [*]	1.20 [#]	2.02 [*]
90	2.55	-0.07 [#]	0.27 [#]	0.30 [#]	2.69 [*]	3.04 [*]	2.73 [*]
-90	6.95	-1.72 [#]	-0.93 [#]	0.68 [#]	1.59 [#]	2.42 [#]	2.90 [#]
-75	8.10	-3.93 [*]	-2.44 [*]	-0.70 [#]	0.32 [#]	1.00 [#]	4.99 [*]
-60	8.56	-3.93 [*]	-3.55 [*]	-1.69 [#]	-1.30 [#]	-0.62 [#]	2.40 [#]
-45	8.22	-4.23 [*]	-2.34 [*]	-2.10 [#]	-1.36 [#]	-0.21 [#]	0.85 [#]
-30	7.32	-4.03 [*]	-1.88 [*]	-0.96 [#]	-1.15 [#]	1.16 [#]	2.43 [#]
-15	6.42	-2.70 [*]	-1.89 [*]	0.25 [#]	-0.50 [#]	1.45 [#]	5.60 [*]

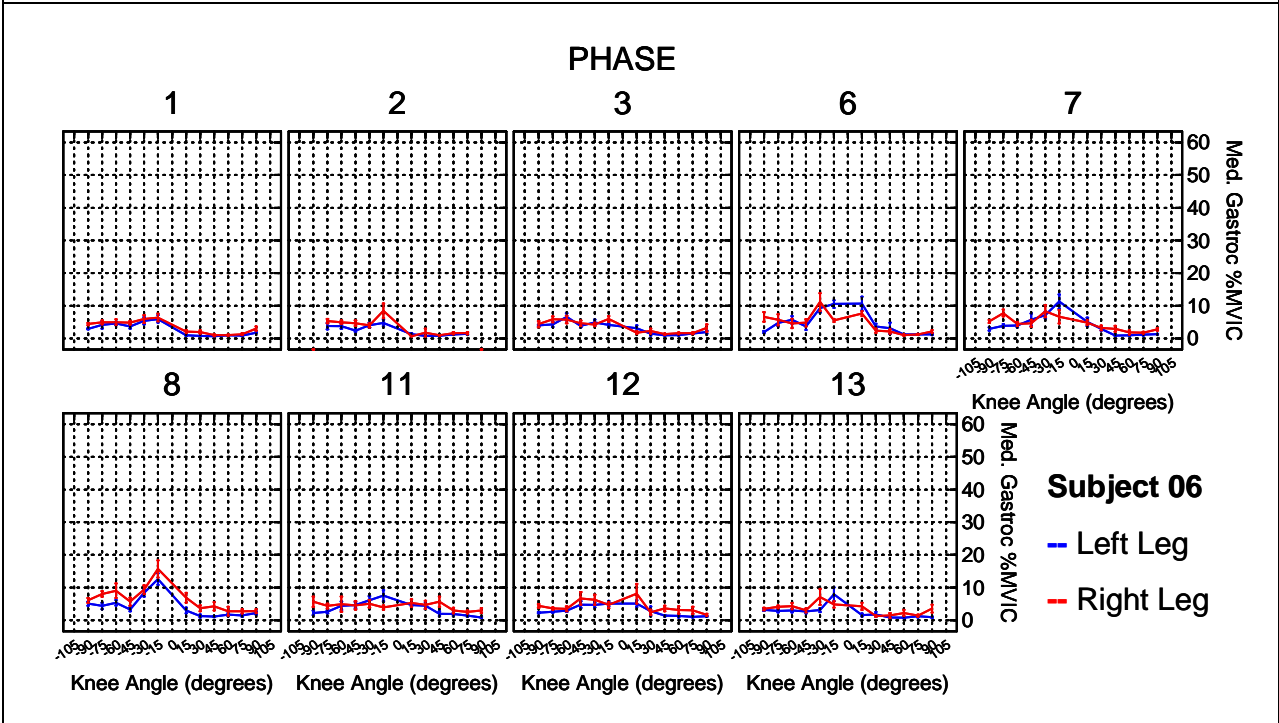
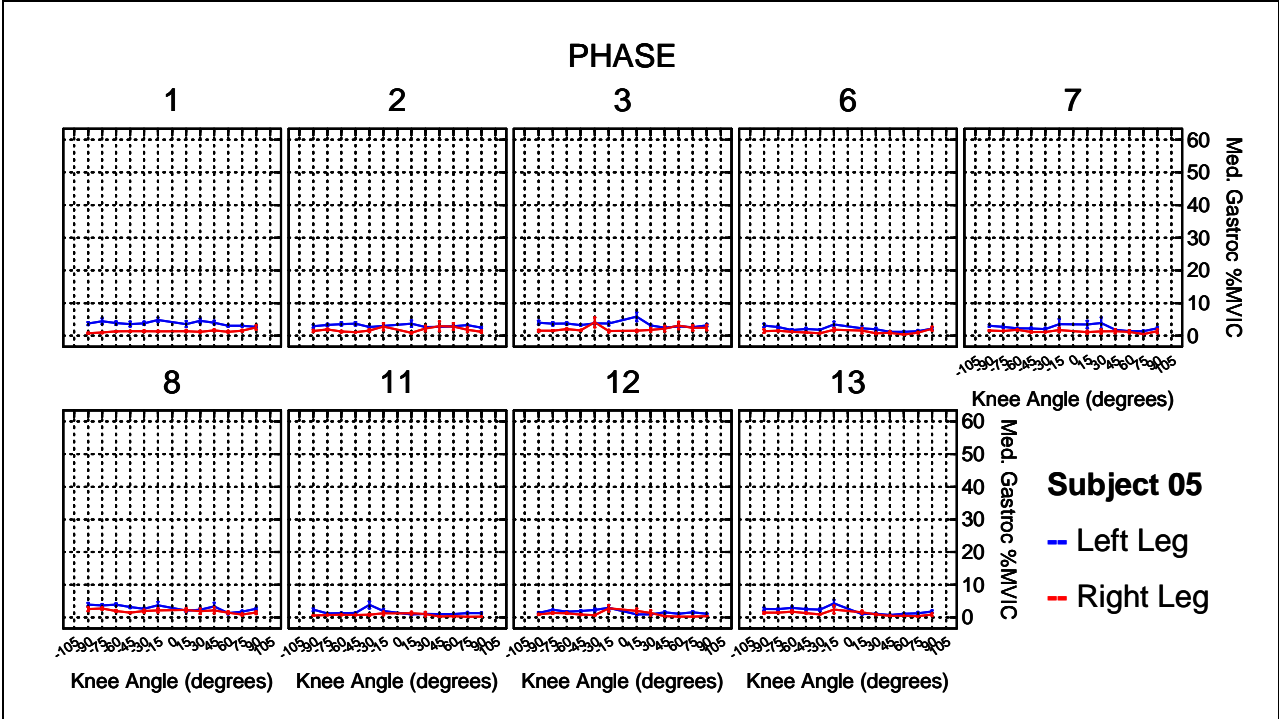
* p < 0.05, # p > 0.05

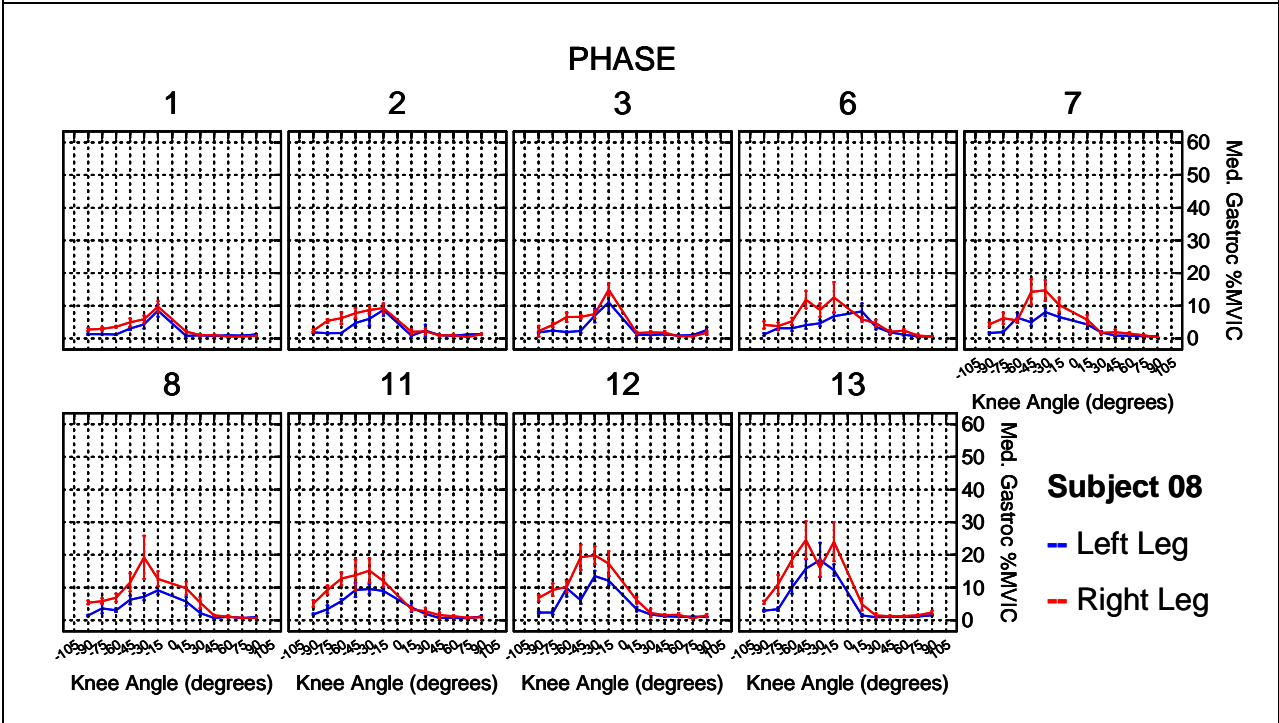
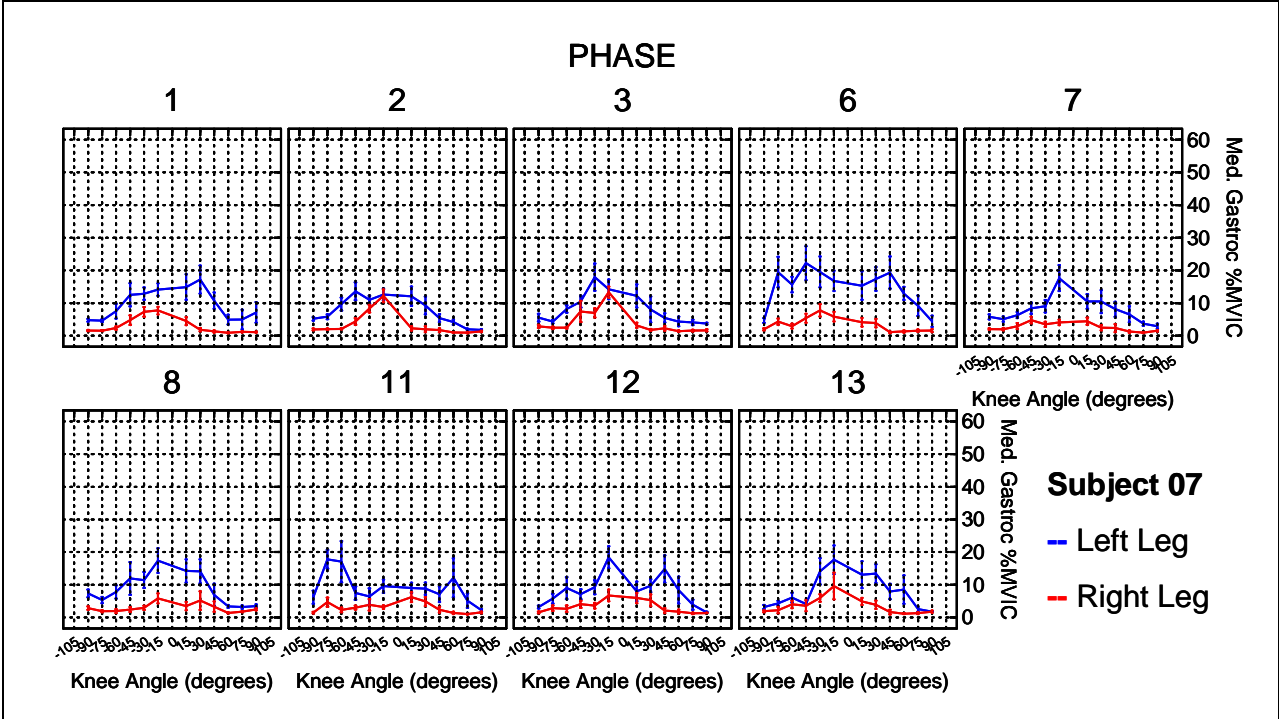
Knee Angle	Up 25%	23-RPM 0%	23-RPM 10%	23-RPM 25%	30-RPM 0%	30-RPM 10%	30-RPM 25%
15	2.70	0.39 [#]	-0.29 [#]	0.46 [#]	0.39 [#]	0.06 [#]	0.46 [#]
30	3.20	0.74 [#]	-0.67 [#]	-1.06 [*]	1.04 [#]	0.05 [#]	0.14 [#]
45	2.78	0.61 [#]	-0.49 [#]	-0.56 [#]	0.84 [#]	0.50 [#]	0.92 [#]
60	2.82	-0.08 [#]	-0.76 [#]	-0.89 [#]	1.33 [#]	0.99 [#]	1.03 [#]
75	3.50	-0.56 [#]	-1.25 [#]	-0.97 [#]	2.19 [#]	0.23 [#]	1.05 [#]
90	2.91	-0.43 [#]	-0.09 [#]	-0.06 [#]	2.34 [*]	2.68 [*]	2.37 [*]
-90	5.78	-0.55 [#]	0.25 [#]	1.85 [#]	2.76 [*]	3.59 [*]	4.07 [*]
-75	8.36	-4.20 [*]	-2.70 [*]	-0.96 [#]	0.06 [#]	0.73 [#]	4.72 [*]
-60	9.24	-4.60 [*]	-4.22 [*]	-2.36 [*]	-1.97 [#]	-1.29 [#]	1.72 [#]
-45	8.29	-4.30 [*]	-2.42 [*]	-2.17 [*]	-1.43 [#]	-0.28 [#]	0.78 [#]
-30	7.13	-3.83 [*]	-1.68 [#]	-0.76 [#]	-0.95 [#]	1.36 [#]	2.63 [#]
-15	7.06	-3.33 [*]	-2.52 [*]	-0.38 [#]	-1.13 [#]	0.82 [#]	4.97 [*]

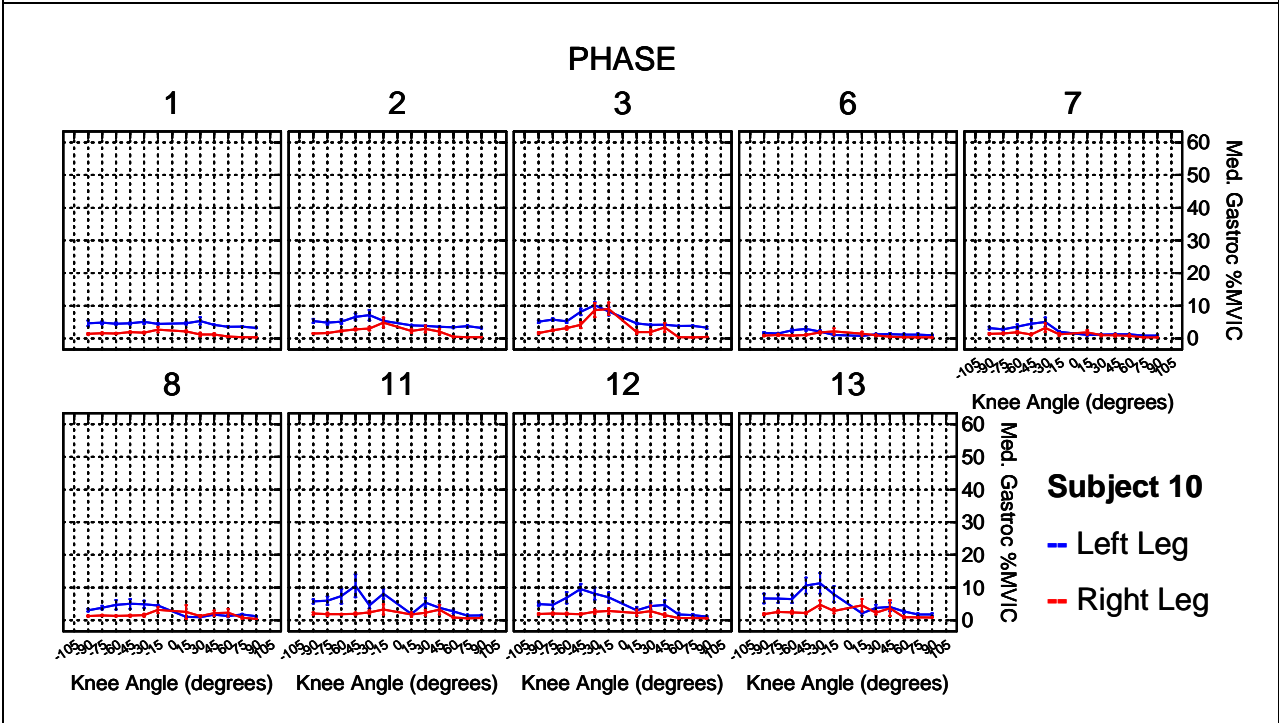
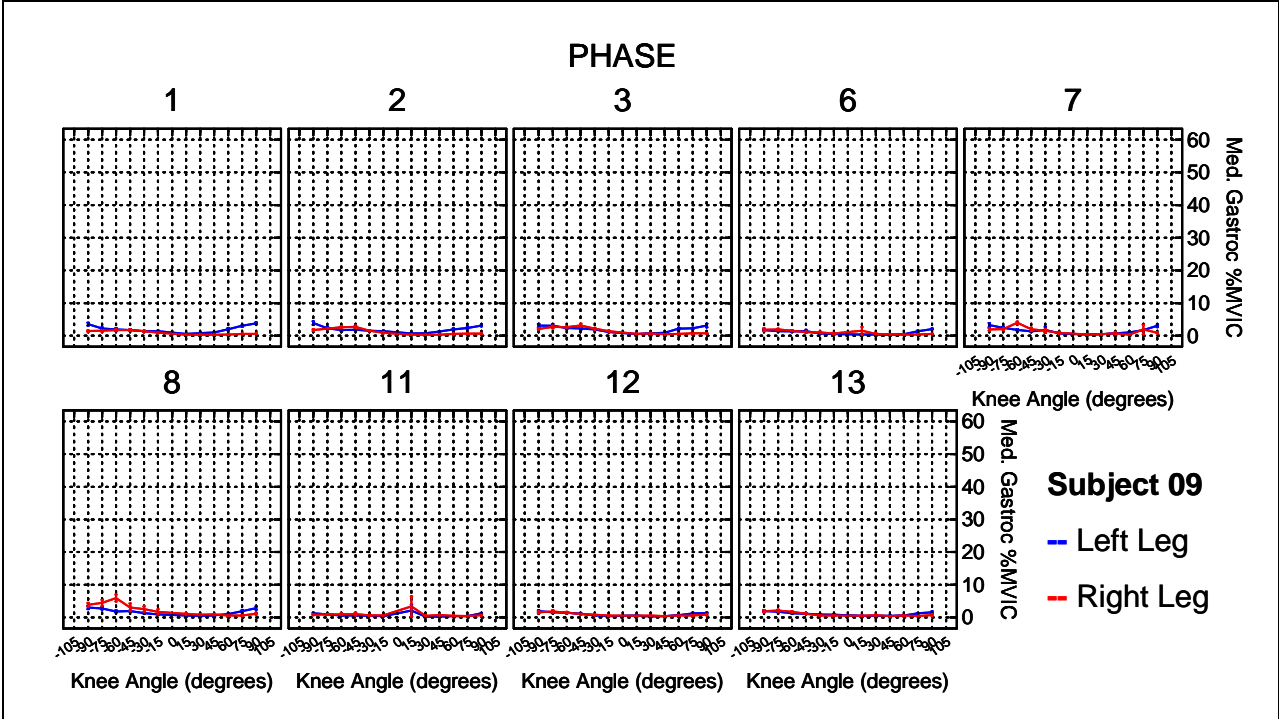
* p < 0.05, # p > 0.05

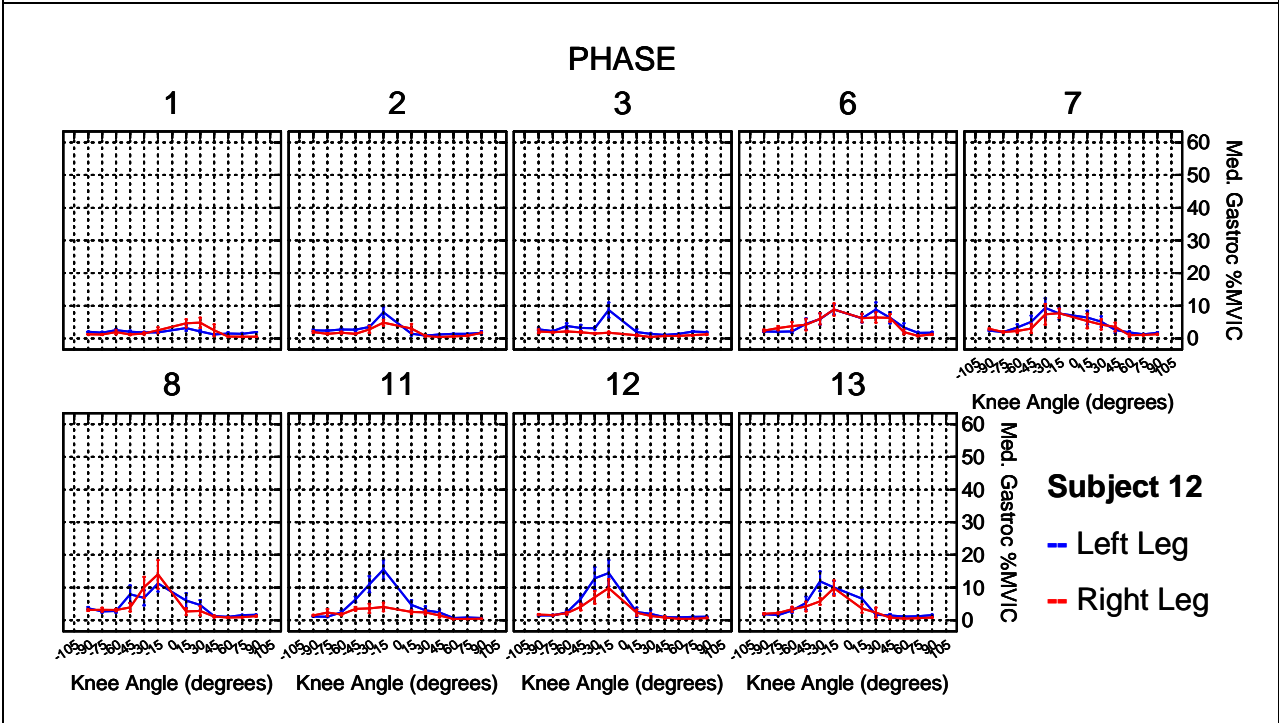
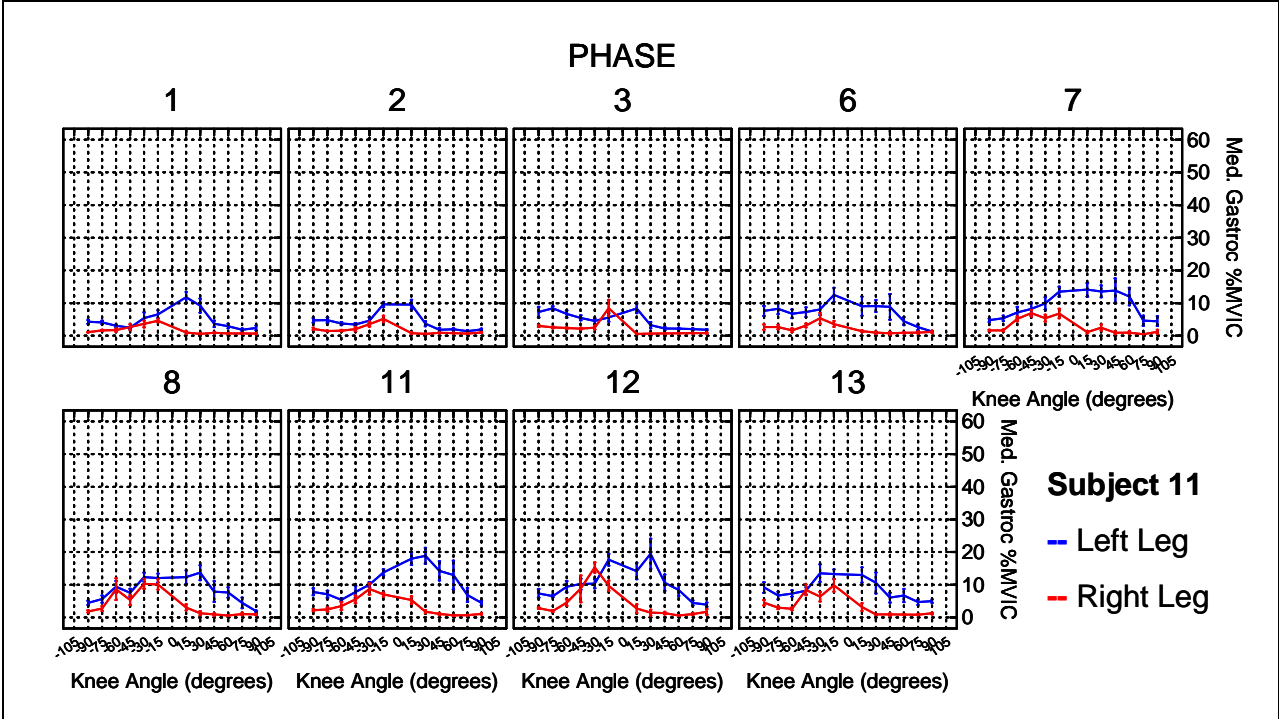


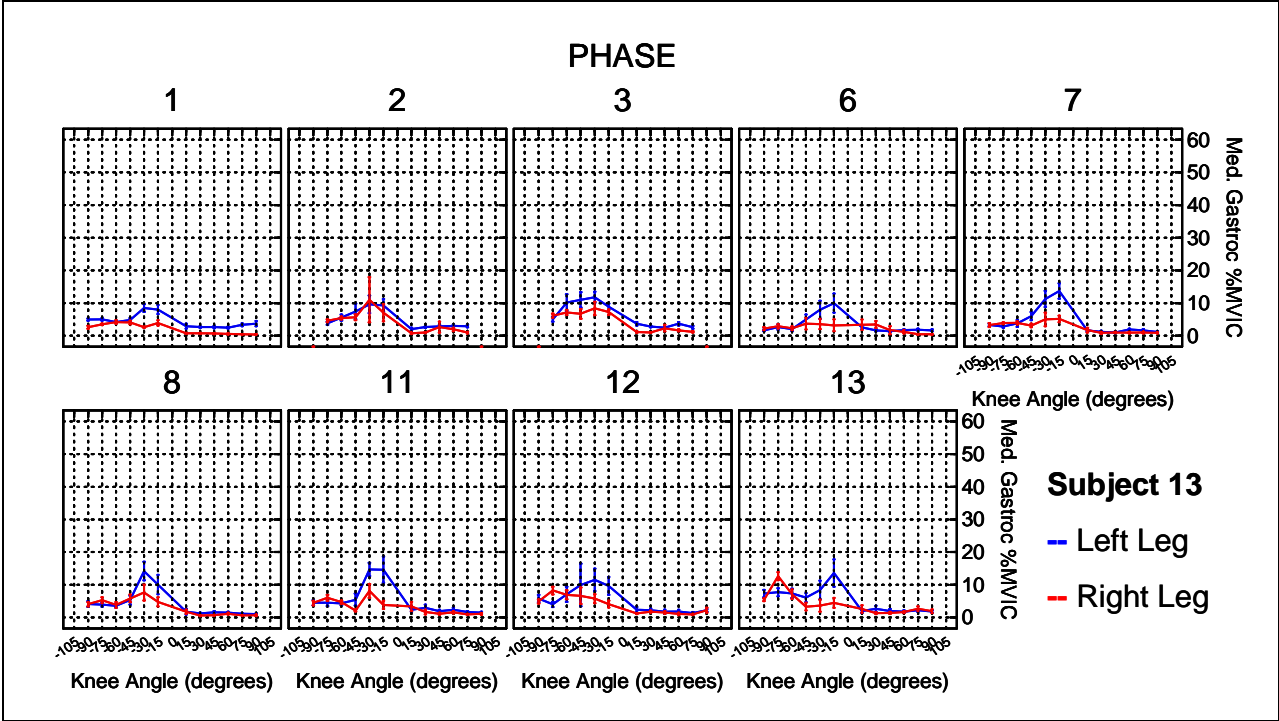












Left Medial Gastrocnemius

Knee Angle	Up 0%	23-RPM 0%	23-RPM 10%	23-RPM 25%	30-RPM 0%	30-RPM 10%	30-RPM 25%
15	4.46	-0.61#	-0.81#	-0.45#	1.87*	0.91#	0.52#
30	4.37	-1.40*	-1.28#	-0.90#	1.53#	1.71#	-0.33#
45	3.22	-0.78#	-0.02#	-0.98#	1.54#	0.71#	-0.48#
60	2.52	-0.22#	0.03#	-0.34#	1.05#	0.21#	-0.27#
75	2.51	-0.91*	-0.69*	-0.90*	0.18#	0.35#	-0.29#
90	2.95	-1.65*	-1.39*	-1.55*	-0.61#	0.98#	-0.22#
-90	3.84	-0.85*	-0.85*	-0.57#	0.31#	1.81*	1.92*
-75	3.98	0.05#	-0.75*	-0.13#	1.65*	0.51#	1.69*
-60	4.07	0.39#	0.28#	0.49#	1.76*	1.51*	2.64*
-45	4.56	0.40#	1.00#	0.46#	2.71*	2.38*	3.45*
-30	5.48	0.19#	1.91*	2.81*	3.38*	3.07*	5.40*
-15	6.33	0.97#	1.67#	2.58*	3.43*	2.70*	5.70*

* p < 0.05, # p > 0.05

Knee Angle	Up 10%	23-RPM 0%	23-RPM 10%	23-RPM 25%	30-RPM 0%	30-RPM 10%	30-RPM 25%
15	3.64	0.20#	0.00#	0.36#	2.68*	1.11#	1.33#
30	2.80	0.17#	0.29#	0.67#	3.10*	1.88*	1.24#
45	2.27	0.17#	0.93#	-0.03#	2.49*	0.88*	0.48#
60	2.39	-0.09#	0.16#	-0.21#	1.17*	0.13#	-0.14#
75	2.22	-0.63*	-0.41#	-0.61*	0.47#	-0.27#	0.00#
90	2.57	-1.27*	-1.01*	-1.17*	-0.23#	-0.29#	0.16#
-90	4.37	-1.37*	-1.37*	-1.09*	-0.21#	0.44#	1.40*
-75	4.25	-0.22#	-1.01*	-0.40#	1.38*	0.29#	1.42*
-60	4.87	-0.41#	-0.52#	-0.31#	0.96#	1.10#	1.85*
-45	6.06	-1.10#	-0.50#	-1.04#	1.21#	1.28#	1.95*
-30	6.22	-0.54#	1.17#	2.08*	2.65*	2.53*	4.67*
-15	7.12	0.18#	0.88#	1.79*	2.64*	2.88*	4.91*

* p < 0.05, # p > 0.05

Knee Angle	Up 25%	23-RPM 0%	23-RPM 10%	23-RPM 25%	30-RPM 0%	30-RPM 10%	30-RPM 25%
15	4.35	-0.51#	-0.71#	-0.35#	1.97*	0.40#	0.62#
30	2.87	0.10#	0.22#	0.60#	3.03*	1.81*	1.17#
45	2.38	0.06#	0.82#	-0.14#	2.38*	0.77#	0.36#
60	2.32	-0.02#	0.23#	-0.14#	1.25*	0.20#	-0.07#
75	2.44	-0.84*	-0.63*	-0.83*	0.25#	-0.49*	-0.22#
90	3.25	-1.95*	-1.69*	-1.85*	-0.91#	-0.97*	-0.52#
-90	4.96	-1.96*	-1.97*	-1.69*	-0.80#	-0.16#	0.803#
-75	4.96	-0.93#	-1.73*	-1.11*	0.67#	-0.42#	0.71#
-60	5.88	-1.42#	-1.53*	-1.32*	-0.05#	0.09#	0.84#
-45	6.53	-1.57*	-0.97#	-1.51*	0.74#	0.81#	1.49#
-30	7.70	-2.03*	-0.31#	0.59#	1.16#	1.04#	3.18*
-15	7.83	-0.53#	0.17#	1.08#	1.93*	2.17*	4.20*

* p < 0.05, # p > 0.05

Right Medial Gastrocnemius

Knee Angle	Up 0%	23-RPM 0%	23-RPM 10%	23-RPM 25%	30-RPM 0%	30-RPM 10%	30-RPM 25%
15	2.25	1.19*	0.43#	0.74#	1.43*	-0.76#	0.71#
30	1.84	0.43#	-0.21#	0.05#	0.44#	-0.37#	0.28#
45	1.43	0.10#	-0.25#	-0.37#	0.39#	0.16#	0.58#
60	0.99	0.13#	0.09#	0.20#	0.22#	0.16#	0.62#
75	0.89	0.03#	0.08#	0.05#	0.28#	0.33#	0.68*
90	1.23	-0.29#	-0.21#	-0.08#	0.28#	0.78*	0.74*
-90	2.46	0.73#	0.87#	0.87*	1.58*	1.23*	2.34*
-75	2.59	0.64#	1.30*	2.22*	3.08*	2.50*	4.48*
-60	3.04	0.02#	0.64#	2.05*	2.24*	3.41*	4.45*
-45	3.40	0.81#	1.67*	1.98*	2.49*	3.07*	3.69*
-30	3.95	0.85#	1.69*	3.49*	4.20*	3.42*	5.77*
-15	5.11	0.29#	1.73*	3.61*	2.72*	2.32*	5.31*

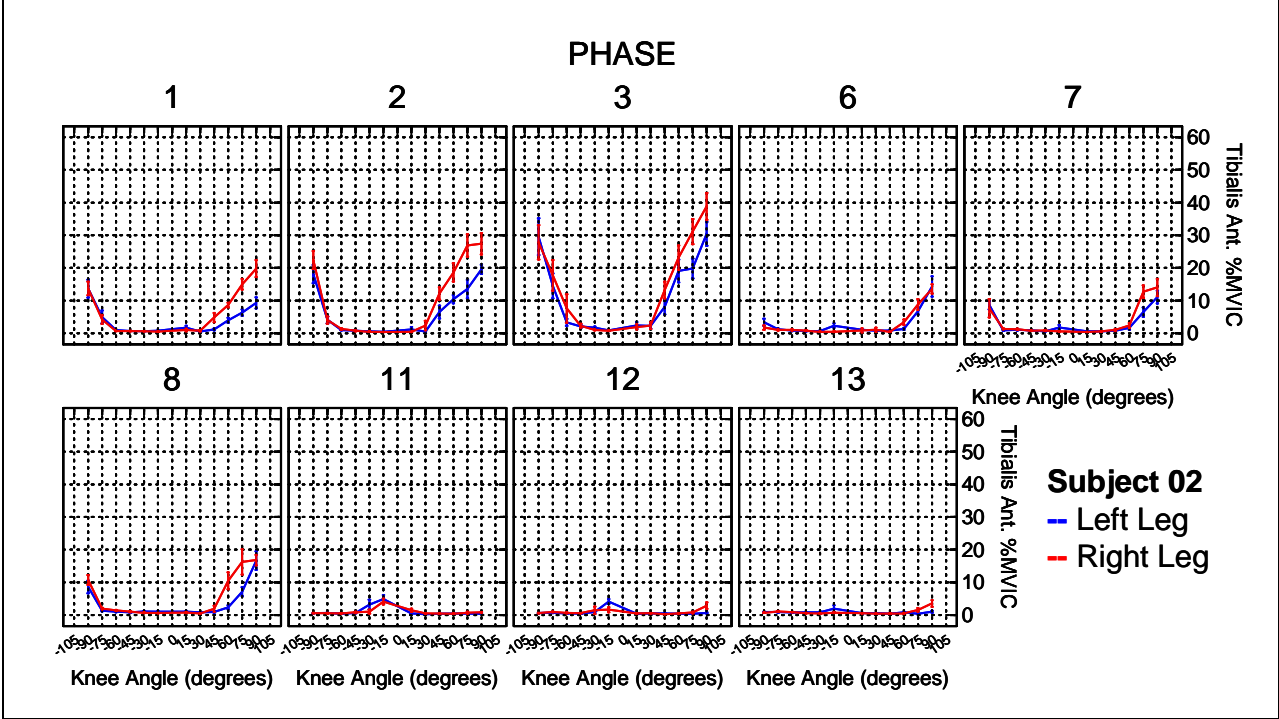
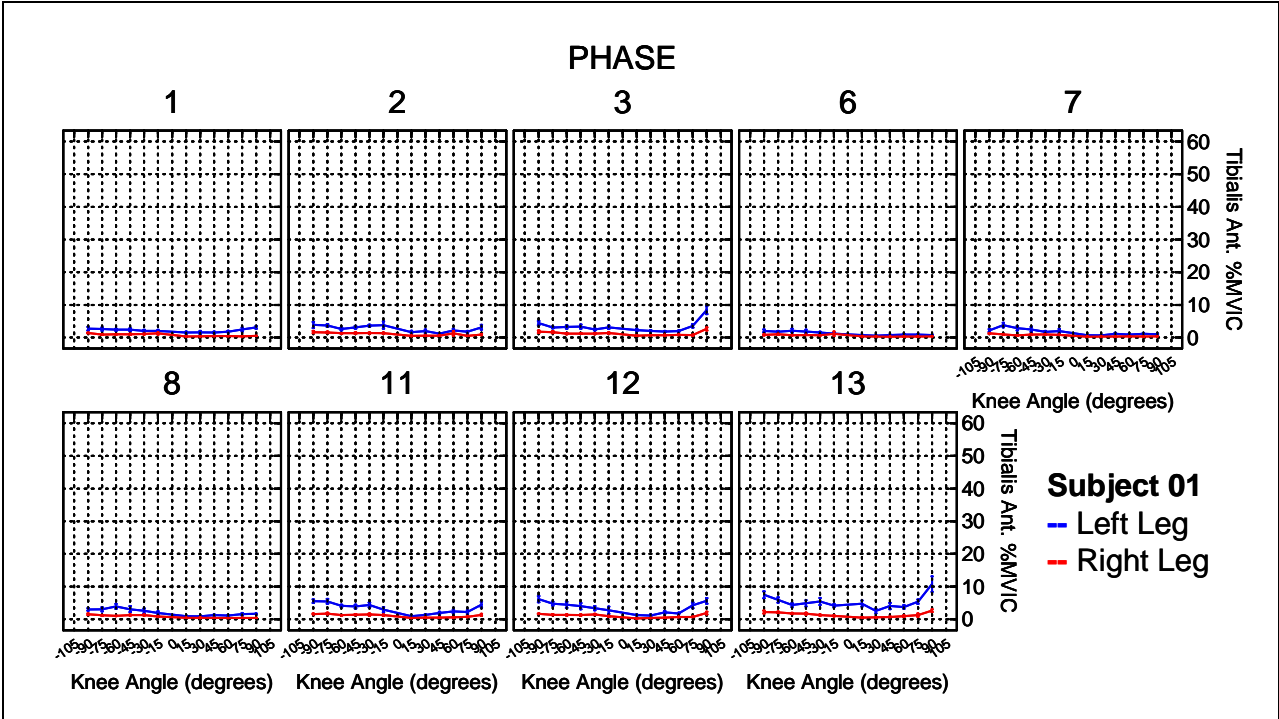
* p < 0.05, # p > 0.05

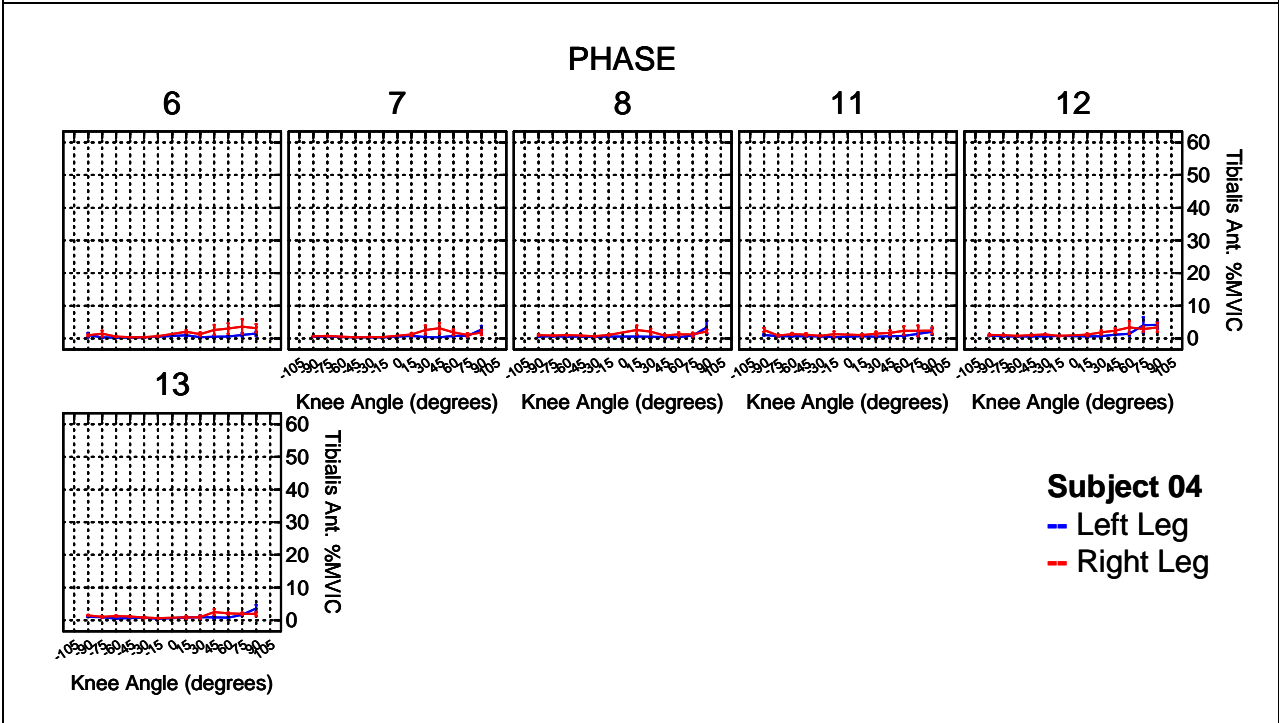
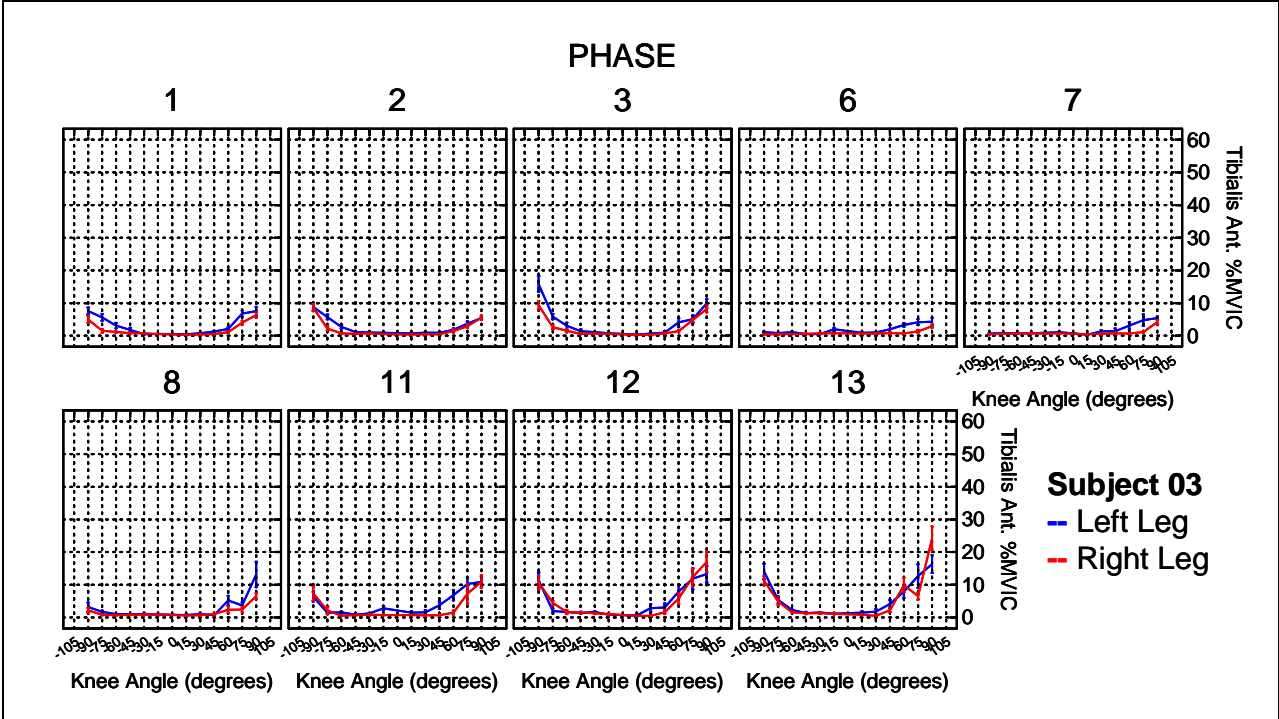
Knee Angle	Up 10%	23-RPM 0%	23-RPM 10%	23-RPM 25%	30-RPM 0%	30-RPM 10%	30-RPM 25%
15	1.60	1.84*	1.08*	1.39*	2.07*	1.08*	1.36*
30	1.61	0.65*	0.01#	0.27#	0.66*	0.28#	0.50#
45	1.53	0.00#	-0.35#	-0.47#	0.29#	0.16#	0.49#
60	1.33	-0.20#	-0.25#	-0.14#	-0.12#	-0.05#	0.28#
75	1.10	-0.18#	-0.13#	-0.16#	0.07#	0.15#	0.47*
90	1.50	-0.55*	-0.47*	-0.35#	0.02#	0.22#	0.47*
-90	2.70	0.49#	0.64#	0.63#	1.35*	1.72*	2.11*
-75	3.53	-0.29#	0.36#	1.28*	2.15*	2.21*	3.54*
-60	3.78	-0.71#	-0.10#	1.31*	1.50*	2.69*	3.71*
-45	4.46	-0.25#	0.61#	0.91#	1.43#	2.82*	2.63*
-30	5.52	-0.73#	0.12#	1.91*	2.62*	2.69*	4.20*
-15	6.26	-0.86#	0.57#	2.46*	1.56*	1.46#	4.16*

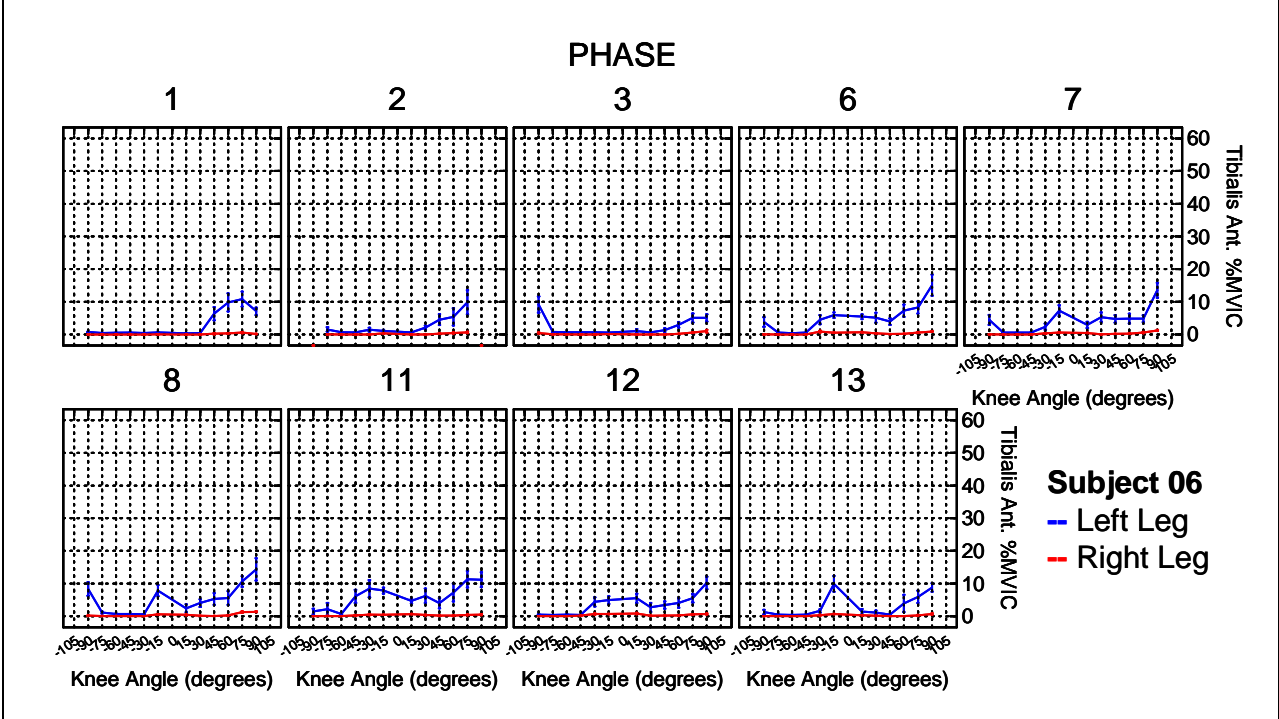
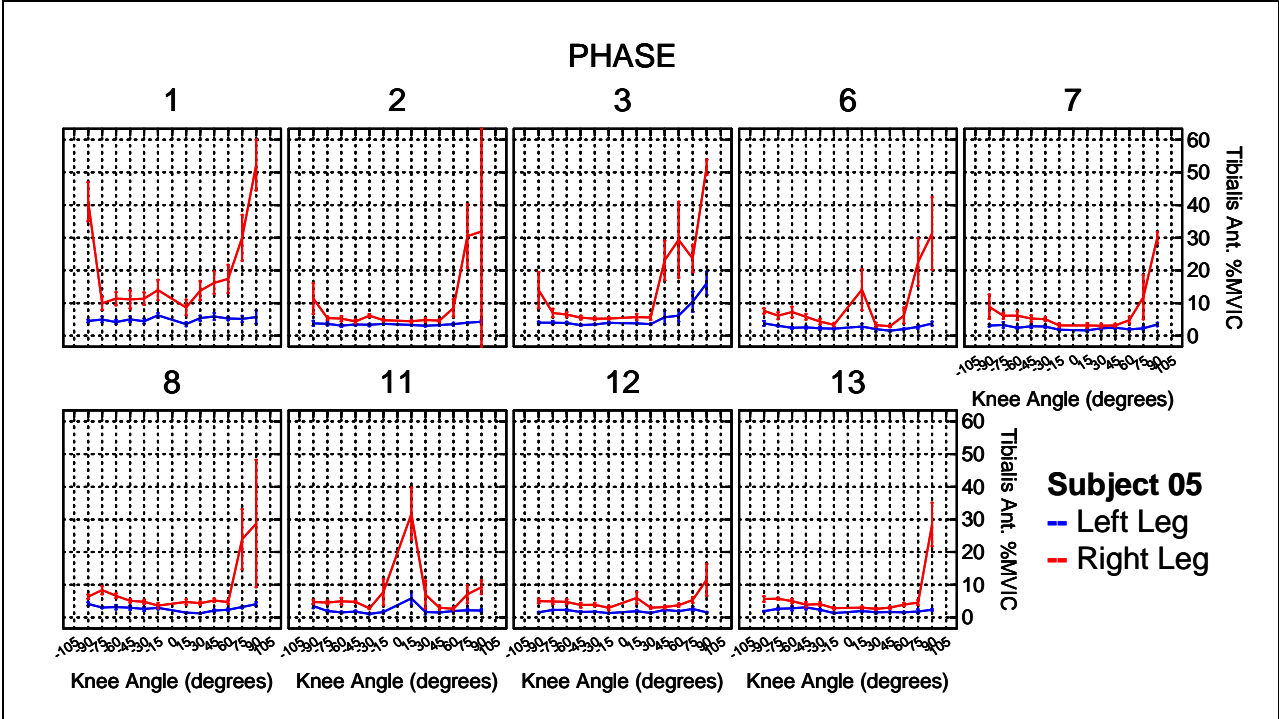
* p < 0.05, # p > 0.05

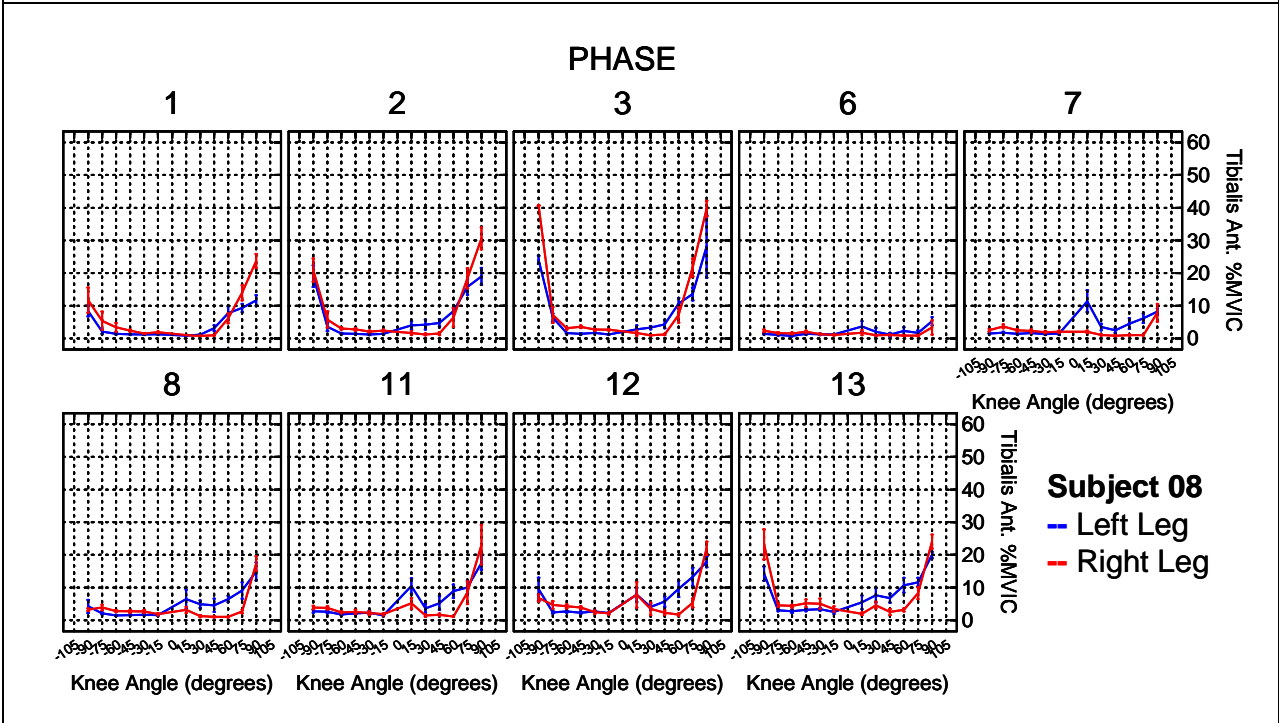
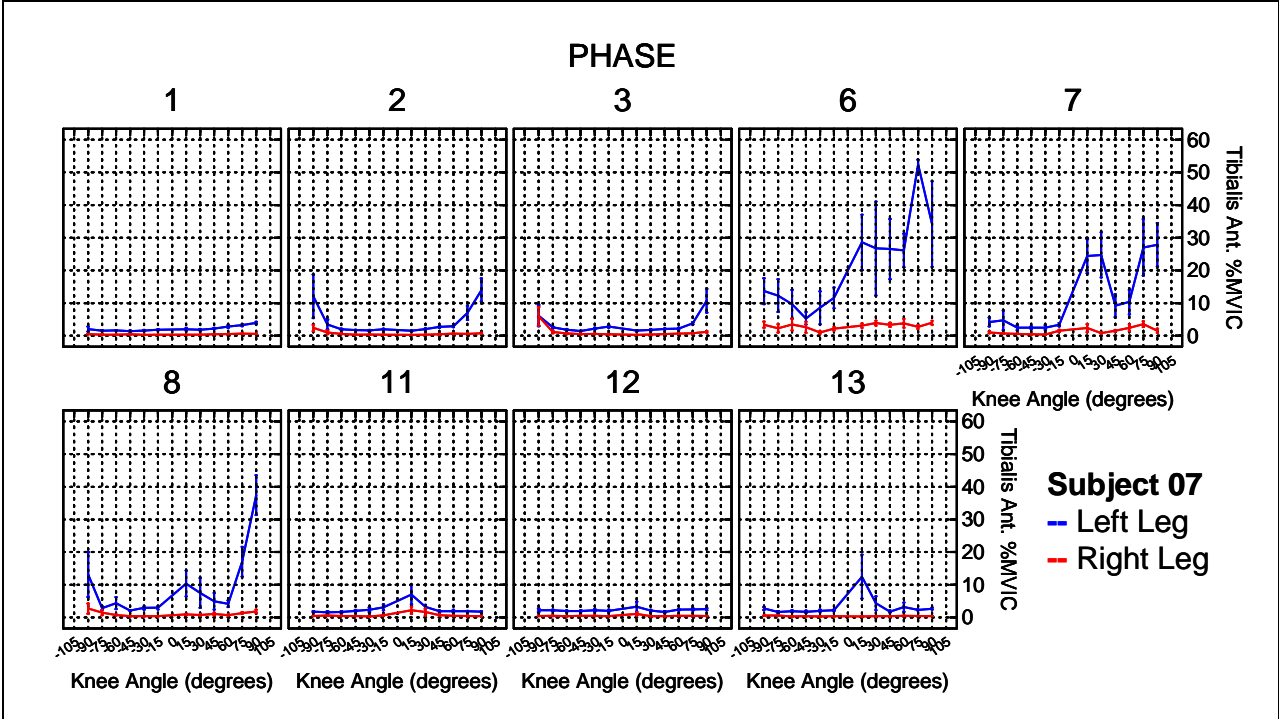
Knee Angle	Up 25%	23-RPM 0%	23-RPM 10%	23-RPM 25%	30-RPM 0%	30-RPM 10%	30-RPM 25%
15	1.85	1.59*	0.83*	1.14*	1.82*	0.83*	1.11*
30	1.76	0.51#	-0.13#	0.13#	0.52#	0.14#	0.36#
45	1.82	-0.28#	-0.63*	-0.75*	0.00#	-0.12#	0.20#
60	1.45	-0.33#	-0.37#	-0.23#	-0.24#	-0.17#	0.15#
75	1.66	-0.73*	-0.69*	-0.71*	-0.48#	-0.40#	-0.08#
90	2.27	-1.33*	-1.24*	-1.12*	-0.75*	-0.55#	-0.30#
-90	2.87	0.32#	0.47#	0.46#	1.18*	1.55*	1.94*
-75	3.76	-0.53#	0.13#	1.05#	1.91*	1.98*	3.31*
-60	4.13	-1.07*	-0.46#	0.95#	1.14#	2.33*	3.35*
-45	5.00	-0.79#	0.08#	0.38#	0.89#	2.28*	2.09*
-30	5.91	-1.11#	-0.27#	1.52#	2.23#	2.31*	3.81*
-15	8.00	-2.60*	-1.17#	0.72#	-0.18#	-0.28#	2.41#

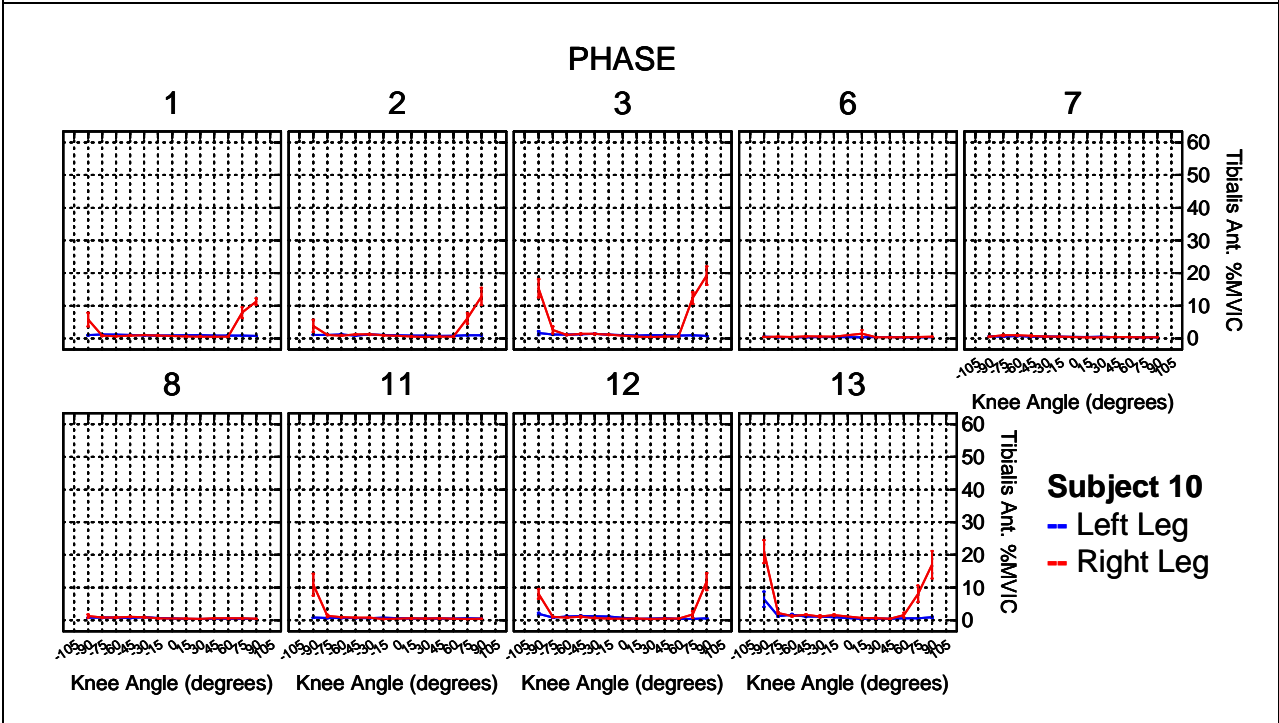
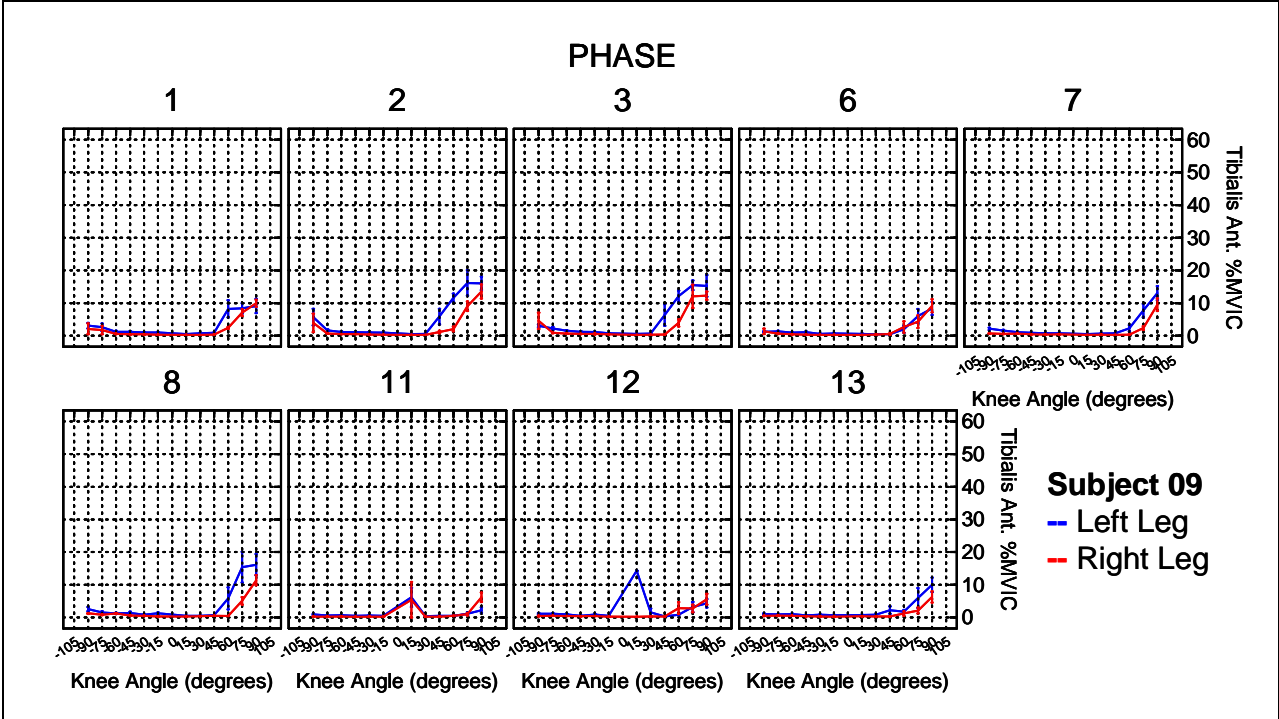
* p < 0.05, # p > 0.05

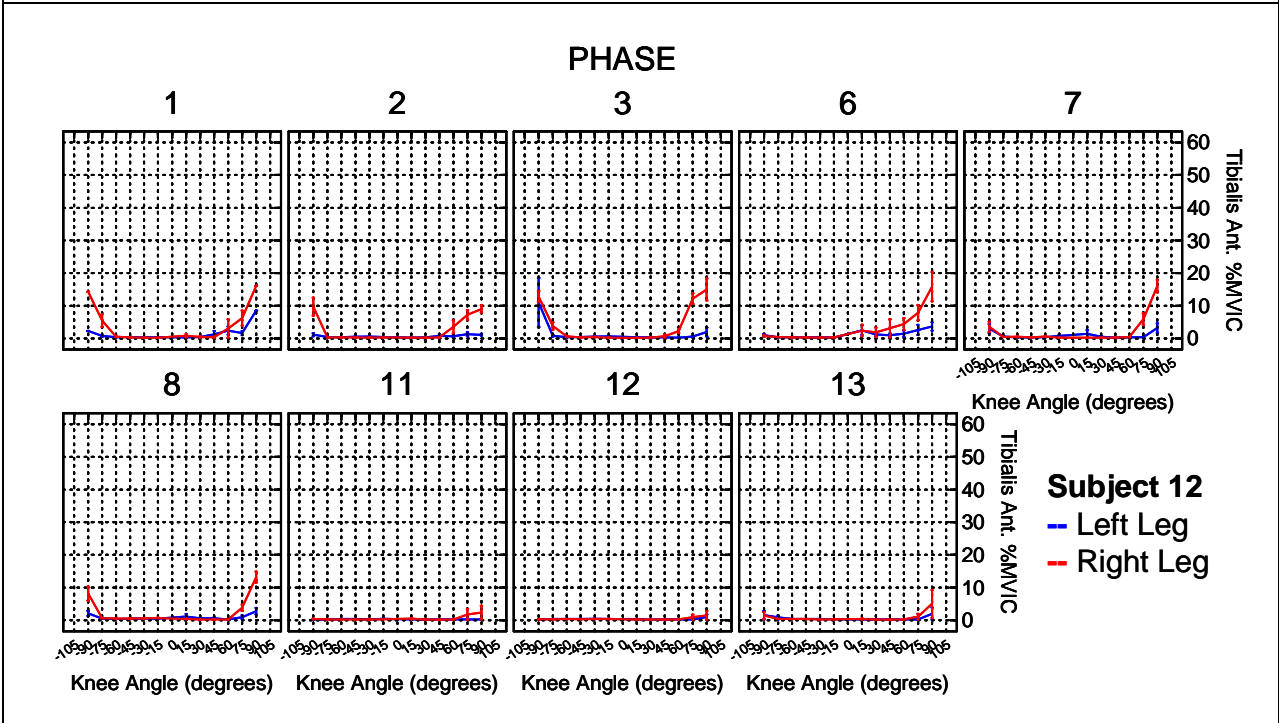
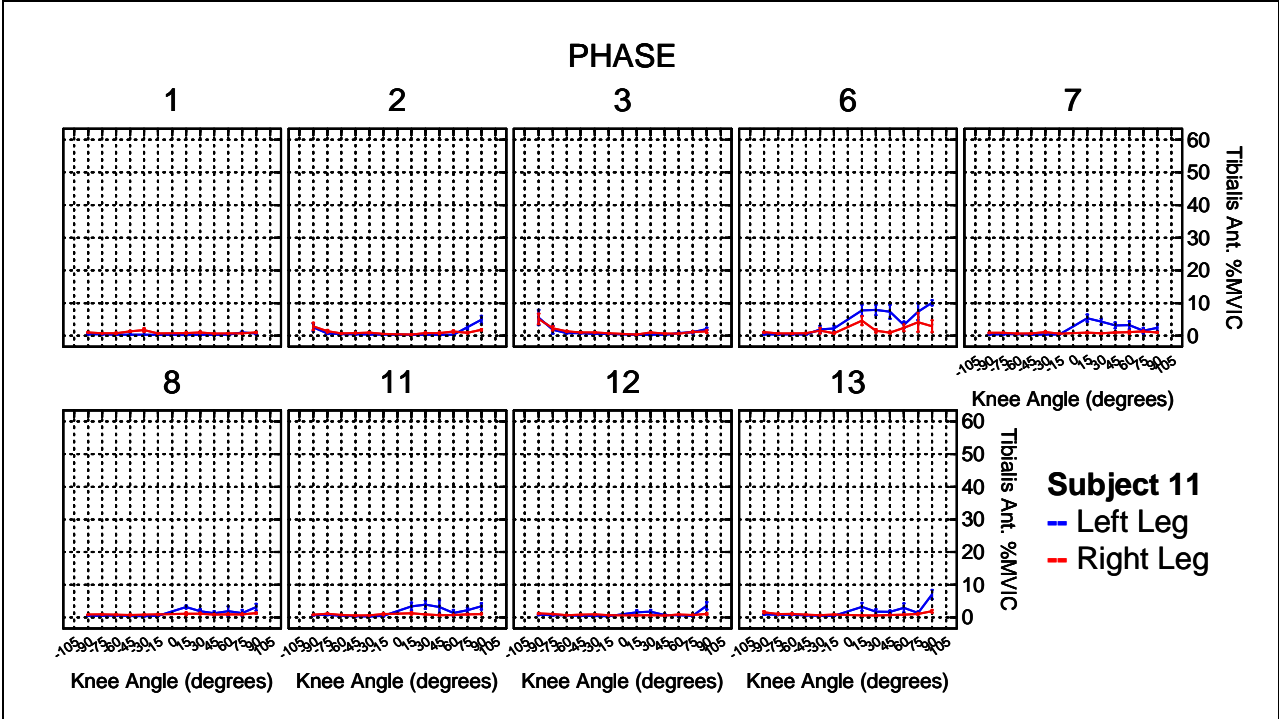


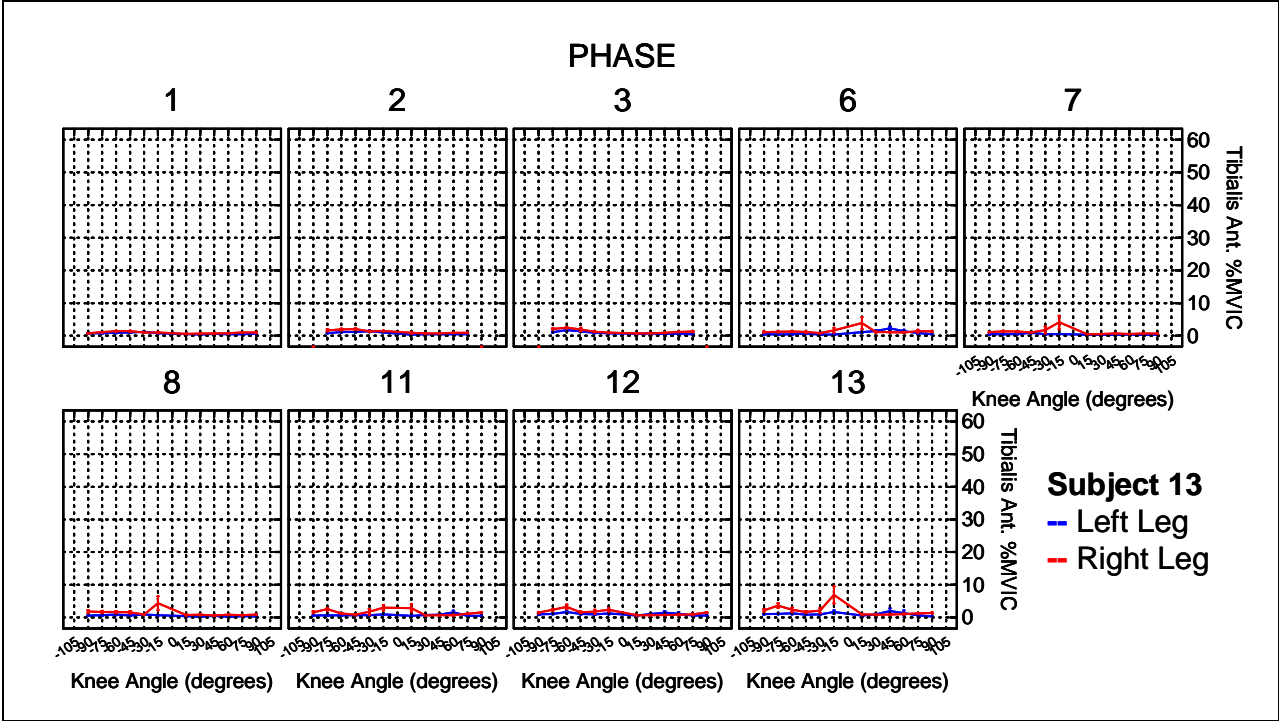












Left Tibialis Anterior

Knee Angle	Up 0%	23-RPM 0%	23-RPM 10%	23-RPM 25%	30-RPM 0%	30-RPM 10%	30-RPM 25%
15	1.10	1.98*	2.38*	1.24*	5.00*	0.35*	1.50*
30	1.24	0.77*	0.27#	0.19#	4.37*	1.92*	1.14*
45	2.14	-0.36#	-0.76*	-0.90*	3.05*	0.77#	0.53#
60	3.84	-1.95*	-2.03*	-1.74*	2.23*	1.53#	-0.09#
75	4.73	-2.11*	-2.45*	-1.53#	3.51*	4.43#	2.78*
90	5.62	-2.47*	-2.48*	-0.68#	5.11*	6.88*	6.89*
-90	4.24	-3.05*	-3.25*	-2.53*	-0.77#	3.22#	2.23*
-75	2.36	-1.39*	-1.17*	-1.04*	0.07#	0.91#	-0.14#
-60	1.54	-0.68*	-0.46*	-0.26#	1.08#	0.75#	0.35#
-45	1.46	-0.13#	-0.48*	-0.29#	1.42#	0.18#	0.19#
-30	1.24	0.49#	0.03#	-0.01#	2.15*	-0.15#	0.47*
-15	1.40	0.64*	0.13#	0.40#	3.37*	-0.11#	0.76*

* p < 0.05, # p > 0.05

Knee Angle	Up 10%	23-RPM 0%	23-RPM 10%	23-RPM 25%	30-RPM 0%	30-RPM 10%	30-RPM 25%
15	1.29	1.78*	2.19*	1.04#	4.80*	2.13*	1.30*
30	1.47	0.53#	0.04#	-0.04#	4.13*	2.46*	0.90*
45	2.69	-0.91*	-1.31*	-1.45*	2.50#	-0.13#	-0.02#
60	4.06	-2.17*	-2.26*	-1.96*	2.01#	-0.64#	-0.31#
75	6.44	-3.83*	-4.17*	-3.25*	1.79#	0.60#	1.06#
90	9.28	-6.14*	-6.14*	-4.34*	1.45#	0.74#	3.23*
-90	7.98	-6.78*	-6.99*	-6.27*	-4.51*	-3.56*	-1.50#
-75	2.55	-1.58*	-1.36*	-1.23*	-0.12#	-0.67#	-0.33#
-60	1.52	-0.66*	-0.44*	-0.24#	1.10#	0.09#	0.38#
-45	1.38	-0.06#	-0.41*	-0.21#	1.49#	0.12#	0.26#
-30	1.48	0.25#	-0.20#	-0.24#	1.91#	0.11#	0.24#
-15	1.46	0.59*	0.08#	0.34#	3.32*	0.49#	0.70*

* p < 0.05, # p > 0.05

Knee Angle	Up 25%	23-RPM 0%	23-RPM 10%	23-RPM 25%	30-RPM 0%	30-RPM 10%	30-RPM 25%
15	1.45	1.62*	2.03*	0.89#	4.64*	1.97*	1.15*
30	1.46	0.55#	0.05#	-0.03#	4.15*	2.47*	0.91#
45	2.75	-0.97#	-1.37*	-1.51*	2.44#	-0.19#	-0.08#
60	5.16	-3.27*	-3.35*	-3.05*	0.91#	-1.74*	-1.41#
75	6.68	-4.07*	-4.41*	-3.49*	1.55#	0.36#	0.82#
90	11.17	-8.03*	-8.04*	-6.24*	-0.45#	-1.15#	1.33#
-90	12.08	-10.88*	-11.08*	-10.36*	-8.60*	-7.66*	-5.60*
-75	3.71	-2.74*	-2.52*	-2.39*	-1.28#	-1.83*	-1.49*
-60	1.96	-1.10*	-0.88*	-0.68*	0.66#	-0.35#	-0.07#
-45	1.58	-0.26#	-0.60*	-0.41*	1.30#	-0.08#	0.06#
-30	1.52	0.22#	-0.24#	-0.28#	1.88#	0.07#	0.20#
-15	1.45	0.60*	0.08#	0.35#	3.32#	0.49#	0.71*

* p < 0.05, # p > 0.05

Right Tibialis Anterior

Knee Angle	Up 0%	23-RPM 0%	23-RPM 10%	23-RPM 25%	30-RPM 0%	30-RPM 10%	30-RPM 25%
15	1.26	3.55*	-0.12#	-0.16#	1.35*	-0.38#	-0.18#
30	1.64	-0.37#	-0.79#	-0.78#	-0.32#	-0.24#	-0.46#
45	2.21	-1.27*	-1.29*	-1.44*	-0.88#	0.23#	-0.73#
60	3.53	-2.49*	-2.43*	-2.45*	-1.34#	1.85*	-0.71#
75	7.31	-5.48*	-6.00*	-5.83*	0.06#	3.43*	-0.52#
90	14.90	-11.77*	-11.89*	-9.19*	-3.26#	0.40#	0.46#
-90	8.99	-7.92*	-7.88*	-7.37*	-5.61*	3.01*	-0.97#
-75	2.70	-1.66*	-1.42*	-1.26*	-0.83#	0.91#	-0.17#
-60	1.85	-0.89*	-0.77*	-0.62#	-0.22#	0.73#	0.03#
-45	1.76	-0.73*	-0.78*	-0.61#	-0.36#	0.41#	-0.12#
-30	1.69	-0.81*	-0.55#	-0.61#	-0.47#	0.47#	-0.18#
-15	1.82	-0.24#	-0.61#	-0.61#	-0.52#	-0.41#	-0.14#

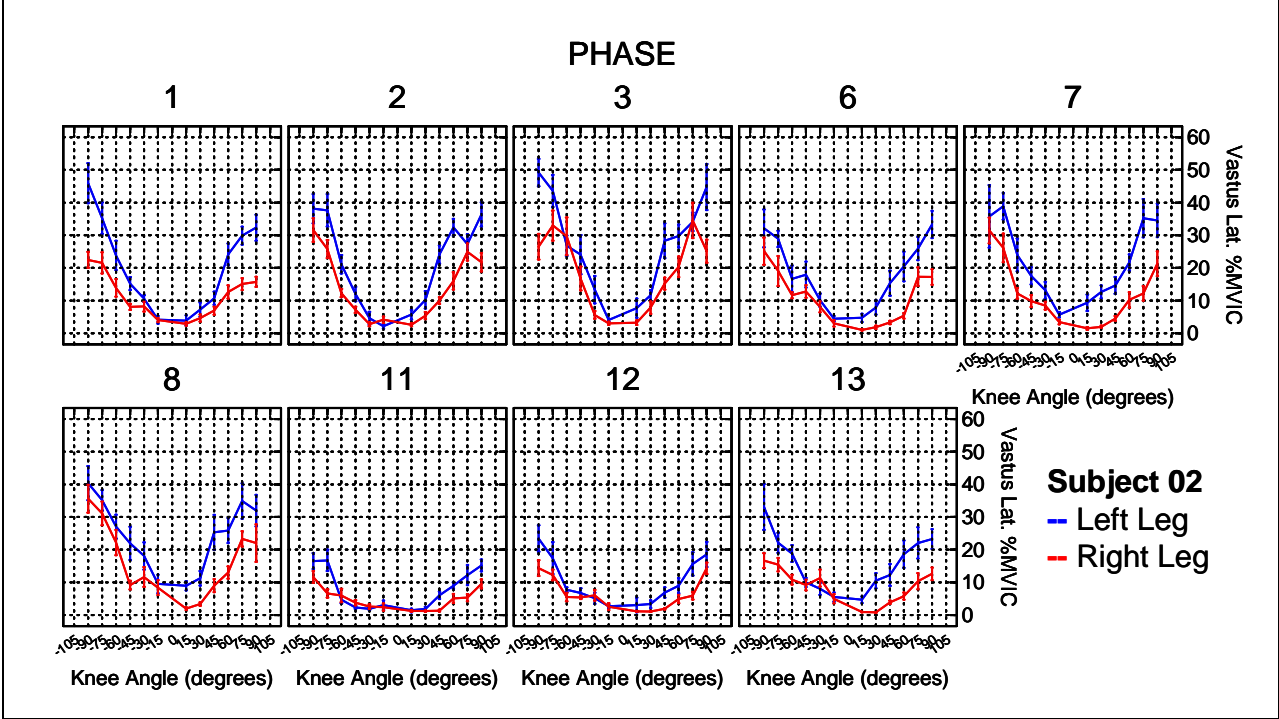
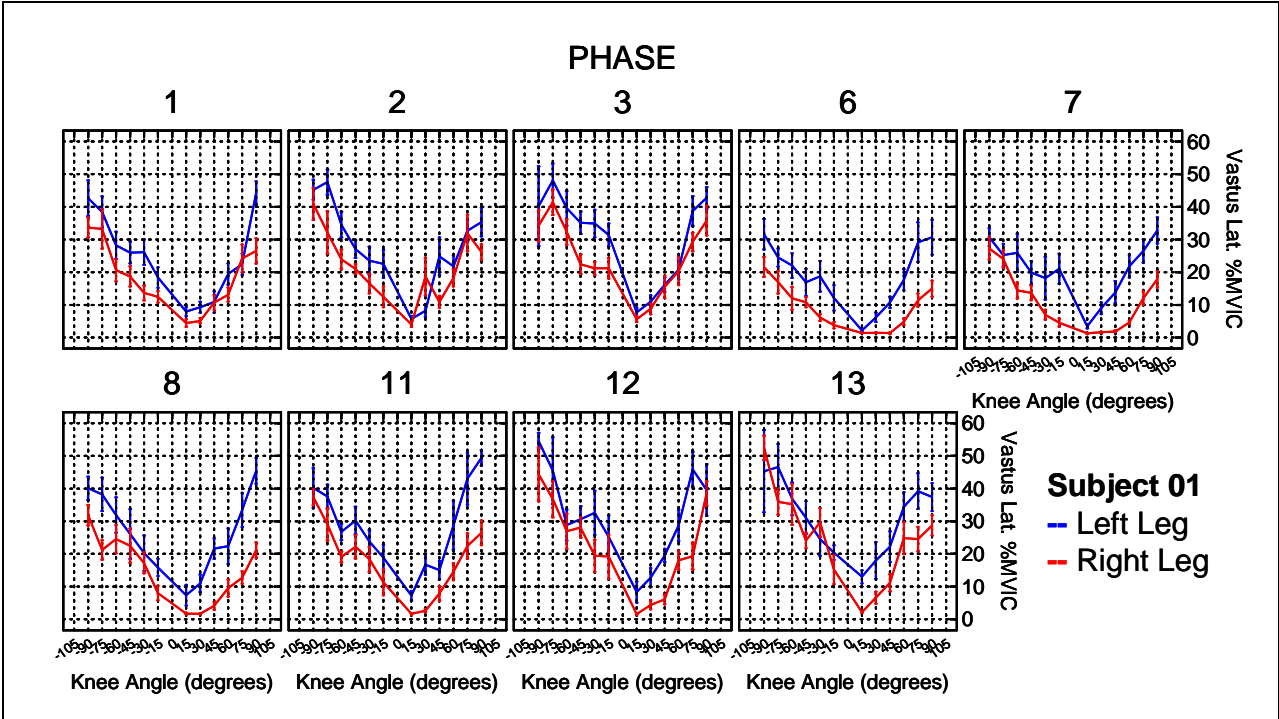
* p < 0.05, # p > 0.05

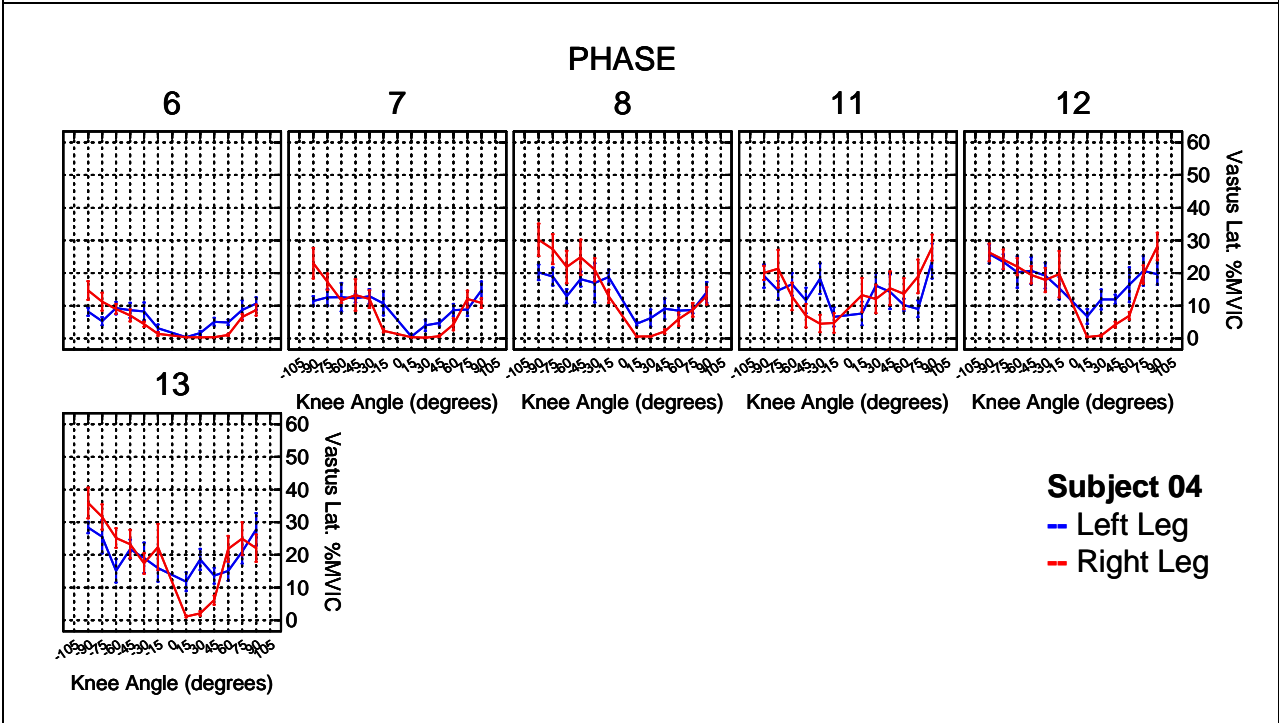
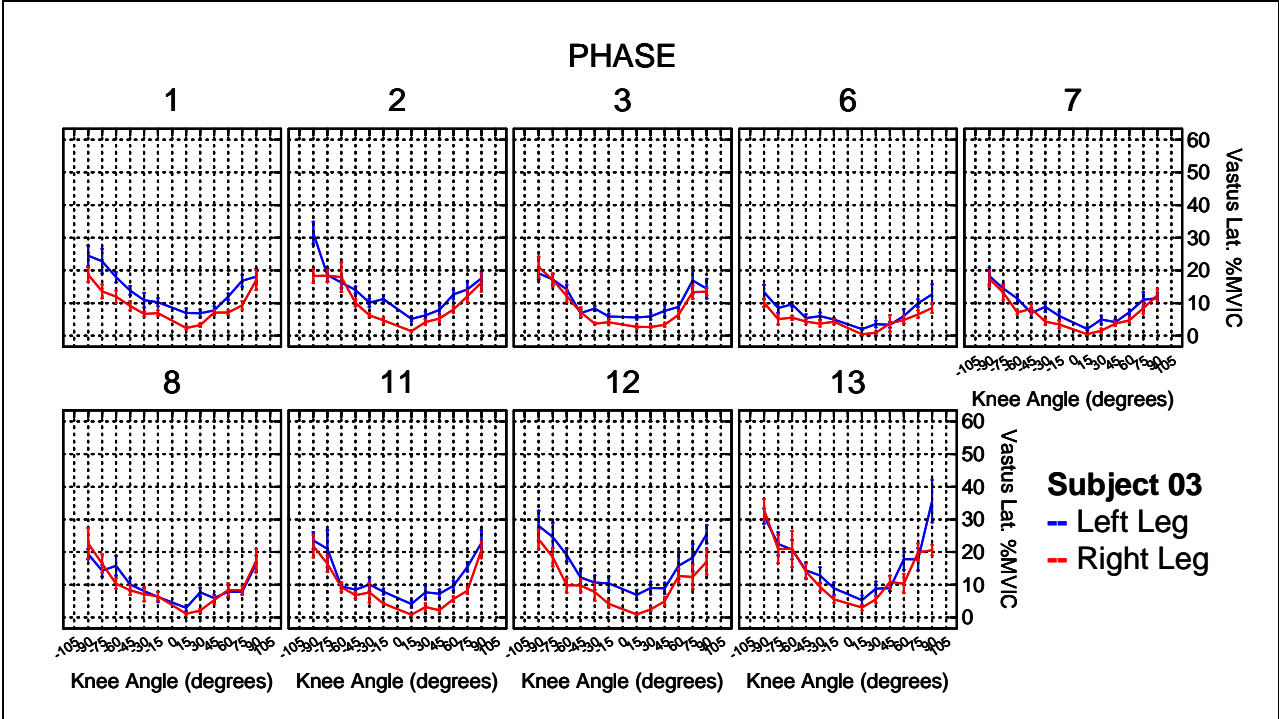
Knee Angle	Up 10%	23-RPM 0%	23-RPM 10%	23-RPM 25%	30-RPM 0%	30-RPM 10%	30-RPM 25%
15	0.86	3.95*	0.28#	0.23#	1.75*	0.57#	0.22#
30	1.05	0.22#	-0.20#	-0.19#	0.27#	-0.02#	0.12#
45	1.99	-1.05*	-1.07*	-1.23*	-0.66#	-0.82*	-0.52#
60	3.83	-2.79*	-2.74*	-2.76*	-1.65*	-1.94*	-1.02#
75	9.65	-7.83*	-8.34*	-8.18*	-2.29#	-4.40*	-2.86#
90	19.50	-16.37*	-16.49*	-13.80*	-7.86*	-4.97#	-4.14#
-90	9.86	-8.78*	-8.74*	-8.24*	-6.48*	-5.78*	-1.84#
-75	2.12	-1.08*	-0.84*	-0.68*	-0.26#	-0.17#	0.41#
-60	1.41	-0.45*	-0.33#	-0.17#	0.22#	0.29#	0.47#
-45	1.27	-0.25#	-0.29#	-0.13#	0.12#	0.16#	0.36#
-30	1.32	-0.44*	-0.18#	-0.24#	-0.10#	0.03#	0.19#
-15	1.16	0.42#	0.05#	0.06#	0.14#	0.01#	0.52#

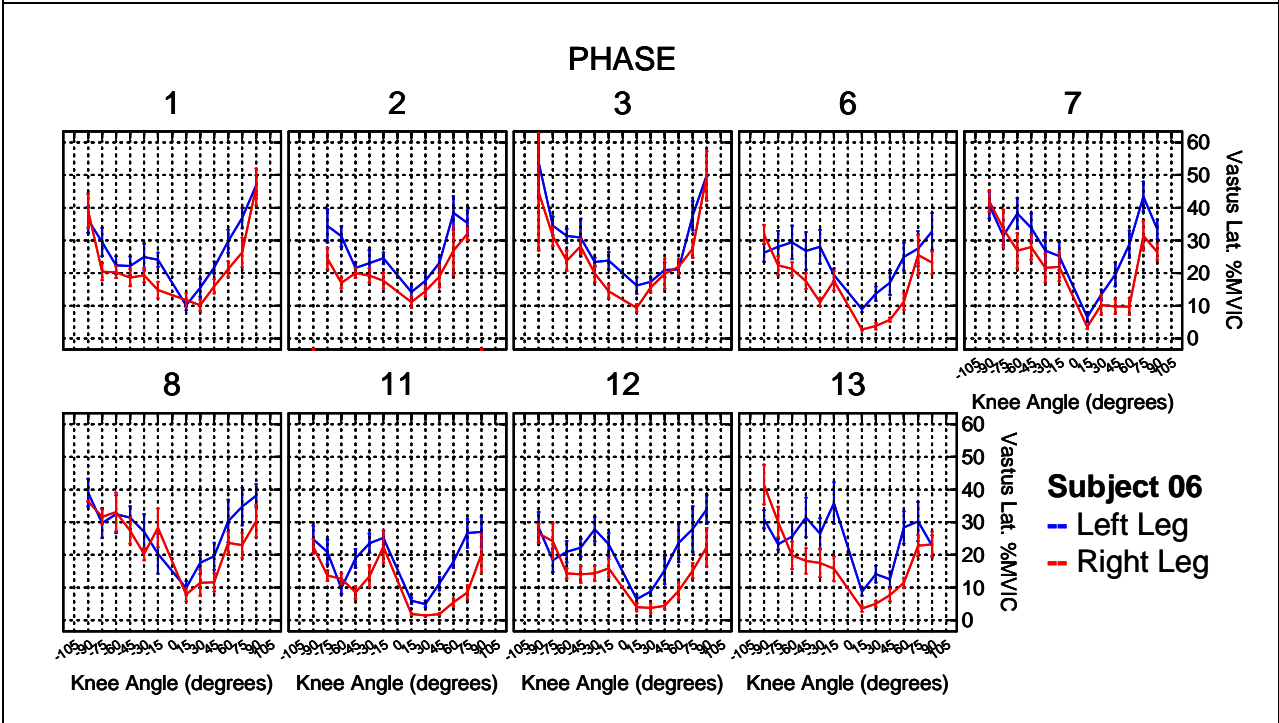
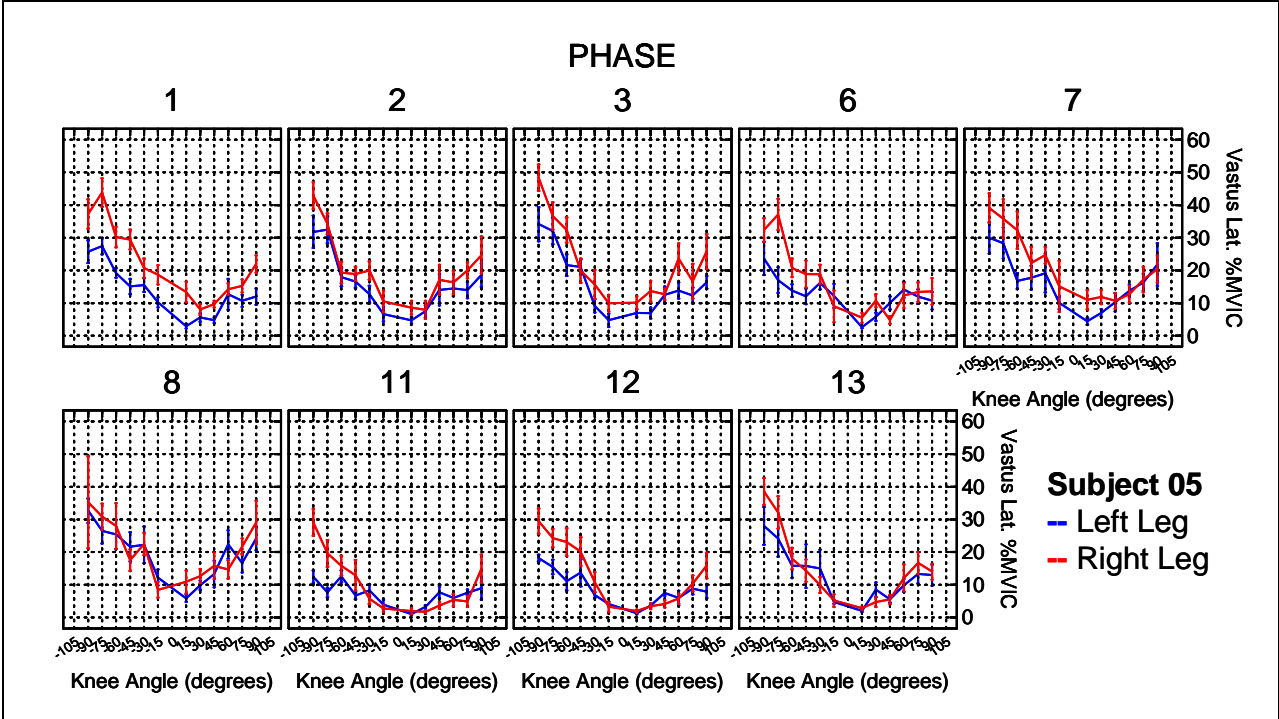
* p < 0.05, # p > 0.05

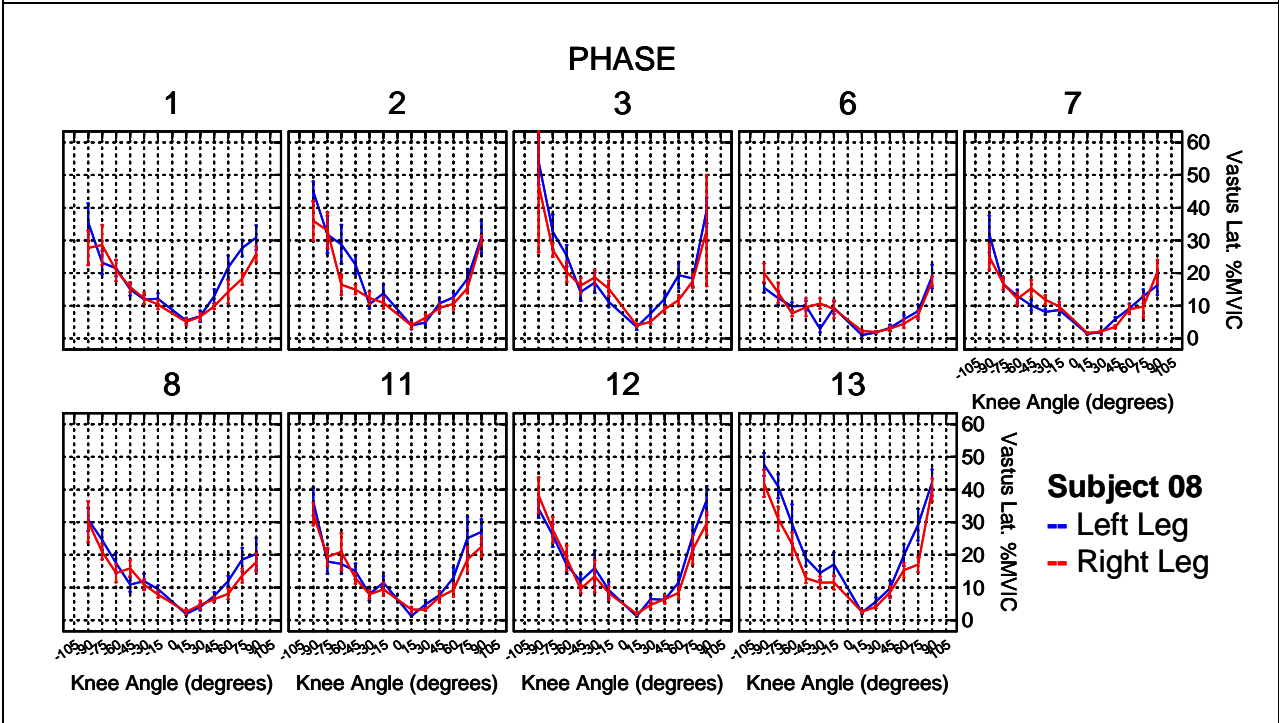
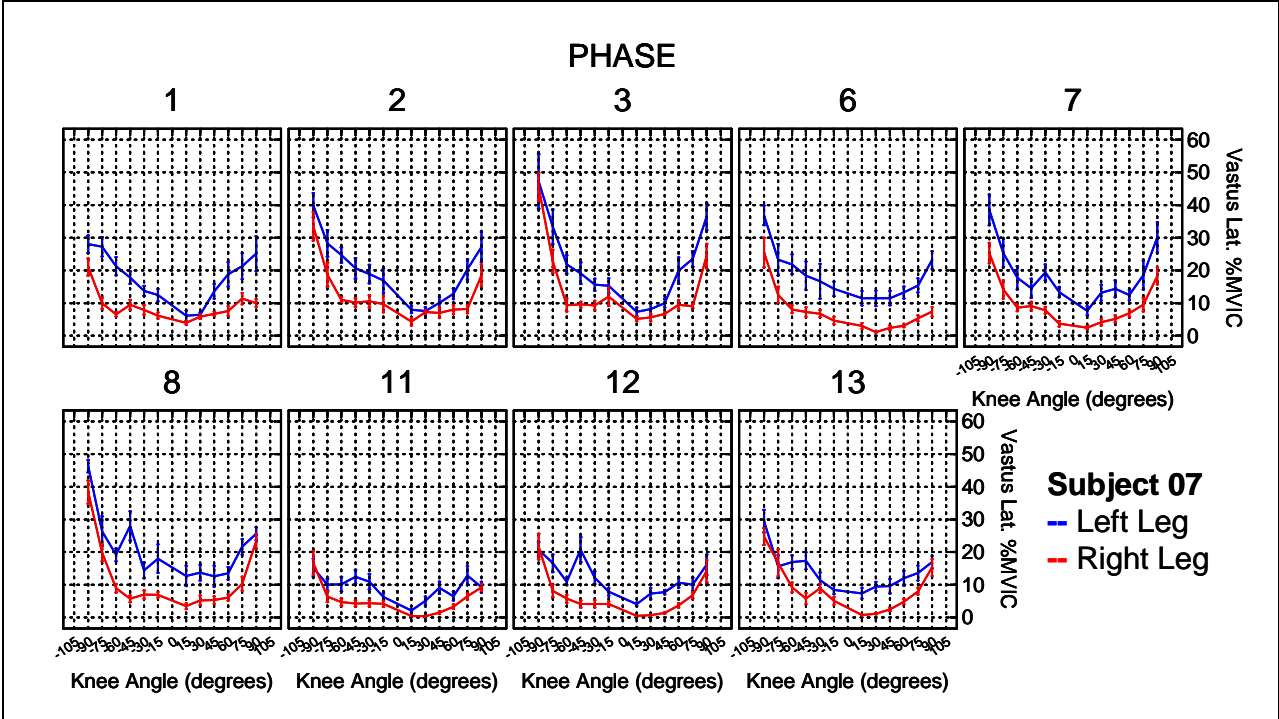
Knee Angle	Up 25%	23-RPM 0%	23-RPM 10%	23-RPM 25%	30-RPM 0%	30-RPM 10%	30-RPM 25%
15	1.07	3.74*	0.07#	0.02#	1.54*	0.36#	0.01#
30	1.12	0.14#	-0.27#	-0.26#	0.20#	-0.09#	0.05#
45	3.58	-2.64*	-2.66*	-2.81*	-2.25*	-2.40*	-2.10*
60	8.44	-7.41*	-7.35*	-7.37*	-6.26*	-6.55*	-5.63*
75	15.91	-14.08*	-14.60*	-14.44*	-8.55*	-10.66*	-9.12*
90	21.19	-18.06*	-18.18*	-15.48*	-9.55*	-6.66#	-5.83#
-90	11.42	-10.34*	-10.30*	-9.80*	-8.04*	-7.33*	-3.39#
-75	4.11	-3.07*	-2.83*	-2.66*	-2.24*	-2.15*	-1.57*
-60	2.25	-1.29*	-1.17*	-1.02*	-0.62#	-0.56#	-0.37#
-45	1.60	-0.57*	-0.62*	-0.45*	-0.20#	-0.16#	0.04#
-30	1.36	-0.47*	-0.21#	-0.27#	-0.13#	-0.01#	0.15#
-15	1.25	0.33#	-0.04#	-0.04#	0.05#	-0.09#	0.43#

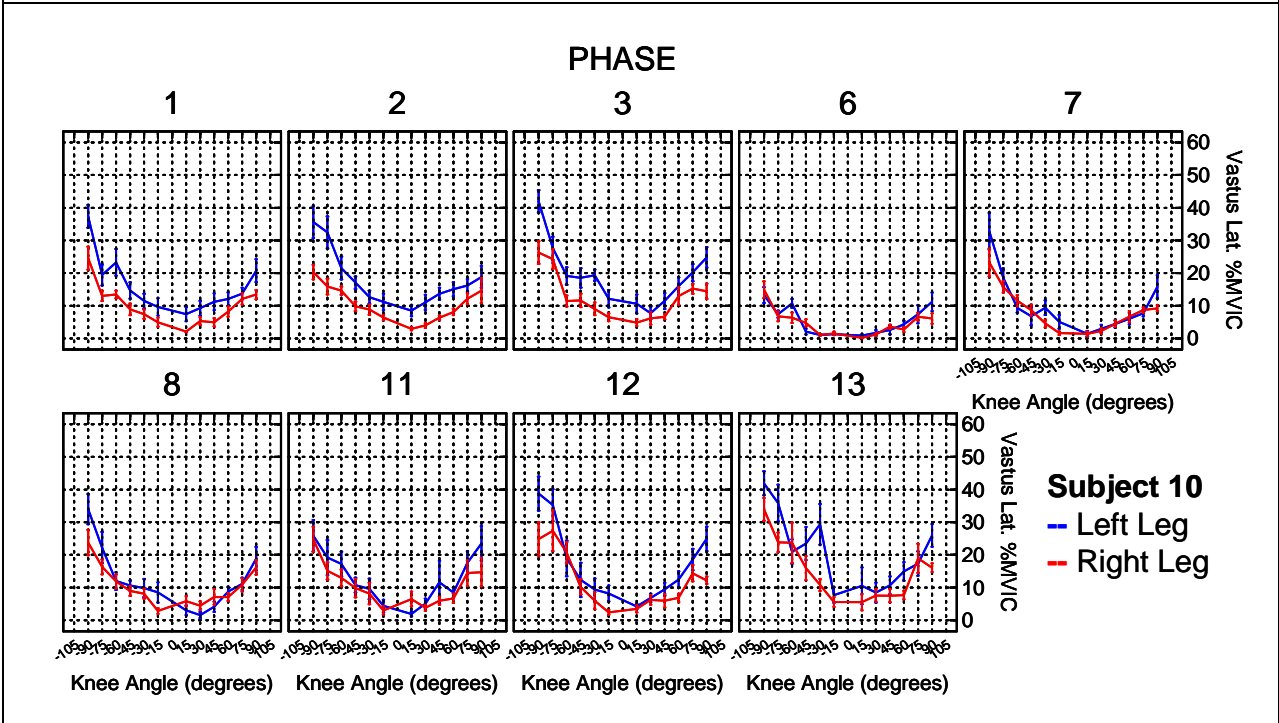
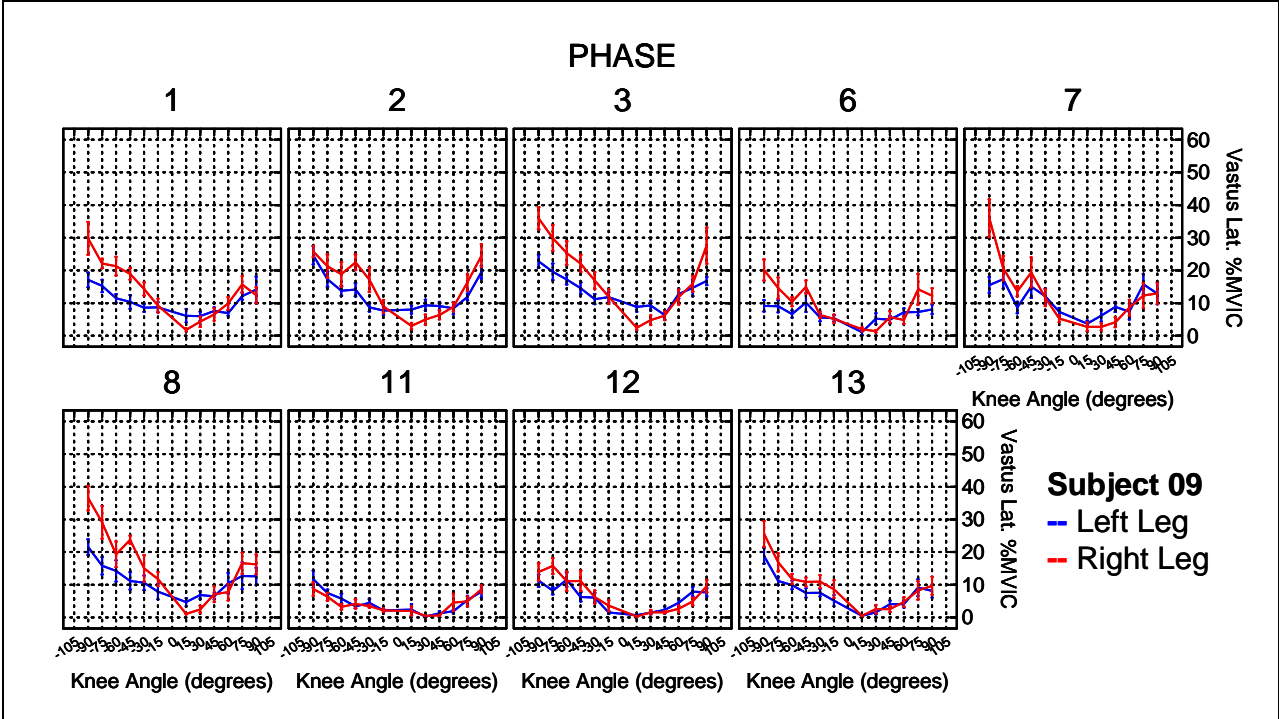
* p < 0.05, # p > 0.05

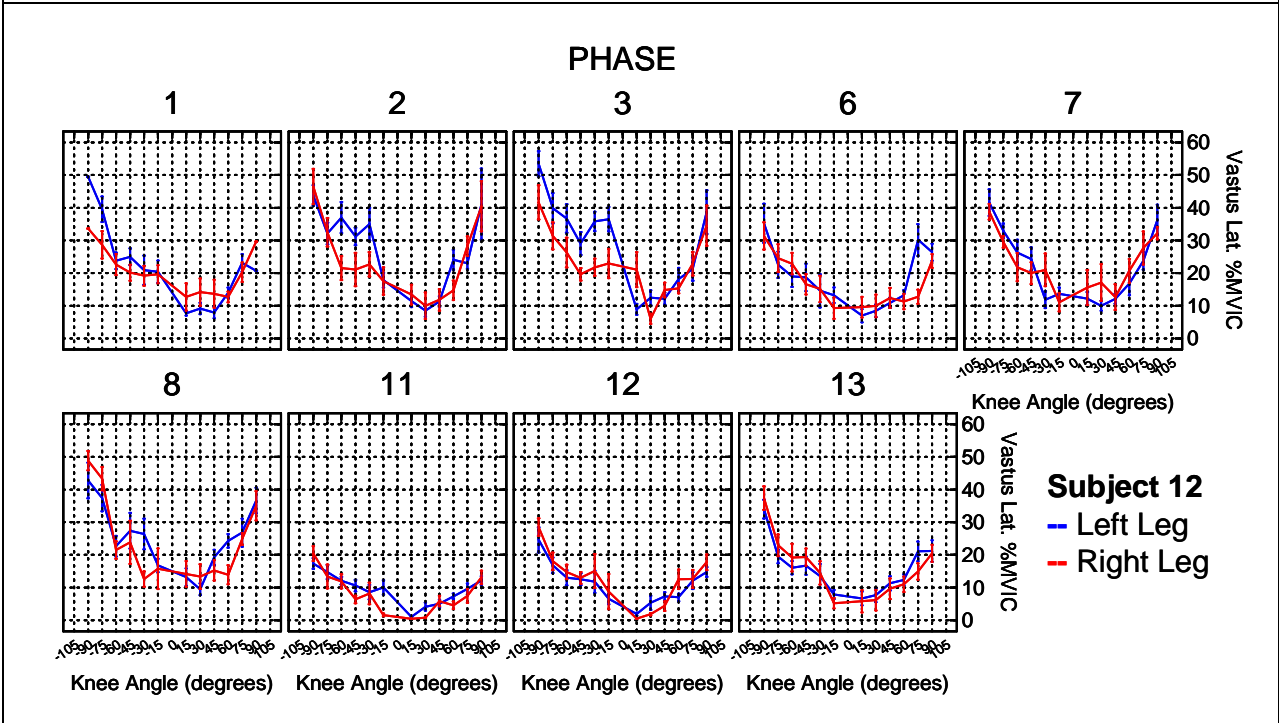
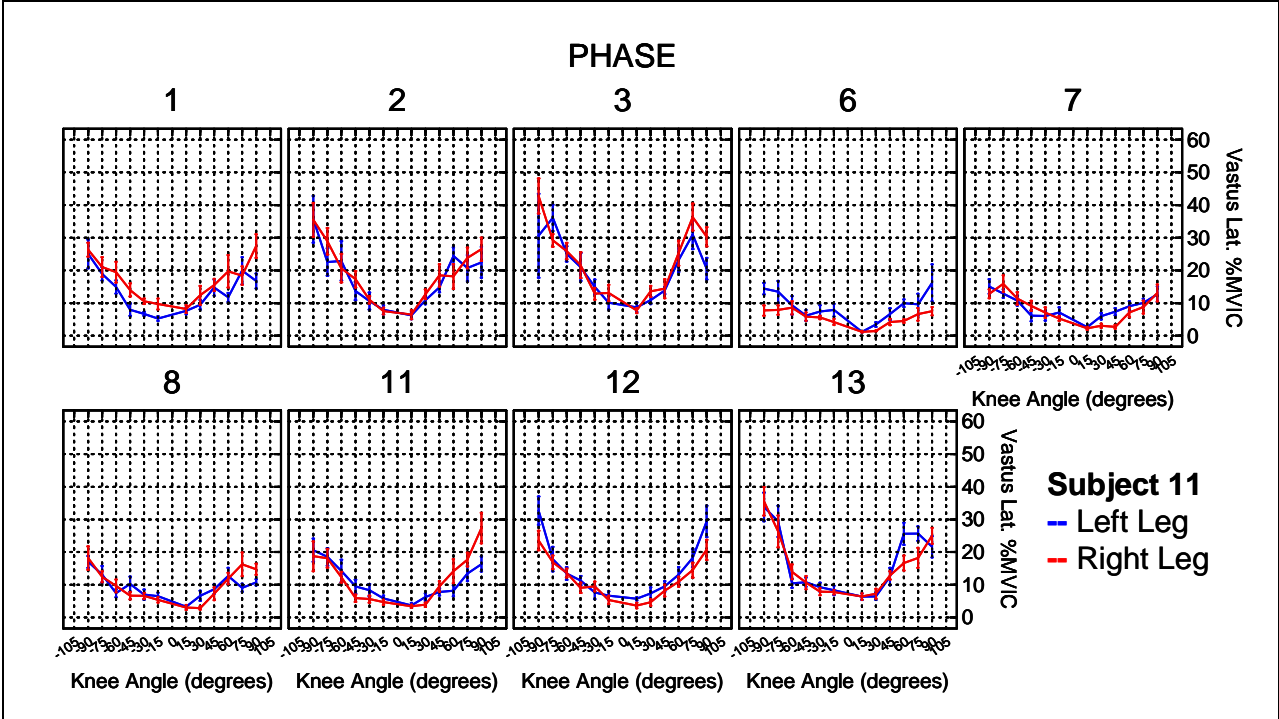


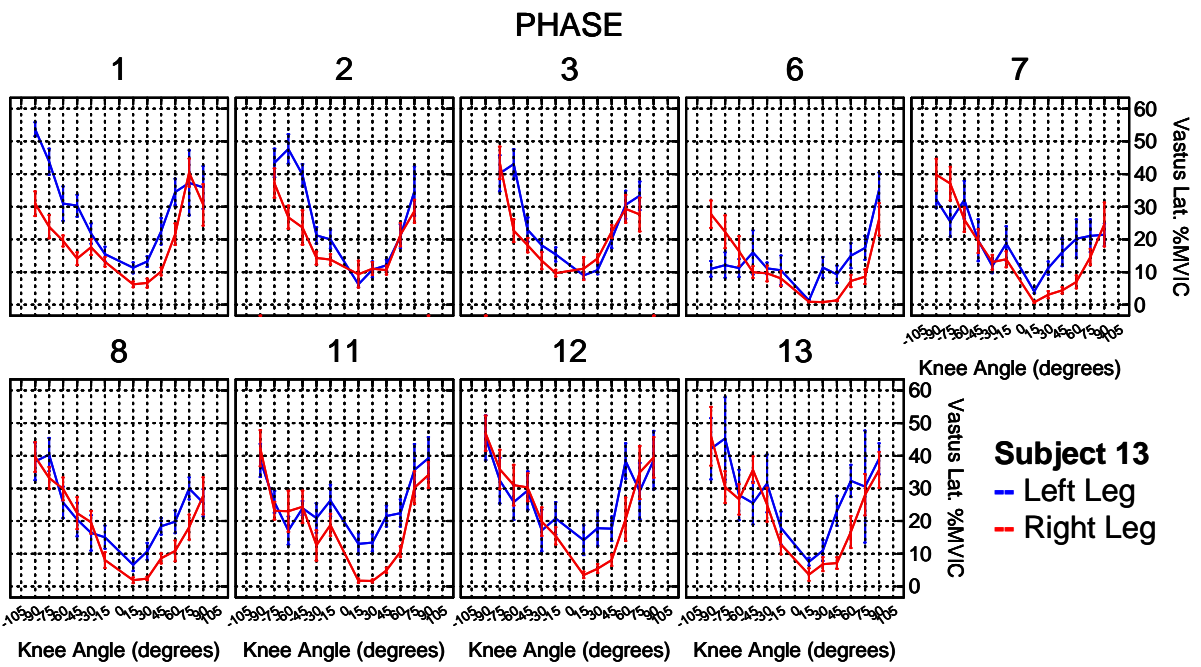












Left Vastus Lateralis

Knee Angle	Up 0%	23-RPM 0%	23-RPM 10%	23-RPM 25%	30-RPM 0%	30-RPM 10%	30-RPM 25%
15	6.99	-5.20*	-4.43*	-2.38*	-1.25#	0.52#	1.66*
30	8.75	-4.94*	-3.37*	-1.06#	0.64#	1.60#	2.47*
45	12.20	-5.92*	-4.19*	-2.15*	0.20#	0.38#	3.44*
60	18.47	-9.83*	-7.47*	-4.46*	-2.15#	1.47#	5.19*
75	24.15	-11.45*	-9.28*	-6.58*	-1.12#	2.50#	5.27*
90	27.25	-10.61*	-10.00*	-7.05*	0.61#	6.36*	5.94*
-90	34.05	-17.65*	-10.12*	-2.75#	-3.41#	8.24*	12.72*
-75	29.73	-16.97*	-12.91*	-7.29*	-7.84*	1.77#	8.53*
-60	21.58	-11.02*	-6.92*	-3.24#	-4.18*	-0.41#	4.14*
-45	17.82	-8.61*	-5.18*	-1.34#	-1.34#	2.92#	4.31*
-30	15.29	-6.55*	-4.10*	-1.51#	-0.68#	1.27#	6.03*
-15	12.61	-4.91*	-3.10*	-0.04#	-0.98#	0.57#	2.05#

* p < 0.05, # p > 0.05

Knee Angle	Up 10%	23-RPM 0%	23-RPM 10%	23-RPM 25%	30-RPM 0%	30-RPM 10%	30-RPM 25%
15	7.34	-5.55*	-4.78*	-2.73*	-1.60*	0.17#	1.31#
30	9.43	-5.61*	-4.05*	-1.74*	-0.03#	0.93#	1.79#
45	14.66	-8.38*	-6.66*	-4.62*	-2.26#	-2.08#	0.98#
60	19.85	-11.21*	-8.85*	-5.85*	-3.53#	0.09#	3.81#
75	23.88	-11.18*	-9.01*	-6.31*	-0.85#	2.77#	5.54*
90	26.53	-9.89*	-9.28*	-6.33*	1.34#	7.08*	6.66*
-90	41.46	-25.06*	-17.53*	-10.16*	-10.82*	0.83#	5.31#
-75	33.12	-20.35*	-16.29*	-10.67*	-11.22*	-1.61#	5.15#
-60	26.92	-16.35*	-12.26*	-8.58*	-9.52*	-5.75*	-1.20#
-45	21.08	-11.87*	-8.44*	-4.60*	-4.60*	-0.34#	1.04#
-30	15.97	-7.23*	-4.78*	-2.19#	-1.36#	0.59#	5.35*
-15	13.56	-5.86*	-4.06*	-0.99#	-1.93#	-0.38#	1.10#

* p < 0.05, # p > 0.05

Knee Angle	Up 25%	23-RPM 0%	23-RPM 10%	23-RPM 25%	30-RPM 0%	30-RPM 10%	30-RPM 25%
15	8.43	-6.65*	-5.87*	-3.83*	-2.69*	-0.92#	0.22#
30	9.98	-6.17*	-4.60*	-2.29*	-0.59#	0.38#	1.24#
45	14.31	-8.03*	-6.30*	-4.26*	-1.91#	-1.73#	1.33#
60	20.23	-11.59*	-9.23*	-6.23*	-3.91*	-0.29#	3.43#
75	26.11	-13.42*	-11.25*	-8.55*	-3.09#	0.53#	3.31#
90	36.58	-19.94*	-19.33*	-16.38*	-8.71*	-2.97#	-3.39#
-90	54.14	-37.74*	-30.21*	-22.84*	-23.50*	-11.85*	-7.37#
-75	38.27	-25.50*	-21.44*	-15.82*	-16.37*	-6.76*	0.00#
-60	28.62	-18.06*	-13.97*	-10.29*	-11.22*	-7.45*	-2.90#
-45	22.30	-13.09*	-9.67*	-5.83*	-5.82*	-1.56#	-0.18#
-30	18.74	-10.00*	-7.56*	-4.97*	-4.13*	-2.19#	2.58#
-15	15.22	-7.51*	-5.71*	-2.64#	-3.58*	-2.03#	-0.55#

* p < 0.05, # p > 0.05

Right Vastus Lateralis

Knee Angle	Up 0%	23-RPM 0%	23-RPM 10%	23-RPM 25%	30-RPM 0%	30-RPM 10%	30-RPM 25%
15	6.26	-5.11*	-4.97*	-3.85*	-2.14*	-2.20*	-1.33#
30	7.23	-6.13*	-5.18*	-4.20*	-2.74*	-1.31#	-0.41#
45	9.82	-7.31*	-6.79*	-4.22*	-3.18*	-2.83*	0.67#
60	14.73	-10.23*	-8.41*	-6.12*	-4.78*	-2.93#	0.09#
75	18.90	-11.88*	-8.86*	-5.83*	-2.05#	0.37#	3.22#
90	23.20	-10.49*	-7.64*	-6.00*	-1.92#	2.51#	4.85*
-90	29.01	-11.62*	-5.49*	1.16#	-0.22#	8.58*	20.57*
-75	23.69	-12.13*	-4.98*	-1.09#	-2.69#	3.75#	9.75*
-60	18.40	-9.16*	-5.41*	-2.14#	-2.55#	1.48#	6.37*
-45	15.46	-8.34*	-2.90*	-1.05#	-1.77#	1.87#	4.26*
-30	13.18	-7.08*	-3.74*	-0.57#	-3.03*	1.38#	2.27#
-15	10.86	-5.62*	-4.75*	-2.99*	-2.73*	-0.45#	1.49#

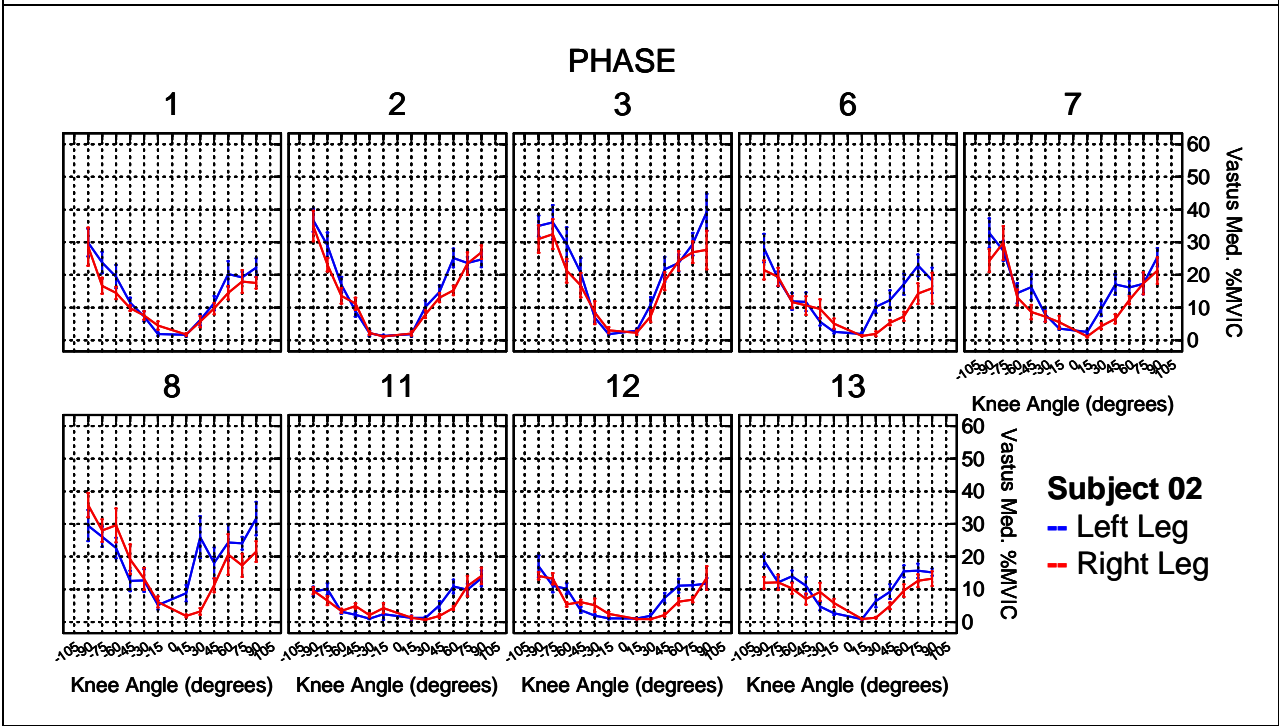
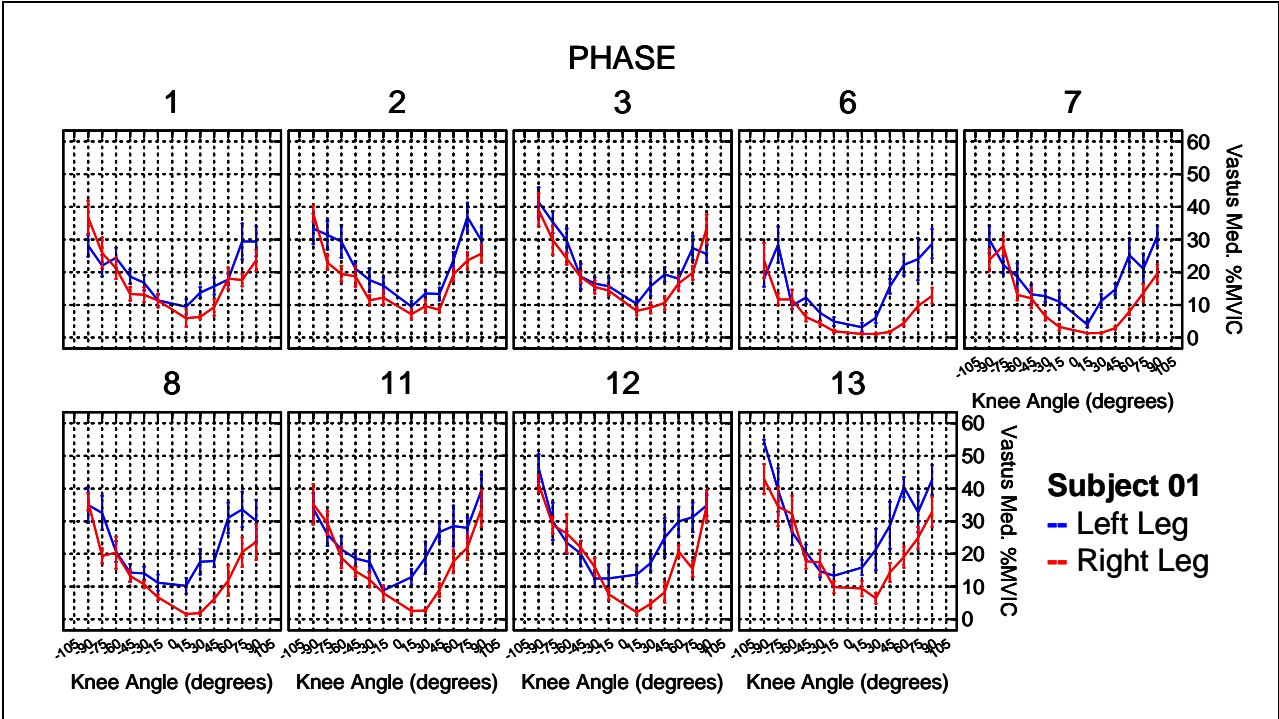
* p < 0.05, # p > 0.05

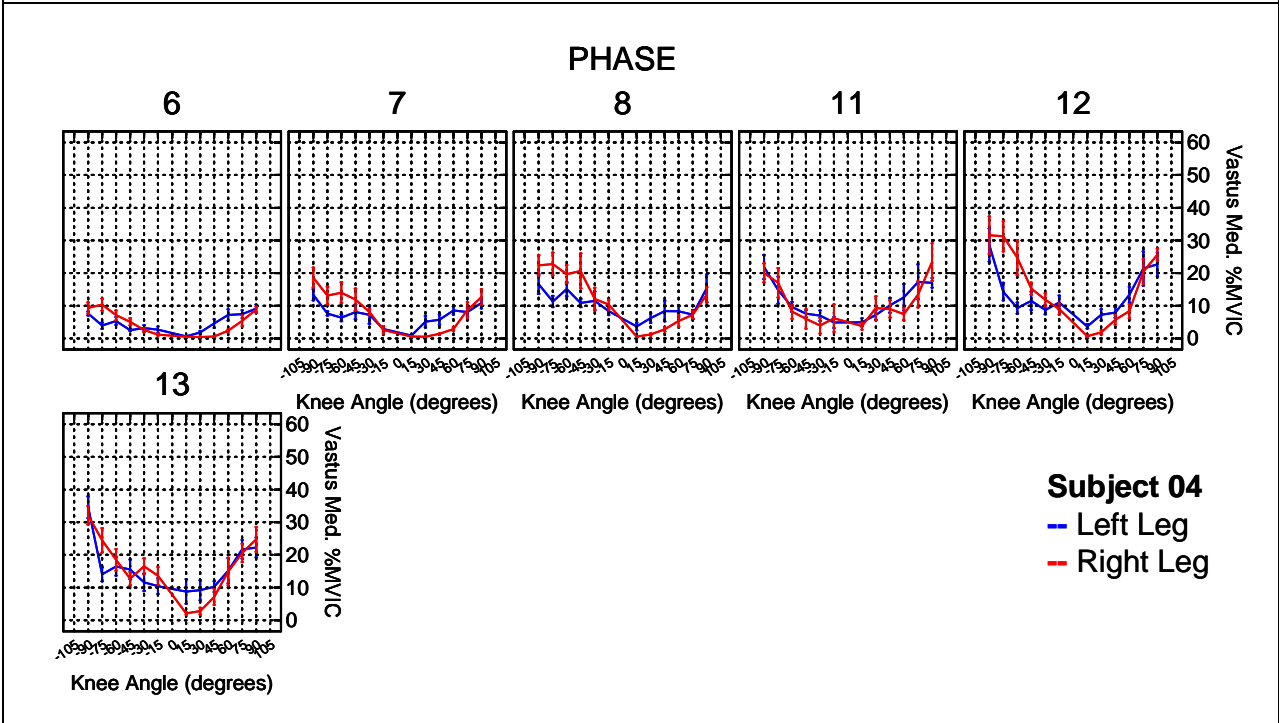
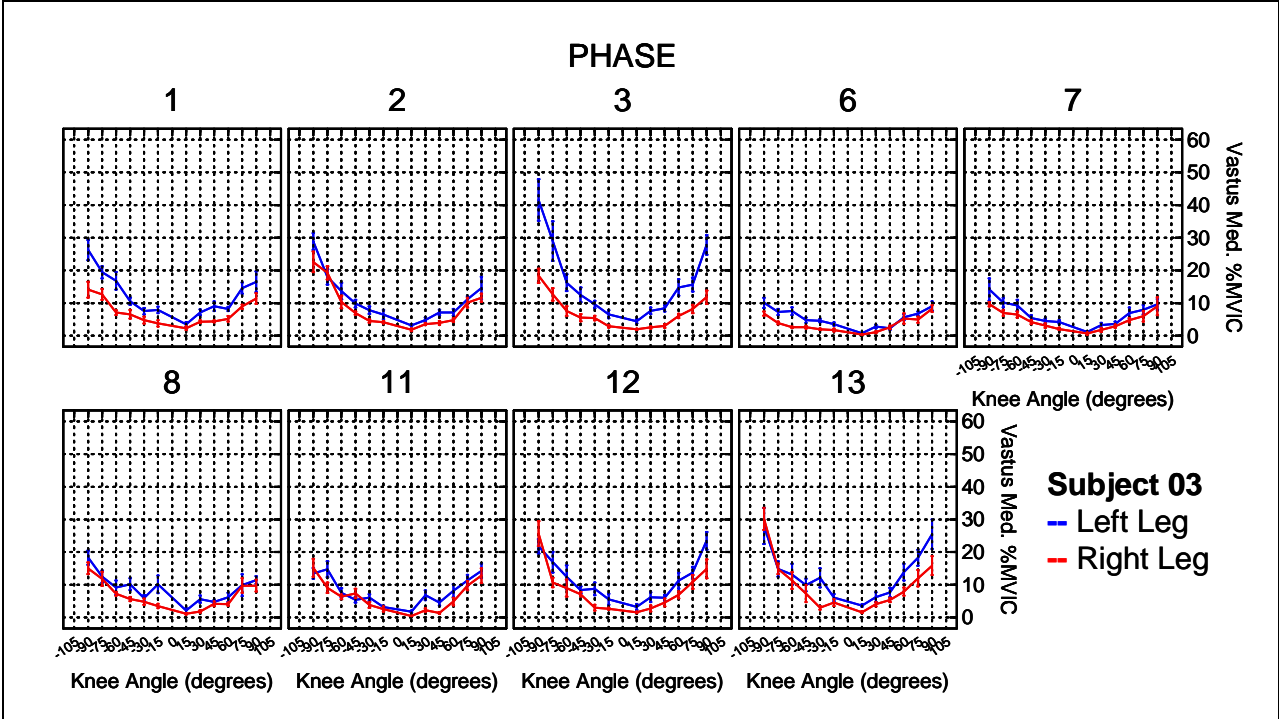
Knee Angle	Up 10%	23-RPM 0%	23-RPM 10%	23-RPM 25%	30-RPM 0%	30-RPM 10%	30-RPM 25%
15	5.94	-4.79*	-4.65*	-3.54*	-1.82#	-1.89*	-1.02#
30	8.93	-7.82*	-6.88*	-5.89*	-4.43*	-3.01*	-2.11*
45	11.03	-8.52*	-8.00*	-5.43*	-4.39*	-4.03*	-0.53#
60	16.35	-11.86*	-10.04*	-7.75*	-6.41*	-4.56*	-1.54#
75	21.71	-14.69*	-11.67*	-8.64*	-4.86*	-2.44#	0.41#
90	24.35	-11.64*	-8.78*	-7.15*	-3.07#	1.36#	3.70#
-90	34.07	-16.68*	-10.54*	-3.89#	-5.27*	3.52#	15.52*
-75	27.82	-16.25*	-9.11*	-5.21*	-6.82*	-0.37#	5.62*
-60	18.38	-9.14*	-5.39*	-2.12#	-2.53*	1.50#	6.39*
-45	16.40	-9.28*	-3.84*	-1.99#	-2.71*	0.92#	3.32*
-30	13.49	-7.40*	-4.05*	-0.89#	-3.34*	1.07#	1.95#
-15	10.39	-5.15*	-4.28*	-2.52*	-2.26*	0.02#	1.96#

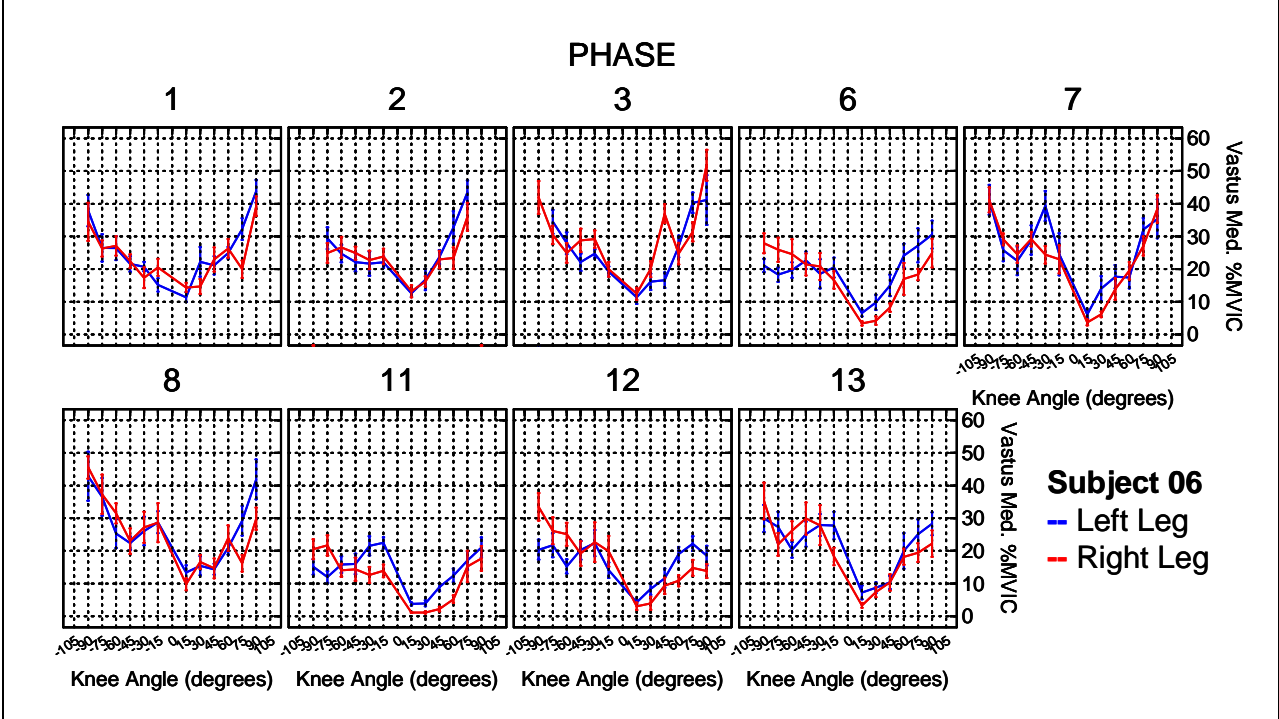
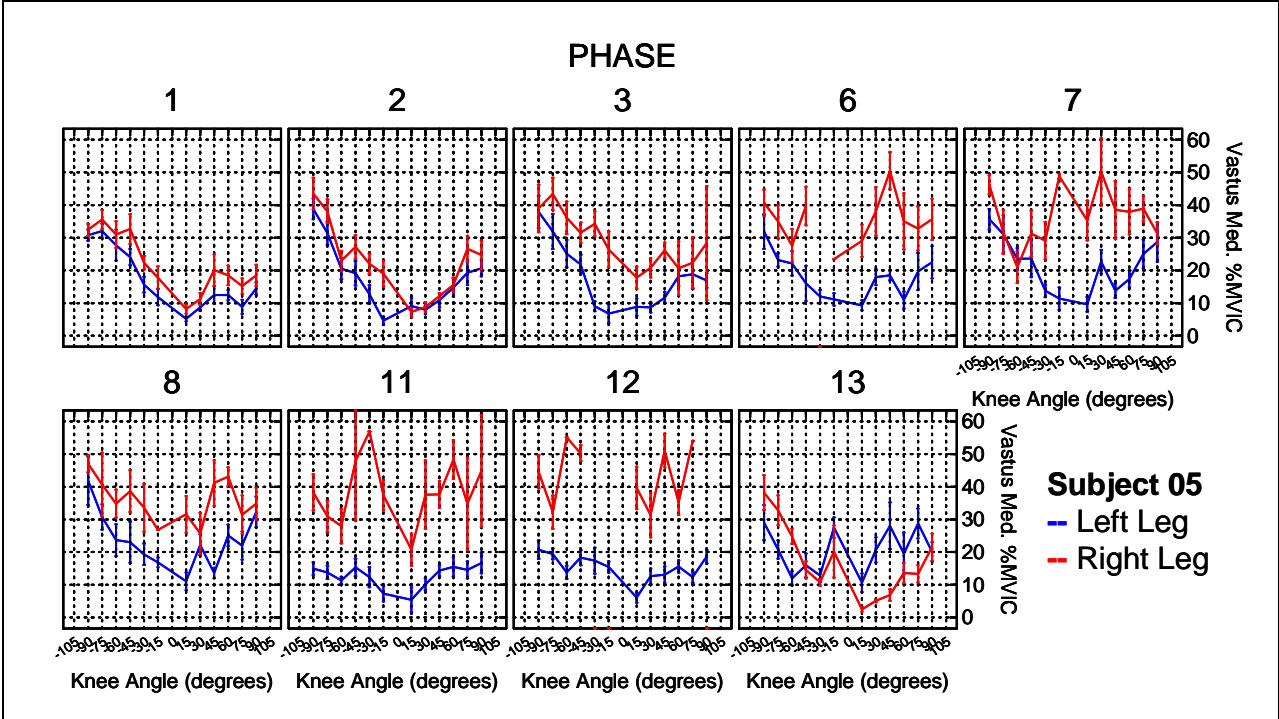
* p < 0.05, # p > 0.05

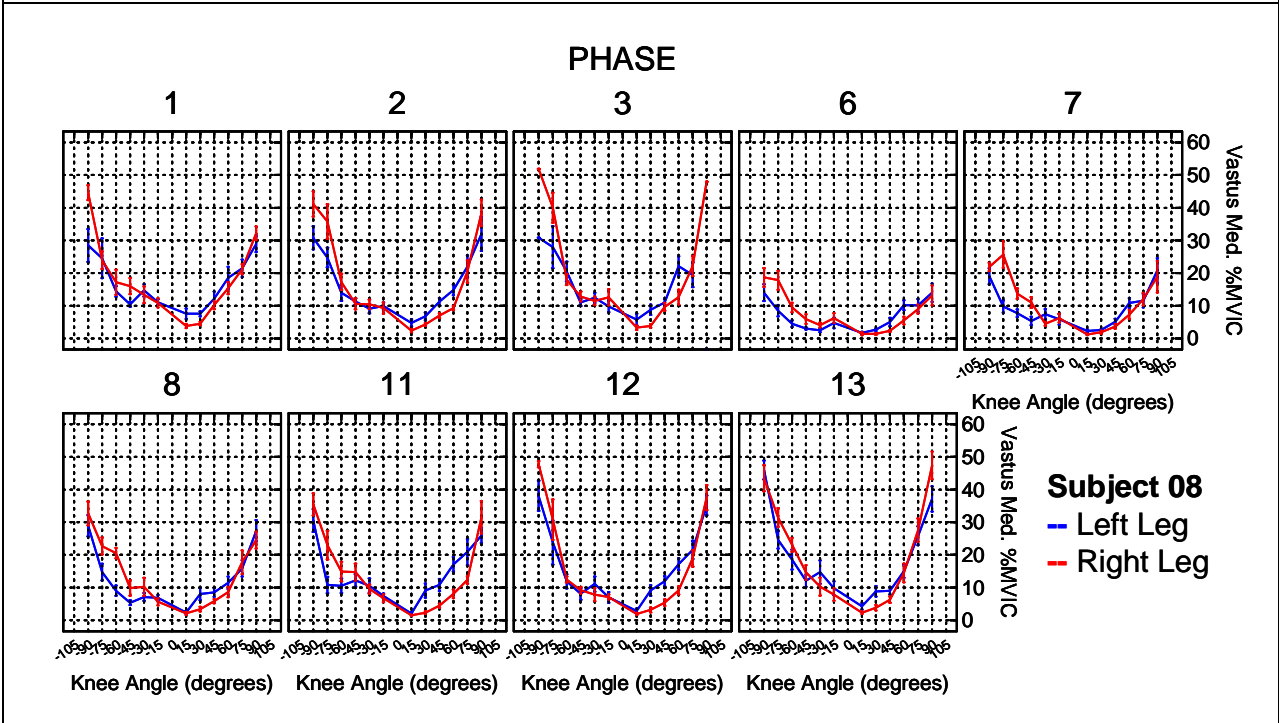
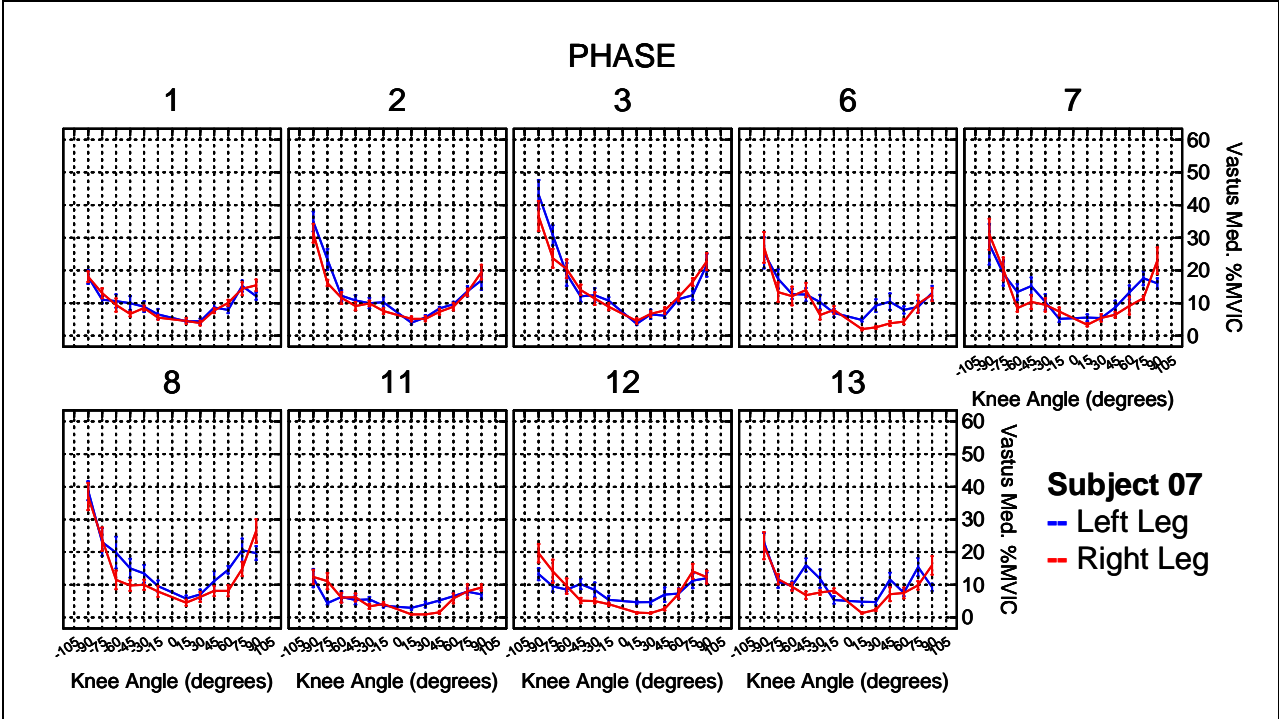
Knee Angle	Up 25%	23-RPM 0%	23-RPM 10%	23-RPM 25%	30-RPM 0%	30-RPM 10%	30-RPM 25%
15	7.30	-6.15*	-6.01*	-4.89*	-3.18*	-3.24*	-2.37*
30	8.68	-7.57*	-6.63*	-5.64*	-4.18*	-2.75*	-1.85*
45	12.24	-9.72*	-9.20*	-6.63*	-5.59*	-5.24*	-1.74#
60	17.40	-12.90*	-11.09*	-8.80*	-7.46*	-5.60*	-2.58#
75	23.11	-16.09*	-13.07*	-10.04*	-6.26*	-3.84*	-0.99#
90	27.11	-14.39*	-11.54*	-9.90*	-5.83*	-1.39#	0.95#
-90	42.47	-25.08*	-18.94*	-12.30*	-13.67*	-4.88#	7.11*
-75	32.97	-21.40*	-14.26*	-10.37*	-11.97*	-5.53*	0.47#
-60	22.65	-13.41*	-9.66*	-6.39*	-6.80*	-2.77#	2.12#
-45	17.82	-10.70*	-5.26*	-3.41*	-4.13*	-0.49#	1.90#
-30	14.02	-7.93*	-4.58*	-1.42#	-3.87*	0.54#	1.42#
-15	12.03	-6.79*	-5.92*	-4.16*	-3.90*	-1.62#	0.32#

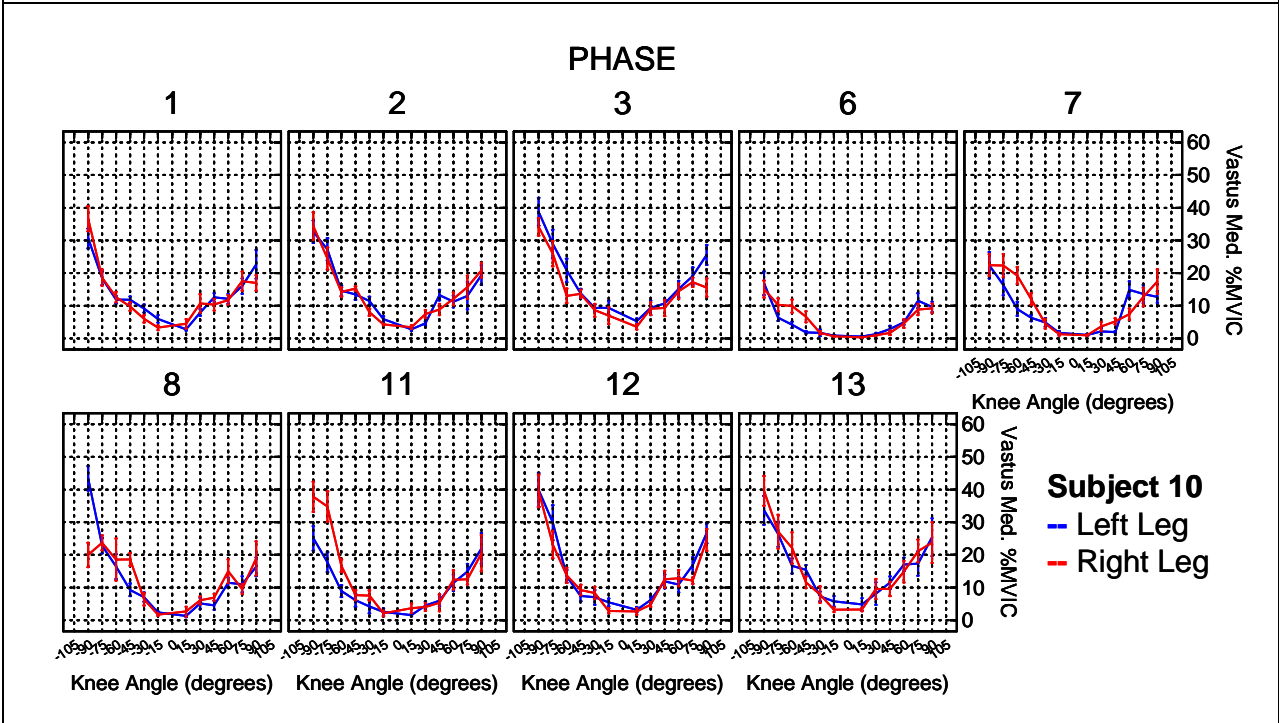
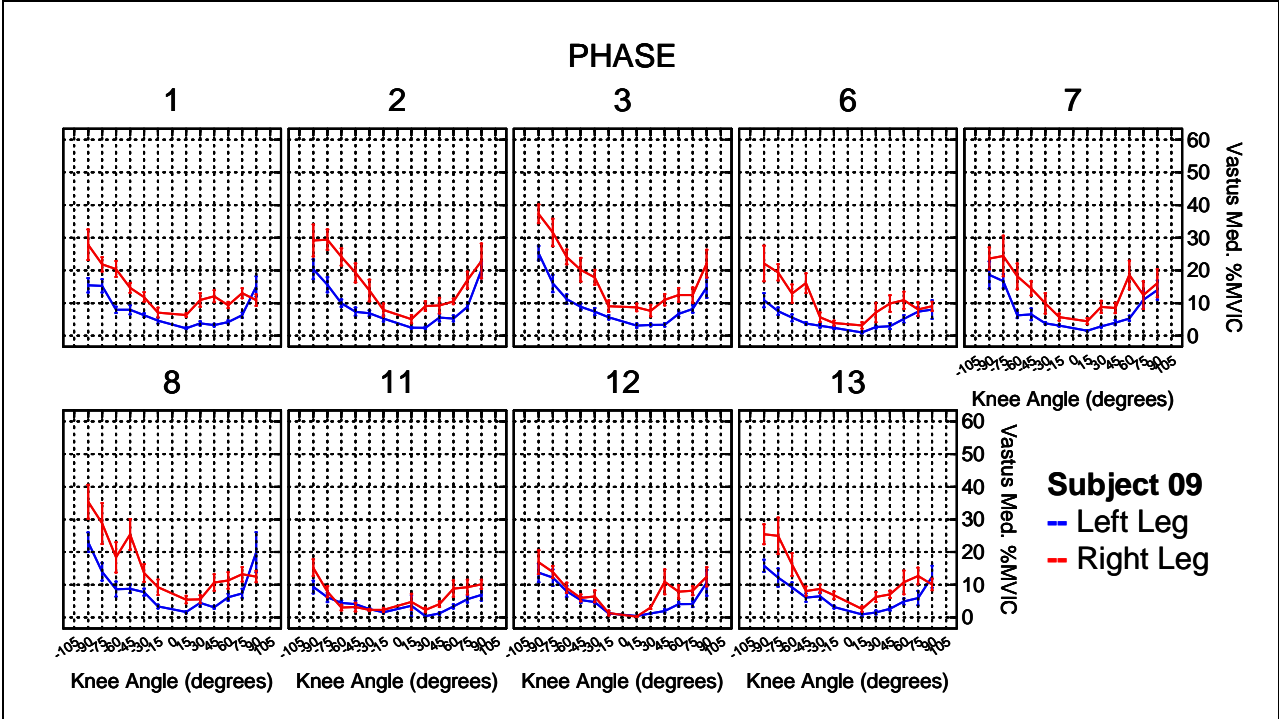
* p < 0.05, # p > 0.05

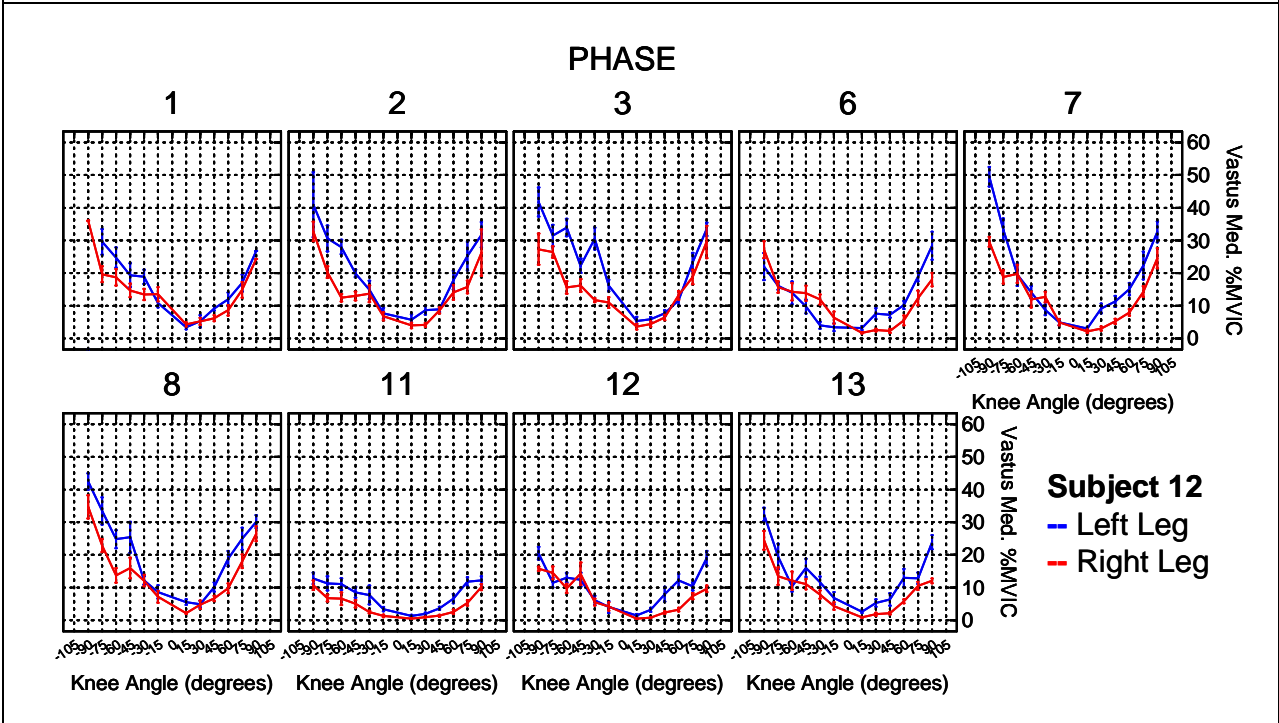
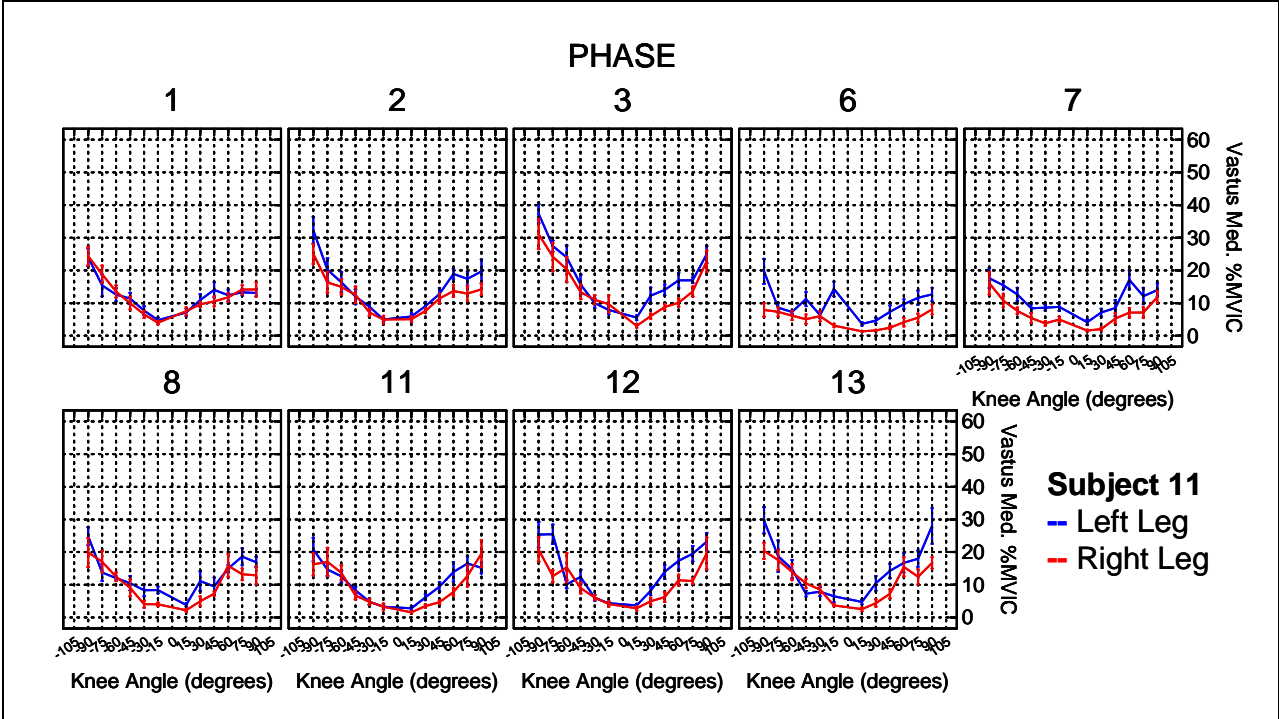


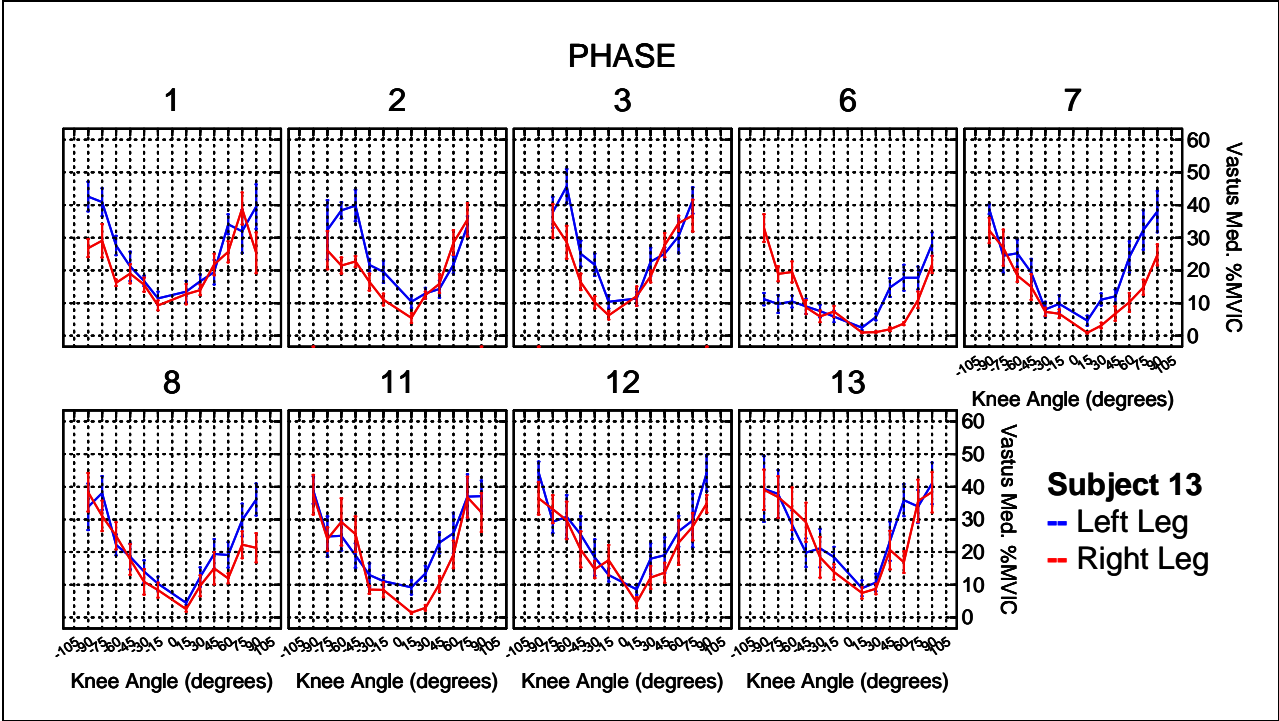












Left Vastus Medialis

Knee Angle	Up 0%	23-RPM 0%	23-RPM 10%	23-RPM 25%	30-RPM 0%	30-RPM 10%	30-RPM 25%
15	6.04	-3.62*	-3.25*	-1.79*	-1.25#	-0.85#	1.45#
30	9.57	-5.95*	-3.83*	-0.83#	-0.03#	0.88#	3.15*
45	12.44	-5.43*	-4.67*	-1.55#	-0.35#	0.54#	1.41#
60	15.43	-5.19*	-1.81#	-0.95#	-0.54#	1.81#	5.22*
75	19.67	-7.21*	-5.24*	-0.96#	0.71#	2.80#	3.70*
90	23.04	-8.19*	-4.82*	-2.11#	-0.19#	6.01*	9.11*
-90	29.81	-16.63*	-8.92*	-0.61#	-3.87#	8.41*	13.40*
-75	24.27	-14.22*	-9.52*	-4.58*	-6.94*	1.31#	4.49*
-60	18.74	-10.94*	-6.60*	-4.21*	-4.29*	-2.50#	1.61#
-45	14.91	-7.49*	-4.40*	-1.45#	-3.04*	0.34#	1.45#
-30	12.55	-6.06*	-3.75*	-1.50#	-3.54*	-0.53#	1.37#
-15	8.65	-2.66*	-2.04*	1.89#	-1.84*	-0.05#	2.33*

* p < 0.05, # p > 0.05

Knee Angle	Up 10%	23-RPM 0%	23-RPM 10%	23-RPM 25%	30-RPM 0%	30-RPM 10%	30-RPM 25%
15	6.05	-3.63*	-3.26*	-1.80*	-1.26#	-0.86#	1.44#
30	8.64	-5.02*	-2.89*	0.10#	0.90#	1.81#	4.08*
45	12.02	-5.01*	-4.25*	-1.13#	0.07#	0.96#	1.84#
60	16.95	-6.70*	-3.33*	-2.46#	-2.05#	0.29#	3.71*
75	22.65	-10.19*	-8.22*	-3.94#	-2.28#	-0.18#	0.72#
90	22.51	-7.66*	-4.29*	-1.58#	0.33#	6.54*	9.64*
-90	33.04	-19.86*	-12.14*	-3.83#	-7.09*	5.18*	10.18*
-75	28.08	-18.03*	-13.33*	-8.38*	-10.74*	-2.49#	0.69#
-60	19.94	-12.14*	-7.80*	-5.41*	-5.49*	-3.69*	0.41#
-45	17.31	-9.90*	-6.80*	-3.85*	-5.44*	-2.06#	-0.95#
-30	12.08	-5.60*	-3.28*	-1.03#	-3.07*	-0.06#	1.84#
-15	9.52	-3.52*	-2.91*	1.02#	-2.71*	-0.92#	1.47#

* p < 0.05, # p > 0.05

Knee Angle	Up 25%	23-RPM 0%	23-RPM 10%	23-RPM 25%	30-RPM 0%	30-RPM 10%	30-RPM 25%
15	6.52	-4.10*	-3.72*	-2.26*	-1.73*	-1.33*	0.98#
30	10.67	-7.05*	-4.93*	-1.93#	-1.13#	-0.23#	2.04#
45	13.00	-5.99*	-5.23*	-2.12#	-0.91#	-0.02#	0.85#
60	18.38	-8.14*	-4.76*	-3.90*	-3.49*	-1.14#	2.27#
75	22.72	-10.26*	-8.29*	-4.01#	-2.34#	-0.25#	0.65#
90	28.31	-13.46*	-10.08*	-7.38*	-5.46*	0.74#	3.84#
-90	44.10	-30.92*	-23.21*	-14.89*	-18.15*	-5.88*	-0.89#
-75	32.36	-22.31*	-17.62*	-12.67*	-15.03*	-6.78*	-3.60#
-60	25.94	-18.15*	-13.81*	-11.41*	-11.50*	-9.70*	-5.60*
-45	17.10	-9.69*	-6.60*	-3.64*	-5.23*	-1.85#	-0.74#
-30	14.23	-7.74*	-5.42*	-3.18*	-5.22*	-2.21#	-0.31#
-15	10.04	-4.05*	-3.44*	0.50#	-3.23*	-1.44#	0.94#

* p < 0.05, # p > 0.05

Right Vastus Medialis

Knee Angle	Up 0%	23-RPM 0%	23-RPM 10%	23-RPM 25%	30-RPM 0%	30-RPM 10%	30-RPM 25%
15	6.38	-3.63*	-1.17#	-4.51*	-1.76#	-0.91#	2.04#
30	8.45	-1.61#	-2.45#	-4.34*	0.74#	1.42#	1.57#
45	12.11	-7.31*	-3.37#	-5.43*	-1.71#	-0.08#	1.31#
60	14.62	-4.60*	-2.48#	-3.99*	-0.09#	2.42#	3.22#
75	17.83	-3.22#	-0.31#	-4.07*	-0.09#	1.89#	4.45*
90	21.18	-3.25#	0.49#	-4.27*	1.52#	6.57*	7.67*
-90	30.39	-13.38*	-7.35*	-2.11#	-0.88#	5.29*	12.60*
-75	21.86	-9.13*	-0.13#	-1.15#	0.92#	3.70*	10.68*
-60	17.43	-5.65*	1.79#	-0.28#	-1.11#	0.74#	5.70*
-45	14.65	-2.76#	1.17#	-1.39#	2.13#	1.41#	4.13*
-30	11.73	-1.66#	1.14#	-1.63#	6.75#	1.60#	5.51*
-15	9.31	1.32#	-3.43*	-0.92#	2.35#	4.67#	5.40*

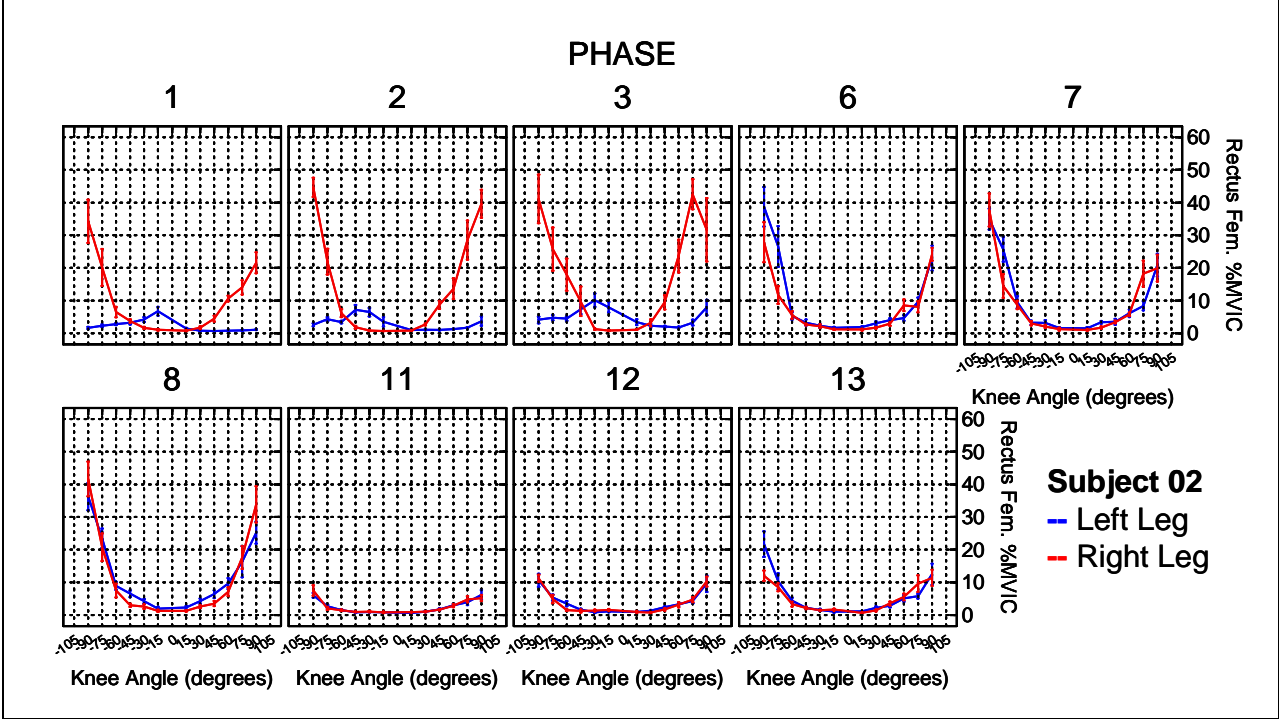
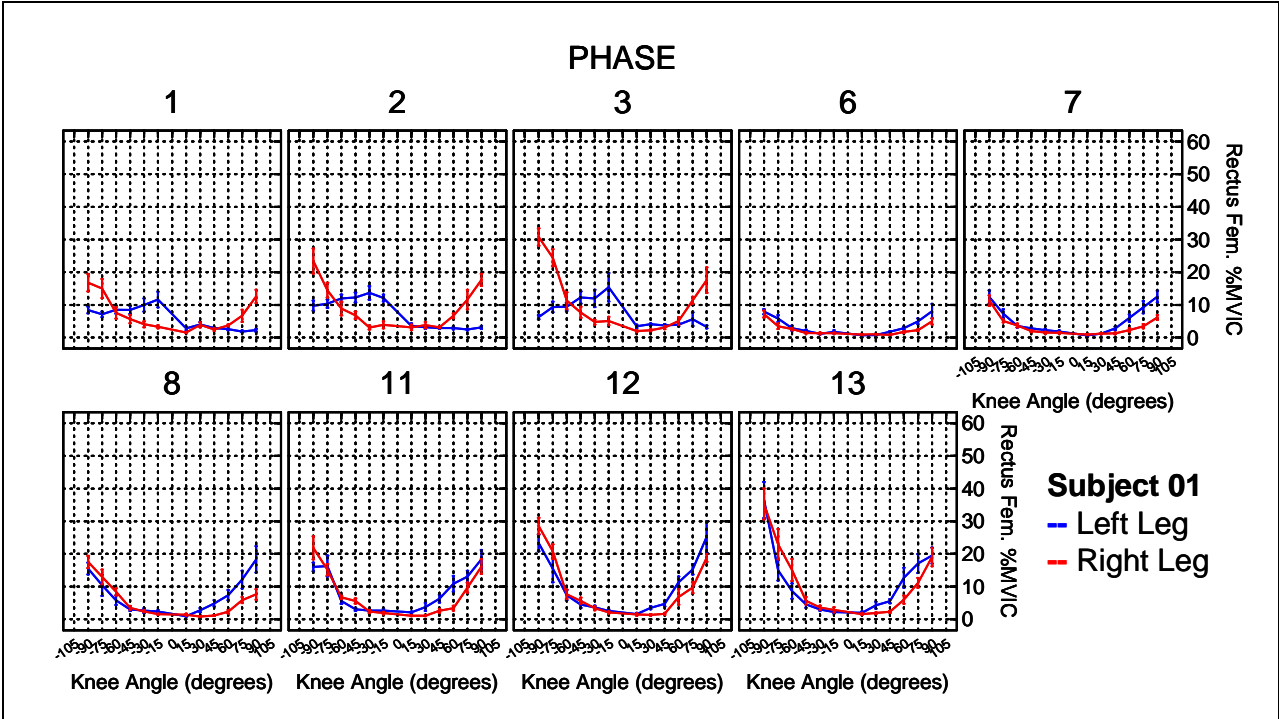
* p < 0.05, # p > 0.05

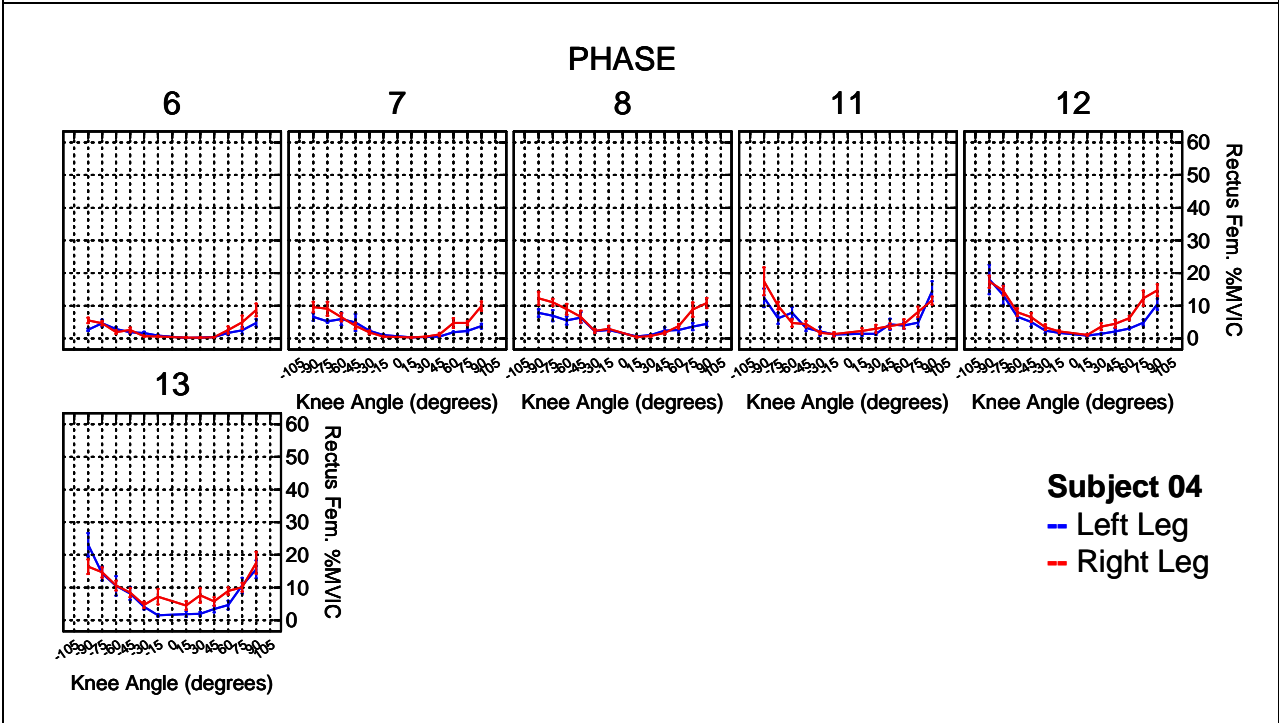
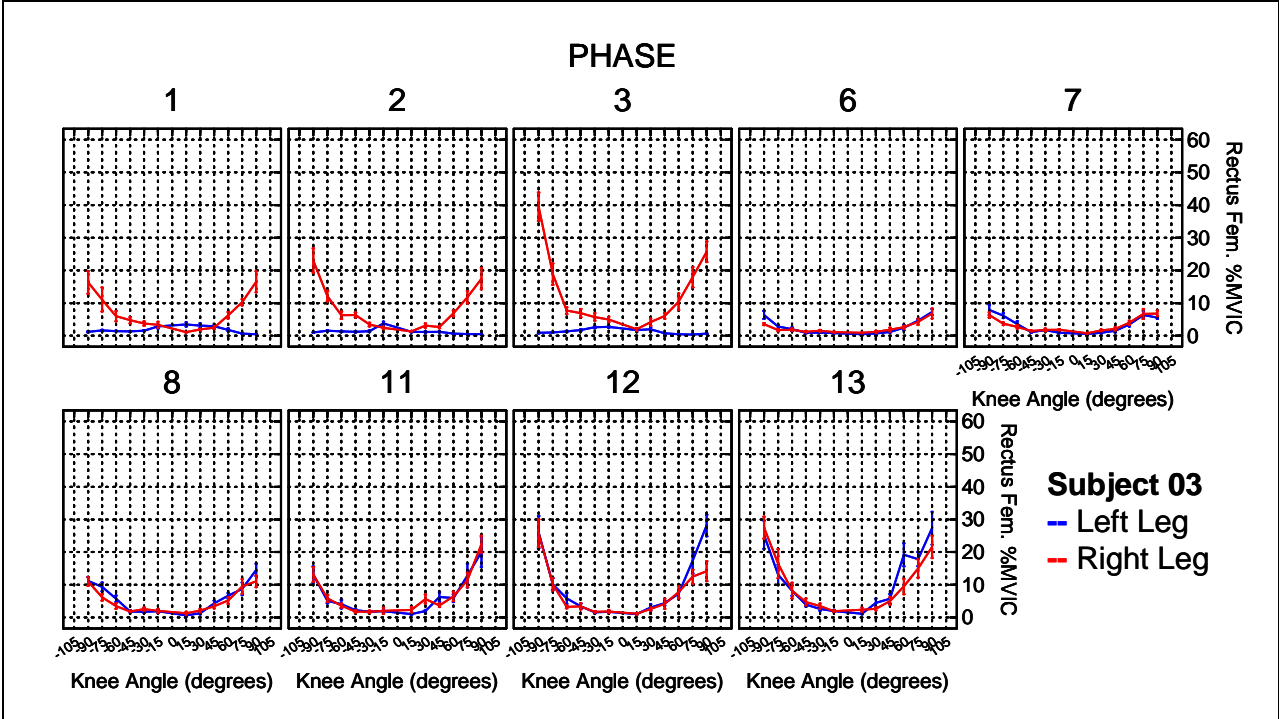
Knee Angle	Up 10%	23-RPM 0%	23-RPM 10%	23-RPM 25%	30-RPM 0%	30-RPM 10%	30-RPM 25%
15	5.19	-2.44*	0.01#	-3.32*	-0.57#	0.28#	3.23#
30	8.06	-1.22#	-2.06#	-3.95*	1.13#	1.81#	1.96#
45	10.76	-5.96*	-2.02#	-4.07*	-0.36#	1.28#	2.67#
60	14.64	-4.62*	-2.50#	-4.01*	-0.10#	2.40#	3.21#
75	20.89	-6.28*	-3.38#	-7.14*	-3.16#	-1.18#	1.38#
90	24.79	-6.86*	-3.12#	-7.88*	-2.09#	2.96#	4.06#
-90	34.91	-17.90*	-11.87*	-6.63*	-5.40*	0.76#	8.08*
-75	25.31	-12.58*	-3.58#	-4.60*	-2.53#	0.25#	7.23*
-60	17.45	-5.66*	1.78#	-0.29#	-1.12#	0.73#	5.69*
-45	16.34	-4.45#	-0.51#	-3.07*	0.45#	-0.28#	2.44#
-30	11.88	-1.81#	0.99#	-1.78#	6.60#	1.44#	5.36*
-15	9.37	1.26#	-3.49*	-0.98#	2.29#	4.61#	5.34*

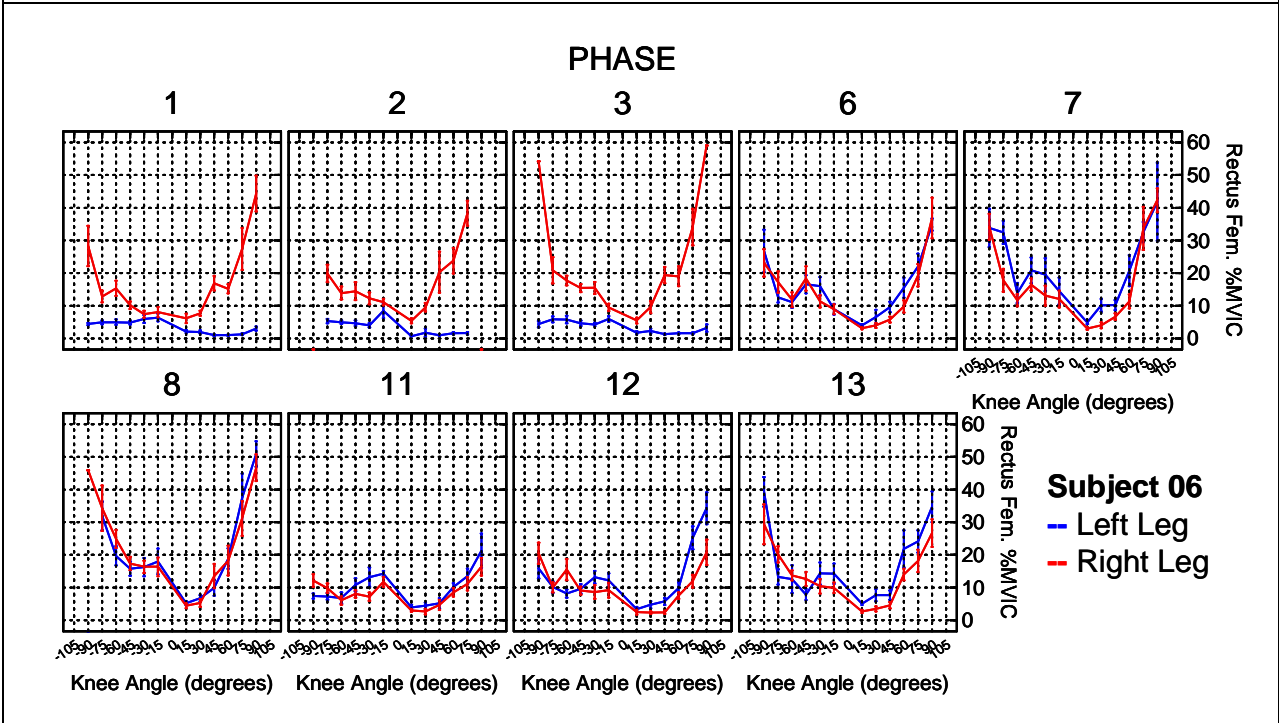
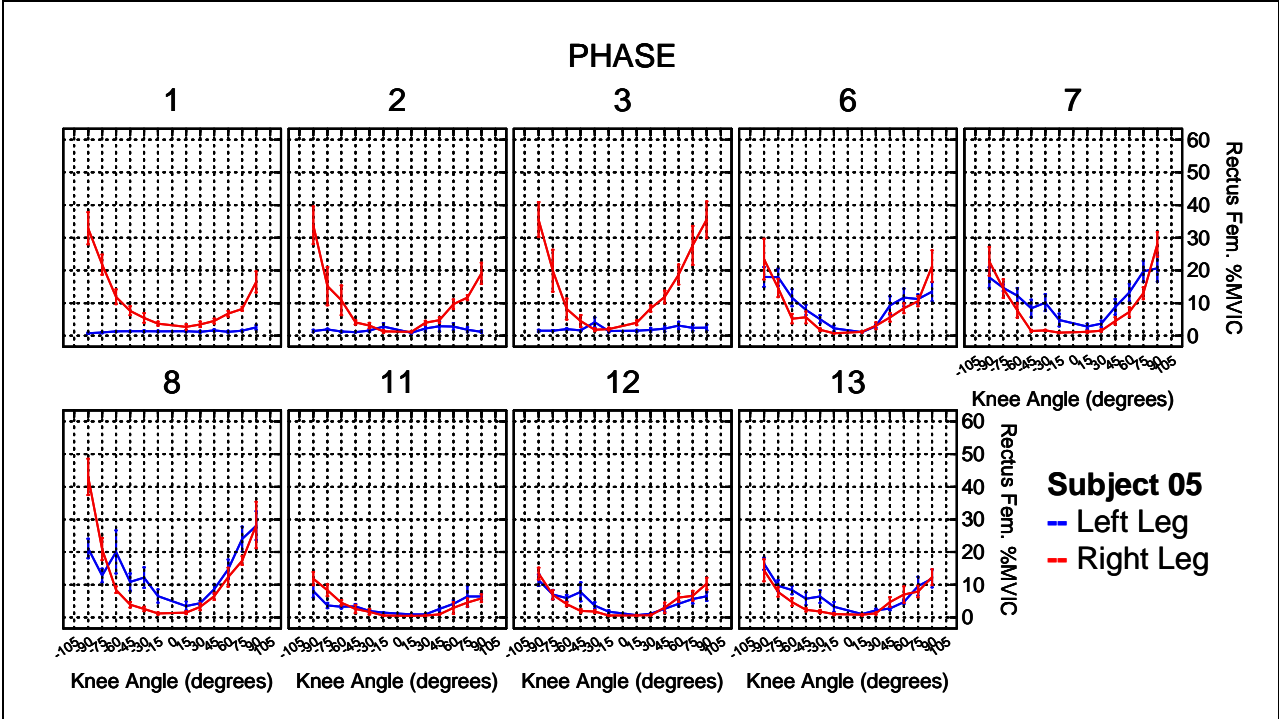
* p < 0.05, # p > 0.05

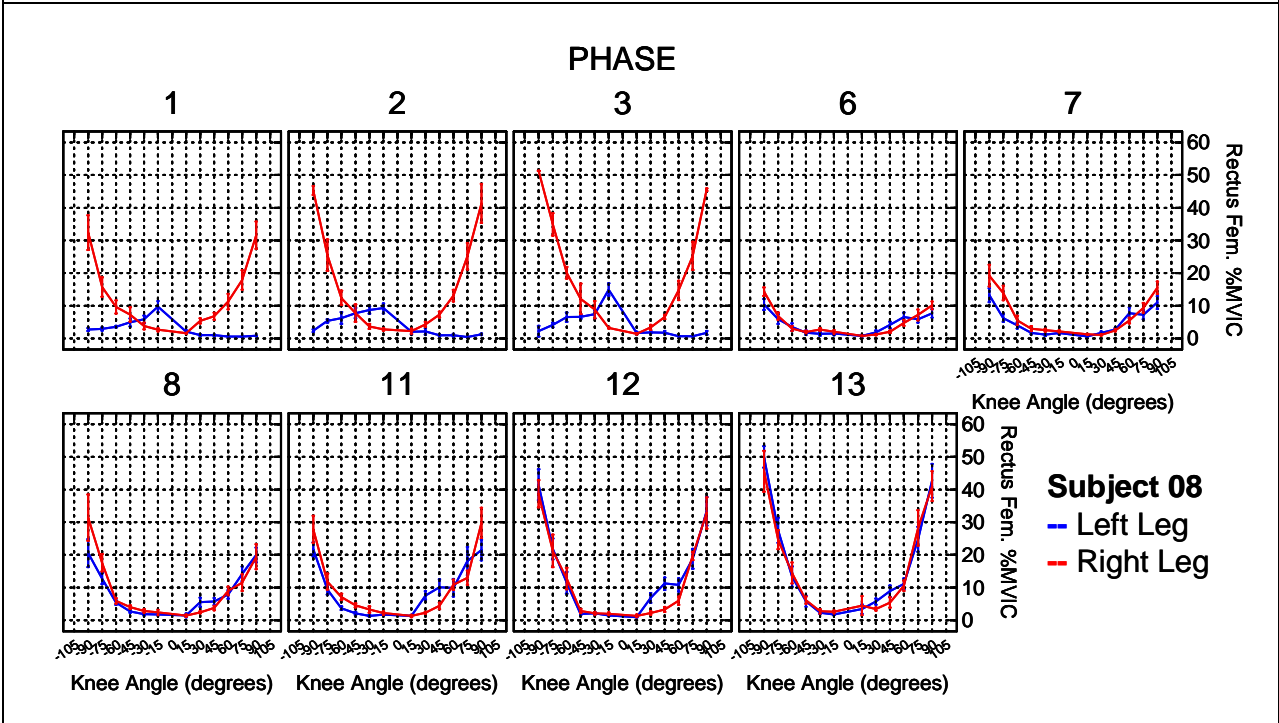
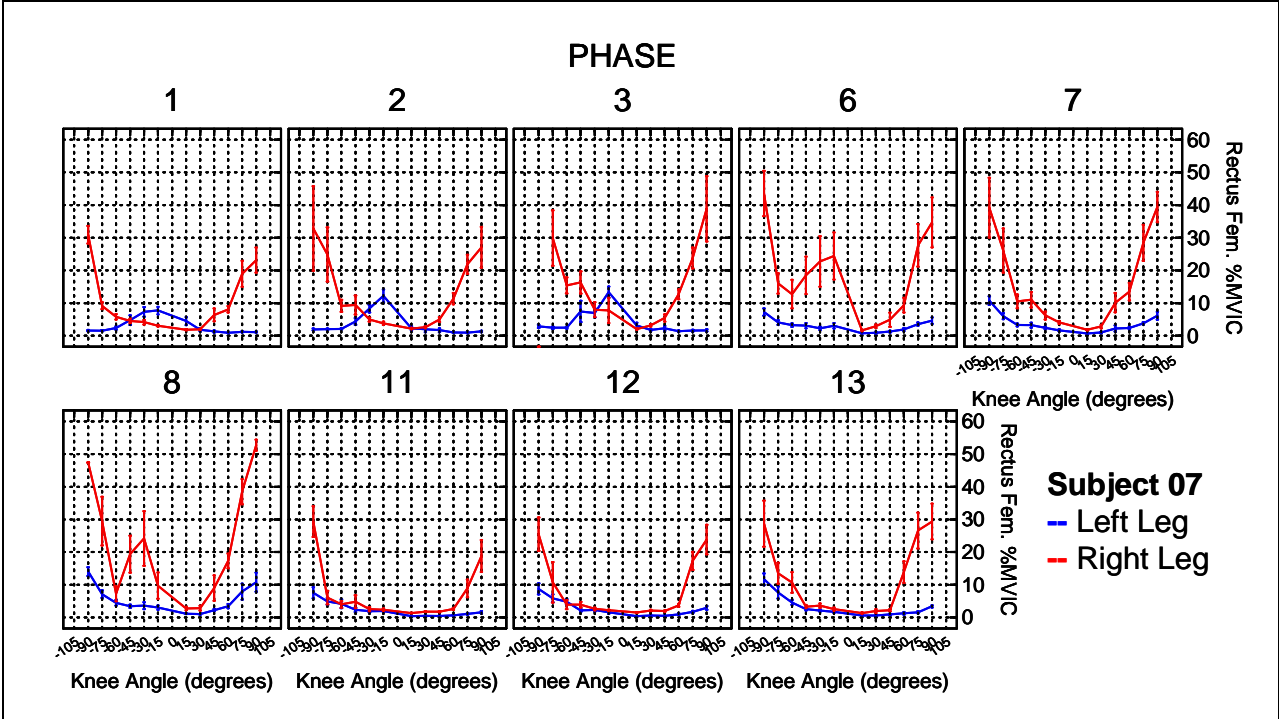
Knee Angle	Up 25%	23-RPM 0%	23-RPM 10%	23-RPM 25%	30-RPM 0%	30-RPM 10%	30-RPM 25%
15	6.80	-4.05*	-1.60#	-4.93*	-2.18#	-1.33#	1.62#
30	9.65	-2.81#	-3.65#	-5.54*	-0.46#	0.22#	0.37#
45	15.91	-11.10*	-7.16*	-9.22*	-5.50*	-3.87#	-2.48#
60	19.00	-8.98*	-6.86*	-8.37*	-4.46*	-1.96#	-1.15#
75	23.86	-9.24*	-6.34*	-10.10*	-6.12*	-4.14#	-1.58#
90	33.46	-15.53*	-11.79*	-16.55*	-10.76*	-5.71#	-4.61#
-90	37.43	-20.42*	-14.39*	-9.15*	-7.92*	-1.75#	5.56*
-75	30.01	-17.29*	-8.28*	-9.30*	-7.23*	-4.45*	2.52#
-60	21.59	-9.80*	-2.36*	-4.43*	-5.27*	-3.41*	1.55#
-45	17.37	-5.48*	-1.55#	-4.10*	-0.59#	-1.31#	1.41#
-30	14.61	-4.54#	-1.74#	-4.51*	3.87#	-1.28#	2.63#
-15	10.95	-0.32#	-5.07*	-2.56*	0.71#	3.03#	3.76#

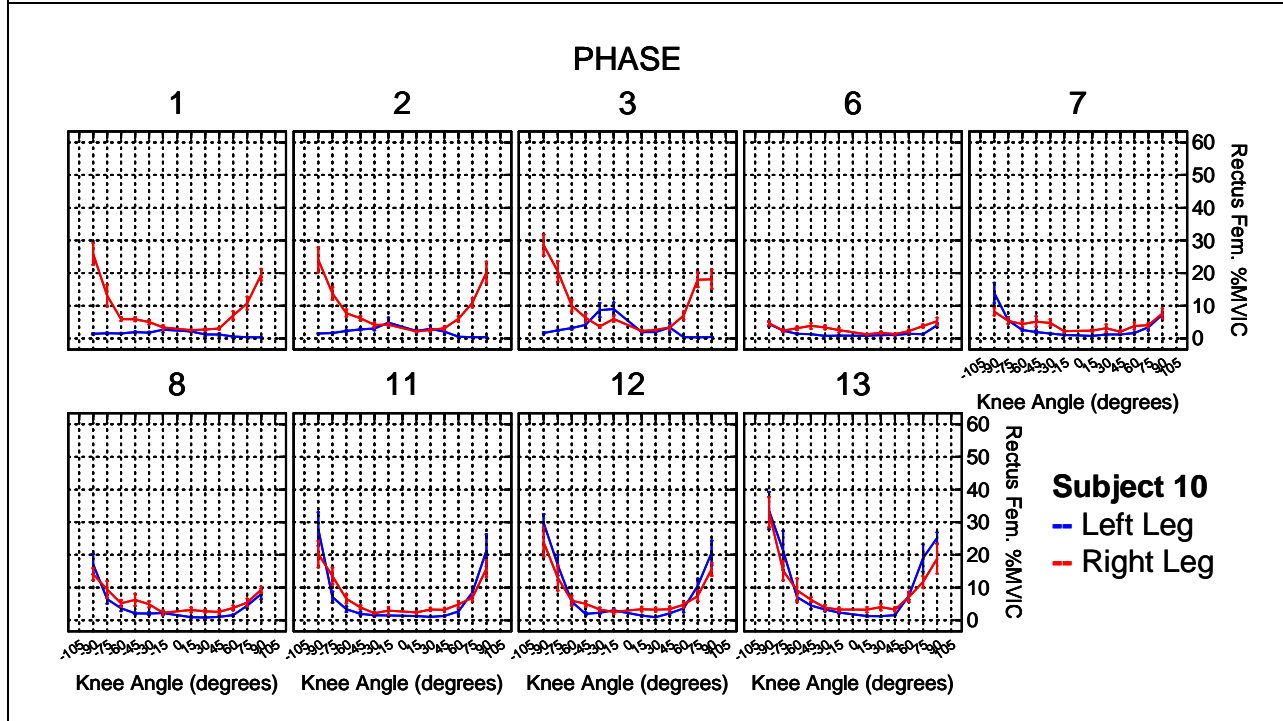
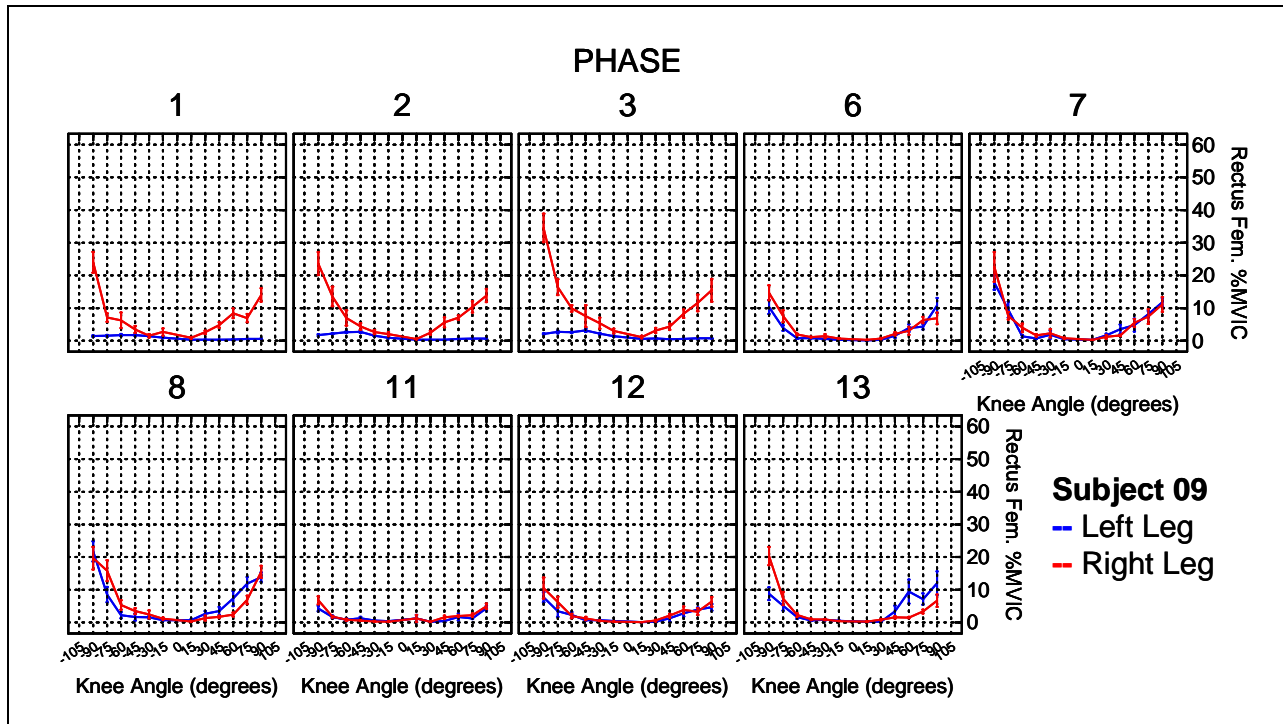
* p < 0.05, # p > 0.05

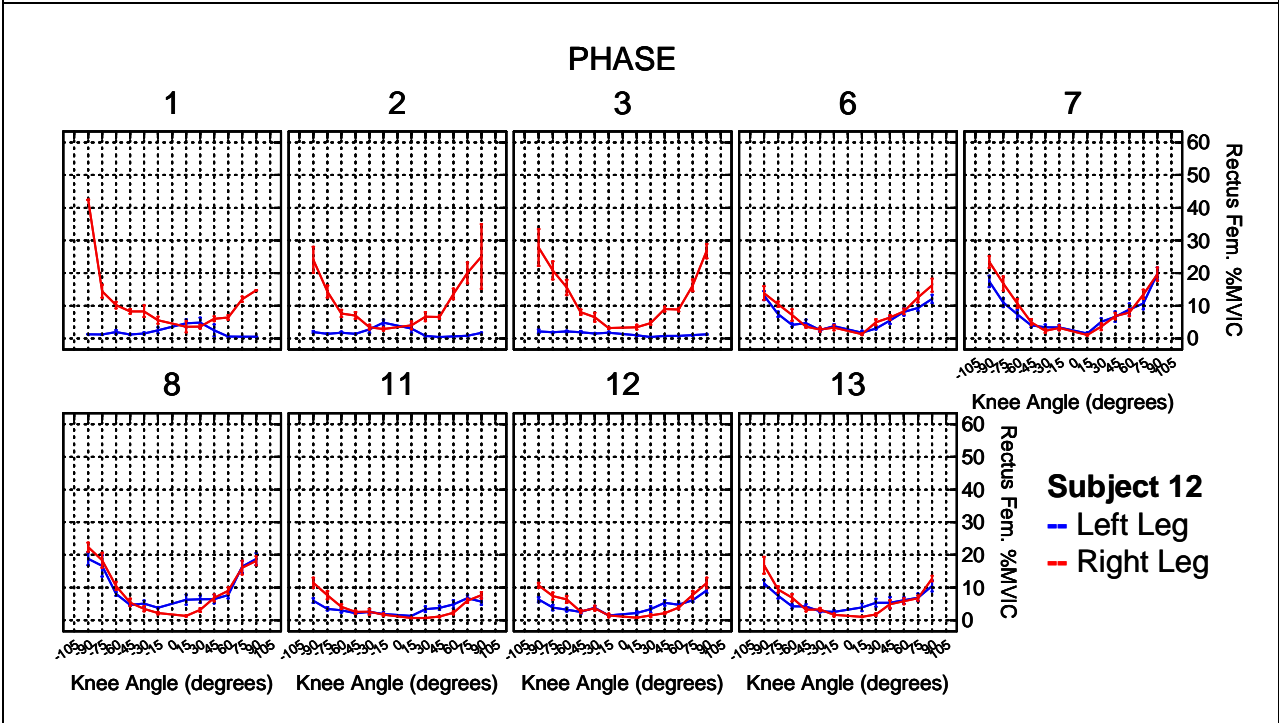
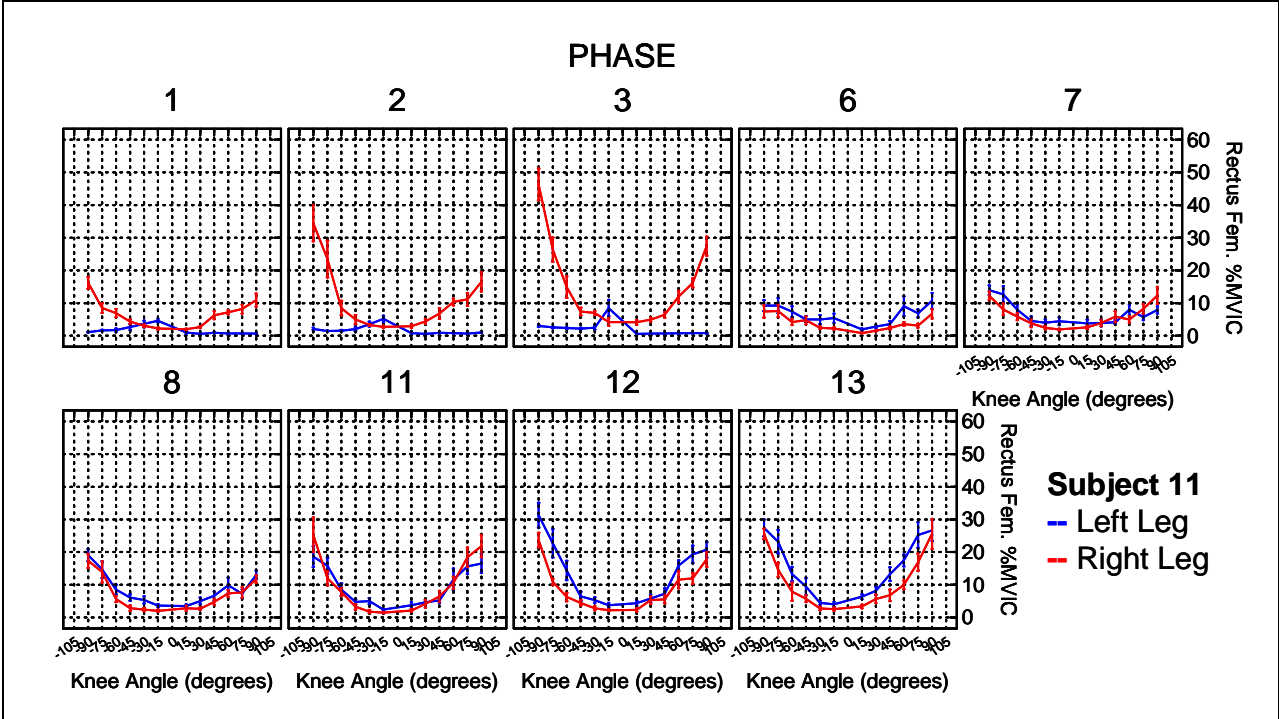


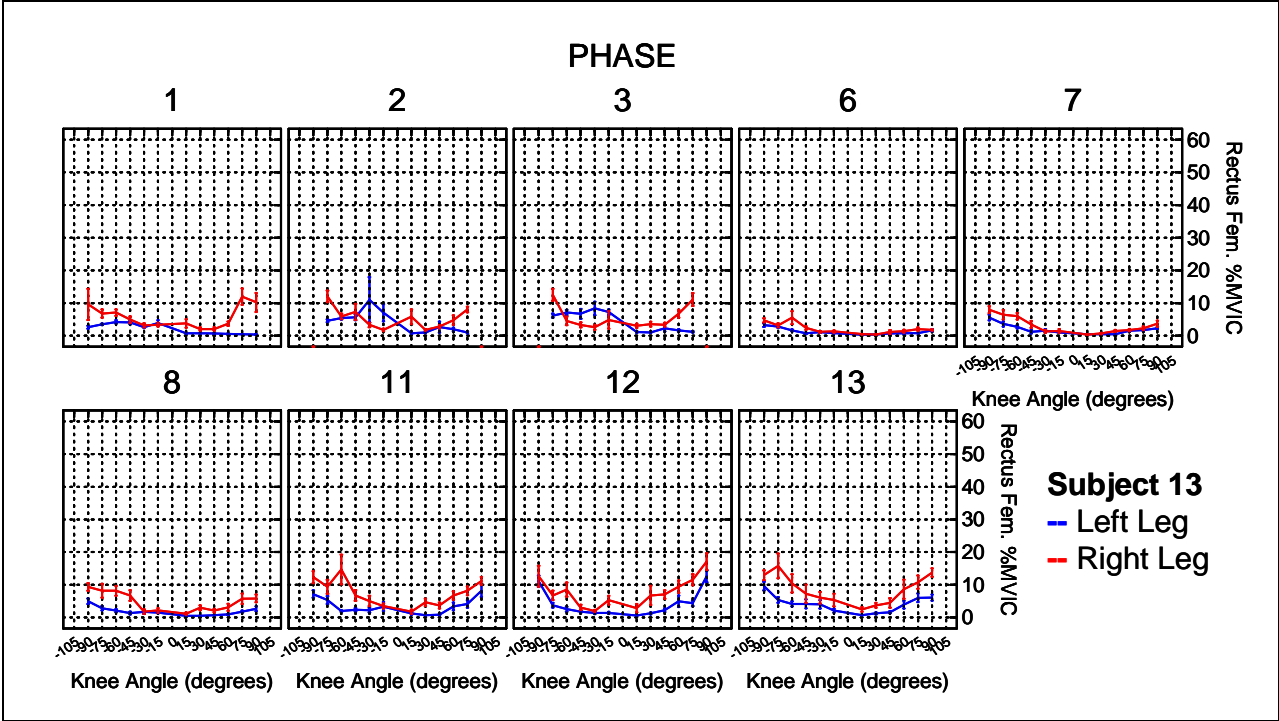












Left Rectus Femoris

Knee Angle	Up 0%	23-RPM 0%	23-RPM 10%	23-RPM 25%	30-RPM 0%	30-RPM 10%	30-RPM 25%
15	2.39	-1.33*	-1.22*	-0.80*	-0.70#	-0.64#	0.38#
30	3.32	-1.91*	-1.68*	-0.62*	-0.39#	0.35#	0.71#
45	5.54	-3.45*	-3.10*	-1.79*	-0.47#	-0.21#	0.41#
60	7.90	-4.09*	-3.57*	-1.34*	-0.62#	0.80#	2.73#
75	13.37	-8.75*	-6.97*	-5.10*	-2.75#	0.01#	5.39*
90	20.95	-14.04*	-11.93*	-8.08*	-3.29#	1.39#	4.58*
-90	25.43	-18.98*	-15.09*	-9.33*	-7.60*	0.27#	10.41*
-75	13.51	-9.09*	-7.17*	-4.51*	-2.86#	2.15#	4.01*
-60	8.28	-5.08*	-3.78*	-2.68*	-2.81#	-0.45#	1.64#
-45	5.91	-3.24*	-2.61*	-2.33*	-1.58#	-0.86#	0.53#
-30	4.30	-1.75*	-1.30*	-0.80*	-0.78#	0.26#	0.83#
-15	3.56	-1.01*	-1.18*	-0.53*	-0.87#	-0.30#	0.30#

* p < 0.05, # p > 0.05

Knee Angle	Up 10%	23-RPM 0%	23-RPM 10%	23-RPM 25%	30-RPM 0%	30-RPM 10%	30-RPM 25%
15	2.67	-1.61*	-1.50*	-1.08*	-0.98#	-0.92#	0.10#
30	4.02	-2.60*	-2.38*	-1.31*	-1.08#	-0.34#	0.02#
45	6.41	-4.32*	-3.98*	-2.66*	-1.34#	-1.09*	-0.47#
60	10.59	-6.78*	-6.26*	-4.03*	-3.30*	-1.89*	0.05#
75	17.81	-13.20*	-11.41*	-9.54*	-7.19*	-4.43*	0.95#
90	25.90	-18.99*	-16.88*	-13.03*	-8.24*	-3.56*	-0.37#
-90	42.82	-36.37*	-32.48*	-26.72*	-24.99*	-17.12*	-6.98*
-75	19.03	-14.61*	-12.69*	-10.03*	-8.38*	-3.37#	-1.51#
-60	8.73	-5.53*	-4.23*	-3.13*	-3.26#	-0.90#	1.19#
-45	6.74	-4.07*	-3.43*	-3.16*	-2.41#	-1.69#	-0.29#
-30	4.03	-1.48*	-1.03*	-0.52*	-0.51#	0.53#	1.11#
-15	3.33	-0.78*	-0.95*	-0.30*	-0.64#	-0.07#	0.53#

* p < 0.05, # p > 0.05

Knee Angle	Up 25%	23-RPM 0%	23-RPM 10%	23-RPM 25%	30-RPM 0%	30-RPM 10%	30-RPM 25%
15	2.69	-1.63*	-1.51*	-1.10*	-1.00#	-0.93#	0.08#
30	4.44	-3.02*	-2.79*	-1.73*	-1.50#	-0.76#	-0.40#
45	7.39	-5.29*	-4.95*	-3.63*	-2.31#	-2.06*	-1.44#
60	12.28	-8.47*	-7.95*	-5.72*	-4.99*	-3.58*	-1.64*
75	21.33	-16.71*	-14.93*	-13.06*	-10.71*	-7.95*	-2.57#
90	35.93	-29.02*	-26.91*	-23.06*	-18.27*	-13.59*	-10.40*
-90	47.85	-41.41*	-37.51*	-31.75*	-30.02*	-22.16*	-12.01*
-75	25.82	-21.40*	-19.47*	-16.82*	-15.17*	-10.16*	-8.30*
-60	12.79	-9.59*	-8.29*	-7.20*	-7.32*	-4.96*	-2.87#
-45	8.81	-6.13*	-5.50*	-5.22*	-4.47*	-3.76*	-2.36#
-30	5.93	-3.37*	-2.92*	-2.42*	-2.40#	-1.36#	-0.79#
-15	4.57	-2.03*	-2.19*	-1.54*	-1.89#	-1.32#	-0.71#

* p < 0.05, # p > 0.05

Right Rectus Femoris

Knee Angle	Up 0%	23-RPM 0%	23-RPM 10%	23-RPM 25%	30-RPM 0%	30-RPM 10%	30-RPM 25%
15	2.39	-1.36*	-1.22*	-0.96*	-0.69*	-0.68*	0.20#
30	3.32	-2.21*	-1.77*	-1.38*	-0.13#	-0.23#	0.33#
45	5.54	-3.86*	-3.23*	-2.38*	-1.25*	-0.68#	0.18#
60	7.90	-4.80*	-3.63*	-1.57*	-0.57#	0.09#	1.89*
75	13.37	-8.34*	-6.39*	-3.05*	-0.98#	1.98#	4.72*
90	20.95	-13.00*	-9.79*	-7.64*	0.65#	4.75#	9.97*
-90	25.43	-15.32*	-12.14*	-5.57*	-1.38#	6.24*	15.06*
-75	13.51	-8.47*	-5.97*	-2.28*	-1.05#	1.47#	7.50*
-60	8.28	-4.93*	-3.03*	-1.54*	-0.87#	-0.14#	2.49*
-45	5.91	-3.00*	-2.61*	-1.56*	0.29#	-0.54#	1.54#
-30	4.30	-2.09*	-1.60*	-1.17*	0.38#	-0.72#	1.77#
-15	3.56	-1.34*	-1.48*	-1.04*	0.69#	-0.42#	0.88#

* p < 0.05, # p > 0.05

Knee Angle	Up 10%	23-RPM 0%	23-RPM 10%	23-RPM 25%	30-RPM 0%	30-RPM 10%	30-RPM 25%
15	2.67	-1.64*	-1.50*	-1.24*	-0.97*	-0.96*	-0.08#
30	4.02	-2.90*	-2.47*	-2.08*	-0.83*	-0.93*	-0.37#
45	6.41	-4.73*	-4.11*	-3.25*	-2.13*	-1.56*	-0.70#
60	10.59	-7.49*	-6.32*	-4.26*	-3.26*	-2.59*	-0.79#
75	17.81	-12.78*	-10.83*	-7.50*	-5.42*	-2.46#	0.28#
90	25.90	-17.95*	-14.74*	-12.59*	-4.30#	-0.20#	5.02#
-90	42.82	-32.70*	-29.53*	-22.96*	-18.77*	-11.15*	-2.33#
-75	19.03	-13.99*	-11.49*	-7.80*	-6.57*	-4.05*	1.98#
-60	8.73	-5.38*	-3.49*	-1.99*	-1.32#	-0.59#	2.04*
-45	6.74	-3.82*	-3.44*	-2.39*	-0.54#	-1.37#	0.71#
-30	4.03	-1.82*	-1.33*	-0.90*	0.66#	-0.45#	2.04*
-15	3.33	-1.11*	-1.25*	-0.81*	0.91#	-0.19#	1.11#

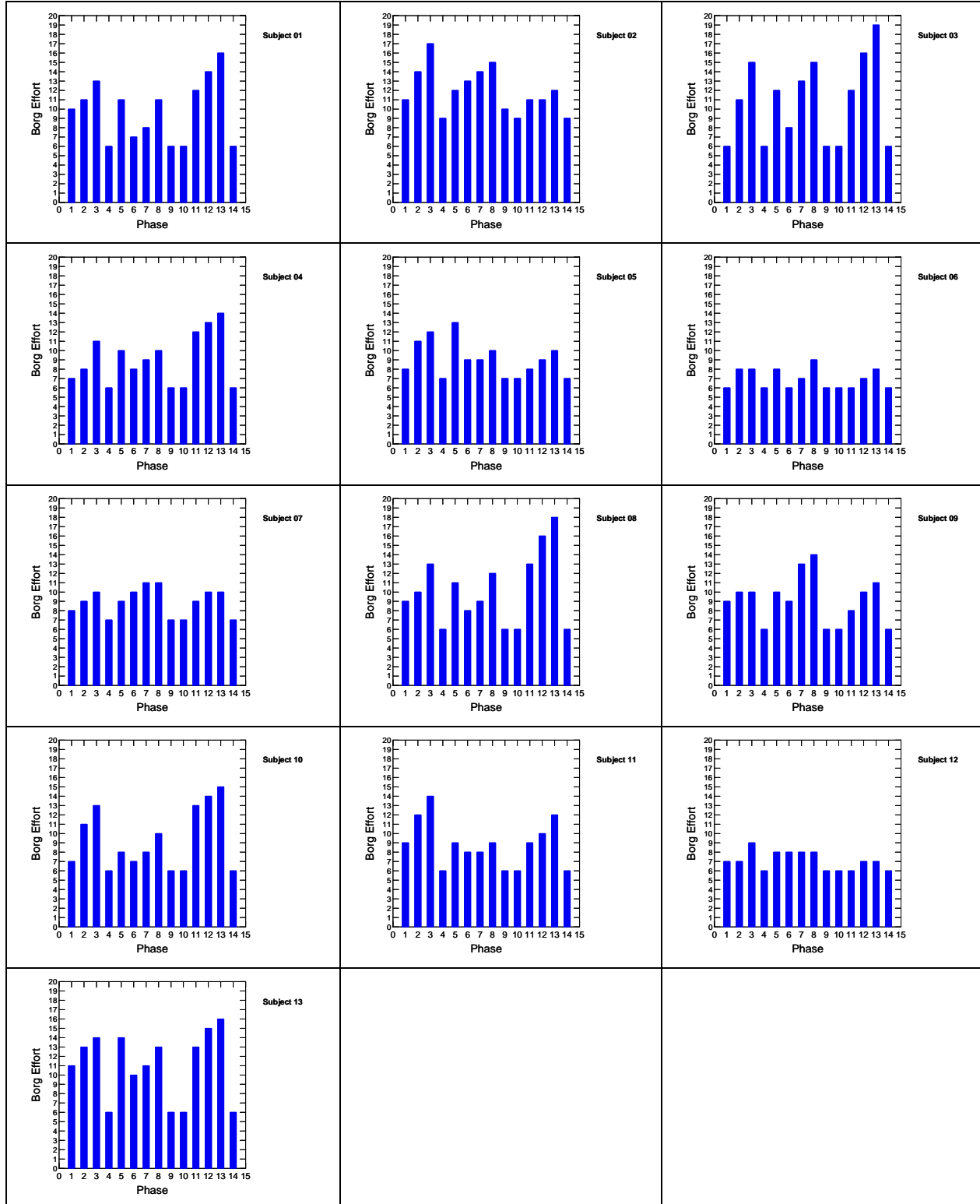
* p < 0.05, # p > 0.05

Knee Angle	Up 25%	23-RPM 0%	23-RPM 10%	23-RPM 25%	30-RPM 0%	30-RPM 10%	30-RPM 25%
15	2.69	-1.66*	-1.51*	-1.25*	-0.98*	-0.97*	-0.09#
30	4.44	-3.32*	-2.88*	-2.49*	-1.24*	-1.34*	-0.78#
45	7.39	-5.70*	-5.08*	-4.22*	-3.10*	-2.53*	-1.67*
60	12.28	-9.18*	-8.01*	-5.95*	-4.95*	-4.28*	-2.48*
75	21.33	-16.30*	-14.35*	-11.01*	-8.94*	-5.98*	-3.24#
90	35.93	-27.98*	-24.77*	-22.62*	-14.33*	-10.23*	-5.01#
-90	47.85	-37.74*	-34.56*	-27.99*	-23.80*	-16.18*	-7.36*
-75	25.82	-20.78*	-18.28*	-14.59*	-13.36*	-10.84*	-4.80*
-60	12.79	-9.44*	-7.55*	-6.06*	-5.39*	-4.65*	-2.03#
-45	8.81	-5.89*	-5.50*	-4.45*	-2.60*	-3.44*	-1.35#
-30	5.93	-3.71*	-3.23*	-2.80*	-1.24#	-2.34*	0.15#
-15	4.57	-2.35*	-2.49*	-2.06*	-0.33#	-1.44*	-0.13#

* p < 0.05, # p > 0.05

Borg Effort

Subjective ratings of effort on the Borg scale. The ratings are plotted against the Experiment Phase. To determine whether Phases 6-8 or 11-13 are at 23 or 30 RPM, the Group assignment must be determined from the identifiers at the beginning of the Experiment 2 data.



Motion Sickness

Subjective ratings of motion sickness. The ratings are plotted against the Experiment Phase. To determine whether Phases 6-8 or 11-13 are at 23 or 30 RPM, the Group assignment must be determined from the identifiers at the beginning of the Experiment 2 data.

